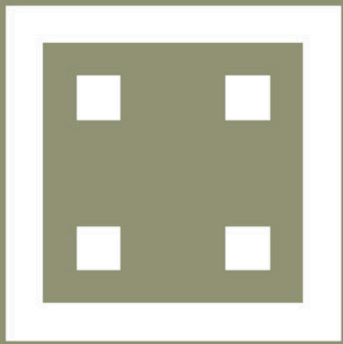


HA

HORMIGÓN y ACERO

REVISTA CUATRIMESTRAL DE **ACHE** ASOCIACIÓN ESPAÑOLA DE INGENIERÍA ESTRUCTURAL

Enero - Agosto 2023 | Volumen 74 - Número 299-300



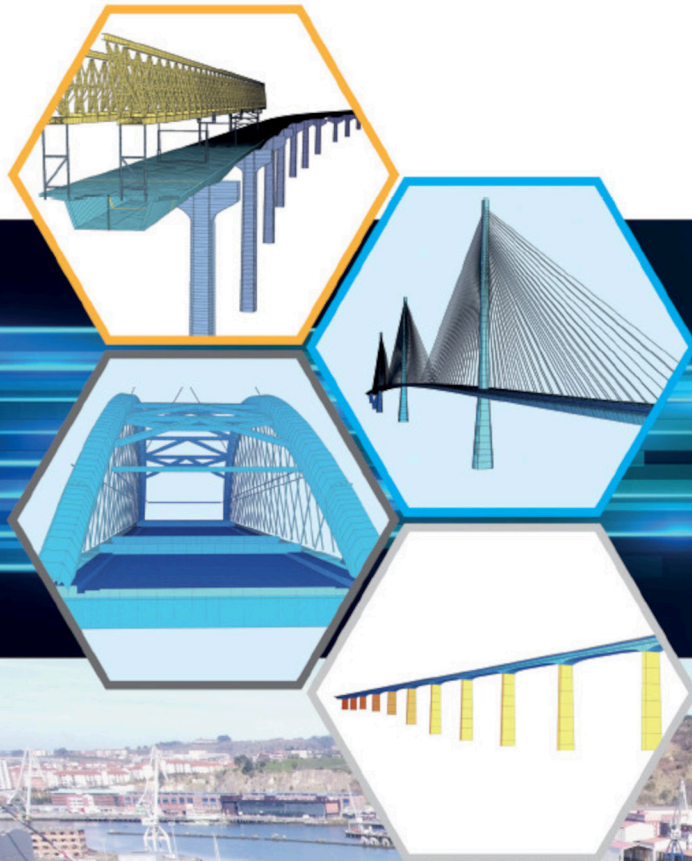
EUROCODES

EN 1992

Design of concrete structures



SOFISTIK



DISEÑO DE PUENTES



sbp  **calter**
schlich
beigermann partner

 **calter**
ingeniería de estructuras

www.sofistik.es
sofistik@calter.es



FOTO DE PORTADA: "Design of concrete structures. Eurocodes. EN 1992".

CONSEJO EDITORIAL:

DIRECTOR:

Gonzalo Ruiz López (ETSI CAMINOS, C. y P. – UCLM, Ciudad Real, España)*

SUBDIRECTOR:

Julio Sánchez Delgado (FHECOR, Madrid, España)*

SECRETARIO:

Dorys C. González Cabrera (E. POLITÉCNICA SUPERIOR – Universidad de Burgos, Burgos, España)*

EDITOR JEFE:

Valentín Alejándrez Piñuela (CINTER, Madrid, España)*

ASESOR EDITORIAL:

José Manuel Ráez Cano (SCIDOC, Madrid, España)*

VOCALES:

Víctor Alvaro Benítez (LEONHARDT, ANDRÄ UND PARTNER BERATENDE INGENIEURE VBI AG, Stuttgart, Alemania)

Juan Luis Bellod Thomas (CESMA INGENIEROS, Madrid, España)

Héctor Bernardo Gutiérrez (GGRAVITY S.A., Madrid, España)

Ángel Castillo Talavera (ISTITUTO E. TORROJA – CSIC, Madrid, España)

Héctor Cifuentes Bulté (ETS INGENIERÍA – Universidad de Sevilla, Sevilla, España)*

Antoni Cladera Bohigas (UNIVERSIDAD DE LAS ISLAS BALEARES, Palma, España)

David Fernández Montes (ETS INGENIERÍA CIVIL – UPM, Madrid, España)

Luisa María Gil Martín (ETSI CAMINOS, C. y P. – UGR, Granada, España)

Beatriz Martín Pérez (UNIVERSITY OF OTTAWA, Ottawa, Canadá)

Pedro Miguel Sosa (ETSI CAMINOS, C. y P. – UPV, Valencia, España)

Alejandro Pérez Caldentey (FHECOR, Madrid, España)

Lisbel Rueda García (ICITECH – UPV, Valencia, España)

Jacinto Ruiz Carmona (MECANISMO INGENIERÍA, Madrid, España)

Abraham Sánchez Corriols (CONSULTOR INDEPENDIENTE, Stuttgart, Alemania)

Álvaro Serrano Corral (MC 2 ESTUDIO DE INGENIERÍA, Madrid, España)

Juan Antonio Sobrino Almunia (PEDELTA CANADA INC., Toronto, Canadá)

Carlos Thomas García (ETSI CAMINOS, C. y P. – Universidad de Cantabria, Santander, España)

* Miembro del Comité de Redacción

CONSEJO ASESOR CIENTÍFICO**

António Adão da Fonseca (UNIVERSIDADE DO PORTO, FACULDADE DE ENGENHARIA, Oporto, Portugal)

Antonio Aguado de Cea (ETSI CAMINOS, C. y P. – UPC, Barcelona, España)

Pilar Alaejos Gutiérrez (CEDEX, Madrid, España)

M^a Carmen Andrade Perdrix (CIMNE, Madrid, España)

Ángel Aparicio Bengoechea (ETSI CAMINOS, C. y P. – UPC, Barcelona, España)

José M^a Arrieta Torrealba (PROES, Madrid, España)

Miguel Ángel Astiz Suárez (ETSI CAMINOS, C. y P. – UPM, Madrid, España)

Gustavo Ayala Milián (INSTITUTO DE INGENIERÍA – UNAM, Coyoacán, México D.F.)

Alex Barbat Barbat (ETSI CAMINOS, C. y P. – UPC, Barcelona, España)

Pilar Crespo Rodríguez (MINISTERIO DE TRANSPORTES, MOVILIDAD Y AGENDA URBANA, Madrid, España)

Paulo J. S. Cruz (UNIVERSIDADE DO MINHO, SCHOOL OF ARCHITECTURE, Guimarães, Portugal)

Luis Fernández Luco (UNIVERSIDAD DE BUENOS AIRES, FACULTAD DE INGENIERÍA, Buenos Aires, Argentina)

Miguel Fernández Ruiz (ETSI CAMINOS, C. y P. – UPM, Madrid, España)

Jaime Carlos Gálvez Ruiz (ETSI CAMINOS, C. y P. – UPM, Madrid, España)

Ravindra Gettu (INDIAN INSTITUTE OF TECHNOLOGY MADRAS, Chennai, India)

Gian Carlo Giuliani (REDESCO PROGETTI SRL, Milán, Italia)

Enrique González Valle (INTEMAC, Madrid, España)

Paulo R. L. Helene (ESCOLA POLITÉCNICA, UNIVERSIDADE DE SÃO PAULO, São Paulo, Brasil)

José Antonio Llombart Jaques (EIPSA, Madrid, España)

Antonio Mari Bernat (ETSI CAMINOS, C. y P. – UPC, Barcelona, España)

Francisco Millanes Mato (IDEAM, Madrid, España)

Santiago Pérez-Fadón Martínez (FADÓN INGENIERÍA S.L., Madrid, España)

Carlos A. Prato (UNIVERSIDAD NACIONAL DE CORDOBA, Córdoba, Argentina)

António Reis (IST – UNIVERSIDADE TÉCNICA DE LISBOA, Lisboa, Portugal)

Jesús Rodríguez Santiago (ETS DE ARQUITECTURA, UPM, Madrid, España)

José Manuel Roesset (NATIONAL ACADEMY OF ENGINEERING, Washington DC, EE.UU.)

Ana M. Ruiz-Terán (IMPERIAL COLLEGE LONDON, FACULTY OF ENGINEERING, London, Reino Unido)

Juan Sagaseta Albajar (UNIVERSITY OF SURREY, FACULTY OF ENGINEERING AND PHYSICAL SCIENCES, Guildford, Surrey, Reino Unido)

Mike Schlaich (SCHLAICH BERGERMANN UND PARTNER, Stuttgart, Alemania)

Carlos Siegrist Fernández (SIEGRIST Y MORENO, Madrid, España)

Peter J. Stafford (IMPERIAL COLLEGE LONDON, FACULTY OF ENGINEERING, London, Reino Unido)

** Incluye además a los Presidentes de las Comisiones Técnicas de ACHE

El Consejo Editorial de la revista tiene como misión la definición de la política editorial (estilo de la revista, redacción, normas de presentación de originales, diseño, creación y orientación de las distintas secciones). El Comité de Redacción se constituye como un comité permanente del Consejo Editorial y se encarga de dirigir y supervisar la gestión diaria de la revista, controlar la selección de contribuciones y tomar las decisiones sobre los contenidos que han de conformar cada número de la revista. La función del Consejo Asesor Científico es la de velar por el prestigio científico y técnico de la revista, promoviendo e impulsando su difusión internacional.

Una descripción más amplia puede consultarse en www.hormigonyacero.com

ÍNDICES Y SERVICIOS DE INFORMACIÓN: *Hormigón y Acero* está indexada en las bases de datos siguientes: Emerging Sources Citation Index/Web of Science Core Collection (ESCI/WoS) - Journal Citation Reports (JCR) – Pascal – Índices-CSIC – Dialnet-Sumaris – Catálogo Latindex 2.0 – ScienceDirect.

Todos los contenidos se publican como artículos de acceso abierto, bajo la licencia *Creative Commons Reconocimiento-No Comercial-Sin Obra Derivada* (CC BY-NC-ND 4.0). No se admite el uso de los artículos con fines comerciales. Si permite copiar, distribuir e incluir el artículo en un trabajo colectivo (por ejemplo, una antología), siempre y cuando no exista finalidad comercial, no se altere ni se modifique el artículo y se cite apropiadamente el trabajo original.

Ni Cinter Divulgación Técnica ni la Asociación Española de Ingeniería Estructural (ACHE) tendrán responsabilidad alguna por las lesiones y/o daños sobre personas o bienes que sean el resultado de presuntas declaraciones difamatorias, violaciones de derechos de propiedad intelectual, industrial o privacidad, responsabilidad por producto o negligencia. Tampoco asumirán responsabilidad alguna por la aplicación o utilización de los métodos, productos, instrucciones o ideas descritos en el presente material. Aunque el material publicitario se ajusta a los estándares éticos, su inclusión en esta publicación no constituye garantía ni refrendo alguno de la calidad o valor de dicho producto, ni de las afirmaciones realizadas por su fabricante.

ISSN 0439-5689

Publicación cuatrimestral (3 números al año)

www.hormigonyacero.com

Protección de datos: CINTER DIVULGACIÓN TÉCNICA, S.L. declara cumplir lo dispuesto por la Ley orgánica 15/1999, de 13 de diciembre, de Protección de Datos de Carácter Personal.

Suscripciones y atención al cliente

 CINTER DIVULGACIÓN TÉCNICA, S.L.
C/Doctor Santero, 7, 28039 Madrid (España)
Teléfono: 913191200
Correo electrónico: cinter@cinter.es

Impresa en España por Gráficas Muriel
Diseño gráfico y maquetación: mgrafico.com

Déposito legal: M-853-1958

The Origins and Some Highlights on the New Proposal for Eurocode 2 <i>Los orígenes y temas principales en la nueva propuesta del Eurocódigo 2</i> José María Arrieta, Jesús Rodríguez, & Hans Ganz.....	7
Durability and Cover Depth Provisions in Next Eurocode 2. Background Modelling and Calculations <i>Capítulo sobre durabilidad y recubrimientos en el próximo Eurocódigo 2. Documento de fundamentos y cálculos</i> Carmen Andrade, & David Izquierdo.....	19
Shear Resistance of Members Without Shear Reinforcement in Presence of Axial Forces in the Next Eurocode 2 <i>Resistencia a cortante de elementos sin armadura de cortante en presencia de esfuerzos axiales en el próximo Eurocódigo 2</i> Pedro F. Miguel, Miguel Ángel Fernández, Josef Hegger, & Maximilian Schmidt.....	41
A Mechanical Approach for the Punching Shear Provisions in the Second Generation of Eurocode 2 <i>El tratamiento del punzonamiento en la segunda generación del Eurocódigo 2 basado en un modelo mecánico</i> Aurelio Muttoni, João T. Simões, Duarte M.V. Faria, & Miguel Fernández Ruiz.....	61
Stress Fields and Strut-and-tie Models as a Basic Tool for Design and Verification in Second Generation of Eurocode 2 <i>Campos de tensiones y modelos de bielas y tirantes: herramientas fundamentales para el proyecto y comprobación de estructuras de hormigón en la segunda generación del Eurocódigo 2</i> Miguel Fernández Ruiz, Linh Cao Hoang, & Aurelio Muttoni.....	79
Serviceability Limit States According to the New Eurocode 2 Proposal: Description and Justifications of the Proposed Changes <i>Estados Límite de Servicio de acuerdo con la propuesta del nuevo Eurocódigo 2: Descripción y justificación de los cambios introducidos</i> Alejandro Pérez Caldentey, Juan Luis Bellod Thomas, Lluís Torres, & Terje Kanstad.....	91
Fatigue in Structural Concrete According to the New Eurocode 2 <i>La fatiga en hormigón estructural según el nuevo Eurocódigo 2</i> Carlos Ríos, Juan Carlos Lancha, & Miguel Ángel Vicente.....	109
Design Provisions for Anchorages and Laps in the Revised EC2 <i>Disposiciones de diseño para anclajes y solapes en la revisión del EC2</i> John Cairns.....	123
Contributions of the Future Eurocode for the Assessment of Existing Concrete Structures <i>Aportaciones del futuro Eurocódigo 2 para la evaluación de estructuras existentes de hormigón</i> Eduardo Díaz-Pavón Cuaresma, Raúl Rodríguez Escribano, Jorge Ley Urzaiz, & Pedro López Sánchez.....	139
Strengthening Existing Concrete Structures with Fibre Reinforced Polymers (FRP) in the New Version of Eurocode 2 <i>Refuerzo de estructuras existentes de hormigón con polímeros reforzados con fibras (PRF) en la nueva versión del Eurocódigo 2</i> Eva Oller, Ana de Diego, Lluís Torres, & Pedro Madera.....	151
Design of Steel Fibre Reinforced Concrete Structures According to the Annex L of the Eurocode-2 2023 <i>Diseño de estructuras de hormigón reforzado con fibras de acero según el Anejo L del nuevo Eurocódigo-2:2023</i> Albert de la Fuente, Andrea Monserrat-López, Nikola Tošić, & Pedro Serna.....	169
Compressive Behaviour of Steel-Fiber Reinforced Concrete in Annex L of New Eurocode 2 <i>Comportamiento en compresión del hormigón reforzado con fibras de acero según el Anejo L del nuevo Eurocódigo 2</i> Gonzalo Ruiz, Ángel De la Rosa, Elisa Poveda, Riccardo Zanon, Markus Schäfer, & Sébastien Wolf.....	187
Embedded Fibre Reinforced Polymers (FRP) in Concrete Structures According to the New Version of Eurocode 2 <i>Armadura de polímeros reforzados con fibras (PRF) para estructuras de hormigón en la nueva versión del Eurocódigo 2</i> Eva Oller, Lluís Torres, & Ana de Diego.....	199
Eurocode Practice: Design of Fastenings for Use in Concrete in Accordance with EC2, Part 4 (EN 1992-4) <i>Eurocódigo práctico: diseño de fijaciones para su uso en hormigón de acuerdo con EC2, parte 4 (EN 1992-4)</i> Jörg Appl, & Antonio Cardo Fernández.....	211
Some Highlights on the New Version of EN 1992-1-2 (Eurocode 2, Fire Part) <i>Algunos aspectos destacados de la nueva versión de la norma EN 1992-1-2 (Eurocódigo 2, parte de fuego)</i> Sergi Carrascón, Fabienne Robert, & Carlos Villagrà.....	223

MIEMBROS PATROCINADORES DE LA ASOCIACIÓN ESPAÑOLA DE INGENIERÍA ESTRUCTURAL (ACHE)

Según los Estatutos de la Asociación existen dos tipos de miembros, uno para personas jurídicas y otro para personas físicas. De entre los primeros, y por la importancia que tienen para la Asociación por su contribución económica, destacan los miembros Patrocinadores y los Protectores. Hasta la fecha de cierre del presente número de la Revista, figuran inscritos como **Miembros Patrocinadores** los que a continuación se indican, citados por orden alfabético:



MIEMBROS PROTECTORES DE LA ASOCIACIÓN ESPAÑOLA DE INGENIERÍA ESTRUCTURAL (ACHE)

Según los Estatutos de la Asociación existen dos tipos de miembros, uno para personas jurídicas y otro para personas físicas. De entre los primeros, y por la importancia que tienen para la Asociación por su contribución económica, destacan los miembros Patrocinadores y los Protectores. Hasta la fecha de cierre del presente número de la Revista, figuran inscritos como **Miembros Protectores** los que a continuación se indican, citados por orden alfabético:



LETTER FROM THE DIRECTOR

This *Hormigón y Acero* monographic issue focuses on the new Eurocode 2. Jesús Rodríguez served as its Associate Editor. He is a member of the Scientific Advisory Council of our Journal and Coordinator of the UNE CTN140/SC2 Committee, formed by the Spanish experts who participated in the new Eurocode 2 development. The work of the Committee took a long time and was extensive in matters covered. It included the participation of some of its members in all the international subcommittees, who made relevant contributions to many of the proposed improvements.

The issue is excellent. We obtained exceptional articles explaining some of the most relevant novelties in Eurocode 2, written by members of the Spanish Committee and with notable contributions from authors from other countries. As usual, the articles followed peer reviews involving many other experts to ensure the high level of quality we want for *Hormigón y Acero*. All the editing steps were supervised by the Associate Editor. We hope the scientific and technological community of structural concrete enjoys this issue and considers it practical for getting acquainted with the new Eurocode 2.

Hormigón y Acero and ACHE are also preparing a one-day workshop to present this issue, scheduled for Tuesday, October 17, 2023, in the *ETSI Caminos, C. y P.* of the Polytechnic University of Madrid. A selection of authors will take part in it. There will also be four invited lecturers: Hans Ganz, who is the general coordinator

of CEN TC250/SC2 Eurocode 2, will speak on the scope and main changes of the new Eurocode 2; Aurelio Muttoni, who will talk on the new shear and punching model based on his critical shear crack theory; John Cairns, on anchoring and overlapping of reinforcing bars; and Patrick Bamonte, whose lecture deals on design against fire. We will give more information on the event as it gets closer. Please, reserve the date if you are interested in attending the workshop.

Some other monographic issues are being produced. David Fernández Montes is editing one on the shear in structural concrete elements. There are already seven papers published online, available at www.hormigonyacero.com, and we will likely have another three by the end of 2023. Similarly, Juan José Jorquera is editing an issue about the legacy of Jörg Schlaich in Spanish Structural Engineering. Alejandro Pérez Caldentey is preparing another one on the resistance of structures to blast loads.

Finally, let me remind you that *Hormigón y Acero* is in the Web of Science. Soon—in July this year—we will have our first impact factor in the Journal of Citation Reports. We hope that the aforesaid monographic issues—and the regular ones too—are of interest to our readership and new readers in Spain and abroad. Enjoy your reading of this one!

Gonzalo Ruiz
DIRECTOR OF HORMIGÓN Y ACERO

LETTER OF THE ASSOCIATED EDITOR

This issue No. 299-300 from the Spanish journal Hormigón y Acero has been prepared to inform the worldwide technical community on some of the relevant changes in the final proposal for the 2nd generation of Eurocode 2 on concrete structures, to be approved and published as EN standards within 2023.

This 2nd generation corresponds to an updated version with the most recent consolidated knowledge on concrete structures regarding the previous standards approved in 2004. Besides, the field of application has been extended to cover the assessment and strengthening of existing structures, steel fibre concrete structures and reinforcing bars made of stainless steel or fibre polymers.

This work started more than 12 years ago in the CEN TC250/SC2 “Eurocode 2”, currently under the chairmanship of Hans Ganz and with the active participation of most European countries. Mikael Hallgren, Aurelio Muttoni, Fabienne Robert and Craig Giaccio chaired Working Group 1 (WG1) and three project teams, respectively.

In Spain, the following experts have participated in the framework of CEN TC250/SC2:

- Alejandro Pérez, Jose María Arrieta and Jesús Rodríguez at CEN TC250/SC2 and WG1
- Eva Oller on strengthening of existing structures and structures with FRP reinforcement
- Gonzalo Ruiz (with Elena Vidal in the last year) on fibre steel reinforced concrete
- Carmen Andrade on assessment of existing structures
- Antoni Cladera, in the first years, and Pedro Miguel and Miguel Angel Fernández, in the last one, on shear and punching
- Sergio Carrascón on fire design
- Alejandro Pérez on structural analysis and time dependent effects
- Carlos Ríos on fatigue design
- Antonio Martínez Cutillas on bridges
- Carmen Andrade and David Izquierdo on durability

Besides, the Spanish Mirror Group UNE CTN140/SC2 met regularly during the last 12 years with about 30 attendees to follow up the progress in the preparation

of the new versions of Eurocode 2, giving support to the previously mentioned experts.

This monographic issue includes 15 papers that have been written by some members of the Spanish Mirror Group on Eurocode 2 (UNE CTN140/SC2) and some members of the European subcommittee CEN TC250/SC2 Eurocode 2.

The first paper introduces the future new version of two EN standards on Eurocode 2 Design of concrete structures “Part 1-1: General rules, Rules for buildings, bridges and civil engineering structures” and “Part 1-2: “Structural fire design”.

The second paper presents the durability and the new approach on Exposure Resistance Classes for classifying the concrete durability.

Subsequently, five papers deal with Ultimate Limit States on shear, punching, stress fields, strut-and-tie models, fatigue, laps and anchorages. Other one presents the Service Limit States, summarising the content on cracking and deflection.

In addition, five papers discuss some of the new annexes concerning the assessment of existing structures, strengthening with fibre reinforced polymers (FRP), steel fibre reinforced concrete (SFRC) (2 papers) and embedded fibre reinforced polymers (FRP).

Finally, one paper deals with fastenings for concrete structures and the last one, on fire design.

I would like to thank warmly to the 44 authors of the 15 papers and the 40 reviewers, for their excellent contribution during the last 12 months preparing this monographic issue, and I sincerely hope to have contributed to the worldwide technical community through the diffusion of the future new version of Eurocode 2.

JESÚS RODRÍGUEZ
CHAIRMAN

SPANISH MIRROR GROUP ON EUROCODE 2
(UNE CTN140/SC2 “EUROCÓDIGO 2”)

The Origins and Some Highlights on the New Proposal for Eurocode 2

Los orígenes y algunos aspectos destacados en la nueva propuesta del Eurocódigo 2

José María Arrieta^{*,a}, Jesús Rodríguez^b, Hans Rudolf Ganz^c,

^a Secretary of UNE CTN140/SC2 Eurocódigo 2, Proes consultores S.A. / Universidad Politécnica de Madrid

^b Chairman of UNE CTN140/SC2 Eurocódigo 2

^c Chairman of CEN TC250/SC2 Eurocode 2

Recibido el 14 de noviembre de 2022; aceptado el 7 de febrero de 2023

ABSTRACT

This paper presents a summary of the Eurocode development procedures which began in the last two decades of the 20th century, with some emphasis in the Eurocode 2 on concrete structures. Besides, a general scope of the technical content of the new proposal for Eurocode 2 is commented and the main changes are highlighted.

KEYWORDS: Eurocodes, concrete structures, mandates, compressive concrete strength.

©2023 Hormigón y Acero, the journal of the Spanish Association of Structural Engineering (ACHE). Published by Cinter Divulgación Técnica S.L. This is an open-access article distributed under the terms of the Creative Commons (CC BY-NC-ND 4.0) License

RESUMEN

Este artículo presenta un resumen de los procedimientos para la preparación de los Eurocódigos, trabajo que se inició en las últimas dos décadas del Siglo XX, con especial énfasis en el Eurocódigo 2 de estructuras de hormigón. Asimismo, se comenta el alcance de la nueva propuesta para el Eurocódigo 2, destacándose los cambios más relevantes.

PALABRAS CLAVE: Eurocódigos, estructuras de hormigón, mandatos, resistencia del hormigón a compresión.

©2023 Hormigón y Acero, la revista de la Asociación Española de Ingeniería Estructural (ACHE). Publicado por Cinter Divulgación Técnica S.L. Este es un artículo de acceso abierto distribuido bajo los términos de la licencia de uso Creative Commons (CC BY-NC-ND 4.0)

1. INTRODUCTION

1.1. Origins and history

The Eurocodes have been developed to enable the design of structural construction works (building and civil engineering works) in order to comply with the Essential Requirement No.1 (mechanical resistance and stability) and partially Essential Requirements No.2 (safety in case of fire) and No.4 (safety in use), and to determine the performance of structural construction products.

In 1975, the Commission of the European Community decided to launch an action program in the field of construction,

based on article 95 of the Treaty. The objective of the program was the elimination of the technical barriers to trade and the harmonization of construction-related technical specifications among the Member States. Within this programme, the Commission took the initiative to establish a set of harmonized technical rules for the structural design of construction works, which, in a first level, would serve as an alternative to the national regulations in the Member States and, finally, would replace them.

For fifteen years, the Commission, with the help of a Management Committee made up of representatives of the Member States, managed the development of the Eurocode Program and the publication of an experimental version of these European standards in the 1980s.

* Persona de contacto / Corresponding author.
Correo-e / e-mail: josemaria.arrieta@proes.es (José María Arrieta).

In 1989, the Commission and the Member States decided to transfer to the European Committee for Standardization (CEN), the preparation and publication of the Eurocodes through a Mandate, by which in the future the Eurocodes would acquire the status of European standards (EN).

Originally, the Eurocodes were developed by CEN as 62 experimental European standards (ENV). Most of them were published between 1992 and 1998 but, due to the difficulties in harmonizing all aspects in the calculation methods, the ENV versions of the Eurocodes included "box values" for some parameters that allowed Member States to choose different values in their territories. The values that each Member State adopted were collected in the so-called "National Application Documents (NAD)", which allowed the application of the ENV Eurocodes in each Member State.

In 1998, CEN began the conversion of the ENV Eurocodes (experimental standards) to European Standards EN (first generation), in accordance with Mandate 265. In this conversion process, the national comments to experimental ENV standards, input and suggestions from users and editorial inconsistencies and, finally, the elimination or minimization of the "box values" were considered. In principle, the conversion was not intended to include significant alterations to the technical content, unless necessary for security reasons. The publication of the different parts of the EN Eurocodes, has taken place between 2002 and 2007.

The EN Eurocodes have been published by the National Standardization Bodies (NSB), which participate in the program developed by CEN (in the Spanish case, the Spanish Association for Standardization UNE), in their own language, and have been made up of the technical text of the Eurocode itself and a National Annex (NA). This National Annex contains the "Nationally Determined Parameters" (equivalent to the "box values" of the "National Application Documents"), the specific geographic and climatic data of the Member State and a reference to the national regulations dealing with the matter. The final pursued objective is the implementation and use of the EN Eurocodes in the Member States.

The technical aspects from the Eurocodes are both considered by the Technical Committees of CEN/TC250 and others responsible for Product Standards, for the purpose of achieving full compatibility between product specifications and EN Eurocodes.

Currently, within the Eurocodes programme, the following ten Eurocodes have been developed:

Eurocode 0	EN 1990: Basis of Structural Design [1]
Eurocode 1	EN 1991: Actions on structures [2]
Eurocode 2	EN 1992: Design of concrete structures [3]
Eurocode 3	EN 1993: Design of steel structures [4]
Eurocode 4	EN 1994: Design of composite steel and concrete structures [5]
Eurocode 5	EN 1995: Design of timber structures [6]
Eurocode 6	EN 1996: Design of masonry structures [7]
Eurocode 7	EN 1997: Geotechnical design [8]
Eurocode 8	EN 1998: Design of structures for earthquake resistance [9]
Eurocode 9	EN 1999: Design of aluminium structures [10]

Each Eurocode, except Eurocode 0 [1], is made up of a certain number of parts (58), which have been published as European Standards EN by June 2007. Most of these parts already existed as experimental standards (ENV).

1.2. Eurocode system: documents and committees

It has previously been indicated that CEN (European Committee for Standardization) is the body in charge of European standardization work. CEN is structured in several Technical Committees, with Committee CEN/TC250 "Structural Eurocodes" in charge of the development of all Eurocodes. This Committee, in turn, is made up of independent subcommittees for working on each specific Eurocode (for example, the CEN/TC250/SC2 Subcommittee "Design of Concrete Structures", is the one that deals with the Eurocode 2). Within these subcommittees, the work of drafting and reviewing the draft standards is developed by Working Groups made up of experts, who represent the different countries, and Project Teams made up of a set of experts contracted under the Mandate.

At the national level, the National Standardization Bodies participating in the program of Eurocodes are configured in a parallel and interrelated organization with CEN. In Spain, the UNE Committee mirroring CEN/TC250 is the Technical Committee for Standardization UNE/CTN 140 "Eurocódigos estructurales". The president and the secretary of this Committee attend the meetings of the Committee CEN/TC250 as national representatives.

UNE/CTN 140 Committee also has a series of Subcommittees that deal with the follow-up of a specific Eurocode (for example, UNE/CTN 140 subcommittee dealing with Eurocode 2 is the subcommittee UNE/CTN 140/SC2). Membership in any of these subcommittees is based only on the expertise. The chairs and secretaries of each of these subcommittees are members of the corresponding CEN subcommittees, whose meetings they attend as national representatives. As an example, at the Spanish level, the Mirror Group UNE CTN140/SC2 met regularly during the last 10-12 years with about 30 members to follow up the progress in the preparation of the new version of Eurocode 2 and several experts participated in Project Teams and Working Groups of TC250/SC2.

The activities that take place within them, include tasks as varied as:

- Attendance at European meetings as a national representative and/or expert.
- Participation in European working groups focused on the analysis of some part of the Eurocodes, developing the drafts and generating proposals.
- Participation in national working groups focused on the analysis of some part of the Eurocodes, reviewing the drafts generated by the European Subcommittees and proposing alternatives and modifications to them.
- Holding conferences for the presentation and dissemination of the new regulations.
- Translation of the Eurocodes into the national language.
- Carrying out calibration studies to check the applicability of the standard, or to find out the differences between the new standards and the old ones.
- Preparation of manuals and guides that ease the application of Eurocodes by technicians, preparation of comput-

er developments, dissemination in technical schools, etc. The final draft of a part of Eurocode is generated as follows:

- First, the National Standardization Bodies nominate the experts who are going to constitute the Working Groups and the responsible CEN Subcommittee selects the members of the Project Teams in charge of the conversion of a part of a Eurocode. In the composition of these groups, the expertise of members essentially prevails.
- These groups thus constituted, begin their conversion work of the European standard. Experts in working groups prepare technical input which is then considered and integrated by the Project Team into drafts of the revised standard. In addition, the CEN Subcommittee is informed about the development of the work, gives strategic guidance and takes decisions.
- In parallel the new documents are analysed and discussed in the National Subcommittees (Mirror Groups) to generate comments and proposals, that are sent and discussed in the European Subcommittees by the national representatives. The work is developed based on successive drafts, which are modified considering the comments and suggestions of the Member States, until an acceptable-to-all final draft is reached.
- Once the final draft of an EN Eurocode is available, it is sent by CEN for Enquiry to the National Subcommittees (NSBs) which have a period to review it and send comments. The European Subcommittee considers the national comments, modifies the document which is sent to CEN for the Formal Vote (FV). As the documents are drawn up in English, they must be translated into the two other official CEN languages (French and German) and formally verified by CEN before the Formal Vote takes place. If the document is approved in FV, it is sent to the NSBs before the Date of Availability (DAV) (4 months after FV). At this moment, the document can be translated into the national language and the National Annex can be elaborated by each country before the Date of Publication (DoP) (for 2nd generation Eurocodes set to October 2027). The National Annex will contain mainly the Nationally Determined Parameters (NDPs) and the Non-Contradictory Complementary Information (NCCI) for each country and allows to apply the Eurocode in the country. There is another important date, the Date of Withdrawal (DoW), which establishes when the old version must be withdrawn (6 months after DoP).

2. MANDATE M515

2.1. Introduction

Commission Recommendation 2003/887/EC [11] encourages Member States to adopt the Eurocodes and to maintain the Eurocodes at the forefront of engineering knowledge and developments in structural design (research on new materials, products and construction methods). Recommendation indicates the need to assess the variations of the Nationally Determined Parameters (NDPs) between countries with the aim of further harmonization.

A sustained development of the Eurocodes programme is necessary to preserve the users' confidence:

- Encourage/accompany innovation (materials, products, construction techniques and design methods).
- Meet the new demands and needs of society.
- Harmonise national technical initiatives on new topics of interest for the construction sector.

They shall at least cover:

- Assessment, re-use and retrofitting of existing structures.
- Strengthening the requirements for robustness.
- Improving the practical use for day-to-day calculations.
- New Eurocode on structural glass.
- Fibre Reinforced Polymer (FRP) structures and tensile surface structures.
- Incorporation of ISO (International Organization for Standardization) Standards into the Eurocodes family, such as atmospheric icing of structures and actions from waves and currents on coastal structures.

2.2. Mandate content

Beyond the maintenance work considering the comments from the systematic review, the following tasks are established for Eurocode 2 [3]:

General

- Extension of existing rules for the assessment of existing structures and their strengthening.
- Extension of existing horizontal rules for robustness.

Further development

- Reduction of the number of Nationally Determined Parameters (NDPs).
- Improvement the "ease of use" of Eurocodes for practical users.
- Incorporation of recent results relevant to innovation and contribution of structural design to sustainability.
- Adoption, where relevant, of ISO standards to complement the Eurocodes.
- Developing auxiliary guidance documents.
- Providing a clear and complete list of background documents.
- Developing a technical report, analysing and providing guidance for potential amendments for Eurocodes regarding structural design addressing relevant impacts of future climate change (general and material specific).
- Assessing the link to harmonized Product Standards or other European standards.

2.3. The Mandate in Eurocode 2

Model Code 2010 [12] has been extensively used as a basis for this revision. A great work of updating knowledge has been done, including some specific research works and many calibrations of expressions against experimental data bases. In addition, a large set of background documents (near 1000 pages) has been generated.

The preference for formulations irrespective of the type of structural member and based on physical models more than on

empirical ones, has been a general criterion all over the development of the documents. Physical models are easier to understand and facilitate the task of extrapolating the formulations to other conditions.

A refinement of many formulations has been done that may reduce the quantity of materials in the concrete design, and goes in favour of sustainability.

As in other Eurocodes, the numbering of the sections has changed from the actual version, as two new sections have appeared: 2. Normative references and 3. Terms, definitions and symbols. In general, the new number of a section can be obtained adding two to the old one.

An important number of design clauses of the Bridge Part have disappeared since new formulations are independent of the type of structure; some others were not specific for bridges and have been incorporated into the General Part; others have been transferred to Eurocode 1 [2] (actions during the construction) or Eurocode 3 [4] (cable stayed bridges, extradosed bridges). As the remaining content of Bridge Part is quite small, it has been decided to suppress this part and incorporate its content into a normative annex (Annex K, Bridges).

Similarly, the contents of current Eurocode EN 1992-3 Containment Structures, has been integrated into informative annexes of the 2nd generation EN 1992-1-1: Verification of early age cracking into Annex D, and leak tightness into Annex H.

The specific tasks performed in the revision of EC2 are the following:

General Part

- Reduction of the number of Nationally Determined Parameters [13], in particular those NPD that are not related to safety or geographic/climatic conditions of a country.
- Enhancement the ease of use [14] [15] by means of:
 - Improving the clarity.
 - Simplifying navigation routes through the Eurocodes.
 - Limiting, where possible, the inclusion of alternative application rules.
 - Avoiding or removing rules of little practical use in design:
 - "A code should be very easy to use for all common cases, but should also suitably address the remaining (less common) ones".
 - "An easy-to-use code should start with clear provisions for simple cases (sufficient and on the safe side, with clear limits for their applicability) and give the necessary rules for more general or less common cases in the following provisions."
 - Allowing not only for an ease of use enhancement in case of simple cases, but also for:
 - Optimization of solutions (economic optimization, optimization of required dimensions, simplification of details, simplification of execution etc.).
 - Assessment of existing structures (Annex I) not complying with geometric or mechanical requirements given in sections 8 and 9 (see chapter 3 of this document).
 - Avoiding unnecessary strengthening (or minimizing it) in case of assessment of existing structures not complying with simple rules.

- Development of new technical contents on the following issues:
 - Performance based on durability design (section 6).
 - Design by non-linear FEM.
 - Consideration of size effect.
 - Early age thermo-mechanical design (Annex D).
 - Stainless Steel (additional clauses to EN 1992-1-1). [16]
 - Assessment of concrete structures (Annex I).
 - Strengthening with Fibre Reinforced Polymers (Annex J).
 - Steel Fibre Reinforced Concrete Structures (Annex L).
 - Recycled Aggregates Concrete Structures (Annex N).
 - Embedded FRP reinforcement (Annex R).

Fire Part

- Improving the ease-of-use within EN 1992-1-2 [17].
- Reduction of NDPs.
- Improvements and amendments of EN 1992-1-2 [17]:
 - Updating design rules.
 - New section for structural overall behaviour.
 - Improvement for braced/unbraced columns.
 - Ensuring consistency between tabulated data, simplified design, and advanced design provisions.
 - Thermal conductivity of concrete.
 - Spalling of concrete.
 - Robustness criteria.
 - Reducing the number of alternative methods.

3.

MAIN CONTENTS OF THE NEW EUROCODE 2

The new FprEN 1992-1-1 [18] is organized into a main part which contains 15 sections (from Section 0 to Section 14) and 19 annexes (from Annex A to Annex R), covering the following content:

0. Introduction.
1. Scope.
2. Normative references.
3. Terms, definitions, and symbols.
4. Basis of design.
5. Materials.
6. Durability and cover.
7. Structural analysis.
8. Ultimate Limit States (ULS).
9. Serviceability Limit States (SLS).
10. Fatigue.
11. Detailing of reinforcement and post-tensioning tendons.
12. Detailing of members and particular rules.
13. Additional rules for precast concrete elements and structures.
14. Plain and lightly reinforced concrete structures.

Annex A (informative) Adjustment of partial factors for materials.
Annex B (normative) Time dependent behaviour of materials: Creep, shrinkage and elastic strain of concrete and relaxation of prestressing steel.

Annex C (normative) Requirements to materials.

Annex D (informative) Evaluation of early-age and long-term cracking due to restraint.

Annex E (normative) Additional rules for fatigue verification.
 Annex F (informative) Non-linear analyses procedures.
 Annex G (normative) Design of membrane, shell and slab elements.
 Annex H (informative) Guidance on design of concrete structures for watertightness.
 Annex I (informative) Assessment of Existing Structures.
 Annex J (informative) Strengthening of Existing Concrete Structures with CFRP.
 Annex K (normative) Bridges.
 Annex L (informative) Steel Fibre Reinforced Concrete Structures.
 Annex M (normative) Lightweight aggregate concrete structures.
 Annex N (informative) Recycled aggregates concrete structure.
 Annex O (informative) Simplified approaches for second order effects.
 Annex P (informative) Alternative cover approach for durability.
 Annex Q (normative) Stainless reinforcing steel.
 Annex R (informative) Embedded FRP Reinforcement.
 Annex S (informative) Minimum reinforcement for crack control and simplified crack control.
 Bibliography.

The new FprEN 1992-1-2 on structural fire design [19] is organized in a main part which contains 10 sections (from Section 0 to Section 9) and 5 annexes (from Annex A to Annex E), covering the following content:

0. Introduction.
1. Scope.
2. Normative references.
3. Terms, definitions and symbols.
4. Basis of design.
5. Material properties.
6. Tabulated design data.
7. Simplified design methods.
8. Advanced design methods.
9. Detailing.
10. Rules for spalling.

Annex A (normative) Lightweight aggregate concrete structures.
 Annex B (informative) Steel fibre reinforced concrete structures.
 Annex C (informative) Recycled aggregate concrete structures.
 Annex D (normative) Buckling of columns under fire conditions.
 Annex E (informative) Load-bearing solid walls — complementary tables.
 Bibliography.

4. IMPROVEMENT OF OLD CONTENT

An important effort has been made to update and improve the content of the previous version of the Eurocode 2, adapting it to the new knowledge, and some few examples are presented in this chapter.

4.1. Green concretes

Green concretes are produced replacing a portion or all the cement content by another binder, like fly ashes for exam-

ple, to reduce the carbon footprint. Consequently, in order to benefit from the slower strength development of these concretes, 2nd generation EC2 permits to test the control specimens at a higher age. The new version of EC2 doesn't regulate these concretes, but leaves the door open to use them, as 5.1.3 (2) [18] allows ages t_{ref} higher than 28 days:

- (2) The value for t_{ref}
- (i) should be taken as 28 days in general; or
 - (ii) may be taken between 28 and 91 days when specified for a project.

4.2. Unification of the design compressive strength of concrete

A new formulation of the design compressive strength of concrete f_{cd} has been defined in 5.1.6 (1) that unifies this strength among the different behaviours: bending, axial force, shear, punching...

5.1.6. Design assumptions

(1) The value of the design compressive strength shall be taken as:

$$f_{cd} = \eta_{cc} k_{tc} \frac{f_{ck}}{\gamma_c} \quad (5.3)$$

where

η_{cc} is a factor to account for the difference between the undisturbed compressive strength of a cylinder and the effective compressive strength that can be developed in the structural member. It shall be taken as:

$$\eta_{cc} = \left(\frac{f_{ck,ref}}{f_{ck}} \right)^{\frac{1}{3}} \leq 1,0 \quad (5.4)$$

k_{tc} is a factor considering the effect of high sustained loads and of time of loading on concrete compressive strength.

NOTE The following values apply, unless a National Annex gives different values:

- $f_{ck,ref} = 40$ MPa;
- $k_{tc} = 1,00$ for $t_{ref} \leq 28$ days for concretes with classes CR and CN and $t_{ref} \leq 56$ days for concretes with class CS where the design loading is not expected for at least 3 months after casting;
- $k_{tc} = 0,85$ for other cases including when f_{ck} replaced by $f_{tk}(t)$ in accordance with 5.1.3 (4).

The parameters and effects, that are considered in the definition of the design value of the compressive strength of concrete $f_{cd,1}$ are the following:

- a) Material, geometrical and model uncertainties, which are considered in the partial safety factor γ_c (see background document to Annex A [20]),
- b) Difference between the strength of the control specimens $f_{c,cyl}$ and the actual in-situ concrete strength $f_{c,ais}$, due to different casting and curing conditions as well as the different behaviour of fresh concrete in control specimens and in the structure (bleeding and settlement). This effect is considered with coefficient $\eta_{is} = f_{c,ais} / f_{c,cyl}$ which is accounted for in γ_c similarly to EN 1992-1-1:2004 [15] and background document to Annex A [20]),
- c) Sustained loading effect considered with coefficient k_{tc} (see background document to subsection 5.1.6 [21]),

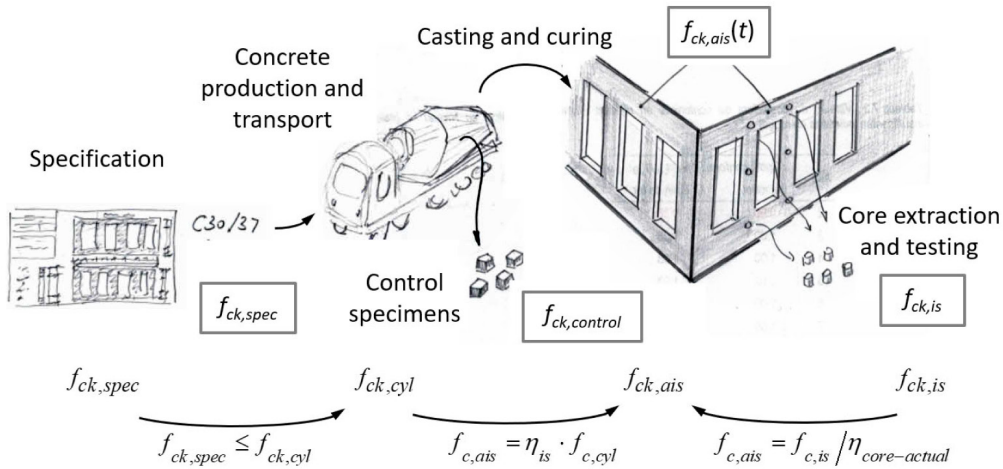


Figure 1. Representation of different compressive concrete strengths.

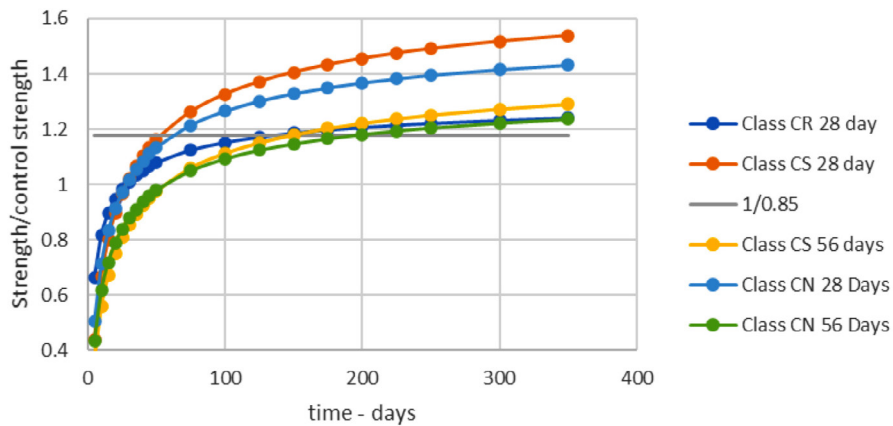


Figure 2. Comparison of strength gain for concretes of $f_{ck} \leq 35$ MPa [21].

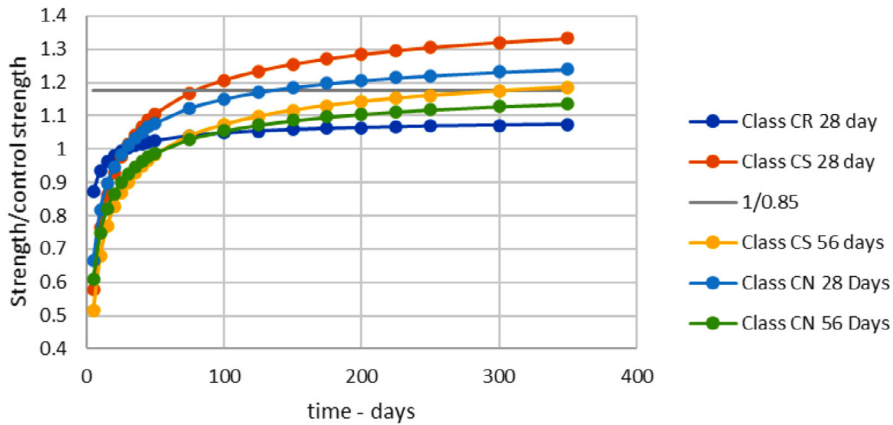


Figure 3. Comparison of strength gain for concretes of $f_{ck} \leq 35$ MPa [21].

d) Influence of increased concrete brittleness of higher strength concretes and stress concentrations related to effects not considered in the analysis, which is taken into account with the strength reduction factor η_{cc} .

In the calculation of structural resistance, strain and stress states are typically simplified (assuming, for instance, that plane sections remain plane) and several local effects are neglected: the stress concentrations related to the interaction with the

reinforcement and its restrained effects, the transversal tensile stresses originated by the local deviation of the stress field due to the presence of a reinforcement or due to the presence of voids under the reinforcement itself resulting from bleeding and settlement of fresh concrete, simplifications of the stress state considered in the analysis, etc.

Because of these effects, the resistance of a member in compression is not directly proportional to the concrete compressive strength measured in control specimens and this is considered

by the coefficient η_{cc} . This coefficient has been calibrated with the resistance of column elements measured in laboratory tests.

As a summary (Figure 1), the compressive strength $f_{c,cyl}$ is obtained from control specimens (or $f_{c,is}$ from drilled core tests), it is converted into undisturbed compressive strength of cylinder (without reinforcement, and with a size effect not taken into account) by the coefficient η_{is} , which is included in γ_c , and then it is converted into effective compressive strength in structural member (with reinforcement) considering brittleness effect by the coefficient η_{cc} (possible splitting). The mentioned size effect on the undisturbed compressive strength of unreinforced cylinders is not taken into account because it is supposed that the minimum reinforcement stated in the Eurocode reduces significantly this effect.

With the introduction of the coefficient η_{cc} considering brittleness effect directly in Formula (5.3) [18] for calculating f_{cd} , the design procedure is simplified since:

- All strength reduction factors ν in section 8 (ULS) [18] are simplified becoming constant values not dependent on f_{ck} anymore.
- The stress distributions in the compression zones (stress block and parabola-rectangle) can be simplified with a constant value of the strain limits, independent of the concrete classes ($\varepsilon_{cz}=0.002$ and $\varepsilon_{cr}=0.035$).
- The constant values for the strains related to the parabola-rectangle distribution even enhance the accuracy of the results.

The factor k_{tc} considers the effect of high sustained loads and the effect of loading time on concrete compressive strength [21]. The effective strength of concrete is reduced under high sustained load, but this may be compensated by the continued increase in concrete strength beyond the normal 28 days, when strength is typically specified. The Code considers a 0.85 reduction in strength under sustained loads as a conservative value, once the nature of testing used to calibrate the codes is considered. When loading is some time after the time of concrete testing, t_{ref} , the reduction in strength, due to high sustained loading, may be offset by continued hydration of the concrete. On this basis, to justify $k_{tc}=1.0$, at the time of loading the relative increase in strength after t_{ref} ($f_{ck,t,load}/f_{ck,t,ref}$) should be at least $1/0.85 = 1.18$ in order to compensate the effect of sustained loads. Thus, the general expression of the coefficient

$$\text{is: } k_{tc} = 0,85 (f_{ck,t,load}/f_{ck,t,ref}) \leq 1,0,$$

where:

$f_{ck,t,load}$: concrete compressive strength at the time of loading.

$f_{ck,t,ref}$: concrete compressive strength at the time of concrete testing, usually 28 days.

On this basis, the coefficient k_{tc} has been calibrated for different cement types and concrete strengths [21], resulting in the values included in the note. In this note, Classes CS, CN and CR stand for slow, normal and rapid strength development of concrete, respectively (Figure 2 and Figure 3)

4.3. Partial factors for materials

Great improvements have been done in the treatment of partial factor for materials:

1) Now, the hypothesis that underlies the values included in Table 1 are clearly given. As it is indicated in the note of this table, these coefficients correspond to Tolerance Class 1 and Execution Class 2 in EN 13670 "Execution of concrete structures" [22].

In Annex A, the statistical data (coefficient of variation and bias factor) of the main variables (concrete and steel strength, dominant geometric values, model uncertainty, etc.) that support these coefficients can be found, see Table 2.

2) In Annex A [18], there is a procedure [A.3(3)] to obtain the partial factors of materials for different values of statistical data of material strength, dominant geometrical value or model uncertainty. This is very important, because if the actual value of this statistical data is known, the partial factors can be modified by NSBs and the design can be adjusted to a particular case. In the following lines, as an example, the procedure to obtain the adjusted partial factor for the compressive strength of concrete γ_c is developed. The compressive capacity R_c of an area of concrete depends on several variables:

$$R_c = f_{c,cyl} \eta_{is} A_c \theta_c \quad [1]$$

where:

$f_{c,cyl}$ is the compressive strength of the control specimen

η_{is} is the coefficient to obtain the in situ compressive strength of concrete

A_c is the area of concrete

θ_c is the model uncertainty

Design situations — Limit states	γ_s for reinforcing and prestressing steel	γ_c and γ_{CE} for concrete	γ_v for shear and punching resistance without shear reinforcement
Persistent and transient design situation	1,15	1,50 ^a	1,40
Fatigue design situation	1,15	1,50	1,40
Accidental design situation	1,00	1,15	1,15
Serviceability limit state	1,00	1,00	—
NOTE The partial factors for materials correspond to geometrical deviations of Tolerance Class 1 and Execution Class 2 in EN 13670.			
^a The value for γ_{CE} applies when the indicative value for the elastic modulus according 5.1.4(2) is used. A value $\gamma_{CE} = 1,3$ applies when the elastic modulus is determined according to 5.1.4(1).			

Table 1. Partial factors for materials (*)

(*) This table corresponds to Table 4.3 in [18].

	Coefficient of variation	Bias factor ^a
Partial factor for reinforcement γ_s		
Yield strength f_y	$V_{fy} = 0,045$	$f_{ym}/f_{yk} = \exp(1,645V_{fy})$
Effective depth d	$V_d = 0,050^b$	$\mu_d = 0,95^b$
Model uncertainty	$V_{\theta_s} = 0,045^c$	$\mu_{\theta_s} = 1,09^c$
Coefficient of variation and bias factor of resistance for reinforcement	$V_{RS} = 0,081^1$	$\mu_{RS} = 1,115^1$
Partial factor for concrete γ_c		
Compressive strength f_c (control specimen)	$V_{fc} = 0,100$	$f_{cm}/f_{ck} = \exp(1,645V_{fc})^d$
Insitu factor $\eta_{is} = f_{c,ais}/f_c^e$	$V_{\eta_{is}} = 0,120$	$\mu_{\eta_{is}} = 0,95$
Concrete area A_c	$V_{Ac} = 0,040$	$\mu_{Ac} = 1,00$
Model uncertainty	$V_{\theta_c} = 0,070^f$	$\mu_{\theta_c} = 1,02^f$
Coefficient of variation and bias factor of resistance for concrete	$V_{RC} = 0,176^i$	$\mu_{RC} = 1,142^i$
Partial factor for shear and punching γ_v (see 8.2.1, 8.2.2, 8.4, 1.8.3.1, 1.8.5)		
Compressive strength f_c (control specimen)	$V_{fc} = 0,100$	$f_{cm}/f_{ck} = \exp(1,645V_{fc})^d$
Insitu factor $\eta_{is} = f_{c,ais}/f_c^e$	$V_{\eta_{is}} = 0,120$	$\mu_{\eta_{is}} = 0,95$
Effective depth d	$V_d = 0,050^b$	$\mu_d = 0,95^b$
Model uncertainty	$V_{\theta_v} = 0,107^g$	$\mu_{\theta_v} = 1,10^g$
Residual uncertainties	$V_{res,v} = 0,046^h$	-
Coefficient of variation and bias factor of resistance for shear and punching (members without shear reinforcement)	$V_{RV} = 0,137^i$	$\mu_{RV} = 1,085^i$
^a The values in this column refer to ratio between mean value and values used in the design formulae (characteristic or nominal). ^b These values are valid for $d = 200$ mm. For other effective depths: $V_d = 0,05(200/d)^{2/3}$ and $\mu_d = 1 - 0,05(200/d)^{2/3}$. ^c The partial factor γ_s is calibrated for the case of pure bending according to 5.2.4 and 8.1. ^d This formula replaces relationship given in Table 5.1 for the purpose of Annex A. ^e Insitu factor η_{is} accounts for the difference between the actual insitu concrete strength in the structure $f_{c,ais}$ and the strength of the control specimen f_c . For strength $f_{c,ais}$ assessed on extracted 2:1 cores according to EN 13791, see (7). ^f The partial factor γ_c is calibrated for the case of axial compression according to 5.1.6 and 8.1. ^g The partial factor γ_v is calibrated for the case of punching according to 8.4 and applies also for the case of shear without shear reinforcement according to 8.2.2 (similar statistical values). ^h The residual uncertainties refer to aggregate size, reinforcement area and spacing and column size. ⁱ Based on the statistical values above and calculated using Formulae (A.2) to (A.7).		

Table 2. Statistical data assumed for the calculation of partial factors (*)
(*) This table corresponds to Table A3 in [18].

Design situations/Limit states	Sensitivity factors for resistance α_R	target value for the 50-year reliability index β_{tgt}
Persistent or transient design situation	0,8	3,8
Fatigue design situation	0,8	3,8
Accidental design situation	0,8	2,0
NOTE 1 These values refer to CC2. For others Consequence Classes, refer to EN 1990.		

Table 3. Sensitivity factors for resistance α_R and target values for the 50-year reliability index β_{tgt} (*)
(*) This Table corresponds to Table A4 in [18].

If the coefficients of variation and bias of the variables described in Table 2 are known, the values of these coefficients for the compressive strength Rc may be calculated using equations (2) (3) and (4) from [18]:

$$V_{Rc} = \sqrt{V_{f_{c,cyl}}^2 + V_{\eta_{is}}^2 + V_{Ac}^2 + V_{\theta_c}^2} \quad [2]$$

$$\mu_{Rc} = \mu_{f_{c,cyl}} \mu_{\eta_{is}} \mu_{Ac} \mu_{\theta_c} \quad [3]$$

$$\text{where } \mu_{f_{c,cyl}} = \frac{f_{cm}}{f_{ck}} = \theta^{1,645V_{fc}} \quad [4]$$

Finally, the adjusted partial factor for the compressive strength of concrete γ_c may be calculated applying equation (5) from [18] as:

$$\gamma_c = \frac{\theta^{\alpha_R \beta_{tgt} V_{Rc}}}{\mu_{Rc}} \quad [5]$$

where:

α_R is the sensitivity factor for resistance according to Table 3 ($\alpha_R = 0,8$)

β_{tgt} is the target value for the 50-year reliability index according to Table 3 (for persistent design situation $\beta_{tgt} = 3,8$)

Condition for adjusted material factors	persistent and transient design situations			accidental design situations		
	γ_s	γ_c	γ_v	γ_s	γ_c	γ_v
a) if the execution ensures that geometrical deviations of Tolerance Class 2 according to EN 13670 are fulfilled	1,08	1,48	1,33	0,97	1,15	1,11
	in case also at least one of the conditions d), e), f) or h) is fulfilled, the partial factors may be calculated according to (3) with the statistical values given in (4) and in (7) for d) or in (8) for e); with the updated values of the resistance model for (f) and with the values given in Table A.4 for h)					
b) if the calculation of design resistance is based on the value of the dominant geometrical data measured in the finished structure and the CoV of the measurement is not larger than the values given in (5)	1,04	1,48	1,29	0,95	1,15	1,08
	in case also at least one of the conditions d), e), f) or h) is fulfilled, the partial factors may be calculated according to (3) with the statistical values given in (5) and in (7) for d) or in (8) for e); with the updated values of the resistance model for (f) and with the values given in Table A.4 for h)					
c) if the calculation of design resistance is based on the design value of the effective depth according to (6)	1,03	1,50	1,29	0,94	1,15	1,07
	in case also at least one of the conditions d), e), f) or h) is fulfilled, the partial factors may be calculated according to (3) with the statistical values given in (6) and in (7) for d) or in (8) for e); with the updated values of the resistance model for (f) and with the values given in Table A.4 for h)					
d) if the insitu concrete strength in the finished structure is assessed according to EN 13791:2019, Clause 8	γ_c and γ_v according to (7)					
e) if the yield strength of the reinforcement is assessed from tests on samples taken from the existing structure	γ_s according to (8)					
f) if the verification of the structure or of the member is conducted according to more refined methods ensuring reduced uncertainties of the resistance model.	γ_s and γ_c according to (3) where the statistical values describing the model uncertainties in Table A.3 are replaced by the actual ones					
g) if the verification of the structure or of the member is conducted using non-linear analysis and the model uncertainty is considered separately according to F.4(1).	1,20	1,46	1,31 ^a	1,09	1,16	1,16 ^a
h) if the target value for the reliability index β_{tgt} given in Table A.4 is modified in accordance with the relevant authority	γ_s and γ_c according to (3) with the statistical values in Table A.5					
^a These values apply for failures modes similar to punching and shear failures in members without shear reinforcement.						

Table 4. Values of adjusted material factors - General (*)

(*) This Table corresponds to Table A1 in [18].

In Table 4, adjusted material factors are defined for different conditions related to:

- Geometrical deviations belong to Tolerance Class 2 instead of Class 1 [22].
- The value of dominant geometrical data has been measured in the finished structure and the covariance (CoV) of the measurement is not larger than the values given in A.3(5) [18].
- Calculation of design resistance is based on the design value of the effective depth according to A.3(6) [18].
- In-situ concrete strength in the finished structure has been assessed on core tests according to EN 13791:2019, Clause 8 [23].
- The yield strength of the reinforcement has been assessed from tests on samples taken from the existing structure.
- Verification of the structure or member is conducted according to more refined methods ensuring reduced uncertainties of the resistance model.

- Verification of the structure or member is conducted using non-linear analysis and the model uncertainty is considered separately according to F.4(1) [18].
- Target value for the reliability index β_{tgt} given in Table 3 has been modified in accordance with the relevant authority.

3) There is a special partial factor γ_v for the shear and punching resistance without shear reinforcement, that replaces γ_c in all formulae for calculating the shear and punching resistance in members without shear reinforcement. This change has been explicitly introduced to take into account the fact that for shear, the model uncertainties become dominant, whereas the influence of the variability of the compressive concrete strength is reduced by the fact that the compressive concrete strength f_{ck} appears with an exponent of 1/3 in the design formulae. In this way a better and more transparent fitting of the formulation with the data bases of tests is achieved, increasing the sustainability.

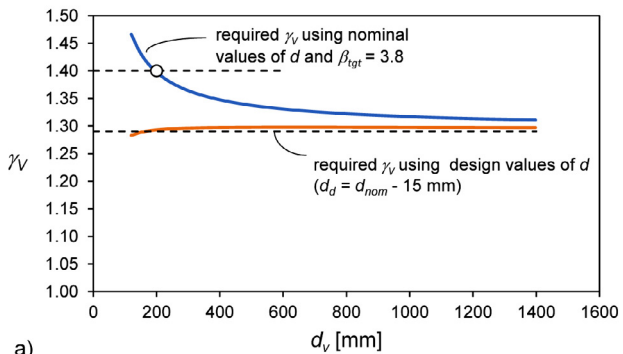
4) It is possible to reduce γ_V and γ_S by using design values for the effective depth: for thin members, geometrical uncertainties govern the calibration of γ_V and γ_S , whereas for deep members, the effect of geometrical uncertainties become almost negligible. For this reason, it is more rational to adopt reduced values of γ_V and γ_S by using design values for the effective depth. This possibility is defined in 4.3.3(2) [18]:

(2) Lower values of partial factor γ_S and γ_V for the verification of the ULS in case of persistent, transient and accidental design situations may be used according to A.3(1) if a design value of the effective depth d_d is considered.

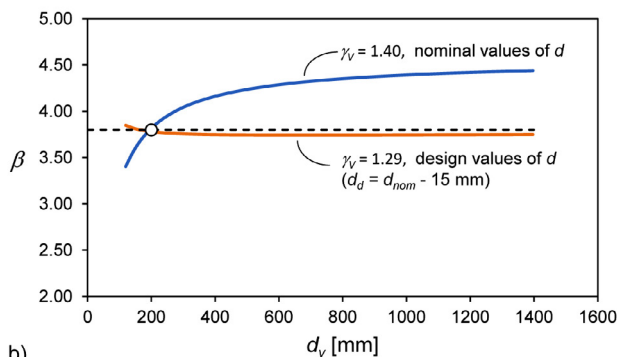
whereas the design value of the effective depth is given in Annex A (A.3(6)) [18]:

(6) The statistical data of the effective depth in Table A.2 may be replaced by $V_d = 0,00$ and $\mu_d = 1,00$ if the calculation of the design resistance is based on the design value of the effective depth d_d :
 $d_d = d_{nom} - \Delta d$ (A.4)
 where
 Δd is the deviation value of the effective depth:
 $\Delta d = 15$ mm for reinforcing and post-tensioning steel,
 $\Delta d = 5$ mm for pre-tensioning steel.
 NOTE: The design value of the effective depth d_d can be used unless a National Annex gives limitations.

and the reduced partial factors $\gamma_S = 1,03$ and $\gamma_V = 1,29$ (Figure 4) can be used.



a)



b)

Figure 4. (a) Required partial safety factors γ_V to obtain $\beta_{req} = 3,8$
 (b) Obtained reliability indexes with the assumed partial safety factors γ_V [20].

4.4. Other changes

- Section 4. Basis of design
 - Improved presentation (imposed deformations, partial safety factors in tables...)
 - References to other Eurocodes and, in particular to EN 1990 [1], suppressing contents that are not specific to Eurocode 2 [3].
 - Definition of partial factors for geometrical deviations of Tolerance Class 1 and Execution Class 2 in EN 13670 [22].
 - Specific partial factor for shear γ_V .
 - Design value of the effective d_d depth that allows to use lower values of partial factors for steel γ_S and concrete γ_V (see 4.3.4), see also text in 4.3 above.
- Section 5. Materials
 - Green concrete has finally been permitted. Green concrete uses fewer resources during production, substituting a portion of cement with more eco-friendly materials (fly ashes, for example) (see 4.1).
 - Cube specimen strength has been suppressed in the definition of concrete classes for design purposes.
 - Unification of the concrete compressive strength among the different behaviours of concrete (bending, shear, punching...) through the factor η_{cc} (see 4.2).
 - Extending the range of material strength classes: for concrete up to $f_{ck} = 100$ MPa, for reinforcing steel up to $f_{yk} = 700$ MPa, and for prestressing steel strand up to $f_{pk} = 2060$ MPa.
- Section 6. Durability and cover [24]
 - New performance-based approach with Exposure Resistance Classes ERCs, that will be defined in the new version of EN 206 Concrete [25], is considered in Section 6 of the new Eurocode 2.
 - Exposure resistance classes ERC are used to classify concrete with respect to resistance against corrosion induced by several attacks (carbonation (class XRC), chlorides (class XRDS XRSD) and freeze/thaw (XRF)).
 - Exposure classes (EC) related to environmental conditions currently given in EN 206 are now defined in this section.
 - For each EC and design service life (50 or 100 years) a combination of ERC and minimum concrete cover may be chosen.
 - Compliance with a particular ERC may be confirmed either following some prescriptive rules for mix composition for conventional/well-known concrete mixes, or by doing some short-term performance tests (carbonation, chloride attack, etc.), for new or also for conventional concrete compositions.
- Section 7. Structural analysis
 - A new analytical method for explicit verification of rotation capacity is given.
 - Consideration of the effects of prestress in analysis and design (as action effects or as resistance) has been clarified.
- Section 8. Ultimate Limit States (ULS) [26] [27] [28]
 - Several formulations for shear without reinforcement in linear members have been developed, and finally

the formulation based on the Critical Shear Crack Theory (CSCT) as in Model Code, was adopted. The decision was to use CSCT also for punching for members without shear reinforcement and to continue use of variable inclination struts / compression field for members with shear reinforcement.

- Provisions for the consideration of transverse bending on the in-plane shear strength have been added.
- Provisions for strut-and-tie models have been amended mainly for verification of struts and nodes.
- Section 9. Serviceability Limit States (SLS) [29]
 - For the cracking control many improvements have been implemented and the result has been a refined formulation, very well fitted to the data base of tests, but somewhat more complex.
 - Simplified methods have been moved to an informative annex.
 - For the deflection control, simplified and refined methods based on zeta procedure (see equation 9.28 of 9.3.4 (3) in FprEN 1992-1-1: 2022 [18]), have been implemented.
- Section 11. Detailing of reinforcement and post-tensioning tendons [30]
 - The section has been significantly updated, simplified and reorganized.
 - The model from fib Bulletin 72 has been adopted for anchorage length of straight bars but updated and calibrated against recently amended test data base. The provisions now consider size effect and the non-linear effect of reinforcement stress on the anchorage length. Bond strength has not been explicitly defined because the great number of factors that influence its value and by the fact that it varies along the bar.
 - Robustness conditions have been included to define the force in the anchorages and the staggering conditions of laps.
 - New methods for anchoring and lapping have been added: U-bar loops, headed bars, post-installed bars.

5. NEW TOPICS

Following the Mandate, new topics have been developed and included in the new version of Eurocode 2 and in this chapter some of them are summarized.

- Stainless steel reinforcement
Alterations for design with stainless steel compared to carbon reinforcing steel have been summarised in normative Annex Q. Nevertheless, for the ease of use, it is permitted to use the same formulations as for carbon steel unless considered significant and relevant. For example, for the stress-strain law, instead of using the Romberg-Osgood Law, a bilinear law has been adopted combined with a reduced value of the elasticity modulus (180 GPa).
- Assessment of existing structures (deteriorated) [31]
Annex I [18], which is informative, contains additional rules for materials and systems not covered in the main

part and additional rules for assessing existing structures where detailing does not comply with the provisions of the main part. Additional rules for the anchorage of plain bars are also included. Some considerations about the deterioration of existing structures are given, but only in a general way. Annex A [18] provides information for modifying materials' partial factors, to consider the information obtained in the tests made on the existing structures.

- Strengthening of Existing Concrete Structures with FRP [32]
Annex J [18] contains rules for strengthening existing structures with Carbon Fibre Reinforced Polymer (CFRP). The reinforcement can be externally bonded to the surface (EBR) or near surface mounted in the concrete (NSM). The reinforcement material can be either in the form of prefabricated strips (EBR or NSM), prefabricated bars (NSM) or in-situ lay-up sheets (EBR). Specific rules for materials, durability, and limit states have been developed and, in particular, those related to bond and anchorage of systems and detailing of CFRP.
- Embedded FRP Reinforcement [33]
In the informative Annex R [18], supplementary information can be found for new structures reinforced with non-prestressed glass and carbon fibre-reinforced bars or meshes subjected to predominantly static loads. It does not apply to lightweight aggregate concrete and to recycled aggregate concrete.
- Steel Fibre Reinforced Concrete Structures (SFRC) [34] [35]
Annex L [18] provides supplementary rules for structures constituted by steel fibre-reinforced concrete with or without reinforcing steel, pre-tensioning or post-tensioning tendons. In section L.5 the way to characterize this material by the residual tensile strengths and the stress-strain relationship in both tension and compression is described. Formulations for bending, shear, punching, torsion and cracking have been adapted to SFRC and detailing rules for members have been developed.

6. MAIN TOPICS IN FIRE PART [36]

Some relevant changes have also been introduced in FprEN1992-1-2 [19] regarding the previous version, dealing with:

- Material properties such as thermal conductivity of concrete, mechanical properties of high strength concrete and steel reinforcement.
- Simplified design methods: tabulated data for buckling of columns, tabulated data for walls, analytical determination of temperature profiles (simplified method) .
 - Rules for concrete spalling.
 - Extending the scope to lightweight aggregate concrete structures, steel fibre reinforced concrete structures and recycled aggregate concrete structures.
- In addition, the structure of the fire part has been harmonised across all Eurocodes' material.

7.

CONCLUSIONS

The first generation of Eurocode 2, consisting of four documents, was published as EN standard by the middle of the first decade of the present century, but works started much earlier in the 1980s.

Since then, a lot of research on concrete structures has been developed, and knowledge has significantly improved, so an updated version of Eurocode 2 was required. On the other hand, the application field has been enlarged and new topics and materials, not included in the first EN versions, have emerged.

This paper summarizes the generation of the first Eurocodes, addressing the organization, the documents and their contents, and how progress has been made with the preparation of the second generation of the Eurocode 2, which will be approved and published as EN new standards within 2023. The scope has been extended, the ease-of-use has been improved and the number of documents has been reduced, simplifying the structure of the code and including sustainability issues.

Main content of new Eurocode 2 is related in a general way in this paper and some issues have been presented in more detail, such as green concretes, unification of the design compressive strength of concrete and reliability of material strength, including existing structures. New topics, as stainless steel reinforcement, assessment of existing structures (deteriorated and non-deteriorated), steel fibre reinforced concrete or fibre reinforced polymer have been covered.

References to other published papers are also included in this paper, describing in detail some of the most relevant technical changes and improvements in the new Eurocode.

Acknowledgements

The authors want to acknowledge the contribution of Antonio Madrid Ramos to section 1 of this paper.

References

- [1] CEN/TC250, Eurocode 0: Basis of structural design, EN 1990
- [2] CEN/TC250, Eurocode 1: Actions on structures, EN 1991
- [3] CEN/TC250, Eurocode 2: Design of concrete structures, EN 1992
- [4] CEN/TC250, Eurocode 3: Design of steel structures, EN 1993
- [5] CEN/TC250, Eurocode 4: Design of composite steel and concrete structures, EN 1994
- [6] CEN/TC250, Eurocode 5: Design of timber structures, EN 1995
- [7] CEN/TC250, Eurocode 6: Design of masonry structures, EN 1996
- [8] CEN/TC250, Eurocode 7: Geotechnical design, EN 1997
- [9] CEN/TC250, Eurocode 8: Design of structures for earthquake resistance, EN 1998
- [10] CEN/TC250, Eurocode 9: Design of aluminium structures, EN1999
- [11] Commission Recommendation of 11 December 2003 on the implementation and use of Eurocodes for construction works and structural construction products (Text with EEA relevance) (notified under document number C(2003) 4639).
- [12] FIB, Model Code for concrete structures 2010
- [13] CEN/TC250, Position paper on reducing the number of Nationally Determined Parameters (NDPs) in the Structural Eurocodes, Document N1493, Technical Committee 250 Eurocodes (*)
- [14] CEN/TC250, Final report on enhancing ease of use of the Structural Eurocodes, Document N1233, Technical Committee 250 Eurocodes (*)
- [15] CEN/TC250, Position paper on enhancing ease of use of the Structural Eurocodes, Document N1239, Technical Committee 250 Eurocodes (*)
- [16] CEN/TC250, Eurocode 2: Design of concrete structures. Part 1-1: General rules and rules for buildings, EN 1992-1-1:2004
- [17] CEN/TC250, Eurocode 2: Design of concrete structures. Part 1-2: Structural fire design EN 1992-1-2: 2004
- [18] CEN/TC250, Eurocode 2: Design of concrete structures, Part 1-1: General rules, Rules for buildings, bridges and civil engineering structures, FprEN 1992-1-1: 2022 (*)
- [19] CEN/TC250, Eurocode 2: Design of concrete structures, Part 1-2: Structural fire design, FprEN 1992-1-2: 2022 (*)
- [20] CEN/TC250, Background document to 4.3.3 and Annex A. Partial safety factors for materials, Document N1116, Working Group 1, Subcommittee TC250/SC2 Eurocode 2 (*)
- [21] CEN/TC250, Background document to subsection 5.1.6 Validation to recommended values for k_{tc} and k_{kt} , Document N1104, Working Group 1, Subcommittee TC250/SC2 Eurocode 2 (*)
- [22] CEN/TC104, Execution of concrete structures, EN13670: 2009
- [23] CEN/TC104, Assessment of in-situ compressive strength in structures and precast concrete components, EN 13791:2019
- [24] Andrade C, Izquierdo D. Durability and cover depth provisions in next Eurocode 2. Background modelling and calculations. *Hormigón y Acero*, Vol.74 No. 299-300 (2023), <https://doi.org/10.33586/hya.2023.3102>
- [25] CEN/TC104, Exposure resistance class concrete. Concrete - Specification, performance, production and conformity". prEN 206, Part 100, 2022 (**)
- [26] Miguel P., Fernández M.A., Hegger J., Schmidt M. Shear resistance of members without shear reinforcement in presence of compressive axial forces in the next Eurocode 2. *Hormigón y Acero*, Vol.74 No. 299-300 (2023), <https://doi.org/10.33586/hya.2023.3112>
- [27] Muttoni, A., Simoes, J.T., Faria, D.M.V., Fernández Ruiz M. A mechanical approach for punching shear provisions in the second generation of Eurocode 2. *Hormigón y Acero*, Vol.74 No. 299-300 (2023), <https://doi.org/10.33586/hya.2022.3091>
- [28] Fernández Ruiz, M., Cao, L., & Muttoni, A. Stress fields and strut-and-tie models as a basic tool for design and verification in second generation of Eurocode 2. *Hormigón y Acero*, Vol.74 No. 299-300 (2023), <https://doi.org/10.33586/hya.2022.3086>
- [29] Pérez Caldentey A., Bellod J.L., Torres Ll., Kanstad T. Serviceability Limit States according to new Eurocode 2 proposal: Description and justifications of the proposed changes. *Hormigón y Acero*, Vol.74 No. 299-300 (2023), <https://doi.org/10.33586/hya.2023.3104>
- [30] Cairns, J. Design provisions for anchorages and laps in the revised Eurocode 2. *Hormigón y Acero*, Vol.74 No. 299-300 (2023), <https://doi.org/10.33586/hya.2023.3118>
- [31] Diaz-Pavón E., Rodríguez R., Ley J., López P. Contributions of the future Eurocode 2 for the assessment of existing concrete structures. *Hormigón y Acero*, Vol.74 No. 299-300 (2023), <https://doi.org/10.33586/hya.2023.3103>
- [32] Oller E., de Diego A., Torres Ll., Madera P. Strengthening of existing concrete structures with fibre reinforced polymers (FRP) in the new version of Eurocode 2. *Hormigón y Acero*, Vol.74 No. 299-300 (2023), <https://doi.org/10.33586/hya.2022.3099>
- [33] Oller E., Torres Ll., de Diego A. Embedded fibre reinforced polymer (FRP) in concrete structures according to the new version of Eurocode 2. *Hormigón y Acero*, Vol.74 No. 299-300 (2023), <https://doi.org/10.33586/hya.2022.3098>
- [34] De La Fuente A., Tosic N., Serna P. Design fundamentals for Steel Fibre Reinforced Concrete within the Eurocode 2 framework. *Hormigón y Acero*, Vol.74 No. 299-300 (2023), <https://doi.org/10.33586/hya.2023.3124>
- [35] Ruiz G., de la Rosa A., Poveda E., Zanon R., Schäfer M., Wolf S. Compressive behavior of steel-fiber reinforced concrete in Annex L of new Eurocode 2. *Hormigón y Acero*, 2 Vol.74 No. 299-300 (2023), <https://doi.org/10.33586/hya.2022.3092>
- [36] Carrascón S., Robert F., Villagra C., Some highlights on the new version of EN 1992-1-2 (Eurocode 2, Fire part). *Hormigón y Acero*, Vol.74 No. 299-300 (2023), <https://doi.org/10.33586/hya.2023.3096>

(*) This document is available through the National members at CEN/TC250/SC Eurocode 2

(**) This document is available through the National members at CEN/TC104 Concrete

Durability and Cover Depth Provisions in Next Eurocode 2. Background Modelling and Calculations

Capítulo sobre durabilidad y recubrimientos en el próximo Eurocódigo 2. Documento de fundamentos y cálculos

Carmen Andrade^{*,a}, David Izquierdo^b

^a CIMNE-International Center of Numerical Methods in Engineering- Barcelona -Spain

^b UPM: Polytechnical University of Madrid-Spain

Recibido el 6 de septiembre de 2022; aceptado el 21 de marzo de 2023

ABSTRACT

Codes contain calculation rules of general acceptance that have demonstrated to enable building safe enough structures with very low probability of failure. Any new method to be introduced, should be based on a consensus among experts and based on the experience. Until now, the durability is treated in the Codes following the so called “prescriptive” approach that is based on selection of constituents and limiting values of their mix-proportions or the characteristic strength, applying a correct curing limiting the presence of deleterious substances such as chlorides and crack widths in serviceability conditions, according to exposure classes. The paper describes the changes introduced in the durability verification in the revision of EN 1992-1-1:2004 currently under formal adoption. The main change is an attempt to design for durability using a performance based approach based on calculating the cover values that avoid reinforcement corrosion. These values were calculated using service life models. The covers are given in function of the “Exposure Resistance classes (ERC)” which substitute current “structural classes”. The calculations are not explicit in the Code, because they do not intrinsically imply a higher precision, but only a more rationale and harmonization. The paper also presents the definition and scope of the ERC’s which will be regulated in a new standard to be named: EN206-100. The current method in EN-206 to verify durability (reproduced in Annex P of the current draft of FprEN 1992-1-1:2023) will be retained for a transition period and it could continue to be applied with acceptable confidence depending on the provisions valid in the place of use. The ERC’s approach is different and its coherence with the present one in EN206 (Annex P) cannot be guaranteed, but the application of one or other route pretends to provide the desired level of durability.

KEYWORDS: Codes, durability, performance, exposure resistance classes, cover depth.

©2023 Hormigón y Acero, the journal of the Spanish Association of Structural Engineering (ACHE). Published by Cinter Divulgación Técnica S.L. This is an open-access article distributed under the terms of the Creative Commons (CC BY-NC-ND 4.0) License

RESUMEN

Los códigos contienen reglas de cálculo de aceptación general que han demostrado permitir la construcción de estructuras lo suficientemente seguras con muy baja probabilidad de fallo. Cualquier nuevo método que se introduzca, debe basarse en un consenso entre expertos y en la experiencia. Hasta el presente, la durabilidad es tratada en las Normas siguiendo el llamado enfoque “prescriptivo,” que se basa en la limitación de los constituyentes del hormigón o su resistencia a compresión, mediante aplicación de un curado correcto y limitación la presencia de sustancias nocivas como los cloruros y de la fisuración relacionada con las condiciones de servicio, en función de las clases de exposición. En el artículo se describen los cambios introducidos en la comprobación de la durabilidad en el nuevo borrador actual de EN -UNE 1992-1-1:2004. Los principales cambios se basan en un primer intento de hacer el cálculo de los recubrimientos a través de un enfoque prestacional a través de modelos de vida útil. Los recubrimientos se especifican en función de un nuevo concepto: las clases de resistencia al ambiente, (ERC), que sustituyen a las actuales “clases estructurales”. Los cálculos no se explicitan en el Código, porque no implican intrínsecamente una mayor precisión, sino más racionalidad y armonización. En el documento también se presenta la definición y el alcance de las ERC que se regularán en un próximo borrador de norma denominada: EN206-100. El método actual para verificar la durabilidad como se indica en la presente EN-206 (reproducido en el Anejo P del borrador actual de la

* Persona de contacto / Corresponding author:
Correo-e / e-mail: candrade@cimne.upc.edu (Carmen Andrade).

FprEN 1992-1-1:2023), se mantendrá durante un período de transición y podrá seguir siendo aplicado. Dado que el nuevo método que introduce las ERC se basa en un nuevo enfoque y formato de seguridad, no se puede garantizar la coherencia con el método anterior, pero la aplicación de una u otra vía dará el nivel de durabilidad deseado.

PALABRAS CLAVE: Códigos, durabilidad, prestaciones, clases-de-resistencia-al-ambiente, recubrimientos.

©2023 Hormigón y Acero, la revista de la Asociación Española de Ingeniería Estructural (ACHE). Publicado por Cinter Divulgación Técnica S.L. Este es un artículo de acceso abierto distribuido bajo los términos de la licencia de uso Creative Commons (CC BY-NC-ND 4.0)

1. INTRODUCTION

The codes on structural concrete contain a set of rules that ensure a level of safety that the experience shows is adequate, as shown by the fact that accidents during construction or use are very rare, showing the very low probability of failure. The duration of the structure in absence of deterioration, without major repair works, during a predefined period of time is called then “service life” (as the serviceability limit states are fulfilled). Experience on durability has shown that it is not adequate in certain exposure conditions if the cover depths or the construction quality are deficient. It is now when codes are trying to incorporate modern methods to calculate service life based on what is termed a “performance approach”, that is, not specifying the material composition, but the material performance. The reason of the delay in incorporating the modelling of the service life in codes is based on the lack of enough experience and calibration of these models, because codes should only incorporate what is proved and enables sufficiently reliable predictions.

Durability prescriptions in current codes are quite basic. They are focused on specifying cover depths as a function of the exposure classes with the simultaneous limitation in each of the following magnitudes:

- the maximum amount of w/c ratio and the minimum value of cement
- alternatively, the minimum concrete strength
- application of a sufficiently long curing regime
- limiting the chloride content in the raw materials used to manufacture concrete
- the maximum crack width in serviceability conditions

The cover depths are aligned with the limitation of the concrete mix proportions or its characteristic strength and the maximum crack width as a function of the aggressivity of the environment. These prescriptions are described in chapter 4 of current EN-1992-1-1:2004 [1] under the heading of “Durability” and EN 206 [2] Annex F.

The draft of the new version of EC2, FprEN-1992-1-1:2023 [3] contains certain evolution towards a performance-based methodology for durability aspects. The main differences are related to that the cover depths were deduced from model calculations, although all models used are valid and the final cover depths proposed were adjusted for a rationale with respect to the classes (ERC’s). This is precisely due to uncertainties in the adequate input parameters for each case and doubts as whether the input data could be generalized. In the new circulated draft for voting [3], durability prescriptions are in chapter 6 instead of chapter 4 [1]. The fact that service life models [5-9] have been used (the calculations are given in the Background Document [10] for Chapter 6) does not imply a higher precision, but a more rational approach and greater harmonization.

The resulting cover depths have been agreed through the use of four different service life models and they are given in Tables 6.3 and 6.4 of the new document [3].

The major change in this new draft is not that such cover depths are calculated through a service life model, but that they are given as a function of a new concept: the exposure resistance classes (ERC) [3,10-11] which substitute the current “structural classes” [1]. They are a way of classifying the expected durability of the concrete mixes. In the current draft the concept is only applied for carbonation and chloride attack to the reinforcement. All other degradation processes continue with the prescriptive approach since background knowledge for modelling these processes is still not fully developed. The durability provisions are defined including a certain period of corrosion propagation within the 50 or 100 years service life; meanwhile, the ERCs correspond to a probability lower than 90% of an unacceptable level of carbonation or chloride ingress under standardized exposure conditions. It is necessary to complement such long-term requirement (performance) with the ones to be fulfilled when the concrete is prepared. Thus, the values of the carbonation rate and of chloride diffusion coefficient to comply with by the concrete specimens at 28 days are now conforming a document which is named EN 206-100 [11] (it is not still finished when writing this paper) that will contain the values to be fulfilled by the specimens for each ERC.

It is worth noting, that although general durability principles are mandatory for all EU members, final NDP (National Determined Parameters) may be adjusted or calibrated by national standardization committees in each country as desired.

This paper briefly describes the changes introduced in the new draft of Eurocode-2, FprEN 1992-1-1:2023 [3] and in the EN 206-100 [11] (not definitively approved) related to durability aspects. The paper is structured according to the following list of contents:

1. Deterioration processes due to environmental actions
2. Table of Exposure classes
3. Concept of ERC’s
4. Cover depths: Calculation procedure from models of service life (contained in the Background Document)
5. Cover depths for stainless steel reinforcements
6. Content of EN 206-100
7. Final comments.

2. DETERIORATION PROCESSES DUE TO ENVIRONMENTAL ACTIONS

Although not providing provisions for all of them, Chapter 6 of new draft of FprEN1992-1-1:2023 [3] lists the concrete

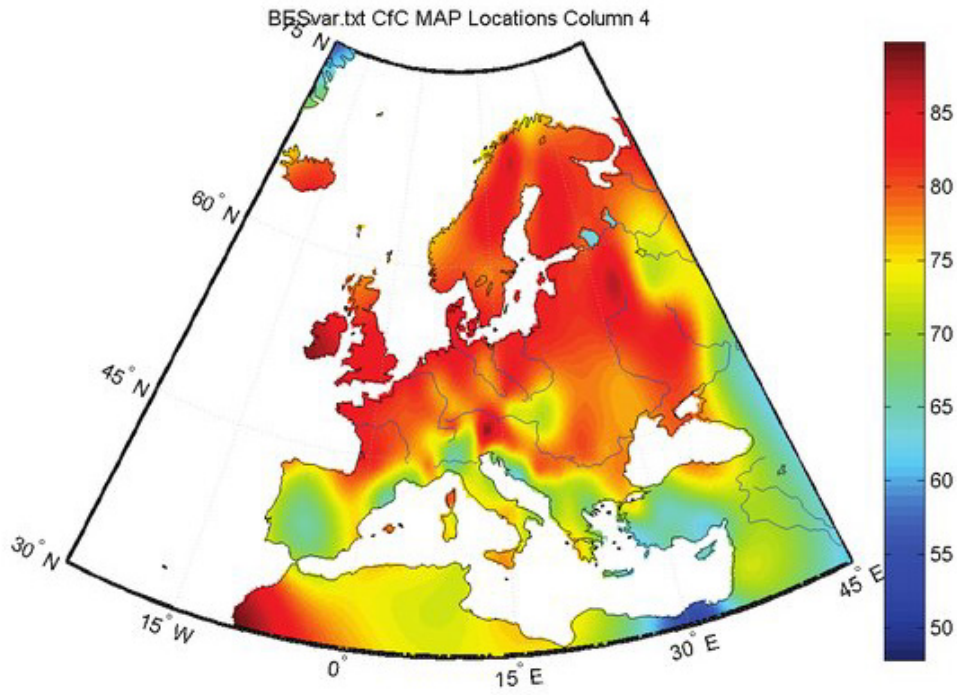


Figure 1. Mean annual external relative humidity [%] [13].

and environmental exposure conditions that may lead into deterioration. The list is the following:

- alkali-aggregate reaction (AA);
- biological attacks arising from e.g.:
 - algae;
 - vegetation;
- chemical attacks arising from e.g. the use of the structure (storage of liquids, etc.):
 - acid solutions;
 - soft water;
 - sulfates;
 - other chemicals;
- delayed ettringite formation (DEF);
- physical attack, arising from e.g.:
 - abrasion;
 - temperature change (including freeze/thaw);
 - water penetration;
- reinforcement corrosion due to carbonation or chlorides ingress;
- reinforcement corrosion that may be due to chlorides present in concrete before exposure;
- stress corrosion cracking.

3. TABLE OF EXPOSURE CLASSES

The new draft provides an updated table of the Exposure classes for reinforcement corrosion. This is shown in Table 1 (Table 6.1 in [3]). The table of other types of attack is not reproduced because it remains essentially unchanged, with only the abrasion classes included. The exposure classes for reinforcement corrosion are the same as in the previous ver-

sion except for the definition of XC1 and XC2. Now XC1 is “dry” conditions alone and not “dry and wet”. The reason for this superseded “dry and wet” classification is because the classes attended to ease of carbonation and they are the conditions where carbonation is minimal or is not produced (wet) and therefore, they were grouped in a single class. However, now the basis for the classification is the risk of corrosion and therefore, the grouping has changed because the carbonation in itself is not considered the limit. The adopted threshold is the corrosion of the reinforcement. Thus, now the risk of corrosion is negligible if the concrete is dry but not, if the concrete is wet. The wet conditions are now under the heading of XC2, XC3 represents the case of concrete exposed to the atmosphere but protected from rain, while XC4 is exposed to rain and with cyclic wet-dry periods.

During internal coordination meetings some doubts arose on how to define XC3 and XC4 exposure. The reason was the mean annual external relative humidity. Northern European countries consider XC3 / XC4 ambient with an average relative humidity of 80 – 85%, southern countries consider values around 65 – 70% (see Figure 1), providing quite different criteria for a durability approach, especially on corrosion onset and propagation [12-13]. These specific topics shall be addressed in NDPs for affected Countries.

4. CONCEPT OF ERC'S

In the current version EN 1992-1-1:2004 [1], the structural classes (from S1 to S6 Table 4.4N and 4.5N) are the intermediate step to select the cover thickness (Table 2). These structural classes have been a concept not fully defined and in

TABLE 1.
Exposure classes related to environmental conditions named Table 6.1 in present draft of [3].

Class	Description of the environment	Informative examples where exposure classes may occur (NDP)
1. No risk of corrosion or attack		
For concrete without reinforcement or embedded metal:		
X0	All exposures except where there is freeze/thaw, abrasion or chemical attack.	Plain concrete members without any reinforcement.
2. Corrosion of embedded metal induced by carbonation		
Where concrete containing steel reinforcement or other embedded metal is exposed to air and moisture, the exposure should be classified as follows:		
XC1	Dry.	Concrete inside buildings with low air humidity, where the corrosion rate will be insignificant.
XC2	Wet or permanent high humidity, rarely dry.	Concrete surfaces subject to long-term water contact or permanently submerged in water or permanently exposed to high humidity; many foundations; water containments (not external). NOTE 1 Leaching could also cause corrosion (see (5), and (6), XA classes).
XC3	Moderate humidity.	Concrete inside buildings with moderate humidity and not permanent high humidity; External concrete sheltered from rain.
XC4	Cyclic wet and dry.	Concrete surfaces subject to cyclic water contact (e.g. external concrete not sheltered from rain as walls and facades).
3. Corrosion of embedded metal induced by chlorides, excluding sea water		
Where concrete containing steel reinforcement or other embedded metal is subject to contact with water containing chlorides, including de-icing salts, from sources other than from sea water, the exposure should be classified as follows:		
XD1	Moderate humidity	Concrete surfaces exposed to airborne chlorides.
XD2	Wet, rarely dry.	Swimming pools; Concrete components exposed to industrial waters containing chlorides. NOTE 2 If the chloride content of the water is sufficiently low then XD1 applies.
XD3	Cyclic wet and dry.	Parts of bridges exposed to water containing chlorides; Concrete roads, pavements and car park slabs in areas where de-icing agents are frequently used.
4. Corrosion of embedded metal induced by chlorides from sea water		
Where concrete containing steel reinforcement or other embedded metal is subject to contact with chlorides from sea water or air carrying salt originating from sea water, the exposure should be classified as follows:		
XS1	Exposed to airborne salt but not in direct contact with sea water.	Structures near to or on the coast.
XS2	Permanently submerged.	Parts of marine structures and structures in seawater.
XS3	Tidal, splash and spray zones.	Parts of marine structures and structures temporarily or permanently directly over sea water.

absence of a precise definition the recommendation was to use the class S4. The exposure resistance classes are a substitution of such structural classes with a more coherent concept behind them, as they are defined to classify the concrete mixes by their durability, measured in specimens in the short term, from carbonation or chloride tests after 28 days of standard curing.

TABLE 2.
Values of minimum cover, $c_{min,dur}$ requirements with regard to durability for reinforcement steel in accordance with EN 1991-1-1: 2004 [1].

Environmental Requirement for $c_{min,dur}$ (mm)							
Structural Class	Exposure Class according to Table 4.1						
	X0	XC1	XC2/XC3	XC4	XD1/XS1	XD2/XS2	XD3/XS3
S1	10	10	10	15	20	25	30
S2	10	10	15	20	25	30	35
S3	10	10	20	25	30	35	40
S4	10	15	25	30	35	40	45
S5	15	20	30	35	40	45	50
S6	20	25	35	40	45	50	55

Because of the lack of agreed models [9] for other than carbonation and chloride ingress, the ERC concept only has

been applied to these two deterioration mechanisms. They have been defined by committee TC250/SC2/WG1/TG10: Durability [10] and expressed in [3] of which, both authors of the paper have been members. The definitions were very much discussed and although not all members fully agreed, they were approved by a majority of the TG10 members. The definition agreed upon was:

- Carbonation: XRC classes for resistance against corrosion induced by carbonation are derived from the carbonation depth [mm] (characteristic value 90% fractile) assumed to be obtained after 50 years under reference conditions (400 ppm CO₂ in a constant 65%-RH environment and at 20 °C). The designation value of XRC has the dimension of a carbonation rate [mm/√(years)].
- Chloride ingress: XRDS classes for resistance against corrosion induced by chloride ingress are derived from the depth of chlorides penetration [mm] (characteristic value 90% fractile), corresponding to a reference chloride concentration

(0,6% by mass of binder (cement + type II additions)), assumed to be obtained after 50 years on a concrete exposed to one-sided penetration of reference seawater (30 g/l NaCl) at 20 °C. The designation value of XRDS has the dimension of a diffusion coefficient [$10^{-13} \text{ m}^2/\text{s}$].

The main aspects considered in relation these definitions it has to be added:

- The performance is defined for a service life of 50 years, although cover depths for 100 years also are given.
- The service life includes a certain level of corrosion attack (initiation and propagation periods) complied with 90% of probability.
- Although the classification is derived by the depth of carbonation or chloride ingress the units of the ERC's are $\text{mm}/\text{year}^{0.5}$ for carbonation rate and cm^2/s for the diffusion coefficient of chlorides.
- The values are calculated for reference conditions that are translated through each service life model to each exposure class. The reference conditions are:
 - 400 ppm CO_2 in a constant 65% RH environment and at 20°C for carbonation attack
 - reference seawater (30 g/l NaCl) at 20°C for chloride ingress.

The fulfillment of the definitions can be achieved by testing for carbonation or chloride attack or by complying with the future EN 206-100 [11] or with Annex P of [3], which reproduces the current EN 206 [2].

These definitions enable the classification by testing under carbonation or chloride ingress of different mixes. However, testing will not be the only way to fulfil the ERC's [11]. They can be also fulfilled through the concrete composition. This was agreed in the committee to induce a "smooth transition" from current situation, where the approach is fully prescriptive (concrete composition), to the new requirements (performance). Additionally, each country should select the manner of incorporating the new concept into their respective standards. The choices will be described later when explaining the new EN 206-100 (in preparation) [11].

4.1. Denomination of ERC's

The ERC classes finally agreed upon are shown in the first column of Tables 3 (carbonation) and 4 (chlorides) [3,10]. Those of carbonation (XRC) have eight and those of chlorides have ten levels. They can be merged or even split into more (obtained by interpolation) as the national standardization bodies decide based on the national concretes and experience.

It is worth to repeat that the cover depths are a function of the ERC's and of the exposure classes. It should be noted, not to mistake the XRC (exposure resistance to carbonation) with the XC (exposure to carbonation), because the last one is the classification of the aggressivity of the environment while the XRC is the level of resistance to such XC.

5.

COVER DEPTHS

Cover depths have been calculated independently using five different service life models in which the input parameters are not identical [10]. The results were however only slightly different because of the selection of different exposure input parameters as mentioned. At the end, the cover depths were then rounded by consensus, based on the experience on the subjects of carbonation and chloride ingress of the persons involved in the calculations [10]. Therefore, the cover depths proposed are not the result of an exact mathematical calculation, but of the application of expert opinion to the calculated values. Because of this, any attempt to reproduce the exact values may fail if the input parameters and the assumptions of each model are not identical to those assumed and specified in the Background document [10]. The agreed cover depths are given in Table 3 for carbonation and Table 4 for chlorides of chapter 6 of [3]. They correspond to the minimum depth which provides the nominal resistance plus an allowance for deviation, Δc_{dev} :

$$c_{nom} = c_{min} + \Delta c_{dev} \quad (1)$$

As is common, the value for c_{min} shall satisfy the requirements for both bond and durability:

$$c_{min} = \max \{c_{min,dur} + \Delta c; c_{min,b}; 10 \text{ mm}\} \quad (2)$$

where:

- $c_{min,dur}$ minimum cover required for environmental conditions;
- Δc sum of the following applicable reductions and additions:
 - $\Delta c_{min,30}$ reduction of minimum cover for structures with design life of 30 years or less;
 - $\Delta c_{min,exc}$ reduction of minimum cover for superior compaction or improved curing;
 - $\Delta c_{min,p}$ additional minimum cover for prestressing tendons;
 - $\Delta c_{dur,red}$ reduction of minimum cover for use of additional concrete protection or use of special measures for protection of reinforcing steel;
 - $\Delta c_{dur,abr}$ additional minimum cover for abrasion;
 - $c_{min,b}$ minimum cover for bond requirement.

For concrete cast directly against soil surface, the minimum cover should be increased by Δc_{min} considering the increased uncertainty and variability of concrete and the reduced compaction against soil.

5.1. Deterioration (condition) limit state

This new limit state, [7,10,14-15] implicitly introduced into the calculations, has been also incorporated into current draft of fib Model Code 2020 [7]. As shown in Figure 2 [10] the deterioration limit state is based on the end of service life not when the chloride threshold is reached or the carbonation front arrives to the external surface of the bar (the nick point in the red curve), but when a certain amount of corrosion is

TABLE 3.
Minimum concrete cover $c_{min,dur}$ for carbon reinforcing steel — Carbonation (Table 6.3 (NDP) of [3]).

ERC	Exposure class (carbonation)							
	XC1		XC2		XC3		XC4	
	Design service life (years)							
	50	100	50	100	50	100	50	100
XRC 0,5	10	10	10	10	10	10	10	10
XRC 1	10	10	10	10	10	15	10	15
XRC 2	10	15	10	15	15	25	15	25
XRC 3	10	15	15	20	20	30	20	30
XRC 4	10	20	15	25	25	35	25	40
XRC 5	15	25	20	30	25	45	30	45
XRC 6	15	25	25	35	35	55	40	55
XRC 7	15	30	25	40	40	60	45	60

NOTE 1 XRC classes for resistance against corrosion induced by carbonation are derived from the carbonation depth [mm] (characteristic value 90% fractile) assumed to be obtained after 50 years under reference conditions (400 ppm CO₂ in a constant 65%-RH environment and at 20 °C). The designation value of XRC has the dimension of a carbonation rate [mm/√(years)].

NOTE 2 The recommended minimum concrete cover values $c_{min,dur}$ assume execution and curing according to EN 13670 with at least execution class 2 and curing class 2.

NOTE 3 The minimum covers can be increased by an additional safety element $\Delta c_{dur,y}$ considering special requirements (e.g. more extreme environmental conditions).

TABLE 4.
Minimum concrete cover $c_{min,dur}$ for carbon reinforcing steel — Carbonation (Table 6.3 (NDP) of [3]).

ERC	Exposure class (chlorides)											
	XS1		XS2		XS3		XD1		XD2		XD3	
	Design service life (years)						Design service life (years)					
	50	100	50	100	50	100	50	100	50	100	50	100
XRDS 0,5	20	20	20	30	30	40	20	20	20	30	30	40
XRDS 1	20	25	25	35	35	45	20	25	25	35	35	45
XRDS 1,5	25	30	30	40	40	50	25	30	30	40	40	50
XRDS 2	25	30	35	45	45	55	25	30	35	45	45	55
XRDS 3	30	35	40	50	55	65	30	35	40	50	55	65
XRDS 4	30	40	50	60	60	80	30	40	50	60	60	80
XRDS 5	35	45	60	70	70	—	35	45	60	70	70	—
XRDS 6	40	50	65	80	—	—	40	50	65	80	—	—
XRDS 8	45	55	75	—	—	—	45	55	75	—	—	—
XRDS 10	50	65	80	—	—	—	50	65	80	—	—	—

NOTE 1 XRDS classes for resistance against corrosion induced by chloride ingress are derived from the depth of chlorides penetration [mm] (characteristic value 90% fractile), corresponding to a reference chlorides concentration (0,6% by mass of binder (cement + type II additions)), assumed to be obtained after 50 years on a concrete exposed to one-sided penetration of reference seawater (30 g/l NaCl) at 20 °C. The designation value of XRDS has the dimension of a diffusion coefficient [10^{-13} m²/s].

NOTE 2 The recommended minimum concrete cover values $c_{min,dur}$ assume execution and curing according to EN 13670 with at least execution class 2 and curing class 2.

NOTE 3 The minimum covers can be increased by an additional safety element $\Delta c_{dur,y}$ considering special requirements (e.g. more extreme environmental conditions).

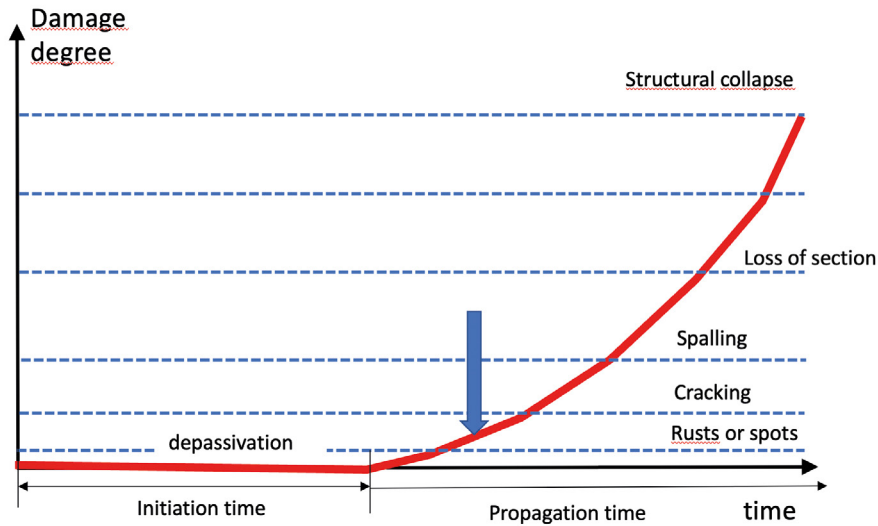


Figure 2. Service life model (Tuutti [5]) that shows with a blue arrow the time corresponding to the deterioration limit state [10,14]: before a crack parallel to the reinforcement appears on the concrete surface.

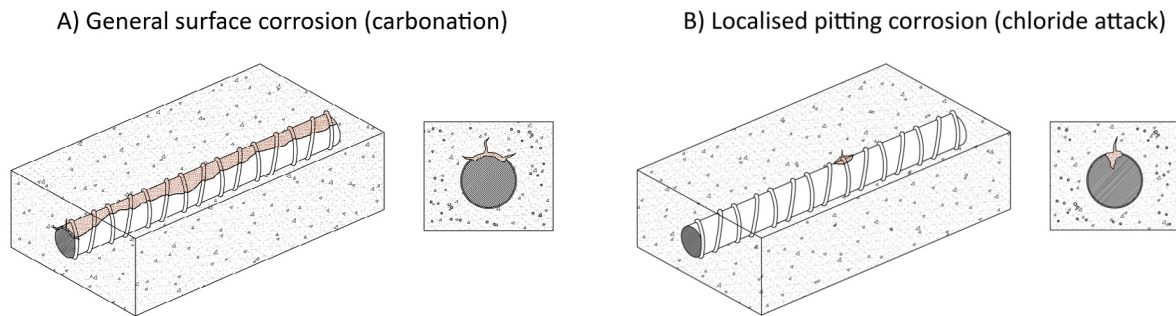


Figure 3. schematic illustration of the limit state of deterioration (condition limit state) regarding general corrosion (carbonation) and regarding localized corrosion (chlorides) [10].

reached (see the blue arrow in Figure 2) [14]. This is because the corrosion onset is not an instant, but it is a period of time in which active corrosion-repassivation may occur and because it is very difficult to identify the moment at which depassivation occurs [15]. However, when the corrosion is active, its identification can be easier from the cracking or rust spots on the outer surface. This new definition of the limit state allows to deal with incongruences generated when thicker covers were required in a dryer environment without causing external damage. A more detailed explanation on this concept can be found in the “introduction” paragraphs of the Background Document [10].

Then, it is only when the corrosion is permanently active that it can be said that the service life foreseen in the design is over. The amount of corrosion that is considered as a limit is 50 μm for general corrosion penetration (carbonation) and of 500 μm for localized attack (pitting) (Figure 3 and 4). These values were adopted by convention and, in reinforced concrete they will affect neither SLS nor ULS. A different case are prestressed steels in which such limits do not apply because smaller corrosion may lead into undesired failure [10,14,15].

The initiation period is modelled by means of diffusion transport models for carbonation and for chloride ingress and

then, the design service life is denoted as the sum of the initiation period and the propagation period [5]:

$$t_{SL} = t_{ini} + t_{prop} \quad (3)$$

The duration of the propagation period depends on the exposure, composition of concrete, concrete cover and bar diameter but for the standard, the limit adopted by convention corresponds to the mentioned corrosion induced loss of thickness equal to 50 μm (homogeneous corrosion) and 500 μm (localized corrosion) Figure 4 [3,15].

$$t_{prop} = P_{corr} / V_{corr} \quad (4)$$

where V_{corr} is the corrosion rate and $P_{corr} = 50 \mu\text{m}$ is the limit value for the average penetration (carbonation-induced corrosion) that is supposed not to cause visible surface cracking. In case of chloride-induced corrosion, pitting depth $P_{pit} = 500 \mu\text{m}$ is deemed to be a lower bound (conservative) estimate of the pitting depth that would not induce cracking in the concrete cover (although P_{pit} up to 1000 μm has been observed without cracking). This pitting depth limit P_{pit} has been allocated on an averaged corrosion depth P_{corr} between 50 mm and 100 mm assuming a pitting factor of 10.

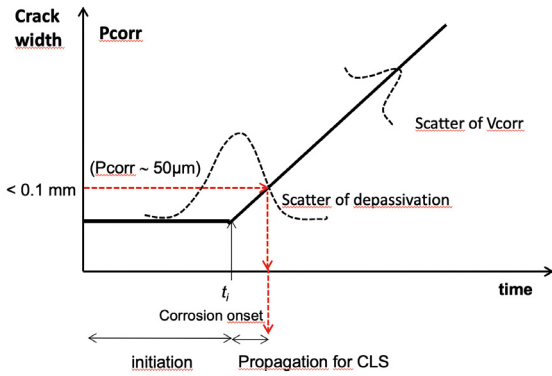


Figure 4. Representation of the Condition/ Deterioration/Corrosion limit state (CLS) [10,14,15]. It means that the service life is not only the initiation period, but also an initial part of the propagation period, that for corrosion is nominally ascribed to a corrosion penetration of $P_{corr} = 50 \mu\text{m}$ of averaged uniform corrosion depth, assuming equivalent to have crack widths in the concrete surface smaller than 0.1 mm.

5.2. Reliability associated to the end of design service life

Methods of establishing the reliability may follow the general principles for probabilistic service life design of concrete struc-

tures outlined in ISO 2394 [16], EN 1990 [17] and ISO 13823 [18] and, for deterministic calculations or semi-probabilistic approaches, include margins to reach the same target reliability.

The probability of exceeding a given limit state (failure probability) is quantitatively expressed by the reliability index, bi-univocally related to the previous through the cumulative Gauss function:

$$P_f = \Phi^{-1}(-\beta) \quad (5)$$

where

P_f is the failure probability,

Φ^{-1} is the Gauss inverse cumulative distribution and,

β is the reliability index.

The failure probability selected was derived after a benchmark examination of the estimated reliability level for the current design criteria in Spanish code EHE-08 [19] and the German prescription for concrete DIN 1045-1 [20]. The adopted target value was $\beta = 1.5$ which corresponds to a nominal probability of 7% as is illustrated in Figures 5 and 6 [21].

Hence, a target value of $\beta = 1.5$ at a life time of 50 years has been used to elaborate the recommended cover depths, $C_{min,dur}$.

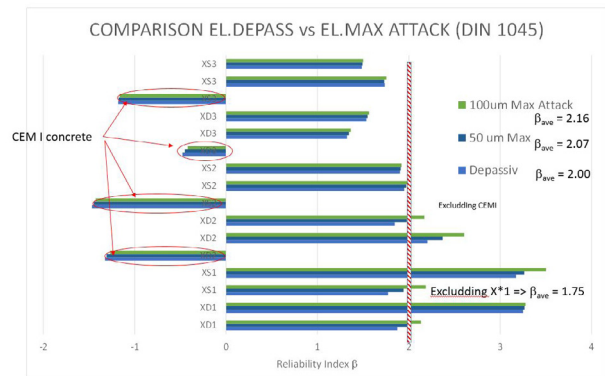
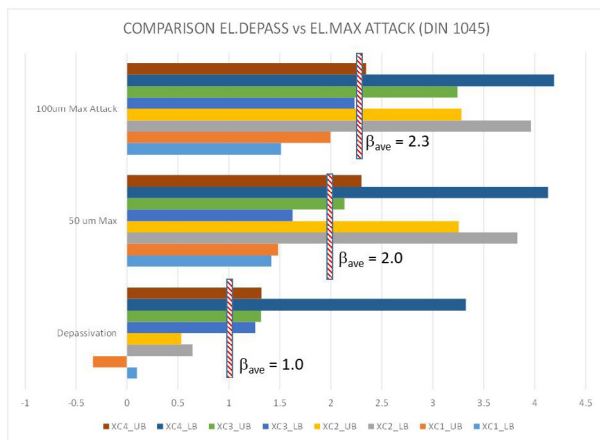


Figure 5. Reliability index for current deemed to satisfy rules in DIN 1045-1 [21] calculated following the procedure of Annex 1 and 2 of present paper. As more positive is the β value, less probability of that the aggressive front reaches the bar position with the cover depths considered in DIN standard. Negative β values indicate probabilities of failure higher than 50%.

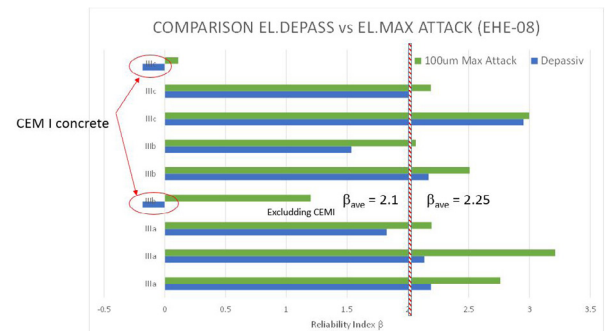
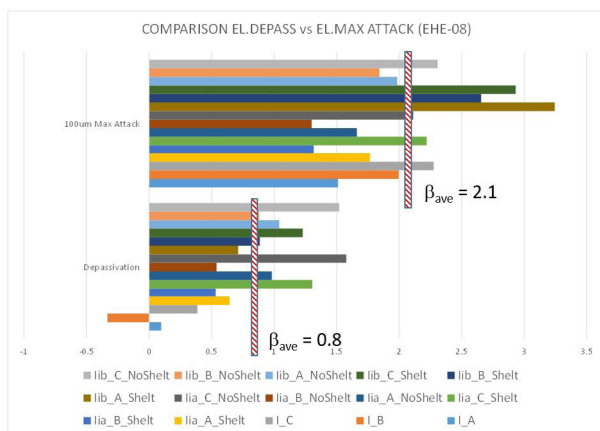


Figure 6. Reliability index for current deemed to satisfy rules in Spanish EHE-08 [21] calculated following the procedure of Annex 1 and 2 of present paper. As more positive is the β value, less probability of that the aggressive front reaches the bar position with the cover depths considered in EHE08 standard. Negative β values indicate probabilities of failure higher than 50%.

This target value $\beta=1.5$ represents a failure probability around 7% for the undesirable event of depassivation of the steel reinforcement followed by a limited part of the propagation period [10,14,15,22,23].

A target reliability of $\beta=1.3$ is often used for the depassivation limit state [7,10,14], which is consistent with a slight increase to 1.5 [9] for considering the durability limit state as initiation followed by a certain part of the corrosion phase. This $\beta = 1.5$ value was also considered as being compatible with current normally used cover depths [1]. This difference in reliability should be considered when comparison between the cover depths proposed in EC2-draft and other code is made.

A single target value for β has been used for the durability limit state of reinforced concrete structures, without specifically taking account of the ease of access for inspection and maintenance. This level of the reliability index is considered acceptable for most types of concrete structures and components. An additional recommended cover depth has been given for the corrosion of prestressing steel, because of the higher severity of the consequences of failure and differences in the corrosion mechanism. Interpretation in terms of reliability is detailed in a specific chapter. Although the description of the calculation of the failure probabilities may require a dedicated text, a short summary is included in one of the methods used in the Background Document [10] included at the end of this paper as annex 1 and 2.

6. COVER DEPTHS FOR STAINLESS-STEEL REINFORCEMENTS

The use of stainless steel has been introduced with the same rationale as normal steel reinforcements. That is, the cover depths will depend on the ERC's and on the type of steel itself, because not all the stainless steels used as reinforcement have the same resistance against corrosion. Table 5 (Table Q.3 in the draft of FprEN1992-1-1:2023 [3]) shows the cover depths for this type of reinforcements.

7. PROVISIONAL CONTENT OF EN 206-100

The current draft 10 of EN 206-100 [11], submitted to comments and not yet approved, contains mainly:

- The definition of ERC.
- The testing methodology for carbonation and chloride ingress.
- The levels of compliance and assessment of concrete mixes.
- The values of the carbonation rate and chloride diffusion coefficient to comply with each ERC.

TABLE 5.
Minimum concrete cover $c_{min,dur}$ to stainless steel reinforcement (Table Q.3 (NDP) of [3]).

Exposure Class	Exposure resistance class ERC	Stainless steel resistance class ^a			
		SSRC1	SSRC2	SSRC3	SSRC4
XC1	≤ XRC7	0	0	0	0
XC2		0	0	0	0
XC3	≤ XRC4	0	0	0	0
	≤ XRC7	15	0	0	0
XC4	≤ XRC4	15	0	0	0
	≤ XRC7	20	0	0	0
XD1, XS1	≤ XRDS0,5	10	0	0	0
	≤ XRDS1,5	20	10	0	0
	≤ XRDS3	25	15	10	0
	≤ XRDS6	35	25	15	0
	≤ XRDS10	45	35	25	15
XD2, XD3, XS2, XS3	≤ XRDS0,5	15	10	10	0
	≤ XRDS1,5	25	20	15	0
	≤ XRDS3	35	30	20	10
	≤ XRDS6	50	40	30	20
	≤ XRDS10	65	50	40	30

NOTE 1 The tabulated cover values apply for a design service life of 50 years unless a National Annex excludes some classes or gives other values.

NOTE 2 For a design service life of 100 years $c_{min,dur}$ in Table Q.3 (NDP) should be increased by +10 mm for all ERC classes unless a National Annex excludes some classes or gives other values.

NOTE 3 In case of combined action of carbonation and chloride induced corrosion, $c_{min,dur}$ in Table Q.3 (NDP) should be increased by 20 mm or a higher stainless steel resistance class should be chosen unless a National Annex gives other values.

NOTE 4 As alternative to the class system of Table Q.3 a performance-oriented service life design may be applied if the input parameters out of technical product specifications are available.

^a For stainless steel corrosion resistance classes see Table Q.2.

ERC's are defined by performance using either (see Figure 7):

- testing, using a European reference test method and criteria given in the standard; or,
- testing, using a European test method or National test method, with criteria specified by provisions valid in the place of use; or,
- limiting values for composition and properties of concrete.

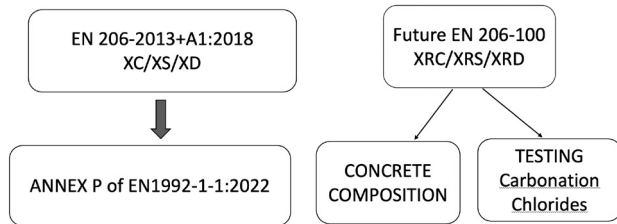


Figure 7. Routes of verifying the XRC's [11].

With the values of each ERC the structure is expected to achieve the design service life provided:

- the appropriate ERCs were selected;
- the concrete has the minimum cover to reinforcement in accordance with FprEN 1992-1-1:2023 [3];
- the concrete is properly placed, compacted and cured, e.g. in accordance with current EN 13670 [24] and EN 13369 [25];
- the appropriate maintenance is applied during the service life.

The standard gives four levels of testing and assessment (Table 6) (Table 1 in the draft of EN206-100) [11]. These levels range from selecting a pre-defined concrete and then accepting that any variability is reliably assessed by the standard EN 206 procedures [11], to specifying standard procedures with additional testing where greater reassurance of constancy of performance is required.

The denomination of ERC is through the letters XRC for carbonation and XRDS for chlorides, both sea water and deicing salts. The letters are followed by a number that represents the classification from more to less resistant to the attack.

7.1. Resistance classes by testing

The preliminary proposal being discussed on Initial type testing ITT, is summarized:

- carbonation classes, XRC, can be verified using the reference test method, EN 12390-10 chamber test [26]. National provisions may use other accelerated carbonation test (EN 12390-12) [27] providing the factor of conversion to natural conditions are given
- chlorides the assessment is made through the reference test method given in EN 12390-11 [28]. The EN 12390-18 chloride migration test [29], or test methods permitted by the provisions valid in the place of use, may be used to define the performance of XRDS concrete with the corresponding factor for natural conditions.

TABLE 6.

Levels of testing and assessment [11] (preliminary proposal not yet approved) (Table 1 in the draft 10 of EN206-100).

*Initial type testing

Task	Level 0	Level 1	Level 2	Level 3
Initial type testing	Not required ^a	In accordance with 5.2		
Confirmation of ITT*		Every four years ^b	Every four years ^b	Not required ^c
Additional routine testing		As required to confirm that any change in the source of a constituent does not adversely affect durability.	As level 1 plus resistivity as frequently as compressive strength testing.	As level 2 and additional tests The frequency of testing specified in provisions valid in the place of use or as otherwise specified.

^a Conforming to 4.1 (1) and (2), and limiting values and concrete properties to 4.3

^b And where there is a significant unexplained change in fresh or hardened concrete properties

^c May be specified

TABLE 7.

ITT criteria for the XRC classes based on the EN 12390-10 chamber test [26] (Table 4 in draft 11*** of EN-206-100)

*proposed by the CEN/TC104/SC1/WG1/ADG not yet approved

** mean values used in the probabilistic calculations of the authors of this paper (see Annex 1)

*** New draft in discussion

XRC class	Mean carbonation rate,* mm/√years	Mean carbonation rate in the ITT,** mm/√years
XRC0,5	0.36	0.5
XRC1	0.72	1.0
XRC2	1.44	2.0
XRC3	2.17	3.0
XRC4	2.89	4.0
XRC5	3.61	5.0
XRC6	4.33	6.0
XRC7	5.06	7.0

TABLE 8.

Mean value for the XRDS classes based on the EN 12390-11 diffusion test [28] (named Table 6 in draft 11** of EN-206-100).

* proposed by the CEN/TC104/SC1/WG1/ADG not yet approved

** New draft in discussion

XRDS class	Mean diffusion coefficient for various ageing factors, $\times 10^{12} \text{ m}^2/\text{s}^*$			
	$\alpha \geq 0,3$	$\alpha \geq 0,4$	$\alpha \geq 0,5$	$\alpha \geq 0,6$
XRDS 0,5	0.17	0.28	0.47	0.78
XRDS 1	0.34	0.56	0.93	1.56
XRDS 1,5	0.50	0.84	1.40	2.33
XRDS 2	0.67	1.12	1.87	3.11
XRDS 3	1.00	1.68	2.80	4.67
XRDS 4	1.34	2.24	3.73	6.22
XRDS 5	1.68	2.80	4.66	7.78
XRDS 6	2.01	3.35	5.59	9.33
XRDS 8	2.68	4.47	7.46	12.4
XRDS 10	3.51	5.59	9.33	15.6

Where the use of non-reference test to assess the performance of an XRDS concrete is accepted, then all parties should confirm assessment criteria to try and avoid the possibility of dispute if the performance is questioned at a later date.

7.2. Levels of XRC's to comply with

The current tables, not yet approved for carbonation and chlorides, are given in Table 7 (Table 4 in the EN206-100 draft-11) and 8 (Table 6 in the draft-11) (please notice that it is mentioned the draft 11 and not the draft 10 of EN206-100 because the values are in continuous change). They show the preliminary ITT mean value (x_n is the mean value of 3 ITT results) that testing results should comply with.

8.

FINAL COMMENTS

The chapter on Durability in EN 1991-1-1 has been renewed more in the fundamentals than in the resulting text. The changed aspects were mainly based on:

- A more rational identification of the possible deterioration processes.
- For the case of reinforcement corrosion, in the calculation of the cover depths through service life models of carbonation and chloride ingress adopting as the onset of corrosion a certain period of propagation, introducing “de facto” a new limit state “condition or deterioration limit state” whose compliance should not affect the serviceability or ultimate limit states. That is, the propagation period allowed should not produce cracks in the cover beyond their value for SLS. This new limit state corrects some anomalies and contradictions caused using the traditional depassivation criterion.
- The introduction of the exposure resistance classes that is a method for ranking the potential durability of the concrete using performance tests in early stages.

The new concept of exposure resistance class defined in the EN206-100 and applicable to concrete mixes, enables to rank their expected durability and link it to the cover depths. This is expected to contribute to the introduction of new types of binders, very demanded for the goal of concrete decarbonation.

A final comment is that the new concrete classification should be used it its own, because it is based on different safety criteria and concepts than current codes. The old and new concepts should not be mixed. Thus use: a) current EN 206-2013+A1:2018 (referred to in Annex P in FprEN1992-1-1:2023) [2] or alternatively b) the new FprEN1992-1-1:2023 (chapter 6) [3] and EN 206-100 [11]. The mixing or comparison of both systems may lead into erroneous or incoherent results. Concrete producers deciding to fit into the new system should work on adjusting their concrete mix proportions to the ERC's, with independence of the current EN 1991-1-1:2004.

Acknowledgements

The authors would like to recognize the interesting contributions of several members of the European committees CEN/TC250/SC2/WG1/TG10 and CEN/TC104/SC1/WG1 and also are grateful to the centers they were or are members of (IETcc: Institute of Construction Sciences- CSIC-Spain, CIMNE and the UPM: Polytechnical University of Madrid) for the permission for attending the volunteer work that standardization always represents.

References

- [1] CEN (2010) EN 1992-1-1:2004. Eurocode 2: Design of concrete structures - Part 1-1: General rules and rules for buildings.
- [2] CEN (2018) EN 206-2013+A1:2018: Concrete — Part 1: Specification, performance, production and conformity.
- [3] CEN (2023). FprEN1992-1-1:2023 Eurocode 2: Design of concrete structures - Part 1-1: General rules and rules for buildings, bridges and civil engineering structures. (*) This document is available through the National members at CEN TC250/SC2.

- [4] Duracrete Project 95-1347, E. C. (1998). Probabilistic performance based durability design of concrete structures.
- [5] Tuutti K., (1982) "Corrosion of steel in concrete", Swedish Cement and Concrete Institute (CBI) n° 4-82. Stockholm.
- [6] fib (2012) MC 2010 Model Code 2010. International Federation for Structural Concrete, fib, Lausanne Switzerland
- [7] fib (2022)-in press- Model Code 2020. International Federation for Structural Concrete, fib, Lausanne Switzerland
- [8] fib. (2006) *Bulletin 34. Model Code for service life design.*
- [9] fib (2015) *Benchmarking of deemed-to-satisfy provisions in standards. Bulletin 76.* Brussels.
- [10] CEN (2021) prEN1992-1-1 Background Document of Chapter 6. Committee CEN/TC250/SC2/WG1/TG10: Durability. (*) *This document is available through the National members at CEN TC250/SC2.*
- [11] CEN (2021) prEN206-100 (draft 10 submitted to NSBs for comments). Concrete - Specification, performance, production and conformity. (*) *This document is available through the National members at CEN TC250/SC2.*
- [12] Izquierdo D.A.C. (2001). Caracterización de la durabilidad de elementos prefabricados mediante ensayos de tipo. En A. C. (ACHE), *Primer Congreso de Prefabricación.* Madrid.
- [13] Schijndel J. V. (2013). The simulation and mapping of building performance indicators based on European weather stations. *Frontiers of Architectural Research*, 121-133.
- [14] Izquierdo D.A.C. (2001): Basis of design for a probabilistic treatment of reinforcement corrosion processes- PhD. Polytechnic University of Madrid. Faculty of Civil Engineering
- [15] Andrade C. (2017). Reliability of corrosion onset: initiation limit state. *Journal of Structural Integrity and Maintenance* Vol01, 200-208.
- [16] ISO 2394 (2015) *General principles of reliability for structures.*
- [17] CEN. (2019) *EN 1990 Eurocode - Basis of structural design.*
- [18] ISO 13823 (2008) *General principles on the design of structures for durability.*
- [19] EHE-08 Ministerio Fomento (2008). *Instrucción de Hormigón Estructural EHE-08.*
- [20] DIN 1045 (2001 - 07). Concrete, reinforced and prestressed concrete structures - Part 1: Design and construction.
- [21] Izquierdo D. (2019). Summary for Reliability analysis of German & Spanish DtS Rules for Durability vs Maximum Corrosion Threshold. Internal documents N92 and N118 of CEN/TC250/SC2/WG1/TG10. (*) *This document is available through the National members at CEN TC250/SC2.*
- [22] Gonzalez J.A., Andrade C., Alonso C., Feliú S. Comparison of rates of general corrosion and maximum pitting penetration on concrete embedded steel reinforcement. *Cement and Concrete Research* 1995; 25(2): 257-264
- [23] CONTECVET - A validated user's manual for assessing the residual life of concrete structures, DG Enterprise, CEC, (2001). (The manual can be downloaded from the web site https://www.ietcc.csic.es/wp-content/uploads/1989/02/manual_contecvet.pdf)
- [24] CEN (2009) EN 13670 -Execution of concrete structures
- [25] CEN (2018) EN 13369 - Common rules for precast concrete products
- [26] CEN (2018) EN12390-10 Testing hardened concrete- Part 10: Determination of the carbonation resistance of concrete at atmospheric levels of carbon dioxide.
- [27] CEN (2020) EN 12390-12 Testing hardened concrete - Part 12: Determination of the carbonation resistance of concrete - Accelerated carbonation method
- [28] CEN (2015) EN 12390-11 Testing hardened concrete - Part 11: Determination of the chloride resistance of concrete, unidirectional diffusion
- [29] CEN (2021) EN 12390-18 Testing hardened concrete - Part 18: Determination of the chloride migration coefficient.

ANNEXES: CALCULATIONS SUPPORTING THE COVER DEPTHS GIVEN IN *FprEN1992-1-1:2023*

As mentioned in chapter 4 of present paper cover depths given in Tables 3 and 4 have been independently calculated by several members of the CEN/TC250/SC2/WG1/TG10 using different service life models, in which the input parameters are not identical [10]. These calculations are incorporated into the Background Document of Chapter 6 of *FprEN 1992-1-1:2023*.

Next as Annexes 1 and 2 are reproduced the chapters 2.2 (carbonation) and 3.2 (chlorides) prepared by the authors of present paper to that Background Document. The models used for the calculations have been in fib Model Code (MC2010) and in JCSS Probabilistic Model Code. Each Annex has the corresponding bibliography used for their preparation.

These Annexes have not been reviewed for present paper and are exclusive responsibility of the authors. The numbering of the chapters is the original of the Background Document mentioned.

ANNEX 1

BACKGROUND DOCUMENT

CHAPTER 2.2

Carbonation induced corrosion

By David IZQUIERDO and Carmen ANDRADE

2.2.1 Objective

The objective of present document consists in establishing the cover depths for 50 and 100 years that fulfil the definition of the exposure resistance classes (ERC) given in chapter 1.2.6. Additionally, it has been calculated the values of the ERC designations at short term (V_{CO_2}) coherent with those values for the case at 50 years.

For achieving that objective, the steps followed are:

- Time-explicit mathematical models for calculating the progress of the carbonation front, and of the corrosion propagation phase, are selected.
- A corrosion propagation period is added to the initiation one in such a length that no external damage is detected in the concrete surface. This assumption makes the service life to be composed of an initiation (t_i) period and a propagation (t_p) one:

$$t_{SL} = t_i + t_p \quad \text{Eq. 2.2.1}$$

The definition of the end of service life is shown in Figure 1.1.

- Probabilistic characterization of the input parameters of the models selected
- Formulation of the limit state function (LSF) in which the adequate cover depth is higher than the initiation plus the corresponding propagation periods.
- Selection of the reliability level of compliance of the LSF. In present document the reliability factor $b=1.5$ has been adopted.
- Calculation of the cover depths complying with the ranking of ERC defined in the chapter 1.2.6 and final proposal of the c_{min} by subtracting 10 mm.

- Rounding of the cover thickness values in order to fit into stepped round values.

Additionally, calculations were repeated with other probabilistic methods as well as deterministic calculation in order to check whether the values of cover depth are the same or they depend on the calculation method.

Finally, for the objective of the back-extrapolation at short term the same methodology has been followed with the difference of calculating the V_{CO_2} instead of the cover thickness.

2.2.1 Carbonation induced corrosion

2.2.1.1. Model of the initiation period

For the carbonation model that included in the *fib* MC2010 [*fib* Model Code 2010] has been simplified by “embodying” the input parameters in a smaller number of them. That is the model is reduced to a “square root” one as it is a full simplification, in which all the input parameters, except logically that of the lifetime, are embodied in velocity of carbonation V_{CO_2} [Izquierdo 2001]. This simplification is made in order to avoid the need to calibrate the six variables of *fib* carbonation model whose uncertainty and statistical distributions are unknown.

The *fib* model of carbonation [MC2010, *fib* Bulletin 34, Gehlen 2000, Izquierdo 2001] is the following:

$$x_c = \sqrt{2 k_e k_c \frac{D_{CO_2}}{a} \left(\frac{t_0}{t} \right)^w} = \sqrt{\frac{2 k_e k_c}{R_{carb}} \left(\frac{t_0}{t} \right)^w} \quad \text{Eq. 2.2.2}$$

x_c = carbonation depth [mm]

k_e = environmental parameter

k_c = factor for curing regime

D_{CO_2} = diffusion coefficient of carbon dioxide

a = reactive alkaline material in the concrete

t_0 = time were testing is started

t = design service life

R_{carb} = Inverse effective carbonation resistance of concrete

w = wetness factor

This expression is reduced by assuming:

$$V_{CO_2} = \sqrt{\frac{2 k_e k_c}{R_{carb}} \left(\frac{t_0}{t} \right)^w} \quad \text{Eq. 2.2.3}$$

V_{CO_2} rate of carbonation

Equation 2.2.2. can yield to the following simplified equation In the case that the k_e , k_c , t_0 and w are set to=1, V_{CO_2} is coincident with the average value of the designation number of the XRC.

$$x_c = V_{CO_2} t^{\frac{1-2w}{2}} \quad \text{Eq. 2.2.4}$$

Considering the time to depassivation as the independent variable:

$$t_{dep} = \left(\frac{c}{V_{CO_2}} \right)^{\frac{2}{(1-2w)}} \quad \text{Eq. 2.2.5}$$

c = depth of carbonation

The rate of carbonation will be ranked following the ERC's.

2.2.1.1 Input Parameters of the carbonation model and their statistical characterization

2.2.1.1.1 Values of V_{CO_2} and their coefficient of variation (CoV)

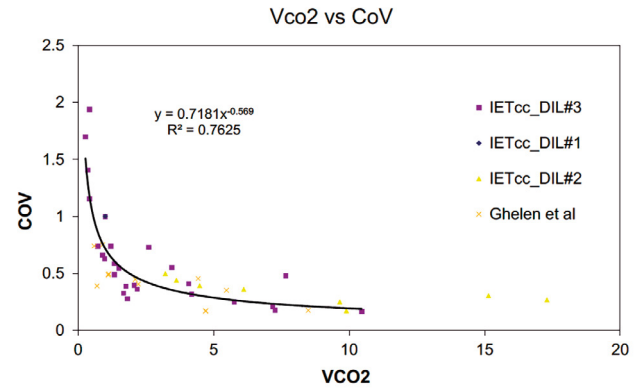


Figure 2.2.1. Relationship between averaged carbonation rate V_{CO_2} and its Coefficient of Variation (expressed as percent per one, thus 1= 100% variation) measured in real structures.

Regarding the CoV of the carbonation rate in tests performed in real structures [Izquierdo 2001, Gehlen 2000] enable to deduce the relationship between average value of carbonation depth and the measured scatter (CoV) when measured in the same zone. The relation between averaged value of the carbonation rate and its scatter is shown in Figure 2.2.1. The CoV is larger logically as smaller is the value, being above 100% (higher than 1 in the figure) for the very low values.

2.2.2.1.1.2 Wetness factor “w” and its CoV

The wetness factor “w” represents the effect of direct rain into the concrete surface [Gehlen 2000] and the delay of the carbonation due to this surface wetness. Eq. 2.2.6 provides its expression:

$$W = \frac{(p_{SR} T_0 W)^{b_w}}{2} \quad \text{Eq. 2.2.6}$$

where p_{SR} is probability of driving rain and b_w is an exponent of regression [*fib* Bulletin 34, MC2010, Gehlen 2000].

In order to have an order of magnitude of the scatter (in terms of CoV) due to it is not provided in the MC2010, it has been made a Montecarlo simulation whose result is shown in Figure 2.2.2. It shows the values distribution shape and expected coefficient of variation, depending on average value of w. For each exposure class, input values for w and variation coefficient are shown in Table.2.2.1:

TABLE 2.2.1. Values of the time of Wetness (averaged per year) and their Coefficient of Variation for the assumptions of exposure classes with averaged low (LH) and high (HH) relative humidities.

Exposure ¹	W_w	CoV (%)
XC1	0	0
XC2	0.4	6.2
XC3_LH	0	0
XC3_HH	0	0
XC4_LH	0.15	65
XC4_HH	0.24	25

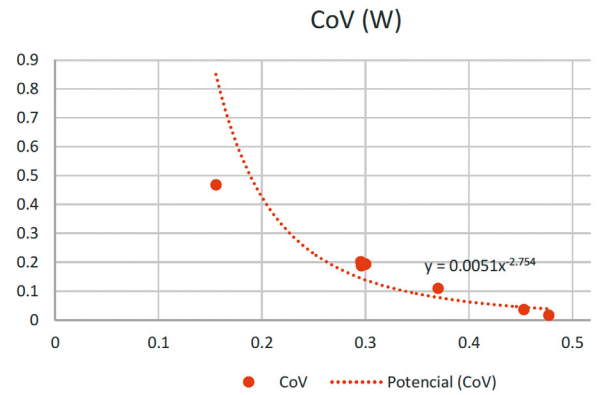
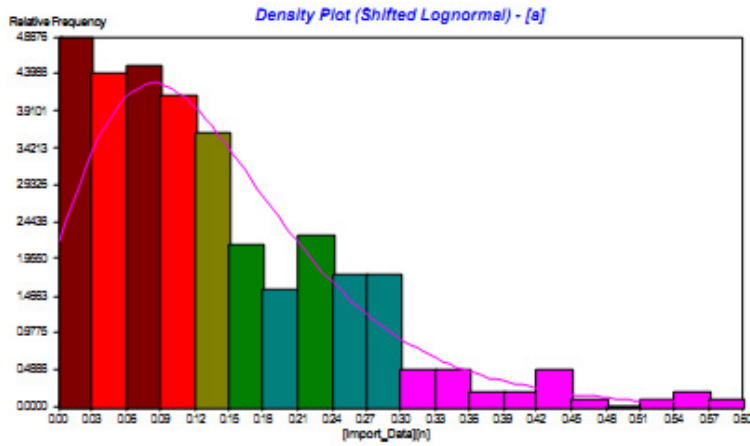


Figure 2.2.2 Left: Distribution values of values of w (value of w in X axis and number of simulations in Y axis). Right Values of w (X axis) from the simulation (coefficient of variation as percent per one in Y axis).

LH accounts for low humidity conditions (e.g.: 65%RH) and HH accounts for high humidity (e.g.: 75%RH).

2.2.2.1.1.3 Environmental parameter k_e

The parameter k_e in equation 2.2.3 can be calculated through Eq.2.2.7 being $f=5$ and $g=2.5$ obtained from regression analysis [Izquierdo 2001]. However as shown in the Figure 2.2.3 the fitting is not good and then, in Table 2.2.2 are given values calculated from the equation 2.2.7 but assuming average values of RH in each exposure class obtained from the meteorological information in different climates.

$$K_e = \frac{\left[1 - \left(\frac{RH}{100}\right)^f\right]^g}{\left[1 - \left(\frac{65}{100}\right)^f\right]^g} \quad \text{Eq. 2.2.7}$$

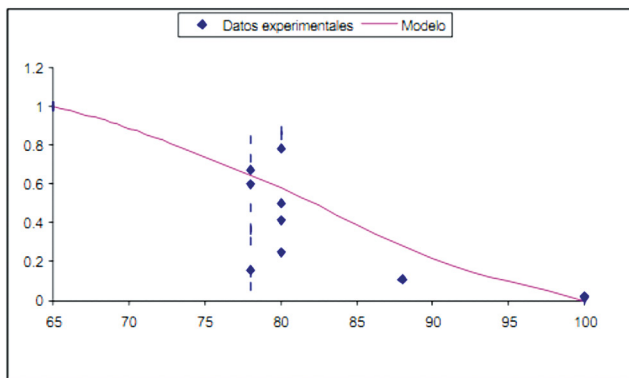


Figure 2.2.3 Fitting of Eq. 8 into values of environmental parameter in real structures The Y axis is the probability and the X axis is the RH.

Table 2.2.2 Values of the environmental parameter in function of the averaged RH obtained from meteorological information for each exposure class

Parameter	XC1	XC2	XC3		XC4	
RH (%)*	65	85	65	75	65	75
k_e	1	0.4	1	0.75	1	0.75

2.2.2.1.1.4. Summary of input parameters of initiation of carbonation

They are given in Table 2.2.3

Table 2.2.3 Summary of the parameters used in the carbonation model

Symbol	Parameter	Units	Equation	Distribution
V_{CO_2}	Velocity of carbonation	[mm/Year ^0.5]	$V_{CO_2} = \sqrt{\frac{2 k_e k_c}{R_{carb}}} \left(\frac{t_0}{t}\right)^w$	Log-Nor
$W(t)$	Wetness factor	[days]	$W = \frac{(p_{SR} ToW)^{b_w}}{2}$	D
k_c	environmental function	[-]	$K_e = \frac{\left[1 - \left(\frac{RH}{100}\right)^f\right]^g}{\left[1 - \left(\frac{65}{100}\right)^f\right]^g}$	Calculated for average RH values

2.2.2.2. Model for calculation the corrosion propagation

The corrosion rate V_{corr} is assumed to be constant (averaged annually) and then, the propagation model is given by [Andrade et al. 1989, Andrade 2019]:

$$t_{pro} = \frac{(\phi_0 - \phi_i)}{V_{corr}} = \frac{P_{corr}}{V_{corr}} \quad \text{Eq. 2.2.8}$$

where t_p is the corrosion propagation time in years, ϕ_0 is the initial diameter of the bar in mm and ϕ_i is the remaining diameter after corrosion in mm, P_{corr} (mm) is the accumulated corrosion or penetration of attack after a certain period of time and V_{corr} (mm/year) is the annually averaged corrosion rate.

The calculations were made considering the end of service life as described in the chapter 1.2.3 when a $P_{corr} = 50 \mu\text{m}$ for homogeneous corrosion as expected in carbonated structures.

2.2.2.2.1 Input Parameters of the propagation model and their statistical characterization

For propagation period, and following principles shown in [Andrade et al 1989, Andrade 1998, Contecvet 2001, Duracrete 2000, Andrade 2020] values are given in Table 2.2.4.

TABLE 2.2.4.

Values of the corrosion rate adopted in the exposure classes and their corresponding CoV.

Exposure	V_{corr} [mm/y]	CoV (%)	$V_{corr,d}$ $c=1,5$	t_{pro} [yr] $\beta=1,5$
XC1	1	65	2.0	25
XC2	4	65	5.4	9
XC3	2	65	4.0	13
XC4	5	90	12.9	4

V_{corr} is the average corrosion rate in the particular exposure class

CoV is the assumed coefficient of variation

$V_{corr,d}$ is the design value of the corrosion rate calculated through Eq. 2.2.17

t_{pro} is the propagation period calculated through Eq. 2.2.16.

For scatter quantification, after [Izquierdo 2001], it can be shown that 60% of variation can be expected for those exposure cases with constant conditions (e.g.: XC1/XC2/ XC3) for all other cases 90% to 120% of variation is used.

2.2.3. Formulation of Limit State Function

The probabilistic and partial factor methodology used next are those of the Probabilistic Model Code of the JCSS (Joint Committee of Structural Safety).

The Limit State considered is mathematically expressed as the probability that the corrosion depth at the time of the Design Service Life (DSL) is smaller than the P_{max} (50µm):

$$P_X(t_{DSL}) \leq P_{max} \tag{Eq. 2.2.9}$$

This eq. can be rewritten in terms of Limit State function $G(\cdot)$ as:

$$G(t) = P_{max} - P_X(t_{DSL}) \tag{Eq. 2.2.10}$$

where

$P_X(t_{DSL})$ is the achieved corrosion degree at the end of the design service life:

$$P_X(t) = \begin{cases} 0 & \text{if } t \leq t_{dep} \\ V_{corr}(t - V_{corr}) & \text{otherwise} \end{cases} \tag{Eq. 2.2.11}$$

V_{corr} is the corrosion rate (µm/y)

V_{corr} is the depassivation time

Depassivation and corrosion rate will be different for each exposure class as per EN206, as well as its respective mathematical expressions (as indicated in Table 2.2.4).

2.2.3.1 Reliability analysis and method

In order to calculate the probability of P_x being higher of P_{max} a whole probabilistic analysis can be performed, however for this calibration the suggested procedure by EN1990:2002 or the previous background document [annex C prEN 1990-2:2020]. This procedure is based on the determination of design point, which is the most probable combination of variables that provokes reaching limit state, see figure 2.2.4.

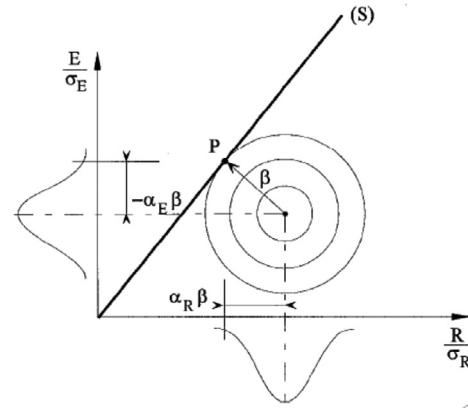


Figure 2.2.4. Design point and reliability index beta according to FROM method for Normally distributed variables.

Where: (S) is the failure boundary $g = R - E = P_{max} - P_x$

(P) is the design point

The design value for every variable can be calculated such that the probability of having more unfavourable values is as follows:

$$X_d = X^* = F^{-1}(-\alpha\beta) \tag{Eq. 2.2.12}$$

Where α 's are the values of the FORM sensitivity factors. The value of α is negative for unfavourable variables (actions) and positive for favourable variables (resistances). Following from FORM probabilistic method, it can be shown that:

$$\sum \alpha^2 = 1 \tag{Eq. 2.2.13}$$

In case of multivariate analysis and for calibration purposes [annex C prEN 1990-2:2020] the following values of Table 2.2.5 can be adopted:

TABLE 2.2.5.

Values of sensitivity factors of resistance and action variables.

Resistance Variables		Action Variables	
Leading	a = 0.70	Leading	a = -0.80
Accompanying	a = 0.28	Accompanying	a = -0.32

For calibration purposes only simplified distributions will be adopted: Normal, log-normal, uniform, exponential.

2.2.3.2 Sensitivity factors

A full probabilistic study was carried out with all described values during the TC250/SC2/WG1/TG10 work calibrating present Deemed-to-Satisfy rules in Germany and Spain in order to obtain sensitivity factors, and target – reliability values [Izquierdo 2001]. Conclusions from this study in terms of sensitivity factors is as follows:

For the case of carbonation induced corrosion, resistance variable is essentially concrete cover (C) whereas action variable is corrosion rate (V_{corr}) calculated values of α 's are shown in 2.2.5.

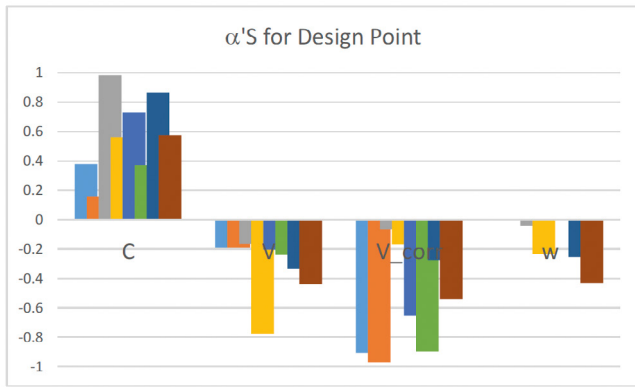


Figure 2.2.5 Sensitivity factor for Carbonation induced corrosion (max. 50µm loss of rebar section).

Thus, following from this analysis, following values will be adopted for concrete cover calculation:

TABLE 2.2.6. Sensitivity factors adopted in the carbonation calculations

Variable	Name	a	Type
Cover	C	0.8	Resistance
Carbonation rate	V _{CO2}	-0.32	Action
Corrosion rate	V _{corr}	-0.70	Action
Wetness factor	w	0.28	Resistance

It can be easily deduced from the table that $\sum \alpha > 1$ (app. 1.32) what implies that followed approach is slightly conservative. If a further refinement would be required, reported values for a could be divided by $\sum \alpha$ in order to normalize the values. However, for this application and in order to follow EN1990 procedure, no normalization was adopted.

2.2.4 Design values

2.2.4.1 Design values for propagation period

Since the definition of service life is now composed of initiation + propagation periods and because the concrete cover is only affecting the first one, it is necessary to calculate first the propagation period:

$$t_{dep}(cover) = service\ life - t_{prop} \quad Eq. 2.2.14$$

Therefore, design values for several reliability levels shall be obtained for propagation period. Applying design values to Eq. 2.2.14, yields:

$$t_{prop,d}(cover) = service\ life - t_{prop,d} \quad Eq. 2.2.15$$

This can be easily made considering a log-normal distribution, 50µm as maximum rebar loss in Eq. 2.2.8 above together with the a values provided in previous Table 2.2.6:

$$t_{prop,d} = \frac{50}{V_{corr,d}} \quad Eq. 2.2.14$$

Where $V_{corr,d}$ can be calculated as [annex C prEN 1990-2:2020, Tanner et al. 2019]:

$$V_{corr,d} = V_{corr,\mu} e^{\frac{0.70}{0.30} \beta C_{cov}} \quad Eq. 2.2.17$$

Where $\alpha = -0.70$ is adopted for XC cases and -0.30 for XS cases. Derived values for corrosion rate and propagation period in years, were given in Table 2.2.4.

It has to be emphasized, the importance of adequate calculation of the propagation period at national or local level, providing its impact in the initiation period.

2.2.4.2. Cover depths for Carbonation induced corrosion

As per agreement in the TC250/SC2/WG1/TG10, results will be presented in terms of the mean carbonation rate in constant chamber conditions ($k_c = w = k_e = 1$) for a value of reliability index of 1.50. The values in Table 2.2.7 are given in terms of $c_{min,dur}$ (where 10 mm for tolerance is subtracted from the calculated design value of concrete cover).

Following table 2.2.8 shows obtained crude values (in mm) for 50 yrs for reliability indexes of $\beta = 1$, to 1.5 and 2. These values shall be truncated by the minimum cover for other requirements such as anchorage or construction (e.g: 10 mm).

TABLE 2.2.7. Values of $c_{min,dur}$ obtained from the design calculated values by subtracting 10 mm.

K	$\beta = 1,5$					
	XC1	XC2	XC3_LH	XC3_HH	XC4_LH	XC4_HH
XRC 0.5	0	0	0	0	0	0
XRC 1	0	0	0	0	1	0
XRC 2	0	0	7	6	8	1
XRC 3	1	0	14	13	14	5
XRC 4	4	0	22	20	20	8
XRC 5	8	0	29	26	26	12
XRC 6	11	0	36	33	32	15
XRC 7	14	0	43	40	38	19
K	$\beta = 2,0$					
	XC1	XC2	XC3_LH	XC3_HH	XC4_LH	XC4_HH
XRC 0.5	0	0	0	0	3	2
XRC 1	0	0	3	2	7	3
XRC 2	2	0	13	11	15	7
XRC 3	7	0	22	19	23	11
XRC 4	13	0	32	27	31	15
XRC 5	18	1	41	35	38	19
XRC 6	24	2	50	43	46	23
XRC 7	29	4	59	51	53	27
K	$\beta = 2,5$					
	XC1	XC2	XC3_LH	XC3_HH	XC4_LH	XC4_HH
XRC 0.5	0	3	1	1	14	13
XRC 1	0	0	8	6	17	11
XRC 2	5	1	20	17	26	15
XRC 3	12	2	32	27	36	20
XRC 4	19	4	44	37	46	25
XRC 5	26	6	56	47	55	30
XRC 6	33	7	67	56	65	35
XRC 7	40	9	79	66	74	40

Table 2.2.8.

Rounded values of $c_{min,dur}$ for 50 and 100 years for $\beta=1.5$

Exposure class	XC 1		XC 2 low HR (65%)		XC 3				XC 4			
					High HR (75%)		Low HR (65%)		High HR (75%)			
Design Service life (years)	50	100	50	100	50	100	50	100	50	100	50	100
XRC 0.5	10	10	10	10	10	10	10	10	10	15	10	10
XRC 1	10	10	10	10	10	10	10	10	10	20	10	10
XRC 2	10	20	10	10	15	20	15	15	15	25	10	20
XRC 3	10	20	10	10	20	35	20	25	25	35	10	25
XRC 4	15	30	10	10	35	45	25	35	30	45	15	35
XRC 5	20	35	10	10	40		45	35			20	45
XRC 7	25		10									

Rounded values of $c_{min,dur}$ are given in Table 2.2.8.

2.2.6 References Carbonation

- Andrade, C., Alonso, C., Rodríguez, J., "Remaining service life of corroding structures", Proceedings IABSE Symposium on Durability, Lisbon (Sep. 1989), pp. 359-363.
- Andrade C., Diez J.M., Alonso C., (1997) "Mathematical modelling of a concrete surface "skin effect" on Diffusion in chloride contaminated media". Advances Cement Based Materials, vol.6 39-44
- Alonso C, Andrade C, Rodríguez J, Diez JM (1998) Factors controlling cracking of concrete affected by reinforcement corrosion. Materials and Structures 31:435-441.
- Andrade C., Arteaga A. (1998)- Duracrete Report of Subtask 4.3.1: Statistical Quantification of the Propagation Period - Brite/EuRam Project BE95-1347 Dec.
- Andrade C. and Tavares F. (2012) LIFEPROB. Program for the Probabilistic calculation of service life due to chloride ingress.
- Andrade, C. (2014). Probabilistic Treatment of the Reinforcement Corrosion. 2013 W.R. Whitney Award Lecture: Corrosion vol. 70, No. 6.
- Andrade C. (2017) -Reliability analysis of corrosion onset: initiation limit state- Journal of Structural Integrity and Maintenance- Nov Vol. 2, no. 4, 200-208
- Andrade C. - Propagation of reinforcement corrosion: principles, testing and modelling Materials and Structures 2 (2019) 1-26.
- Andrade C., Izquierdo D. (2020) - Statistical considerations of corrosion initiation and propagation – Proceedings of the fib CACRCS DAYS 2020 (online event) December 1-4 Edited by B. Belletti and D- Coronelli- CTE Ed.
- CONTECVET (2001) -A validated user's manual for assessing the residual life of concrete structures, DG Enterprise, CEC, (The manual can be downloaded from the web site of <http://www.iectc.csic.es/index.php/es/publicaciones-2/manual-contecvet>
- DuraCrete (2000) Statistical quantification of the variables in the limit state functions. The European Union – Brite EuRam III, Project No. BE95-1347, Probabilistic Performance -based Durability Design of Concrete Structures. Subtask 4.3.1: Statistical Quantification of the Propagation Period-Report BE95-1347 / TG4 / E EN 206:2013+A1:2016: "Concrete - Specification, performance, production and conformity"
- Enquiry draft- Eurocode 0, prEN 1990:2020. Annex C
- prEN 1990-2:2020, Eurocode – Basis of assessment and retrofitting of existing structures: general rules and actions, CEN TC 250/WG2/WG2.T2 Project Team Version, European Committee for Standardization, CEN, Brussels, September 2020
- fib Bulletin 34 (2006): Model code for service life design of concrete structures. Model Code. Fédération Internationale du Béton, Lausanne, Switzerland,
- fib MC 2010 - The fib Model Code for concrete structures 2010. fib (2013). Model Code. Fédération Internationale du Béton, Lausanne, Switzerland, 2013. Ernst & Sohn, Berlin. <http://www.fib-international.org/fib-model-code-2010>
- fib bulletin 76:(2015) Benchmarking of Deemed-to-Satisfy Provisions in Standards – Durability of Reinforced Concrete Structures Exposed to Chlorides. Prepared by fib Task Group 8.6: Gehlen, C., Greve-Dierfeld, S. v., Gulikers, J., Helland, S., Rahimi, A. et al. Fédération Internationale du Béton, Lausanne, Switzerland, 2015.
- Gehlen, C. (2000), Probability-based service life design of reinforced concrete structures – Reliability studies for prevention of reinforcement corrosion. DAFStb Heft 510, Berlin, Beuth, (in German).
- Gehlen C. (2000) Probabilistische Lebensdauerbemessung von Stahlbetonbauwerken-Zuverlässigkeitsbetrachtungen zur wirksamen Vermeidung von Bewehrungskorrosion“, PhD thesis. RWTH Aachen, 2000.
- González J.A., Algaba S. and Andrade C. (1980) - Corrosion of reinforcing bars in carbonated concrete- British Corrosion Journal, 3 135-139.
- Izquierdo D., Andrade C., Arteaga A. (2000) - Risk analysis of crack width limit state due to reinforcement corrosion- International RILEM Workshop on Life Prediction and Aging Management of Concrete Structures. Paris. Dan Naus Editor. Rilem Publications
- Izquierdo D. (2001): Basis of design for a probabilistic treatment of reinforcement corrosion processes- 2001 Polytechnic University of Madrid. Faculty of Civil Engineering.
- Joint Committee of Structural Safety. Probabilistic Model Code
- Siemes A.J.M., Vrouwenvelder A.C.W.M., Van den Beukel A (1985) Durability of buildings: a reliability analysis. Heron 30(3):3-48.
- Tanner P, Lara C, Bellod JL, Sanz D. (2019) "The plastic cathedral": Innovation to extend the service life of a heritage structure. Structural Concrete. 1–16.

ANNEX 2

BACKGROUND DOCUMENT

CHAPTER 3.2 - CHLORIDE INDUCED CORROSION

3.2.1 Objective

The objective of present document consists in establishing the cover depths for 50 and 100 years that fulfil the definition of the Exposure Resistance Classes (ERC) given in chapter 1 in the Introduction. For that objective the principles given in the Probabilistic Model Code of the JCSS and the carbonation model of the fib MC2010 have been used.

For achieving that objective, the steps followed are:

- Description of the Time-explicit mathematical model used for calculating the service life to fulfil the definition of ERC
- Phases of the model and selected input parameters
- Statistical characterization of the input parameters.
- Formulation of the Limit state function (LSF). Reliability level of compliance of the LSF. In present document the reliability factor $b=1.5$ has been adopted.
- Probabilistic calculations of the cover depths complying with the ranking of ERC defined in the chapter 1 of Introduction.

3.2.2 Chloride induced corrosion

3.2.1.1 Model the initiation period in marine environments

The time explicit chloride model selected is that of fib MC2010. It is based on the classical 2nd Ficks law with time variant diffusion coefficient and a skin zone Dx . Hence, the chloride concentration at a depth x can be calculated through:

$$C(x, t) = C_0 + (C_s - C_0) \left[1 - \operatorname{erf} \left(\frac{x - \Delta x}{2 \sqrt{D_{ap}(t)} t} \right) \right] \quad \text{Eq. 3.2.1}$$

Where:

C_0 is the initial chloride concentration of chloride in concrete in %

C_s is the concentration at the surface (a fitted value not a real one)

erf is the error function

$D_{app}(t)$ is the apparent diffusion coefficient for chlorides at time t , which usually is estimated with Eq. 3.2.2:

$$D_{ap}(t) = D_0 \left(\frac{t_0}{t} \right)^n \quad \text{Eq. 3.2.1}$$

Where:

t_0 is the reference time for D_{app} evaluation and,

n is the so-called ageing factor, that accounts for the apparent decrement of D_{app} with time.

Probabilistic evaluation of all the input parameters in Eq. 3.2.1 is complex, since a total number of 5 variables has to be calibrated in a posterior analysis. The equation is then simplified as was made that of the carbonation model by embodying several parameters in the velocity of chloride ingress, V_{cl} . The rearranged equation supposes the following mathematical change of variables:

Being the C_{cr} the critical chloride content (in %) it can be used to define the variable ζ :

$$\zeta = \frac{C_{cr} - C_0}{C_s - C_0} \quad \text{Eq. 3.2.3}$$

and then,

$$V_{cl}(t) = \operatorname{erf}^{-1}(1 - \zeta) \left[2 \sqrt{D(t_0)} (t_0)^n \right] \quad \text{Eq. 3.2.4}$$

In consequence the time to depassivation can be calculated as

$$t_{dep} = \left(\frac{C - \Delta x}{C_{cl}(t)} \right)^{\frac{2}{1-n}} \quad \text{Eq. 3.2.5}$$

For calculation, all scatter is merged into V_{cl} and n in order to make calibration easier and feasible.

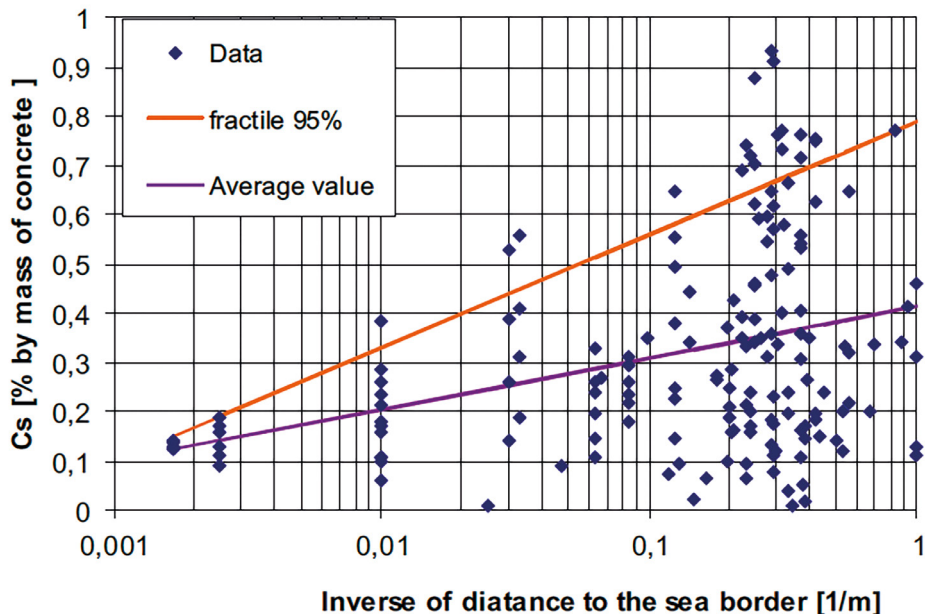


Figure 3.2.1. Relation between distance to shoreline and superficial concentration of chlorides (the X axis shows the inverse to the distance to the seashore).

3.2.2.1.1 Input parameters of the chloride model and their statistical characterization

It consists of calculating or adopting the coefficient of variation to be applicable to each mean value of the input parameter. Calculations are made based on mean values.

3.2.2.1.1.1 Surface chloride concentration

For XS2 and XS3 classes the chloride surface concentration is made to depend on the cement type (Izquierdo, D. Andrade, C., 2011) and ((fib), 2015).

TABLE 3.2.1.
Values of the surface concentration in function of cement type considered in the calculations for XS2 and XS3.

Cement type	C _s [%Con]
CEM I	0.35
CEM III/B	0.35
CEM II/A-V	0.55
CEM II/A-D	0.50

For exposure case XS1, surface concentration is dependent on many parameters (seashore distance, height of exposure, wind direction, wave height, etc.). In Figure 3.2.1 are shown the data used for the calculation of the scatter and due to it a simplified ranking approximation was made (Izquierdo, D. Andrade, C., 2011).

The exposure class XS1 is not defined in detail in the EN206 and in reality covers a wide range of distances and locations with respect to the shoreline. For the sake of this exercise a value of 100 m is adopted and therefore average value of 0.2% by weight of concrete of surface chloride concentration with respect to the concrete mass is taken for the calculations.

A CoV = 50% was taken in all exposure classes.

3.2.2.1.1.2 Critical chloride content (C_{cr})

Critical chloride content is widely characterized in the literature (Izquierdo et al. 2004). In present calculations an averaged value of C_{cr} = 0.6% by cement weight and a CoV = 30% are adopted, with a normal distribution.

3.2.2.1.1.3. Ageing factor n

Ageing factor is in many cases the most influencing variable in Eq. 3.2.1. Hence a proper calibration of this variable is essential. For this exercise several data sources have been used in order to account for the longest exposure periods because at short periods the aging factor *n* may be still evolving and then, with a high uncertainty. In Table 3.2.2 is provided the values considered and their bibliographic source, together with the CoV recorded.

These data enabled to propose in all cases a CoV = 20% (upper boundary of recorded values) for being adopted in the calculations.

TABLE 3.2.2.
Values of aging factors used in the calculations and references.

Cem type	Source	n _p (XS2/XS3)	n _p (XS1)
CEM I	((fib), 2015), (Izquierdo, D. Andrade, C., 2011), (Polder, R.B. Rooij, M.R., 2005)	0.45	0.60
CEM II/A-V	(Izquierdo, D. Andrade, C., 2011), (Polder, R.B. Rooij, M.R., 2005)	0.80	0.60
CEM III/B	((fib), 2015), (Polder, R.B. Rooij, M.R., 2005)	0.50	0.70
CEM II/A-D	((fib), 2015)	0.40	0.65

3.2.2.1.1.4 Skin zone (Δx)

It is named “convection zone” in MC2010, however the mechanisms acting are not only convection and then in pre-set exercise will be named “skin zone”. It is considered only in XS3 environment, where it has been shown that the combination of carbonation and chloride ingress more often leads to a non-fickian diffusion profile (with a maximum in the interior of the concrete). For the calculations, an average value of 10 mm ((fib), 2015) and CoV = 50% were adopted.

3.2.2.1.1.5 Chloride velocity V_{Cl} (t)

The simplified Eq. 3.2.5 embodying several input parameters and resulting in a V_{Cl} is used for the calculations.

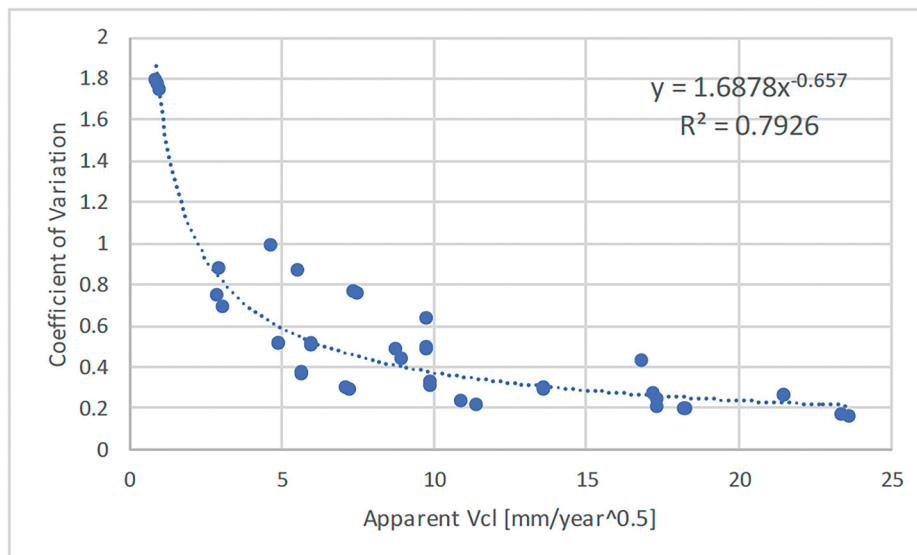


Figure 3.2.2. Average and CoV for apparent chloride ingress rate.

Chloride ingress is dependent of cement type, exposure conditions and concrete quality and then in a parallel manner than in the case of the carbonation rate, the VCl value has been found to depend on its average values, as shown in Figure 3.2.2. It is a hyperbolic function whose formula will be used in the calculations for the CoV.

$$CoV_{VCl} = 1.6878 C_{Cl}^{-0.657} \quad Eq. 3.2.6$$

3.2.2.1.1.6. Concrete cover

The same CoV = 30% than in chapter 2.2 for carbonation is adopted in present calculations ((*fib*), 2015) (Izquierdo, D. Andrade, C., 2011) (Izquierdo, D, 2001).

Table 3.2.3 .
Adopted Coefficient of variation of the concrete cover thickness.

Type of execution	Dist. Type	Bias	CoV
in situ – normal conditions	Log-normal	1.0	30%
Precast – dedicated quality control	Normal	1.0	10%

3.2.3.2 Summary of input parameters of initiation of corrosion due to chloride ingress

TABLE 3.2.4.
Input parameters for the chloride modelling.

Parameter	Units	Average value	CoV (%)	Statistical distribution
C_0	[wt.-%/cem]	0.01	20	Log-Nor
$C_{s,Dx}$	[wt.-%/conc]	See Table 3.2.1 for XS2/XS3 And 0.2% for XS1	50	Log-Nor
C_{crit}	[wt.-%/conc]	0.1	30	Normal
Dx	[mm]	10mm only in XS3	50	D
c	[mm]	several	30	See Table 3.2.3
V_{Cl}	[m ² /Ös]	several	See equation 3.2.5	Log-Nor
n	[-]	See Table 3.2.2.	30	
t_0	[years]	28 days	-	-
t	[years]	50 and 100 years	-	-

3.2.2.2 Model of the propagation period

The propagation model is the same than for carbonation described in (Andrade 1989):

$$t_{pro} = \frac{P_{corr}}{V_{corr}} \quad Eq. 3.2.6$$

where t_p is the corrosion propagation time in years, P_{corr} (μm) is the accumulated corrosion or attack penetration after a certain period of time and V_{corr} ($\mu\text{m}/\text{year}$) is the annually averaged corrosion rate.

3.2.2.2.1. Input Parameters of the propagation period and their statistical characterization

For propagation period, the values considered taken are those given in Table 3.2.5 (Andrade, C., 1999). For scatter quantification, after (Izquierdo, D. Andrade, C., 2011), it was obtained that 60% of CoV variation is shown in exposure cases with constant conditions (e.g.: XS1/XS2) and 90% in XS3 with wet-dry cycles.

Table 3.2.5.
Values of the corrosion rate adopted in exposure class and their corresponding CoV. Propagation periods until $P_{corr} = 500 \mu\text{m}$.

Exposure	V_{corr} [$\mu\text{m}/\text{y}$]	CoV (%)	$V_{corr,D}$ b=1,5	t_p [yr] b=1,5
XS1	30	60	56.3	1
XS2	10	60	13.1	4
XS3	70	90	105.0	0

3.2.2.3 Service life model

The service life is composed of an initiation (t_i) period and a propagation (t_p) one:

$$t_{SL} = t_i + t_p \quad Eq. 3.2.7$$

3.2.3. Formulation of Limit State Function

The probabilistic and partial factor methodology used next are those recommended in the Probabilistic Model Code of the JCSS.

The method is the same than that described in chapter 2.2.3 for carbonation

3.2.3.1 Sensitivity factors

Sensitivity factors and target – reliability values (Izquierdo, 2019) have been calculated for the input parameters of the model. The results obtained are the following:

- For the case of chloride induced corrosion (seawater source), the sensitivity factors are shown in Figure 3.2.3 can be deduced that, on the resistance side Cover and ageing factors are leading values, whereas chloride ingress rate (V_{Cl}) is the leading variable on the action side.

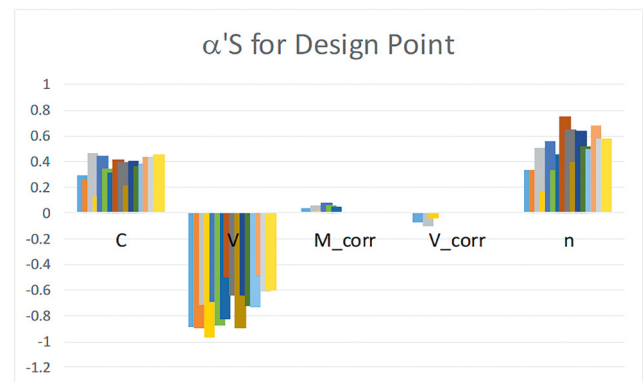


Figure 3.2.3. Sensitivity factors for Chloride induced corrosion (max. 50 μm loss of rebar section).

For calculation purposes the parameters given in Table 3.2.6 are adopted.

TABLE 3.2.6.
Sensitivity factors of the input service life parameters in the case of carbonation

Variable	Name	a	Type
Cover	C	0.40	Resistance
Chloride Ingress rate	V_{Cl}	-0.80	Action
Corrosion rate	V_{Corr}	~0	Action
Ageing factor	n	0.60	Resistance

In the same manner than in the case of carbonation, the summatory $\sum \alpha > 1$, that implies that the values are slightly con-

TABLE 3.2.7. Calculated minimum values (10 mm were subtracted from the nominal cover used in the calculations) for 50 and 100 years of service life)

Calculated minimum cover depths						
b=1.50	XS1		XS2		XS3	
	50 years	100 years	50 years	100 years	50 years	100 years
XRD 0.5	16.0	18.1	19.0	24.7	32.0	37.4
XRS 1	22.0	24.8	30.0	36.7	42.0	51.0
XRS 2	30.0	34.1	45.0	54.5	56.0	69.5
XRS 3	35.0	41.0	56.0	68.7	68.0	83.4
XRS 4	40.0	46.8	66.0	81.0	78.0	94.9
XRS 5	44.0	51.8	75.0	92.0	85.5	104.8
XRS 6	48.0	56.3	83.0	103.0	92.5	113.8
XRS 7	51.2	60.4	90.0	111.5	98.5	121.9
XRS 8	55.0	64.2	97.0	120.3	104.5	129.4
XRS 8.5	56.3	66.0	100.0	124.5	107.0	133.0

TABLE 3.2.8. Rounded minimum values of cover depths

Rounded minimum cover depths						
b=1.50	XS1		XS2		XS3	
	50 years	100 years	50 years	100 years	50 years	100 years
XRD 0.5	20	25	20	25	35	40
XRS 1	25	30	30	40	45	55
XRS 2	30	35	45	55	60	70
XRS 3	35	40	55	70	70	N.R.*
XRS 4	40	50	65	N.R.*	N.R.*	N.R.*
XRS 5	45	55	75	N.R.*	N.R.*	N.R.*
XRS 6	50	60	N.R.*	N.R.*	N.R.*	N.R.*
XRS 7	55	65	N.R.*	N.R.*	N.R.*	N.R.*
XRS 8	60	N.R.*	N.R.*	N.R.*	N.R.*	N.R.*
XRS 8.5	65	N.R.*	N.R.*	N.R.*	N.R.*	N.R.*

*Not recommended

servative. If a further refinement would be required reported values for a could be divided by $\Sigma\alpha=1$ to normalize the values. However, for this application and in order to follow EN1990 procedure, no normalization to 1 was adopted.

Another conclusion from this sensitivity analysis is that the most sensitive parameter are the chloride ingress rate and the aging factor. Then corrosion rate in this case is not predominant as the values are very high resulting in relatively short propagation periods not impacting significantly in the total service life except as will be justified in next paragraphs.

3.2.4 Design values

3.2.4.1 Design values for propagation period

Since the additive definition of service life: initiation + propagation period and given the fact that concrete cover is only affecting the first one, in order to determine the required cover for each exposure class and concrete property will be obtained by subtraction of propagation period from the total required service life.

$$t_{dep}(cover) = Service\ Life - t_{prop} \quad Eq. 3.2.8$$

Applying design values to Eq. 3.2.8, yields:

$$t_{dep,d}(cover) = Service\ Life - t_{prop,d} \quad Eq. 3.2.9$$

Therefore, design values for several reliability levels are obtained considering a log-normal distribution, 500 μm as maximum pitting attack giving:

$$t_{prop,d} = \frac{50}{V_{corr,d}} \quad Eq. 3.2.10$$

Where $V_{corr,d}$ can be calculated as:

$$V_{Corr,d} = V_{Corr,\mu} e^{0.3\beta Cov} \quad Eq. 3.2.11$$

Where $\alpha = -0.30$ is adopted for XS cases. Calculated values for corrosion rate and propagation period until $P_{corr} = 500 \mu\text{m}$ (pitting and end of service life) were given in Table 3.2.5. In view of the short design propagation periods, no propagation has been discounted from the initiation in the calculation of service life.

3.2.4.2. Cover depths for Chloride induced corrosion

The cover depth values are given in terms of $c_{min,dur}$ (where 10 mm for tolerance is subtracted from the design value of concrete cover). Table 3.2.7 shows the calculated minimum cover depth values (in mm) for 50 and 100 years for each ERC (from 0.5 to 7) and exposure classes XS1 to XS3). They should be rounded to the closest value ranked every 5 mm. The rounded values are shown in Table 3.2.8.

3.2.5 References Chlorides

- Andrade, C., Alonso, M.C., y Gonzalez, J.A., (1990) "An initial effort to use the corrosion rate measurements for estimating rebar durability", in Corrosion Rates of Steel in Concrete, ASTM STP 1065, eds. N.S. Berke, V. Chacker, y D. Whiting, Philadelphia, USA, pp.29-37
- Andrade, C. (2014). Probabilistic Treatment of the Reinforcement Corrosion. 2013 W.R. Whitney Award Lecture: Corrosion vol. 70, No. 6.
- Andrade C. (2017) -Reliability analysis of corrosion onset: initiation limit state- Journal of Structural Integrity and Maintenance- Nov Vol. 2, no. 4, 200–208. <https://doi.org/10.1080/24705314.2017.1388693>
- DAfStb Heft 601 Durability design of reinforce concrete structures for reinforcement corrosion – Part 1: System relevant parameter of reinforcement corrosion. (Dauerhaftigkeitsbemessung von Stahlbetonbauteilen auf Bewehrungskorrosion – Teil 1: Systemparameter der Bewehrungskorrosion) Authors: M. Beck, A. Burkert, A. Faulhaber, C. Gehlen, J. Harnisch, B. Isecke, J. Lehmann, K. Osterminski, M. Raupach, P. Schießl, W. Tian, J. Warkus.
- DAfStb Heft 602 Durability design of reinforced concrete structures for reinforcement corrosion– Part 2: Durability design (Dauerhaftigkeitsbemessung von Stahlbetonbauteilen auf Bewehrungskorrosion: Teil 2: Dauerhaftigkeitsbemessung) Authors: E. Bohner, C. Fischer, C. Gehlen, H. S. Müller, K. Osterminski, J. Özbolt, P. Schießl, S. von Greve-Dierfeld
- CEN/TS 17440 2020, *Technical Specification – Assessment and retrofitting of existing structures*, European Committee for Standardization, CEN, Brussels, July 2020.
- CONTECVET – (2000) *A validated user's manual for assessing the residual life of concrete structures*, DG Enterprise, CEC. (The manual can be downloaded from the web site: https://www.ietcc.csic.es/wp-content/uploads/1989/02/manual_contecvet_ingles.pdf)
- EN 1992-1-1:2004 Eurocode 2: Design of concrete structures - Part 1-1: General rules and rules for buildings
- Gehlen C.(2000) Probabilistische Lebensdauerbemessung von Stahlbetonbauwerken-Zuverlässigkeitsbetrachtungen zur wirksamen Vermeidung von Bewehrungskorrosion“, PhD
- Izquierdo D. (2001): Basis of design for a probabilistic treatment of reinforcement corrosion processes- PhD. Polytechnic University of Madrid. Faculty of Civil Engineering
- Izquierdo D., Alonso C., Andrade C., Castellote M. (2004) "Potentiostatic determination of chloride threshold values for rebar depassivation. Experimental and statistical study". *Electrochimica Acta* 49 pp. 2731–2739.
- IZQUIERDO D. ANDRADE C. (2009) CALIBRATION OF MODELS FOR ESTABLISHING THE DURABILITY LIMIT STATE)- 7TH COLLOQUIA OF MANAGERS AND TECHNICIANS OF CEMENT PLANTS NOVEMBER -MÁLAGA – SPAIN
- Izquierdo D., Andrade C., Arteaga A., Tanner P. (2003) Economical optimization of appraising concrete degradation processes3rd International IABMAS Workshop on Life –Cycle Cost Analysis and Design of Civil Infrastructure Systems and the fib WP 5.3-1, TG 5.6 and the Joint Committee on Structural Safety Workshop on Probabilistic Modelling of Deterioration Processes in Concrete Structures- Lausanne- Switzerland- March 24-26.
- Izquierdo D., Andrade C., Arteaga A. (2000) - Risk analysis of crack width limit state due to reinforcement corrosion- International RILEM Workshop on Life Prediction and Aging Management of Concrete Structures. Paris. Dan Naus Editor. Rilem Publications
- JCSS (2000), JCSS probabilistic model code Part 1: Basis of design. Joint Committee on Structural Safety.
- MC2010 fib Model Code for Concrete Structures 2010
- prEN 1990:2020 (E), *Eurocode – Basis of structural and geotechnical design*, CEN TC 250 Enquiry Draft, European Committee for Standardization, CEN, Brussels, September 2020.
- prEN 1990-2:2020, *Eurocode – Basis of assessment and retrofitting of existing structures: general rules and actions*, CEN TC 250/WG2/WG2.T2 Project Team Version, European Committee for Standardization, CEN, Brussels, September 2020.
- Tanner P, Lara C, Bellod JL, Sanz D. (2019) "The plastic cathedral": *Innovation to extend the service life of a heritage structure*. *Structural Concrete*; 1–16. <https://doi.org/10.1002/suco.201900365>
- Tuutti, K. (1982) "Corrosion of steel in concrete", Swedish Cement and Concrete Institute (CBI) n° 4-82. Stockholm.

Shear Resistance of Members Without Shear Reinforcement in Presence of Compressive Axial Forces in the Next Eurocode 2

Resistencia a cortante de elementos sin armadura de cortante en presencia de esfuerzos axiales de compresión en el próximo Eurocódigo 2

Pedro F. Miguel^a, Miguel A. Fernández^a, Josef Hegger^b, Maximilian Schmidt^c

^a Professor. Universitat Politècnica de València

^b Professor. RWTH Aachen University

^c Research Associate. RWTH Aachen University

Recibido el 23 de octubre de 2022; aceptado el 30 de enero de 2023

ABSTRACT

The second generation of Eurocode 2 incorporates formulations based on physical models which are general enough for the assessment of existing structures but can be simplified for the design of new structures, in order to improve the ease-of-use. One of the areas where these improvements are addressed is the shear verification of members without shear reinforcement, such as solid slabs, walls, cut-and-cover tunnels, precast ribs or hollow core slabs, which in some cases are prestressed or subjected to external axial loading.

In current Eurocode 2, the shear verification of these structures is based on an empirical formulation proposed by Zsutty in 1968. The final draft of the new version of Eurocode 2 has adopted the Critical Shear Crack Theory (CSCT) as the theoretical basis for the formulation of the shear resistance, which allows a better understanding of structural behaviour in many different conditions, not only for the design of new structures, but also for the assessment of existing structures. This formulation accounts for some aspects that are not well considered in current Eurocode 2, which have been underlined as shortcomings in recent years.

The formulation for design of new structures in the final draft of the new version of Eurocode 2 (General Model) is easy to use for the verification of the shear resistance, but requires an iterative process to calculate the shear capacity of sections in the presence of axial forces. For this reason, the final draft of the new version of Eurocode 2 also provides an alternative non-iterative formulation (Linear Approach) to calculate the shear capacity in presence of compressive axial forces, based on the linearisation of the CSCT shear failure criterion and formulated with the same additive structure as in the current Eurocode 2, useful for the most common cases.

This paper presents the General Model formulation provided in the next Eurocode 2 for the shear verification of axially loaded members without shear reinforcement, as well as the alternative formulation (linear approach). In addition, the agreement of both formulations with experimental results from an available shear test database on prestressed concrete beams is shown and the consistency of the safety treatment between the two formulations is also discussed.

KEYWORDS: Shear, shear resistance, concrete structures, prestressing, axial force.

©2023 Hormigón y Acero, the journal of the Spanish Association of Structural Engineering (ACHE). Published by Cinter Divulgación Técnica S.L. This is an open-access article distributed under the terms of the Creative Commons (CC BY-NC-ND 4.0) License

RESUMEN

La segunda generación del Eurocódigo 2 incorpora formulaciones basadas en modelos físicos suficientemente generales para la evaluación de estructuras existentes, pero que pueden simplificarse para el diseño de nuevas estructuras, con el fin de mejorar la facilidad de uso. Uno de los ámbitos en los que se abordan estas mejoras es la verificación a cortante de elementos sin armadura de cortante, como losas macizas, muros, marcos, viguetas prefabricadas o losas alveolares, que en algunos casos están pretensados o sometidos a cargas axiales externas.

En el actual Eurocódigo 2, la verificación a cortante de estas estructuras se basa en una formulación empírica propuesta por Zsutty en 1968. El borrador final de la nueva versión del Eurocódigo 2 ha adoptado la denominada Critical Shear Crack Theory (CSCT) como

* Persona de contacto / Corresponding author:
Correo-e / e-mail: pmiguel@cst.upv.es (Pedro F. Miguel).

base teórica para la formulación de la resistencia a cortante, lo que permite una mejor comprensión del comportamiento estructural en muchas condiciones diferentes, no sólo para el diseño de nuevas estructuras, sino también para la evaluación de las estructuras existentes. Esta formulación tiene en cuenta algunos aspectos que no están bien considerados en el actual Eurocódigo 2, los cuales han sido subrayados como deficiencias en los últimos años.

La formulación para el diseño de nuevas estructuras en el borrador final de la nueva versión del Eurocódigo 2 (Modelo General) es fácil de usar para la verificación de la resistencia a cortante, pero requiere un proceso iterativo para calcular la capacidad resistente a cortante de secciones en presencia de esfuerzos axiales. Por este motivo, el borrador final de la nueva versión del Eurocódigo 2 también proporciona una formulación alternativa que no requiere iteración (Aproximación Lineal) para calcular la capacidad resistente a cortante en presencia de esfuerzos axiales de compresión, basada en la linealización del criterio de fallo por cortante del CSCT y formulada con la misma estructura aditiva que en el actual Eurocódigo 2, útil para los casos habituales.

En este trabajo se presenta la formulación del Modelo General previsto en el próximo Eurocódigo 2 para la verificación a cortante de elementos sin armadura de cortante sometidos a esfuerzos axiales, así como la formulación alternativa (Aproximación lineal). Además, se muestra la concordancia de ambas formulaciones con los resultados experimentales de una base de datos disponible de ensayos de cortante en vigas de hormigón pretensado y la consistencia del tratamiento de seguridad entre ambas formulaciones.

PALABRAS CLAVE: Cortante, resistencia a cortante, estructuras de hormigón, pretensado, esfuerzo axial.

©2023 Hormigón y Acero, la revista de la Asociación Española de Ingeniería Estructural (ACHE). Publicado por Cinter Divulgación Técnica S.L. Este es un artículo de acceso abierto distribuido bajo los términos de la licencia de uso Creative Commons (CC BY-NC-ND 4.0)

1. INTRODUCTION

Many common structures, such as solid slabs, walls, cut-and-cover tunnels, precast ribs, hollow core slabs, which are subjected to shear forces, are designed without shear reinforcement. These elements can be subjected to axial forces either due to prestressing or external loads.

In current Eurocode 2 [1], the shear resistance verification of members without shear reinforcement is based on an empirical formulation proposed by Zsutty in 1968 [2] from test on non-axially loaded reinforced concrete beams, but including a coefficient k to account for the size effect and an additive term to account for the axial force effect, and setting a specific value for the shear slenderness a/d . The influence of axial force on the shear resistance is based on the proposal of Hedman and Losberg [3], according to which a prestressed concrete beam has the same shear resistance as a reinforced concrete beam but adding the shear force acting when the decompression moment is reached. On the other hand, both the original Zsutty's formulation and the Hedman and Losberg proposal depend on the shear slenderness a/d . However, this influence has been removed in the current Eurocode 2 [1] by assuming a fixed value for a/d .

The availability of experimental databases with a large number of tests [4] on beams without stirrups and the research work carried out by various authors have shed light on some of the shortcomings of this formulation, which have been highlighted by Muttoni *et al.* [5] and Herbrand and Hegger [6]:

- The k -factor does not adequately account for the influence of the size effect. A discussion on the factor to consider the size effect in different standards can be found in [7], where it concludes that the factor proposed by ACI-446 is the one that best fits the experimental results. Compared to this factor, the k -factor in current Eurocode 2 [1] gives unsafe values for large values of the effective depth;
- The additive term included to consider the influence of the axial force gives too conservative or even negative values of the shear resistance in case of tensile force. This behaviour has been also investigated and pointed out by Adam and Hegger [8];

- The influence of eccentricity is not explicitly accounted for, which can lead to unsafe results for members with normal force instead of prestressing or less eccentricity (for example in members with additional external normal force or prestressing [6]);
- The influence of aggregate size on shear resistance is not considered. However, aggregate interlock, initially described by Fenwick and Paulay [9], Taylor [10] and Paulay and Loeber [11] could be the main shear transfer action in elements without shear reinforcement [12], [13] and [14]. This mechanism depends on the roughness of the shear crack and, consequently, on the aggregate size;
- The current version of Eurocode 2 [1] does not take advantage of the increase of shear resistance in members with small values of shear slenderness.

Different models have been proposed for the calculation of shear resistance in elements without shear reinforcement in the last decades. Among others: tooth models, such as those proposed by Kani [15], Hamadi and Regan [16], Reineck [17] and Yang [18]; models based on the compressed chord resistance, such as those proposed by Zararis and Papadakis [19], Hegger and Görtz [20], Park *et al.* [21] and Mari *et al.* [22], [23] and [24]; model based on the Critical Shear Crack Theory (CSCT) proposed by Muttoni *et al.* [25], [26], [12] and [27]; models based on fracture mechanics, such as that proposed by Carmona and Ruiz [28]; models based on crack propagation by Classen [29] and Schmidt [30]; and model based on the Modified Compression Field Theory (MCFT) proposed by Vecchio and Collins [31] and [32].

The final draft of the new version of Eurocode 2 (FprEN 1992-1-1:2023) [33] has adopted the CSCT [25] and [26] as the basis for the formulation of the detailed verification of shear and punching shear resistance in members without transverse reinforcement.

The main assumption of the CSCT [25] is that the shear stress resistance in reinforced concrete elements without shear reinforcement depends on the width and roughness of the critical shear crack developed along the web and on the concrete compressive strength (Formula (1) and Figure 1). The crack width (w) is proportional to the product of a control longitudinal strain (ϵ) by the effective depth of the

section (d). The strain ϵ is evaluated at a depth of $0.6d$ from the outermost compressed fibre in the critical section whose location depends on the external loading distribution. The roughness is taken into account by the aggregate size d_g and $d_{g0} = 16$ mm is the reference value of the aggregate size.

$$\frac{V_R}{\sqrt{f_c} b d} = \frac{1}{3} \frac{1}{1+120 \frac{\epsilon d}{d_g + d_{g0}}} \quad (1)$$

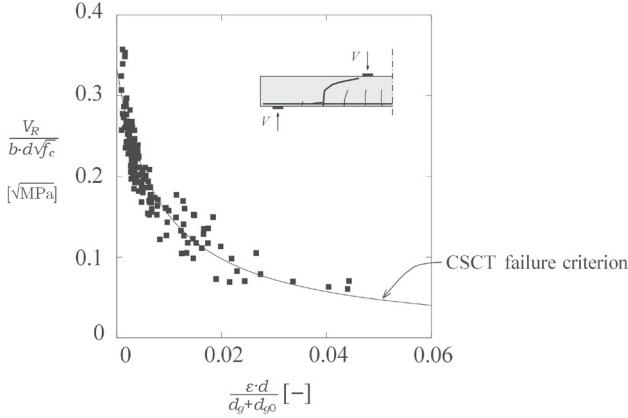


Figure 1.- CSCT failure criterion and comparison to tests (adapted from [34]).

This formulation accounts for the aforementioned main parameters. The size effect and the aggregate size are directly considered and the influence of the shear slenderness and the axial force through the longitudinal strain due to the bending and axial forces concomitant with the acting shear.

This hyperbolic failure criterion has been considered in Annex I of the FprEN 1992-1-1:2023 [33] for the assessment of existing structures. However, to simplify the verification of the shear resistance of new structures, a closed-form equation has been proposed, which allows the verification of the shear resistance in a straightforward manner. Such closed-form equation requires nevertheless an iterative process to calculate the shear capacity of the section in presence of axial forces. Alternatively, the FprEN 1992-1-1:2023 [33] provides a non-iterative method for the calculation of the shear capacity in presence of compressive axial forces, formulated with the same additive structure as in the current Eurocode 2 [1], useful for the most common cases.

This paper presents how the CSCT has been drafted in the next generation of Eurocode 2 to provide a General Model for the shear verification of members not requiring shear reinforcement in the presence of axial forces, as well as the alternative formulation (Linear Approach) based on the linearisation of the shear failure criterion used for the General Model. The paper also shows that both methods (General Model and Linear Approach) have similar agreement with experimental results from an available shear test database on prestressed concrete beams. On the other hand, a discussion shows the consistency on the safety treatment between both formulations. Finally, an example has been included to show the use of the general model and the linear approach in a practical case.

2. GENERAL MODEL

2.1. formulation

The formulation to calculate the shear resistance of members without shear reinforcement is based on the Critical Shear Crack Theory, using the longitudinal tensile reinforcement strain (ϵ_v) instead of the reference strain at the control depth (ϵ) [35]. According to this, the shear resistance can be expressed as the following hyperbolic law:

$$V_{R,c} = \frac{0.3}{1+48 \frac{\epsilon_v d}{d_{dg}}} \sqrt{f_c} b_w d \quad (2)$$

where:

- ϵ_v strain of the longitudinal tensile reinforcement. In case of prestressing, strain increase in the prestressing steel.
- b_w width of the cross-section
- d effective depth of the cross-section
- f_c compressive strength of concrete
- $d_{dg} = 16 \text{ mm} + D_{\text{lower}} \leq 40 \text{ mm}$ for concrete with $f_{ck} \leq 60 \text{ MPa}$
- $= 16 \text{ mm} + D_{\text{lower}} (60/f_{ck})^2 \leq 40 \text{ mm}$ for concrete with $f_{ck} > 60 \text{ MPa}$

According to FprEN 1992-1-1:2022 [33], D_{lower} is the smallest value of the upper sieve size D in an aggregate for the coarsest fraction of aggregates in the concrete permitted by the specification of concrete according to EN206 [36].

The reinforcement strain ϵ_v can be calculated by a sectional analysis for the bending moment M_E and axial force N_E acting at the control section. To this aim, a non-linear sectional analysis can be performed.

However, in order to provide an easy-to-use formulation for design of new structures, FprEN 1992-1-1:2023 [33] introduces some simplifications:

- The hyperbolic shear failure criterion (2) is replaced by the following power-law [12],

$$V_{R,c} = k \left(\frac{f_c d_g}{\epsilon_v d} \right)^{1/2} b_w d \quad (3)$$

$$\text{with } k = 0.015 \left(\frac{a_{cs}}{d} \right)^{1/4}$$

where a_{cs} is the effective shear span with respect to the control section.

- The reinforcement strain ϵ_v can be calculated by a simplified flexural analysis at the control section assuming a linear elastic behaviour of the tension reinforcement (Figure 2)

$$\epsilon_v = \frac{|M_E| + N_E e_c}{E_s A_{sl} z} = \left(1 + \frac{N_E e_c}{|M_E|} \right) \frac{|M_E|}{E_s A_{sl} z} = k_{vp} \frac{|M_E|}{E_s A_{sl} z} \quad (4)$$

Introducing the definition of the effective shear span at control section as $a_{cs} = |M_E| / V_E = d$, the reinforcement strain is a linear function of the acting shear force.

$$\epsilon_v = k_{vp} \frac{|V_E| a_{cs}}{E_s A_{sl} z} \quad (5)$$

where $k_{vp} = 1 + \frac{N_E e_c}{|M_E|}$ is a coefficient that allows to account for the effect of the axial force in the effective shear span $a_{cs,N} = k_{vp} a_{cs}$, which physically means that the presence of an compressive

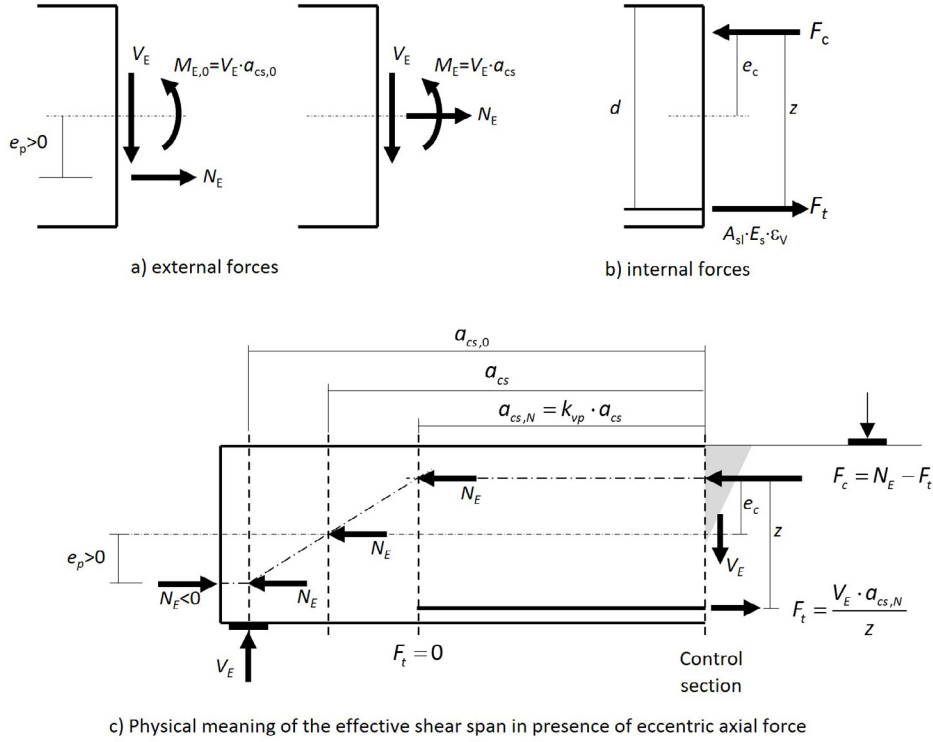


Figure 2. Simplified sectional analysis.

axial force reduces the length where the flexural reinforcement is in tension (Figure 2c). The value of k_{vp} is equal to 1 when there is no axial force applied, less than 1 for compressive axial forces and greater than 1 for tension axial forces. Since only tensile reinforcement strains are allowed in the shear failure criterion, k_{vp} must be greater than 0. This means that, for members subjected to compression forces, the eccentricity of the applied forces $-\frac{|M_E|}{N_E}$ must be greater than e_c . Considering $\frac{|M_E|}{-N_E} \geq \frac{e_c}{0.9}$, the minimum value of k_{vp} is 0.1.

On the other hand, the value of e_c can be approximated by a constant value equal to $d/3$. Therefore, the coefficient k_{vp} can be expressed as

$$k_{vp} = 1 + \frac{N_E}{|V_E| a_{cs}} \frac{d}{3} \geq 0.1 \quad (6)$$

Replacing (5) in (3) and considering that at failure $V_E = V_{R,c}$, it follows

$$V_{R,c} = 0.015^{2/3} \left(\frac{E_s \rho_l f_c d_g}{k_{vp} \sqrt{a_{cs} d}} \frac{z}{d} \right)^{1/3} b_w d \quad (7)$$

where $\rho_l = \frac{A_d}{b_w d}$

and considering $E_s = 200000 \text{ N/mm}^2$ and $z/d = 0.9$, Formula (7) can be rewritten as

$$V_{R,c} = 0.6 \left(\frac{100 \rho_l f_c d_{dg}}{k_{vp} a_v} \right)^{1/3} b_w d \quad (8)$$

where $a_v = \sqrt{\frac{a_{cs} d}{4}}$ is the mechanical shear span.

When the longitudinal tensile reinforcement is composed by both ordinary A_{si} and prestressed A_{pi} reinforcement located at

d_{si} and d_{pi} respectively from the outermost compressed edge of the section, an equivalent reinforcement A_{si} can be considered. This equivalent reinforcement provides a tensile force F_t equal to the sum of all tensile forces (increase in case of prestressing) of the reinforcements, located at a distance d from the outermost compressed edge of the section which provides a bending moment equal to the sum of all bending moments (increase in case of prestressing) of the reinforcements.

$$d = \frac{\sum A_{pi} d_{pi}^2 + \sum A_{si} d_{si}^2}{\sum A_{pi} d_{pi} + \sum A_{si} d_{si}} \quad (9)$$

$$A_{si} = \frac{\sum A_{pi} d_{pi} + \sum A_{si} d_{si}}{d} \quad (10)$$

Figure 3 illustrates the power-law shear failure criterion and the load-deformation path, when no axial force is applied, for different values of a_{cs}/d . For a given value of a_{cs}/d , the point of intersection between the shear failure criterion (Formula (3)) and the load-deformation relationship (Formula (5)) depicts the shear resistance (Formula (8)) for this value of a_{cs}/d . Therefore, the thicker solid line that links these points depicts the relationship between the shear resistance and the reinforcement strain obtained by varying a_{cs}/d . As can be seen, the shear resistance decreases as a_{cs}/d increases. Since for $a_{cs}/d \geq 4$ the variation of the shear resistance is small, a constant value of the shear resistance can be assumed for $a_{cs}/d \geq 4$, leading to the following easy-to-use formulation included in the new Eurocode 2 (FprEN1992-1-1:2022) [33].

$$V_{R,c} = 0.6 \left(\frac{100 \rho_l f_c d_{dg}}{d} \right)^{1/3} b_w d \quad (11)$$

In presence of an axial force N_E and for a given value of $a_{cs,0}/d$ ($a_{cs,0}$ is the effective shear span when no axial force is applied,

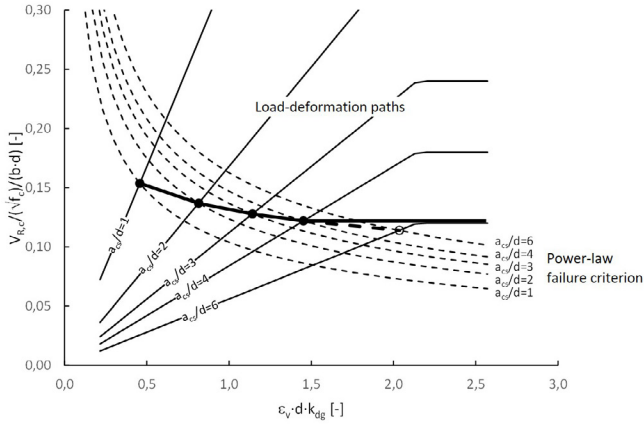


Figure 3. Shear resistance for different a_{cs}/d values when no axial force is applied.

see Figure 2c), as when there is no axial force, the shear resistance is given by the intersection between the load-deformation relationship and the shear failure criterion for this given value of $a_{cs,0}/d$. Figure 4 illustrates how this resistance is obtained for two values of $a_{cs,0}/d$. The load-deformation relationship can be expressed as a function of $a_{cs,0}/d$ (see Figure 2 and Formula (4))

$$V_E = -\frac{N_E(e_p + e_c)}{a_{cs,0}} + \frac{E_s A_{st} z}{a_{cs,0}} \varepsilon_v$$

which is a straight line when a constant value of $z = 0.9 \cdot d$ is considered. The failure criterion for a given value of $a_{cs,0}/d$ can be obtained from (3) substituting a_{cs} by $a_{cs,0} + \frac{N_E e_p}{V_{R,c}}$ in the expression of k .

By repeating this process for different values $a_{cs,0}/d$, the thicker solid line in Figure 5 is obtained, which depicts the relationship between the shear resistance and the reinforcement strain for a constant value of the axial force by varying $a_{cs,0}/d$. As can be seen, each point of this line corresponds to a different value of a_{cs}/d . As in the case of no axial forces, FprEN1992-1-1:2022 [33] considers a constant value of the shear resistance for $a_{cs}/d \geq 4$.

In summary, the shear resistance, accounting for the effect of axial force and the effective shear span, can be expressed as follows

$$V_{R,c} = 0.6 \left(\frac{100 \rho_l f_c d_{dg}}{k_{vp} a_v} \right)^{1/3} b_w d \quad (12)$$

where:

$$k_{vp} = 1 + \frac{N_E}{|V_E| a_{cs}} \frac{d}{3} \geq 0.1 \quad (13)$$

$$\frac{d}{2} \leq a_v = \sqrt{\frac{a_{cs} d}{4}} \leq d \quad (14)$$

The limits of $k_{vp} \geq 0.1$ and $a_{cs} \geq d$ (i.e. $a_v \geq d/2$) are in fact an upper bound on the shear strength.

2.2. Minimum shear resistance

Experimental evidences [37] have proven that the shear resistance decreases as the reinforcement strain increases, even when they are larger than the yielding strain. However, only in case of designs with plastic redistributions of internal forces in statically indeterminate structures, shear failures with rein-

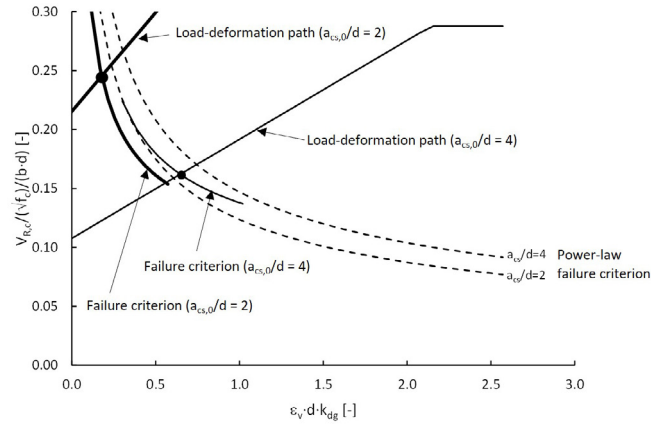


Figure 4.- Shear resistance for different $a_{cs,0}/d$ values in presence of a compressive axial force.

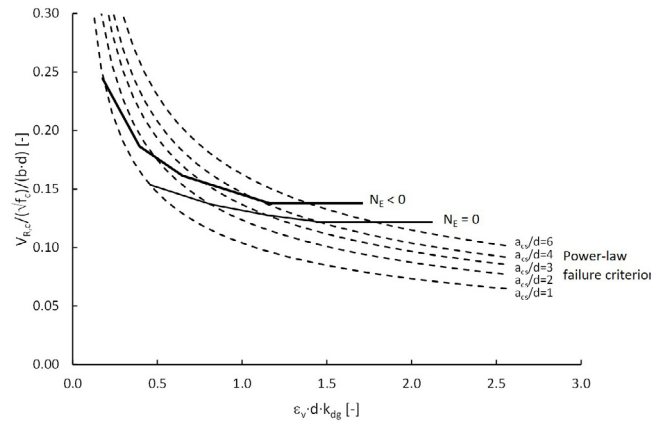


Figure 5. Shear resistance for $N_E=0$ and $N_E<0$.

forcement strains larger than yielding strain can occur [38]. Therefore, for the sake of simplicity, the maximum reinforcement strain has been taken equal to the yielding strain. Thus, the minimum shear resistance can be expressed from Formula (3) as

$$V_{R,min} = 0.015 \left(\frac{a_{cs}}{d} \right)^{1/4} \left(\frac{E_s f_c d_{dg}}{f_y d} \right)^{1/2} b_w d \quad (15)$$

And considering $E_s = 200000 \text{ N/mm}^2$ and a value of $a_{cs}/d = 4$, Formula (15) can be rewritten as

$$V_{R,min} = 10 \left(\frac{f_c d_{dg}}{f_y d} \right)^{1/2} b_w d \quad (16)$$

In case of prestressed members without ordinary reinforcement, f_y must be taken as the difference between the yielding stress and the prestress of the tendon after losses.

It is worth noting that the minimum shear resistance is not dependent on the applied axial force. This is because the minimum shear resistance is defined assuming that the flexural reinforcement yields at the load level that produces the shear failure, that is, the available flexural reinforcement is equal to that required for the bending and axial forces concomitant with the shear force applied at the control section.

On the other hand, it should also be noted that the minimum shear resistance given by (16) is not proportional to d , but to the square-root of d . This does not only mean that a size effect is being considered but also a combined size and strain

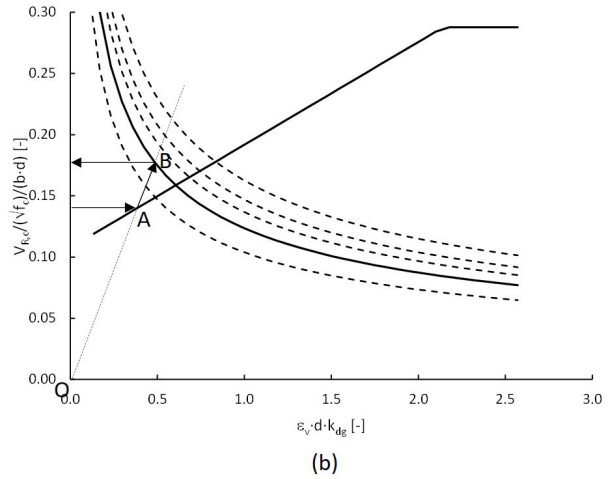
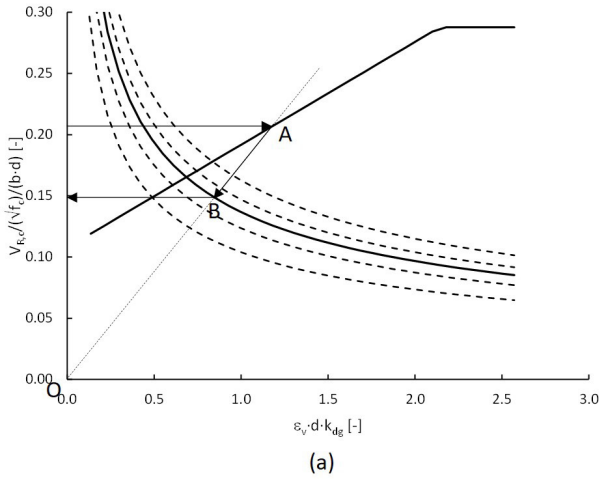


Figure 6. Verification procedure. (a) Section does not resist the applied shear. (b) Section resists the applied shear

effect. Thus, as the member size increases, the flexural reinforcement ratio required to reach the yield strength at the load level that produces the minimum shear resistance decreases.

2.3. Verification procedure and resistance capacity

When there is no axial force, $k_{vp}=1$ and Formula (12) becomes an explicit expression to obtain directly the shear resistance, while in presence of axial forces, k_{vp} depends on the acting shear force and Formula (12) is thus an expression in function of the acting shear force.

In a verification problem, Formula (12) can be used directly (refer to Figure 6). For given values of the applied forces N_E , M_E y V_E at the control section, the effective shear span a_{cs} and the coefficient k_{vp} can be calculated, which define the straight-line OA in Figure 6. The intersection of this line with the shear failure criterion (Formula (12)) for the calculated value of a_{cs} gives the shear resistance V_R (point B in Figure 6). If $V_E > V_{R,c}$, shear failure is predicted to occur for a shear force lower than the applied force (Figure 6(a)) and, conversely, $V_E < V_{R,c}$ means that section resists the applied shear force (Figure 6(b)).

In summary, the flow chart for the detailed verification of the shear resistance is as follows (Figure 7):

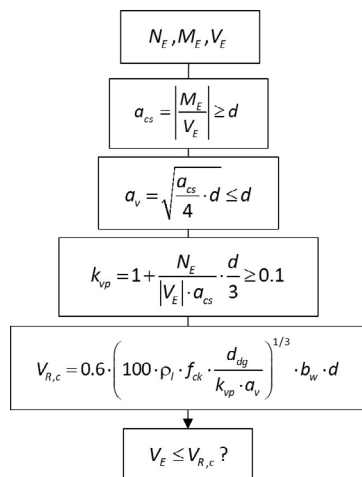


Figure 7. Flow chart for the verification of the shear resistance.

However, when the shear capacity of the control section is required, the applied shear force V_E must be taken equal to shear resistance V_R . Therefore, Formula (12) becomes an equation of the unknown V_R , which cannot be solved explicitly and thus needs an iterative process, as illustrated in Figure 8.

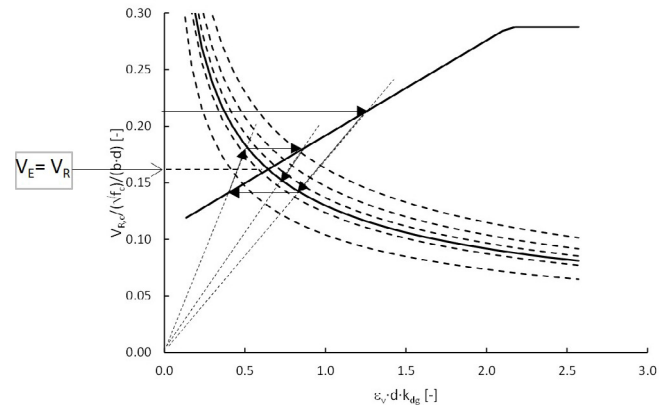


Figure 8. Iterative process to obtain the shear capacity in sections subjected to axial force.

3. LINEAR APPROACH

To avoid the iterative process described in the previous section, FprEN1992-1-1:2022 [33] provides a simplified formulation (Linear Approach) which is derived by linearizing the power law shear failure criterion used in the General Model for compressive axial forces.

3.1. Linearization of the power law shear failure criterion

In statically determinate structures subjected to a point or uniformly distributed load (Figure 9), the ratio $(a_{cs,0})$ between the bending moment and the shear force at the control section does not depend on the magnitude of the applied load.

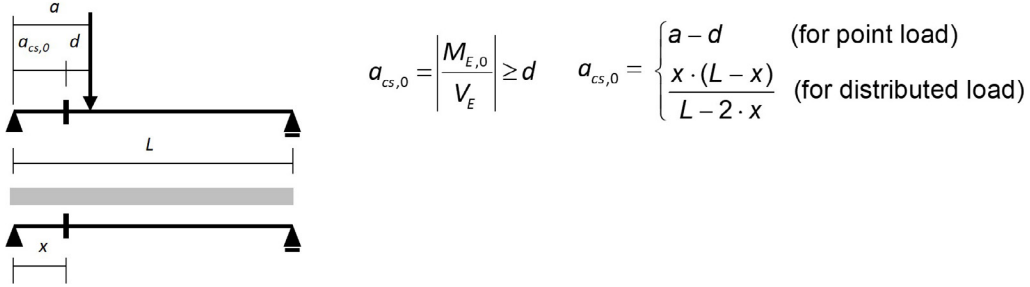


Figure 9. Definition of the $a_{cs,0}$ in statically determinate structures

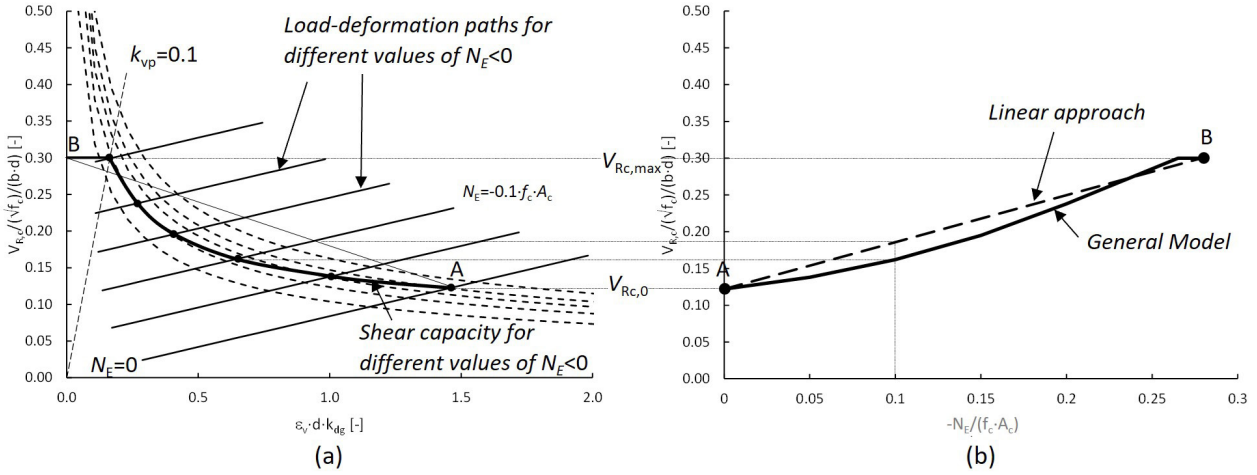


Figure 10.- Shear capacity for different compressive axial forces and a constant value of $a_{cs,0}$ (solid line: general model) (dashed line: linear approach): (a) Shear capacity vs reinforcement strain; (b) Shear capacity vs axial force.

When, in addition to the above load, a load (external or prestressing) producing an axial force N_E with an eccentricity e_p (refer to Figure 2) is acting, the ratio (a_{cs}) between the total bending moment and the applied shear force (effective shear span) depends on the axial and shear forces and is given by the following expression

$$a_{cs} = \left| \frac{M_E}{V_E} \right| = \left| a_{cs,0} + \frac{N_E e_p}{V_E} \right| \geq d \quad (17)$$

For a given value of $a_{cs,0}$ and N_E , the shear capacity $V_{R,c}$ is obtained by the iterative process defined in 2.3 (Figure 8) and the strain of the reinforcement (ϵ_v) can be calculated from (5). For different values of N_E the relationships $V_{R,c} - \epsilon_v$ and $V_{R,c} - N_E$, keeping constant the value of $a_{cs,0}$, can be obtained (thicker solid lines in Figure 10(a) and Figure 10(b) respectively).

This thicker solid line can be linearized for compressive axial forces by the dashed line in Figure 10(b), which is defined by two points:

- Point A: which corresponds to the shear capacity of the section without applying axial force ($V_{R,c,0}, \epsilon_{v,0}$).
- Point B: which is given by the shear capacity corresponding to $k_{vp}=0.1$ ($V_{R,c,max}$) and $\epsilon_v=0$.

This linear approach is given by the following expression:

$$V_{R,c} = V_{R,c,0} + \frac{V_{R,c,max} - V_{R,c,0}}{\epsilon_{v,0}} (\epsilon_v - \epsilon_{v,0}) \leq V_{R,c,max} \quad (18)$$

where

$V_{R,c,0}$ is the shear resistance obtained from the General Model without considering axial force,

$\epsilon_{v,0}$ is the reinforcement tensile strain for $V_{R,c,0}$, and $V_{R,c,max}$ is the upper limit of the shear resistance defined in the General Model by taking $k_{vp}=0.1$ and the corresponding value of a_{cs} .

The tensile strains ϵ_v and $\epsilon_{v,0}$ of the longitudinal reinforcement can be obtained from the same simplified sectional analysis as that used in the General Model in section 2.1 (Figure 2 with $e_c=d/3$):

$$\epsilon_v = \frac{V_E a_{cs,0} + N_E \left(e_p \frac{d}{3} \right)}{A_{sl} E_s z} \quad (19)$$

$$\epsilon_{v,0} = \frac{V_{R,c,0} a_{cs,0}}{A_{sl} E_s z} \quad (20)$$

Substituting (19) and (20) in (18) and taking $V_E = V_{R,c}$, an explicit expression can be derived to calculate the shear resistance in presence of compressive axial forces

$$V_{R,c} = V_{R,c,0} - k_N N_E \leq V_{R,c,max} \quad (21)$$

where

$$k_N = \left(1 - \frac{V_{R,c,0}}{V_{R,c,max}} \right) \frac{e_p + \frac{d}{3}}{a_{cs,0}} \quad (22)$$

$V_{R,c,max}$ can be approximated by the following formula (see annex 1)

$$V_{R,c,max} = 2.15 \left(\frac{a_{cs,0}}{d} \right)^{1/6} V_{R,c,0} \leq 2.71 V_{R,c,0} \quad (23)$$

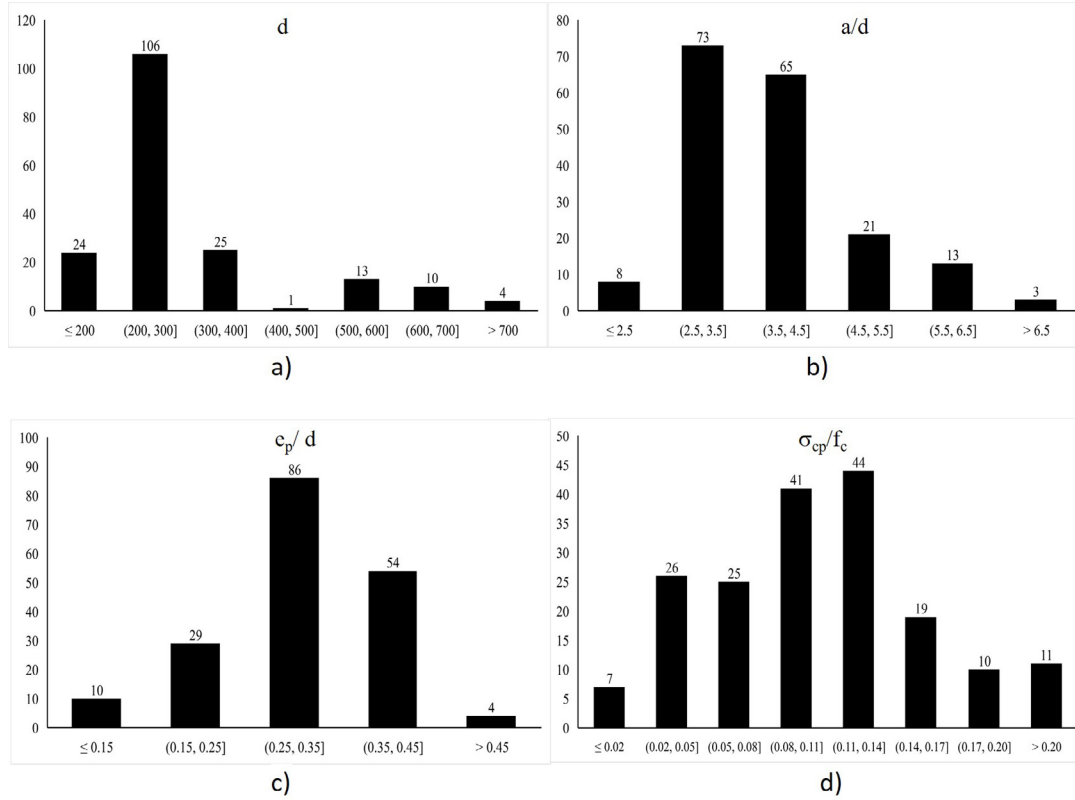


Figure 11. Histograms of the main parameters: a) Effective depth; b) shear span to effective depth ratio; c) eccentricity of axial force to effective depth ratio; d) compressive stress to concrete strength ratio.

And k_N (Formula (22)) can be simplified by taking the minimum value of $\frac{V_{Rc,max}}{V_{Rc,0}}=2.15$, since $a_{cs,0} \geq d$. Therefore,

$$k_N = 0.54 \frac{e_p + \frac{d}{3}}{a_{cs,0}} \leq 0.18 \quad (24)$$

The upper-bound of k_N is justified also in annex 1.

3.2. Linear Approach formulation

In summary, rounding the factor 0.54 in k_N to 0.5 and taking into account the minimum value of the shear resistance (Formula (16)), the Linear Approach formulation is expressed as

$$V_{Rc,min} \leq V_{Rc} = V_{Rc,0} - k_N N E \leq V_{Rc,max} \quad (25)$$

where

$$k_N = 0.5 \frac{e_p + \frac{d}{3}}{a_{cs,0}} \leq 0.18 \quad (26)$$

$$V_{Rc,max} = 2.15 \left(\frac{a_{cs,0}}{d} \right)^{1/6} V_{Rc,0} \leq 2.71 V_{Rc,0} \quad (27)$$

4.

COMPARISON WITH EXPERIMENTAL TEST RESULTS

4.1. Selected database

A comparison of the shear resistance calculated using the General Model and the Linear Approach with the experimental re-

sults of a selected database (see annex 2) has been performed in order to check the agreement between both formulations. This selected database is based on the ACI-DAFStb-Database of PC beams without stirrups (vuct-PC) [39][40], removing the tests for which no aggregate size is provided, those reported as flexural or anchorage failure and those with shear reinforcement, and adding the tests reported by De Wilder et al. [41] as well as Joergensen and Fisker [42].

The total number of tests is 183, 85 with rectangular cross-section and 98 with profiled cross-section. All tests are subjected to compressive axial forces.

Table 1 and Figure 11 present the range and the histogram of each of the main parameters.

TABLE 1.
Range of the main parameters.

Parameter	Min	Max
d [mm]	109	1025
a/d [-]	2.42	7.30
e_p/d [-]	0.13	0.51
$ \sigma_{cp} /f_c$ [-]	0.004	0.258

4.2. Statistical values

The formulations described in section 2 for the General Model (GM) (Formulae (12)-(14)) and in section 3 for the Linear Approach (LA) (Formulae (25)-(27)), taking into account the minimum value of the shear resistance given by Formula (16), as well as the current EN1992-1-1:2004 [1], have been ap-

Table 2. Statistical values for the ratio experimental to predicted shear strength (V_{test}/V_{cal})

Num	All tests			Rectangular sections			Profiled sections		
	183			85			98		
Method	EC2	GM	LA	EC2	GM	LA	EC2	GM	LA
AVG	1.59	1.52	1.51	1.32	1.47	1.40	1.84	1.56	1.60
SD	0.481	0.367	0.365	0.408	0.415	0.408	0.403	0.315	0.297
CoV	0.302	0.242	0.242	0.311	0.282	0.291	0.220	0.203	0.186
Max	3.40	2.67	2.59	2.39	2.67	2.59	3.40	2.51	2.54
Min	0.70	0.82	0.78	0.70	0.82	0.78	1.00	0.91	1.01
$V_{test}/V_{cal} < 1$	17	5	4	17	3	4	0	2	0

EC2: Current Eurocode 2 [1]
 GM: General Model
 LA: Linear Approach

plied to the tests in the selected database to obtain the ratio experimental to predicted shear strength (V_{test}/V_{cal}). The statistical values of this ratio are the followings:

As can be seen in Table 2, the statistical values of V_{test}/V_{cal} provided by the General Model (GM) and Linear Approach (LA) are almost the same for all tests and very similar when they are evaluated for rectangular sections or profiled sections separately. On the other hand, the values of CoV obtained with current Eurocode 2 [1] are higher than those provided by GM and LA formulations, both for rectangular and profiled sections and especially for all tests. Furthermore, the difference between the mean values calculated for rectangular sections and for profiled sections is much higher when using the current Eurocode 2 than when GM and LA formulations are used.

It should be noted that the tests where shear failures do not develop from a flexural crack have not been removed from the selected database. When these formulations are applied to these tests the calculated values are much less than the test results. If the 19 tests with $V_{test}/V_{cal} > 2$ are removed from the 183 tests of the selected database, CoV decrease significantly from 0.242 to 0.172, which is in line with the CoV obtained for members without axial force [5].

Figure 12 shows the experimental results against those provided by current Eurocode 2 [1], GM and LA formulations. As can be seen, the scatter and the R^2 coefficient is practically the same for GM and LA formulations and this R^2 coefficient (0.88) is better than that of the current Eurocode 2 (0.76).

Figure 13 to Figure 16 show the ratio V_{test}/V_{cal} as a function of the main parameters. As can be seen, the General model and the Linear Approach give similar results and trends for all these parameters.

In addition, it is worth noting that these formulations provide improvements with respect to current Eurocode 2 related to the influence of shear span to effective depth ratio and axial force on the shear resistance in presence of compressive axial force. While the current EC2 gives V_{test}/V_{cal} values below 1 for $a/d > 6$ and very conservative for small values of a/d , GM and LA formulations better capture the influence of this variable (Figure 14). Likewise, Figure 16 shows that the current EC2 gives many V_{test}/V_{cal} values below 1 for Σ_{cp}/f_c between 0.05 and 0.15 and is very conservative for high values of this variable. However, GM and LA captures more accurately the influence of this variable.

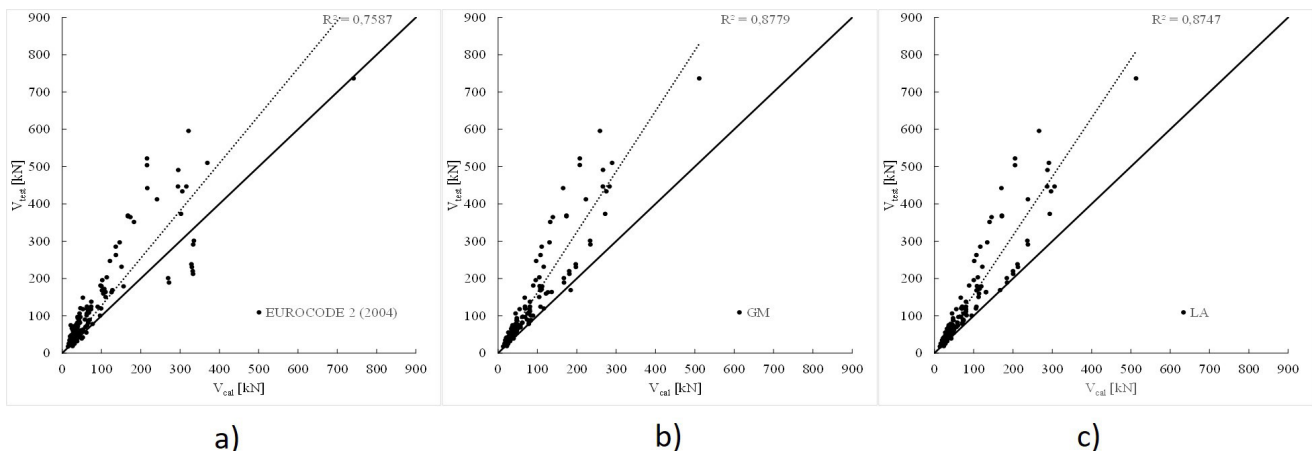


Figure 12. V_{test} vs. V_{cal} . a) Eurocode 2 (2004). b) General Model. c) Linear approach.

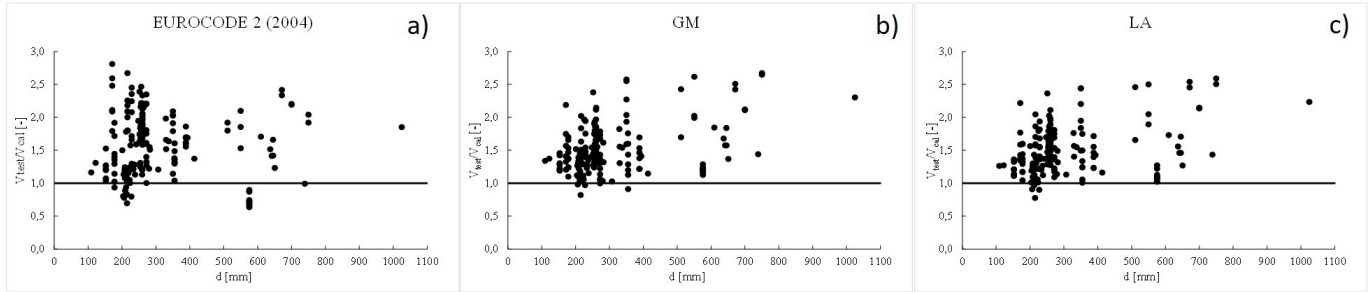


Figure 13.- Ratio V_{test}/V_{cal} vs. effective depth. a) Eurocode 2 (2004). b) General Model. c) Linear approach.

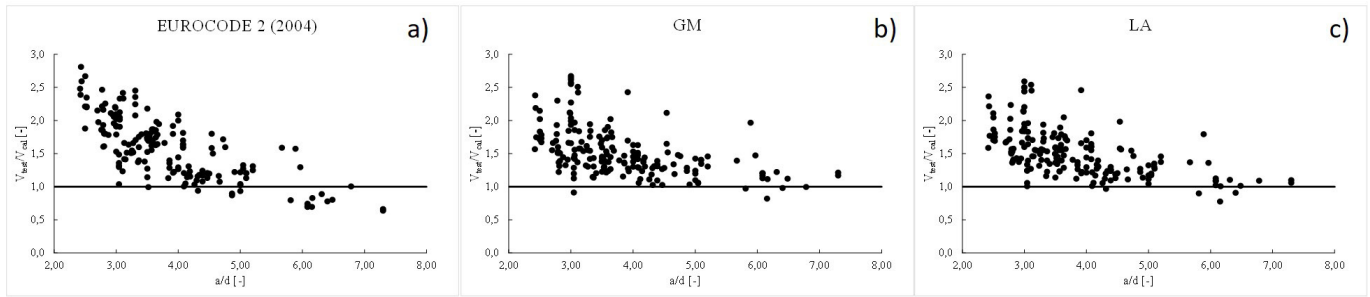


Figure 14. Ratio V_{test}/V_{cal} vs. shear span to effective depth ratio. a) Eurocode 2 (2004). b) General Model. c) Linear approach.

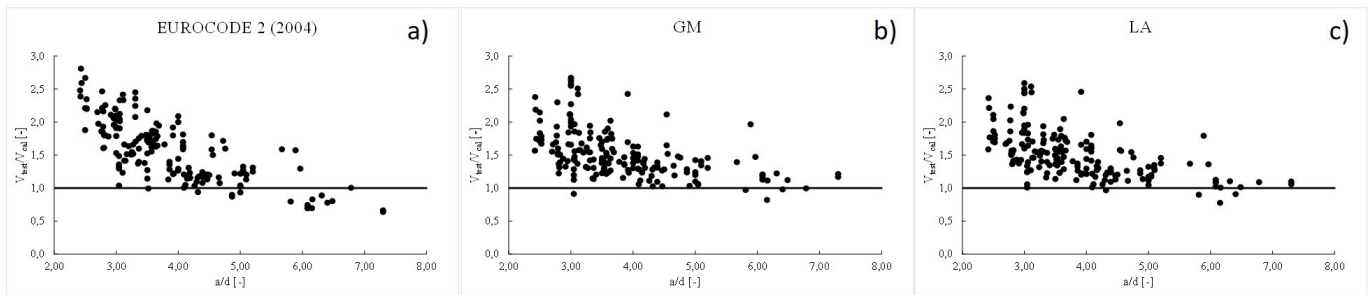


Figure 14. Ratio V_{test}/V_{cal} vs. shear span to effective depth ratio. a) Eurocode 2 (2004). b) General Model. c) Linear approach.

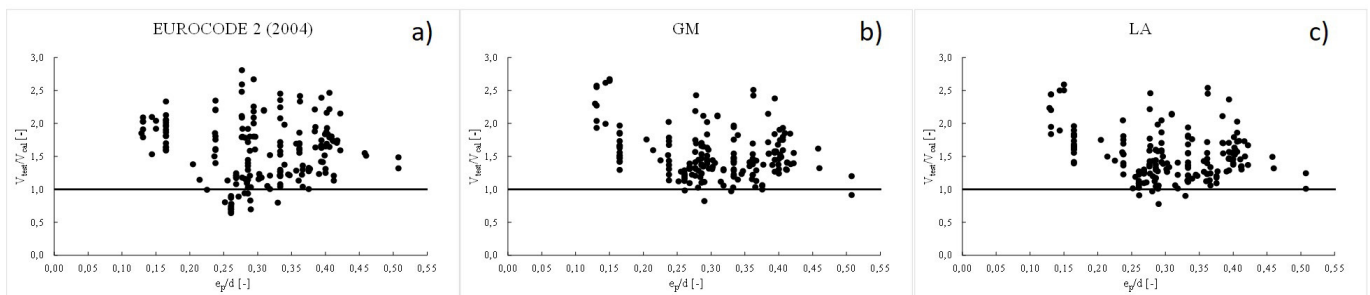


Figure 15. Ratio V_{test}/V_{cal} vs. eccentricity of axial force to effective depth ratio. a) Eurocode 2 (2004). b) General Model. c) Linear approach.

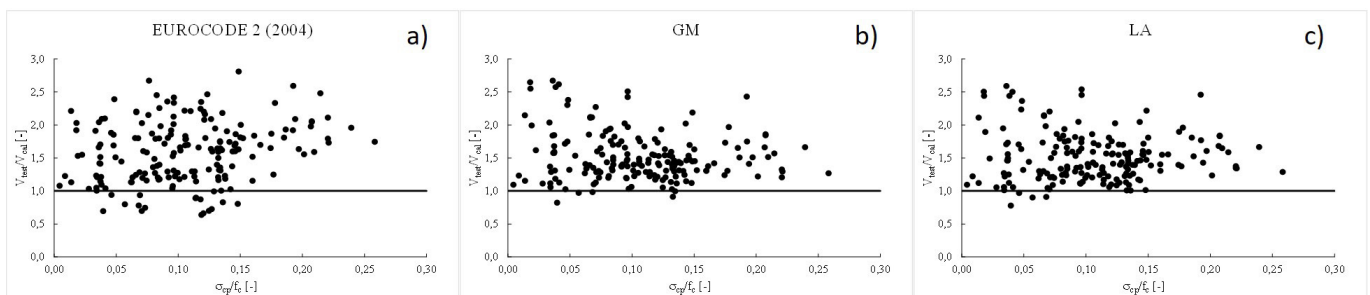


Figure 16. Ratio V_{test}/V_{cal} vs. compressive stress to concrete strength. a) Eurocode 2 (2004). b) General Model. c) Linear approach.

5. SAFETY FORMAT FORMULATION

The design shear resistance power law criterion can be expressed from (3) using a partial safety factor γ_R

$$\frac{V_{Rd,c}}{b_w d} = \frac{1}{\gamma_R} \frac{V_{Rk,c}}{b_w d} = \frac{k}{\gamma_R} \left(\frac{f_{ck} d_{dg}}{\epsilon_{vd} d} \right)^{1/2} \leq \frac{V_{Rdc,max}}{b_w d} \quad (28)$$

In absence of axial forces, a partial factor, γ_{def} can be assumed to account for the uncertainties related to the calculation of the deformation. Therefore, the design simplified load-deformation relationship can be obtained from (5) with $k_{vp}=1$ and applying the partial factor γ_{def}

$$\epsilon_{vd} = \gamma_{def} \frac{|V_{Ed}| a_{cs,0}}{E_s A_{sl} z} \quad (29)$$

The design value of the shear resistance $V_{Rd,c}$ can be obtained by substituting (29) in (28) and making $V_{Ed}=V_{Rd,c}$

$$\frac{V_{Rd,c}}{b_w d} = \frac{0.60}{\gamma_R^{2/3} \gamma_{def}^{1/3}} \left(100 \rho_l f_{ck} \frac{d_{dg}}{\sqrt{\frac{a_{cs,0}}{4} d}} \right)^{1/3} \quad (30)$$

The product $\gamma_R^{2/3} \gamma_{def}^{1/3}$ can be considered as a single safety factor γ_V , which involves all the uncertainties related to the model, the material and the geometry. So, the expression (30) can be written as

$$\frac{V_{Rd,c}}{b_w d} = \frac{0.60}{\gamma_V} \left(100 \rho_l f_{ck} \frac{d_{dg}}{\sqrt{\frac{a_{cs,0}}{4} d}} \right)^{1/3} \quad (31)$$

The partial safety factor γ_V is calibrated according to annex A of FprEN 1992-1-1:2023 [33] and the background document to Annex A [43] on the basis of the statistical values of the most sensitive random variables appearing in this Formula.

In presence of axial force, as in the case without axial force, to take into account the uncertainties related to the reinforcement strain, a partial safety factor γ_{def} could be assumed. Therefore, the design value ϵ_{vd} can be expressed from (5), as

$$\epsilon_{vd} = \gamma_{def} \frac{|V_{Ed}| a_{cs} k_{vp}}{E_s A_{sl} z} \quad (32)$$

$$\text{where } k_{vp} = 1 + \frac{N_E}{|V_E| a_{cs}} \frac{d}{3} \geq 0.1 \quad \text{and } a_{cs} = \left| \frac{M_{Ed}}{V_{Ed}} \right| \geq d$$

To calculate the design value of the shear resistance $V_{Rd,c}$ by means of Formula (28), the design value of the applied shear force V_{Ed} must be taken equal to $V_{Rd,c}$.

$$V_{d,c} = \frac{0.6}{\gamma_V} \left(\frac{100 \rho_l f_{ck} d_{dg}}{k_{vp} a_v} \right)^{1/3} b_w d \quad (33)$$

Since the coefficients k_{vp} and a_v are function of V_{Ed} , Formula (33) becomes a non-linear equation of $V_{Rd,c}$. Thus, unlike the case without presence of axial force, this Formula is not an explicit function of the random variables that governs this mode of failure. However, for the sake of simplicity FprEN 1992-1-1:2023 [33] assumes the same value of the partial factor γ_V as for members without axial force. This assumption is conservative since the scatter of the ratio V_{test}/V_{cal} decreases as γ_{cp}/f_c increases, as can be seen in Figure 16b.

It should be noted that the ratio $V_{Rk,c}/V_{Rd,c}$ which results by applying the General Model with $\gamma_V=1$ for $V_{Rk,c}$ and γ_V for $V_{Rd,c}$ is variable with N_{Ed} because Formula (33) is a non-linear equation.

Similarly, in the Linear Approach, the design shear failure criterion is obtained from (18) using the design values of the shear resistance

$$V_{Rd,c} = V_{Rdc,0} + \frac{V_{Rdc,max} - V_{Rdc,0}}{\epsilon_{vd0} - \epsilon_{vd}} (\epsilon_{vd0} - \epsilon_{vd}) \geq V_{Rdc,max} \quad (34)$$

The design simplified load-deformation relationship used in this approach is the same expression (32) as that used by the General Model

$$\epsilon_{vd} = \gamma_{def} \frac{|V_{Ed}| a_{cs} k_{vp}}{E_s A_{sl} z} = \gamma_{def} \frac{|V_{Ed}| a_{cs,0} + N_{Ed} \left(e_p + \frac{d}{3} \right)}{E_s A_{sl} z} \quad (35)$$

The tensile reinforcement strain ϵ_{vd0} is given by

$$\epsilon_{vd0} = \gamma_{def} \frac{|V_{Rdc,0}| a_{cs,0}}{E_s A_{sl} z} \quad (36)$$

The shear capacity $V_{Rd,c}$ can now be obtained by substituting (36) and (35) in (34) and making $V_{Ed}=V_{Rd,c}$

$$V_{Rd,c} = V_{Rdc,0} - \frac{V_{Rdc,max} - V_{Rdc,0}}{V_{Rdc,max}} \frac{e_p + \frac{d}{3}}{a_{cs,0}} N_{Ed} \geq V_{Rdc,max} \quad (37)$$

$$\text{Taking into account that } \frac{V_{Rdc,max} - V_{Rdc,0}}{V_{Rdc,max}} = \frac{V_{Rc,max} - V_{Rc,0}}{V_{Rc,max}}$$

$$\text{and } \frac{V_{Rc,max}}{V_{Rc,0}} = 2.154 \left(\frac{a_{cs,0}}{d} \right)^{1/6} \leq 2.71 \quad (\text{see annex 1}), \text{ Formula (37)}$$

can be written as

$$V_{Rd,c} = V_{Rdc,0} - k_N N_{Ed} \leq 2.15 \left(\frac{a_{cs,0}}{d} \right)^{1/6} V_{Rdc,0} \leq 2.71 V_{Rdc,0} \quad (38)$$

where k_N is given by Formula (26).

$$\text{Therefore, the coefficient } k_N = 0.54 \frac{e_p + \frac{d}{3}}{a_{cs,0}} \text{ that multiplies } N_{Ed}$$

does not include any partial safety factor.

6. EXAMPLE OF APPLICATION

Figure 17 presents a simply supported prestressed beam subjected to two point-loads used as an example for the detailed shear verification by the General Model (see Figure 6) and for the calculation of the shear capacity by both the General Model (see Figure 8) and the Linear Approach.

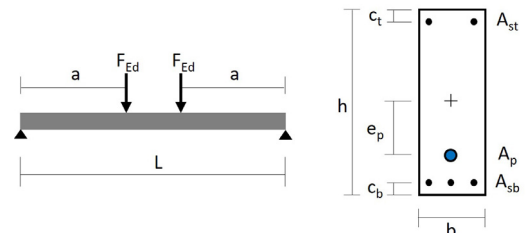


Figure 17. Example of application.

Geometrical data (mm)

L	a	h	b	e _p	c _b	c _t	A _{sb}	A _{st}	A _p
10000	4000	700	250	150	60	60	942	628	1050

Material data:

- Concrete: $f_{ck} = 60$ MPa. $D_{lower} = 16$ mm
- Reinforcement: $f_{yk} = 500$ MPa
- Prestressing steel: $f_{py} = 1560$ MPa

Design value of the prestressing force: $P_d = 1155$ kN.
External load: $F_{Ed} = 200$ kN

6.1. Preliminary calculations:

Effective depth of the ordinary reinforcement:

$$d_s = h - c_b = 700 - 60 = 640 \text{ mm}$$

Effective depth of the prestressed reinforcement:

$$d_p = \frac{h}{2} + e_p = 350 + 200 = 550 \text{ mm}$$

Effective depth:

$$d = \frac{d_s^2 A_s + d_p^2 A_p}{d_s A_s + d_p A_p} = \frac{640^2 \cdot 942 + 500^2 \cdot 1050}{640 \cdot 942 + 500 \cdot 1050} = 575 \text{ mm}$$

Size parameter:

$$d_{dg} = 16 + D_{lower} = 16 + 16 = 32 \text{ mm} \leq 40 \text{ mm}$$

Reinforcement ratio:

$$\rho_l = \frac{d_s A_s + d_p A_p}{d_w d^2} = \frac{640 \cdot 942 + 500 \cdot 1050}{250 \cdot 575^2} = 0.01365$$

Minimum shear stress resistance:

$$\tau_{Rdc,min} = \frac{V_{Rdc,min}}{b_w z} = \frac{11}{\gamma_v} \sqrt{\frac{f_{ck}}{f_{yd}}} \frac{d_{dg}}{d} = \frac{11}{1.4} \sqrt{\frac{60}{500}} \frac{32}{575} = 0.689 \text{ MPa}$$

The control section is located at a distance from the support axis.

In this control section, the design forces are:

$$N_{Ed} = -P_d = -1100 \text{ kN}$$

$$M_{Ed} = F_{Ed} x - P_d e_p = 200 \cdot 3.45 - 1100 \cdot 0.15 = 520 \text{ kN m}$$

$$\tau_{Ed} = \frac{V_{Ed}}{b_w z} = \frac{200000}{250 \cdot (0.9 \cdot 575)} = 1.54 \text{ MPa}$$

Since is greater than, detailed verification of the shear resistance cannot be omitted.

6.2. Verification procedure using the General Model

(see Figure 6)

The design value of the shear stress resistance can be obtained by dividing Formula (33) by $b_w \cdot z$ and taking $d/z=1.1$.

$$\tau_{Rdc} = \frac{0.66}{\gamma_v} \left(100 \rho_l f_{ck} \frac{d_{dg}}{k_{vp} a_v} \right)^{1/3} = \tau_{Rdc,min}$$

where:

$$k_{vp} = 1 + \frac{N_{Ed}}{|V_{Ed}|} \frac{d}{3 a_{cs}} = 1 + \frac{-1000}{200 \cdot 2600} \frac{575}{3} = 0.595 \geq 0.1$$

$$a_v = \sqrt{\frac{a_{cs,0}}{4}} d = \sqrt{\frac{2600}{4}} \cdot 575 = 611 \text{ mm} \neq d = 575 \text{ mm}$$

with

$$a_{cs} = \frac{|M_{Ed}|}{|V_{Ed}|} = \frac{575}{200} \cdot 1000 = 2600 \text{ mm} \geq d = 575 \text{ mm}$$

By substituting these values:

$$\tau_{Rdc} = \frac{0.66}{\gamma_v} \left(100 \cdot 0.01365 \cdot 60 \cdot \frac{32}{0.595 \cdot 575} \right)^{1/3} = 0.929 \text{ MPa} \geq \tau_{Rdc,min} = 0.689 \text{ MPa}$$

Since $\tau_{Ed} = 1.54$ MPa is greater than $\tau_{Rdc} = 0.929$ MPa, shear reinforcement should be provided in this control section.

6.3. Shear capacity using the General Model

(see Figure 8)

The calculations performed in this section are not needed when it deals with a verification problem, because they do not change the result of this verification related to the calculation performed in the section 6.2. They are only needed when the value of the shear capacity of the section is required.

To obtain the shear capacity in the control section, as indicated in section 2.3, the design shear force V_{Ed} must be equal to the design value of the shear resistance V_{Rdc} , which requires an iterative process applying the expressions given in section 6.2, since k_{vp} and a_{cs} depend on the design shear force. The result of this iterative process gives the following results:

x	V _{Ed}	M _{Ed}	a _{cs}	a _v	k _{vp}	τ _{Rdc}	V _{Rdc}
m	kN	kN·m	m	m	[-]	MPa	kN
3.425	143.311	325.86	2.274	0.572	0.353188	1.108	143.311

As can be seen, the shear capacity is 1.108 MPa.

6.4. Shear capacity using the Linear Approach

The design value of the shear stress resistance can be obtained by dividing Formula (38) by $b_w \cdot z$ and taking $d/z=1.1$:

$$\tau_{Rdc,min} \leq \tau_{Rdc} = \tau_{Rdc,0} - k_1 \sigma_{cp} \leq \tau_{Rdc,max}$$

where:

$$\tau_{Rdc,0} = \frac{0.66}{\gamma_v} \left(100 \rho_l f_{ck} \frac{d_{dg}}{a_{v,0}} \right)^{1/3} = 0.782 \text{ MPa}$$

$$k_1 = \frac{0.5}{a_{cs,0}} \left(e_p + \frac{d}{3} \right) \frac{A_c}{b_w z} = 0.067 \leq 0.18 \frac{A_c}{b_w z} = 0.185$$

$$\sigma_{cp} \leq \frac{N_{Ed}}{A_c} = -6.286 \text{ MPa}$$

$$\tau_{Rdc,max} = 2.15 \tau_{Rdc,0} \left(\frac{a_{cs,0}}{d} \right)^{1/6} = 2.264 \text{ MPa} \leq 2.71 \tau_{Rdc,0} = 2.119 \text{ MPa}$$

with

$$a_{cs,0} = a - d = 3425 \text{ mm} \geq d = 575 \text{ mm}$$

$$a_{v,0} = \sqrt{\frac{a_{cs,0}}{4}} d = 702 \text{ mm} \not\geq d = 575 \text{ mm}$$

By substituting these values:

$$\tau_{Rd,min} = 0.689 \text{ MPa} \leq \tau_{Rd,c} = 0.782 + 0.067 \cdot 6.286 = 1.203 \text{ MPa} \leq \tau_{Rd,max} = 2.119 \text{ MPa}$$

The shear capacity is 1.20 MPa, which is lower than $\tau_{Ed} = 1.54$ MPa. Thus, shear reinforcement should be provided in this control section.

7. CONCLUSIONS

1. The final draft of the new version of Eurocode 2 provides a General Model formulation to calculate the shear resistance of members without shear reinforcement in the presence of axial forces (prestressing or external load) based on the Critical Shear Crack Theory, as a theoretical extension of the formulation of shear resistance without axial force, by including a single coefficient k_{vp} .
2. Another feature of the final draft of the new version of Eurocode 2 is the explicit incorporation of the influence of the shear slenderness in the formulation of the shear resistance for members without shear reinforcement.
3. In addition, a new partial safety factor γ_V has been introduced. This partial factor account for both the uncertainties of the variables involved in the shear resistance and the model uncertainties, allowing it to be adjusted to appropriate values by means of Annex A provisions of the final draft of the new version of Eurocode 2.
4. The General Model formulation is easy to use in practice for verification problems in presence of axial force both for tension and compression, although it requires an iterative process when the shear capacity is required.
5. Alternatively, the final draft of the new version of Eurocode 2 provides a Linear Approach formulation to calculate the shear resistance in presence of compressive axial forces that is derived by linearising the shear failure criterion based on the Critical Shear Crack Theory and is therefore consistent with the General Model.
6. This Linear Approach allows to calculate the shear capacity without iteration for the most practical common cases.
7. The agreement of the shear resistance predicted by both formulations (General Model and Linear Approach) to the experimental results are similar and have a lower dispersion than that provided by the current Eurocode 2.
8. The shear resistance formulation provided by the Linear Approach has a similar format to that of the current Eurocode 2, although it introduces the main variables on which the axial effects on the shear resistance depends: the shear slenderness, the eccentricity of the axial force and the shape of the section.

Notation

A_c	Cross-sectional area of concrete
A_{pi}	Cross-sectional area of longitudinal prestressed reinforcement i located in the tensile zone due to bending at a distance d_{pi} from the outermost compressed fibre of the cross-section.
A_{si}	Cross-sectional area of the longitudinal ordinary reinforcement i located in the tensile zone due to bending at a distance d_{si} from the outermost compressed fibre of the cross-section.
A_{sl}	Equivalent cross-sectional area of the reinforcement in the tensile zone due to bending.
D_{lower}	Smallest value of the upper sieve size in an aggregate for the coarsest fraction of aggregates in the concrete permitted by the specification of concrete
E_s	Modulus of elasticity of the flexural reinforcement
M_E	Acting bending moment
$M_{E,0}$	Acting bending moment without considering the effect of prestressing or external load that produces axial forces
N_E	Applied axial force
N_{Ed}	Design value of the applied axial force
V_E	Applied shear force
V_{Ed}	Design value of the applied shear force
$V_{R,c}$	Shear resistance of members without shear reinforcement
$V_{R,c,0}$	Shear resistance of members without shear reinforcement without considering the effect of prestressing or external load that produces axial force
$V_{R,c,max}$	Maximum shear resistance of members without shear reinforcement
$V_{R,c,min}$	Minimum shear resistance of members without shear reinforcement
$V_{Rd,c}$	Design value of the shear resistance of members without shear reinforcement
$V_{Rd,c,0}$	Design value of the shear resistance of members without shear reinforcement without considering the effect of prestressing or external load that produces axial forces
$V_{Rd,c,max}$	Design value of the maximum shear resistance of members without shear reinforcement
$V_{Rk,c}$	Characteristic value of the shear resistance of members without shear reinforcement
a_{cs}	Effective shear span with respect to the control section
$a_{cs,0}$	Effective shear span with respect to the control section without considering the effect of prestressing or external load that produces axial forces
a_v	Mechanical shear span
b_w	Minimum width of the cross-section between tension and compression chords
d	Effective depth of a cross-section
d_{dg}	Size parameter describing the crack and the failure zone roughness taking account of concrete type and its aggregate properties
d_{pi}	Distance from outermost compressed fibre of the cross-section to the prestressed reinforcement i

d_{si}	Distance from outermost compressed fibre of the cross-section to the ordinary reinforcement i
e_c	Distance from centroid of the cross section to the resultant of the normal compressive stresses.
e_p	Eccentricity of the axial forces related to the centroid of the cross-section, positive when the eccentricity is on the side of the flexural reinforcement in tension
f_c	Cylinder compressive strength of concrete
f_{ck}	Characteristic cylinder compressive strength of concrete
k_1	Coefficient to take into account the influence of axial forces on the shear stress resistance in the Linear approach
k_N	Coefficient to take into account the influence of axial forces on the shear resistance in the Linear approach
k_{vp}	Coefficient to take into account the influence of axial forces on the shear resistance in the General Model
z	Inner lever arm of internal forces
γ_{def}	Partial safety factor which covers the uncertainties related to the calculation of the strain in the longitudinal tensile reinforcement
γ_R	Partial safety factor which covers the uncertainties related to the shear failure criterion
γ_V	Partial safety factor for shear resistance without shear reinforcement
ϵ_v	Strain in the longitudinal tensile reinforcement
ϵ_{vd}	Design value of the strain in the longitudinal tensile reinforcement
ϵ_{v0}	Strain in the longitudinal tensile reinforcement without considering the effect of prestressing or external load that produces axial forces
ϵ_{vd0}	Design value of the strain in the longitudinal tensile reinforcement without considering the effect of prestressing or external load that produces axial forces
ρ_1	Reinforcement ratio for bonded longitudinal reinforcement in the tensile zone referred to the nominal concrete area $b_w d$
σ_{cp}	Compressive stress in the concrete from axial load or prestressing

References

- [1] CEN, "Eurocode 2: Design of Concrete Structures-Part 1-1: General rules and rules for buildings, EN 1992-1-1," Brussels (Belgium), 2004.
- [2] T. Zsutty, "Beam Shear Strength Prediction by Analysis of Existing Data," *Journal Proceedings*, vol. 65, no. 11, pp. 943–951, Nov. 1968, <https://doi.org/10.14359/7526>.
- [3] O. Hedman and A. Losberg, "Design of concrete structures with regard to shear forces," in *Bulletin d'Informacion n° 126 Shear and Torsion*, CEB, 1978, pp. 183–210.
- [4] K. H. Reineck, E. C. Bentz, B. Fitik, D. A. Kuchma, and O. Bayrak, "ACI-DAF-Stb Database of Shear Tests on Slender Reinforced Concrete Beams without Stirrups," *Structural Journal*, vol. 110, no. 5, pp. 867–876, Sep. 2013, <https://doi.org/10.14359/51685839>.
- [5] A. Muttoni, M. Fernández Ruiz, F. Cavagnis, and J. T. Simoes, "Background document to subsections 8.2.1 and 8.2.2 Shear in members without shear reinforcement," *Report EPFL-IBETON 16-06-R2*, pp. 1–17, 2021.
- [6] M. Herbrand and J. Hegger, "Experimentelle Untersuchungen zum Einfluss einer externen Vorspannung auf die Querkrafttragfähigkeit vorgespannter Durchlaufträger," *Bauingenieur*, vol. 88, no. 12, pp. 428–437, 2013.
- [7] Q. Yu, J. L. Le, M. H. Hubler, R. Wendner, G. Cusatis, and Z. P. Bažant, "Comparison of main models for size effect on shear strength of reinforced and prestressed concrete beams," *Structural Concrete*, vol. 17, no. 5, 2016, <https://doi.org/10.1002/suco.201500126>.
- [8] V. Adam, M. Claßen, and J. Hegger, "Versuche zum Querkrafttragverhalten bei gleichzeitiger Zugnormalkraft," *Beton- und Stahlbetonbau*, vol. 115, no. 10, pp. 821–831, Oct. 2020, <https://doi.org/10.1002/BEST.202000003>.
- [9] R. C. Fenwick and T. Paulay, "Mechanisms of Shear Resistance of Concrete Beams," *Journal of the Structural Division*, vol. 94, no. 10, pp. 2325–2350, Oct. 1968, <https://doi.org/10.1061/JSDEAG.0002092>.
- [10] H. Taylor, *Investigation of the forces carried across cracks in reinforced concrete beams in shear by interlock of aggregate*. London : Cement and Concrete Association, 1970.
- [11] T. Paulay and P. J. Loeber, "Shear Transfer By Aggregate Interlock," *Special Publication*, vol. 42, pp. 1–16, Jan. 1974, <https://doi.org/10.14359/17277>.
- [12] F. Cavagnis, M. Fernández Ruiz, and A. Muttoni, "A mechanical model for failures in shear of members without transverse reinforcement based on development of a critical shear crack," *Eng Struct*, vol. 157, pp. 300–315, Feb. 2018, <https://doi.org/10.1016/J.ENGSTRUCT.2017.12.004>.
- [13] P. Huber, T. Huber, and J. Kollegger, "Investigation of the shear behavior of RC beams on the basis of measured crack kinematics," *Eng Struct*, vol. 113, pp. 41–58, Apr. 2016, <https://doi.org/10.1016/J.ENGSTRUCT.2016.01.025>.
- [14] A. Monserrat López, M. Fernández Ruiz, and P. F. Miguel Sosa, "The influence of transverse reinforcement and yielding of flexural reinforcement on the shear-transfer actions of RC members," *Eng Struct*, vol. 234, May 2021, <https://doi.org/10.1016/J.ENGSTRUCT.2021.111949>.
- [15] G. N. J. Kani, "The Riddle of Shear Failure and its Solution," *Journal Proceedings*, vol. 61, no. 4, pp. 441–468, Apr. 1964, <https://doi.org/10.14359/7791>.
- [16] Y. D. Hamadi and P. E. Regan, "Behaviour in shear of beams with flexural cracks," *Magazine of Concrete Research*, vol. 32, no. 111, pp. 67–78, Jun. 1980, <https://doi.org/10.1680/MACR.1980.32.111.67>.
- [17] K. H. Reineck, "Ultimate shear force of structural concrete members Without Transverse Reinforcement Derived From a Mechanical Model (SP-885)," *Structural Journal*, vol. 88, no. 5, pp. 592–602, Sep. 1991, <https://doi.org/10.14359/2784>.
- [18] Y. Yang, "Shear behaviour of reinforced concrete members without shear reinforcement: A new look at an old problem," 2014, <https://doi.org/10.4233/UUID:AC776CF0-4412-4079-968F-9EACB67E8846>.
- [19] P. D. Zararis and G. Ch. Papadakis, "Diagonal Shear Failure and Size Effect in RC Beams without Web Reinforcement," *Journal of Structural Engineering*, vol. 127, no. 7, pp. 733–742, Jul. 2001, [https://doi.org/10.1061/\(ASCE\)0733-9445\(2001\)127:7\(733\)](https://doi.org/10.1061/(ASCE)0733-9445(2001)127:7(733)).
- [20] J. Hegger, A. Sherif, and S. Görtz, "Investigation of Pre- and Postcracking Shear Behavior of Prestressed Concrete Beams Using Innovative Measuring Techniques," *ACI Struct J*, vol. 101, no. 2, pp. 183–192, Mar. 2004, <https://doi.org/10.14359/13015>.
- [21] H. G. Park, K. K. Choi, and J. K. Wight, "Strain-Based Shear Strength Model for Slender Beams without Web Reinforcement," *ACI Struct J*, vol. 103, no. 6, pp. 783–793, Nov. 2006, <https://doi.org/10.14359/18228>.
- [22] A. Mari, J. Bairán, A. Cladera, E. Oller, and C. Ribas, "Shear-flexural strength mechanical model for the design and assessment of reinforced concrete beams," *Structure and Infrastructure Engineering*, vol. 11, no. 11, pp. 1399–1419, Nov. 2015, <https://doi.org/10.1080/15732479.2014.964735>.
- [23] A. Cladera, A. Mari, C. Ribas, J. Bairán, and E. Oller, "Predicting the shear-flexural strength of slender reinforced concrete T and I shaped beams," *Eng Struct*, vol. 101, pp. 386–398, Oct. 2015, <https://doi.org/10.1016/J.ENGSTRUCT.2015.07.025>.
- [24] A. Mari, J. M. Bairán, A. Cladera, and E. Oller, "Shear Design and Assessment of Reinforced and Prestressed Concrete Beams Based on a Mechanical Model," *Journal of Structural Engineering*, vol. 142, no. 10, p. 04016064, Oct. 2016, [https://doi.org/10.1061/\(ASCE\)ST.1943-541X.0001539](https://doi.org/10.1061/(ASCE)ST.1943-541X.0001539).
- [25] A. Muttoni and M. F. Ruiz, "Shear Strength of Members without Transverse Reinforcement as Function of Critical Shear Crack Width," *ACI Struct J*, vol. 105, no. 2, pp. 163–172, Mar. 2008, <https://doi.org/10.14359/19731>.
- [26] A. Muttoni, "Punching Shear Strength of Reinforced Concrete Slabs without Transverse Reinforcement," *ACI Struct J*, vol. 105, no. 4, pp. 440–450, Jul. 2008, <https://doi.org/10.14359/19858>.
- [27] F. Cavagnis, J. T. Simões, M. F. Ruiz, and A. Muttoni, "Shear Strength of Members without Transverse Reinforcement Based on Development of Critical Shear Crack," *ACI Struct J*, vol. 117, no. 1, pp. 103–118, Jan. 2020, <https://doi.org/10.14359/51718012>.
- [28] J. R. Carmona and G. Ruiz, "Bond and size effects on the shear capacity of RC beams without stirrups," *Eng Struct*, vol. 66, pp. 45–56, May 2014, <https://doi.org/10.1016/J.ENGSTRUCT.2014.01.054>.

- [29] M. Classen, "Shear Crack Propagation Theory (SCPT) – The mechanical solution to the riddle of shear in RC members without shear reinforcement," *Eng Struct*, vol. 210, p. 110207, May 2020, <https://doi.org/10.1016/J.ENGSTRUCT.2020.110207>.
- [30] M. Schmidt, P. Schmidt, S. Wanka, and M. Classen, "Shear Response of Members without Shear Reinforcement—Experiments and Analysis Using Shear Crack Propagation Theory (SCPT)," *Applied Sciences* 2021, Vol. 11, Page 3078, vol. 11, no. 7, p. 3078, Mar. 2021, <https://doi.org/10.3390/APP11073078>.
- [31] F. J. Vecchio and M. P. Collins, "THE MODIFIED COMPRESSION-FIELD THEORY FOR REINFORCED CONCRETE ELEMENTS SUBJECTED TO SHEAR.," *Journal of the American Concrete Institute*, vol. 83, no. 2, pp. 219–231, Mar. 1986, <https://doi.org/10.14359/10416>.
- [32] M. P. Collins, D. Mitchell, P. Adebare, and F. J. Vecchio, "A General Shear Design Method," *ACI Struct J*, vol. 93, no. 1, pp. 36–45, Jan. 1996, <https://doi.org/10.14359/9838>.
- [33] CEN/TC250, "Eurocode 2: Design of concrete structures — Part 1-1:General rules — rules for buildings, bridges and civil engineering structures, FprEN 1992-1-1:2023," Brussels, Belgium, 2023.
- [34] M. Fernández Ruiz, A. Muttoni, and J. Sagaseta, "Shear strength of concrete members without transverse reinforcement: A mechanical approach to consistently account for size and strain effects," *Eng Struct*, vol. 99, 2015, <https://doi.org/10.1016/j.engstruct.2015.05.007>.
- [35] A. Muttoni, "Schubfestigkeit und Durchstanzen von Platten ohne Querkraftbewehrung," *Beton-und-Stahlbetonbau*, vol. 98, 2003.
- [36] "EN 206:2013 Concrete - Specification, performance, production and conformity," Brussels, Belgium, 2013.
- [37] R. Vaz Rodrigues, A. Muttoni, and M. F. Ruiz, "Influence of Shear on Rotation Capacity of Reinforced Concrete Members Without Shear Reinforcement," *ACI Struct J*, vol. 107, no. 5, pp. 516–525, Sep. 2010, <https://doi.org/10.14359/51663902>.
- [38] A. Monserrat López, P. F. Miguel Sosa, J. L. Bonet Senach, and M. Á. Fernández Prada, "Experimental study of shear strength in continuous reinforced concrete beams with and without shear reinforcement," *Eng Struct*, vol. 220, Oct. 2020, <https://doi.org/10.1016/J.ENGSTRUCT.2020.110967>.
- [39] K.-H. Reineck and D. Dunkelberg, "ACI-DAFStb databases 2015 with shear tests for evaluating relationships for the shear design of structural concrete members without and with stirrups".
- [40] Karl-Heinz Reineck; Birol Fitik, Beuth Verlag, and DAFStb, "ACI-DAFStb databases 2020 with shear tests on structural concrete members without stirrups - Volume 1: Part 1 to Part 2.5 and Volume 2: Part 2.6 to Part 7".
- [41] K. de Wilder, G. de Roeck, and L. Vandewalle, "Experimental analysis of the shear behaviour of prestressed and reinforced concrete beams," *European Journal of Environmental and Civil Engineering*, vol. 22, no. 3, pp. 288–314, Mar. 2018, <https://doi.org/10.1080/19648189.2016.1194321>.
- [42] H. B. Joergensen and J. Fisker, "Experimental Study on the Shear Behaviour of Post-Tensioned Beams without Shear Reinforcement," in *Concrete Structures: new trends for a eco-efficiency and performance. Proceedings of the fib symposium 2021*, 2021.
- [43] A. Muttoni, "Background document to 4.3.3 and Annex A. Partial safety factors for materials (prEN 1992-1-1:2020(D7))," *Report EPFL-IBETON 16-06-R11*, pp. 1–22, May 2021.
- (*) *This document is available through the National members at CEN TC250/SC2 Eurocode 2*

ANNEX I

Derivation of $V_{Rc,max}$ and the upper bound of coefficient k_N in the Linear Approach

Expression for $V_{Rc,max}$

The maximum shear resistance can be expressed by Formula (12) for the shear resistance of the general model by taking the minimum values for k_{vp} and a_{cs} ($k_{vp}=0.1$ and $a_{cs}=d$)

$$V_{Rc,max} = 0.6 \left(100 \rho_l f_c \frac{d_{dg}}{0.1 \frac{d}{2}} \right)^{1/3} b_w d \quad (39)$$

On the other hand, the shear resistance obtained from the General Model without considering axial force is given by Formula (12) by taking $k_{vp}=1$

$$V_{Rc,0} = 0.6 \left(100 \rho_l f_{ck} \frac{d_{dg}}{\sqrt{\frac{a_{cs,0} d}{4}}} \right)^{1/3} b_w d \quad (40)$$

Dividing (39) by (40) it follows

$$\frac{V_{Rc,max}}{V_{Rc,0}} = 2.15 \left(\frac{a_{cs,0}}{d} \right)^{1/6} \leq 2.71 \quad (41)$$

which has an upper limit of 2.71 because $\frac{a_{cs,0}}{d} \leq 4$

Upper bound of k_N

The coefficient

$$k_N = 0.54 \frac{e_p + \frac{d}{3}}{a_{cs,0}}$$

is upper-bounded to 0.18 because the condition $a_{cs} \geq d$ entails that

$$\frac{e_p + \frac{d}{3}}{a_{cs,0}} \leq \frac{1}{3}$$

This condition can be easily understood by means of Figure 18.

As can be seen in the graph on the left of Figure 18, for a given value of $a_{cs,0}$, for different compressive axial forces, the corresponding shear resistances are obtained by intersection of the linearized failure criterion (thinner solid line) with the load-deformation relationships from Formula (19) (thicker solid lines), which can be rewritten in function of a_{cs} as

$$\varepsilon_v = \frac{V_E a_{cs} + N_E \frac{d}{3}}{E_s A_{sl} z} \quad (42)$$

When the compressive axial force increases, a_{cs} decreases and it can become equal to the effective depth for a certain value of the compressive axial force N^* . For $N_E < N_E^*$, the load-deformation relationship changes and becomes defined by the condition $a_{cs} = d$, which is expressed by

$$\varepsilon_v = \frac{V_E d + N_E \frac{d}{3}}{E_s A_{sl} z} \quad (43)$$

and depicted with the thicker dashed lines in Figure 18, which have different slope than the thicker solid lines.

The graph on the right in Figure 18 shows the relationship between the shear resistance and the axial force, which is defined by two segments: A-B (from 0 to $-N_E^*$) given by Formula (42) and B-C (from $-N_E^*$ to $-3 V_{Rc,max}$) given by Formula (43). This bilinear law is simplified by the thicker solid line (A-C) which slope is

$$k_{N,max} = \frac{V_{Rc,max} - V_{Rc,0}}{3 V_{Rc,max}} \quad (44)$$

The minimum value of $k_{N,max}$ is equal to 0.18 since the minimum value of $\frac{V_{Rc,max}}{V_{Rc,0}}$ is 2.154, according to Formula (41) for $a_{cs,0}=d$.

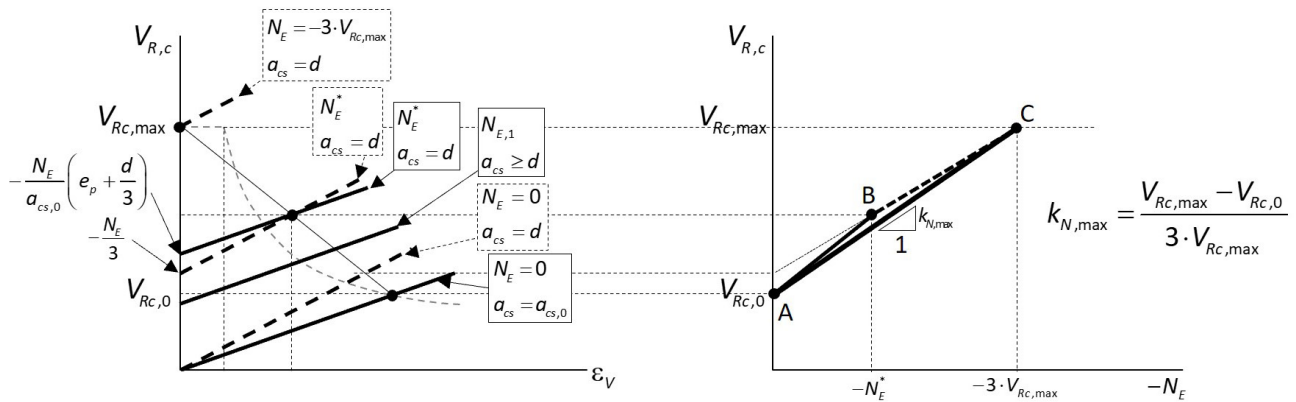


Figure 18.- Upper bound of coefficient k_N .

ANNEX 2
Selected database

Notation	Concrete cross section			Reinforcement		Prestressing						Concrete		LOAD	
	Type	A _c	b _w	d _s	A _s	d _p	A _p	f _{pp}	P	e _p	σ _p	f _c	D _{lower}	a	V _{test}
		mm ²	mm	mm	mm ²	mm	mm ²	MPa	kN	mm	MPa	MPa	mm	mm	kN
Arthur_1965_002_A2	P	21935	51	0	0	201	77	1459	-91.2	47.4	924	31.44	9.5	914	25.4
Arthur_1965_027_B1	P	25806	51	0	0	272	142	1334	-150.3	64.6	824	45.74	9.5	914	45.9
Arthur_1965_028_B2	P	25806	51	0	0	272	142	1334	-145.9	64.6	800	42.30	9.5	914	49.0
Arthur_1965_029_B3	P	25806	51	0	0	272	142	1334	-143.2	64.6	785	46.88	9.5	686	66.4
Arthur_1965_031_B5	P	25806	51	0	0	272	142	1334	-160.1	64.6	878	51.45	9.5	686	66.4
Arthur_1965_034_B8	P	25806	51	0	0	272	142	1334	-145.9	64.6	800	51.45	9.5	686	64.2
Arthur_1965_035_B9	P	25806	51	0	0	272	142	1334	-143.2	64.6	785	42.30	9.5	914	38.8
Arthur_1965_054_E1	P	30968	76	0	0	272	142	1334	-142.3	64.6	780	45.16	9.5	762	58.1
Arthur_1965_055_E2	P	30968	76	0	0	272	142	1334	-145.9	64.6	800	51.45	9.5	762	67.4
Elzanaty_1985_001_CW1	P	54193	51	432	214	369	568	1749	-606.7	140.3	1069	76.55	12.7	1071	137.7
Elzanaty_1985_002_CW3	P	54193	51	432	214	369	568	1749	-596.5	140.3	1051	76.55	12.7	1847	117.4
Elzanaty_1985_003_CW2	P	54193	51	432	214	369	568	1749	-603.1	140.3	1062	76.55	12.7	1385	124.5
Elzanaty_1985_005_CW5	P	54193	51	432	1164	369	568	1749	-605.8	140.3	1067	77.93	12.7	1385	124.1
Elzanaty_1985_006_CW7	P	54193	51	432	214	369	395	1799	-443.9	140.3	1124	77.59	12.7	1385	105.9
Elzanaty_1985_007_CW6	P	54193	51	432	214	369	568	1749	-455.0	140.3	801	77.93	12.7	1385	112.1
Elzanaty_1985_008_CW9	P	54193	51	432	214	369	568	1749	-447.0	140.3	787	61.03	12.7	1385	101.0
Elzanaty_1985_009_CW8	P	54193	51	432	214	369	568	1749	-451.5	140.3	795	41.38	12.7	1385	89.8
Elzanaty_1985_010_C11	P	58710	76	330	214	242	568	1749	-604.9	102.1	1066	76.55	12.7	1845	77.8
Elzanaty_1985_013_C14	P	58710	76	0	0	242	568	1749	-610.3	102.1	1075	78.62	12.7	1372	108.5
Elzanaty_1985_014_C15	P	58710	76	330	1164	242	568	1749	-604.5	102.1	1065	77.93	12.7	1372	119.7
Elzanaty_1985_015_C17	P	58710	76	330	214	242	395	1799	-443.0	102.1	1122	77.59	12.7	1372	81.4
Elzanaty_1985_016_C16	P	58710	76	330	214	242	568	1749	-455.0	102.1	801	77.93	12.7	1372	89.0
Elzanaty_1985_017_C19	P	58710	76	330	214	242	568	1749	-446.6	102.1	787	61.03	12.7	1372	87.2
Evans_1963_002_S2	R	30968	102	0	0	251	514	621	-58.3	99.1	113	38.83	6.4	610	106.1
Evans_1963_019_S19	P	23226	51	0	0	257	506	621	-91.6	104.1	181	30.00	6.4	940	48.1
Evans_1963_025_S25	P	23613	53	0	0	257	388	621	-92.5	104.1	238	36.90	6.4	940	53.5
Evans_1963_027_S27	P	23226	51	0	0	257	508	621	-86.3	104.1	170	35.38	6.4	711	66.7
Evans_1963_029_S29	P	23226	51	0	0	257	388	621	-81.8	104.1	211	28.55	6.4	711	64.9
Evans_1963_043_S43	P	11177	56	0	0	122	506	621	-52.0	46.0	103	48.34	6.4	508	29.0
Evans_1963_046_S46	R	12000	79	0	0	109	77	1241	-52.5	33.0	680	33.03	6.4	508	17.7
Kar_1968_001_A1	R	32258	127	0	0	178	101	1386	-80.1	50.8	790	35.93	19.1	889	27.1
Kar_1968_003_A4	R	32258	127	0	0	178	194	1476	-82.7	50.8	427	28.83	19.1	622	55.6
Kar_1968_004_A5	R	32258	127	0	0	178	194	1476	-104.8	50.8	541	34.48	19.1	533	69.3
Kar_1968_005_A6	R	32258	127	0	0	178	155	1476	-48.9	50.8	316	28.03	19.1	711	38.9
Kar_1968_006_A7	R	32258	127	0	0	178	194	1476	-82.6	50.8	427	30.21	19.1	686	45.8
Kar_1968_007_A8	R	32258	127	0	0	178	194	1476	-125.9	50.8	650	34.14	19.1	737	43.8
Kar_1968_008_A9	R	32258	127	0	0	178	194	1476	-145.8	50.8	753	33.79	19.1	686	54.6
Kar_1968_009_A10	R	32258	127	0	0	178	194	1476	-145.8	50.8	753	31.79	19.1	889	40.8
Kar_1968_010_A12	R	32258	127	0	0	178	155	1476	-102.7	50.8	664	34.90	19.1	711	44.3
Kar_1968_011_B3	R	20645	102	0	0	152	155	1476	-48.9	50.8	316	29.17	19.1	533	28.8
Kar_1968_012_B4	R	20645	102	0	0	152	155	1476	-48.3	50.8	312	32.00	19.1	610	29.3
Kar_1968_013_B5	R	20645	102	0	0	152	155	1476	-41.2	50.8	266	28.03	19.1	686	25.8
Kar_1968_014_B6	R	20645	102	0	0	152	194	1476	-59.6	50.8	308	30.21	19.1	711	27.3
Kar_1968_015_B7	R	20645	102	0	0	152	155	1476	-65.5	50.8	423	33.17	19.1	533	38.6
Kar_1968_016_B9	R	20645	102	0	0	152	155	1476	-65.5	50.8	423	33.31	19.1	762	26.3
Kar_1968_017_B10	R	20645	102	0	0	152	155	1476	-82.7	50.8	534	35.45	19.1	762	33.7
Kar_1968_018_I-10	P	35806	76	0	0	229	194	1476	-104.5	76.2	540	35.34	19.1	756	69.3

Notation	Concrete cross section			Reinforcement		Prestressing						Concrete		LOAD	
	Type	A _c	b _w	d _s	A _s	d _p	A _p	f _{py}	P	e _p	σ _p	f _c	D _{lower}	a	V _{test}
		mm ²	mm	mm	mm ²	mm	mm ²	MPa	kN	mm	MPa	MPa	mm	mm	kN
Kar_1968_019_I-11	P	35806	76	0	0	229	194	1476	-126.2	76.2	652	38.62	19.1	756	71.7
Kar_1968_020_I-14	P	35806	76	0	0	229	194	1476	-145.5	76.2	752	34.48	19.1	756	69.8
Kar_1968_021_I-15	P	35806	76	0	0	216	194	1476	-83.2	63.5	430	30.41	19.1	540	66.5
Kar_1968_024_I-19	P	35806	76	0	0	229	194	1476	-146.3	76.2	756	33.79	19.1	756	64.4
Kar_1968_025_I-20	P	35806	76	0	0	216	194	1476	-106.8	63.5	552	35.17	19.1	610	62.0
Kar_1968_026_I-21	P	35806	76	0	0	229	194	1476	-127.7	76.2	660	35.17	19.1	864	49.7
Kar_1968_029_D3	P	28064	51	0	0	216	194	1476	-123.6	63.5	638	30.76	19.1	540	74.6
Kar_1968_030_D4	P	28064	51	0	0	216	194	1476	-123.6	63.5	638	34.83	19.1	864	47.1
Kar_1968_031_D5	P	28064	51	0	0	216	155	1476	-117.0	63.5	756	30.76	19.1	756	44.7
Kar_1968_033_D7	P	28064	51	0	0	216	194	1476	-145.5	63.5	752	34.48	19.1	864	47.6
Kar_1968_034_D8	P	28064	51	0	0	229	194	1476	-142.8	76.2	738	34.83	19.1	1080	42.1
Kar_1968_035_D9	P	27016	51	0	0	229	194	1476	-106.5	76.2	550	34.83	19.1	1364	29.2
Mahgoub_1975_002_A2	P	33438	75	0	0	260	192	1560	-225.7	42.9	838	38.58	10.0	930	78.2
Mahgoub_1975_014_A7-1	P	33438	75	0	0	260	192	1560	-251.5	42.9	933	36.24	10.0	795	87.8
Mahgoub_1975_015_A7-2	P	33438	75	0	0	260	192	1560	-251.5	42.9	933	36.24	10.0	770	88.2
Mahgoub_1975_017_A8-2	P	33438	75	0	0	260	192	1560	-248.4	42.9	922	31.05	10.0	770	75.9
Mahgoub_1975_022_A11-2	P	33438	75	0	0	260	192	1560	-179.9	42.9	668	29.06	10.0	905	64.9
Mahgoub_1975_025_B2	P	29250	50	0	0	260	192	1560	-206.8	42.9	768	35.88	10.0	1060	49.5
Mahgoub_1975_039_B11-2	P	29250	50	0	0	260	192	1560	-229.9	42.9	853	38.01	10.0	705	62.6
Mahgoub_1975_012_C12	P	38438	75	0	0	260	192	1560	-200.3	42.9	743	24.87	10.0	1060	53.6
Mahgoub_1975_012_C17	P	38438	75	0	0	225	245	1570	-98.0	75.0	399	26.43	10.0	1325	41.5
Mahgoub_1975_012_C19	P	38438	75	0	0	260	245	1570	-94.2	75.0	384	36.24	10.0	1180	55.3
Mahgoub_1975_015_D5	P	35250	50	0	0	260	192	1560	-187.2	42.9	695	31.97	10.0	1060	44.6
Mahgoub_1975_015_D6	P	35250	50	0	0	260	192	1560	-188.6	42.9	700	38.44	10.0	795	52.1
Mahgoub_1975_015_D8	P	35250	50	0	0	260	245	1570	-95.9	75.0	391	32.54	10.0	1325	27.3
Mahgoub_1975_015_D9	P	35250	50	0	0	260	245	1570	-95.2	75.0	388	36.24	10.0	1180	36.8
Mahgoub_1975_016_E1-1	P	43438	75	0	0	260	192	1560	-190.3	42.9	706	45.54	10.0	795	77.0
Mahgoub_1975_016_E1-2	P	43438	75	0	0	260	192	1560	-190.3	42.9	706	45.54	10.0	795	72.9
Mahgoub_1975_019_E4	P	43438	75	0	0	260	192	1560	-225.0	42.9	835	35.53	10.0	1060	58.8
Mahgoub_1975_019_E5-1	P	43438	75	0	0	260	192	1560	-245.9	42.9	913	37.73	10.0	1060	69.9
Mahgoub_1975_020_E6	P	43438	75	0	0	260	192	1560	-274.5	42.9	1019	35.53	10.0	795	93.4
Mahgoub_1975_021_F2	P	41250	50	0	0	260	192	1560	-193.5	42.9	718	35.03	10.0	1060	41.9
Olesen_1967_003_B1434	P	35039	79	0	0	262	117	1572	-92.6	109.2	793	19.76	9.5	914	41.3
Olesen_1967_004_B1441	P	34639	76	0	0	254	156	1572	-122.7	101.6	786	20.31	9.5	914	44.5
Sozen_1959_001_A1143	R	46452	152	0	0	209	284	1434	-227.0	56.9	800	42.90	38.1	1321	54.8
Sozen_1959_002_A1151	R	46452	152	0	0	214	161	1503	-126.3	62.0	786	20.00	38.1	1321	31.6
Sozen_1959_003_A1153	R	46452	152	0	0	204	241	1503	-206.6	51.3	858	30.07	38.1	1321	42.2
Sozen_1959_005_A1223	R	47226	155	0	0	237	161	1503	-126.4	84.6	787	38.97	38.1	914	60.8
Sozen_1959_006_A1231	R	46452	152	0	0	219	201	1503	-157.7	67.1	786	40.00	9.5	914	60.1
Sozen_1959_007_A1234	R	46452	152	0	0	208	284	1434	-215.3	55.9	758	55.10	38.1	914	74.4
Sozen_1959_008_A1236	R	47226	155	0	0	233	150	1421	-117.5	81.0	785	23.72	38.1	914	48.9
Sozen_1959_009_A1242	R	46452	152	0	0	211	284	1434	-202.4	58.4	713	43.17	38.1	914	70.0
Sozen_1959_010_A1246	R	46452	152	0	0	208	227	1434	-205.7	55.9	906	32.14	38.1	914	63.1
Sozen_1959_012_A1253	R	46452	152	0	0	218	201	1503	-149.8	66.0	747	23.45	9.5	914	54.8
Sozen_1959_013_A1256	R	46452	152	0	0	218	234	1472	-194.0	65.8	831	26.14	9.5	914	59.7
Sozen_1959_018_A1439	R	46452	152	0	0	212	141	1503	-113.5	59.7	807	23.10	38.1	610	65.2
Sozen_1959_019_A1444	R	46452	152	0	0	216	161	1503	-130.7	63.5	814	23.10	38.1	610	72.0
Sozen_1959_020_A1455	R	46452	152	0	0	217	201	1503	-161.8	64.3	807	22.90	38.1	610	81.5
Sozen_1959_022_A2129	R	46452	152	0	0	215	101	1503	-42.4	62.2	421	23.10	38.1	1321	18.6
Sozen_1959_023_A2139	R	46452	152	0	0	227	141	1503	-57.1	74.9	406	21.59	38.1	1321	24.9

Notation	Concrete cross section			Reinforcement		Prestressing						Concrete		LOAD	
	Type	A _c	b _w	d _s	A _s	d _p	A _p	f _{py}	P	e _p	σ _p	f _c	D _{lower}	a	V _{test}
		mm ²	mm	mm	mm ²	mm	mm ²	MPa	kN	mm	MPa	MPa	mm	mm	kN
Sozen_1959_024_A2151	R	46452	152	0	0	206	301	1503	-122.8	53.8	407	38.83	38.1	1321	38.9
Sozen_1959_025_A2220	R	46452	152	0	0	215	114	1434	-47.9	62.2	422	36.90	38.1	914	33.2
Sozen_1959_026_A2224	R	46452	152	0	0	224	95	1434	-38.5	71.1	406	23.93	38.1	914	32.2
Sozen_1959_028_A2227	R	46452	152	0	0	213	114	1434	-47.0	60.5	414	26.55	38.1	914	31.8
Sozen_1959_029_A2228	R	47226	155	0	0	222	114	1434	-38.6	69.9	340	24.00	38.1	914	29.7
Sozen_1959_030_A2231	R	46452	152	0	0	205	114	1434	-70.0	52.3	616	24.34	38.1	914	34.2
Sozen_1959_031_A2234	R	46452	152	0	0	212	151	1434	-61.4	59.5	407	28.62	38.1	914	31.6
Sozen_1959_032_A2236	R	46452	152	0	0	212	114	1434	-68.9	59.7	607	19.93	38.1	914	33.7
Sozen_1959_033_A2239	R	46452	152	0	0	224	114	1434	-28.3	71.1	249	17.79	38.1	914	24.8
Sozen_1959_034_A2240	R	46452	152	0	0	208	246	1434	-122.0	55.9	496	39.93	38.1	914	59.7
Sozen_1959_035_A2249	R	46452	152	0	0	208	246	1434	-96.3	55.9	392	32.83	38.1	914	52.0
Sozen_1959_036_A3222	R	46452	152	0	0	238	114	1434	-18.8	85.9	165	29.59	38.1	914	32.2
Sozen_1959_037_A3227	R	46452	152	0	0	233	114	1434	-7.8	80.3	69	19.31	38.1	914	28.8
Sozen_1959_038_A3237	R	46452	152	0	0	208	246	1434	-8.5	55.9	34	42.21	38.1	914	40.0
Sozen_1959_039_A3249	R	46452	152	0	0	208	246	1434	-57.6	55.9	234	32.83	38.1	914	47.5
Sozen_1959_041_B1120	P	33952	75	0	0	259	115	1628	-97.8	106.9	851	31.21	9.5	1321	31.0
Sozen_1959_042_B1129	P	34064	75	0	0	254	154	1372	-131.8	101.6	855	28.90	9.5	1321	38.7
Sozen_1959_043_B1140	P	34064	75	0	0	254	232	1372	-186.8	101.6	807	31.03	9.5	1321	46.6
Sozen_1959_045_B1210	P	34692	78	0	0	282	78	1472	-66.2	129.8	848	38.62	9.5	914	35.8
Sozen_1959_049_B1226	P	35095	77	0	0	256	150	1462	-114.0	103.1	758	30.76	9.5	914	52.6
Sozen_1959_050_B1229	P	34452	76	0	0	248	154	1628	-128.8	95.5	839	28.83	9.5	914	56.6
Sozen_1959_051_B1234	P	35483	78	0	0	259	225	1462	-166.7	106.2	740	33.28	9.5	914	64.6
Sozen_1959_052_B1235	P	35894	78	0	0	254	154	1628	-128.1	101.3	834	22.14	9.5	914	51.5
Sozen_1959_053_B1250	P	34292	75	0	0	259	193	1372	-154.3	106.7	800	20.34	9.5	914	51.6
Sozen_1959_054_B1261	P	34452	76	0	0	251	232	1372	-182.8	99.1	789	20.55	9.5	914	53.8
Sozen_1959_056_B1316	P	34452	76	0	0	264	115	1372	-99.9	111.3	865	38.21	9.5	711	59.6
Sozen_1959_057_B1326	P	34212	75	0	0	255	154	1372	-131.8	102.4	855	31.72	9.5	711	65.0
Sozen_1959_058_B1341	P	34052	74	0	0	255	232	1372	-189.2	102.6	817	29.79	9.5	711	71.2
Sozen_1959_059_B2126	P	34292	75	0	0	259	154	1628	-66.0	106.9	430	30.83	9.5	1321	27.9
Sozen_1959_060_B2209	P	34292	75	0	0	281	77	1628	-33.6	128.8	438	43.59	9.5	914	32.1
Sozen_1959_061_B2223	P	34639	76	0	0	255	154	1628	-58.5	102.4	381	35.31	9.5	914	42.1
Sozen_1959_062_B2230	P	35453	79	0	0	258	113	1462	-44.1	105.4	391	19.10	9.5	914	34.1
Sozen_1959_063_B2241	P	36027	80	0	0	255	150	1462	-53.1	102.1	353	18.69	9.5	914	39.5
Sozen_1959_065_B2268	P	34452	76	0	0	251	232	1372	-94.2	99.1	407	18.41	9.5	914	42.7
PWRI_1995_001_H3-35-30	R	85000	200	0	0	350	837	1799	-136.4	45.8	122	89.11	20.0	1050	247.0
PWRI_1995_002_H3-35-60	R	85000	200	0	0	350	837	1799	-272.8	45.8	244	83.60	20.0	1050	285.3
PWRI_1995_003_H3-35-90	R	85000	200	0	0	350	837	1799	-409.2	45.8	367	68.12	20.0	1050	296.9
PWRI_1995_004_H3-55-30	R	125000	200	0	0	550	837	1799	-193.5	79.2	173	81.32	20.0	1650	231.4
PWRI_1995_005_H3-55-60	R	125000	200	0	0	550	837	1799	-387.1	79.2	347	75.81	20.0	1650	364.5
PWRI_1995_006_H3-75-30	R	165000	200	0	0	750	837	1799	-251.7	112.5	226	85.69	20.0	2250	351.3
PWRI_1995_007_H3-75-60	R	165000	200	0	0	750	837	1799	-503.4	112.5	451	84.65	20.0	2250	442.2
PWRI_1995_008_H3-95-60	R	220000	200	0	0	1025	2093	1778	-728.1	131.9	307	69.16	20.0	2850	595.8
PWRI_1995_010_L3-35-30	R	85000	200	0	0	350	837	1778	-136.4	45.8	122	48.17	20.0	1050	195.4
PWRI_1995_011_L3-35-60	R	85000	200	0	0	350	837	1778	-272.8	45.8	244	39.33	20.0	1050	203.3
Funakoshi_1981_006_10	P	23800	70	200	121	160	400	1226	-294.4	47.3	736	83.22	15.0	416	148.4
Funakoshi_1981_008_14	P	23800	70	200	121	160	400	1226	-259.0	47.3	648	56.53	15.0	417	120.5
Funakoshi_1981_009_19	P	23800	70	200	121	160	400	1226	-259.0	47.3	648	56.05	15.0	504	96.9
Funakoshi_1982_006_38	P	23800	70	200	121	160	390	1236	-211.9	47.3	543	41.52	15.0	414	96.9
Funakoshi_1982_007_39	P	23800	70	200	121	160	390	1236	-211.9	47.3	543	40.38	15.0	499	81.2
Funakoshi_1982_008_40	P	23800	70	200	121	160	390	1236	-211.9	47.3	543	40.38	15.0	583	68.9

Notation	Concrete cross section			Reinforcement		Prestressing						Concrete		LOAD	
	Type	A_c	b_w	d_s	A_s	d_p	A_p	f_{py}	P	e_p	σ_p	f_c	D_{lower}	a	V_{test}
		mm ²	mm	mm	mm ²	mm	mm ²	MPa	kN	mm	MPa	MPa	mm	mm	kN
Sato_1987_001_3-4	P	90000	150	375	860	330	804	1010	-294.3	180.0	366	40.47	15.0	1080	163.7
Sato_1987_004_3-7	P	90000	150	375	860	330	804	1010	-490.5	180.0	610	41.04	15.0	1080	168.6
Sato_1987_007_3-11	R	67500	150	375	860	330	804	1010	-196.2	105.0	244	40.47	15.0	990	172.2
Sato_1987_009_3-13	R	67500	150	0	0	330	804	1010	-392.4	105.0	488	36.39	15.0	1080	159.3
Sato_1987_011_4-6	R	60000	150	375	142	330	804	1010	-294.3	130.0	366	38.86	15.0	1080	171.0
Sato_1987_012_4-7	R	60000	150	0	0	330	804	1010	-294.3	130.0	366	42.18	15.0	1080	168.0
Sato_1987_013_4-10	R	60000	150	375	860	330	804	1010	-98.1	130.0	122	39.62	15.0	1080	100.3
Sato_1987_014_4-11	R	60000	150	375	860	330	804	1010	-196.2	130.0	244	41.04	15.0	1080	150.4
Sato_1987_015_4-12	R	60000	150	375	860	330	804	1010	-294.3	130.0	366	44.18	15.0	1080	163.1
Ito_1996_001_NC-50	R	45000	150	275	143	250	227	1197	-33.1	100.0	146	54.06	15.0	650	117.8
Ito_1996_002_NC-100	R	45000	150	275	143	250	227	1197	-111.6	100.0	491	54.06	15.0	650	119.3
Ito_1997_001_M-B 100	P	62000	100	400	253	270	454	1158	-213.7	111.6	471	40.19	20.0	1200	124.8
Saqan_2009_003_V-4-2.37	R	265187	373	660	1529	610	395	1676	-480.4	254.0	1217	53.45	19.1	2019	373.1
Saqan_2009_005_V-7-1.84	R	257419	362	664	1187	610	691	1676	-490.6	254.0	710	53.10	19.1	2019	490.8
Saqan_2009_006_V-7-2.37	R	252903	356	660	1529	610	691	1676	-490.6	254.0	710	53.10	19.1	2019	433.7
Saqan_2009_007_V-10-0	R	257419	362	0	0	610	987	1676	-494.2	254.0	501	51.72	19.1	2019	412.1
Saqan_2009_008_V-10-1.51	R	257419	362	663	974	610	987	1676	-494.2	254.0	501	51.72	19.1	2019	446.7
Saqan_2009_009_V-10-2.37	R	257419	362	660	1529	610	987	1676	-494.2	254.0	501	51.72	19.1	2019	446.7
Choulli_2007_S1E	P	188900	100	0	0	671	1773	1776	-1805.9	243.4	891	99.15	12.0	2091	503.8
Choulli_2007_S1W	P	188900	100	0	0	671	1773	1776	-1805.9	243.4	891	99.15	12.0	2087	521.7
Choulli_2007_S2E	P	188900	100	0	0	700	1013	1776	-1205.2	216.5	951	96.34	12.0	2091	366.8
Choulli_2007_S2W	P	188900	100	0	0	700	1013	1776	-1205.2	216.5	951	96.34	12.0	2087	368.7
Zink_2000_SV-2	R	70000	175	350	1256	350	140	1570	-274.4	75.0	980	105.28	11.0	1225	178.9
Zink_2000_SV-4	R	140000	350	357	1963	345	560	1570	-1086.4	72.5	970	93.67	16.0	1225	509.7
Zink_2000_SV-5	R	280000	350	763	402	733	1680	1570	-3225.6	166.5	960	89.53	16.0	2600	736.5
Wilder_2014_B103	P	84670	70	511	0	511	744	1737	-1261.8	141.9	1488	77.50	12.0	2000	262.8
Wilder_2014_B106	P	84670	70	511	0	511	744	1737	-636.0	141.9	750	88.90	12.0	2000	179.7
Wilder_2014_B109	P	84670	70	550	0	550	373	1737	-710.4	130.4	1488	89.30	12.0	2000	181.0
Joergensen 2021 PB5-750A	R	175000	250	641	942	500	1050	1560	-750.0	150.0	714	58.50	16.0	3500	200.9
Joergensen 2021 PB5-750B	R	175000	250	641	942	500	1050	1560	-750.0	150.0	714	60.70	16.0	3500	189.2
Joergensen 2021 PB5-1250A	R	175000	250	641	942	500	1050	1560	-1250.0	150.0	1190	56.30	16.0	3500	238.4
Joergensen 2021 PB5-1250B	R	175000	250	641	942	500	1050	1560	-1250.0	150.0	1190	57.30	16.0	3500	230.7
Joergensen 2021 PB4-1250A	R	175000	250	641	942	500	1050	1560	-1250.0	150.0	1190	60.60	16.0	2800	290.9
Joergensen 2021 PB4-1250B	R	175000	250	641	942	500	1050	1560	-1250.0	150.0	1190	62.50	16.0	2800	301.1
Joergensen 2021 PB6-1250A	R	175000	250	641	942	500	1050	1560	-1250.0	150.0	1190	59.40	16.0	4200	219.9
Joergensen 2021 PB6-1250B	R	175000	250	641	942	500	1050	1560	-1250.0	150.0	1190	60.20	16.0	4200	212.3

Type: P (profiled section); R (rectangular section)

A_c : cross-sectional area of concrete

b_w : minimum width of the cross-section between tension and compression chords

d_s : distance from outermost compressed fibre of the cross-section to the centroid of the ordinary reinforcement

A_s : cross-sectional area of the longitudinal ordinary reinforcement located in the tensile zone due to bending

d_p : distance from outermost compressed fibre of the cross-section to the centroid of the prestressed reinforcement

A_p : cross-sectional area of the longitudinal prestressed reinforcement located in the tensile zone due to bending

f_{py} : yield strength of prestressing steel

P: prestressing force

e_p : eccentricity of the prestressing force related to the centroid of the cross-section, positive when the eccentricity is on the side of the flexural reinforcement in tension

σ_p : stress in prestressing steel

f_c : cylinder compressive strength of concrete

D_{lower} : Smallest value of the upper sieve size in an aggregate for the coarsest fraction of aggregates

a: shear span

V_{test} : shear force at failure

A Mechanical Approach for the Punching Shear Provisions in the Second Generation of Eurocode 2

El tratamiento del punzonamiento en la segunda generación del Eurocódigo 2 basado en un modelo mecánico

Aurelio Muttoni^a, João T. Simões^b, Duarte M. V. Faria^c, Miguel Fernández Ruiz^{*,d}

^a Professor, Ecole Polytechnique Fédérale de Lausanne, Switzerland

^b Dr, Strutlantis Engineering, Portugal / Muttoni et Fernández, ingénieurs conseils SA, Switzerland

^c Dr, Muttoni et Fernández, ingénieurs conseils SA, Switzerland

^d Professor, Universidad Politécnica de Madrid, Spain

Recibido el 15 de julio de 2022; aceptado el 2 de noviembre de 2022

ABSTRACT

The revision of a code is a long-term project that shall fulfil several aims, comprising the enhancement of the ease-of-use and incorporating updated state-of-the-art. With respect to the revision of Eurocode 2 concerning the punching shear provisions, this task allowed also for the opportunity to enhance the understanding of the code and physical phenomenon by designers. The original EN1992-1-1:2004 punching provisions were adapted from an empirical equation for design based on the regression analyses performed by Zsutty in the 1960s for shear in beams and later reworked in Model Code 1990 for punching shear. These expressions did not show any link to the physical response of a structure, making difficult to designers to clearly understand how to engineer their designs. Instead of continuing with this approach, CEN/TC250/WG1 took the decision in 2016 to ground the punching provisions on a mechanical model that could be explained to engineers, allowing for a transparent understanding of the design equations and phenomena. To that aim, the Critical Shear Crack Theory, already implemented in Model code 2010 at that time, was selected as representative of the state-of-the-art. Following that decision, a large effort has been performed to implement this theory into the Eurocode, keeping its simplicity of use and generality. This paper is aimed at presenting the theoretical grounds of the theory as well as the manner in which it is drafted for the future generation of Eurocode 2.

KEYWORDS: Punching, shear, reinforced concrete, slabs, column bases, mechanical model.

©2023 Hormigón y Acero, the journal of the Spanish Association of Structural Engineering (ACHE). Published by Cinter Divulgación Técnica S.L. This is an open-access article distributed under the terms of the Creative Commons (CC BY-NC-ND 4.0) License

RESUMEN

La revisión de una norma es un proyecto que debe cumplir varios objetivos, entre los que se encuentran la mejora de la facilidad de uso y la consideración del estado del conocimiento más avanzado y robusto. En el marco de la revisión de las disposiciones relativas al punzonamiento de placas para el futuro Eurocódigo 2, se dedicaron también amplios esfuerzos para mejorar la coherencia entre las expresiones de diseño y los fenómenos físicos asociados, con el objetivo de facilitar la comprensión de la norma por los proyectistas. Debe observarse que las expresiones originales de la norma EN1992-1-1:2004 se desarrollaron a partir de una ecuación empírica para el diseño de vigas a cortante basada en los trabajos de Zsutty en la década de 1960. Dicha expresión fue posteriormente modificada e introducida en el Código Modelo de 1990 para la resistencia a punzonamiento. Estas expresiones empíricas, a pesar de ser sencillas de aplicar, no permiten comprender la respuesta mecánica de una estructura ni los mecanismos físicos que llevan a su fallo a punzonamiento. Esta pérdida de conexión con la física del fenómeno dificulta a los proyectistas comprender de manera clara cómo mejorar sus diseños o cuestiona la aplicación de las expresiones fuera de los rangos en los que han sido calibradas. En lugar de continuar con un enfoque empírico, el CEN/TC250/WG1 tomó la decisión en 2016 de basar las disposiciones para el punzonamiento de placas en un modelo mecánico que pudiera ser explicado a los ingenieros. Para ello, se seleccionó la Teoría de la Fisura Crítica, implementada previamente en el Código Modelo 2010 como referente del estado del conocimiento. Tras esa decisión, la implementación de la Teoría de la Fisura Crítica en el Eurocódigo ha requerido diversas consideraciones específicas con el objetivo de mantener el formato del Eurocódigo 2 pero respetando la simplicidad de uso y generalidad de la teoría. Este artículo presenta así los fundamentos de la Teoría de la Fisura Crítica, así como la manera en que se ha incorporado en la futura generación del Eurocódigo 2.

PALABRAS CLAVE: Punzonamiento, cortante, hormigón armado, placas, conexiones columna-placa, modelo mecánico.

©2023 Hormigón y Acero, la revista de la Asociación Española de Ingeniería Estructural (ACHE). Publicado por Cinter Divulgación Técnica S.L. Este es un artículo de acceso abierto distribuido bajo los términos de la licencia de uso Creative Commons (CC BY-NC-ND 4.0)

* Persona de contacto / Corresponding author: Correo-e / e-mail: miguel.fernandezruiz@upm.es (Miguel Fernández Ruiz).

How to cite this article: Muttoni, A., Simoes, J.T., Faria, D.M.V., & Fernández Ruiz, M. (2023) A Mechanical Approach for the Punching Shear Provisions in the Second Generation of Eurocode 2, *Hormigón y Acero* 74(299-300):61-77, <https://doi.org/10.33586/hya.2022.3091>

I. INTRODUCTION

Punching shear is a brittle failure mode associated to the penetration of a loaded area in a concrete slab. Slab-column connections where punching occurs experience in general a sudden loss of load-carrying capacity and this can trigger punching failures at other regions (which is a typical situation in flat slabs supported by columns) leading to a progressive collapse [1]. Despite being a phenomenon well-known and having attracted many research efforts in the past [2-6], scanty approaches have been developed so far to lead to physically-based design approaches. As a consequence, design has been traditionally performed on the basis of empirical equations [7-10]. For instance, Eurocode 2 (EN1992-1-1:2004) [8] based its punching design formulation on the approach of one-way slabs and beams failing in shear by adopting the empirical formulation established by Zsutty in 1968 [11]. Such approach had the advantage of keeping a consistent unitary resistance for both verifications (one- and two-way shear). However, it required to define a control perimeter relatively far from the supported area (typically the column) and not linked to the mechanics of the phenomenon. Also, adapting the empirical formulation to other cases that were observed to be relevant from a practical point of view and whose different response was confirmed experimentally (for instance different yield strength of the reinforcement or considering the influence of the slenderness) was not possible. The engineer had, in fact, little help from the empirical formula on the physics of the phenomenon and how to design suitably and in a robust manner.

With respect to physical design models, Kinnunen and Nylander in Sweden proposed in the 1960s [12] an approach that constituted a significant advancement in the understanding of the phenomenon and its prediction. This model considered shear to be carried by a conical strut whose failure in compression leads to the punching failure of the slab-column connection. According to Kinnunen and Nylander [12], failure was assumed to occur for a given level of the compressive tangential strain developing in the soffit of the slab in vicinity of the supported area. By adopting a kinematics defined by a conical deformation in the outer region of the slab, a failure criterion was established as a function of the rotation of the slab. The theory of Kinnunen and Nylander [12] allowed for relatively accurate predictions and was later adapted by other researchers and extended to a number of cases. Amongst these approaches consistent with the principles established by Kinnunen and Nylander [12], a theory named the Critical Shear Crack Theory (CSCT) was developed in 1985 [13] for the Swiss code for structural concrete SIA 162 [14] and later elaborated by Muttoni and Schwartz in 1991 [15]. Originally developed for punching of slab-column connections without shear reinforcement, it was later extended to one-way slabs failing in shear [16] and also to punching of connections with shear reinforcement [17], prestressing [18, 19], footings [20], fibre reinforced concrete [21] and slabs strengthened with post-installed shear reinforcement [22] or fibre reinforced polymers [23].

The formulation of the CSCT allowed to be implemented into design codes following simple design expressions, showing in a transparent manner the various parameters implied

in the phenomenon. These parameters can be evaluated in simple and safe manners or following accurate analyses. On that basis, the CSCT was successfully formulated in terms of a Levels-of-Approximation (LoA) approach [24] and implemented into *fib* Model Code 2010 [25], constituting a significant advance with respect to previous approaches. The LoA approach is a design philosophy [24,26] very much aligned to engineering daily practice. Safe and simple estimates are first performed with a limited amount of work, whose accuracy can be refined upon necessity, requiring some additional work to better evaluate the parameters. For the punching formulation of the CSCT in *fib* Model Code 2010 [25], these levels were structured as follows:

- LoA I: Aimed at a preliminary check and identification of potentially-critical regions. When the resistance of this level is satisfied, bending and not punching is expected to govern the design.
- LoA II: Aimed at typical design for a slab-column connection failing in punching. Implemented by means of analytical formulae exclusively.
- LoA III: Refinement of the previous level, by evaluating several physical parameters on the basis of a linear-elastic finite element analysis. This level is only intended for design of unusual cases or for assessment of existing structures.
- LoA IV: Procedure considering both the failure criterion of the CSCT for the resistance and a demand curve (load-rotation relationship) established on the basis of a nonlinear flexural analysis of the slab. Such level is the most accurate prediction. It allows considering in a consistent manner a number of effects traditionally neglected for design (such as membrane action) but is relatively time-consuming and intended mostly for the assessment of critical cases.

The *fib* Model Code 2010 [25] constituted a significant advancement in design procedures. The expressions for punching design were also checked in numerous scientific works performed all over the world, verifying its accuracy or helping to refine it. The formulation of the *fib* Model Code 2010 is also very practical, allowing for a direct design procedure [26] by verifying that the design value of the resistance V_{Rd} is not lower than the design shear force V_{Ed} . For the explicit calculation of the punching resistance, performing an iterative procedure (intersection of failure criterion and load-rotation relationship) is however required.

Within the revision of Eurocode 2, several deficiencies of the empirical design formula of EN1992-1-1:2004 [8] were highlighted [e.g. 28-37] as well as the limitations of the approach in terms of generality to address relevant topics, such as new materials, unusual geometries or the assessment of existing structures. In addition, the necessity to move to more rational and physically-based models was early identified. After careful analysis of potential approaches, the CSCT was eventually selected as the basic model for the new provisions concerning punching shear. The physical grounds of the CSCT and its flexibility for implementation into design expressions were largely appreciated. However, a relatively direct transcription of the *fib* Model Code 2010 [25] was not considered appropriate within the Eurocode 2 design philosophy. Thus,

it was decided to implement the CSCT following a different approach:

- The preliminary check, identifying regions where shear failures are not expected to be governing was implemented in the definition of the minimum shear resistance.
- The general procedure for punching shear verification had to be based on analytical formulae. This has analogies with the LoA II of Model Code 2010, but its design expressions shall be written a closed-form manner, avoiding iterative procedures for calculation of the punching resistance
- The Annex for assessment of existing structures (Annex I, of informative nature in FprEN1992-1-1:2022 [42]) could elaborate more detailed solutions, comprising the results of nonlinear analyses and verification procedures

With this task in mind, the Task Group 4 (TG4; “Shear, Punching and Torsion”) of CEN/TC250/SC2/WG1 tailored the formulation of the CSCT to the needs of the Eurocode 2. This task required efforts in a number of fields, from the definition of the failure criterion to the verification of the level of safety of the design expressions. The current provisions FprEN1992-1-1:2022 [42] reflect the work performed during the last seven years incorporating the comments and advices of the various participants of CEN.

In this paper, a review of the EN1992-1-1:2004 [8] is first presented, showing also the reasons for change. Then, the theoretical principles of the CSCT are introduced. The main formulae and simplifications introduced for the derivation of the closed-form expressions of FprEN1992-1-1:2022 [42] are also shown and justified. Finally, a practical example is presented, showing the simplicity of the approach and its generality.

2. PUNCHING DESIGN ACCORDING TO FIRST GENERATION OF EUROCODE 2 (EN 1992-1-1:2004)

2.1 Code formulation

The design approach of current Eurocode 2 (EN 1992-1-1:2004) [8] with respect to punching is formulated in terms of closed-form equations, where the action and resistance are evaluated on the basis of a number of geometrical and mechanical parameters. The different formulae have in fact an empirical nature. Namely, the one referring to design of members without shear reinforcement can be considered as a direct adaption of the works of Zsutty [11] for the shear resistance of beams to the punching resistance of two-way slabs:

$$v_{Rd,c} = C_{Rd,c} k (100 \rho_l f_{ck})^{1/3} + k_1 \sigma_{cp} \geq (v_{min} + k_1 \sigma_{cp}) \quad [\text{MPa}] \quad (1)$$

where

- $C_{Rd,c}$, v_{min} and k_1 are NDPs, whose proposed values are $C_{Rd,c} = 0.18/\gamma_C$, $v_{min} = 0.035 k^{3/2} f_{ck}^{1/2}$ and $k_1 = 0.1$.
- $k = 1 + \sqrt{\frac{200}{d}} \leq 2.0$ with d in [mm] is the factor accounting for the size effect
- f_{ck} is the cylinders characteristic concrete compressive strength in [MPa]

- $\rho_l = \sqrt{\rho_{ly} \rho_{lz}} \leq 0.02$ is the geometric mean of the steel reinforcement ratio relating to the bonded tension steel in y - and z - directions respectively (calculated on a band of width equal to $3d$ on each side of the column plus the column size)
- $\sigma_{cp} = \frac{\sigma_{cy} + \sigma_{cz}}{2}$, with σ_y and σ_z being the normal concrete stresses [MPa] in the y - and z - directions (positive if compression)

As it can be noted, the original expression of Zsutty [11] has been somewhat adapted to include other relevant effects as the size effect (parameter k). Also, corrections were proposed to account for the influence of compression and tension forces (term σ_{cp}) [38]. In order to maintain a uniform approach with the verification for shear (based on the same unitary resistance), the location of the control perimeter was thus tailored to a distance equal to $2d$ from the edge of the column (for typical verifications corresponding to the previous formula).

The approach followed is in fact very much inspired on the formulation proposed in Model Code 1990 [7]. The formula had served during almost 20 years, with a format that is apparently simple and accounting for a limited number of parameters, which is convenient for design. Although no major criticism was raised on its simplicity for use for standard cases in flat slabs, several theoretical inconsistencies were raised and partly amended in the EN 1992-1-1:2004 corrigenda [40, 41]. Some of the most important critics, justifying an update of the provisions, are presented in the next section.

2.2. Criticism of EN 1992-1-1:2004 and reasons for change

The section dedicated to the punching shear design in current EN 1992-1-1:2004 [8] was one of the parts that received more systematic review comments in 2013 before starting the revision for the 2nd generation of Eurocodes. Many reasons supported an in-depth revision, mostly addressing scientific concerns (state-of-the-art) and ease-of-use [28-37]. Some relevant critics are summarized below:

- A different methodology is prescribed for the verification of punching shear resistance of flat slabs and footings. For flat slabs, the control section is located at a nominal distance $2d$, lacking of physical meaning (control section too far away from the critical region where punching develops). For footings, the location of the control section is calculated by minimization of the resistance, requiring lengthy and unpractical analyses (even if the use of software and spreadsheets can simplify the calculations).
- The size effect law included in the EN1992-1-1:2004 [8] approach does not suitably describe the phenomena [37]. The size effect can in fact be severely underestimated for thick slabs (too small decrease on the unitary strength for increasingly larger sizes) and the formula does not comply to any reasonable size-effect law [37].
- The current approach does not consider any slenderness effect [28]. The level of strains (and corresponding crack widths) is governed by the flexural deformations in bending [28] which is in turn represented by the flexural reinforcement ratio. However, the same amount of flexural reinforcement can lead to different crack openings and

associated punching resistances for varying slenderness. This effect was already observed by empirical analysis of data [6] and also by theoretical reasoning [28], and named in many cases strain-effect.

The level of safety when compared to available test data is not uniform with respect to the various parameters implied (and also between footings and slender slabs). This has been observed by analysis of large experimental programmes performed since the 2000s (see a detailed overview in [43]).

In addition to these reasons, which suggest deficiencies in the formulae used, there is still a more significant one. It relates to the generality of the approach and its potential to adapt to new situations. The Zsutty's formula is in fact of empirical nature, obtained by regression of parameters compared to test results (as honestly stated in the title of that paper [11]). Every parameter or physical phenomena that has not been calibrated into the original formula is not reflected and the designer has no orientation on how to address it. This fact, which could be limiting but perhaps sufficient for a new design following a number of restrictions (detailing rules), is however very unsuitable for the assessment of existing structures. For instance, the formula does not provide guidance on how to account for the influence of reinforcement with higher or lower yield strength than usually arranged. This can however be relevant for design of new structures (use of new materials) and particularly for assessment of existing ones (in many cases with lower-resistance reinforcement). A similar situation happens with respect to other parameters, such as aggregate size or even influence of level of load when strengthening is performed [75]. The loss of physical meaning does not allow the designer to understand the potential detrimental or favourable effects and how to account for them (which can unfortunately be seen as new patches or coefficients in the existing formula).

In order to overcome these difficulties, it was decided by CEN/TC250/SC2/WG1 to ground the punching shear design provisions on the basis of a mechanical model. This shall allow to transparently clarify the role of the different parameters and

their influence in the punching design formulae and to show also the relationship between them (as for instance between size and strain effects). Such approach should also allow for a sufficient level of generality, so that it can be safely applied to both unusual design situations (enhancing the freedom of the designer) and for assessment of existing structures.

3.

A MECHANICAL MODEL FOR THE SECOND GENERATION OF EUROCODE 2 – THE CRITICAL SHEAR CRACK THEORY

As previously mentioned, after detailed analysis of several state-of-the-art models, TG4 of CEN/TC250/SC2/WG1 decided to adopt the Critical Shear Crack Theory (CSCT) as the grounds for the new provisions for punching shear design of FprEN 1992-1-1:2022 [42]. The theoretical bases of the CSCT are briefly presented in this section. A detailed description can be consulted elsewhere [17, 28, 45-49]. In the following sections, the adaptations introduced to implement it into FprEN 1992-1-1:2022 [42] and to respect the format of the Eurocode will be discussed.

3.1. Members without shear reinforcement

Two-way slabs subjected to concentrated loading develop both cracking associated to radial and tangential bending moments. Due to the presence of shear forces, tangential cracks develop in an inclined manner and can disturb the inclined compression struts carrying shear [28]. One of these cracks is named as the Critical Shear Crack (CSC), being the one intercepting the compression strut near the supported area (shear-critical region).

The mechanical and geometrical properties of the CSC govern the punching resistance. It localizes the strains in the shear-critical region due to the strong gradient of bending moments and shear forces close to the concentrated action

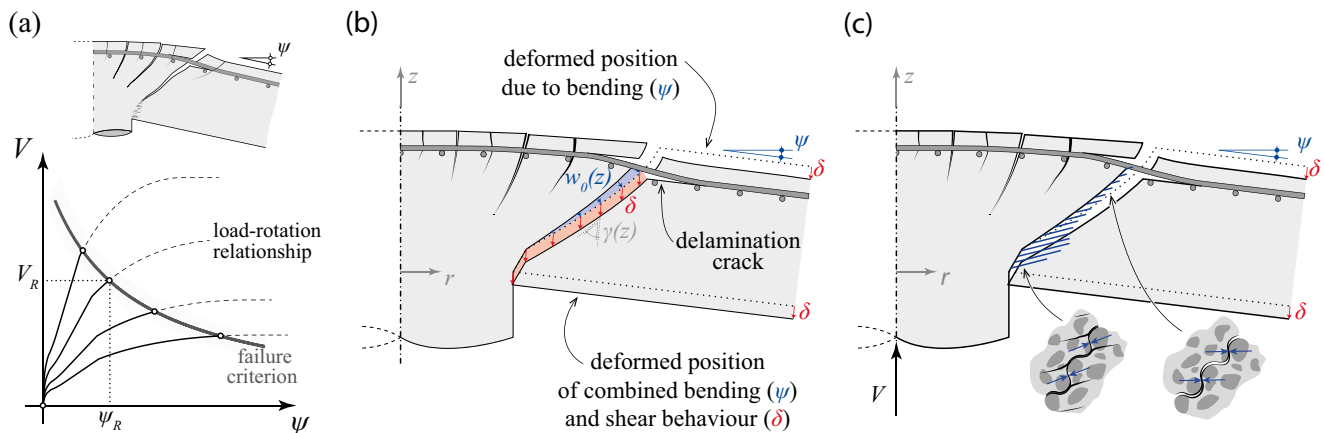


Figure 1. Theoretical principles of the mechanical model of Critical Shear Crack Theory (adapted from [46] and [49]): (a) intersection of load-rotation relationship and a failure criterion; (b) kinematics of the critical shear crack at failure; and (c) resulting internal stresses.

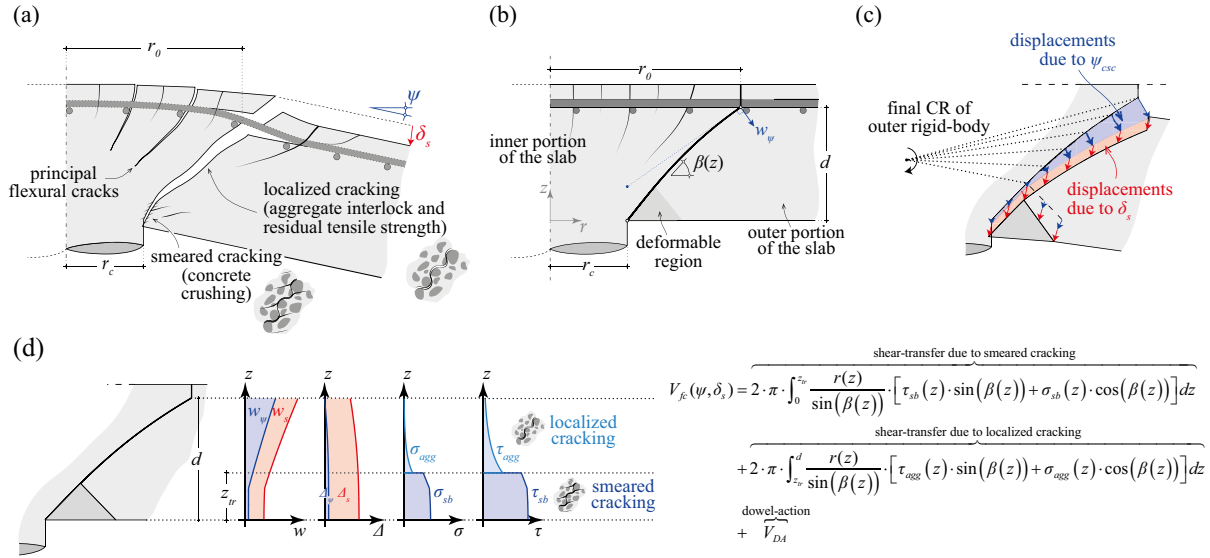


Figure 2. The refined mechanical model of Critical Shear Crack Theory according Simões et al. [48]: (a) observed behaviour; (b) adopted critical shear crack geometry; (c) adopted kinematics; (d) resulting normal and shear stresses (b4 and b5) (figures adapted from [48] and [49]).

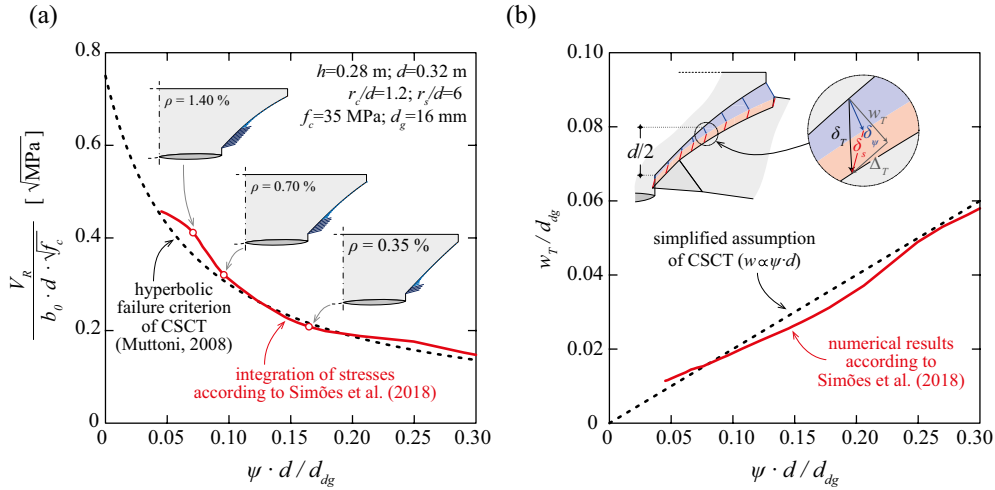


Figure 3. Results of mechanical model by Simões et al. [48] for an investigated case: (a) comparison of the numerically calculated failure criterion with the hyperbolic failure criterion (Eq. (2)) and representation of the resultants of stresses developing along the CSC for different rotations; and (b) numerically calculated crack opening–rotation relationship and comparison with simplified assumption of Muttoni [28].

[28, 47]. The CSC is usually originated at a distance close to one effective depth (d) and propagates in an inclined manner. Its opening is one of its key parameters for the punching resistance, as wider cracks reduce the ability of concrete to transfer shear stresses [51]. For slender members, such opening is mostly governed first by bending deformations but, when approaching to failure, shear deformations become also significant [52, 19, 46, 50, 48]. Eventually, at failure, the critical shear crack starts sliding leading to the development of the punching cone as shown in Figure 1 [52, 19, 50]. Based on these considerations, the Critical Shear Crack Theory (CSCT) considers that the kinematics of the CSC is composed by the sum of flexural (in blue in Figure 1b) and shear (in red in Figure 1b) movements. On that basis, the shear and normal stresses acting along the CSC can be calculated considering suitable material laws, see Figure 1c. This

can be performed in a refined manner based on a numerical integration [52, 19, 48], see Figure 2.

Some results of the mechanical model of the advanced implementation of the CSCT [48] are shown in Figure 3a in terms of normalized punching resistance and normalized rotation. The results show a decrease on the punching resistance with increasing rotations of the slab. This is justified by the fact that larger rotations are associated to wider widths of the critical shear crack, thus reducing the contribution of the different shear-transfer actions (i.e. direct strutting, aggregate interlock, residual tensile strength and dowel action).

The results of this model are in fact in agreement with the model of Kinnunen and Nylander [12], considering the development of an inclined strut carrying shear near the column region (also called compressive cone; see stresses developing along the CSC in Figure 3a according to refined mechanical

model of CSCT). Another interesting result can be obtained if the opening of the critical shear crack (accounting for both flexural and shear deformations) at a height $d/2$ from the slab soffit is represented as a function of the normalized rotation for the investigated case, refer to Figure 3b. The results show that the crack width and the normalized rotation are correlated and that a linear correlation is a fairly good approximation of it. It is interesting to note that Muttoni and Schwartz [15] suggested in 1991 such a linear relationship between the opening of the critical shear crack and the product ψd (linear correlation between crack width w and product of rotation ψ and effective depth d).

Other than the opening of the CSC, also its roughness influences the ability of the CSC to transfer shear forces [53, 54, 55]. In 2003, Muttoni [16] introduced this consideration by including the crack roughness, expressed in terms of the maximum aggregate size d_g . Eventually, Muttoni [16, 28] proposed a hyperbolic failure criterion relating the punching resistance and the crack opening (represented by the product ψd) and roughness (accounting for d_g) as follows [28]:

$$\frac{V_{R,c}}{b_{0,5} d_v} = \frac{0.75 \sqrt{f_c}}{1 + 15 \frac{\psi d}{d_{g0} + d_g}} \quad (2)$$

where $V_{R,c}$ refers to the punching shear resistance (concrete contribution); $b_{0,5}$ to the length of the control perimeter at a distance of $d_v/2$ from the column face (round corners in case of square or rectangular columns); d_v to the shear-resisting effective depth (potentially differing from the effective depth d to account for the penetration of the support and thus reducing the depth available to carry shear); f_c to the cylinders concrete compressive strength; d_{g0} to the reference aggregate size ($d_{g0} = 16$ mm for normal weight concrete).

Eq. (2) suitably represents the response of reinforced concrete slabs failing in punching when compared to available experimental results, see Figure 4a. The theory shows a decreasing punching strength for increasing level of rotations (according also to Kinnunen and Nylander [12]). The punching strength of a slab-column connection can therefore be obtained by intersecting the load-rotation relationship of the slab (defining

the shear demand) and the failure criterion (representing the shear resistance associated to a state of deformations), refer to Figure 4b. One interesting aspect of the CSCT is that the load-rotation relationship of the slab can be calculated with different levels of refinement:

- Analytical formulae for axisymmetric cases based on the model by Kinnunen and Nylander [12]. These formulae were developed considering both a simplified bilinear moment-curvature relationship as well as more sophisticated laws accounting for tension-stiffening (quadri-linear laws) [15, 16, 28];
- Using a simplified formula for practical purposes, derived analytically from the general law [26]):

$$\psi = k_m \frac{a_p}{d} \frac{f_y}{E_s} \left(\frac{m_s}{m_R} \right)^{\frac{3}{2}} \quad (3)$$

where a_p is the distance between the axis of the column and the line of zero radial moment, f_y and E_s are respectively the yield strength and the modulus of elasticity of the flexural reinforcement, k_m is a factor depending on the level of the refinement of the approach used to estimate the acting bending moment in the support width (typically 1.5 for simple analyses and 1.2 when some parameters are known more in detail), m_s is the acting bending moment in the support strip width (b_s) and m_R is the average moment capacity in the support width;

- Nonlinear finite element analyses, considering in detail geometrical and mechanical aspects of the response [56-59].

The selection of the most suitable load-rotation relationship depends on many aspects, such as the level of knowledge of the structure. Very refined analyses, as those resulting from the application of the nonlinear finite element analyses are in principle only possible when the structure can be characterized in detail. This is the case when the resistance of a structure needs to be assessed, when the required geometric data, reinforcement and material properties can be finely evaluated. Otherwise, namely for design, simpler methods are preferable and more consistent with the degree of knowledge or definition of the structure.

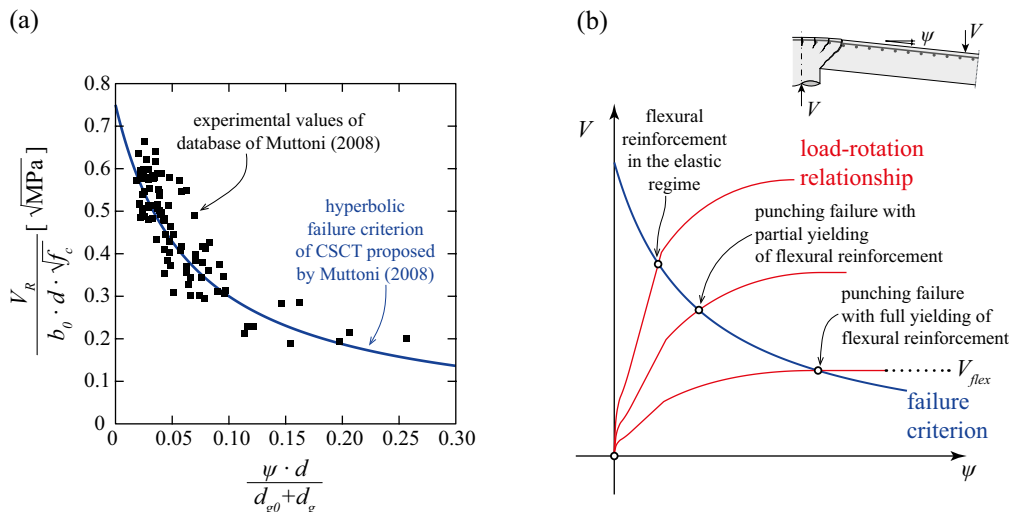


Figure 4. (a) Experimental validation of the hyperbolic failure criterion of CSCT (Eq. (2)) proposed by Muttoni in 2008 [28] and (b) potential punching shear failure regimes (figures adapted from [46]).

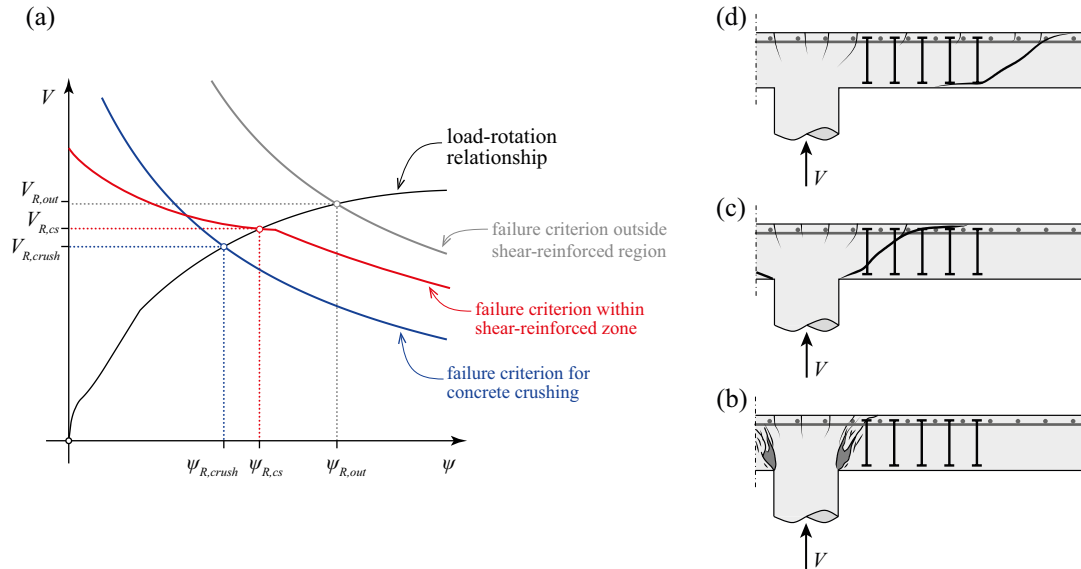


Figure 5. Members with shear reinforcement: (a) load-rotation relationship and intersection with possible governing failure criteria [Eqs. (4) to (7)] associated with (b) crushing of concrete struts, (c) failure within the shear-reinforced region; and (d) failure outside the shear-reinforced region (failure modes adapted from [17]).

3.2. Members with shear reinforcement

The arrangement of shear reinforcement is one of the most suitable solutions to enhance the resistance and deformation capacity of slabs [e.g. 60, 61, 17, 35]. The CSCT was extended consistently to this case maintaining its basic assumptions by Fernández Ruiz and Muttoni [17]. To that aim, when usual detailing rules are respected [25], three potential failure modes can govern [17]: (i) failure within the shear-reinforced area (Figure 5c); (ii) crushing of concrete struts (maximum punching strength; Figure 5b) and (iii) failure outside the shear reinforced area (Figure 5d). The approach proposed by the CSCT [17] allows calculating again the resistance by intersection of the load-rotation curve (assumed to be the same as for members without shear reinforcement, since the shear deformations are neglected) and the pertinent failure criterion for each of these modes.

Failure within the shear-reinforced area

As shown in Figure 6, the punching resistance can be calculated as the sum of concrete $V_{R,c,cs}$ and shear reinforcement $V_{R,s,cs}$ contributions [17]:

$$V_{R,cs} = V_{R,c,cs} + V_{R,s,cs} \quad (4)$$

In this Equation, the concrete contribution $V_{R,c,cs}$ is given by the failure criterion of the corresponding element without shear reinforcement (see Eq. (2)) and the shear reinforcement contribution ($V_{R,s,cs}$) is given for axisymmetric cases by:

$$V_{R,s,cs} = \sigma_{sw} \Sigma A_{sw} \leq f_{yw} \Sigma A_{sw} \quad (5)$$

where σ_{sw} is the average stress in the shear reinforcement intercepted by the punching cone (considered in a simplified manner to develop with an inclination of 45°), ΣA_{sw} is the total area

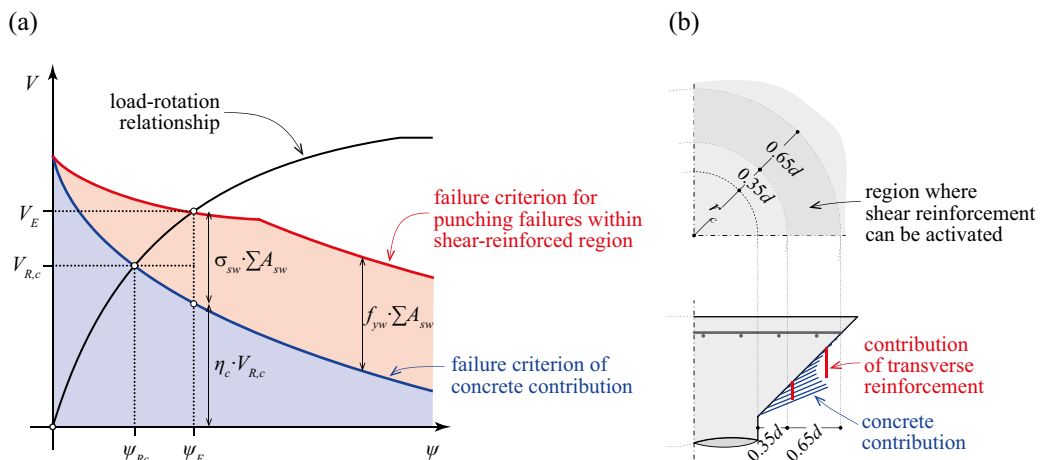


Figure 6. Definition of contributions of concrete and shear reinforcement for punching failure within the shear-reinforced region.

of the activated shear reinforcement in the punching cone (assumed within $0.35d_v$ and d_v) and f_{yw} is the yield strength of the shear reinforcement. The average stress in the shear reinforcement can be calculated as a function of the rotation, by assuming it to be proportional to the opening of the CSC plus a term accounting for bond (details accounting for advanced considerations on bond and anchorage can be consulted elsewhere [17]):

$$V_{sw} = \frac{E_{sw}}{6} \psi + f_b \frac{d_v}{\phi_w} \quad (6)$$

where f_b is the average bond stress, ϕ_w and E_{sw} are respectively the diameter and the modulus of elasticity of the shear reinforcement. For members governed by shear deformations (as footings or prestressed slabs) [62, 67], the maximum punching resistance can be associated to large shear deformations with the concrete contribution vanishing ($V_{R,c,c} \rightarrow 0$) and the stress in the shear reinforcement tending to the yield strength ($\sigma_{sw} \rightarrow f_{yw}$). For these cases, however, the extent where the punching shear reinforcement can be activated can be significantly reduced (steeper angle of the failure cone [29, 62, 63]).

Failure by crushing of concrete struts (maximum punching resistance)

Fernández Ruiz and Muttoni [17] proposed to evaluate the maximum punching resistance (crushing of concrete struts) as an enhancement of the punching strength of the corresponding element without shear reinforcement. This is justified by the fact that the crushing resistance of the concrete strut is, as for members without shear reinforcement, influenced by the opening of the CSC and by its roughness. In addition, it depends strongly on the anchorage conditions, geometry and detailing rules of the shear reinforcement [e.g. 17, 35, 60, 61, 64]. This condition can be expressed as:

$$V_{R,max} = \eta_{sys, sb} V_{R,c} \quad (7)$$

where $V_{R,max}$ is the punching resistance associated to crushing of the concrete struts, $V_{R,c}$ is the failure criterion of the corresponding slab-column connection without shear reinforcement (see Eq. (2)) and $\eta_{sys, sb}$ is an enhancement factor which depends on the type of shear reinforcement.

Failure outside the shear-reinforced area

To calculate the punching resistance of failures outside of the shear-reinforced area, Fernández Ruiz and Muttoni [17] considered in a safe manner that the rotations of the critical shear crack concentrate outside of the shear-reinforced area. This is equivalent to considering the shear-reinforced area as a stiff supported region. On that basis [17], the same failure criterion as for slabs without shear reinforcement can be used, provided a suitable value of the control perimeter is selected:

$$\frac{v_{R,out}}{b_{0.5,out} d_{v,out}} = \frac{0.75 \sqrt{f_c}}{1 + 15 \frac{\psi d}{d_{g0} + d_g}} \quad (8)$$

where $d_{v,out}$ is the shear-resisting effective depth of the outer perimeter of reinforcement (see Figure 5d). On that basis, $b_{0.5,out}$ is the outer control perimeter (defined at $0.5d_{v,out}$ from the last perimeter of shear reinforcement and accounting for some limitations in the distances between the shear reinforcement units).

3.3. Considerations for eccentric punching

The development of a non-uniform distribution of shear forces along the control perimeter in the cases of eccentric punching (internal columns with unbalanced moments, presence of large openings in the vicinity of columns, edge and corner columns) is accounted in the framework of the Critical Shear Crack Theory by setting two different control perimeters (as defined in fib Model Code 2010, see also Figure 7):

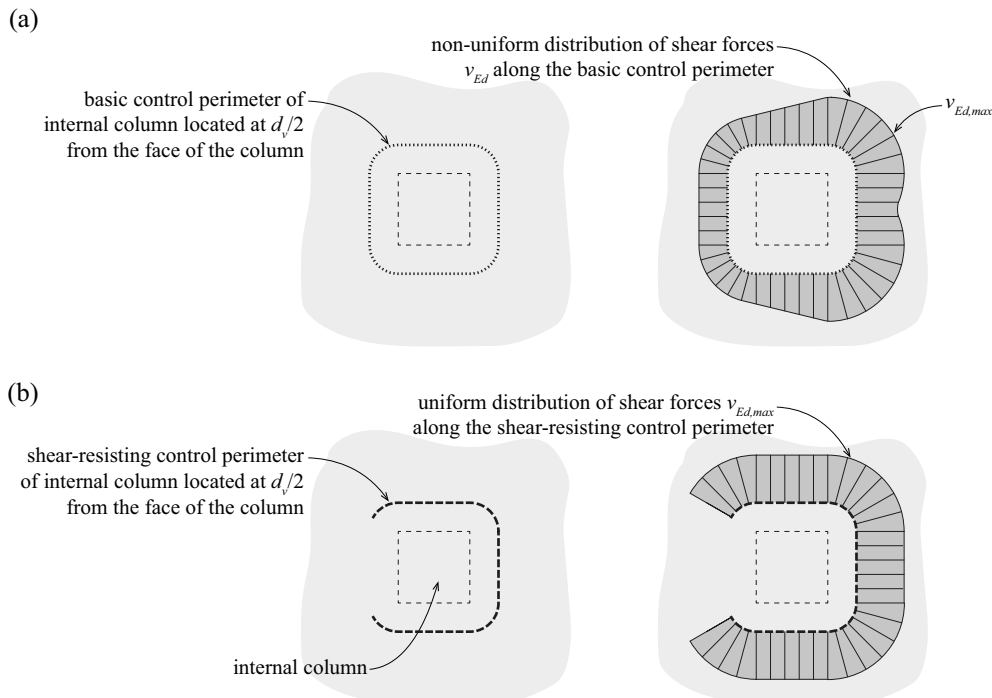


Figure 7. Eccentric punching: (a) non-uniform distribution of shear forces along the basic control perimeter; (b) idealized uniform distribution of shear forces along the reduced control perimeter.

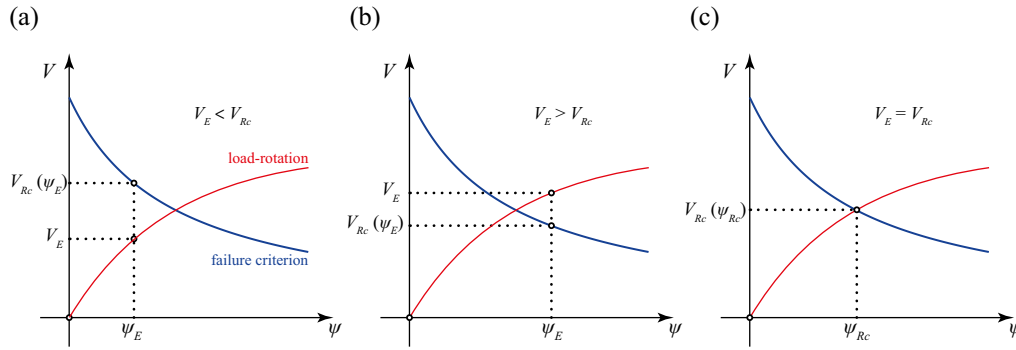


Figure 8. Application of Critical Shear Crack Theory for design and assessment: (a,b) procedure for design with calculation of punching shear resistance V_{Rc} corresponding to the rotation ψ_E associated to acting shear force V_E ; (c) iteration required to calculate the punching resistance.

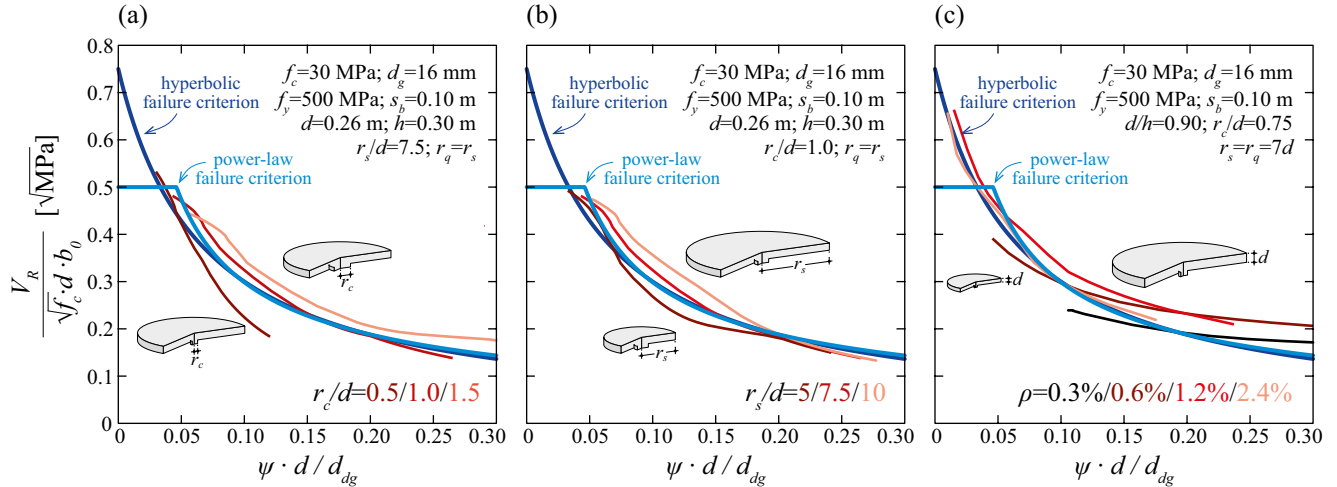


Figure 9. Comparison of original hyperbolic failure criterion (Eq. (2)) and failure criterion based on a power law (Eq. (9)) with the results from the refined mechanical model of CSCT by Simões et al. [48].

- a basic control perimeter, defined purely by geometric considerations, referring to the one located at $d_v/2$ (accounting for discontinuities, edges, opening, inserts and with straight segments limited to $3d_v$ in case of large columns or wall ends and corners).
- A reduced shear-resisting control perimeter which can be obtained by multiplying the basic control perimeter by a reduction factor k_e accounting for the concentrations of shear forces.

In this case, the concentration of shear forces is to be accounted for in the design of shear reinforcement by multiplying also A_{sw} (defined purely on the basis of geometry) by the coefficient k_e in Eq. (5). Further details can be consulted elsewhere [65]. In a similar manner, the consideration of other effects such as elongated columns [66], prestressing [67, 68] or membrane forces [69, 70] can also be consistently accounted for.

3.4. Methodology for design and assessment of existing structures

Within the original formulation of the CSCT and its implementation in *fib* Model Code 2010 [25], it can be noted that the punching verification for design of a new structure is direct. This can be shown in Figures 8a,b, as it only has to be verified if the resistance is higher or equal than the demand for

the rotation calculated by means of the load-rotation relationship. For an explicit calculation of the resistance, however, the two nonlinear curves shall be intersected (Figure 8c), which requires in general following an iterative procedure.

4. SIMPLIFICATIONS FOR DESIGN INTRODUCED IN FPREN 1992-1-1:2022

The implementation of the CSCT into the FprEN 1992-1-1:2022 [42] required several adaptations. The main one was to propose for design purposes a closed-form method for design as per EN 1992-1-1:2004 [8]. Such approach (where details can be consulted in [46]) allows for an analytical evaluation of the punching resistance (being thus direct both for design and assessment purposes) on the basis of a limited number of mechanical and geometrical parameters. For a detailed assessment of existing structures (defined in Annex I of FprEN1992-1-1:2022 [42]), the general method of the CSCT is however allowed, both in terms of failure criterion and general definition of the load-rotation relationship. This allows for a detailed evaluation of the load-rotation relationship accounting for the peculiarities of the structure.

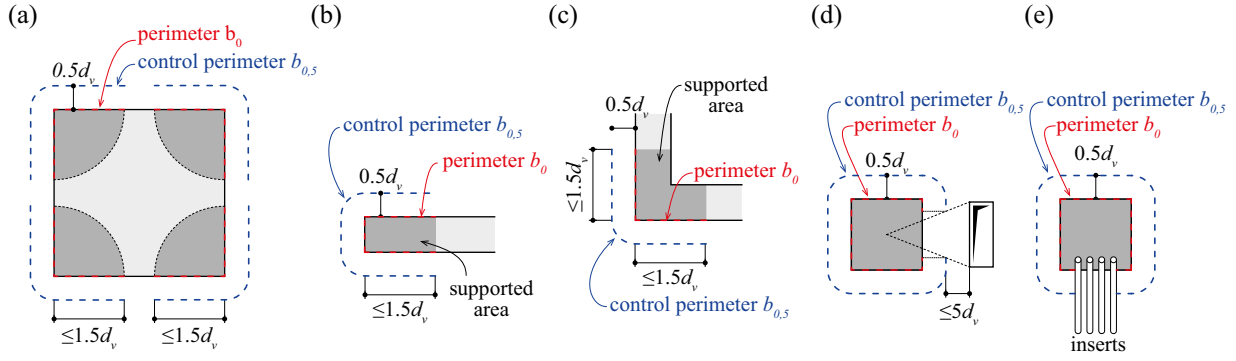


Figure 10. Definition of control perimeter $b_{0,5}$ at $d_v/2$ from the supported area and perimeter b_0 at the face of the supported area

4.1. Members without shear reinforcement

In order to obtain a closed-form expression for punching, the failure criterion was slightly adapted [46, 72] from its hyperbolic form (Eq. (2)) to a power law with very similar results [48] (see Figure 9):

$$V_{R,c} = 0.55 k_e b_{0,5} d_v \sqrt{f_c} \left(\frac{1}{25} \frac{d_{dg}}{\psi d} \right)^{\frac{3}{2}} \leq 0.50 k_e b_{0,5} d_v \sqrt{f_c} \quad (9)$$

where d_{dg} is the reference value of roughness of the critical shear crack and is computed as [46, 71]:

$$d_{gg} = d_{g0} + d_g \min \left(\left(\frac{60}{f_c} \right)^2, 1 \right) \leq 40 \text{ mm} \quad (10)$$

It can be noted that a value 0.50 is used in Eq. (9), instead of the original value of reference [46], for simplicity and yielding to almost identical results.

With respect to the load-rotation relationship, the one defined in Eq. (3) was adopted according to the presumed level of definition of the structure. It was however improved, as recent investigations suggest that the influence of the ratio a_p/d could be slightly modified to better approximate not only the theoretical response (e.g. integration of quadri-linear moment-curvature [28]) but also the punching shear resistance calculated with the refined model of the CSCT [48]. Accounting for such consideration, and assuming $m_s/m_R \approx V_E/V_{flex}$ and $km \approx 1.2$ [28], it results:

$$\psi = k_m \sqrt{8 \frac{a_p}{d} \frac{f_y}{E_s} \left(-\frac{V_E}{V_{flex}} \right)^{\frac{3}{2}}} \quad (11)$$

where V_E refers to the acting punching shear force and V_{flex} to the flexural capacity. The punching shear resistance can thus be directly determined by intersecting Eqs. (11) and (9), resulting into (see reference [74] for a complete derivation):

$$V_{R,c} = 0.16 b_{0,5} d_v \sqrt{a \frac{d}{d_v} \frac{k_e d}{b_{0,5}}} \left(E_s \rho_l f_c \frac{d_{dg}}{\sqrt{d} a_p} \right)^{\frac{1}{3}} \leq 0.50 k_e b_{0,5} d_v \sqrt{f_c} \quad (12)$$

where $a = V_{flex}/m_R$. Eq. (12) can be written in a design format by (see reference [74] for derivation and associated considerations):

- using characteristic values of material strength and the partial safety factor associated to the required reliability index

- by considering additionally that the shear stress concentrations are not accounted for by reducing the control perimeter by a factor k_e (*fib* Model Code 2010 [25] approach) but rather by increasing the average acting shear stress calculated on the basic control perimeter by a coefficient β_e (Eurocode 2 [8] approach).
- for a safe simplified calculation, the parameter a_p can be replaced by a value equal to $8d$.
- replacing the term d by d_v as a safe and simplified assumption (refer to Eq. (12) and see [74] for further details).

In that case, the design punching shear stress (to be compared with the acting shear stress $\tau_{Ed} = \beta_e V_{Ed}/(b_{0,5} d_v)$) becomes:

$$\tau_{Rd,c} = \frac{0.60}{\gamma_V} k_{pb} (100 \rho_l f_{ck} \frac{d_{dg}}{d_v})^{\frac{1}{3}} \leq \frac{0.50}{\gamma_V} \sqrt{f_{ck}} \quad (13)$$

where d_{dg} is calculated according to Eq. (10) (with d_g being replaced by the definition D_{lower}), ρ_l is the longitudinal flexural reinforcement ratio (with $\rho_l = \sqrt{\rho_{l,x} \rho_{l,y}}$, where subscripts x, y refer to two orthogonal directions). With respect to coefficient k_{pb} in Eq. (13), it accounts for the strength enhancement due to the shear field gradient in the control section and can be calculated as (see [74] for further details on the derivation):

$$1 \leq k_{pb} = 3.6 \sqrt{1 - \frac{b_0}{b_{0,5}}} \leq 2.5 \quad (14)$$

where b_0 is the perimeter of the supporting area (perimeter at the column edge, see Figure 10). It should be noted that, for the sake of simplicity, k_{pb} in Eq. (14) is expressed as a function of a geometrical rule using the two main control perimeters defined in FprEN 1992-1-1:2022 [42]: b_0 and $b_{0,5}$. This rule greatly simplifies notations for its practical use, hindering however the true physics of the phenomenon (a mechanical rule, as shown in [74], is replaced by a geometric one). This has to be kept in mind for the understanding of engineers of the design formulation.

It is interesting to note the physical meaning of the shear-gradient enhancement factor k_{pb} . This parameter describes the enhancement on the unitary shear resistance for a punching case with respect to the shear resistance of a beam or one-way slab. When the column (or in general the supporting area) is very large, k_{pb} tends to 1 and the punching shear resistance tends to the shear resistance of one-way slabs. Its value,

otherwise, increases for decreasing column sizes, enhancing the unitary shear resistance. The upper limitation $k_{pb} = 2.5$ is addressed at very small columns.

With respect to the slenderness of the slab, it was stated before that a simplification was made on the load-rotation relationship as a safe bound ($a_p = 8d$) in Eq. (13). This is intended to increase the strains of the reinforcement and thus to reduce the unitary shear resistance. However, this consideration can be easily refined, by introducing a suitable strain effect, by replacing the parameter d_v by $\sqrt{d_v \frac{a_p}{8}}$, where:

$$a_p = \sqrt{a_{p,x} a_{p,y}} \geq d_v \quad (15)$$

where $a_{p,x}$ and $a_{p,y}$ are the distances between the column axis and the locations where the bending moments $m_{Ed,x}$ and $m_{Ed,y}$ are equal to zero.

4.2. Members with shear reinforcement

As it was done for members without shear reinforcement, several adaptations with respect to the CSCT general formulation were required to derive closed-form design expressions. These considerations are presented in the following for the three potential failure modes.

Failure within the shear-reinforced area

As previously introduced, the punching strength in case of failure within the shear reinforced region (VR,cs) is given by the sum of the contributions of concrete and shear reinforcement:

$$V_{R,cs}(\psi_E) = V_{R,c}(\psi_E) + k_e \sigma_{sw}(\psi_E) \Sigma A_{sw} \geq k_e f_{yw} \Sigma A_{sw} \quad (16)$$

where $V_{R,cs}(\psi_E)$ is the concrete contribution calculated with the failure criterion for the level of rotation ψ_E derived from the load-rotation relationship for the acting shear force; the term $\sigma_{sw}(\psi_E)$ is the stress in the shear reinforcement for the level of rotation ψ_E ; the term f_{yw} is the yield strength of the shear reinforcement; k_e the coefficient accounting to the concentration of shear forces and ΣA_{sw} is the total area of shear reinforcement within $0.35 \cdot d_v$ and d_v . In Eq. (16), the right-hand side of the inequality refers to the case where the concrete contribution vanishes ($V_{R,c} \rightarrow 0$) and the stress in the shear reinforcement tends to the yielding strength ($\sigma_{sw} \rightarrow f_{yw}$) [64].

Eq. (16) was however considered not suitable for the punching design within the Eurocode 2 design philosophy since it is strain-based. To overcome that issue, Eq. (16) was simplified following an analytical derivation together with a number of simplifications (a detailed derivation is presented in [74]):

- Replacing $V_{R,c}(\psi_E)$ by the corresponding value (Eq. 9) with ψ_E , but neglecting the upper limit;
- Introducing Eq. (11) (load-rotation) into Eq. (6) (activation of shear-reinforcement)
- Considering that $\eta_c = \frac{\tau_{Rd,c}}{f_{Ed}}$ and that $\tau_{Rd,c}$ is given by Eq. (13)
- Rounding the exponents and retaining only the most influential parameters for design

Following the above-mentioned considerations, Eq. (16) can be rewritten in a design format complying with the Eurocode 2 philosophy as (see [74] for further considerations):

$$\tau_{Rd,c} = \eta_c \tau_{Rd,c} + \eta_c f_{yw} \rho_w \geq f_{yw} \rho_w \quad (17)$$

being:

$$\eta_c = \frac{\tau_{Rd,c}}{f_{Ed}} \quad (18)$$

$$\eta_s = \sqrt{15 \frac{d_{lg}}{d_v} \left(\frac{1}{\eta_c k_{pb}} \right)^{\frac{3}{2}}} + \frac{d_v}{150 \phi_w} \leq 0.80 \quad (19)$$

$$\rho_w = \frac{A_{sw}}{s_r s_t} \quad (20)$$

where A_{sw} is the area of one leg of shear reinforcement; s_r is the radial spacing of shear reinforcement; s_t is the average tangential spacing of perimeters of shear reinforcement measured at control perimeter and f_{ywd} is the yield strength of the shear reinforcement. It should be noted that the factor $d_v/(150 \phi_w)$ in Eq. (19) refers to the enhancement on the activation of the punching reinforcement due to bond, and thus that it can only be considered provided that the shear reinforcement consists of ribbed or indented bars.

Failure by crushing of concrete struts (maximum punching resistance)

According to the general frame of the CSCT [17], the maximum punching shear resistance of shear-reinforced slabs can be calculated by multiplying the concrete failure criterion by a factor ($\eta_{sys, sb}$), whose value accounts for the performance of the shear reinforcement system. Provided that the power-law failure criterion is multiplied by a factor, the resulting strength can also be obtained in a closed-form manner. For convenience, the strength will be expressed in this case on the basis of the one of a member without shear reinforcement:

$$V_{R,max} = \eta_{sys} V_{R,c} \quad (21)$$

where η_{sys} is the factor to enhance the punching resistance of slabs without shear reinforcement. In fact, factors $\eta_{sys, sb}$ and η_{sys} are related and account for the same effects. It shall be noted however that while the former is the multiplication factor to be applied in a strain-based approach (multiplication of the failure criterion), the latter is the multiplication factor to be applied to the punching resistance (their mathematical relationship is a function of the adopted failure criterion and load-rotation relationship).

In order to introduce in an explicit manner, the governing parameters ruling the value of η_{sys} , specific simulations were performed with the refined implementation of the CSCT [73]. It was found that the most influential parameters are (i) the type of punching reinforcement, (ii) the size of the column, (iii) the position of the first perimeter of punching reinforcement and (iv) the detailing of the anchorages (enclosure of the third or fourth layer of flexural reinforcement with the punching reinforcement units and the spacing of the subsequent perimeters). Other factors were also shown to have a certain impact (such as the yield strength and flexural reinforcement ratio), yet with a more limited impact for the daily design cases [73]. Based on this analysis [73], an analytical expression for the value of η_{sys} was formulated within FprEN1992-1-1:2022 [42] as:

$$\eta_{sys} = 1.15 \frac{d_{sys}}{d_v} + 0.63 \left(\frac{b_0}{d_v} \right)^{\frac{1}{4}} - 0.85 \frac{s_0}{d_{sys}} \geq 1.0 \quad (22)$$

where d_{sys} represents the anchorage performance of the punching reinforcement system and its detailing and s_0 is the distance from the column face to the axis of the first perimeter of shear reinforcement. This expression fairly well approximates the results of the refined implementation of the CSCT and accounts for the effect of most detrimental parameters. For ease-of-use in designing new structures complying with the detailing rules of Section 12, constant values for the ratios d_{sys}/d_v and s_0/d_{sys} can be adopted depending on the type of shear reinforcement system, leading to the expressions included in Clause 8 of FprEN1992-1-1:2022 [42]:

$$\eta_{sys} = 0.70 + 0.63 \left(\frac{b_0}{d_v} \right)^{\frac{1}{4}} \geq 1.0 \quad (23a)$$

$$\eta_{sys} = 0.50 + 0.63 \left(\frac{b_0}{d_v} \right)^{\frac{1}{4}} \geq 1.0 \quad (23b)$$

whereas the more general expression of Eq. (22) is defined in Annex I for the assessment of existing structures.

Failure outside the shear-reinforced area

Following the general approach of the CSCT, the punching resistance outside the shear reinforced region should be calculated in accordance to Eq. (13), considering the reduced shear-resisting effective depth (function of the shear reinforcement system) and the outer control perimeter $b_{0,5,out}$ (located at $d_{v,out}/2$ from the outer perimeter of shear reinforcement with a length of the straight segments not exceeding $3d_{v,out}$).

5. COMPARISON OF FPEN 1992-1-1:2022 TO TESTS AND TO FIRST GENERATION OF EUROCODE 2

A systematic comparison of the formulation of FprEN 1992-1-1:2022 [42] against experimental tests was performed and published elsewhere [74]. No remarkable trend was observed, with a uniform level of safety and a relatively constant and low Coefficient of Variation (below or around 14% in all cases), improving the results by EN 1992-1-1:2004 [8]. The values obtained are amongst the lowest that can be found for any design code and comparable to those of the original theory.

6. CONSIDERATIONS FOR ASSESSMENT OF EXISTING STRUCTURES

The previous method was developed in order to provide designers with a simple tool for design, implying only a limited number of parameters and being sufficiently safe in the assumptions covering other (non-explicit) parameters. However, for assessment of existing structures, the different properties of the structure are usually known (in case drawings and documents are available) or can be assessed on-site (as the characteristic strength of concrete or the yield strength of the reinforcement). This allows one to perform more tailored analyses, with potential increases of the strength as the various load-car-

rying actions can be suitably evaluated, avoiding unnecessary strengthening or minimizing it.

To that aim, Annex I of the FprEN 1992-1-1:2022 [42] proposes a more general frame of verification, with an explicit definition of the failure criterion for punching based on the CSCT for members without shear reinforcement:

$$\frac{v_{R,c}}{b_{0,5} d_v} = 0.75 \frac{\gamma_{def}^{\frac{2}{3}}}{\gamma_v^{\frac{2}{3}}} \frac{\sqrt{f_{ck}}}{1+15 \frac{\gamma_{def} \psi d_v}{d_{dg}}} \quad (24)$$

This failure criterion is equivalent to the one defined by the CSCT (refer to Eq. (2)), but accounting for partial safety factors (γ_{def} and γ_v) to comply with the required level of reliability [75] (similar considerations as for the general CSCT approach can be assumed for other failure modes).

The rotation at failure can be estimated by intersection of the failure criterion with the load-rotation -relationship at the slab-column connection. This latter can be calculated accounting for the different geometrical and mechanical conditions. For instance, an analysis based on nonlinear finite elements is a suitable strategy for this purpose [e.g. 58,59], although simpler approaches might be sufficient.

7. EXAMPLE OF APPLICATION

An example is presented in the following referring to the assessment of the punching resistance of an existing structure. To that aim, the geometry and reinforcement layout are considered as known data. The assessment of the resistance is performed first by using the closed-form approach for design provided in Clause 8.4 (Eq. (13)), whose value is later refined by means of the strain-based approach and consideration of membrane action according to Annex I. The example is inspired on a real structure built in Lausanne, Switzerland during the 1990s, serving as a hall for maintenance of vehicles. The most relevant properties for the assessment of the slab without shear reinforcement are listed below:

- **Geometry:** the geometry of the slab considered in the design example is shown in Figure 11.
 - Slab's overall depth: $h = 0.32$ m
 - Spans: $L_x = 7.80$ m; $L_y = 8.00$ m
 - Cover: 20 mm
 - Effective depth: $d = 0.28$ m
 - Shear-resisting effective depth: $d_v = 0.28$ m (0.00 m column penetration)
 - Columns: square 0.50 x 0.50 m
- **Materials**
 - Concrete: $f_{ck} = 42.8$ MPa (measured *in-situ* and calculated according to Annex I of FprEN1992-1-1:2022 [42] on the basis of $f_{ck, is}$ determined with EN 13791 [76]); $D_{max} = 32$ mm
 - Flexural reinforcement: B500; B ductility class; $f_{yd} = f_{ywd} = 435$ MPa
- **Top flexural reinforcement:** $\emptyset 18@0.10$ m in both x- and y- directions
 - Partial safety factors: $\gamma_v = 1.4$; $\gamma_{def} = 1.33$
 - Acting shear force: $V_{Ed} = 1.167$ MN

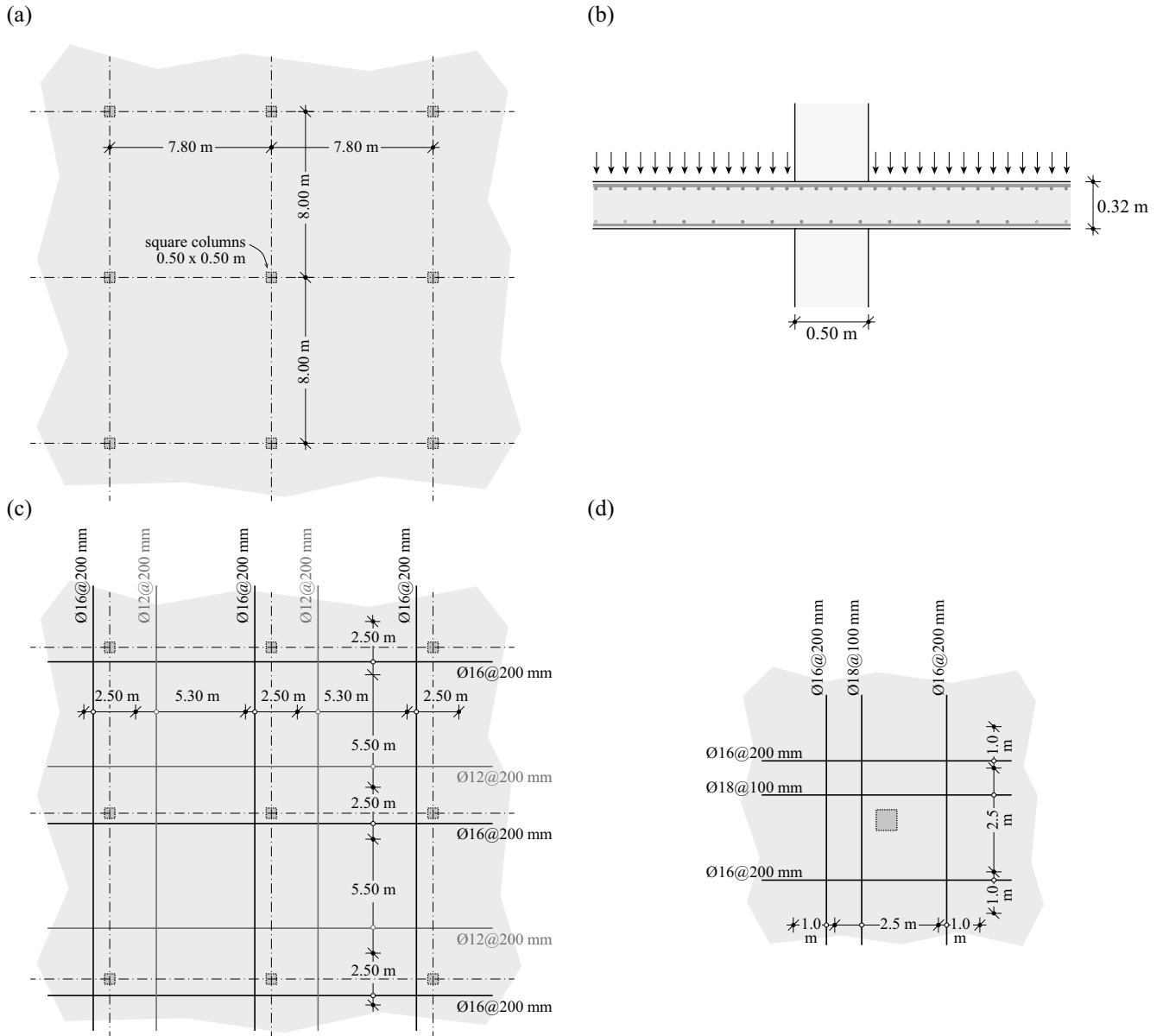


Figure 11. Example of assessment of existing structure: (a) geometry in plan; (b) cross section of slab-column connection; (c) bottom flexural reinforcement ratio; and (d) top flexural reinforcement ratio.

Punching resistance according to Section 8.4 of FprEN 1992-1-1:2022 [42]

The control perimeters b_0 and $b_{0,5}$ are given by:

$$b_0 = 4 \cdot 0.50 = 2.0 \text{ m}$$

$$b_{0,5} = b_0 + 2 \cdot \pi \cdot d_v/2 = 2.0 + \pi \cdot 0.28 = 2.88 \text{ m}$$

The value of the parameter β_e accounting for concentrations of the shear forces due to moment transfer between the slab and the column can be assumed equal to $\beta_e = 1.15$ according to clause 8.4.2(6) (it could also be calculated following a refined methodology). The acting shear stress τ_{Ed} is thus given by:

$$\tau_{Ed} = \frac{\beta_e V_{ed}}{b_{0,5} b_v} = \frac{1.15 \cdot 1.167}{2.88 \cdot 0.28} = 1.66 \text{ MPa}$$

With respect to the shear stress resistance without shear reinforcement, it is given by:

$$d_{dg} = 0.016 + 0.032 = 0.048 \leq 0.040 \Rightarrow d_{dg} = 0.040 \text{ m}$$

$$k_{pb} = 3.6 \sqrt{1 - \frac{b_0}{b_{0,5}}} = 3.6 \sqrt{1 - \frac{2.00}{2.88}} = 1.99 \text{ with } 1 \leq k_{pb} = 1.99 \leq 2.5$$

$$\tau_{Rd,c} = \frac{0.60}{1.40} \cdot 1.99 \left(100 \cdot 0.0091 \cdot 42.8 \cdot \frac{0.040}{0.28} \right)^{\frac{1}{3}} \leq \frac{0.50}{1.40} \sqrt{42.8}$$

$$\Rightarrow \tau_{Rd,c} = 1.51 \leq 2.34 \Rightarrow \tau_{Rd,c} = 1.51 \text{ MPa}$$

As $\tau_{Ed} > \tau_{Rd,c}$, the punching shear resistance without shear reinforcement is insufficient. As $a_p = \sqrt{0.22 \cdot 8.0 \cdot 0.22 \cdot 7.80} = 1.74 \text{ m} < 8d_v = 2.24 \text{ m}$, the punching shear resist-

ance can still be increased with clause 8.4.3(2) adopting

$$a_{pd} = \sqrt{1.74 \frac{0.28}{8}} = 0.247 \text{ m}$$

$$\tau_{Rd,c} = \frac{0.60}{1.40} 1.99 \left(100 \cdot 0.0091 \cdot 42.8 \frac{0.040}{0.28} \right)^{\frac{1}{3}} \leq \frac{0.50}{1.40} \sqrt{42.8}$$

$$\Rightarrow \tau_{Rd,c} = 1.51 \leq 2.34 \Rightarrow \tau_{Rd,c} = 1.57 \text{ MPa}$$

As $\tau_{Ed} > \tau_{Rd,c}$, the punching shear resistance without shear reinforcement is again insufficient following the formulae proposed in Section 8.4 which is tailored for the design of new structures. The Annex I, for existing structures, can be used.

Punching resistance according to Annex I of FprEN 1992-1-1:2022 [42]

Annex I of FprEN 1992-1-1:2022 allows calculating the punching resistance by intersection of the load-rotation relationship and the failure criterion of Eq. (24). This procedure is shown in Figure 12 for the example presented in this section.

In this case, the most accurate load-rotation relationship (red line) is calculated considering a layered sectional model calculated with finite elements accounting for the non-linear behaviour of the concrete and reinforcement (considering tension-stiffening effects and reinforcement yielding). This approach has been assessed by comparing the calculated load-rotation relationship with the experimental values of several benchmark tests. To that aim, the methodology explained in [59] is followed, where the governing rotation is measured at a distance $2d_v$ from the control perimeter. The design shear stress $\tau_{Ed} = 1.59 \text{ MPa}$ is calculated in accordance to clause 8.4.2(6) with the coefficient accounting for the concentration of shear forces (β_e) computed with the refined approach (Table 8.3 of FprEN 1992-1-1:2022 [42]; $\beta_e = 1 + 1.1 \cdot e_b/b_v = 1.10$).

The design punching shear resistance obtained following this procedure is equal to 1.69 MPa , being approximately 10% larger than the one calculated with the closed-form formulae of Section 8.4 (1.57 MPa). Such value allows verifying that the punching resistance is sufficient. In terms of the compliance factor for punching resistance ($\tau_{Rd,c}/\tau_{Ed}$), it increases from 0.95 to 1.06 using Annex I from FprEN 1992-1-1:2022. This allows justifying the structural safety related to punching failures, avoiding expensive (or unnecessary) strengthening measures. The increase on the resistance is in this case mainly associated to the non-linear response of the slab (which accounts for the slab continuity and membrane action). Such effects lead to a stiffer response when compared to the load-rotation relationship obtained with the parabola of Eq. (11) (represented by the dashed black line in Figure 12). As a consequence of the stiffer response, narrower crack widths can be expected and consequently a higher punching resistance.

It shall be noted that Annex I of FprEN 1992-1-1:2022 [42] also allows accounting for the favourable effect of compressive membrane action around internal columns (in absence of large openings or inserts in the vicinity of the column) based on the closed-form expressions for the punching resistance. This is performed by multiplying the factor k_{pt} by an enhancement factor η_{pm} (Clause I.8.5.1). Applying such clause to the present example leads to a punching resistance equal to 1.75 MPa . This result is comparable to the one obtained based

on the nonlinear analysis. Such good agreement between the nonlinear analysis and the closed-form expression with membrane action enhancement is generally found for typical cases if internal columns (comprising regular geometries and usual reinforcement arrangements). For unusual geometries or reinforcement layouts, as well as for corner or edge columns, the nonlinear analysis of the flat slab allows better considering the actual response of the system and leads generally to higher estimates of the resistance.

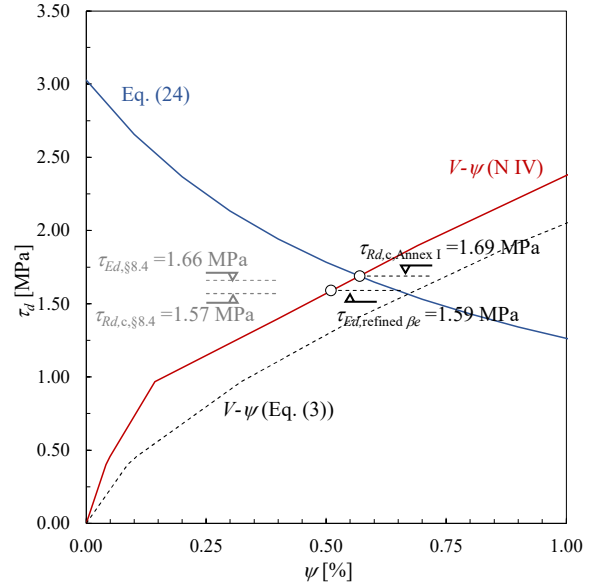


Figure 12. Assessment of existing slab-column connection according to Annex I of FprEN 1992-1-1:2022 [42].

8. CONCLUSIONS

The new provisions for Eurocode 2 (FprEN 1992-1-1:2022 [42]) with respect to punching verification have underwent some major changes. The most significant aspect is that the code, previously based on an empirical formula, has now been based on a mechanical model. This allows for:

- Enhanced consistency of the provisions, with consideration of the different phenomena (such as size and strain effects) in a sound manner
- Allowing for a transparent understanding of the design expressions and the role of the various geometrical and mechanical parameters implied
- Lead to simple formulations for design, but providing a general frame for a more accurate assessment of existing structures

The Critical Shear Crack Theory (CSCT) was selected as the theory to ground the punching shear provisions, but its implementation as performed in *fib* Model Code 2010 was however considered inconvenient for the FprEN 1992-1-1:2022 [42]. Thus, the theory was implemented in an alternative manner considering:

An explicit closed-form formulation for design and simple assessment based on a limited number of physical and me-

chanical parameters. This required some adaptations from the classical formulation, comprising a new definition of the failure criterion and introducing a number of simplifications for ease-of-use.

A general and flexible framework to assess in a detailed manner the punching resistance when the geometrical and mechanical properties of a structure are known in detail. This approach implies intersecting the failure criterion of the CSCT with a suitable load-rotation relationship. Such methodology is typically convenient for assessment of critical existing structures and is provisioned into the Annex I of FprEN 1992-1-1:2022 [42], addressed at existing structures

The proposed approach is shown to lead to consistent results when compared to available test results, and also to be simple to use for practical purposes.

Acknowledgements

The authors of this manuscript want to thank all the members of Task Group 4 of CEN/TC250/WG1 for the fruitful discussions and comments. The authors would also like to thank the help of Diego Hernández Fraile (École Polytechnique Fédérale de Lausanne, Switzerland) for the development of the provisions for maximum punching shear resistance.

References

[1] Fernández Ruiz M., Mirzaei Y., Muttoni A., *Post-Punching Behavior of Flat Slabs*, ACI Structural Journal, V. 110, USA, 2013, pp. 801-812. <https://doi.org/10.14359/51685833>

[2] Silfwerbrand J., Hassanzadeh G., Editors, *International Workshop on punching shear capacity of RC slabs*, Royal Institute of Technology, Stockholm, Sweden, 2000, 527 p.

[3] *fib, Punching of structural concrete slabs*, *fib Bulletin* 12, Lausanne, Switzerland, 2001, 307 p. <https://doi.org/10.35789/fib.BULL.0012>

[4] Polak M. A., Editor, *Punching Shear in Reinforced Concrete Slabs*, SP-232, American Concrete Institute, Farmington Hills, MI, 2005, 302 p. <https://doi.org/10.14359/14960>

[5] *fib, Shear and punching shear in RC and FRC elements*, *fib Bulletin* 57, Lausanne, Switzerland, 2010, 268 p. <https://doi.org/10.35789/fib.BULL.0057>

[6] *fib, Punching shear of structural concrete slabs*, *fib Bulletin* 81, Lausanne, Switzerland, 2017, 378 p.

[7] Comité Euro-International du béton, CEB-FIP Model Code 1990: Design Code, Thomas Telford Ltd., London, England, 1993, 460 p.

[8] CEN, *Eurocode 2: Design of Concrete Structures—Part 1-1: General Rules and Rules for Buildings*, EN 1992-1-1, Brussels, Belgium, 2004, 225 pp.

[9] ACI, *Building Code Requirements for Reinforced Concrete* (ACI 318-14), Farmington Hills, USA, 2014, 524 p.

[10] ACI, *Building Code Requirements for Reinforced Concrete* (ACI 318-19), Farmington Hills, USA, 2019, 624 p.

[11] Zsutty, T.C., *Beam Shear Strength Prediction by Analysis of Existing Data*, ACI Journal Proceedings, V. 65, N. 11, 1968, pp. 943-951

[12] Kinnunen S., Nylander H., *Punching of Concrete Slabs Without Shear Reinforcement*, Transactions of the Royal Institute of Technology, N. 158, 1960, 112 p.

[13] Muttoni, A., *Punching shear – Draft code proposal*, SIA 162, Working Group 5, Swiss Society of Engineers and Architects, Zürich, 1985, 15 p.

[14] SIA, *Code 162 for Concrete Structures*, Swiss Society of Engineers and Architects, Zürich, 1993, 86 p.

[15] Muttoni, A., and Schwartz, J., *Behaviour of Beams and Punching in Slabs without Shear Reinforcement*, IABSE Colloquium, V. 62, Zürich, Switzerland, 1991, pp. 703-708

[16] Muttoni A., *Schubfestigkeit und Durchstanzen von Platten ohne Querkraftbewehrung*, *Beton- und Stahlbetonbau* (In German), Beton-und Stahlbetonbau, V. 98, 2003, pp. 74-84 <https://doi.org/10.1002/best.200300400>

[17] Fernández Ruiz M., Muttoni A., *Applications of the critical shear crack theory to punching of R/C slabs with transverse reinforcement*, ACI Structural Journal, V. 106, N. 4, 2009, pp. 485-494 <https://doi.org/10.14359/56614>

[18] Muttoni A., Fernández Ruiz M., Guandalini S., *Poinçonnement des ponts-dalles*, Documentation SIA, 4. FBH/ASTRA Studientagung 'Neues aus der Brückenforschung', 2007, pp. 85-94

[19] Clément T., *Influence de la précontrainte sur la résistance au poinçonnement de dalles en béton armé* (In French), Doctoral Thesis, EPFL, Lausanne, Switzerland, 2012, N. 5516, 222 p.

[20] Simões J. T., *The mechanics of punching in reinforced concrete slabs and footings without shear reinforcement*, Doctoral thesis, EPFL, Lausanne, Switzerland, 2018, N. 8387, 223 p.

[21] Maya Duque L. F., Fernández Ruiz M., Muttoni A., Foster S. J., *Punching shear strength of steel fibre reinforced concrete slabs*, *Engineering Structures*, V. 40, 2012, pp. 93-94. <https://doi.org/10.1016/j.engstruct.2012.02.009>

[22] Fernández Ruiz M., Muttoni A., Kunz J., *Strengthening of flat slabs against punching shear using post-installed shear reinforcement*, ACI Structural Journal, V. 107 N° 4, USA, 2010, pp. 434-442. <https://doi.org/10.14359/51663816>

[23] Faria D. M. V., Einpaul J., Ramos A.P., Fernández Ruiz M., Muttoni A., *On the efficiency of flat slabs strengthening against punching using externally bonded fibre reinforced polymers*, *Construction and Building Materials*, V. 73, 2014, pp. 366-377. <http://dx.doi.org/10.1016/j.conbuildmat.2014.09.084>

[24] Muttoni A., Fernández Ruiz M., *The levels-of-approximation approach in MC 2010: application to punching shear provisions*, *Structural Concrete*, V. 13, N. 1, 2012, pp. 32-41. <https://doi.org/10.1002/suco.201100032>

[25] Fédération internationale du béton, *fib Model Code for Concrete Structures 2010*, Ernst & Sohn, Germany, 2013, 434 p.

[26] Muttoni A., Fernández Ruiz M., Bentz E., Foster S., Sigrist V., *Background to fib Model Code 2010 shear provisions – part II: punching shear*, *Structural Concrete*, V. 14, N. 3, 2013, pp. 204-214 <https://doi.org/10.1002/suco.201200064>

[27] SIA, *Code 262 for Concrete Structures*, Zürich, Switzerland: Swiss Society of Engineers and Architects, 2013, 102 p.

[28] Muttoni A., *Punching shear strength of reinforced concrete slabs without transverse reinforcement*, ACI Structural Journal, V. 105, N. 4, 2008, pp. 440-450. <https://doi.org/10.14359/19858>

[29] Hegger J., Ricker M., Sherif A. G., *Punching Strength of Reinforced Concrete Footings*, ACI Structural Journal, V. 106, N. 5, 2009, pp. 706-716 <https://doi.org/10.14359/51663111>

[30] Vollum R.L., Abdel-Fattah T., Eder M., Elghazouli A.Y., *Design of ACI-type punching shear reinforcement to Eurocode 2*, *Magazine of Concrete Research*, V. 62, N. 1, 2010, pp. 3-16 <https://doi.org/10.1680/mac.2008.62.1.3>

[31] Siburg C., Häusler F., Hegger J., *Flat slab punching design according to German annex of Eurocode 2*, *Bauingenieur*, V. 87, 2012, pp. 216-225

[32] Siburg C., Ricker M., Hegger J., *Punching shear design of footings: critical review of different code provisions*, *Structural Concrete*, V. 15, 2014, pp. 497-508 <https://doi.org/10.1002/suco.201300092>

[33] Ricker M., Siburg C., *Punching shear strength of flat slabs – critical review of Eurocode 2 and fib Model Code 2010 design provisions*, *Structural Concrete*, V. 17, 2016, pp. 457-468 <https://doi.org/10.1002/suco.201500106>

[34] Einpaul, J., Bujnak, J., Fernández Ruiz, M., Muttoni, A., *Study on influence of column size and slab slenderness on punching strength*, ACI Structural Journal, V. 113, N. 1, 2016, pp. 135-145 <https://doi.org/10.14359/51687945>

[35] Einpaul J., Brantschen F., Fernández Ruiz M., Muttoni A., *Performance of Punching Shear Reinforcement under Gravity Loading: Influence of Type and Detailing*, ACI Structural Journal, V. 113, N. 4, 2016, pp. 827-838 <https://doi.org/10.14359/51688630>

[36] Kueres D., Siburg C., Herbrand M., Classen M., Hegger J., *Uniform Design Method for punching shear in flat slabs and column bases*, *Engineering Structures*, V. 136, 2017, pp. 149-164

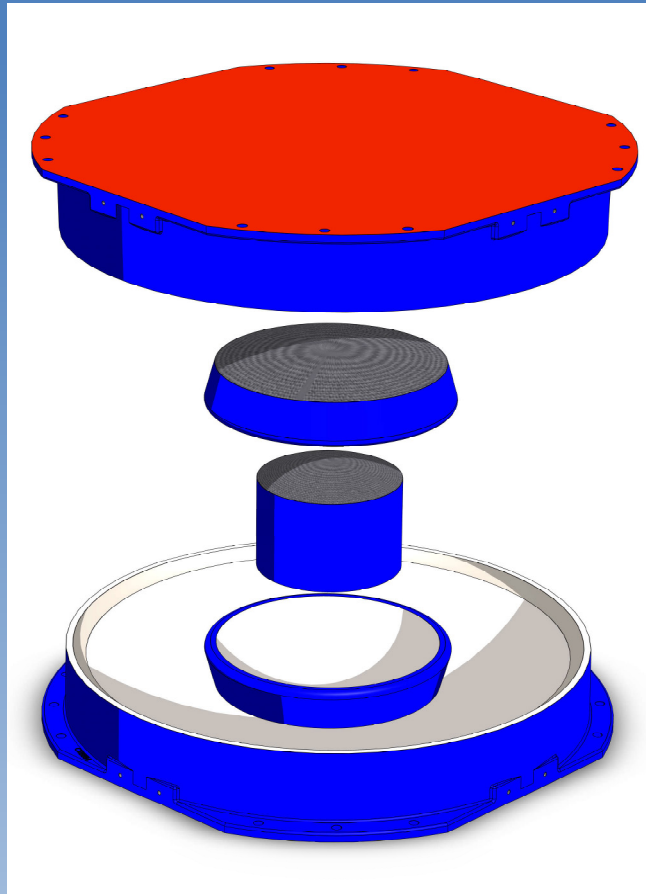
<https://doi.org/10.1016/j.engstruct.2016.12.064>

- [37] Fernández Ruiz M., Muttoni A., *Size effect in shear and punching shear failures: differences between statically determinate members and redundant structures*, Structural Concrete, V. 19, 2018, pp. 65-75, <https://doi.org/10.1002/suco.201700059>
- [38] ECP, *Eurocode Commentary (rev A 31-03-2017)*, European Concrete Platform, Brussels, Belgium, 2008, 220 p.
- [39] HILTI, *Fastening Technology Manual, Post-installed punching reinforcement Hilti HZA-P*, Hilti, 2019, 33 p.
- [40] CEN, *Eurocode 2: Design of Concrete Structures—Part 1-1: General Rules and Rules for Buildings*, Corrigendum, EN 1992-1-1:2004+AC:2010, Brussels, Belgium, 2010, 23 pp.
- [41] CEN, *Eurocode 2: Design of Concrete Structures—Part 1-1: General Rules and Rules for Buildings*, EN 1992-1-1:2004+A1:2014, Brussels, Belgium, 2014, 6 pp.
- [42] CEN/TC 250, *Eurocode 2: Design of Concrete Structures—Part 1-1: General Rules - Rules for buildings, bridges and civil engineering structures*, FprEN 1992-1-1:2022, Brussels, Belgium, 2022-05, 408 pp (this document is available through the National members at CEN TC250/SC2).
- [43] Walkner R., *Kritische Analyse des Durchstanznachweises nach EC2 und Verbesserung des Bemessungsansatzes (In German)*, Doctoral Thesis, Innsbruck University, 2014, 458 p.
- [44] Muttoni A., Fernández Ruiz M., Simões J.T., *The theoretical principles of the Critical Shear Crack Theory for punching shear failures and derivation of consistent closed-form design expression*, Structural Concrete, V. 19, 2018, pp. 174-190, <https://doi.org/10.1002/suco.201700088>
- [45] Fernández Ruiz M., Sagaseta Albajar J., Muttoni A., *La teoría de la fisura crítica como base teórica para el diseño de losas frente a punzonamiento en el nuevo Código Modelo 2010*, Hormigón Y Acero, V.63, N. 263, pp. 49-63, 2012.
- [46] Muttoni A., Fernández Ruiz M., Simões J.T., *The theoretical principles of the Critical Shear Crack Theory for punching shear failures and derivation of consistent closed-form design expression*, Structural Concrete, V. 19, 2018, pp. 174-190, <https://doi.org/10.1002/suco.201700088>
- [47] Muttoni A., Fernández Ruiz M., *Shear in slabs and beams: should they be treated in the same way?*, fib bulletin 57, Lausanne, Switzerland, 2010, pp. 105-128 <https://doi.org/10.35789/fib.bull.0057.ch07>
- [48] Simões J.T., Fernández Ruiz M., Muttoni A., *Validation of the Critical Shear Crack Theory for punching of slabs without transverse reinforcement by means of a refined mechanical model*, Structural Concrete, V. 19, 2018, pp. 191-216, <https://doi.org/10.1002/suco.201700280>
- [49] Muttoni A., Fernández Ruiz M., Simões J. T., *Recent improvements of the Critical Shear Crack Theory for punching shear design and its simplification for code provisions*, Proceedings of 5th fib Symposium, Melbourne, 2018, 14 p.
- [50] Einpaul J., Fernández Ruiz M., Muttoni A., *Measurements of internal cracking in punching tests slabs without shear reinforcement*, Magazine of Concrete Research, V. 70, N. 15, 2018, pp. 798-810 <https://doi.org/10.1680/jmacr.16.00099>
- [51] Vecchio F.J., Collins M.P., *The Modified Compression-Field Theory for Reinforced Concrete Elements Subjected to Shear*, ACI Journal Proceedings, V. 83, N. 2, 1986, pp. 219-231 <https://doi.org/10.14359/10416>
- [52] Guidotti R., *Poinçonnement des planchers-dalles avec colonnes superposées fortement sollicitées (In French)*, Doctoral Thesis, EPFL, Lausanne, Switzerland, 2010, N. 4812, 189 p.
- [53] Walraven J.C., *Fundamental Analysis of Aggregate Interlock*, Journal of Structural Engineering, ASCE, V. 107, N. 11, 1981, pp. 2245-2270
- [54] Tirassa M., Fernández Ruiz M., Muttoni A., *An interlocking approach for the rebar-to-concrete contact in bond*, Magazine of Concrete Research, V. 73, N. 8, 2021, pp. 379-393 <https://doi.org/10.1680/jmacr.20.00209>
- [55] Fernández Ruiz M., *The influence of the kinematics of rough surface engagement on the transfer of forces in cracked concrete*, Engineering Structures, V. 231, N. 15, 2021, 17 p. <https://doi.org/10.1016/j.engstruct.2020.111650>
- [56] Belletti B., Walraven J.C., Trapani F., *Evaluation of compressive membrane action effects on punching shear resistance of reinforced concrete slabs*, Engineering Structures, V. 95, 2015a, pp. 25-39 <https://doi.org/10.1016/j.engstruct.2015.03.043>
- [57] Belletti B., Pimentel M., Scolari M., Walraven J.C., *Safety assessment of punching shear failure according to the level of approximation approach*, Structural Concrete, V. 16, N. 3, 2015b, pp. 366-380 <https://doi.org/10.1002/suco.201500015>
- [58] Setiawan A., Vollum R.L., Macorini L., Izzuddin B.A., *Numerical modelling of punching shear failure of reinforced concrete flat slabs with shear reinforcement*, Magazine of Concrete Research, V. 73, N. 23, 2021, pp. 1205-1224 <https://doi.org/10.1680/jmacr.19.00562>
- [59] Setiawan A., Viúla Faria D.M., Hernández Fraile D., Fernández Ruiz M., Muttoni A., *On the behaviour of exterior slab panels of flat slab buildings*, fib Symposium, Lisbon, June 2021, 12 p.
- [60] Beutel R., Hegger J., *The effect of anchorage on the effectiveness of the shear reinforcement in the punching zone*, Cement and Concrete Composites, V. 24, 2002, pp. 539-549 [https://doi.org/10.1016/S0958-9465\(01\)00070-1](https://doi.org/10.1016/S0958-9465(01)00070-1)
- [61] Lips S., Fernández Ruiz M., Muttoni A., *Experimental Investigation on Punching Strength and Deformation Capacity of Shear-Reinforced Slabs*, ACI Structural Journal, V. 109, 2012, pp. 889-900 <https://doi.org/10.14359/51684132>
- [62] Simões J.T., Bujnak J., Fernández Ruiz M., Muttoni A., *Punching shear on compact footings with uniform soil pressure*, Structural Concrete, V. 17, N. 4, 2016, pp. 603-617 <https://doi.org/10.1002/suco.201500175>
- [63] Simões J.T., Viúla Faria D.M., Fernández Ruiz M., Muttoni A., *Strength of reinforced concrete footings without transverse reinforcement according to limit analysis*, Engineering Structures, V. 112, 2016, pp. 146-161 <https://doi.org/10.1016/j.engstruct.2016.01.010>
- [64] Brantschen F., Viúla Faria D.M., Fernández Ruiz M., Muttoni A., *Bond Behaviour of Straight, Hooked, U-Shaped and Headed Bars in Cracked Concrete*, Structural Concrete, V. 17, N. 5, 2016, pp. 799-810 <https://doi.org/10.1002/suco.201500199>
- [65] Sagaseta J., Muttoni A., Fernández Ruiz M., Tassinari L., *Non-axis-symmetrical punching shear around internal columns of RC slabs without transverse reinforcement*, Magazine of Concrete Research, V.63, N.6, 2011, pp. 441-457 <https://doi.org/10.1680/macrc.10.00098>
- [66] Sagaseta J., Tassinari L., Fernández Ruiz M., Muttoni A., *Punching of flat slabs supported on rectangular columns*, Engineering Structures, V. 77, 2014, pp. 17-33 <https://doi.org/10.1016/j.engstruct.2014.07.007>
- [67] Clément T., Pinho Ramos A., Fernández Ruiz M., Muttoni A., *Influence of prestressing on the punching strength of post-tensioned slabs*, Engineering Structures, V. 72, 2014, pp. 59-69 <https://doi.org/10.1016/j.engstruct.2014.04.034>
- [68] Clément T., Pinho Ramos A., Fernández Ruiz M., Muttoni A., *Design for punching of prestressed concrete slabs*, Structural Concrete, V. 14, N. 2, 2013, pp. 157-167 <https://doi.org/10.1002/suco.201200028>
- [69] Einpaul J., Ospina C. E., Fernández Ruiz M., Muttoni A., *Punching Shear Capacity of Continuous Slabs*, ACI Structural Journal, V. 113, N. 4, 2016, pp. 861-872 <https://doi.org/10.14359/51688758>
- [70] Einpaul J., Fernández Ruiz M., Muttoni A., *Influence of moment redistribution and compressive membrane action on punching strength of flat slabs*, Engineering Structures, V. 86, 2015, pp. 43-57 <https://doi.org/10.1016/j.engstruct.2014.12.032>
- [71] Cavagnis F., Fernández Ruiz M., Muttoni A., *A mechanical model for failures in shear of members without transverse reinforcement based on development of a critical shear crack*, Engineering Structures, V. 157, 2018, pp. 300-315 <https://doi.org/10.1016/j.engstruct.2017.12.004>
- [72] Muttoni A., Fernández Ruiz M., *The Critical Shear Crack Theory for punching design: from a mechanical model to closed-form design expressions*, ACI/fib International Punching Shear Symposium, Bulletin fib 81, 2017, pp. 237-252
- [73] Hernández Fraile D., Simões J. T., Fernández Ruiz M., Muttoni A., *A mechanical approach for the maximum punching resistance of shear-reinforced slab-column connections*, fib Symposium, Lisbon, June 2021, 12 p.
- [74] Muttoni A., Fernández Ruiz M., Simões J.T., Hernández Fraile D., Hegger J., Siburg C., Kueres D., *Background document to section 8.4 – Punching (FprEN 1992-1-1:2022)*, Report EPFL 17-01-R5, December 2022 (in press)
- [75] Muttoni A., Yu Q., *Partial safety factor for strain-based formulae*, presentation to fib TG3.1. Oslo, June 2022, 12 p.
- [76] CEN, EN 13791: Assessment of in-situ compressive strength in structures and precast concrete components, Brussels, Belgium, 2019, 41 p.

Notation

A_{sw}	area of a unit of shear reinforcement	k_1	NDP from NP EN 1992-1-1:2004 [8] with proposed value equal to 0.1
$C_{Rd,c}$	NDP from NP EN 1992-1-1:2004 [8] with proposed value equal to $0.18/\gamma_C$	m_s	acting bending moment in the support strip width
E_c	modulus of elasticity of the flexural reinforcement	m_R	average moment capacity in the support width
E_{sw}	modulus of elasticity of the shear reinforcement	$v_{Rd,c}$	punching shear resistance in the basic control section [MPa] according to NP EN 1992-1-1:2004 [8]
L	spans (indices referring to directions)	v_{min}	NDP from NP EN 1992-1-1:2004 [8] with proposed value equal to $0.035 k_3/2 f_{ck}^{1/2}$
V_E	acting punching shear force	s_r	radial spacing of shear reinforcement between the first and second unit
V_{Ed}	design acting punching shear force	s_t	average tangential spacing of perimeters of shear reinforcement measured at control perimeter
V_{flex}	flexural capacity	s_0	distance from the column face to the axis of the first perimeter of shear reinforcement
$V_{R,c}$	punching shear resistance for members without shear reinforcement	ΣA_{sw}	total area of the activated shear reinforcement in the punching cone
$V_{R,cs}$	punching shear resistance for failures within the shear-reinforced area (concrete contribution)	β_e	coefficient to increase the average acting shear stress on the basic control perimeter to account for the concentrations of shear stresses in FprEN 1992-1-1:2022 [42]
$V_{R,cs}$	concrete contribution for failures within the shear-reinforced area	γ_C	partial safety factor in NP EN 1992-1-1:2004 [8]
$V_{R,cs}$	steel contribution for failures within the shear-reinforced area	γ_{def}	partial safety factor for the rotation in the strain-based approach in Annex I of FprEN 1992-1-1:2022 [42]
$V_{R,max}$	punching resistance associated to the crushing of the concrete struts	γ_V	partial safety factor for shear design in FprEN 1992-1-1:2022 [42]
$V_{R,out}$	punching resistance of failures outside of the shear-reinforced area	φ_w	diameter of a shear reinforcement unit
a_p	distance between the axis of the column and the line of zero radial moment	η_c	factor accounting for the reduction of the concrete contribution to the punching resistance with increasing rotation
b_s	support strip width	η_{pm}	enhancement factor accounting for the favourable effect of compressive membrane action in Annex I of FprEN 1992-1-1:2022 [42]
b_0	perimeter of the support region (perimeter at the column edge minimised for re-entrant corners and columns near to the edge, see Figure 10)	η_s	factor accounting for the increase of the shear reinforcement contribution to the punching resistance with increasing rotation
$b_{0,5}$	control perimeter at a distance of $d_c/2$ from the column face (round corners in case of square or rectangular columns)	η_{sys}	enhancement factor depending on the type of shear reinforcement to be multiplied on the punching shear resistance to calculate the maximum punching shear resistance
$b_{0,5,out}$	outer control perimeter	$\eta_{sys,ab}$	enhancement factor depending on the type of shear reinforcement to be multiplied on the concrete failure criterion to obtain the failure criterion associated with the crushing of the concrete struts
d	effective depth	ψ	rotation
d_{dg}	reference value of roughness of the critical shear crack	ψ_E	rotation associated to the acting shear force V_E
d_{g0}	reference aggregate size ($d_{g0} = 16$ mm for normal weight concrete)	ρ_l	steel reinforcement ratio relating to the bonded tension steel (indices referring to directions)
d_v	shear resisting effective depth	ρ_w	ratio of the vertical shear reinforcement ratio at the investigated control perimeter
$d_{v,out}$	shear-resisting effective depth of the outer perimeter of reinforcement	σ_{cp}	normal concrete stresses in the critical section (indices referring to directions)
d_{sys}	the anchorage performance of the punching reinforcement system and its detailing	σ_{sw}	average stress in the shear reinforcement intercepted by the punching cone
f_b	average bond stress	τ_{Ed}	acting punching shear stress in FprEN 1992-1-1:2022 [42]
f_c	cylinders concrete compressive strength	$\tau_{Rd,c}$	design punching shear stress of members without shear reinforcement in FprEN 1992-1-1:2022 [42]
f_y	yield strength of the flexural reinforcement	$\tau_{Rd,cs}$	design punching shear stress for failures within the shear-reinforced area in FprEN 1992-1-1:2022 [42]
f_{yw}	yield strength of the shear reinforcement		
f_{ywd}	yield strength of the shear reinforcement		
f_{ck}	cylinders characteristic concrete compressive strength		
$f_{ck, is}$	cylinders characteristic concrete compressive strength measured in-situ		
k	factor accounting for the size effect in NP EN 1992-1-1:2004 [8]		
k_m	factor depending on the level of the refinement of the approach used to estimate the acting bending moment in the support width (typically 1.5 for simple analyses and 1.2 when some parameters are known more in detail)		
k_{pb}	punching strength enhancement factor due to the shear field gradient in the control section in FprEN 1992-1-1:2022 [42]		
k_e	reduction factor to be multiplied to the basic control perimeter to account for the concentrations of shear forces		

INGENIERÍA SÍSMICA



JORNADA TÉCNICA

15 JUNIO 2023 | MADRID

PRESENCIAL Y ONLINE

ORGANIZA

ACHE

Asociación Española de
Ingeniería Estructural

www.e-ache-com

COLABORA



POLITÉCNICA

PATROCINAN

MK4 | Innovative
Solutions

Protección frente al Sismo

VSL | A member of
Bouygues Construction

FREYSSINET
SUSTAINABLE TECHNOLOGY

MAURER

WELL LINK
www.wellink.com.tw

mageba
mageba-group.com

Stress Fields and Strut-and-Tie Models as a Basic Tool for Design and Verification in Second Generation of Eurocode 2

Campos de tensiones y modelos de bielas y tirantes: herramientas fundamentales para el proyecto y comprobación de estructuras de hormigón en la segunda generación del Eurocódigo 2

Miguel Fernández Ruiz^{*,a}, Linh Cao Hoang^b, Aurelio Muttoni^c

^a Professor, Universidad Politécnica de Madrid, Spain

^b Professor, Danmarks Tekniske Universitet, Denmark

^c Professor, Ecole Polytechnique Fédérale de Lausanne, Switzerland

Recibido el 1 de julio de 2022; aceptado el 2 de noviembre de 2022

ABSTRACT

Within the frame of the revision of the Eurocode 2 for concrete structures, the section devoted to strut-and-tie design has been updated to enhance its applicability, its consistency with other sections and its ease-of-use. As a result, a number of changes have been introduced. Namely, the use of stress fields and their combination with classical strut-and-tie models has been incorporated. The changes in this section can be seen as an effort to provide a more comprehensive and general tool for designers, that can be transparently applied to any structural member with sufficient reinforcement for crack control. In this paper, the consistency between the strut-and-tie and the stress field methods is clarified as well as the fundamentals of the revision performed in Eurocode 2. The paper also elaborates how the code can be used for advanced analyses, considering in an explicit manner the compatibility of deformations to obtain refined estimates of the structural resistance.

KEYWORDS: Strut-and-tie, stress fields, limit analysis, shear, discontinuity regions, shell design.

©2023 Hormigón y Acero, the journal of the Spanish Association of Structural Engineering (ACHE). Published by Cinter Divulgación Técnica S.L. This is an open-access article distributed under the terms of the Creative Commons (CC BY-NC-ND 4.0) License

RESUMEN

En el marco de la revisión del Eurocódigo 2 para estructuras de hormigón, se ha actualizado el capítulo dedicado al diseño mediante modelos de bielas y tirantes, mejorando su coherencia con otras secciones así como su facilidad de uso. Para ello, se han introducido una serie de cambios, como la consideración del método de campos de tensiones y su combinación con los modelos clásicos de bielas y tirantes. Estos cambios pueden considerarse como un esfuerzo para proporcionar una herramienta más completa y general. En este artículo, se clarifica la coherencia entre los métodos de bielas y tirantes y los campos de tensiones, así como los principios de la revisión efectuada para el Eurocódigo 2. También se explica cómo puede utilizarse dicha norma para realizar análisis avanzados, considerando de manera explícita la compatibilidad de deformaciones con el objetivo de obtener estimaciones precisas de la resistencia.

PALABRAS CLAVE: Bielas y tirantes, campos de tensiones, análisis límite, cortante, regiones de discontinuidad, diseño de lajas.

©2023 Hormigón y Acero, la revista de la Asociación Española de Ingeniería Estructural (ACHE). Publicado por Cinter Divulgación Técnica S.L. Este es un artículo de acceso abierto distribuido bajo los términos de la licencia de uso Creative Commons (CC BY-NC-ND 4.0)

1. INTRODUCTION

Reinforced concrete as a structural material was introduced at the end of the 19th century through a number of patents [1-3].

Almost from the beginning, the engineers realised that traditional design methods rooted in linear elastic theory could not adequately be used to explore the full potential of the new composite material. A new approach was therefore needed and within

* Persona de contacto / Corresponding author.
Correo-e / e-mail: miguel.fernandezruiz@upm.es (Miguel Fernández Ruiz).

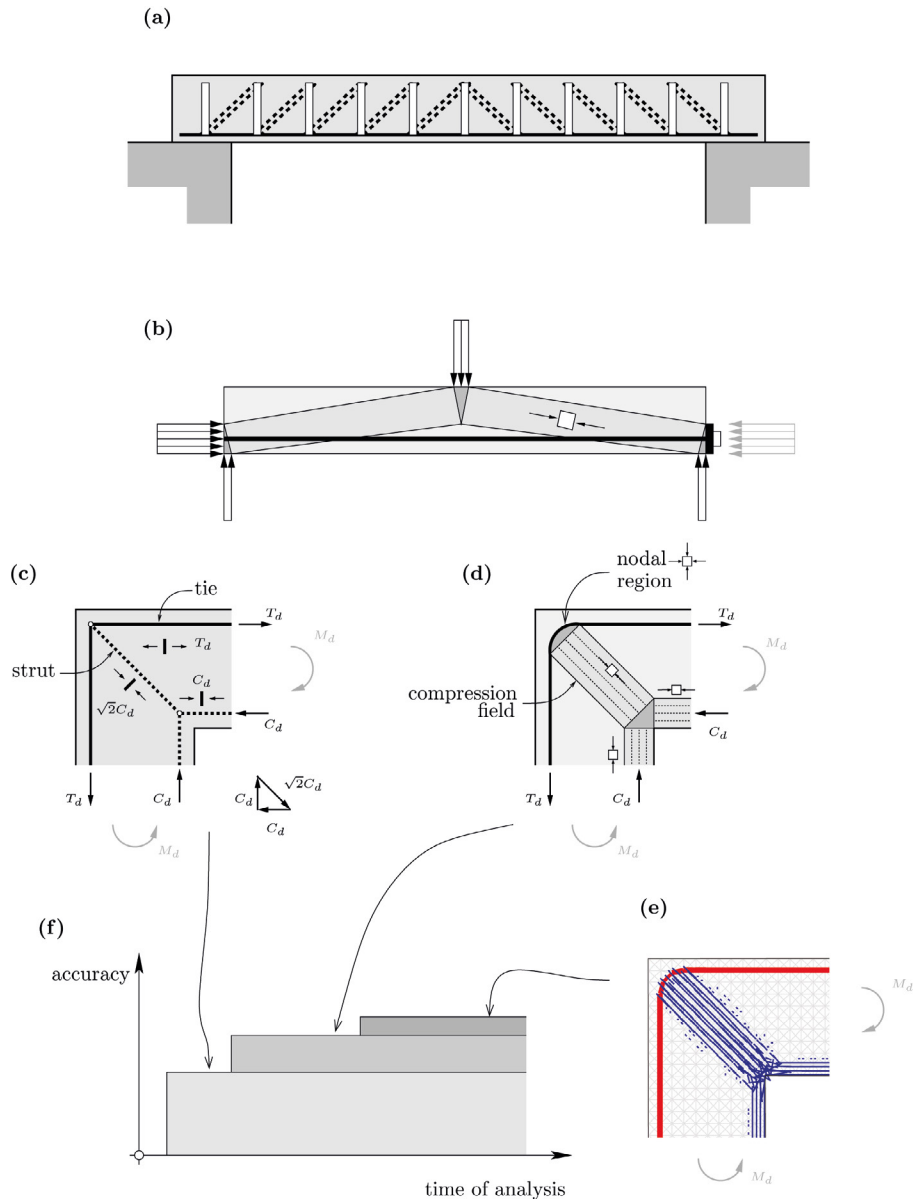


Figure 1. Strut-and-tie and stress fields: (a) truss model (adapted from Ritter [4]); (b) stress field (adapted from Drucker [9]); (c) strut-and-tie model; (d) corresponding rigid-plastic stress field; (e) elastic-plastic stress field; and (f) Levels-of-Approximation approach.

less than a decade, Ritter in 1899 [4] proposed in his pioneering work an engineering approach to characterize the load-carrying actions in cracked reinforced concrete beams. The approach included an idealization of the flow of forces within the cracked concrete element by means of an internal truss system (with concrete struts carrying compression forces and ties representing the reinforcement carrying the tensile forces, see Figure 1a). This concept provided a simple way to understand and to visualize how the element carries loads in the cracked state.

The approach by Ritter was adopted by the community of designers and was given the name *truss analogy* with reference to the widely used steel trusses at that time. The method was further developed by Morsch [5] and later generalised beyond beam design by, amongst others, Leonhardt and co-workers in Stuttgart, (see for instance [6]). The approach was observed to be particularly efficient for design of the so-called *discontinuity regions*, where the Navier-Bernoulli assumption (i.e. plane

sections remain plane) does not hold. Following this school, Schlaich and co-workers systematically developed criteria and guidance on how to arrange appropriate strut-and-tie systems (inspired by the stress trajectories in linear-elastic members and including non-prismatic struts). The work of Schlaich et al. [7-8] had a significant impact in practice and it became clear to the wider engineering community that the method in fact is grounded on the lower-bound theorem of limit analysis and, as such, could be used in a safe manner for design of new structures. During the course of development and generalization of the method, the term *strut-and-tie* was introduced (Figure 1c), representing the resultants of internal stresses and/or forces (the definition “truss analogy” was deliberately abandoned since in many cases, strut-and-tie models become labile trusses which depend on the load configuration).

While strut-and-tie modelling originated from the truss analogy and only in retrospective recognized as a lower bound

method, the concept of stress field modelling for structural concrete was from its infancy directly based on application the lower bound theorem of limit analysis and rigid-plastic theory. The first stress field solutions, and corresponding failure mechanisms, were developed by D. Drucker in 1961 [9] who considered beams without shear reinforcement, see Figure 1b. During the 1960's - 1980's the potential of stress field modelling was utilised extensively, mainly by Thürlimann and co-workers in Zürich and by Nielsen and co-workers in Copenhagen, to address multiple relevant situations in structural concrete (for an overview, see e.g. [10-13]). The method allowed the engineers to take an active role in the design process, by choosing the arrangement of the reinforcement and consequently defining the actual flow of the internal forces.

The classical stress field approach has in recent years experienced a revitalization, where e.g. efficient numerical optimization algorithms have been utilised to solve large-scale problems [14-15]. The approach has furthermore been extended to allow implementation of elastic-plastic [13] as well as nonlinear constitutive laws [16-18], in order to explicitly account for (local) compatibility of deformations (see Figure 1e).

The different origin of classical strut-and-tie modelling and of stress field modelling means that engineers in the past (and perhaps still today due to code formulations) would arrive at different structural layout depending on which of the two concepts/schools they are most acquainted to. Designs based on strut-and-tie models tend to have a discrete nature with extensive use of concentrated reinforcement and with large zones of concrete assumed to be stress-free. On the other hand, designs based on stress fields tend to have a more continuous nature involving potentially smeared stress fields and mesh reinforcement. The different origin of the two methods is also reflected in the way they were implemented during the 1990's into the current version of Eurocode 2 (EN1992-1-1:2004 [19]). In this code, the provisions related to strut-and-tie modelling are very much inspired by the approach formulated by Schlaich et al. [8] and they have almost no connections/references to the plasticity-based methods also implemented in the code for shear design of members with shear reinforcement and for reinforcement design of membrane elements (see e.g. above-mentioned references).

It is, however, important to note that a stress field can always be represented by means of the resultants of stresses (in compression and tension) which in turns leads to a strut-and-tie model (see Figure 1c-d). Both approaches can therefore be seen as complementary tools in the design process [13,20], where the strut-and-tie models are particularly suitable to determine the total amount of reinforcement required in a certain area, while the stress fields allow for a detailed check of the compression fields and nodal regions. The complementary nature of the two methods suits perfectly the so-called Levels-of-Approximation approach, by which successive refinements of the design can be obtained (Figure 1f, [20,21]).

The complementary nature of the two methods will become clearer in the next generation of Eurocode 2 (EN1992-1-1:2004), whose current stable draft is the FprEN1992-1-1:2022 [22]. In this revised version of the

code, the provisions concerning strut-and-tie design have been extensively updated and expanded into a new section named "Design with strut-and-tie models and stress fields". The intention of this new section is to provide the concepts of strut-and-tie models and stress fields in a consistent manner within the plasticity-based framework for ULS design. In this paper, the reasons for improvement of the EN1992-1-1:2004 clauses as well as its implementation and background are presented and discussed. The paper highlights the benefits of the changes, shows a practical design example and discusses on the overall consistency with other parts of FprEN1992-1-1:2022.

2. STRUT-AND-TIE AND STRESS FIELDS: DESIGN AND ASSESSMENT OF CONCRETE STRUCTURES AND REASONS FOR CHANGE IN FprEN1992-1-1

Stress fields and strut-and-tie models are used both for design of new structures as well as for the assessment of existing ones. In the past, codes have been fundamentally oriented towards the design of new structures. However, it can be expected that new generations of codes will meet the demand to have rules and methods explicitly dealing with assessment of existing structures. For instance, FprEN1992-1-1:2022 has a dedicated Annex (Annex I) for the assessment of existing structures, allowing for the use of advanced methods to determine more accurate estimates of the load carrying capacity of members, which e.g. do not fulfil the detailing rules related to new design.

In the frame of limit analysis, design and assessment can be performed following specific considerations taking advantage of the lower- and upper bound theorems of limit analysis [23]. For design, it is convenient to work with different lower bound models (Figure 2a) to decide on the manner to carry the loads within the structure. This gives enhanced freedom to tailor the geometry of the structure and to arrange the reinforcement in the most suitable manner. For assessment of existing structures, the context is different. Here, the geometry and reinforcement arrangement are given and the primary objective is typically to determine the maximum load that can be carried by the structure in order to decide whether the structure needs strengthening. To that aim, upper bounds of the load-carrying capacity based on considerations of different collapse mechanisms

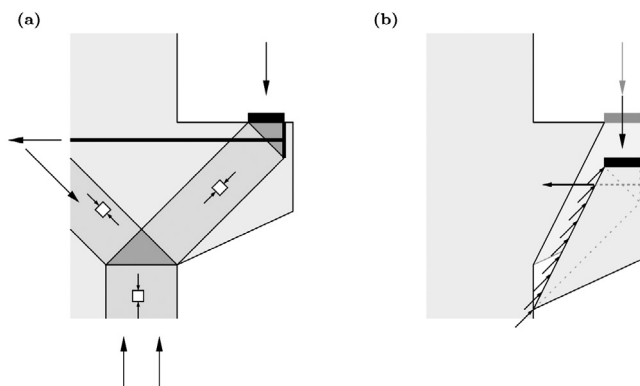


Figure 2. Example of lower- and upper-bound solutions: (a) lower bound (stress field); and (b) upper-bound (mechanism).

(Figure 2b) are particularly useful in the initial phase, as they are easier to establish - especially when dealing with complex geometries and reinforcement arrangements. For more refined estimates of the resistance, supplementary stress fields may be established to determine the gap between the upper- and the lower bound estimates. This strategy allows approaching the exact solution according to limit analysis (when an upper- and a lower bound solution meet [23]).

Exact solutions can be established in simple cases by following hand-made procedures [23]. However, numerical approaches can be needed in complex cases. Such approaches are already available in practice, e.g. efficient optimization procedures to establish the optimum rigid-plastic solution (see e.g. [14-15]) or finite element models based on elastic-plastic material behaviour to determine the load-carrying capacity and the displacement field at collapse (see e.g. [13,24]). The elastic-plastic approach has the advantage of providing equilibrium solutions that fulfil the yield conditions with proper consideration of the strength reduction factors (refer to next section) and at the same time ensuring compatibility of deformations. This eventually leads to a stress field with a corresponding licit failure mechanism and can therefore be interpreted as exact solutions within the frame of limit analysis. Such numerical approaches are state-of-the-art and can be safely used for design [25,26], although they require consideration of more advanced concepts than simple strut-and-tie provisions which can be found in EN1992-1-1:2004.

The necessity for a code addressing the challenges and needs of the structural engineers for the next decades suggested to evolve the provisions of EN1992-1-1:2004 in a series of topics:

- Keeping simplified procedures providing an enhanced freedom for design (lower-bounds), but allowing for ad-

vanced procedures (accounting for compatibility of deformations and consistent with the lower bound methods) to be used in e.g. design optimization and assessment

- Generalizing the strut-and-tie method and considering its combined use with stress fields to verify in a more transparent manner the compression fields and nodal regions
- Providing a more consistent integration of the provisions for design with strut-and-tie and stress field models with other sections of the code. This includes notably the sections on shear, bending and torsion design of linear members with web reinforcement and the Annex on design of membrane, slabs and shell elements

As it can be noted, such changes will enlarge the field of application of the section (with a special significance of assessment). The changes also allow for a progressive refinement of the analysis [21], starting with simple (hand-made) approaches covering most design situations and ending with refined (strain-based) approaches to obtain more accurate estimates, if required.

3. STRESS FIELDS FUNDAMENTALS

The provisions of the FprEN1992-1-1:2022 consider, according to the stress field method, that the external actions are equilibrated by a set of compression fields and tension ties converging at nodal regions. The compression fields, ties and nodal regions can be of concentrated or smeared nature. For instance, in Figure 3a smeared compression fields and ties are considered, while in Figure 3c, they are concentrated elements. On that basis, the corresponding strut-and-tie models can be

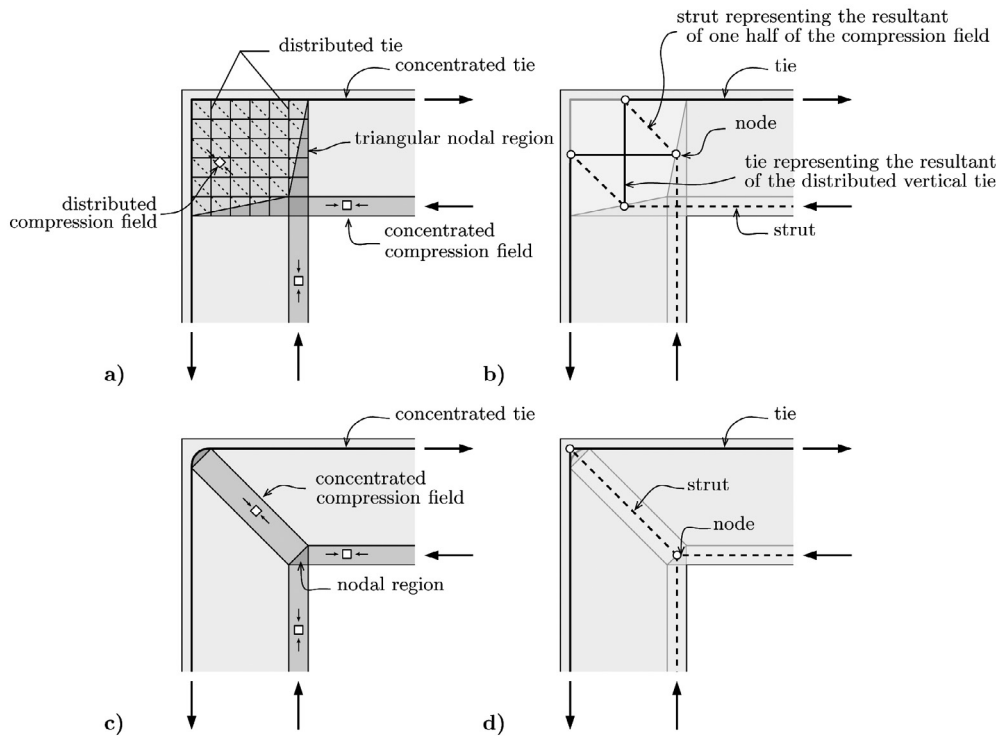


Figure 3. Strut-and-tie and stress fields: (a) stress field considering distributed compression fields and ties; (b) corresponding strut-and-tie model; (c) stress field considering concentrated compression fields and ties; and (d) corresponding strut-and-tie model.

determined, by arranging struts and ties as connectors between nodes of the stress field model (see Figure 3b,d). It can be noted that when a compression field in a panel transfers the forces between its edges (see Figure 3a), the resulting stress field can be designed following a stringer-panel approach [27,28]. In that case, the distributed compression fields result from membrane conditions and the forces at the edges are equilibrated by stringers (concentrated struts and ties).

In order to safely apply approaches based on limit analysis, the structure/member should have sufficient deformation capacity so that redistributions of stresses can occur. In structural concrete, such condition requires normally the member to be provided with a minimum amount of reinforcement (also covering other aspects as the crack localization at serviceability limit state, robustness or to avoid performing other detailed checks) and that the reinforcement has large deformation capacities (normally Ductility Class B or C according to FprEN1992-1-1:2022). These minimum requirements are normally sufficient to prevent crack localization (leading to smeared strains in the member) as well as brittle reinforcement rupture and thereby ensure safe application of the stress field method [20]. It shall be stated that more advanced models can be used to account for reinforcement with limited deformation capacity [20], but the FprEN1992-1-1:2022 does not explicitly suggest methods for so doing. In the following, the methods proposed by FprEN1992-1-1:2022 to verify the resistance of the compression fields and nodal regions will be introduced.

3.1. Compression fields

The verification of compression fields is performed in a direct manner on the basis of the acting stresses and the resistance of the material accounting for its state of strains (as a direct condition for the solution to be considered a lower-bound). This is formulated as follows:

$$\sigma_{cd} \leq v f_{cd} \quad (1)$$

where σ_{cd} is the stress at the location to be verified, f_{cd} is the design value of the compression strength of concrete and v is the strength reduction factor to account for the detrimental influence of transverse strains (the so-called efficiency factor). It shall be noted that in the provisions of EN1992-1-1:2004, the v -factor accounts for strength reduction due to transverse strains as well as concrete brittleness. However, in FprEN1992-1-1:2022, the two effects are separated into two factors, with v solely reflecting the effect of transverse strain (see below) while the effect of brittleness is incorporated into the formulation of f_{cd} :

$$f_{cd} = \frac{f_{ck}}{\gamma_C} \eta_{fc} \quad (2)$$

where f_{ck} and γ_C are, respectively, the characteristic compressive cylinder strength and the partial safety factor. The coefficient η_{fc} is a strength reduction factor, which takes into account the post-peak strain-softening behaviour of concrete, when subjected to uniaxial compression (Figure 4a). This coefficient is in FprEN1992-1-1:2022 given as:

$$\eta_{fc} = \left(\frac{40}{f_{ck}} \right)^{1/3} \leq 1 \quad (3)$$

The formulation of FprEN1992-1-1:2022 adopts the format originally proposed by Muttoni in 1991 [29] and later adopted by Model Code 2010 [30], however with a slightly different reference value (40 MPa instead of 30 MPa). This change is introduced to account for a uniform reliability level for different concrete strengths [31] while keeping a constant value of γ_C .

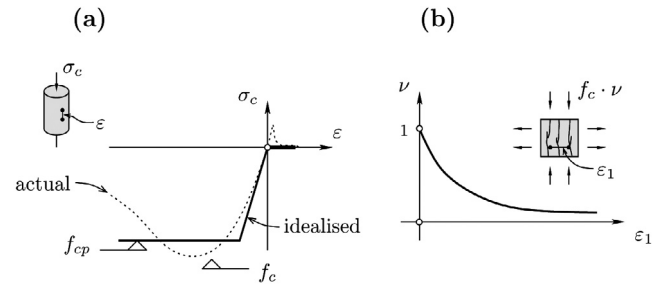


Figure 4. Concrete response: (a) idealised and actual uniaxial response of concrete; and (b) compression softening effect for an element in longitudinal compression and transverse tension.

The influence of transverse cracking on the effective compression strength of concrete is as mentioned above covered by the v -factor (schematically shown in Figure 4b). It was Robinson and Demorieux in 1968 [32] who first documented this phenomenon in tests with membrane elements subjected to biaxial tension-compression. Several researchers have later on studied the phenomenon by means of panel shear tests (as those performed by Vecchio and Collins (1986 [33])), and on that basis suggested constitutive models for concrete which account for the influence of transverse cracking (a detailed state-of-the-art on this topic can be consulted in [20]). It is common in these models, that the first principal tensile strain, ϵ_1 , is adopted as a measure of the level of transverse cracking (thereby assuming the members being sufficiently reinforced to avoid crack localization).

The general approach to account for the influence of strains on the concrete strength is described in the code (FprEN1992-1-1:2022) by means of the following expression:

$$v = \frac{1}{1 + 110 \epsilon_1} \quad (4)$$

where ϵ_1 , as mentioned above, refers to the principal tensile strain (only tensile strains considered, see Figure 4b). This expression is similar to others in the literature and has been developed to suitably fit the results of panels tested under shear and normal forces (refer to Background document to Annex G of FprEN1992-1-1:2022 [34]). It shall be noted that by separating the effect of transverse strains and that of concrete brittleness, it is possible to adopt the same expressions for v and η_{fc} in all of the provisions in FprEN1992-1-1:2022 dealing with strut and tie and stress field modelling. This is an advantage compared to EN1992-1-1:2004. It shall be noted that the evaluation of the v -factor (being dependent on ϵ_1) has to be performed in an indirect manner when rigid-plastic stress fields are used for design purposes. A direct evaluation of ϵ_1 (and thereby of the v -factor) will require methods which are able to determine stress fields that satisfy the compatibility conditions [13], as elastic-plastic methods.

For most cases in practice, however, a direct calculation of ε_1 is unnecessary for design. In fact, it is normally sufficient to assume that the main reinforcement reaches yielding and, on this basis, use the compatibility condition to derive a value for the ν factor. For instance, for beams in bending (Figure 5a) or when a gradient of strains can be assumed through the borders of a panel, the compatibility condition will lead to the following expression (refer to Mohr's circle in Figure 5b):

$$\varepsilon_1 = \varepsilon_x + (\varepsilon_x + 0.001) \cot^2 \theta_{cs} \quad (5)$$

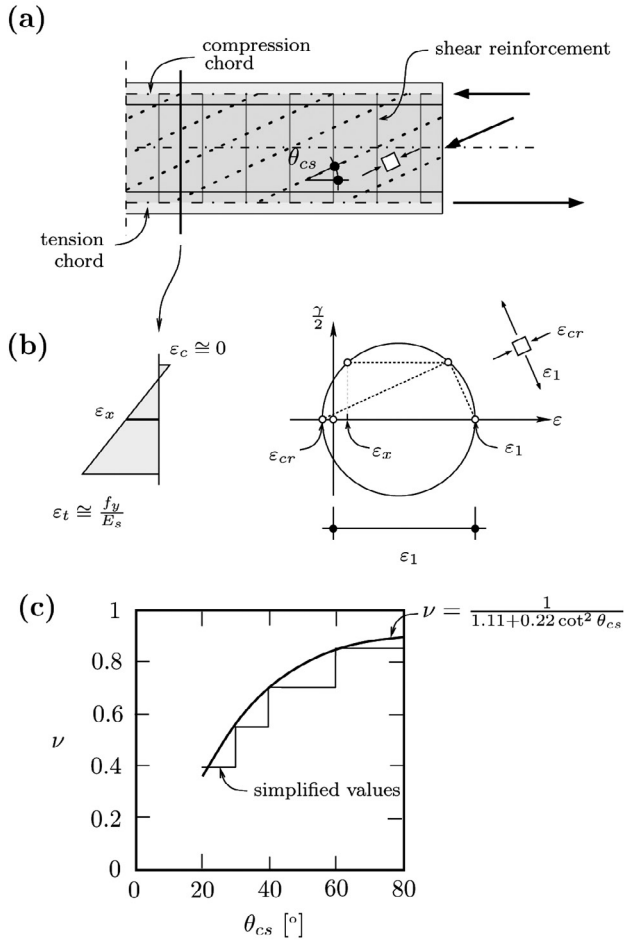


Figure 5. Verification of compression field in webs: (a) variable-angle truss model and direction of compression field; (b) Mohr's circle of strains (at mid-height); and (c) comparison of refined expression for calculation of ν and simplified values.

Where the parameters on which the maximum tensile strain (ε_1) depends are known:

- concrete is assumed at crushing to have a strain equal to approximately -0.1% (for an elastic-plastic response),
- θ_{cs} refers to the angle of the compression field with respect to the x-axis, and
- ε_x refers to the average strain between the top and bottom chords (that, for beams in bending, can be estimated by neglecting the strain of the compressive chord as $\varepsilon_x = \frac{f_y}{2E_s} \cong 0.001$).

And thus, the general expression results in this case:

$$\nu = \frac{1}{1.11 + 0.22 \cot^2 \theta_{cs}} \quad (6)$$

This expression, which is consistent to the one proposed for shear design of beams in FprEN1992-1-1:2022, allows for a detailed calculation of the efficiency factor under the previous assumptions (reinforcement yielding in a panel subjected to a gradient of strains), which covers a large number of cases. It can be further simplified to constant values for convenience, as for instance (figure 5c):

- $20^\circ \leq \theta_{cs} < 30^\circ$ $\nu = 0.40$
- $30^\circ \leq \theta_{cs} < 40^\circ$ $\nu = 0.55$
- $40^\circ \leq \theta_{cs} < 60^\circ$ $\nu = 0.70$
- $60^\circ \leq \theta_{cs} < 90^\circ$ $\nu = 0.85$

For other cases, analogous expressions can be derived depending on the strain conditions of the element. It is also important to note that angles between the strut and the tension ties lower than 20° are not allowed. This ensures that the values of the efficiency factors comply with those stated by the code. However, lower values could be derived if a refined analysis is performed accounting for compatibility of strains.

3.2. Ties

The ties, ensuring the transfer of tensile forces between the loads and/or nodal regions, can be designed or verified by respecting the condition of plasticity (where the acting forces F_{td} shall be lower or equal to the resistance of the ties F_{Rd}):

$$F_{td} \leq F_{Rd} = A_s f_{yd} + A_p f_{pd} \quad (7)$$

Where A_s and f_{yd} refer to the area and yield strength of the reinforcing steel and A_p and f_{pd} to the area and yield strength of the prestressing steel (to be reduced accordingly if the prestressing force is considered as an external action).

3.3. Nodal regions

With respect to the nodal regions, they refer to the zones where the forces are transferred amongst the converging struts and ties. Depending on their configuration (where "C" stands for compression and "T" for tension), they can be classified as:

- CCC nodes: where only compression fields converge to the nodal region
- CCT nodes: in presence of one tie
- CTT nodes: in presence of two ties and one strut
- TTT nodes: with only converging ties

CCC nodes are the most favourable case. They can consist of three or more converging struts, see Figure 6. Such nodal regions are not typically governing for design. Provided that all struts carry the same level of stress, the nodal region can be in a hydrostatic in-plane state of stresses, directly fulfilling the resistance condition ($\nu=1$). In case, where the stresses of the converging struts are not identical, a local spreading of the struts can be assumed (ensured by the minimum reinforcement of the member) or non-hydrostatic nodal regions can be considered. Also, connecting CCC triangular nodal regions by

uniaxial compression fields is a suitable strategy in many cases of complex nodal geometry [35].

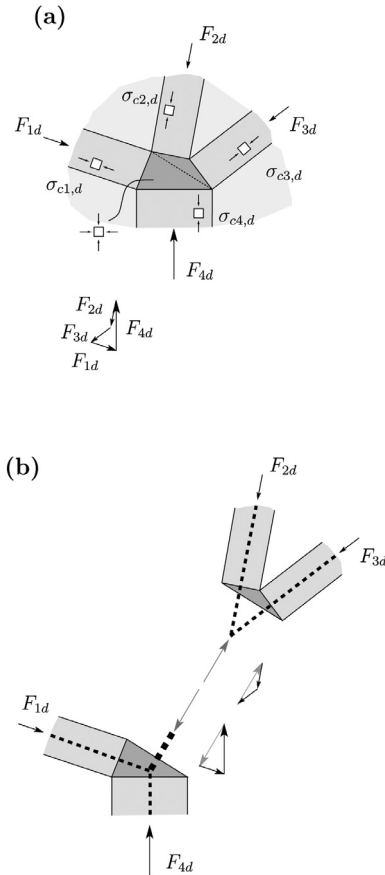


Figure 6. CCC node with four converging struts: (a) detail of the nodal region; and (b) analysis as two CCC nodes of three converging struts.

With respect to CCT nodes and CTT nodes, they can be smeared or concentrated nature. For concentrated nodes, anchorage of the reinforcement can be provided outside of the nodal region, ensuring in-plane hydrostatic conditions ($v=1$ inside the nodal region, see Figure 7a). In this case, the nodal regions are thus governed by the resistance of the converging struts (depending on their angle with the ties). For smeared configurations, the arrangement of the region shall satisfy the anchorage length of the bars, which is usually governing and enhanced by the presence of transverse pressure (see Figure 7c with reduced anchorage length). Intermediate cases of partial

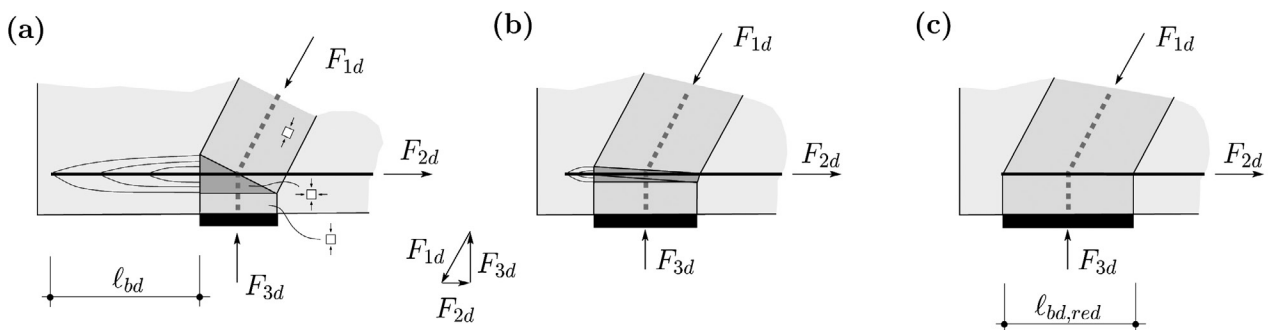


Figure 7. CCT node: (a) concentrated; (b) partly anchored within the nodal region; and (c) fully anchored within the nodal region.

anchorage inside of a nodal region are also accepted (Figure 7b) in FprEN1992-1-1:2022, where the v factor for the node is adopted in a simplified manner as a linear interpolation between the extreme cases (full anchorage outside of the nodal region and full anchorage within the nodal region).

Finally, concerning TTT nodes, its use is discouraged as the evaluation of the v factor is subjected to uncertainties. In case a TTT node is identified, it is advised to modify the layout of the strut-and-tie or stress field model to avoid it (or to pre-stress one direction).

4. REFINED ANALYSES

As previously explained, the approach of stress fields, and particularly its integration within FprEN1992-1-1:2022 allows for an easy implementation by means of numerical analyses. This is explicitly acknowledged in Annex I of FprEN1992-1-1:2022 and can for instance be done following the Elastic-Plastic Stress Field (EPSF) method. Within this approach, the yield conditions of the materials are introduced following an elastic phase [13]. The solution can be obtained in an automated manner based on a classic stiffness-based approach (implemented for instance by means of the Finite Element Method), where a displacement field is calculated fulfilling equilibrium, compatibility of deformations and material constitutive laws (considering the plastic response of concrete).

For the reinforcement, simple link elements can be considered with an elastic-plastic response (with or without strain-hardening), see Figure 8a. This ensures compatibility of deformations as well as respecting the yield conditions of the material. For concrete in uniaxial as well as biaxial compression, an elastic-plastic law can also be adopted. Furthermore, by neglecting the tensile strength of concrete, it is possible to work with a simple quadratic yield surface for plane stress conditions (Figure 8d), corresponding to a Mohr-Coulomb yield condition with a zero-tension cut-off. For plane stress conditions, usual and safe assumption for application of the stress field method, the concrete is subjected to a biaxial state of stresses. Thus, the yield criterion of concrete considers a Mohr-Coulomb yield condition with a tension cut-off (Figure 8d). The plastic strength is reduced consistently with the efficiency factor v (depending on the local state of strains). The stress state is deter-

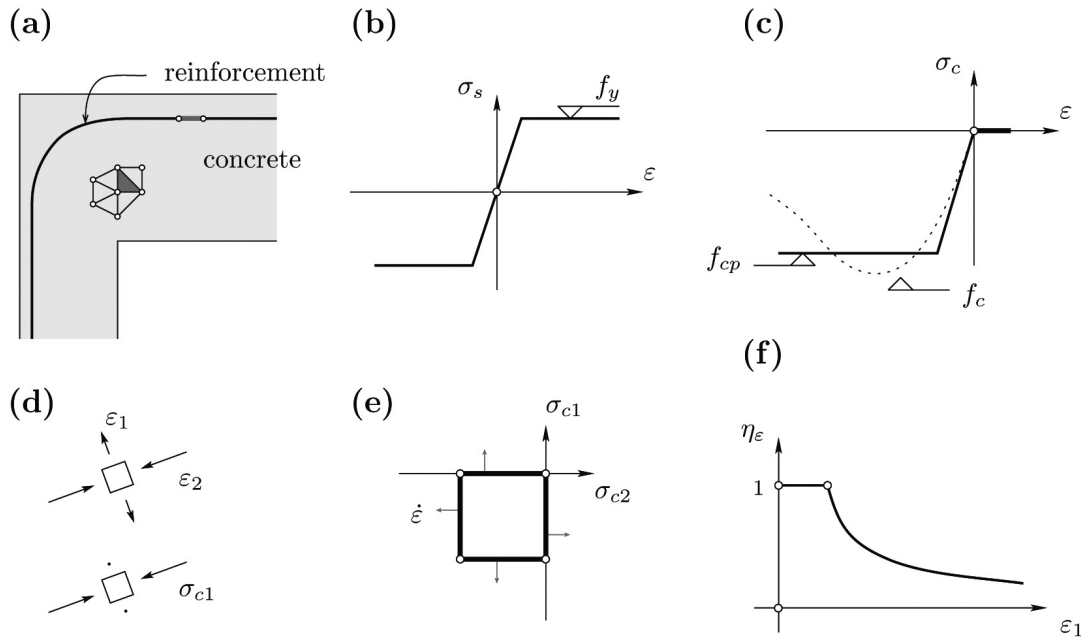


Figure 8. Finite Element Method implementation of Elastic-Plastic Stress Fields: (a) model; (b) constitutive law for steel; (c) strain and stress principal directions; and (d) yield criterion for concrete.

mined considering that the principal directions of the stress tensor and of the strain tensor are coincident, consistently with Nadai [36], Hencky [37] and the tension field model of Wagner [38]. As discussed by Prager [39] and in *fib* [20], for advanced states of deformation (development of a kinematically compatible mechanism), the deformation of the materials in the plastic regions are very large, ensuring convergence to a plastic solution where the stress tensor is considered parallel to the tensor of increment of plastic strains (considering same values for the efficiency factors).

The advantage of this approach is that the compatibility of deformations is respected locally, and thus refined estimates of the strain state and the corresponding v factor can be determined. Also, failure occurs when a kinematically-admissible mechanism develops, ensuring the conditions for an exact solution according to limit analysis (for comparable values of efficiency factors).

The EPSF allows thus for refined estimates of the strength. It considers that the element and materials have sufficient deformation capacity to develop their yield plateau, allowing for potentially large stress redistributions (bounded by the resistance of the materials and namely by the weakening of concrete due to transverse cracking). As discussed above, in order to ensure sufficient deformation capacity of the materials, a minimum amount of reinforcement shall be provided in both directions, avoiding strain localization (associated to brittle failures). This minimum reinforcement shall at least comply with the amount required for elements in shear, and can locally need to respect other conditions depending on the response of the member (such as minimum reinforcement for bending or tension). In addition, the reinforcement shall have sufficient deformation capacity (typically class B or C according to EN1992-1-1:2004). Otherwise, performing a control of its deformation

capacity accounting for the effect of bond on the rupture strain of the reinforcement is required [17,18].

5. EXAMPLE OF APPLICATION

As an example of application, Figure 9a shows the support of a girder built for a project in Lausanne (Switzerland). It refers to a courtyard of a school under refurbishment, where reinforced concrete girders with a slenderness of approximately 13.6 ($= 12.1/0.89$) and 400 mm of width were arranged. The critical detail locates at the left support shown in Figure 9b, where questions arise on how shall such reinforcement be detailed. A rough analysis based on equilibrium considerations (thrust-line analysis), see Figure 9c, shows that, as expected, compression forces develop on the top face, while tension forces develop on the bottom face. However, the thrust line of the compression develops outside of the concrete element, and the thrust line of the tension will require to be deviated to remain within the member.

On that basis, a preliminary strut-and-tie model can be established, see Figure 9d. The model allows locating the main strut and ties and ensuring equilibrium. With this model, the benefits of arranging an inclined reinforcement can be easily acknowledged. Also, it can be noted that the region at the right of the bent of the flexural bar behaves in a similar manner as the end-region of a beam, with a conventional strut-and-tie arrangement. The analysis of the nodal regions shows a CCC node (node B in Figure 9d), a CCT node (node A in Figure 9d) and a CTT node (node C in Figure 9d). It can be noted that for the nodes CCT and CTT, the angle between the strut and the ties does not

respect (at nodes A and C) the minimum angle $\theta_{cs} = 20^\circ$ recommended by the FprEN1992-1-1:2022.

Grounded on these observations, some refinements can be introduced in the strut-and-tie model, Figure 9e, by providing spreading of the struts. Such spreading allows fulfilling the requirements in terms of minimum angles between struts and ties, and needs the arrangement of additional reinforcement in the form of horizontal and vertical bars (stirrups or pins, see Figure 9f). With respect to the region at the right of the bent of the bar, the fan region (with a steeper angle of the resulting strut) and the constant-angle compression field region (with a flatter angle of the resulting strut) can be designed following the standard procedure for shear in members with transverse reinforcement.

Finally, detailed checks can be performed on the basis of stress fields at the critical regions (nodal regions A and B), ensuring that sufficient space is available for development of the struts and nodal regions. To that aim, a constant and safe value of the efficiency factor is adopted ($\nu = 0.55$ ac-

counting for the angles of the struts and ties), allowing to analyse all nodes under plane-stress hydrostatic conditions, see Figure 9f. The results show that this aspect is not critical. Also, detailing of the reinforcement can be consistently established, in terms of type of reinforcement and anchorage lengths.

For a final optimisation, or in case the performance of the detailed needed to be assessed, a refined EPSF analysis could also be performed. The results are shown in Figure 10 for two cases. The first considers only inclined reinforcement and stirrups at the right of the bend (Figures 10a-d), corresponding to the reinforcement layout of Figure 9d. The latter considers also an additional horizontal and vertical reinforcement in the discontinuity region (Figures 10e-h), corresponding to the reinforcement layout of Figure 9f. In all cases, the load was applied by means of a stiff plate, distributing it into the concrete surface.

When only inclined reinforcement is provided in the discontinuity region (Figures 10a-d), a similar response to that of Figure 9d results, with an inclined compression field devel-

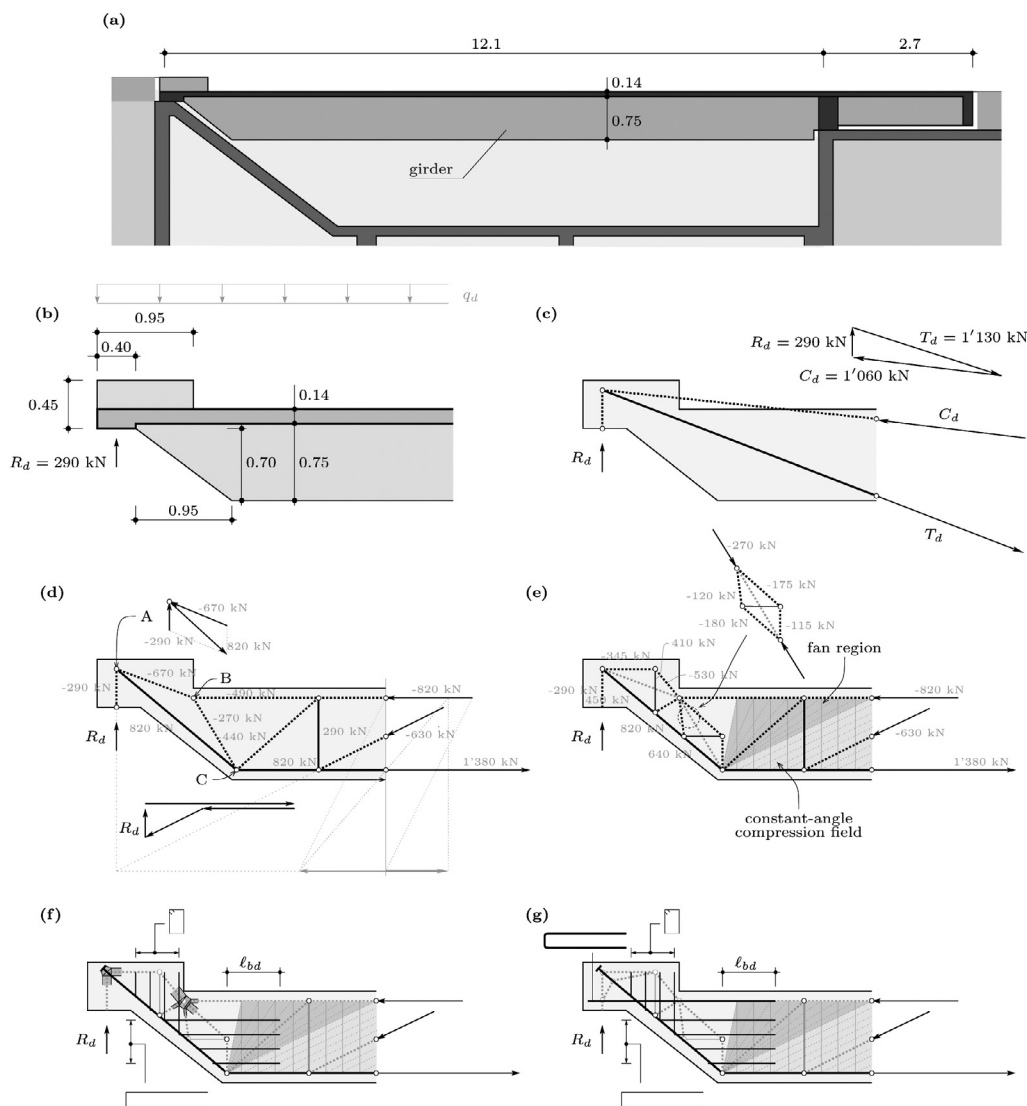


Figure 9. Example of application: (a) element investigated; (b) critical detail; (c) analysis based on thrust line; (d) strut-and-tie model (with lines for analysis with graphic statics shown in light grey); (e) refined strut-and-tie model; (f) stress field verifications and reinforcement layout; and (g) enhanced detailing.

oping between the bent of the reinforcement and the convex corner of the compression face (point B in Figure 9d). As it can be noted, the value of factor ν becomes very low in the region where the compression field is rather parallel to the tie (refer to dark-shaded area in Figure 10c). The member thus fails with a severely reduced concrete strength before yielding of any reinforcement (failure attained at $R_{Rd} = 110$ kN, lower than the applied action $R_d = 290$ kN).

A suitable response is on the contrary confirmed when the reinforcement is arranged according to the strut-and-tie model of Figure 9e. The value of factor ν is consistent with the one proposed by the codes (refer to Figure 10g) and failure occurs by yielding of the flexural reinforcement. It can be noted that the yielded zone of the inclined reinforcement (indicated in brown in Figure 10e) develops at the same location as the critical zone according to the refined strut-and-tie model (Figure 9e). In this case, with the reinforcement designed according to the lower-bound solution of Figure 9f, it results a member resistance equal to $R_{Rd} = 351$ kN. The over-strength with respect to the design load is mainly justified by the activation of the horizontal stirrups as flexural reinforcement in the critical region and by rounding of the required diameters of the flexural bars. It can also be noted the important role of the horizontal reinforcement near to the loading plate, which deviates the load introduction (local yielding in Figure 10e). Such reinforcement can, in fact, be increased to avoid local cracking issues, as shown in Figure 9g. Finally, it shall be considered that verification of the cracking state or other serviceability limit states might be governing, which can be performed according to specific models (fib 2021).

8. CONCLUSIONS

The current draft for the revision of Eurocode 2 (FprEN1992-1-1:2022) maintains the strut-and-tie method as a basic tool for the design of discontinuity regions of concrete structures. Its scope has been enlarged by introducing the stress field method for verification of the compression fields and nodal regions and the full consistency of the two approaches is highlighted in the new standard. As a result, the designer has a consistent tool to design both discontinuity regions (where the assumption that plane sections remain plane does not hold) and beam regions (where deformed sections can be assumed to remain plane). Also, the same method can be consistently applied for the design of membrane elements. The provisioned rules are in addition simple to apply and have clear physical meaning, enhancing the ease-of-use of the code and the understanding of the code by engineers.

The draft for the new Eurocode 2 also encourages the use of refined analyses based on the stress field method. Such analyses consider the compatibility of deformations and allow more accurate estimates of the strength reduction factor accounting for the state of concrete cracking. These analyses are particularly useful for the assessment of existing structures, where the different load-carrying actions can be considered in an explicit manner.

It is the belief of the authors that the changes introduced in the code will address in a more comprehensive manner the challenges of structural engineers in the years to come, providing them with a sound tool for understanding, designing and assessing structural concrete.

Acknowledgements

The authors of this manuscript want to thank the engineers Antonio Garcia Blanco, Dr. João T. Simões and Dr. Duarte V. Faria (Muttoni et Fernández, ingénieurs conseils SA, Switzerland) for their help in preparing the example and for their fruitful discussions during preparation of the manuscript.

Notation

A_p	: cross section area of prestressing
A_s	: cross section area of reinforcement
C_d	: design value of compression force
E_s	: modulus of elasticity of reinforcement
F_{Rd}	: design value of resistance in tension
F_{td}	: design value of tension force
R_d	: design value of reaction
T_d	: design value of tension force
f_{cd}	: design value of uniaxial compressive resistance of concrete
f_{ck}	: characteristic value of uniaxial compressive resistance of concrete
f_{cp}	: plastic strength of concrete in compression
f_{pd}	: design value of the yield strength of the prestressing
f_y	: yield strength of reinforcement
f_{yd}	: design value of the yield strength of reinforcement
l_{bd}	: design value of anchorage length
$l_{bd,red}$: design value of anchorage length (reduce by transverse pressure)
ϵ_1	: principal tensile strain
ϵ_2	: principal compressive strain
ϵ_c	: strain in compression chord
ϵ_{cr}	: crushing strain of concrete
ϵ_t	: strain in tension chord
ϵ_x	: strain in the x direction
γ	: shear strain
γ_C	: partial safety factor of concrete
η_{fc}	: brittleness factor of concrete
ν	: compression softening efficiency factor for concrete cracking
σ_{cd}	: design value of the stress in the concrete
σ_{c1}	: principal tensile stress of concrete
σ_{c2}	: principal compressive stress of concrete
θ_{cs}	: inclination of compression field

References

- [1] Hennebique F. (1892), Combination of steel and ciment to create light and highly resistant beams (in French: Combinaison particulière du métal et du ciment en vue de la création de poutres très légères et de haute résistance), French patent, No 223 546
- [2] Hennebique F. (1893), Combination of steel and ciment to create light and highly resistant beams (in French: Combinaison particulière du métal et du ciment en vue de la création de poutres très légères et de haute résistance), French patent (patent added to the previous patent of 1892), No 223 546
- [3] Coignet E. (1892), New building system with straight or curved beams and flat plates of masonry or iron (in French: Nouveau système de construction avec poutres droites ou courbes et plate-bandes en maçonnerie et fer combinés), French patent, No 226 634.

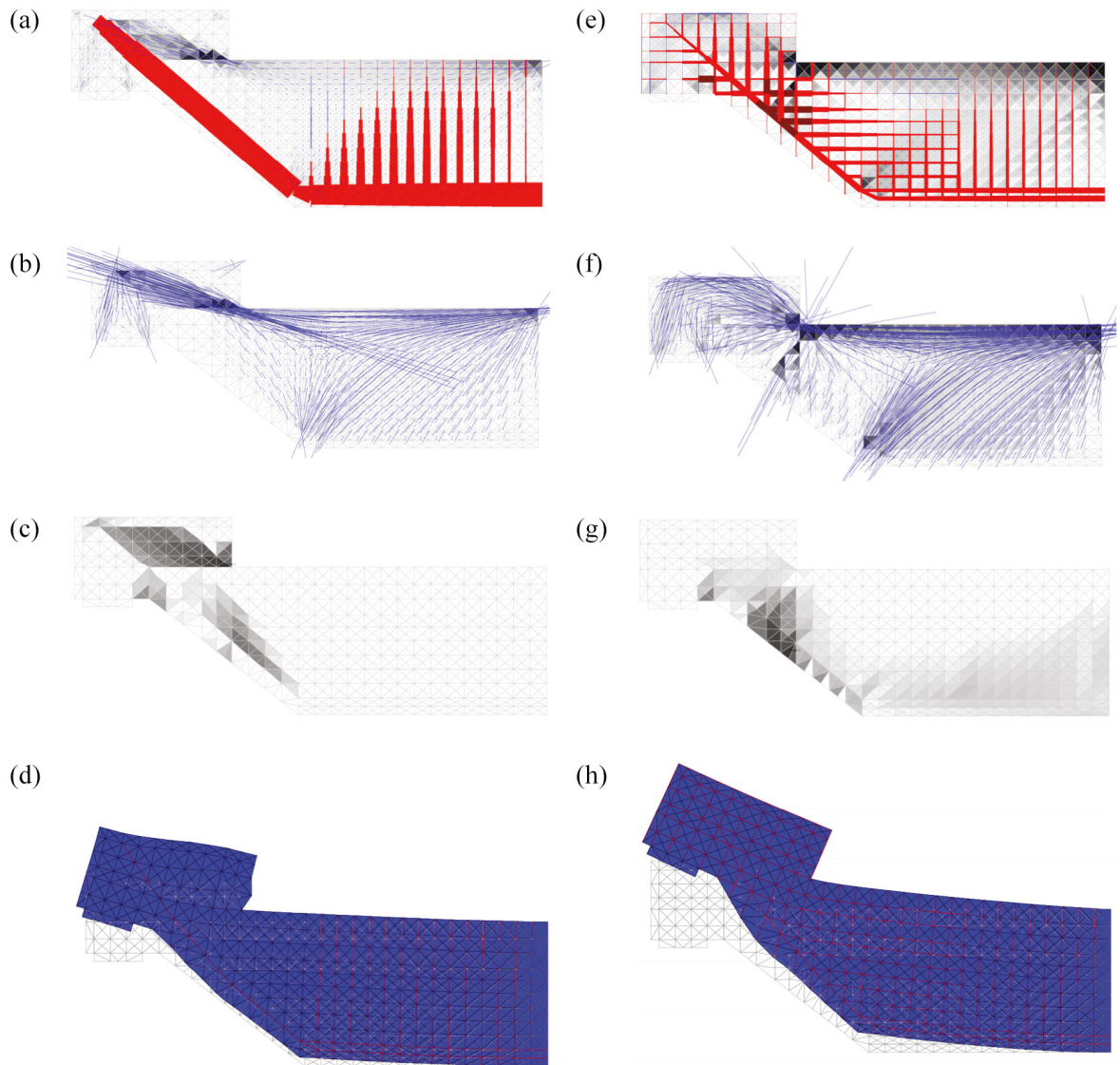


Figure 10. Example of application, use of EPSF: (left column) case with only inclined reinforcement; and (right column) case with additional horizontal and vertical reinforcement. Results at failure: (a,e) relative stresses at the reinforcement and concrete (red refers to tension and blue to compression; for the reinforcement, brown means yielding and for the concrete black means crushing); (b,f) detail of concrete stresses; (c,g) value of ν factor (black means $\nu = 0$, white $\nu = 1$); and (d,h) deformed shapes at failure.

- [4] Ritter, W. (1899), The Hennebique construction method (in German, Die Bauweise Hennebique), Schweizerische Bauzeitung, XXXIII, N° 7, pp. 41-61. <http://doi.org/10.5169/seals-21306>
- [5] Mörsch, E. (1908), Reinforced concrete construction, theory and application, (in German, Der Eisenbetonbau, seine Theorie und Anwendung), 3rd edition, Verlag von Konrad Wittwer, 1908, 376 p.
- [6] Leonhardt F. and Walther, R. (1966), Deep beams (in German, Wandartige Träger), Deutscher Ausschuss für Stahlbeton, Heft 178, Berlin, 159 pp.
- [7] Schlaich, J. and Weischede, D. (1982), "A practical method for methodical design and building in reinforced concrete" (in German, "Ein praktisches Verfahren zum methodischen Bemessen und Konstruieren im Stahlbetonbau"), Bulletin d'Information n° 150, Comité Euro-International du Béton, 163 pp.
- [8] Schlaich, J., Schäfer, K. and Jennewein, M. (1987), "Toward a consistent design of structural concrete", Prestressed Concrete Institute Journal, May-June, pp. 75-150. <https://doi.org/10.15554/pcij.05011987.74.150>
- [9] Drucker, D.C. (1961), On Structural Concrete and the Theorems of Limit Analysis, Publications, International Association for Bridge and Structural Engineering, V.21, Zürich, Switzerland, pp. 49-59.
- [10] Nielsen, M. P., and Hoang, L. C. (2011), Limit Analysis and Concrete Plasticity, 3rd edition, CRC Press, Boca Raton, FL, 796 pp.
- [11] Thürlimann, B., Marti, P., Pralong, J., Ritz, P. and Zimmerli, B. (1983), Application of the plasticity theory to reinforced concrete (in German, Anwendung der Plastizitätstheorie auf Stahlbeton), Institut für Baustatik und Konstruktion, ETH Zürich, 252 pp.
- [12] Muttoni, A., Schwartz, J., Thürlimann, B. (1997), Design of concrete structures with stress fields. Birkhäuser, Basel, Switzerland, 143 p.
- [13] Fernández Ruiz M., Muttoni A. (2007), On Development of Suitable Stress Fields for Structural Concrete, ACI, Structural Journal, Vol. 104 n°4, pp. 495-500. <https://doi.org/10.14359/18780>
- [14] Andersen, H. M. (2017), Numerical Limit Analysis of Precast Concrete Structures - A framework for efficient design and analysis, PhD Thesis, DTU, Rapport No. R-383, 251 p.
- [15] Jensen, TW; Poulsen, PN; Hoang, LC (2019), Layer model for finite element limit analysis of concrete slabs with shear reinforcement. Engineering Structures, Vol. 115, pp. 51-61, 2019. <https://doi.org/10.1016/j.engstruct.2019.05.038>

- [16] Lourenco, M. S., Almeida, J. F. (2013), Adaptive Stress Field Models: Formulation and Validation, *ACI, Structural Journal*, Vol. 110, No. 1, pp. 71-81.
- [17] Ferreira M. (2020), Studies of cyclic behaviour of concrete coupling beams (in Portuguese: Estudo de zonas de descontinuidade de betão estrutural sujeito a ações cíclicas através de modelos de campos de tensões). PhD Thesis. University of Lisbon.
- [18] Kaufmann, W., Mata-Falcón, J., Weber, M., Galkovski, T., Tran, Kabelac, J., Konecny, M., Navrátil, J., Cihal, M., Komarkova, P. (2020) *Compatible Stress Field Design of Structural Concrete: Principles and Validation*. ETH Zurich and IDEA StatiCa s.r.o, ISBN 978-3-906916-95-8, 2020, 158 pp.
- [19] EN1992-1-1:2004 (Eurocode 2), Design of concrete structures-Part 1-1: General rules and rules for buildings, European Committee for Standardization (CEN), 225 p., Brussels, Belgium, 2004.
- [20] fib WP 2.2.4 (2021), M. Serio Lourenço and M., Fernández Ruiz, Editors), "Design and assessment with strut-and-tie models and stress fields: from simple calculations to detailed numerical analysis", *fib, Structural Concrete Federation, Bulletin No 100*, 2021, 235 p.
- [21] Muttoni, A., Fernández Ruiz, M. (2012), Levels-of-Approximation approach in codes of practice, *Structural Engineering International, Journal of the International Association for Bridge and Structural Engineering (IABSE)*, Switzerland, Vol. 2, pp. 190-194. <https://doi.org/10.2749/101686612X13291382990688>
- [22] FprEN 1992-1-1:2022, Design of concrete structures - Part 1-1: General rules, rules for buildings, bridges and civil engineering structures, Version of the draft of the 2nd generation of Eurocode 2 for Formal Vote, European Committee for Standardization (CEN), Brussels, Belgium, 30.05.2022 (this document is available through the National members at CEN TC250/SC2)
- [23] Muttoni, A., Fernández Ruiz, M., Niketic, F. (2015), Design versus assessment of concrete structures using stress fields and strut-and-tie models, *American Concrete Institute, Structural Journal*, Vol. 112, No. 5, pp. 605—615. <https://doi.org/10.14359/51687710>
- [24] Vestergaard, D., Larsen K.P., Hoang, L. C., Poulsen, P.N., Feddersen, B. (2021) Design-oriented elasto-plastic analysis of reinforced concrete structures with in-plane forces applying convex optimization, *Structural Concrete*, Vol. 22, pp. 3272–3287. <https://doi.org/10.1002/suco.202100302>
- [25] Muttoni, A., Fernández Ruiz, M., Niketic, F., Backes, M. R. (2016), Assessment of existing structures based on elastic-plastic stress fields-Modelling of critical details and investigation of the in-plane shear transverse bending interaction, *Département fédéral des transports, des communications et de l'énergie, Office fédéral des routes, Rapport 680*, Bern, Switzerland, 134 p.
- [26] Yu, Q., Valeri, P., Fernández Ruiz, M., Muttoni, A. (2021), A consistent safety format and design approach for brittle systems and application to Textile Reinforced Concrete structures, *Engineering Structures*, Elsevier, Vol. 249, 113306, pp. 1-20. <https://doi.org/10.1016/j.engstruct.2021.113306>
- [27] Blaauwendraad, J. (2018), *Stringer-Panel Models in Structural Concrete applied to D-region design*, SpringerBriefs, Springer, 125 p.
- [28] Fernández Ruiz, M., Hoang, L.C. (2021), The Elastic-Plastic Stress Field method for structural concrete design: a complementary perspective to the use of rigid-plastic design approaches, *Proceedings of the Danish Society for Structural Science and Engineering (Bygningsstatistiske Meddelelser)*, Vol. LXXXIX, Nr. 3-4, 09-2018, Copenhagen, Denmark, pp. 45—73
- [29] Muttoni, A. (1991), The applicability of the theory of plasticity in the design of reinforced concrete (in German: Die Anwendbarkeit der Plastizitätstheorie in der Bemessung von Stahlbeton), PhD thesis, ETH, Zürich, 164 p.
- [30] fib (2013), *Model Code for Concrete Structures 2010*, Ernst & Sohn, 434 p. <https://doi.org/10.1002/suco.202000211>
- [31] Moccia, F., Yu, Q., Fernández Ruiz, M., Muttoni, A. (2020), Concrete compressive strength: from material characterization to a structural value, *Structural Concrete*, Wiley, Vol. 22, pp. 1--21 (<https://doi.org/10.1002/suco.202000211>)
- [32] Robinson, J. R. and Demorieux, J. M. (1968), Test in tension-compression of specimens representing webs of reinforced concrete beams (in French: Essai de Traction-Compression sur Modèles d'Ames de Poutre en Béton Arme), *Compte Rendu Partiel I, U.T.I., Institut de Recherches Appliquées du Béton Arme*, Paris, France, 43 p.
- [33] Vecchio F. J., Collins M. P. (1986) The Modified Compression-Field theory for Reinforced Concrete Elements Subjected to Shear, *ACI Journal Proceedings*, Vol. 83, No. 2, pp. 219-231. <https://doi.org/10.14359/10416>
- [34] Hoang, L.C. (2021), Background Document to Annex G - Design of membrane-, shell- and slab elements, CEN/TC250/SC2/WG1/TG4, Background Document for prEN1992-1-1:2021, 11 p. (this document is available through the National members at CEN TC250/SC2)
- [35] Schlaich, M., Anagnostou, G. (1990) Stress Fields for Nodes of Strut-and-Tie Models, *ASCE, Journal of Structural Engineering*, Vol. 116, No. 1, 1990, pp. 13-23. [https://doi.org/10.1061/\(ASCE\)0733-9445\(1990\)116:1\(13\)](https://doi.org/10.1061/(ASCE)0733-9445(1990)116:1(13))
- [36] Nadai, A (1923) The beginning of yielding regime in bars under torsion (in German: Der Beginn des Fließvorganges in einem tordierten Stab), *Journal of Applied Mathematics and Mechanics/Zeitschrift für Angewandte Mathematik und Mechanik* 3.6 (1923), pp. 442–454.
- [37] Hencky, H. (1924) On a theory of plastic deformations and the corresponding stresses (in German: Zur Theorie plastischer Deformationen und der hierdurch im Material hervorgerufenen Nachspannungen). *Journal of Applied Mathematics and Mechanics/Zeitschrift für Angewandte Mathematik und Mechanik* 4.4 (1924), pp. 323–334.
- [38] Wagner, H. (1929). Flat plate beams with very slender webs (in German: Ebene Blechwandträger mit sehr dünnen Stegblech), *Zeitschrift für Flugtechnik und Motorluftschiffahrt*, Vol. 20, pp. 200-207, 227-233, 279-284, 306-314.
- [39] Prager, W. (1948), The theory of plastic flow versus theory of plastic deformation, *Journal of Applied Physics*, Vol. 19, pp. 540-543. <https://doi.org/10.1063/1.1698170>

Serviceability Limit States According to the New Eurocode 2 Proposal: Description and Justification of the Proposed Changes

Estados Límite de Servicio de acuerdo con la propuesta del nuevo Eurocódigo 2: Descripción y justificación de los cambios introducidos

Alejandro Pérez Caldentey^{*,a}, Juan Luis Bellod Thomas^b, Lluís Torres^c, Terje Kanstad^d

^aTechnical University of Madrid (UPM). FHECOR Consulting Engineers

^bCesma, Technical University of Madrid (UPM)

^cUniversitat de Girona (UdG)

^dNorwegian University of Science and Technology (NTNU)

Recibido el 8 de septiembre de 2022; aceptado el 26 de enero de 2023

ABSTRACT

In this paper the main changes introduced into FprEN 1992-1-1:2023¹ [1] with respect to the current version of EC2 (EN 1992-1-1:2004) [2] with regard to cracking and deflection calculations are introduced and justified. The changes introduced into the cracking formulation account for the variation of stresses in the tensioned zones for bending, the effect of the casting position and the influence of curvature on the increase of surface crack widths. The introduction of these effects, together with a reformulation of the effective area allow for a reduction of scatter in the model when compared to experimental data. For deflections, a simplified method is introduced which is fully consistent with the general method and allows practical application by providing correction factors to be applied to linear elastic calculations. From this method a formulation for the slenderness limits is deduced. This formulation is the basis for the table-based method to avoid deflection calculations. Finally, coefficients are derived to translate the slenderness limits of beams to the slenderness limits of slabs supported on isolated columns and slabs supported on walls

KEYWORDS: cracking, flexure, tension, deflections, EN 1992-1-1, MC 2010, bond conditions, slabs.

©2023 Hormigón y Acero, the journal of the Spanish Association of Structural Engineering (ACHE). Published by Cinter Divulgación Técnica S.L. This is an open-access article distributed under the terms of the Creative Commons (CC BY-NC-ND 4.0) License

RESUMEN

En este trabajo se introducen y justifican los principales cambios introducidos en la norma FprEN 1992-1-1:2023² [1] con respecto a la versión actual del EC2 (EN 1992-1-1:2004) [2] en relación con los cálculos de fisuración y flechas. Los cambios introducidos en la formulación de la abertura de fisura tienen en cuenta la variación de las tensiones en la zona traccionada en flexión, el efecto de la posición de hormigonado y la influencia de la curvatura en el aumento de la abertura de fisura entre el nivel de la armadura y la fibra más traccionada. La introducción de estos efectos, junto con una reformulación del área efectiva, permiten reducir la dispersión del modelo respecto de los datos experimentales. Para las flechas, se introduce un método simplificado que es totalmente coherente con el método general y permite la aplicación práctica al proporcionar factores de corrección que se aplican a los cálculos elástico-lineales. De este método se deduce una formulación para los límites de esbeltez. Esta formulación es la base del método basado en tablas para evitar los cálculos de flechas. Por último, se obtienen coeficientes para extrapolar los límites de esbeltez de las vigas a los límites de esbeltez de losas apoyadas en pilares aislados y de losas apoyadas en muros.

PALABRAS CLAVE: fisuración, flexión, tracción, flechas, EN 1992-1-1, MC 2010, posición de hormigonado, losas.

©2023 Hormigón y Acero, la revista de la Asociación Española de Ingeniería Estructural (ACHE). Publicado por Cinter Divulgación Técnica S.L. Este es un artículo de acceso abierto distribuido bajo los términos de la licencia de uso Creative Commons (CC BY-NC-ND 4.0)

1.- FprEN 1992-1-1:2023 is available through the National members of CEN TC250/SC2 until approval as EN.

2.- El documento FprEN 1992-1-1:2023 puede obtenerse a través de los miembros nacionales del comité CEN TC250/SC2 hasta que sea aprobado como norma EN.

* Persona de contacto / Corresponding author:
Correo-e / e-mail: apc@fhecor.es (Alejandro Pérez Caldentey).

1. INTRODUCTION

The work on the revision of Eurocode 2 started in 2012. The technical content of the revised document was approved by CEN-TC-250/SC2 in June 2022. The revision has therefore taken about 10 years. It is expected that the current draft will be ready for a formal vote in April 2023, but it will still not be fully operational until 2027 since the countries need to draft the National Annexes and there will be a transition period. This standard, when approved, will replace the standard approved in 2004. It can therefore be stated that between revisions of the European standards a period of 25 to 30 years can easily go by.

Some of the goals of the revision were to update the code incorporating the latest state-of-the-art, improve ease-of-use and reduce the number of nationally determined parameters.

In the revision of Section 7 Serviceability Limit States of EN 1992-1-1:2004 [2] (Section number updated to Section 9), significant changes have been made to the cracking model that allow a reduction in scatter by introducing important effects which have been neglected up to now and can be credited with significant discrepancies between calculated and observed crack width values. These effects have to do with the distribution of stresses (tension or flexure), with the effect of casting position, and with the effects of curvature. These effects will be explained in detail and be illustrated using experimental evidence below. Also, since this is still a matter of controversy in some countries, the importance of accounting for the effect of cover will also be dealt with.

Additionally, content from EN 1992-3:2006 [3] has been incorporated into EN 1992-1-1, particularly considerations regarding the boundary conditions of elements subjected to imposed strains (whether a wall or a slab is restrained at the ends or at the edges.) This should help designers to better understand cracking and how when the restraint is on the edges, the differential strain between steel and concrete is mainly determined by the imposed strain whereas when the element is restrained at the ends, it depends on the cracking load.

Regarding deflections, the general method (ζ -method) has been kept as it was, since it provides relatively good approximations to tests [4] and relies on a robust model. However, in order to improve ease of use, a simplified formulation has been introduced which is consistent with the general method but is much easier to apply by practitioners. This method allows performing a linear elastic calculation to obtain the deflection and correct this calculation to account for cracking and tension stiffening effects. This method also forms the basis for the definition of slenderness limits (span-to-depth ratios).

2. JUSTIFICATION OF THE MODEL FOR THE DETERMINATION OF CRACK WIDTHS

2.1. Main changes in the model

The main changes introduced in the model (see Eq. (1)) are a factor to account for distribution of stresses (k_{β}) and a factor to account for casting position (k_b), both of which affect

the bond term of the crack spacing equation, the introduction into the crack formulation of the curvature factor ($k_{1/r}$) and the formulation of the model in terms of mean values, with an explicit coefficient (k_w) to go from mean crack width values to characteristic values. The reason for this last change is that calibrations can only be meaningfully performed considering the mean values measured in the tests.

Note that the predicted crack width is the crack at the surface of concrete. In the authors' opinion it is important that the formulation describes a magnitude that can be measured so that the formulation may be tested against experimental evidence, which is the basis of the scientific method.

$$s_{r,m,cal} = 1.5c + \frac{1}{7.2} k_{\beta} k_b \frac{\phi}{\rho_{s,eff}}$$
$$\varepsilon_{sm} - \varepsilon_{cm} = \frac{\sigma_s - k_t \frac{f_{ctm}}{\rho_{eff}} (1 + \alpha \rho_{eff})}{E_c} \geq 0.6 \frac{\sigma_s}{E_c} \quad (1)$$

$$w_{k,cal} = k_w k_{1/r} s_m (\varepsilon_{r,m,cal} - \varepsilon_{c,m}) \geq 1.7 k_{1/r} s_{r,m,cal} (\varepsilon_{sm} - \varepsilon_{cm})$$

In the following the need for these change will be discussed in detail.

2.2. The importance of accounting for cover

There is overwhelming evidence that cover is a significant factor to explain the crack spacing ([5] [6] [7] [8]) and should be explicitly accounted for. This is done by adding a cover term to the bond term when determining the crack spacing. Deniers of this fact have argued that this effect is already accounted for in the definition of the effective area, which, in fact, depends on the cover. However, the tests carried out at the Universidad Politécnica de Madrid in 2009¹ ([7]), clearly demonstrated that this was not enough by testing three pairs of otherwise identical elements (specimens 25-20-XX and 25-70-XX where XX stands for the stirrup spacing in cm going from 00 (no stirrups) to 10 cm and 30 cm) having very different covers (32 and 82 mm) but the nearly same effective area as per the definition included in EN 1992-1-1:2004. The specimens with the higher cover had a maximum crack width opening which was twice as large as that of the specimens with the smaller cover. It was quite notable that for a service stress in reinforcement of only 250 MPa (determined on the basis of a cracked section) the maximum measured crack width was around 0.6 mm, much higher than the values normally deemed admissible (see Figure 1).

There has been an attempt ([9]) to explain this difference by claiming that in Specimens 25-70 the stabilised cracking was not reached whether as in specimen 25-20 it was and therefore different values of the bond strength could explain this behaviour. Unfortunately, this hypothesis is not supported by the experimental data which shows that for both tests

1 All specimens were RC sections subjected to a constant bending zone, having a width of 350 mm, a height of 450 mm, all reinforced with 4 bars in tension. The naming of the specimens is AA-BB-CC, where AA is the bar diameter in mm, BB is the cover to the stirrups in mm (12 mm stirrups) and CC is the stirrup spacing in cm in the constant moment zone area. CC=00 means there are no stirrups.

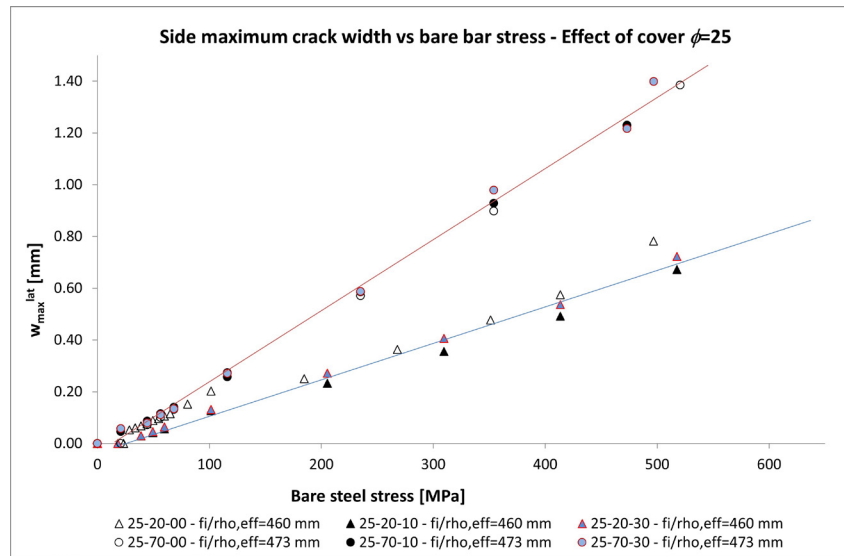


Figure 1. Maximum crack width measured in identical specimens with different covers and nearly the same effective area [7]. The maximum crack within the specimens with larger cover doubles the maximum crack width in the specimens with the smaller cover. The crack width, w_{max}^{lat} is measured at the side of the beam at the level of the tension reinforcement.

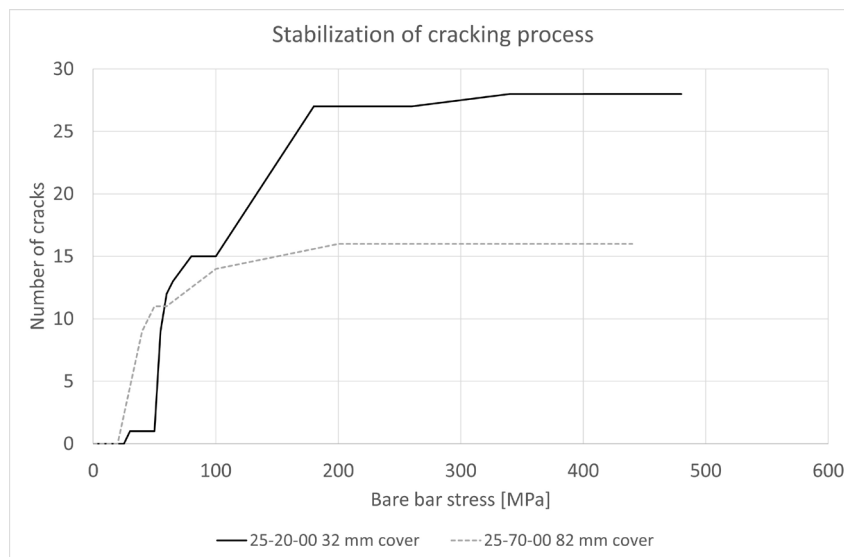


Figure 2. Number of cracks as a function of the steel stress for specimens 25-20-00 and 25-70-00. The crack pattern is stabilized for a stress in steel of about 200 MPa.

stabilized cracking is reached at a stress in the reinforcement of about 200 MPa, as shown in Figure 2.

Given this information, the authors of this paper consider the need for an additive cover term to be a settled matter. The physical explanation for this term is that internal cracks (Goto cracks) form at each rib. A larger proportion of these cracks tend to close before reaching the surface for elements with larger covers. This effect is not modelled by bond theory and thereby requires the corresponding correction in the form of an additive cover term.

2.3. Effect of casting position

It is a well-established fact (e.g., see [2], [10], and [11]) that casting position affects the required anchorage length of reinforcing bars. In ULS, the anchorage length has traditionally

been increased by a factor of 1.4 for bars in horizontal elements which are close to the top surface. This modification has to do with the appearance of voids under the top bars due to plastic settlement and bleeding, which reduces the bond perimeter of the bar. Even though cracking has to do with bond (and a bond factor has been present in codes – for instance factor k_l in EN 1992-1-1:2004 which accounts for the different bond properties of ribbed and smooth bars) casting position has – to the knowledge of the authors – never been considered in models dealing with crack spacing [12].

However, tests carried out at the Universidad Politécnica de Madrid (UPM), show strong evidence that casting position has a substantial effect on crack spacing. The flexural specimens 12-70-00 and 12-70-F tested in 2009 [7] and 2017 [13], respectively, with identical geometry (though slightly different concrete mix proportions), showed substantial differences in crack spacing

Comparison of beams 12-70 (tested in 2017 and in 2009)

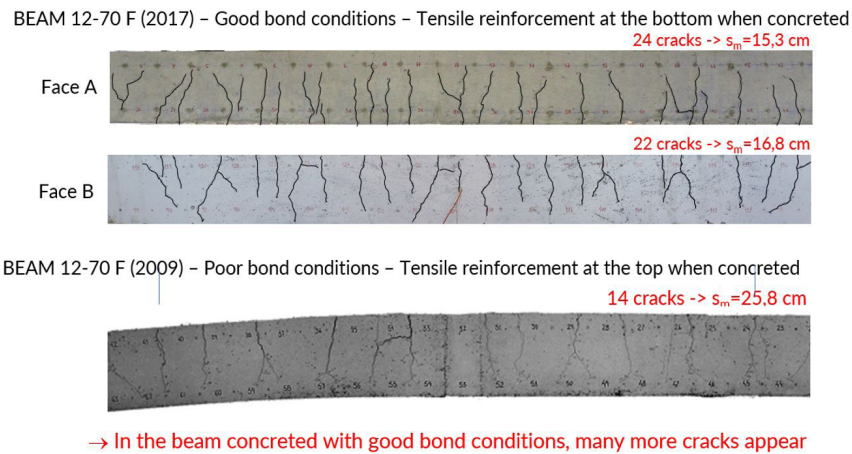


Figure 3. Cracking patterns of beams cast in 'good' casting position (top) and 'poor' casting position (bottom).

TIE 16-20 T

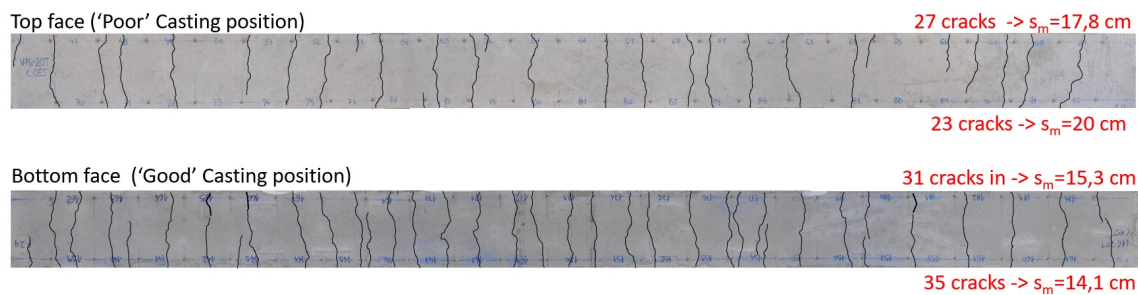


Figure 4. Cracking pattern of a tie showing different crack spacing on different faces.

(see Figure 3). Besides the concrete mix (which is known not to have an important effect on cracking), the only difference was the casting position of the tension reinforcement. In the beam tested in 2009, the tensile reinforcement was cast in 'poor' casting position (top), while in the test carried out in 2017, it was cast in 'good' casting position (bottom). The beam tested in 2009 showed a mean crack spacing of 258 mm, while the element tested in 2017 showed a mean crack spacing of only 161 mm.

The effect of casting position has been confirmed by analysis of the cracking pattern of ties, where the face cast in good casting position has a definite tendency to develop a cracking pattern with more closely spaced cracks. Figure 4² also illustrates this fact using results of specimen 16-20-T tested in 2017.

Given this evidence a more systematic study was undertaken at the Universidad Politécnica de Madrid [14]. In this study companion flexural tests were performed in good casting conditions for flexural specimens previously tested in poor casting conditions. Additionally for one of the tests, 25-20-B, the earlier with poor bond conditions was repeated. The results of this study, which includes tests carried out in 2009, 2017, 2018 and 2020, are summarized in Table 1. In all cases, the face concreted in poor conditions showed a larger

crack spacing when compared to the face of the corresponding specimen concreted in good bond conditions. Additionally, the table shows that workmanship has a significant influence on this effect. For specimen 25-20-B, the increase in elements concreted in the laboratory is only 11.3%, while the effect is 51.1% when comparing with an element cast on site with poor bond conditions.

While the effect of bond conditions on cracking is clear from these results, it has not been studied before. Because of this the evidence is still scant and does not allow the formulation of an experimentally validated model, even though the results clearly show an effect of the workmanship, as noted above, and possibly an effect of the bar diameter and the cover. Because of the lack of data, the new formulation proposes fixed-value coefficients which are meant to be a recognition that this effect exists and that need to be improved in the future as further data becomes available. The effect is therefore accounted for by a coefficient k_b , which affects the bond term of the crack spacing equation and adopts a value of 0.9 for good bond conditions and 1.2 for poor bond conditions.

2.4. Effect of the distribution of stresses

A new coefficient is suggested to model the effect of uneven distribution of stresses when dealing with elements subjected to bending.

² The beam was rotated when tested so that the two faces shown were subjected to identical forces from self-weight.

TABLE 1.
Effect of casting position as measured in tests carried out at UPM (taken from [4]).

SPECIMEN	Mean Crack Spacing according to Bond Condition (mm)				
	Good	Poor Lab.	Increase	Poor On-site	Increase
12-20-B-X	115	-	-	173	50.4%
16-20-T-X	147	170.5	16.0%	-	-
16-20-B-X	105	109.8	4.6%	-	-
25-20-T-X	115	171	48.7%	-	-
25-20-B-X	86.7	96.5	11.3%	131	51.1%
12-70-B-X	162	-	-	236	45.7%
16-70-T-X	220	232	5.5%	-	-
16-70-B-X	183	188	2.7%	-	-
25-70-T-X	184	230	25.0%	-	-
25-70-B-X	148.3	-	-	227	53.1%
Average	-	-	16.2%	-	50.1%

To account for this effect, in EN 1992-1-1:2004 [2], the model for crack spacing includes coefficient k_2 defined as follows (Eq. (2)):

$$k_2 = \frac{(\varepsilon_1 + \varepsilon_2)}{2\varepsilon_1} \quad (2)$$

where ε_1 and ε_2 are the greater and lesser tensile strains in the section ($\varepsilon_2=0$ if part of the section is compressed.) With this definition $k_2=1.0$ in tension and 0.5 in flexure.

The rationale behind the above factor is that, in bending, the transfer length will be shorter because the tension force per meter of width (coloured area in Figure 5) that has to be transferred by bond to the effective concrete area from an existing crack to produce a new crack will be half that in pure tension because the strain of the least tensioned fibre is zero, and therefore the transfer length would also be half. The current Eurocode 2 (EN 1992-1-1:2004) formulation, however, instead of providing small crack spacings in flexure, is calibrated in such a way that the model results in notoriously exaggerated crack spacings for tension elements (see [15] Figure 1).

The above reasoning, as shown in Figure 5, is not sound because what matters is not the stress gradient within the full tensile zone itself but rather the tensile gradient within

the effective area around the bar. In a bending element of significant height, the effective area can represent only a small part of the cross-section in tension and the approximation of a tie, as done in MC 2010 [16] can be reasonable. However, in small elements, the model of EC2 would be better. Figure 6 demonstrates that, for tension, the mean stress, σ_{mean} , in the effective area will be f_{ctm} when the next crack occurs. However, in the case of flexure with the simplifying assumption of a linear distribution, the mean stress can be determined as shown in Eq. (3):

$$\begin{aligned} \sigma_{mean} &= \frac{1}{2} (f_{ct,eff} + \sigma_{c,min,ef}) = \frac{1}{2} \left(f_{ct,eff} + \frac{f_{ct,eff}}{h-x_g} (h-x_g - h_{c,eff}) \right) = \\ &= f_{ct,eff} \frac{1}{2} \underbrace{\left(1 + \frac{(h-x_g - h_{c,eff})}{h-x_g} \right)}_{k_{fl}} \end{aligned} \quad (3)$$

where x_g is the depth of the neutral axis in the uncracked section and k_{fl} is the coefficient accounting for the distribution of stresses. This expression results in a value for k_{fl} of 1.0 for pure tension ($x_g=\infty$) and of 0.5 in pure flexure if $h_{c,eff}$ is equal to $(h-x_g)$.

For a rectangular cross section and pure bending, the expression for k_{fl} of Eq. (3) simplifies to Eq. (4):

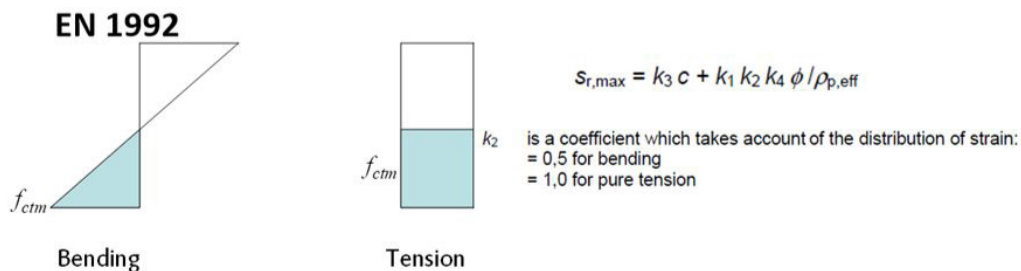


Figure 5. Effect of distribution of stresses prior to cracking on transfer length according to EN 1992-1-1:2004.

Flexure – stress in effective area is variable

Tension – stress in effective area is constant

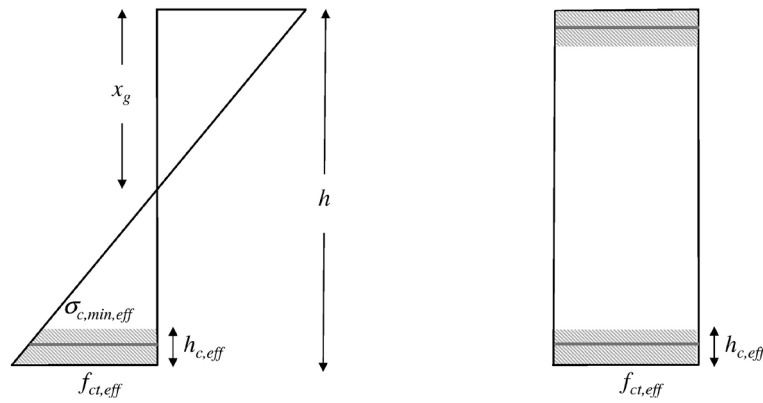


Figure 6. Consideration of the effective tensile area around a bar in flexural elements.

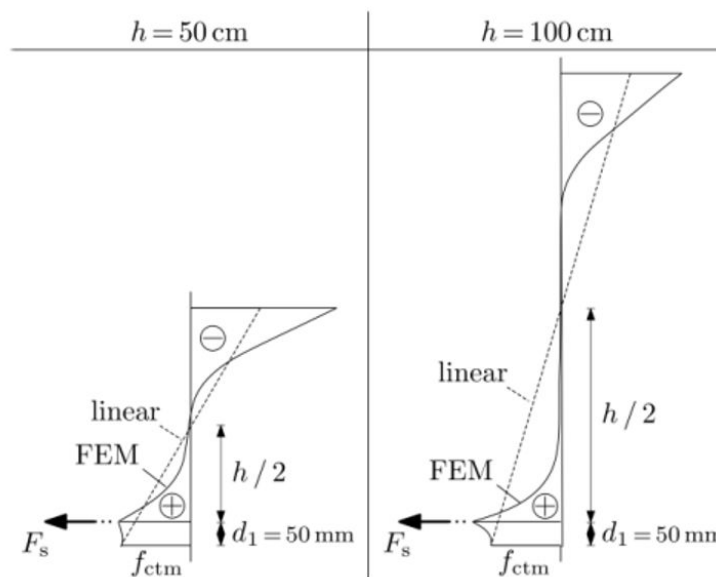


Figure 7. FEM estimate of stresses between cracks [9]. For smaller heights, the stress distribution tends to be triangular whereas for larger elements the is a stronger stress concentration. This behaviour is consistent with the simplified proposal for k_{fl} .

$$k_{fl} = \frac{1}{2} \left(1 + \frac{(h-x_g - h_{c,eff})}{h-x_g} \right) = \frac{1}{2} \left(1 + \frac{\left(\frac{h}{2} - h_{c,eff} \right)}{\frac{h}{2}} \right) = \frac{1}{2} \left(2 - \frac{2h_{c,eff}}{h} \right) = \frac{h-h_{c,eff}}{h} \quad (4)$$

This approach is, of course simplified, since it assumes that the distribution of stresses within the effective area is linear and follows Navier's law. This, of course, is not strictly true. Nonetheless, recent FEM calculations [9] show that the assumption of a constant stress within the effective area is not correct and that the actual distribution of stresses becomes more similar to a triangular distribution as the height of the section is reduced, while it becomes more concentrated as the height increases (see Figure 7). The proposed simplified model is consistent with these findings.

The need to distinguish between elements subjected to flexure and tension has been shown very clearly in [14] from which Table 2 is adapted. The table shows results from several tests, all involving a $b \times h = 350 \times 450$ mm rectangular section coded with the bar diameter in tension (4 bars), followed by the cover to the stirrups (for the cover to the longitudinal bars, add 12 mm), type of test (B=bending, T=tension) and the casting position (G=good, PL=Poor in Laboratory conditions).

In Model Code 2010 [16], this effect is accounted for, in an obscure way, by limiting the height of the effective area around a bar in bending to $(h-x)/3$, whereas there is no such limit in tension. As far as the authors are aware there is no published justification for this factor which seems to be originating from curve fitting to test data. Besides the lack of clarity regarding where this factor comes from, it provides very strange differences for the effective area depending on the type of force applied. Figure 8 shows the effective area for one

TABLE 2.

Experimental results comparing stabilized crack spacing in bending and tension tests and predictions by the new version of EN 1992-1-1, the Model Code 2010 and the current version of EN 1992-1-1 (adapted from [14]).

BEAMS	Measured mean crack spacing (mm)			FprEN 1992-1-1:2022			MC 2010			EN 1992-1-1:2004		
	B	T	Inc. (T-B)/B	B	T	Inc. (T-B)/B	Predicted mean crack spacing (mm)			B	T	Inc. (T-B)/B
							B	T	Inc. (T-B)/B			
12-20-B/T-G	115	162	0.41	137	162	0.18	182	182	0.00	152	240	0.58
16-20-B/T-G	105	147	0.40	125	152	0.22	151	151	0.00	134	203	0.52
16-70-B/T-G	183	220	0.20	213	262	0.23	233	352	0.51	248	477	0.93
16-20-B/T-PL	109.8	170.5	0.55	150	187	0.25	151	151	0.00	134	203	0.52
16-70-B/T-PL	188	232	0.23	243	309	0.27	233	352	0.51	248	477	0.93
25-20-B/T-G	86.7	115	0.33	105	135	0.29	113	119	0.05	110	163	0.48
25-70-B/T-G	148.3	184	0.24	186	245	0.32	175	260	0.49	212	365	0.72
25-20-B/T-PL	96.5	171	0.77	124	164	0.32	113	119	0.05	110	163	0.48
Average	129	175	0.39	160	202	0.26	169	211	0.20	168	287	0.64

of the tests reinforced with 4 25 mm bars and having a cover of 82 mm. The ratio between effective heights is larger than 2.00. This is because the $(h-x)/3$ limits the height of the effective area for the element subjected to bending. The difference is hard to justify from physical considerations or from what the effective area stands for (i.e. the area of concrete that is effectively tensioned by a bar (or group of bars), or the equivalent area of concrete that has to reach the tensile resistance of concrete for form a new crack adjacent to an existing one, assuming that Navier's hypothesis is valid).

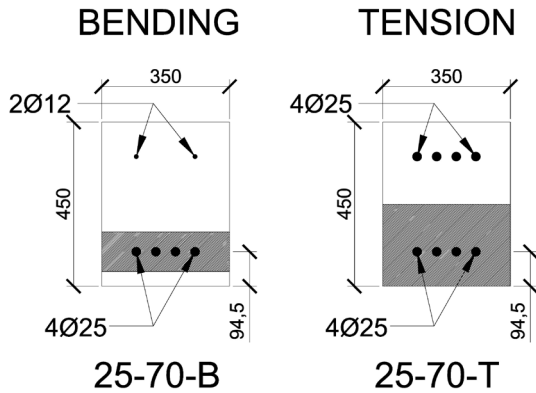


Figure 8. Effective area for specimens with 25 mm diameter and 82 mm cover in bending and tension [7].

Table 2 shows that this factor has no influence for small covers, whereas experimental results report a spacing that is 40% higher in tension than in bending. On the other hand, for large covers, the effect seems to be too large (50% compared to 20 to 33% in experimental results).

In the same table the same results provided by EN 1992-1-1:2004 are given. This model is accounting for the effect of the distribution of stresses twice, once through the limit to the effective area height $(h-x)/3$ and again through factor k_2 . This results in a significant overestimation of the effect of distribution of stresses with the (T-B)/B coefficients ranging from 58% to 72%, much higher than the experimental values.

It is clear that current formulations do not properly account

for this effect. Looking at the performance of the proposed method, at first glance, it would seem that while it performs better than the model of EN 1992-1-1:2004 and MC 2010, it still provides rather poor performance. However, it must be considered that this comparison is measuring not only the error in k_{fl} , but also in k_b , the effective area and the calibration coefficients of the cover and bond terms. The comparison can be improved by considering the experimental values of k_b for comparisons referring to the face concreted in poor bond conditions. These values can be obtained from Table 3, below.

The experimental value of k_{fl} can then be obtained for the coarse value of k_b , assuming that this value is the same for the tension and flexural tests as follows ($k_{\phi/\rho}$ is a calibration factor for the slip term):

$$\left. \begin{aligned} s_{r,m,cal,B} - k_c c &= k_{\phi/\rho} k_{fl} k_b \frac{\phi}{\rho_{s,eff}} \\ s_{r,m,cal,T} - k_c c &= k_{\phi/\rho} 1.00 k_b \frac{\phi}{\rho_{s,eff}} \end{aligned} \right\} \rightarrow k_{fl} = \frac{s_{r,m,cal,B} - k_c c}{s_{r,m,cal,T} - k_c c} \quad (5)$$

where:

$s_{r,m,cal,B}$ is the calculated mean crack spacing in bending

$s_{r,m,cal,T}$ is the calculated mean crack spacing in tension

The fact is, however, that the experimental k_b factor for the specific tie of the specific flexural element is not the same, so, in order to eliminate this noise from tests performed in poor bond conditions, the k_{fl} can, instead, be obtained accounting for this difference:

$$\left. \begin{aligned} s_{r,m,cal,T} - k_c c &= k_{\phi/\rho} 1.00 k_{b,exp,B} \frac{\phi}{\rho_{s,eff}} \\ s_{r,m,cal,T} - k_c c &= k_{\phi/\rho} 1.00 k_{b,exp,T} \frac{\phi}{\rho_{s,eff}} \end{aligned} \right\} \rightarrow k_{fl} = \frac{(s_{r,m,cal,B} - k_c c) k_{b,exp,T}}{(s_{r,m,cal,T} - k_c c) k_{b,exp,B}} \quad (6)$$

Table 3 shows how the “experimental” value of k_{fl} compares with the theoretical value when the noise due to errors in k_b is compensated for in the tests having bars in poor bond position. In the table the ratio of the theoretical value over the experimental value of k_{fl} (th/exp) is given for the case where the value of k_b is taken as either 0.9 or 1.2 (“coarse” value if k_b), as well as for the case when a measured value for k_b is available

TABLE 3.
Evaluation of k_{fl} , accounting for experimental values of k_b , tests referring to poor bond conditions.

	coarse value of k_b				exp value of k_b			
	kfl, th	kb	kfl, exp	th/exp	kb, F	kb, T	kfl,exp,2	th/exp
12-20-B/T-G	0.782	0.9	0.588	1.33	0.90	0.90	0.588	1.33
16-20-B/T-G	0.733	0.9	0.576	1.27	0.90	0.90	0.576	1.27
16-70-B/T-G	0.644	0.9	0.619	1.04	0.90	0.90	0.619	1.04
16-20-B/T-PL	0.733	1.2	0.504	1.45	0.98	1.11	0.571	1.28
16-70-B/T-PL	0.644	1.2	0.596	1.08	0.98	1.01	0.615	1.05
25-20-B/T-G	0.654	0.9	0.578	1.13	0.90	0.90	0.578	1.13
25-70-B/T-G	0.512	0.9	0.415	1.24	0.90	0.90	0.415	1.24
25-20-B/T-PL	0.654	1.2	0.394	1.66	1.13	1.65	0.576	1.14
			Mean =	1.28			Mean =	1.19
			CoV =	16%			CoV =	9%

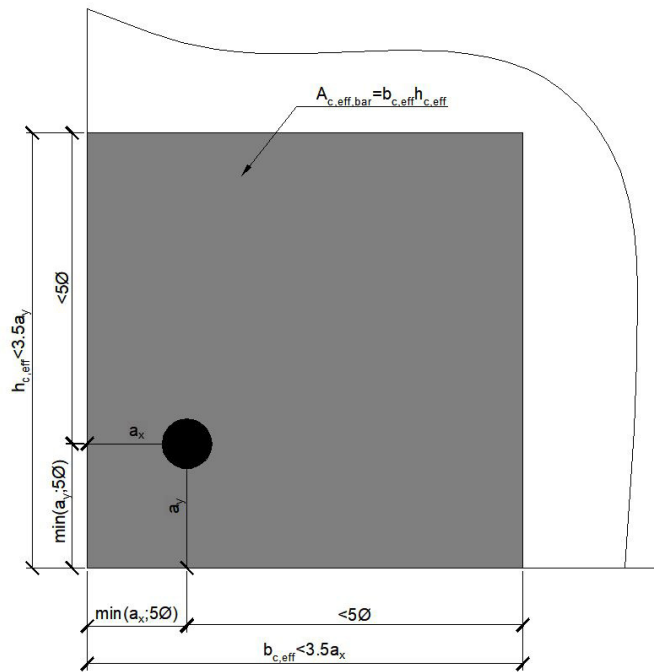


Figure 9. Effective tension area of concrete around an isolated bar, $A_{c,eff,bar}$.

(exp value of k_b). For elements with bars in good bond position this factor does not change, and the base value remains the same. The improvement is significant with the mean value of the ratio between theoretical and experimental results going from 1.28 to 1.19 and the coefficient of variation reducing from 16% to 9%. If anything, these results seem to indicate that the correction for type of loading should be even stronger (lower values of k_{fl}).

2.5. Definition of the effective area of concrete in tension

The definition of the effective tensioned area is changed to account for the removal of the $(h-x)/3$ limit, to deal with some inconsistencies in its current definition (limit to the area of concrete that is influenced by the presence of the bar) and to contribute to reduce scatter.

For an isolated bar, the proposed definition of the effective area is given in Figure 9 and the following equation:

$$A_{c,eff,bar} = b_{c,eff} h_{c,eff} \quad (7)$$

$$h_{c,eff} = \min(a_y + 5\phi; 10\phi; 3.5a_y) \leq |h-x|$$

$$b_{c,eff} = \min(a_x + 5\phi; 10\phi; 3.5a_x)$$

When individual tension areas of different bars overlap, the effective reinforcement ratio should be considered for the group of bars, as shown in Figure 10 and the following equation:

$$A_{c,eff,group} = b_{c,eff} h_{c,eff} \quad (8)$$

$$h_{c,eff} = \min(a_y + 5\phi; 10\phi; 3.5a_y) + s_y \leq |h-x|$$

$$b_{c,eff} = b$$

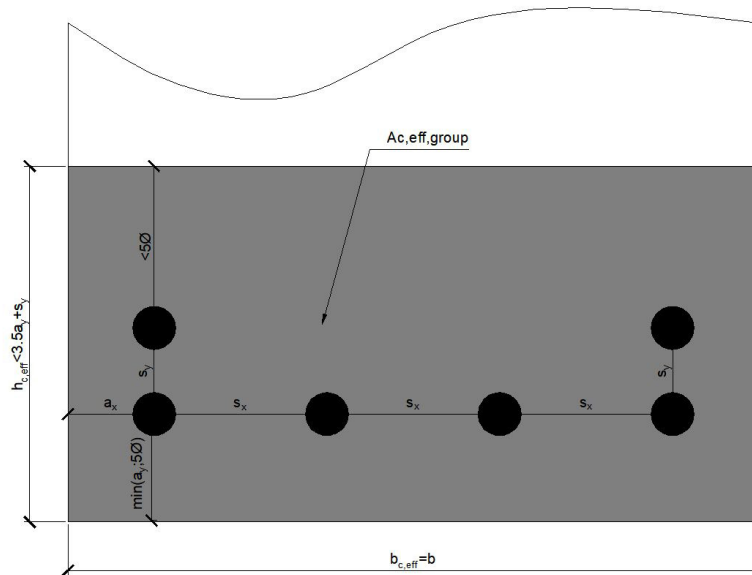


Figure 10. Effective tension area of concrete around a group of bars, $A_{c,eff,group}$ (to be applied when effective tension areas of adjoining bars overlap).

Even though for the example of Figure 10, the strict definition given for the isolated bar would result in a U shape for the effective area, this has been simplified (on the conservative side) by a rectangle, to improve ease of use.

As mentioned above, a limit on the effective area around a bar is given as a linear function of the bar diameter. This condition accounts for the fact that a bar can only control cracks within its proximity. With the definition of the effective area given in MC 2010 and EN 1992-1-1:2004, a single bar placed in the middle of a large rectangle of concrete would have an effective area equal to the area of concrete, and the value of the effective area would increase indefinitely with the dimensions of the cross section. This does not make sense and a limit is therefore necessary for consistency.

2.6. Effect of curvature on crack width

Regarding crack width, it has been well established that, in bending, the value of the crack opening increases from the

level of the reinforcement towards the most tensioned face (see for instance the tests reported in reference [7]). The increase in the crack opening is proportional to coefficient $k_{1/r}$, defined, as follows:

$$k_{1/r} = \frac{h-x}{d-x} \quad (9)$$

where:

- h is the section height
- d is the effective depth, and
- x is the depth of the neutral axis of the cracked section

As an illustration, Figure 11 shows a typical example of the accuracy of this correction using one of the tests carried out at UPM (specimen 25-20-00 [7]). The maximum crack width measured at the level of the reinforcement on the side of the beam is plotted against the maximum crack width measured over the exterior bar at the top of the section, both vertical and horizontal covers being the same (32 mm). A nearly per-

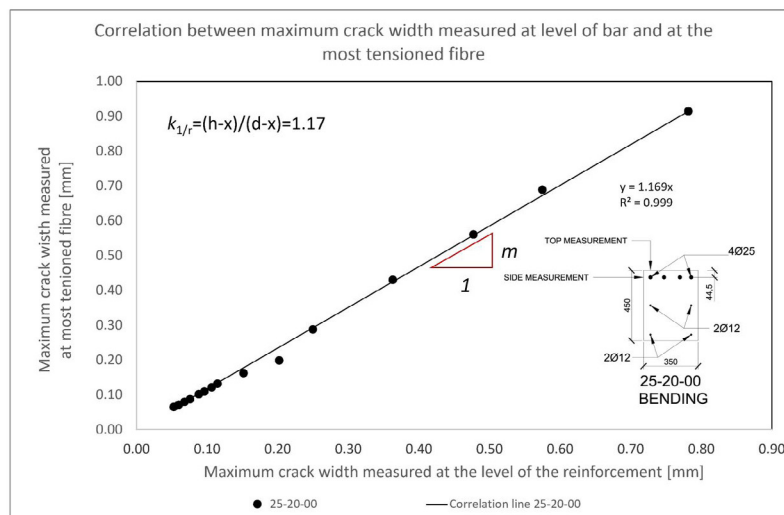


Figure 11. Illustration of the performance of factor $k_{1/r}$ on one of the tests.

TABLE 4.
Comparison between the slope of the correlation line (m) and factor $k_{1/r}$, for all flexural tests performed at UPM (s_i is the stirrup spacing).

Test	c [mm]	Reinf.	st [m]	h [m]	d [m]	x [m]	$k_{1/r}$	m	R^2	$m/k_{1/r}$
12-20-00	32	4•12	-	0.45	0.412	0.077	1.11	1.09	0.998	0.98
12-20-10	32	4•12	0.2	0.45	0.412	0.077	1.11	1.15	0.995	1.03
12-20-30	32	4•12	0.3	0.45	0.412	0.077	1.11	1.10	1.000	0.99
12-70-00	82	4•12	-	0.45	0.362	0.071	1.30	1.29	1.000	0.99
12-70-10	82	4•12	0.2	0.45	0.362	0.071	1.30	1.32	1.000	1.01
12-70-30	82	4•12	0.3	0.45	0.362	0.071	1.30	1.32	1.000	1.01
16-20-00	32	4•16	-	0.45	0.410	0.094	1.13	1.13	0.993	1.00
16-70-00	82	4•16	-	0.45	0.360	0.089	1.33	1.34	0.985	1.00
25-20-00	32	4•25	-	0.45	0.406	0.141	1.17	1.17	1.000	1.00
25-20-10	32	4•25	0.2	0.45	0.406	0.141	1.17	1.24	0.997	1.06
25-20-30	32	4•25	0.3	0.45	0.406	0.141	1.17	1.26	1.000	1.08
25-70-00	82	4•25	-	0.45	0.356	0.132	1.42	1.40	0.995	0.98
25-70-10	82	4•25	0.2	0.45	0.356	0.132	1.42	1.41	1.000	0.99
25-70-30	82	4•25	0.3	0.45	0.356	0.132	1.42	1.32	1.000	0.93
$\mu =$ 1.00										
$\sigma =$ 0.036										
$CoV =$ 3.6%										

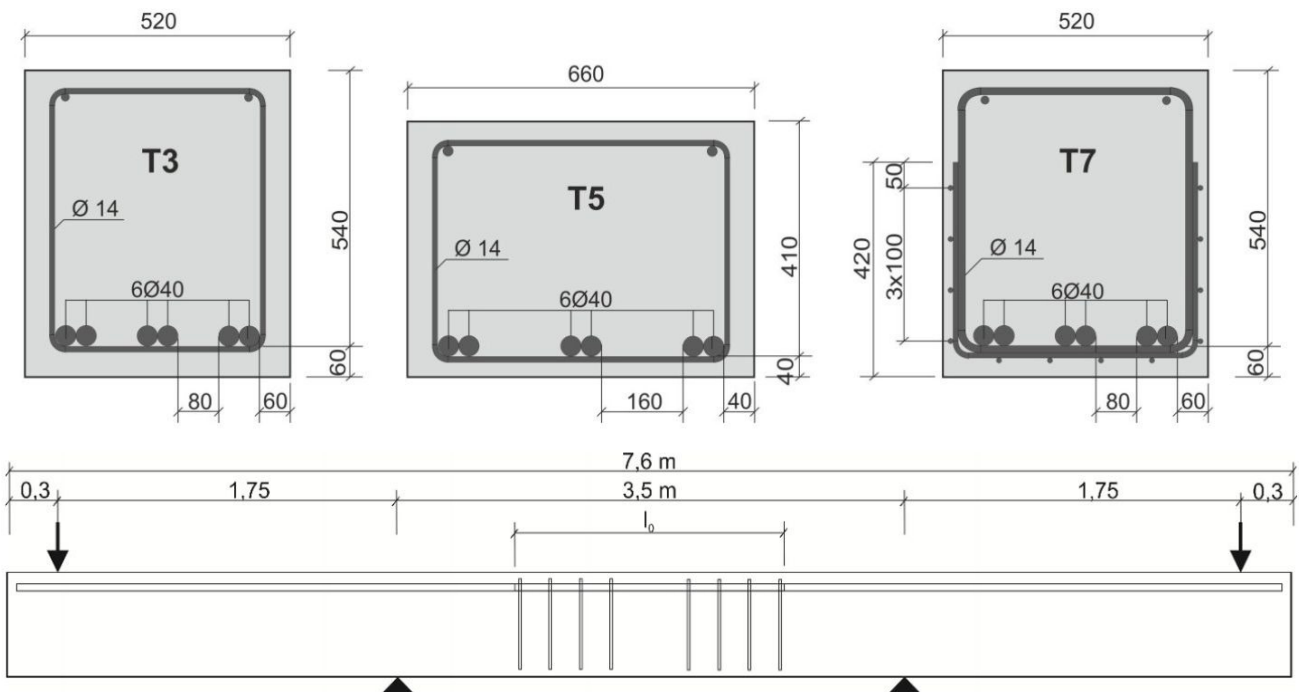


Figure 12. Test set-up and cross section of tests. Figure taken from [18]. Note that the elements were tested with the large reinforcement bars on the top (rotated 180° with respect to the cross sections shown).

fect linear correlation is obtained with a slope which closely mirrors the result obtained by applying the definition of the $k_{1/r}$ factor. This result is not the fruit of chance. Table 4 shows a comparison between the slope of the correlation line, m , determined as in Figure 11 and the value of the $k_{1/r}$ factor for all the flexural tests carried out at UPM until now (14 tests). The ratio between these two values is always very close to 1.00 and the coefficient of variation is only 3.6%. This is a clear indication that this factor is quite accurate and very necessary if an adequate estimate of the surface crack is to be obtained.

This factor is particularly necessary when estimating the crack width of flexural elements with large bars. Typically,

such elements have large covers and large reinforcement ratios resulting in large values of x , and thereby in large values of the $k_{1/r}$ factor. This can be illustrated with the tests carried out by Hegger *et al.* [17] (also reported in [18]). These tests involve large bar diameters (from 40 to 60 mm) and covers ranging from 40 to 75 mm. Figure 12 shows the test set-up as well as the definition of the sections. Figure 13 shows the comparison between mean crack openings predicted by the model of FprEN1992-1-1:2022 and those actually measured. A good approximation is obtained with the correlation slope being close to 1.00 and having a high coefficient of determination. The mean value of the ratio of mean calculated to mean

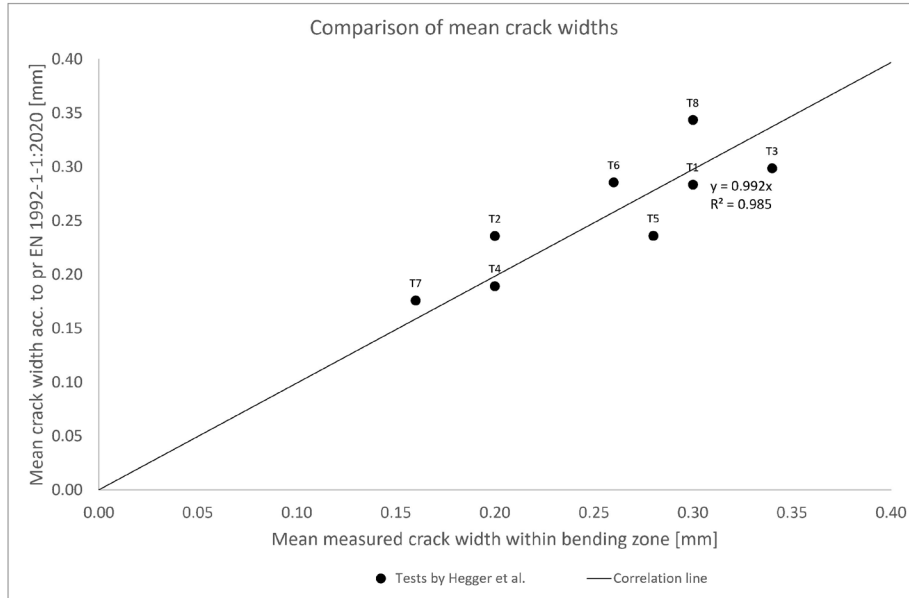


Figure 13. Comparison between mean crack width predicted by the model of FprEN1992-1-1:2022 [1] and the values measured experimentally.

experimental crack width ($w_{m,calc}/w_{m,exp}$) is 1.01 and the CoV is 12.4%. This result is independent experimental confirmation of the performance of the model since these tests were not considered for the calibration of the model.

This model can also easily account successfully for the effect of adding surface reinforcement to control crack width in elements reinforced with large diameter bars and can be used to justify experimental rules (see [19]). The main reasons why the introduction of surface reinforcement reduces the crack widths are the reduction of cover, the reduction in factor $k_{1/r}$, the increase in the effective reinforcement ratio, and, to a lesser extent the reduction in the equivalent bar diameter and the increase in total reinforcement, this last factor having a very minor effect. Also note that k_{η} increases because $h_{c,eff}$ decreases.

2.7. Type of restraint

It is well known that elements that are subjected to imposed deformation and restrained at ends are subjected, at most, to the cracking force. This is because the magnitude of the imposed strains that are found in normal structural concrete applications are small enough for the element to be in the crack formation stage. As the imposed strain increases, when the stress in concrete between cracks reaches the tensile strength of concrete, a new crack forms and the forces are reduced because the stiffness is reduced. New cracks will form each time this happens as the imposed strain increases. Therefore, the cracking force is the maximum force that can develop in the element with restrained ends. This behaviour is possible because the formation of a new crack affects the distribution of forces in the whole element.

When the element is restrained at the edges, the behaviour is different, because compatibility cannot be achieved globally as in the previous case but has to be met locally because the length of the edge does not change. The formation of a crack does not relieve stresses at a certain distance from the crack so that cracks form independently from one another. Figure 14

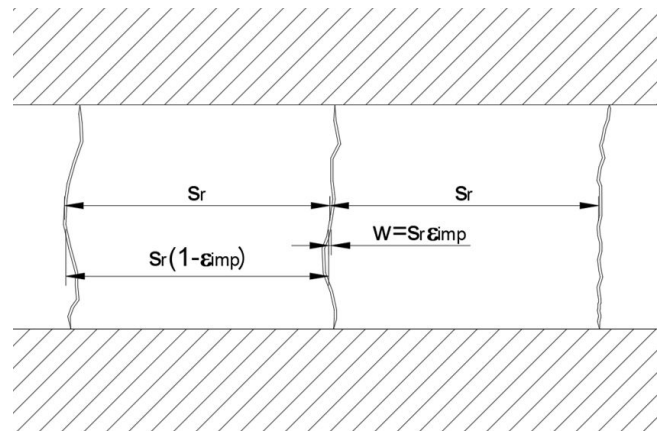


Figure 14. Cracking: behaviour of an element restrained at the edges. It is assumed that the edges are fully restrained. Tension stiffening effects are not included.

shows the behaviour in this case³. Ignoring tension stiffening effects, if s_r is the distance between two cracks the concrete between the cracks would shrink a length equal to the imposed deformation and therefore the crack opening would be $s_r \cdot \epsilon_{imp}$. So, the crack opening is no longer a function of the steel stress but a function of the imposed deformation. Accounting for tension stiffening effects, the relative strain between steel and concrete can be expressed as in Eq. (10). If the edges are not totally restrained the imposed deformation is obtained by multiplying the free imposed strain by a restraint factor which is determined from a linear elastic analysis which accounts for the flexibility of the restraint in which the free strain is applied on the structure. The restraint factor is a function of the ratio between the strain that develops freely in the element and the imposed strain.

³ The behaviour is simplified here for the purpose of explanation. In actual structures the stabilized crack pattern will normally not have been achieved and the adjacent cracks would normally not be formed. s_r would represent the transfer length in such a case.

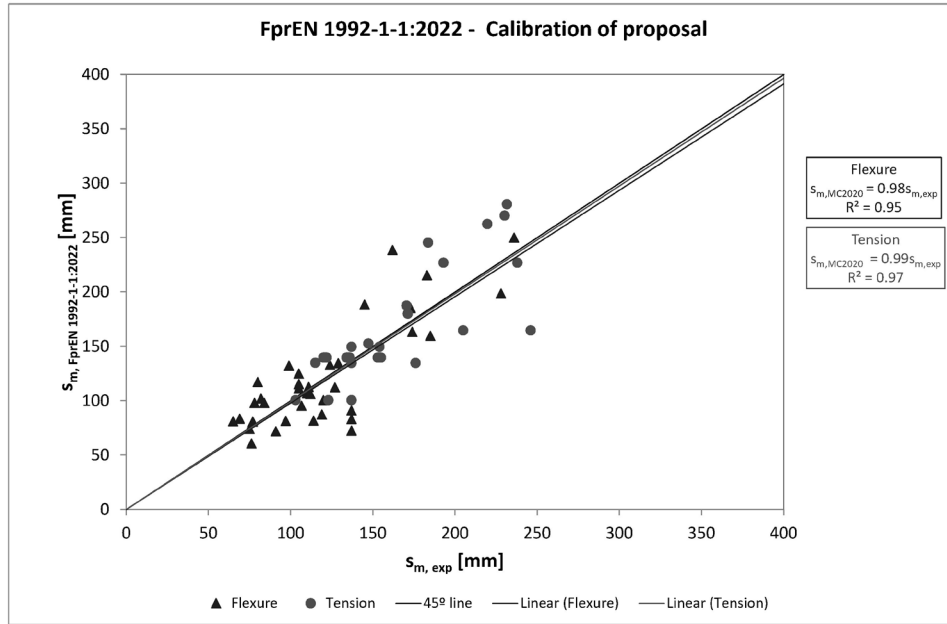


Figure 15. Comparison between predicted and measured crack spacing, separated according to type of load.

$$\begin{aligned} \varepsilon_{sm} - \varepsilon_{cm} &= \varepsilon_{imp} - k_t \frac{f_{ct,eff}}{E_{cm}} \\ \varepsilon_{imp} &= R_{ax} \varepsilon_{free} \end{aligned} \quad (10)$$

where:

R_{ax} is the restraint factor, which is obtained as $R_{ax} = 1 - \frac{\varepsilon_{restr}}{\varepsilon_{imp}}$, where ε_{restr} is the strain that develops freely in the restrained element and ε_{imp} is the imposed strain (e.g. free shrinkage, free temperature strain).

2.8. Calibration and comparison

The formulation has been calibrated to determine the coefficients to be applied to the cover term and the bond term. The expressions for the mean crack spacing can be written as follows:

$$s_{r,m,cal} = k_c c + k_{\phi/\rho} k_{\beta} k_b \frac{\phi}{\rho_{s,eff}}, \quad (11)$$

where:

k_c is an empirical parameter account for the influence of the concrete cover not accounted for in the bond term; as a simplification, $k_c = 1.5$ can be assumed;

c is the maximum concrete cover. The maximum value has been adopted because recent research [20] confirms that, when vertical and horizontal covers are different, crack spacing is much better correlated to the maximum cover than to minimum cover. When the effective area concept applies to a single bar located in the perimeter of the section, the maximum cover of this bar applies. When the effective area applies to a group of bars, the most unfavourable value of cover of the bars located in the perimeter of the section should be considered;

$k_{\phi/\rho}$ is an empirical parameter to account for the influence of bond; as a simplification, $k_{\phi/\rho} = 1/7.2$ can be assumed.

The design crack width is obtained from Eq. (12).

$$w_{k,cal} = k_w k_{1/r} s_{r,m,cal} (\varepsilon_{sm} - \varepsilon_{cm}) \quad (12)$$

where:

k_w is a factor to obtain a design value of the crack width from the mean value, which can be taken as 1.7;

ε_{sm} is the average steel strain over the length $s_{r,m,cal}$;

ε_{cm} is the average concrete strain over the length $s_{r,m,cal}$;

For members subjected to direct loads (stabilized crack- ing) or for members subjected to imposed strains (crack formation phase) restrained at the ends, $\varepsilon_{sm} - \varepsilon_{cm}$ can be determined as in Eq. (13).

$$\varepsilon_{sm} - \varepsilon_{cm} = \frac{1}{2} \left(\sigma_s - k_t \frac{f_{ct,eff}}{\rho_{ct,eff}} (1 + \alpha_e \rho_{eff}) \right) \quad (13)$$

where:

E_s is the modulus of elasticity of steel;

σ_s is the stress of steel at the crack;

k_t is an empirical coefficient to assess the mean strain over the transfer length, equal to 0.6 for short-term analysis and equal to 0.4 for long-term analysis or repeated loading;

$f_{ct,eff}$ is the effective tensile strength of concrete, which in practical cases can be taken as the mean tensile strength $f_{ct,m}$;

α_e is the modular ratio $= E_s/E_c$;

For members subjected to imposed strains and restrained at the ends, the applied load is assumed to be the cracking force and the parenthesis in Eq. (13) simplifies to:

$$\left(\sigma_s - k_t \frac{f_{ct,eff}}{\rho_{eff}} (1 + \alpha_e \rho_{eff}) \right) = \frac{f_{ct,eff}}{\rho_{s,eff}} (1 + \alpha_e \rho_{eff}) (1 - k_t) \quad (14)$$

TABLE 5.
Statistical analysis of crack spacing.

	MC 2010		EN 1992-1-1:2004		FprEN 1992-1-1:2022		
	Flexure	Tension	Flexure	Tension	Flexure	Tension	
n° of tests	37	36	37	36	37	36	
$\sqrt{(\Sigma \varepsilon^2/N)}$	38.28	37.96	35.25	83.01	29.01	30.97	
Model/Exp.	$\min(s_{m,model}/s_{m,exp})=$	0.46	0.51	0.6	0.68	0.53	0.67
	$\max(s_{m,model}/s_{m,exp})=$	1.78	1.51	1.74	2.04	1.47	1.34
	$\mu =$	1.04	1.05	1.08	1.43	1.00	1.01
	$\sigma =$	0.29	0.22	0.27	0.30	0.24	0.16
	COV =	27.68%	21.18%	24.69%	21.25%	23.57%	15.62%

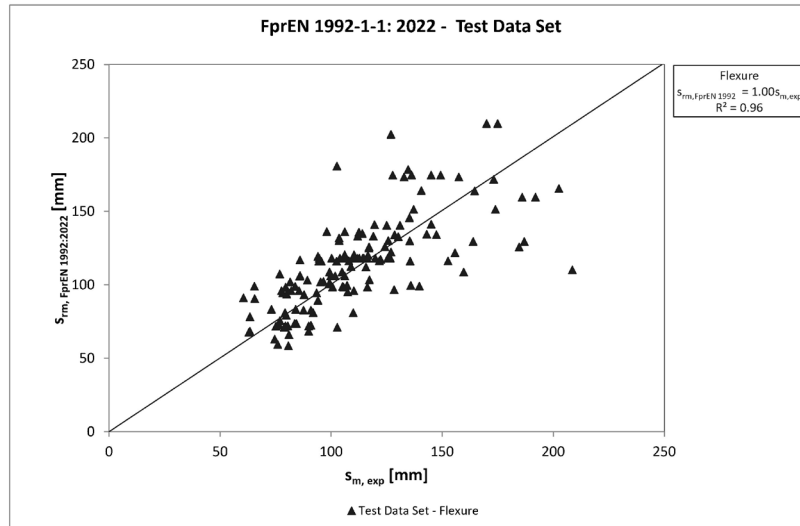


Figure 16. Comparison between predicted and measured crack spacing for the independent test series.

For members subjected to imposed strains and restrained at the edges, $\varepsilon_{sm} - \varepsilon_{cm}$ can be determined as in Eq. (10).

Figure 15 shows the comparison between predicted values, $s_{m, FprEN1991-1:2022}$, and experimental values of crack spacing, $s_{m, exp}$. The correlation lines show a coefficient of determination of 0.95 in flexure and 0.97 in tension and a slope close to 1.00. Contrary to the current version of EC2, for which the crack width in tension specimen is overestimated, there is no skew between tension and flexure in the new proposal. This is due to the deletion of the $(h-x)/3$ limit and the introduction of factor k_{fl} .

Table 5 shows the statistical parameters referred to the 73 tests used for the calibration for crack spacing which includes tests by [21], [22], [23], [24], [7], [13], [25], [26], [27] (see [28]). The table includes the mean squared error, the minimum value of the ratio of model prediction and experimental values (min), its maximum value (max), its mean value (μ), its standard deviation (σ) and its coefficient of variation (COV).

It can be seen the proposed corrections improve the prediction quality in statistical terms, for all the considered statistical parameters, both in flexure and in tension with respect to both the formulation of MC 2010 and EN 1992-1-1:2004. The improvement in tension is related to the changes introduced in the definition of the effective tension area.

2.9. Verification of the calibration using an alternative data set

The model has been calibrated with the same data set (calibration set) as was used for the original calibration of MC 2010, with the addition of several experimental series, as mentioned above. The robustness of this calibration was verified using a separate set of data (test set – see [28]). The independent database includes a total of 144 specimens. This database consists of the following tests:

- Clark (54 specimens) [22]
- Rehm&Rüsch (30 specimens) [25]
- Gribniak (6 specimens) [29]
- Gilbert & Nejadi (12 specimens) [30]
- Calderón (14 specimens) cast in poor casting position [31]
- Wu (4 specimens) – 2 Tests with excessive side cover were discarded [32]
- Frosch (2 specimens) – Other tests with excessive side cover were discarded – Poor casting position [33]
- Case, Beeby (16 specimens) – Tests with mild reinforcement were discarded [34]
- Klakauskas (6 specimens) [35]

The details of the specimens are available in [28].

Figure 16 demonstrates the performance of the proposed model on the independent test set. Even though there is scatter, the model proves to be well-calibrated. Table 6 shows

TABLE 6.
Statistical analysis of crack spacing for the independent data set.

	MC 2010	EN 1992-1-1:2004	FprEN 1992-1-1:2022	
n° of tests	144	144	144	
$\sqrt{(\sum \varepsilon^2/N)}$	26.97	26.3	23.55	
Model/Exp.	$\min(s_{m,model}/s_{m,exp})=$	0.54	0.51	0.53
	$\max(s_{m,model}/s_{m,exp})=$	1.87	1.63	1.76
	$\mu =$	1.05	0.99	1.04
	$\sigma =$	0.24	0.24	0.2
	COV =	23.04%	24.56%	18.85%

the corresponding statistical parameters. It can be observed that the application of the proposed modification reduces the coefficient of variation from 23.0% for MC 2010 and 24.6% for EN 1992-1-1:2004 to 18.9%. This result corroborates the need for the corrections proposed to account for differences between flexure and tension.

3. DEFLECTIONS

3.1. Simplified method for deflection control

The general method for determining deflection (ζ -method) has been left untouched in the FprEN1992-1-1:2022 [1], because there was no reason to change it as it provides satisfactory results and has a solid basis. However, it is notorious among practicing engineers that this method is not easy to apply to real projects, for which linear models with complex geometries are used. The current practice consists in determining a certain factor to apply to linear elastic calculation in order to obtain an estimate of the deflection considering creep and shrinkage effect. Up to now the determination of this coefficient has been done using approximate methods whose basis is not fully clear. In order to improve ease-of-use, and provide a common basis for this practice, a simplified approach is provided, in which the long term cracked deflection can be easily obtained by taking the linear elastic deflection and correcting with simple coefficients that account for cracking and tension stiffening effects as shown in Eq (15).

$$\delta = k_l [\delta_{LOADS} + k_s \delta_{cs}] \quad (15)$$

The basis of this procedure is an approximation to the long-term ratio between the cracked and uncracked sectional inertia. It results that this ratio can be approximated with significant precision with a fairly simple formulation for rectangular sections. Figure 17 shows this approximation. Note that $\alpha_{e,eff}$ is the long term modular ratio, which accounts for creep (see Eq. (16)).

$$\alpha_{e,eff} = \frac{E_s}{E_c} (1 + \varphi) = \frac{E_s}{E_{c,eff}} \quad (16)$$

The creep coefficient can be taken as weighted mean value (φ_{mean}) according to the following expression:

$$\varphi_{mean} = \frac{\varphi(t, t_0)g_{SW} + \varphi(t, t_1)g_{SDL} + \varphi(t, t_2)\psi_2 q_{LL}}{g_{SW} + g_{SDL} + \psi_2 q_{LL}} \quad (17)$$

where:

- g_{SW} is the self-weight, applied when the concrete age is t_0 ;
- g_{SDL} is the superimposed dead load applied when the concrete age is t_1 ;
- $\psi_2 q_{LL}$ is the quasi-permanent live load applied when the concrete age is t_2 ;
- t is the age of concrete corresponding to the service life of the structure.

Using the approximation to the ratio I_{cr}/I_g shown in Figure 17, and applying the methodology of the ζ -method which consists in interpolating a stiffness between the fully cracked and uncracked values, factor k_l is determined as shown in Eq. (18).

$$\zeta = \left(1 - 0.5 \left(\frac{M_{cr}}{M_k} \right)^2 \right)$$

$$K_I = \zeta \frac{I_g}{I_{cr}} + (1 - \zeta) = \zeta \frac{1}{2.7 (\alpha_{e,eff} \rho)^{0.6}} \left(\frac{h}{d} \right)^3 + (1 - \zeta) \quad (18)$$

The deflection due to shrinkage is obtained by applying a constant shrinkage strain on the structure, determining the elastic deflection, and correcting this by a coefficient that takes into account how the ratio between the equivalent and the uncracked first order moment of the reinforcement with respect to the centroid of the cross section changes due to cracking and tension stiffening effects. The correction in this case is given in Eq. (19). Figure 18 shows calculated values of this ratio for 3 different concrete strengths and the proposed approximation as a function of the reinforcement ratio.

$$k_s = 455\rho^2 - 35\rho + 1.6 \quad (19)$$

3.2. Slenderness limits for beams

Eq. (15) can easily be converted into a general formulation to determine the slenderness limit. Eq. (20) shows the condition for the slenderness limit, i.e., that the deflection be limited to a fraction ($1/a$) of the span (where a is usually taken as 250). It also shows the expressions of the deflections due to a uniformly distributed load and to a constant curvature due to shrinkage.

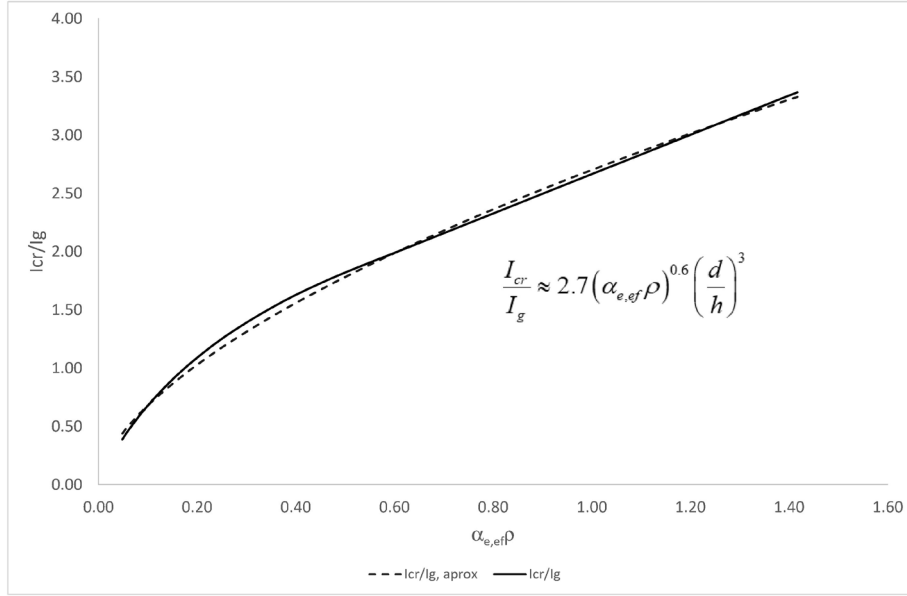


Figure 17. Ratio between long term cracked inertia and gross cross sectional inertia as a function of the long-term transformed reinforcement ratio.

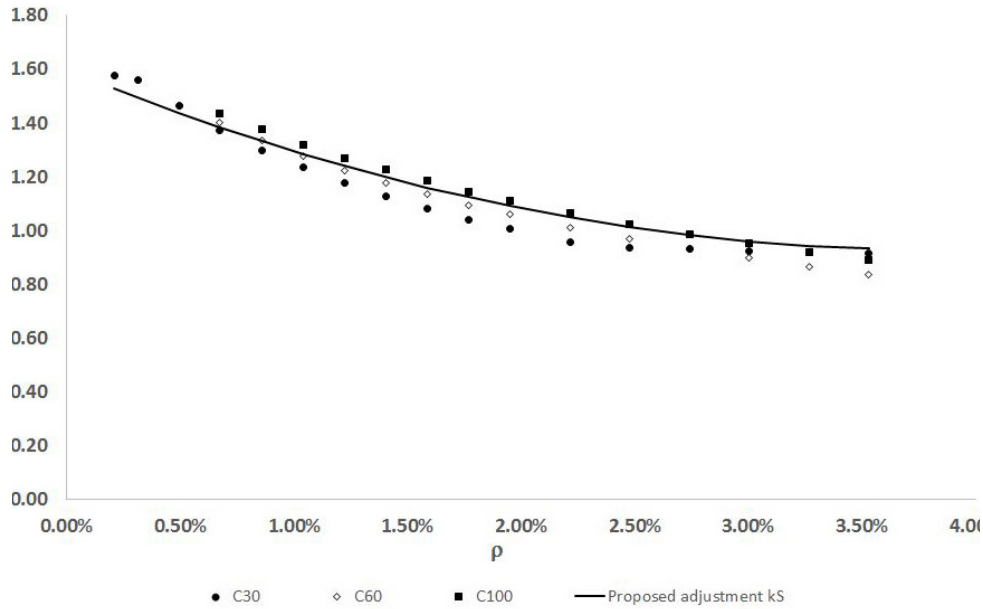


Figure 18. Ratio between the equivalent and the uncracked first order moment of the reinforcement with respect to the centroid of the section as a function of the reinforcement ratio for different concrete strengths.

$$\delta = k_I [\delta_{LOADS} + k_S \delta_{cs}] \leq \frac{L}{a}$$

$$\delta_{LOADS} = K \frac{5}{384} \frac{q_{ap} L^4}{E_{c,eff} \frac{1}{12} b h^3} \quad (20)$$

$$\delta_{cs} = K_{cs} \epsilon_{cs} \frac{E_s}{E_{c,eff}} \frac{A_s \left(d - \frac{h}{2} \right) - A_s \left(\frac{h}{2} - (h-d) \right)}{\frac{1}{12} b h^3} \frac{L^2}{8}$$

where:

K is a factor that considers the support conditions for the deflection due to uniformly distributed loads and can be determined from Eq. (21) (for a detailed derivation see [36]):

$$K = \sqrt[3]{\frac{f_{simply,sup}}{f_{real,sup,cond}}} \quad (21)$$

where:

$f_{simply,sup}$ is the linear elastic deflection of the simply supported member of arbitrary span subjected to a uniformly distributed load, and

$f_{real,sup,cond}$ is the linear elastic deflection of the member with the actual support conditions with the same arbitrary span and subjected to the same uniformly distributed load.

K_{cs} is a factor that considers the support conditions for the deflection due to shrinkage and can be determined from Expression (22) (for a detailed derivation see [36]):

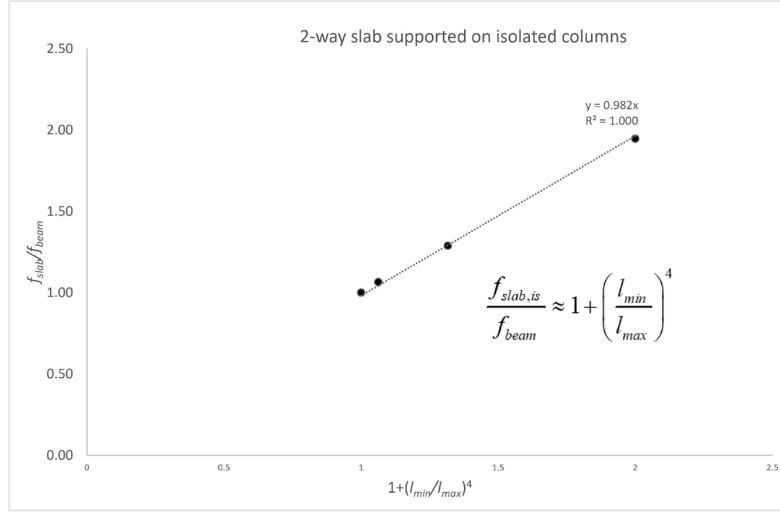


Figure 19. Ratio of the elastic deflection of a slab supported on 4 isolated columns and a simply supported beam as a function of parameter $1+(l_{min}/l_{max})^4$.

$$K_{cs} = \frac{f_{cs, simply, sup}}{f_{cs, real, sup, cond}} \quad (22)$$

where:

$f_{cs, simply, sup}$ is the linear elastic deflection of the simply supported member of arbitrary span subjected to a constant curvature, and

$f_{cs, real, sup, cond}$ is the linear elastic deflection of the member with the actual support conditions with the same arbitrary span and subjected to a constant curvature.

Assuming that the provided reinforcement is that strictly needed in ULS, the value of the quasi-permanent load of a simply supported element can be determined from the ultimate bending resistance as shown in Expression (23) as the product of the ultimate load and coefficient k_{DL} ($q_{ap} = k_{DL} q_{Rd}$).

$$M_{Rd} = q_{Rd} \frac{L^2}{8} = A_s f_{yd} \left(d - 0.5 \frac{A_s f_{yd}}{b f_{cd}} \right)$$

$$q_{Rd} = A_s f_{yd} d \left(1 - 0.5 \frac{A_s f_{yd}}{b f_{cd}} \right) \frac{8}{L^2} \quad (23)$$

$$\frac{q_{ap}}{q_{Rd}} = \frac{G + \psi_2 Q}{\gamma_G G + \gamma_Q Q} = \frac{\frac{1 - \frac{LL}{TL}}{\frac{LL}{TL}} + \psi_2}{\gamma_G \left(\frac{1 - \frac{LL}{TL}}{\frac{LL}{TL}} \right) + \gamma_Q \frac{LL}{TL}} = \frac{\left(1 - \frac{LL}{TL} \right) + \psi_2 \frac{LL}{TL}}{\gamma_G \left(1 - \frac{LL}{TL} \right) + \gamma_Q \frac{LL}{TL}} = k_{DL}$$

$$\frac{LL}{TL} = \frac{Q}{G+Q} \rightarrow G = \frac{\left(1 - \frac{LL}{TL} \right)}{\frac{LL}{TL}} Q$$

In Expression (23) it is assumed that there is no need for compression reinforcement in ULS.

Introducing the value of q_{ap} into Expression (20), and developing, the slenderness limit can be obtained as shown in Expression (24). This expression also assumes that there is

no compression reinforcement but can be easily generalized for this case (see [36]). However, the effect of compression reinforcement on deflections is limited, and the increase in precision for this rare case is not worth the complication.

$$k_l \left[K \frac{5}{384} \frac{k_{DL} A_s f_{yd} d \frac{8}{L^2} (1-0.5\omega) L^4}{E_{c,eff} \frac{1}{12} b h^3} + k_s K_{cs} \varepsilon_{cs} \frac{E_s}{E_{c,eff}} \frac{A_s \left(d - \frac{h}{2} \right) - A'_s \left(\frac{h}{2} - (h-d) \right)}{\frac{1}{12} b h^3} \frac{L^2}{8} \right] \leq \frac{L}{a} \quad (24)$$

$$\left. \begin{aligned} q_{ap} &= k_{DL} q_{Rd} = k_{DL} A_s f_{yd} d (1-0.5\omega) \frac{L^2}{8} \\ A'_s &= 0 \end{aligned} \right\} \rightarrow$$

$$\frac{L}{d} \leq \frac{E_{c,eff}}{k_l 12 a} \left(\frac{h}{d} \right)^3 \left[\frac{1}{K k_{DL} \frac{5}{48} f_{cd} \omega (1-0.5\omega) + k_s K_{cs} \varepsilon_{cs} \frac{E_s}{8} \rho \left(1 - \frac{h}{2d} \right)} \right]$$

The values included in Table 9.3 of FprEN 1992-1-1:2022 are derived from this expression assuming that the concrete class is C30, that a is 250 and that the quasipermanent live load is 30% of the total live load. The creep coefficients implicit in k_l were determined assuming the following conditions:

- The self-weight is applied at 7 days
- The superimposed dead load is 15% of the self-weight and is applied at 60 days
- The quasi-permanent live load is applied at 365 days
- The relative humidity is 50%
- The deflection is determined for a design life of 100 years

3.3. Slenderness limits for slabs

The Slenderness limits for slabs on isolated supports and on continuous supports can be obtained by multiplying the values

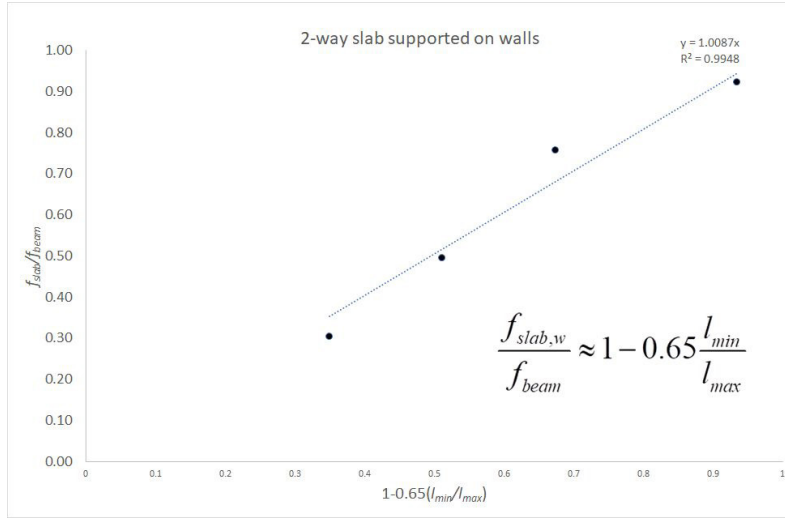


Figure 20. Ratio of the elastic deflection of a slab supported on walls and a simply supported beam as a function of parameter $1-0.65l_{min}/l_{max}$

of Table 9.3 by coefficients which are determined from the ratio of the linear elastic deflections of the slab and a simply supported beam of the same span.

Figure 19 shows that the ratio is a linear of the fourth power of the ratio between the shorter and longer spans. The ratio corresponding to the slenderness limits of the two support conditions (factor K) can be easily determined as shown in Eq. (25):

$$f_{slab, is} \approx \left(1 + \left(\frac{l_{min}}{l_{max}}\right)^4\right) f_{beam, l_{max}} = f_{beam, l_{beam}} \quad (25)$$

$$\rightarrow \left(1 + \left(\frac{l_{min}}{l_{max}}\right)^4\right) k \frac{ql_{max}^4}{EI} = k \frac{ql_{beam}^4}{EI} \rightarrow \frac{l_{min}}{l_{beam}} = \sqrt[4]{\frac{1}{1 + \left(\frac{l_{min}}{l_{max}}\right)^4}}$$

$$\rightarrow \frac{\frac{l_{max}}{d}}{\frac{l_{beam}}{d}} = \sqrt[4]{\frac{1}{1 + \left(\frac{l_{min}}{l_{max}}\right)^4}}$$

$$\rightarrow \frac{l_{max}}{d} = \frac{l_{beam}}{d} \sqrt[4]{\frac{1}{1 + \left(\frac{l_{min}}{l_{max}}\right)^4}}$$

For a slab supported on walls, Figure 20 shows the ratio of the deflection of the slab to the deflection of the simply supported beam as a function of $1-0.65 (l_{min}/l_{max})$. The correlation line has a slope very close to 1.00 and a high coefficient of determination. With identical reasoning as above, the slenderness limit for slabs supported on walls is given in Eq. (26):

$$\frac{l_{max}}{d} = \frac{l_{beam}}{d} \sqrt[4]{\frac{1}{1 - 0.65 \frac{l_{min}}{l_{max}}}} \quad (26)$$

4. CONCLUSIONS

In this paper, the main changes in the formulations for cracking and deflections introduced in FprEN 1992-1-1:2022 have been presented and justified.

The main changes in the cracking formulation introduce relevant factors to consider several effects that have been ignored or misrepresented in previous formulations. The main effects are the effect of the bond conditions, the uneven distribution of stresses in elements subjected to bending, and the increase in the crack width due to curvature from the level of the bar to the most tensioned fibre. It is shown that their consideration leads to a reduction the scatter of the model when compared to experiments.

For deflection control, the main changes consist in the inclusion of correction for the slenderness limits to deal with slabs supported on columns and supported at the edges and the introduction of a simplified method which allows to obtain a justified value of the deflection from results of a linear elastic calculation. Globally, the changes lead to an improvement of ease-of-use.

Acknowledgements

The authors wish to thank Gintaris Klakauskas and Aleksandr Sokolov for providing the independent test set for the model.

References

- [1] CEN, FprEN 1992-1-1:2023 Eurocode 2: Design of concrete structures — Part 1-1: General rules Rules for buildings, bridges and civil engineering structures, Brussels: CEN, 2022. This document is available through the National members of CEN TC250/SC2.
- [2] CEN, EN 1992-1-1. Eurocode 2 Design of concrete structures - Part 1-1: General rules and rules for buildings, Brussels: Comité Européen de Normalisation, 2004.
- [3] CEN, "EN 1992-3: Eurocode 2 - Design of concrete structures - Part 3: Liquid retaining and containment structures," CEN, Brussels, 2006.

- [4] V. Gribniak, D. Bacinskas, R. Kacianauskas, G. Kaklauskas and L. Torres, "Long-term deflections of reinforced concrete elements: accuracy analysis of predictions by different methods," *Mech Time-Depend Mater*, vol. 17, p. 297–313, 2013. <https://doi.org/10.1007/s11043-012-9184-y>
- [5] F. Carneiro Pacheco Marques Guedes and R. Vaz Rodrigues, "The effect of concrete cover on the crack width in reinforced concrete members—a code perspective," in *2nd International Conference on Recent Advances in Nonlinear Models-Design and Rehabilitation of Structures*, Coimbra, 2017.
- [6] V. Gribniak, A. Rimkus, A. Pérez Caldentey and A. Sokolov, "Cracking of concrete prisms reinforced with multiple bars in tension—the cover effect," *Engineering Structures*, vol. 220, p. 110979, 2020.
- [7] A. Pérez Caldentey, H. Corres Peiretti, J. Peset Iribaren and A. Giraldo Soto, "Cracking of RC members revisited: influence of cover, ϕ/ρ , ϵ_f and stirrup spacing – an experimental and theoretical study," *Structural Concrete*, vol. 16, no. 1, pp. 69–78, 2013. <https://doi.org/10.1002/suco.201200016>
- [8] C. Naotunna, S. Samarakoon and K. Fossa, "Identification of the Influence of Concrete Cover Thickness and ϕ/ρ parameter on crack spacing," in *15th International Conference on Durability of Building Materials and Composites*, Online, 2020.
- [9] T. Nguyen Viet and D. Schlicke, "Chapter 9.2 - Crack control of prEN1992-1-1: A critical view," in *Meeting of CEN-TC-250/SC2/WG1 March 28-29, 2022, On-line Meeting*, 2022.
- [10] L. Steyl, Plastic cracking of concrete and the effect of depth. PhD thesis, Stellenbosch: Stellenbosch University, 2016.
- [11] R. Combrinck, L. Steyl and P. Boshoff, "(2018), Interaction between settlement and shrinkage cracking in plastic concrete," *Construction and Building Materials*, vol. 185, pp. 1–11, 2018.
- [12] A. Borosnyói and G. Balázs, "Models for flexural cracking in concrete: the state of the art," *Structural Concrete*, vol. 6, no. 2, pp. 53–62, 2005. <https://doi.org/10.1680/STCO.2005.6.2.53>
- [13] R. García and A. Pérez Caldentey, "Cracking of reinforced concrete: Tension vs. Flexure. Report on cracking tests of large ties," Technical University of Madrid, Madrid, Spain, 2018.
- [14] R. García and A. Pérez Caldentey, "Influence of casting position on cracking behavior of reinforced concrete elements and evaluation of latest proposal for EN-1992 and MC2020: Experimental study," *Structural Concrete*, 08 April 2022. <https://doi.org/10.1002/suco.202100639>
- [15] A. Pérez Caldentey, A. García, V. Gribniak and A. Rimkus, "Background document to subsection 9.2.4," CEN TC 2650, Madrid, 2020.
- [16] fib, Model Code for Concrete Structures 2010, Lausanne: Fédération Internationale du Béton, 2013, p. 434.
- [17] H. Hegger, M. Empelmann and S. J. (2015.), "Weiterentwicklung von Bemessungs- und Konstruktionsregeln bei großen Stabdurchmessern ($d > 32$ mm, B500). Verbundfestigkeit und Übergreifungsstöße. Institutsbericht-Nr.: 341/2015," Instituts für Massivbau der RWTH, Aachen, 2015.
- [18] J. Schoening and H. Hegger, "Concrete elements reinforced with large diameters. Bond behaviour and lapped joints," in *fib Symposium 2015*, Copenhagen, Denmark, 2015.
- [19] A. Pérez Caldentey, "Background document to subsection S.5. Surface reinforcement for large bar diameters," CEN, Brussels, 2022.
- [20] A. Beldholm Rasmussen, Modelling of reinforced concrete in the serviceability limit state: A study of cracking, stiffness and deflection in flexural members. PhD Thesis, Aarhus: Aarhus University, 2019.
- [21] B. B. Broms, "Crack Width and Crack Spacing in Reinforced Concrete Members," *ACI Journal Proceedings*, vol. 62, no. 10, pp. 1237–1256, 1965. <http://dx.doi.org/10.14382/epitoanyag-jsbcm.2010.14>
- [22] A. Clark, "Cracking in Reinforced Concrete Flexural Members," *ACI Journal, Proc.*, vol. 27, no. 8, p. pp.851–862., 1956.
- [23] CUR Dutch Centre for Civil Engineering, "Scheurvorming en Doorbiting in gewapend Beton bij Toepassing van geribd Staal. Research and Codes Report no. 37," Dutch Centre for Civil Engineering, 1968.
- [24] E. Hognestad, "High Strength Bars as Concrete Reinforcement – Part 2: Control of Flexural," *Journal, PCA Research and Development Laboratories*, vol. 4, pp. 46–63, 1962.
- [25] E. Rüschi and G. Rhem, "Versuche mit Betonformstählen. (1963), pt. II (1963), pt. III (1964).," *Deutscher Ausschuss für Stahlbeton*, no. 140, 1963–1964.
- [26] J. Farra and J. Jaccoud, "Rapport des Essais de Tirants sous déformation imposée de courte durée," EPFL, Lausanne, 1996.
- [27] A. Rimkus and V. Gribniak, "Experimental Investigation of cracking and deformations of concrete ties reinforced with multiple bars," *Construction and Building Materials*, vol. 148, pp. 49–61, 2017. <http://dx.doi.org/10.1016/j.conbuildmat.2017.05.029>
- [28] A. Pérez Caldentey, R. García, V. Gribniak and A. Rimkus, "Tension versus flexure: Reasons to modify the formulation of MC 2010 for cracking," *Structural Concrete*, vol. 21, p. 2101–2123, 2020. <https://doi.org/10.1002/suco.202000279>
- [29] V. Gribniak, R. Jakubovskis, A. Rimkus, P.-L. Ng and D. Hui, "Experimental and numerical analysis of strain gradient in tensile concrete prisms reinforced with multiple bars," *Construction and Building Materials*, vol. 187, pp. 572–583, 2018. <https://doi.org/10.1016/j.conbuildmat.2018.07.152>
- [30] R. I. Gilbert and S. Nejadi, "An experimental study of flexural cracking in reinforced concrete members under short term loads. Report.," University of New South Wales, Sydney, Australia, 2015.
- [31] E. Calderón Bello, "Estudio experimental de la fisuración en piezas de hormigón armado sometidas a flexión pura. PhD Thesis," Technical University of Madrid (UPM), Madrid, Spain, 2008.
- [32] M. Wu, Tension stiffening in reinforced concrete – instantaneous and time-dependent behaviour. PhD Thesis, Cardiff, Wales: The University of South Wales., 2010.
- [33] R. J. Frosch, B. D.T and R. Radabaugh, Investigation of bridge deck cracking in various bridge superstructure systems. Report No. FHWA/IN/JTRP-2002/25., West Lafayette, Indiana: Purdue University, 2003.
- [34] C. Base, A. Beeby and P. Taylor, An investigation of the crack control characteristics of various types of bar in reinforced concrete beams. Research report 18., Cement and Concrete Association., 1966.
- [35] Klaklauskas, "Personal communication (unpublished)," 2019.
- [36] A. Pérez Caldentey, J. Mendoza Cembranos and H. Corres Peiretti, "Slenderness Limits for deflection control: a new formulation for flexural RC elements," *Structural Concrete*, vol. 18, no. 1, pp. 118–127, 2016. <https://doi.org/10.1002/suco.201600062>

Fatigue in Structural Concrete According to the New Eurocode 2

La fatiga en hormigón estructural según el nuevo Eurocódigo 2

Carlos Ríos^{*a}, Juan C. Lancha^b, and Miguel Á. Vicente^c

^a IDEAM, C/ Jorge Juan, 19 – 3º, 28001, Madrid, Spain.

^b Neos Maritime Consulting S.L, C/José Echegaray, 8 28232, Las Rozas, Madrid, Spain.

^c Universidad de Burgos, Dpto. de Ingeniería Civil, C/ Villadiego s/n, 09001 Burgos, Spain.

Recibido el 29 de agosto de 2022; aceptado el 20 de marzo de 2023

ABSTRACT

The new Eurocode 2 represents a significant advance in the treatment of fatigue in structural concrete, compared to the old Eurocode. Fatigue acquires greater relevance and visibility in the new standard, and the field of application of this limit state is extended.

This paper shows the most relevant changes in the fatigue chapter of the new Eurocode 2, in which there has been an important formal and/or conceptual change with respect to the old Eurocode 2. The first difference is that in the new Eurocode 2, fatigue has its own chapter and annex, which shows how important this phenomenon has become in recent years. On the other hand, the new proposed fatigue formulation significantly improves the mechanical capacity of the material, which allows an optimisation of those concrete structures in which fatigue is a critical phenomenon.

KEYWORDS: Fatigue, structural concrete, S-N curves, Palmgren Miner rule, bridges.

©2023 Hormigón y Acero, the journal of the Spanish Association of Structural Engineering (ACHE). Published by Cinter Divulgación Técnica S.L. This is an open-access article distributed under the terms of the Creative Commons (CC BY-NC-ND 4.0) License

RESUMEN

El nuevo Eurocódigo 2 supone un avance significativo en el tratamiento de la fatiga en hormigón estructural, en comparación con el antiguo Eurocódigo. La fatiga adquiere una mayor relevancia y visibilidad en la nueva norma, y se amplía el campo de aplicación de este Estado Límite.

Este artículo muestra los cambios más relevantes del capítulo de fatiga en el nuevo Eurocódigo 2, en los que se ha producido un importante cambio, formal y/o conceptual, respecto al antiguo Eurocódigo 2. La primera diferencia es que en el nuevo Eurocódigo 2, la fatiga tiene su propio capítulo y anexo, lo que muestra la importancia que este fenómeno ha adquirido en los últimos años.

Por otra parte, la nueva formulación de fatiga propuesta mejora de forma significativa la capacidad mecánica del material, lo que permite una optimización de aquellas estructuras de hormigón en las que la fatiga sea un fenómeno crítico.

PALABRAS CLAVE: Fatiga, hormigón estructural, curvas S-N, regla de Palmgren Miner, puentes.

©2023 Hormigón y Acero, la revista de la Asociación Española de Ingeniería Estructural (ACHE). Publicado por Cinter Divulgación Técnica S.L. Este es un artículo de acceso abierto distribuido bajo los términos de la licencia de uso Creative Commons (CC BY-NC-ND 4.0)

1. INTRODUCTION

From the 1990s to today, many things have changed in the world and in Europe; in all areas: social, cultural, economic, environmental, etc., as well as scientific and technological. The world of concrete and structures has been no exception, and in the last 30 years there have been significant advances in

many fields. These include, for example, the development of the High-Speed Railway network that has been carried out in Spain (with the construction of some 3,000 km of new lines during this time) and throughout Europe, with the help of European Funds. Also noteworthy is the development of wind energy in Spain (with a total of approximately 21,500 wind turbines installed in almost 1,300 wind farms) and worldwide. The vast majority of wind turbines are steel towers, but in recent years different concrete-based solutions have been appearing due to the exigent dynamic requirements of the wind

* Persona de contacto / Corresponding author.
Correo-e / e-mail: carlos.rios@ideam.es (Carlos Ríos).

turbines, and larger turbines will lead to a more extensive use of the concrete tower as the standard solution.

However, one thing has not changed in recent years, and that is Eurocode 2, which remains broadly the same structure as that document published at the beginning of the 2000s.

In the field of structural fatigue, and more specifically in the field of concrete fatigue, the evolution in the last 30 years has been more than remarkable, both in the knowledge of the fatigue response of concrete (both in its mass concrete version and in its reinforced, prestressed, fibre-reinforced, etc.) and in the importance of fatigue as a structural design criterion. In this respect, the concrete towers of wind turbines are a good example. For these structural elements, the most restrictive limit state, the one that conditions their design, is fatigue. This is due, in part, to the fact that the international standards and recommendations that regulate it are highly conservative, which makes it less competitive than other structural solutions.

The Eurocode 2, EN 1992-1-1, [1], currently in force, dated 2004, was an important advance in the field of concrete fatigue, but it was based on the state of the art of the 1990s. 20 to 30 years of intense scientific and technological development have rendered it obsolete in certain aspects. A profound change was needed. The new version of Eurocode 2, in its Fatigue chapter, represents a more than remarkable update.

The first change that can be observed is that, in the case of the new version of Eurocode 2, FprEN1992-1-1:2023, [5], fatigue has its own chapter and its own annex, whereas in the equivalent document of 2004 [1], fatigue is included in clause 6, a clause dealing with every Ultimate Limit State. It is necessary to go to the Eurocode 2 part 2 [2] to find a section (not a chapter) and an annex dedicated to fatigue. At that time, end of 1990s, bridges were the only structures where fatigue could be considered as a relevant structural effect. For the rest of the structures, it was not usually taken into account.

The fact that in the new version of Eurocode 2 [5], fatigue in concrete occupies an entire chapter shows the importance that this limit state has acquired in recent years.

In the field of concrete fatigue, the new Eurocode 2 [5] follows a different line from the Model Code 2010 [3], a document that has been a reference in the world of structural concrete in many aspects, and also in fatigue. It also follows a different approach from the one presented in the technical document recently published by the American Concrete Association "ACI PRC-215-21" [4]. The new Eurocode 2 [5] includes a new formulation of the fatigue strength in compression, based on the new formulation introduced for the static compressive strength in Ultimate Limit States, ULS, which leads to remarkable increases of the fatigue strength of concrete in compression, especially for those concretes with strength class above C50, compared to the formulation of the still current version of Eurocode 2 [1].

The changes introduced by the new version of Eurocode 2 [5] in the formulation used to verify the fatigue strength of concrete make it possible to exploit the material's strength capacity between 10% and 20% more than the old formulation allowed, and this change will make it possible to reduce the volume of concrete structures subjected to wind by 5% to 10%.

This will give a decisive boost to the implementation of wind energy production facilities, both on-shore and off-shore,

which will reduce the price of energy and simultaneously reduce energy dependence on the outside world.

Furthermore, the use of renewable energy sources helps to reduce the carbon footprint and, consequently, contributes to the fulfilment of one of the Sustainable Development Goals promulgated by the United Nations.

This paper presents, in detail, the most relevant aspects of the fatigue chapter of the new Eurocode 2 [5], in which a major change, formal and/or conceptual, has taken place with respect to the Eurocode 2 currently in force [1].

3.

CASES TO BE CONSIDERED

Fatigue is not a common concern in structures under predominantly static loads, such as standard buildings. On the other hand, most of live loads are always dynamic loads, even in case of building structures. Therefore, it could be possible to affirm that almost any structure is subjected to dynamic loads, being most of them cyclic loads.

However, depending on the number of cycles and the load amplitude or range of these loads, their impact on the structure may be negligible and therefore the verification of the ULS of fatigue not required. Concretely the new Eurocode, FprEN1992-1-1:2023, 10.1, [5], states: "*Structures and structural components subjected to significant numbers of repeated load or deformation induced significant stress cycles shall be verified to endure the expected cyclic actions during the required design life*".

Key issues are when a cyclic load can be considered fatigue non-relevant, a structural type can be considered non-sensitive to cyclic action or when the number of cycles is non-significant. Current Eurocode EN 1992-1-1, [1], states, 6.8.1 (2):

"A fatigue verification should be carried out for structures and structural components which are subjected to regular load cycles (e.g., crane-rails, bridges exposed to high traffic loads)".

Hence, it does not provide specific cases to avoid fatigue verification but leave it to the engineer's judgment.

Regarding [5], the following list of cases for which a fatigue verification is not required is provided in clause 10, which is a novelty compared to [1], although not to EN 1992-2 [2], as commented below:

- common buildings subjected to a total number of significant load cycles $\leq 2 \cdot 10^4$,
- prestressing and reinforcing steel, in sections where, under the frequent combination of actions and P_k (prestressing actions), only compressive stresses occur at the extreme concrete fibres;
- external and unbonded tendons, lying within the depth of the concrete section".

Regarding a), the maximum number of cycles to avoid fatigue check is very low. For instance, any building resisting wind actions will be loaded by far more cycles. In EN 1991-1-4, B.3 [6], a relation between the number of cycles N_g and the amplitude of the wind gust, ΔS_k , is provided (Figure 1). It is shown than for $2 \cdot 10^4$ cycles the corresponding load amplitude

of the gust, ΔS_k , would be around 35% of the characteristic load S_k , which is a non-negligible value and could be fatigue relevant (Figure 1). Of course, engineering judgment, again, is fundamental.

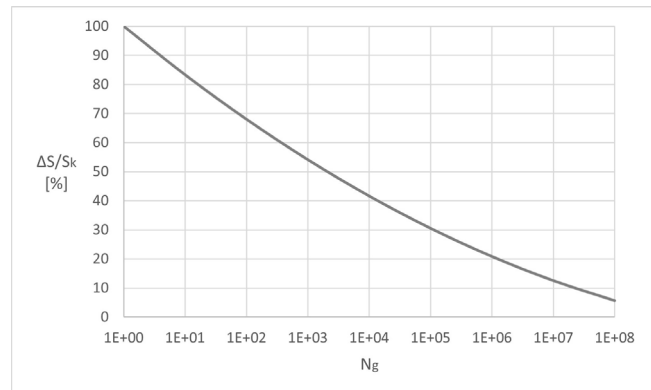


Figure 1. Number of gust loads N_g for an effect $\Delta S/S_k$ during a 50 years period [6].

Background for b) is clear. Prestressing and reinforcing steel in sections compressed under the frequent load combination will not have significant amplitudes, due to the uncracked condition of the section, and the compressive stress ranges are far less damaging than tensile ones. For instance, EN 1993-1-9 [7] states that compressive ranges of non-welded details shall be multiplied by 0.60. This provision b) was included in [2], but not in the general part [1].

Last, c), is based on the well-known fact that internal unbonded and external tendons will not have significant stress increments under service loads. These stress ranges depend on the deformations of the whole structure, there is no strain compatibility between concrete and steel, and this deformation must be controlled under SLS loads. According to the author's experience, this is generally true for bridges and other horizontal structures resisting primarily gravity loads. For support structures for Wind Turbine Generators, where deformations are not usually controlled under SLS loads, fatigue of external tendons should be verified due to the increasingly slenderness of the towers and the subsequent large displacements of the upper anchor of the post-tensioning system as well as the bending stresses at the anchors or other devices such deviators if specific measures are not taken to avoid them.

In EN 1992-2, [2], part of bridges, it is stated:

A fatigue verification is generally not necessary for the following structures and structural elements:

- footbridges, with the exception of structural components very sensitive to wind action;
- buried arch and frame structures with a minimum earth cover of 1.00 m and 1.50 m respectively for road and railway bridges;
- foundations;
- piers and columns which are not rigidly connected to superstructures;
- retaining walls of embankments for roads and railways;
- abutments of road and railway bridges which are not rigidly connected to superstructures, except the slabs of hollow abutments;

- prestressing and reinforcing steel, in regions where, under the frequent combination of actions and P_k only compressive stresses occur at the extreme concrete fibres.

Hence, [2] does provide a list of cases where fatigue can be assumed as negligible. But this list is kept in Annex K, [5], which is an Annex specific for bridges. Just point g) of the above list has been removed, but it is included in the general part, chapter 10, as already commented.

Other proposed exclusions were finally not included in [5], either in chapter 10 or Annex K. For instance a specific and interesting claim of U.K was related to fatigue of reinforcement of deck slabs bridges designed by conventional means. This claim is implemented in the UK National Annex of [2], where it is stated that fatigue verification is not required if the deck slab complies with certain requirements. According to UK's research, fatigue of reinforcement due to live load is typically around 10% of elastic predictions due to compressive membrane action work. This proposal was finally excluded, but the possibility of its inclusion, as well as other national claims, by means of an NCCI (Non-Contradictory Complementary Information for the use of EN Eurocodes at the National level) is allowed.

3. METHODS OF VERIFICATION

Whereas in [1] there is not a summary of the methods for the verification of the Ultimate Limit State, ULS, of fatigue, in [5] such summary is provided in 10.1:

- Simplified methods given in paragraphs 10.4 to 10.7.
- Refined methods:
 - Using damage equivalent stresses in Annex E, E.4 and Annex K, K.10 where applicable or
 - Explicit method using Palmgren-Miner rule in Annex E, E.5 where applicable.

Hence, levels of approximation are provided, being the more accurate the application of the Palmgren-Miner rule.

Damage equivalent stress method is only feasible if damage equivalent stresses, or loads, are provided. These equivalent loads are provided exclusively for bridges in Annex K, both railway and road bridges, and their calculation is based on several simplifications. Nevertheless, it is a more accurate method for standard elements of the bridge, i.e., beams, decks, girders, etc., than the simplified methods.

Palmgren-Miner rule requires the knowledge of the history or time series of the stress or load of interest. Alternatively, it is possible to apply a counting method (rainflow, reservoir) to these time series and get the stress histograms or the corresponding Markov matrices. This is the more accurate method, and the standard one in case of structures for wind turbines and non-standard elements of bridges.

It is noteworthy that damage equivalent stress range and Palmgren-Miner rule were included in [2], part for bridges, but not in the general part, [1]. Main reason could be that, at the time of the elaboration of [1] and [2], bridges were the main concrete structures subjected to cyclic loading, whereas wind turbines were not in the close horizon and offshore structures

were specifically excluded of the current Eurocodes. Including these refined methods in the general part is clearly more rational.

4. COMBINATIONS OF ACTIONS

In [1] the following specific combination of actions is provided, 6.8.3. (Eq. 1):

$$(\sum_{j \geq 1} G_{kj} + P + \psi_{1,1} Q_{k,1} + \sum_{i \geq 1} \psi_{2,1} Q_{k,i}) + Q_{fat} \quad (1)$$

The proposed combination is the frequent combination of actions for transient or persistent situations plus the relevant fatigue load, Q_{fat}

Definition of Q_{fat} is explicitly given:

" Q_{fat} is the relevant fatigue load (e.g. traffic load as defined in EN 1991 or other cyclic load)"

In [5] the "fatigue" combination of actions is slightly modified (Eq. 2):

$$\Sigma F_d = \Sigma_i G_{k,i} + \Sigma_j \psi_{2,j} Q_{k,j} + (P_K) + F_{fat,d} \quad (2)$$

We can identify the proposed combination as the quasi-permanent combination of actions for transient or persistent situations plus the design value of the fatigue action, $F_{fat,d}$, as leading action. $F_{fat,d}$ is defined as the cyclic component of the frequent load.

$F_{fat,d}$ is explicitly defined for road and railway bridges in [5]. Concretely, for road bridges, $F_{fat,d}$ can be taken as the frequent load of Load Model 1 and for railway bridges as the frequent load of Load Model 71 according to EN 1991-2 [8]. For other cyclic loads, definition of $F_{fat,d}$ is not explicitly given, and its election shall be based in engineering judgment but always using the frequent value.

It is important to notice that the above values of $F_{fat,d}$ for bridges, frequent values of Load Model 1 and Load Model 71, are only valid for the simplified verification of fatigue according to paragraphs 10.4 to 10.7 of [5]. More refined methods, such damage equivalent stress range or Palmgren Miner rule requires a different definition of $F_{fat,d}$. For the damage equivalent stress approach, $F_{fat,d}$ shall be precisely the equivalent load, which is defined in Annex K for both road and railway bridges. In case of road bridges, the specific fatigue load model from which the equivalent load is calculated is the Fatigue Load Model 3, whereas for railway bridges is the Load Model 71 (or SW/0 when required).

Regarding the differences between combinations proposed in the current version and in the draft, it would seem that the combination in [5] is more favourable than the current one, quasipermanent versus frequent load combination. A closer look yields only small differences.

The reason is that the definition of the cyclic load doesn't change, frequent value of the cyclic action, and this load is the main source of fatigue damage. Nevertheless, other actions may have an impact. This impact is due to the inherent non-linearity of concrete cross sections due to cracking. For

structural steel, the amplitude or range of the cyclic load would be the only source of fatigue damage, but in case of concrete, reinforced or prestressed, the cross section shall be considered cracked, and therefore the stress assessment of concrete and reinforcing and prestressing steel shall take into account every force defined in the combination, especially if axial forces are involved. Besides, fatigue of concrete does depend not only on the stress range but also on the mean stress, what, again, oblige to include every force acting on the cross section.

However, impact of changing frequent values of the non-cyclic actions by their quasipermanent value will not have a significant impact. Usually, the more significant non-cyclic action, at least for bridges, would be the thermal load if the structure is statically indeterminate or the cross section is composite. But the difference between ψ_1 , frequent value specified in [1], and ψ_2 , quasipermanent value specified in [5], is very small. According to EN1991-2 [8], $\psi_1 = 0.6$ and $\psi_2 = 0.5$. Hence the impact on the fatigue verification is minimal, and on the other hand, it seems more correct to consider the quasi-permanent value for fatigue verification.

Regarding wind actions, the scenario is slightly different. ψ_1 is taken as 0.5 and ψ_2 is taken as zero, EN1991-2 [8]. Hence, the proposed combination in [5] does not include wind in the fatigue combination whereas the current one does, with the frequent value. If cyclic action of wind is not considered relevant, neglecting the static value as [5] does for the fatigue combination is rational. Of course, wind can be adopted as the leading cyclic action in several cases, clearly in support structures for wind turbines but also in case of other type of structures where wind may induce significant stress ranges and number of cycles, including specific aerodynamic effects such vortex shedding, and this requires engineering judgment.

One last consideration is that this fatigue combination shall not be adopted as a limit for consideration of cracking. Cross sections or structural elements shall be considered cracked, as explained in the next paragraph.

5. INTERNAL FORCES AND STRESSES

First, it is important to note that cyclic internal forces and stresses shall be calculated under service conditions. Appropriate stress-strain relationships shall be adopted, although linear relationship is recommended, and strain compatibility must be assumed. For assessment of stresses, assumption of cracked concrete is prescribed. It is worth to point out that, in prestressed members, according to paragraph 9.2.2 (7), [5], if, under the characteristic combination of actions the tensile stress in the concrete is below $f_{ct,eff}$, effective concrete tensile strength, the section can be considered uncracked. This would be beneficial for reinforcing and prestressing steel, as well as for concrete, but then fatigue of concrete under tensile stress ranges must be verified. This verification is not covered in [5], which just covers, as [1] does, concrete fatigue under compressive stresses, not under tensile stresses or compressive-tensile stresses. Hence, the assumption of cracked concrete is the only possible one. This assumption is correct if no stress reversals occur in the fiber under

TABLE 1.
Ratio of bond strength ξ between tendons and reinforcing steel

prestressing steel	ξ		
	pre-tensioned	bonded, post-tensioned	
		$\leq C50/60$	$\geq C70/85$
smooth bars and wires	Not applicable	0.3	0.15
Strands	0.6	0.5	0.25
indented wires	0.7	0.6	0.30
ribbed bars	0.8	0.7	0.35

Note: For intermediate values between C50/60 and 70/85 interpolation may be used

study, i.e., if the fiber is always subjected to tensile stresses, as usually happens in bridges. If stress reversals occur, i.e., if the fiber is subjected to compression-tension stress ranges, for instance in structures for wind turbines, consideration of cracked cross sections shall be carefully analysed, specially if concrete has a significant humidity and other codes and standards should be applied.

Regarding the different bond behaviour of prestressing and reinforcing steel, which has an impact in their stress assessment, the approach has slightly changed. The current formulation in [1] is correct only if reinforcing and prestressing steel are in the same position. The new approach allows to calculate stresses for different locations of reinforcing and prestressing steel. For this, an equivalent area of prestressing steel, A_e , is defined, (Eq. 3), function of the bond strength ratio between tendons and reinforcing steel, implemented by means of parameter ξ . This different bond strength is equivalent to a larger stiffness of the reinforcing steel compared to prestressing steel and therefore techniques for composite cross section analysis, i.e., equivalent sections, can be used:

$$A_e = A_p \sqrt{\xi \frac{\phi}{\phi_p}} \quad [3]$$

Please note that in Table 10.1, Note 2 [5], it is stated that provided ξ values are valid just for “tendons directly cast into concrete or contained within corrugated metal ducts”, which means that plastic ducts, widely used, are excluded. If such ducts are used, no provisions are given. This could be problematic since in the European Technical Assessment or Approval of prestressing systems this value is generally not given, but if the tendons are intended to be bonded the plastic ducts must be corrugated, not being expected large differences between the ξ values of metallic ducts which, additionally, are affected by a square root. Table 1 show the values of ξ considered in [5].

A very important novelty is the consideration of the redistribution of stresses in concrete in the compression zone. This redistribution allows to consider a reduction of the concrete stresses, which can be of importance for reinforced concrete and less significant for prestressed concrete.

Application is straight forward; the stress calculation shall be carried out at the fibre located 100 mm from the most compressed edge but limiting the 100 mm distance to 1/3 of the cross-section depth and limiting the calculated value of the stress to 2/3 of the maximum stress at the extreme fibre of the cross-section. This is a simplified approach in general, and sometimes conservative compared to the approach of Model Code 2010, [3].

Redistribution of stresses under fatigue loading has experimental background. Most loaded fiber under cyclic stress will soft and the less stressed fibers will absorb more stress. According to Zanuy [10], redistributions in reinforced concrete beams, not over-reinforced, practically avoid any failure of compressed concrete under cyclic loads, so that the typical fatigue failure takes place in the reinforcement. This is not true, according to [10], in prestressed members, over-reinforced cross sections, columns or piers or when the cyclic concrete stresses are very high.

In the author’s opinion, the formulation for redistribution of stresses provided in [5] is quite conservative. Besides the importance of this redistribution for a proper assessment of highly variable stress zones, is undoubtful. Lack of experimental work on this matter effectively prevents more refined approaches, and this is reflected in [5].

6. REINFORCING AND PRESTRESSING STEEL. S-N CURVES. SIMPLIFIED VERIFICATION

General approach for fatigue verification for steel, reinforcing and prestressing, has not been changed. Simplified and refined methods can be used, both based on the S-N curves. However, these curves have been updated. Below new S-N curves, new corresponding results of the simplified verification and other changes are described.

S-N curves for reinforcing steel are provided in [1], Table 6.3N, which is reproduced below, (Table 2):

TABLE 1.
Ratio of bond strength ξ between tendons and reinforcing steel

Type of reinforcement	N^*	Stress exponent		$\Delta\sigma_{Rsk}$ (MPa) at N^* cycles
		k_1	k_2	
Straight and bent bars ¹	10^6	5	9	162.5
Welded bars and wire fabrics	10^7	3	5	58.5
Splicing devices	10^7	3	5	35

Note 1: Values for $\Delta\sigma_{Rsk}$ are those for straight bars. Values for bent bars should be obtained using a reduction factor $\xi = 0.35 + 0.026 D/\phi$, where:
D: diameter of the mandrel.
 ϕ : bar diameter.

[5] provides different S-N curves for reinforcing steel in Annex E, Table E.4, given below as Table 3:

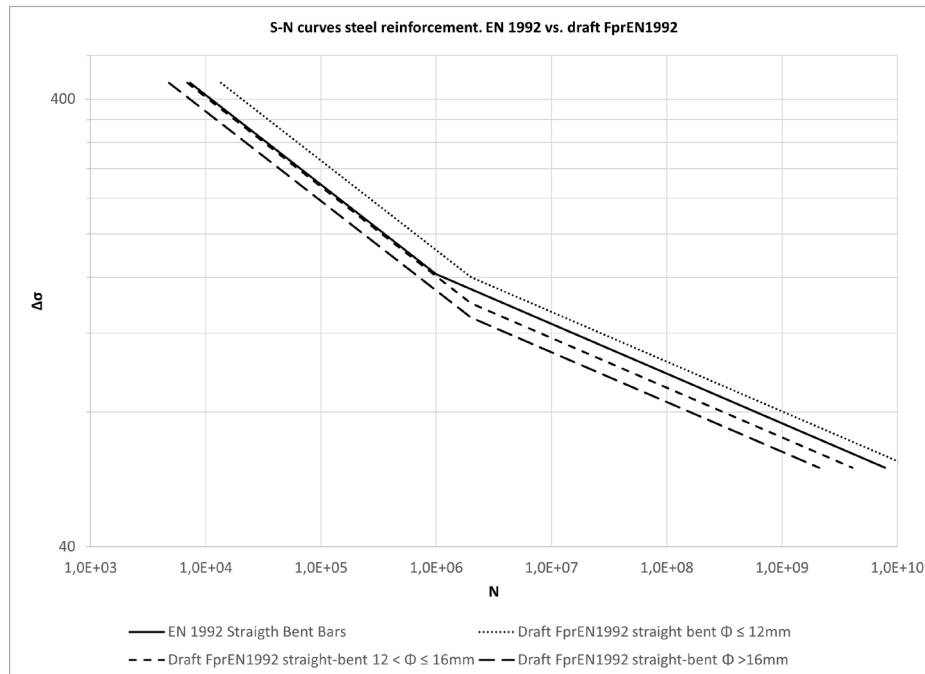


Figure 2. Comparison between S-N curves for non-welded reinforcement [5].

TABLE 3. Parameters of S-N curves for carbon reinforcing steel [5].

Type of reinforcing steel	Diameter	$\Delta\sigma_{Rsk}$ 5%-quantile (Test $\sigma_{max}=0,6f_{yk}$)			
		$\Delta\sigma_{Rsk}$ [MPa]	N^*	Stress exponent	
				$k_{\rho 1}$	$k_{\rho 2}$
Bars ^a	$\phi \leq 12$ mm	160	$2 \cdot 10^6$	5	9
	12 mm < $\phi \leq 16$ mm	140			
	16 mm < $\phi \leq 20$ mm	130			
	$\phi > 20$ mm	130			
	$\phi \leq 12$ mm	100		3	5
Type of reinforcing steel	$\phi > 12$ mm	80			
Couplers ^c	-	35	3	5	

a Values for bent parts of bars should be obtained using a reduction factor $\zeta=0.35 + 0.026 \phi_{mand}/\phi$. The reduction factor ζ may be omitted for shear reinforcement with 90° stirrups $\phi \leq 16$ mm and depth $h \geq 600$ mm.

b Values for $\Delta\sigma_{Rsk}$ of tack welded apply for a distance of 5ϕ at each side of the weld.

c Values for couplers apply unless more accurate S-N curves are available and confirmed by testing.

NOTE: The 10% quantile values for material according to table C1.a and C2.a are based on a confidence level of 90% whereas confidence levels probabilities for design $\Delta\sigma_{Rsk}$ (5% quantile values) are 75% according to EN 1990:2010, Annex D

Hence, S.N curves for rebars has changed. In [15], the corresponding background document for these new S-N curves, the two main reasons for these changes are explained. First, it is stated that bar diameters equal or below 16 mm are more relevant regarding fatigue because of the increasing application of post- and pre-tension, and these smaller bars, 6 to 20 mm, are today efficiently produced as mechanical straightened bars from coils (de-coiled bar). De-coiling has a negative influence in the fatigue properties of the bars, and it must be addressed

in the corresponding S-N curves, effectively ruling out other production methods regarding fatigue verifications.

Secondly, tack welding, instead of binding the bars with wires, has become the standard method for efficient prefabricated construction, and of course it has an impact in fatigue design and it must be addressed.

Hence, more than 500 test were carried out, mainly of 12 and 16mm bars, mechanically straightened and cross-welded bars by resistance welding and CO₂ tack welding.

These test campaign led to the modifications of the S-N curves in [5] shown in Table 3. Concretely, to the change of the knee from $N^* = 10^6$ (straight bars and bent bars) and $N^* = 107$ (welded bars and wire fabrics, as well as splicing devices) to $N^* = 2 \cdot 10^6$ in [5] for every type of reinforcement.

A quick comparison of the S-N curves for straight and bent unwelded bars shows that the proposed S-N curves in [5] are more conservative for $\phi > 16$ mm, as shown in Figure 2, where characteristic S-N curves are shown. For diameters from 12mm up to 16mm the proposed S-N curves are also more conservative, especially for low ranges, however for diameters lower than 12 mm cycles are clearly better.

Regarding welded bars, S-N curves are compared (Figure 3). For diameters less or equal than than 12 mm S-N curves in [5] are more favourable for low stress ranges and match the current S-N curve in [1] for stresses above the knee. For diameters larger than 12mm, the proposed S-N curve is less favourable stresses above the knee and matches the S-N curve in [1] below the later. Note that just tack weld and welded fabrics are included in [5], whereas in [1] the S-N curves are given for welded bars in general. On the other hand, in paragraph 10.4 of [5], the stress range limit to avoid fatigue verification is given for butt and tack welds, i.e., it can be deduced that butt welded bars may be verified by the S-N curve of Table 3. Other types of welded reinforcement, such as lap or cruciform joints, admitted in [1], would be excluded. Here, a more refined analysis would be required.

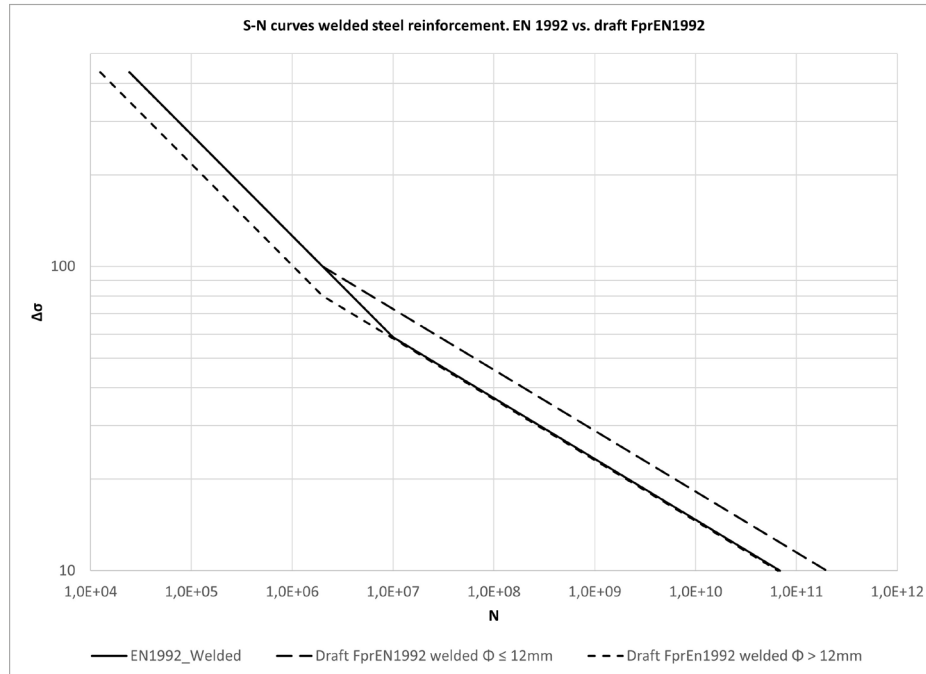


Figure 3. Comparison between S-N curves for welded reinforcement.

It is worth to comment the footnote in Table 3, “The 10% quantile values for material according to Table C1.a and C2.a are based on a confidence level of 90% whereas confidence levels probabilities for design $\Delta\sigma_{Rsk}$ (5% quantile values) are 75% according to EN 1990:2010, Annex D”. This note can produce some confusion and a brief comment is given below.

In the mentioned tables C.1 and C.2 10% quantile values of $\Delta\sigma_{Rsk}$, i.e., $2 \cdot \sigma_a$, are given, but these values are obtained from testing on bare reinforcing bars. In Table E.1, values of $\Delta\sigma_{Rsk}$ are the same than in tables C.1 and C.2, but for a 5% quantile. These values apply for reinforcement embedded in concrete.

Embedment in concrete will improve the fatigue behaviour of the bars about 10 to 15%, but this won't justify the same values for 10 and 5% quantiles. Hence in the note is specified that values of tables C.1 and C.2 mentioned above are given for a 90% confidence level, whereas values in Table 3 are given for a 75% confidence level, which is the standard confidence level obtained by the statistical methods of design assisted by testing, according to EN 1990 Annex D [11]. In conclusion, values are coherent in both tables.

Regarding the influence of bent parts, of critical importance for the assessment of shear reinforcement and other bent bars, it is treated as in [1], including the same formulation for the reduction factor of $\Delta\sigma_{Rsk}$, ζ . But an important novelty is given in Table 3, note ^a, where it is stated that for shear reinforcement with 90° stirrups, $\zeta \leq 16\text{mm}$ and depth $h \geq 600\text{mm}$, influence of the bent part may be omitted. For standard hook of bars smaller than 20 mm, $\phi_{mand} = 4 \cdot \phi$, the reduction factor is $\zeta = 0.454$, which leads to a drastic reduction of the fatigue life. Hence, neglecting the influence of the bent implies an important improvement. Aside of the maximum bar diameter and 90° angle, an important requirement is that the element depth shall be larger or equal than 600 mm, what allows the anchorage of the compressive strut of the shear force in the straight part of the bar, before reaching the bent part. This is the main

reason to neglect the undoubtable impact of the bent in the fatigue life of the bar. For smaller depths or larger diameters, a detailed analysis of the stress distribution along the bar may also allow some improvement of the fatigue life of bent bars.

For couplers, denoted splicing devices in [1], the S-N curve is modified, being less favourable due to the reduced value of N^* , but it is stated that European Technical Product Specifications can be used, since several suppliers provide special couplers with improved fatigue life.

S-N curves for prestressing steel are subjected to minor changes, which are shown in Table 4.

TABLE 4. Parameters of S-N curves for prestressing steel [5].

S-N curve for prestressing steel	N^*	Stress exponent		$\Delta\sigma_{Rsk}$ (MPa) at N^* cycles ^a
		k_1	k_2	
Pre-tensioning	10^6	5	9	185
Post-tensioning				
- single strands in plastic ducts	10^6	5	9	185
- curved tendons ^b in steel ducts	10^6	5	9	150
- straight tendons ^b or curved tendons ^b in plastic ducts	10^6	3	7	120
- anchoring devices and couplers	10^6	5	5	80

Note 1: Values in Table E.2 (NDP) apply for prestressing steel complying with Table C.3 to C.5 and prestressing systems complying with 5.4.

- a Values correspond to prestressing steel embedded in concrete
- b Applies to tendons with wires and strands; tendons with bars are not covered.

First change can be found in the general footnote. These S-N curves are applicable if prestressing system complies with subclause 5.4 of [5], where it is stated that the prestressing system must comply with the relevant standard for prestressing sys-

tems, being recommended EAD 160004-00-0301 (i.e., former E.T.A.G 013). In practical words, the prestressing system shall be in possession of the corresponding European Technical Assessment Document (E.T.A.).

In footnote b an important provision is given. Prestressing bars are excluded, no S-N curve is given for them. Background for this exclusion is the presence of threads in the bar, worsening the fatigue behaviour of the bars compared to strands or wires. Since cyclic loads on these elements in concrete structures are not uncommon, mostly in connections steel to concrete or concrete to concrete, it is worth to point out that fatigue verification of these bars is usually carried out according to EN 1993-1-9 [7], with a Detail Category (DC) of 50 MPa. This DC is valid if bending stresses in the bar are considered, which is not common unless detailed Finite Element Model of the connection is used. If bending stresses on the bar are not considered in the fatigue verification other codes and standards, [13] and [14] for instance, recommend using a lower DC, 36 MPa, to take into account the additional damage due to the non-contemplated bending stresses.

Regarding simplified verification of reinforcing and prestressing steel is provided in subclause 10.4 of [5], by means of maximum stresses under the fatigue load combination already mentioned. For unwelded and welded reinforcing steel, a comparison with [1], subclause 6.8.6, is given in Table 5.

TABLE 5.
Comparison among simplified verifications for welded and unwelded reinforcing bars in [5] and [1].

New EC2 [5]		Old EC2 [1]	
Type of bars, [5]	$\Delta\sigma_{sd,max}$, [5]	Type of bars, [1]	$\Delta\sigma_{sd,max}$, [1]
Unwelded, $\phi \leq 12\text{mm}$	90 MPa	Unwelded	70 MPa
Unwelded, $\phi > 12\text{mm}$	73 MPa		
Butt and tack welded, $\phi \leq 12\text{mm}$	40 MPa	Welded	35 MPa
Butt and tack welded, $\phi > 12\text{mm}$	30 MPa		
Couplers	24 MPa	Couplers	-

Limits are more relaxed in [5], for unwelded reinforcing bars, better for welded reinforcement with diameters $\phi \leq 12$ mm, and more exigent for welded reinforcements with $\phi > 12$ mm. Limit for couplers is a novelty. Limits for prestressing, differentiating pre and post-tensioning, are also given, which is an important novelty of [5].

Regarding the combination of actions to be used, the one specified in 10.2, [5], shall be adopted, but a maximum number of cycles is provided, 108 cycles. In contrast, in [1], no maximum number of cycles is provided. Specification of number of cycles for the simplified verification allows calculating these limits directly, as shown below.

Concretely, it is easy to check, based on the mentioned S-N curves that the provided values correspond to $N = 108$, being N the number of design cycles. For instance, for straight bars, with $\phi \geq 12\text{mm}$, and applying the corresponding S-N curve (Eq. 4):

$$(1.0 \Delta\sigma_{sd})^9 10^8 \leq \left(\frac{130}{1.15}\right)^9 2 \cdot 10^6 \rightarrow \Delta\sigma_{sd} = 73 \text{ Mpa} \quad (4)$$

the result matches the proposed simplified value, with $y_{Ej} = 1.00$, $y_{Ej} = 1.15$, $k_{f2} = 9$ and $\Delta\sigma_{Rsk} = 130$ MPa, i.e., it has been adopted for this simplified assessment the S-N curve for $\phi > 20$ mm also for diameters between 12 and 20 mm besides diameters larger than 20 mm. Since the number of cycles is given, this simplified verification can be adjusted for diameters larger than 12 mm and up to 20 mm.

7. CONCRETE UNDER COMPRESSION

7.1. The concrete fatigue phenomena

At material lever, the number of compression (or compression-tension) cycles that concrete is able to bear before the material failure is driven by several complex phenomena. Some of these phenomena controlling the material fatigue resistance are concrete compressive strength, concrete tensile strength, fibre amount and orientation (for FRC), water content (humidity), concrete fracture energy, cement type and aggregates type and size among others. Other phenomena control the fatigue action, like the peak compressive stress, the valley compressive, or tensile, stress, the load frequency, the stress gradient, the load path and the load history among others.

7.2. Compression fatigue verification methods

Since there is not a general fatigue formulation covering all the above-mentioned aspects in the state of the art, old Eurocodes [1] and [2], as all other concrete codes, includes in its formulations only a small part of these parameters: the most important; covering the high resulting uncertainty by a set of high safety coefficients and parameters.

The new Eurocode, [5], includes three levels of concrete compression fatigue verifications:

- A first level, called simplified verification, that can be found at clause 10.5 of this standard [5], does not take into account the number of load cycles, as far as they are less than ten million, and just limits the maximum peak stress and stress range, under the fatigue combination of loads, with a simple lineal equation.
- A second level, called damage equivalent stress, that can be found at Annex E chapter E.4.3 of this standard [5], considers, not the maximum stresses as the simplified method but the damage equivalent stresses, through a more detailed formulation.
- A third level, called Palmgren-Miner rule, that can be found at Annex E chapter E.5.3 [5] that allows for a detailed account of the damage induced by each individual load cycle, depending on its peak and valley stresses.

All the three methods evaluate the fatigue resistance of concrete working with the stress level, that is the ratio of the true stress (peak or valley or equivalent) to a notional design fatigue strength of concrete $f_{cd,fat}$.

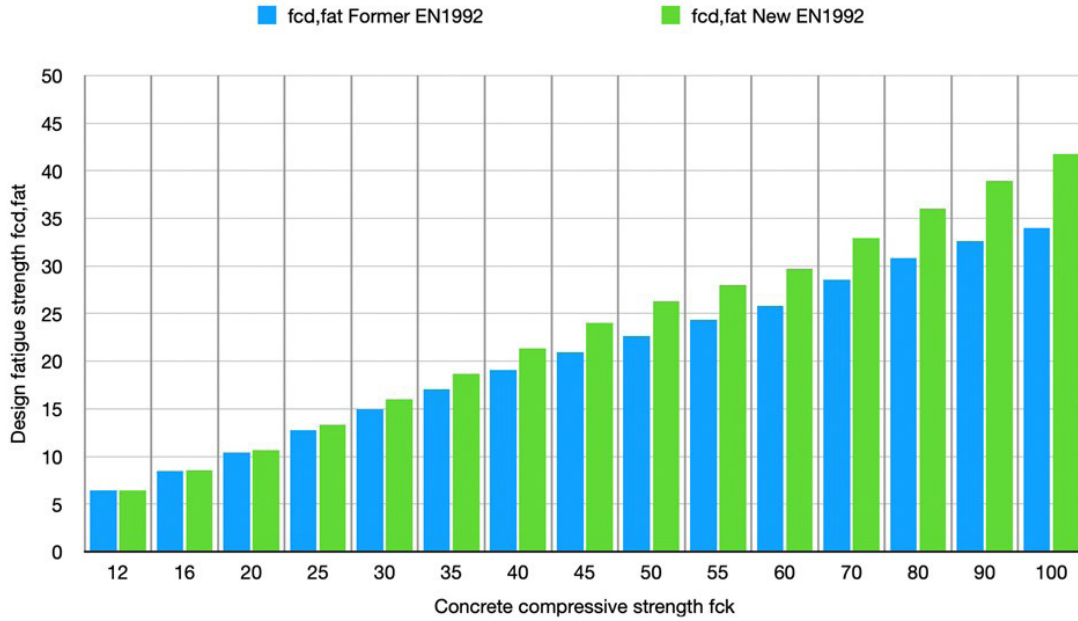


Figure 4. Comparison of $f_{cd,fat}$ between [2] and [5].

7.3. The design fatigue strength $f_{cd,fat}$

The design fatigue stress $f_{cd,fat}$ is a notional stress that is used to normalize the fatigue stress levels for the three methods. Therefore, this is the key parameter controlling the concrete compression fatigue at the code formulation.

Physically, $f_{cd,fat}$, may be understood as a stress such as if being reached in only one cycle it produces the failure of the material; therefore the fatigue peak stress of the loading cycles needs to stay as much under $f_{cd,fat}$ as higher is the number of acting cycles.

The equation used in [5] for $f_{cd,fat}$ is as follows (Eq. 5):

$$f_{cd,fat} = \beta_{cc}(t_0) f_c \frac{f_{ck}}{\gamma_c} \eta_{cc,fat} \quad (5)$$

where:

$\beta_{cc}(t_0)$ is a coefficient of concrete strength at first load application t_0 .

$$\eta_{cc,fat} = \min \{0.85 \eta_{cc} ; 0.8\}$$

The equation used in [1] for $f_{cd,fat}$ is as follows (Eq. 6):

$$f_{cd,fat} = k_1 \beta_{cc}(t_0) f_c (1 - f_{ck} / 250) \quad (6)$$

where:

$\beta_{cc}(t_0)$ is a coefficient of concrete strength at first load application .

t_0 is the time of the start of the cyclic loading on concrete in days.

The value of k_1 for use in a country may be found in its National Annex. The recommended value for $N = 10^6$ cycles is 0.85.

Equation 5 is very similar to the one used in [1] (Eq. 6), being the only difference the $\eta_{cc,fat}$ factor, a coefficient that reduces the fatigue strength for the concrete strength classes over 40 MPa. This new factor $\eta_{cc,fat}$ replaces the former k_1 and $(1 - f_{ck} / 250)$ factors.

This coefficient, in [5], is based in the general η_{cc} coefficient, that applies for static loading. In [1], which lacked this general η_{cc} coefficient for the static compressive strength, the coefficient was obtained directly from the compressive strength.

Figure 4 shows the current and the new resulting design fatigue strengths for the concrete classes covered by the standard. In both cases, former and new Eurocode, the standard recommended values, above mentioned, for k_1 and $\beta_{cc}(t_0)$ have been used to make the comparison.

The new formulation gives slightly lower fatigue strengths for the lower concrete classes and bigger values for the high strength classes, giving a net strength increase of 23% for the C100.

This change in the fatigue compressive strength in [5] is made in the opposite direction of the change in the static design compressive strength, that is reduced in the new code proportionally to the increase in the f_{ck} , being the bigger reduction applied for the C100 with a 25% reduction of the static compressive strength relative to [1].

7.4. Simplified verification

This first method provided in [5], is very similar to the one present in [1]. The criteria is as follows (Eq. 7) [5]:

$$\frac{|\sigma_{cd,max}|}{f_{cd,fat}} \leq 0.5 + 0.45 \frac{|\sigma_{cd,min}|}{f_{cd,fat}} \leq 0.9 \quad (7)$$

where:

$\sigma_{cd,max}$ is the maximum compressive stress at a fibre under the fatigue load combination according to 10.2 [5].

$\sigma_{cd,min}$ is the minimum compressive stress at the same fibre where $\sigma_{cd,max}$ occurs.

$f_{cd,fat}$ is the design fatigue strength of concrete according to 10.5 [5].

Note that, as commented above, if $\sigma_{cd,min}$ is tensile, it shall be considered as null, since concrete must be considered cracked.

The new formula is exactly the same as the one present in [1], being the only difference the absolute limiting value 0.90 for peak the stress level.

This maximum peak stress level was fixed at 0.90 for concrete classes up to 50 MPa and limited to 0.80 for classes over 50 MPa. In [5] the same 0.90 is used for all concrete classes, giving an additional 12% increase in the strength for the higher concrete classes on top of the increase of the design fatigue strength previously described.

Therefore, the global increase in the fatigue strength for a C100, according to the simplified method, is over 38% compared to [1].

7.5. Damage equivalent stress amplitude method

This second method has been moved from the main article 6.8.7 in [1] to the new Annex E in [5]. The formulation used is the same used in [1], and can be found now at subclause E.4.3, [5]:

$$\frac{|\sigma_{cd,max,equ}|}{f_{cd,fat}} + 0.43 \sqrt{1 - \frac{|\sigma_{cd,min,equ}|}{|\sigma_{cd,max,equ}|}} \leq 1 \quad (8)$$

Where:

$f_{cd,fat}$ is the design fatigue strength of concrete according to 10.5 [5].

$|\sigma_{cd,max,equ}|$ is the upper stress of the damage equivalent stress amplitude for $N=10^6$ cycles.

$|\sigma_{cd,min,equ}|$ is the lower stress of the damage equivalent stress amplitude for $N=10^6$ cycles.

Both [1] and [5] use the same term $\sigma_{cd,max,equ}$, nevertheless, the definition for $\sigma_{cd,max,equ}$ in [1] is “the upper stress of the ultimate amplitude for N cycles” and his ratio to $f_{cd,fat}$ was called “maximum compressive stress level” while in [5] the definition for the same term is the more precise “the upper stress of the damage equivalent stress amplitude for $N=10^6$ cycles”; and the same applies for $\sigma_{cd,min,equ}$.

Most of the structures subjected to fatigue coming from wind, wave and traffic loads are subjected to fatigue cycles of different amplitude, usually a random amplitude following some statistical distribution. The “damage equivalent stress amplitude” is a term commonly used in fatigue of metals subjected to this kind of loads, that refers to a notional constant stress amplitude which for a fixed number of cycles ($N=10^6$ cycles in this case) produces exactly the same damage as the true variable (usually random) stress amplitude loads.

In the case of metals this “damage equivalent stress” can be calculated directly for the “damage equivalent loads” that can be obtained by simple calculations over time history loads or loads spectra due to the linear nature (and the almost null influence of the mean stress) of the S-N curves in metals.

In the case of concrete under compression, since there is not such a linear S-N relationship, a precise definition of the “damage equivalent loads” is needed for every structural application (i.e., bridges, towers, sea structures, etc.).

In [5] these equivalent loads are provided for the specific case of railway bridges at the new Annex K article K.11.3 [5].

7.6. Palmgren-Miner rule method

This third, and most precise method, the Palmgren-Miner rule, was present in the old Eurocode only at the bridges part of the code, [2]. Now it is included in the new annex E and can be used for all the structures covered by [2], including some of the structures at which the compression fatigue normally drives the design, like the offshore structures and the wind turbine support structures, previously excluded of the scope of [2].

The Equation E.8 used in [5], Annex E, is exactly the same found in [2] (Eq. 9):

$$N_i = 10^{k_i} \quad (9)$$

where:

N_i is the number of cycles to fatigue failure for each stress-level.

k_i is a coefficient which can be obtained with the following formula (Eq. 10).

$$k_i = C \frac{1 - \frac{|\sigma_{cd,max,i}|}{f_{cd,fat}}}{\sqrt{1 - \frac{|\sigma_{cd,min,i}|}{|\sigma_{cd,max,i}|}}} \quad (10)$$

where:

$C = 14$ may be taken for concrete under compression and not permanently submerged in water.

$\sigma_{cd,max,i}$ is the maximum compressive stress in stress-level “i”,
 $\sigma_{cd,min,i}$ is the minimum compressive stress in stress-level “i”,
 $f_{cd,fat}$ is the design fatigue strength of concrete according to 10.5 [5].

The difference between [2] and [5] comes from two sources:

- As previously mentioned, the current EN 1992-2 [2] is allowed to be applied only to bridges, and under the specific bridge loads combinations defined in the same Part 2 of [2], while [5] allows the application to any kind of structure, but those permanently submerged in water.
- The reference concrete fatigue design strength used to drive the stress level is increased in [5] as explained above, leading to a much higher number of resisting cycles for the same stresses at the higher concrete classes.

This increment in the fatigue compressive strength is very significant, since with [5], some structures whose design is driven by the compression fatigue strength of the concrete, like those under predominantly waves or wind loads, can now be designed with this new formulation.

8. SHEAR

It is possible to split the fatigue verification of members under shear in two cases, members requiring and not requiring shear reinforcement.

8.1. Members not requiring shear reinforcement.

No modifications have been implemented in the simplified verification, except replacing forces, $V_{Ed,max}$ and $V_{Rd,c}$, by stresses, $\tau_{Ed,max}$ and $\tau_{Rd,c}$.

Considering the extensive modification of the shear strength of members not requiring shear reinforcement carried out in [5], it is hard to tell if the simplified verification is more exigent than in [1].

Combination of actions for this simplified verification, and any other one, is the one proposed in 10.2 of [5].

Regarding the methods for refined fatigue assessment, damage equivalent stress range or Palmgren Miner rule, there is no formulation provided for members without shear reinforcement, no S-N curves are given. Model Code 2010 [3], however, provides a S-N curve for fatigue shear strength of members without shear reinforcement (Eq. 11):

$$\log N = 10 (1 - V_{max} / V_{ref}) \quad (11)$$

where:

V_{max} is the maximum shear force under the relevant representative values of permanent loads including prestress and maximum cyclic loading.

$$V_{ref} = V_{Rd,c}$$

This S-N curve was not included in [5], but it will allow the use of Palmgren Miner rule in case that histograms or Markov matrices of shear forces are available.

8.2. Members requiring shear reinforcement.

In members requiring shear reinforcement both shear reinforcement and concrete struts must be verified. Hence simplified and refined methods for fatigue verification of reinforcing steel and concrete under compressive stresses can be applied.

Verification of fatigue for shear reinforcement and concrete struts strongly depends on the value of the angle of the struts to the bending reinforcement, θ . In the current EN 1992-1-1 the following formula is proposed in 6.8.2 (3) [1] for this angle when verifying fatigue (Eq. 12):

$$\cot\theta_{fat} = \sqrt{\cot\theta} \quad (12)$$

This formula considers the fact that the angle of the struts under fatigue loads, which are loads under service conditions, may be significantly larger than the one considered for ultimate loads. For instance, if $\cot\theta = 2.50$ for ULS verifications, $\cot\theta_{fat}$ would yield 1.58 for fatigue checks. Hence fatigue design of shear reinforcement can be more determinant than ULS design, especially if the shear reinforcement presents an additional reduction of its fatigue strength due to the presence of a bent.

But the proposed formula is an estimation and does not consider the actual biaxial stress state in the member if axial force is present. For instance, the prestressing force acting on the member can significantly flatten the angle. Hence, although keeping the formulation in [1] for $\cot\theta_{fat}$ the possibility of a specific calculation of $\cot\theta_{fat}$ by means of the formulation of annex G is allowed by [5], using the maximum shear in the cycle.

Annex G provides information for assessment of SLS stresses, considering cracking, in G.5. Formulation is given for membrane elements, perfectly applicable for thin webs of T beams, box girders, etc., but also for solid cross sections with some adjustments. For this assessment of $\cot\theta$ Annex G allows two approaches, elastic calculation, and the following more refined formula, which implies solving a 4th grade polynomial equation (Eq. 13) and takes into account the reinforcement amount:

$$\frac{|\tau_{Edxy}|}{\rho_x} \cot^4\theta + \frac{\sigma_{Edx}}{\rho_x} \cot^3\theta - \frac{\sigma_{Edy}}{\rho_x} \cot\theta - \frac{|\tau_{Edxy}|}{\rho_x} = 0 \quad (13)$$

Regarding the compression strut, the same $\cot\theta_{fat}$ shall be used. Reduction of compressive fatigue strength $f_{cd,fat}$ due to transverse tensile stresses is considered by means of factor v . A simplified value of $v = 0.5$ is proposed in chapter 8 of [5] and directly recommended for the simplified verification of concrete under shear. A larger value of v may be calculated, according to the formulation given in 8.2.3 (7), [5], if the ductility of reinforcement is B or C. In any case, when adopting the recommended simplified value of v , 0.50, high strength reductions of concrete fatigue strength can be expected, and this can have an impact in the design of thin webs of precast beams and other members under cyclic loads. Hence, it is highly recommended to use the more refined value of v . It is interesting to point out that even these refined values of v are very conservative since the transverse reinforcement won't yield under cyclic loads, whereas the proposed formulation for v assumes a yielded, or close to yield, reinforcement. A more accurate estimation of the strength reduction considering the stress level of the transverse reinforcement can be also found in Annex G. The formulation can be found in G.3, and it allows to consider levels of reinforcement stress lower than the yield strength, increasing consequently the value of v . Of course, this is closely related to the multiaxial stress states, commented below.

8.3. Shear at interfaces

Treatment of shear at interfaces has completely changed in the new FprEN 1992-1-1:2023 [5]. Current provisions just state that value of the cohesion, c , shall be halved in case of fatigue or cyclic loads, 6.2.5 (5) [1].

In the new draft, approach is totally different. First, detailing may allow to avoid fatigue verifications, i.e., if the reinforcement through the joint is fully anchored and the interface is rough or keyed, no fatigue verification of the interface itself is required. Of course, this does not excuse the verification of concrete and reinforcement next to the interface.

If, as sometimes occurs in precast construction, reinforcement crossing the interface cannot be fully anchored, i.e., anchor (or lap) length is not enough to transmit the full design stress of the reinforcement, f_{yd} , or the interface is not at least rough, strength of the interface shall be checked according to the following equation (Eq. 14):

$$\Delta\tau_{Edi} \leq \Delta\tau_{Rdi} = \mu_{v,fat} |\sigma_n| + \rho \frac{\Delta\sigma_{Rsk}}{0.45\gamma_s} (\mu_{v,fat} \sin\alpha + \cos\alpha) \quad (14)$$

Where $\Delta\tau_{Edi}$ would be the stress range according to the fatigue combination already described.

This verification is very favourable, since there is a factor 0.45 dividing the fatigue strength of the reinforcement, $\Delta\sigma_{Rsk}$.

Hence, this in fact an increase of the fatigue strength of the reinforcement.

Main reasoning behind this improvement of the fatigue strength of the reinforcement is that, neglecting the cohesion term, c , the concrete strut at the interface will flatten, and this has a positive impact in the reinforcement stresses.

This approach is not totally clear, at least in the author's opinion. If cohesion is omitted in the verification of ULS of fatigue, it should also be omitted in the standard ULS verification, and it is not.

On the other hand, Model Code 2010, [3], recommends a reduction of the static strength of 40% if cyclic loads were present, and although this reduction may be quite conservative, compared to it the new approach in [5] is much favourable for the fatigue verification.

Of course, zones adjacent to the interface, which shall be checked, will usually be, in this case, determinant.

9. MULTIAXIAL STRESS STATES.

Multiaxial stress states are common in most of the members subjected to cyclic loads, from bridges to support structures for wind turbines, especially in unavoidable geometric transitions or relatively abrupt geometric changes, but there is little experimental or theoretical background regarding fatigue behaviour of concrete under multiaxial cyclic stresses.

On the other hand, [1], and [5], do consider the reduction of concrete compressive strength under fatigue loads, $f_{cd,fat}$, in case of transverse tension, since the factor v shall multiply f_{cd} , when verifying fatigue of the concrete strut under shear. Hence, it is implicitly assumed that tensile stresses will have an impact on the compressive fatigue strength not only for shear but for any biaxial or triaxial stress states with at least one positive principal stress. This means that, although not directly stated, [1] and [5] are assuming that parameters defining concrete strength under static multiaxial ULS stresses shall be also considered for fatigue strength verification of concrete under multiaxial cyclic stresses.

Accepting this assumption as correct, and it is correct according to [1] and [5], for biaxial stress states with at least one positive principal stress refined formulations, instead of simplified assessment, can be used for a calculation of the reduction factor v . Concretely Annex G in [5] allows assessing the reduction of compressive strength considering the real transverse reinforcement stress, and this will have a significant impact since, under cyclic loads, stress levels of transverse reinforcement will be significantly lower than its yield strength whereas the reduction of concrete strength given by the simplified value of factor v considers the reinforcement yielded or close to yield. Old Eurocode 2, part of bridges, [2], in subclause 6.109, also allowed this refined assessment of the strength reduction, but in a much more conservative way. In the author's experience the application of this Annex G will lead to more rational reductions of concrete strength for fatigue verification of concrete under compressive cyclic stresses and transverse tension.

Regarding confinement of concrete under bi or triaxial compressive stress states, no provisions are given in the current draft. There are few experimental results for confined

concrete under cyclic compressive stresses, but several of them indicate an improvement of the fatigue strength, [12]. Additionally, since compressive fatigue strength reduction must be assumed if transverse tensile stresses exist, it seems rational to also consider the improvement of the compressive fatigue strength due to confinement. Despite this, no direct indications to consider confinement are given in [5]. It is worth to mention that in other codes, for instance in [14], it is allowed to consider confinement, but the increase in the fatigue compressive strength is limited to a factor of 1.30.

Last, it shall be pointed out that, as already commented, no provisions for verification of concrete fatigue under tensile or compressive-tensile stresses are given in [5], i.e., concrete shall be considered cracked.

10. APPLICATION TO BRIDGES

No significant changes have been carried out in [5]. Below are described the most important ones.

10.1. λ factors

λ factors are required to calculate the damage equivalent stress range, $\Delta\sigma_{s,eqv}$ for prestressing and reinforcing steel in both road and railway bridges. They consider, according to [5], Annex K:

- $\lambda_{s,1}$: Type of element, e.g., simply supported or continuous beam, as well as the damaging effect of traffic by means of the critical length of the influence line or area
- $\lambda_{s,2}$: Traffic volume
- $\lambda_{s,3}$: Design life of the bridge
- $\lambda_{s,4}$: Number of loaded tracks or lines.

The only λ value that has significantly changed is $\lambda_{s,1}$, although this change is specified just for railway bridges, $\lambda_{s,1}$.

This factor must change since it is function of the shape of the considered S-N curves, and these curves have changed for reinforcing steel, welded and unwelded. Concretely the number of cycles at the knee, N^* , has changed, being now $2 \cdot 10^6$ for any reinforcing steel, welded or unwelded. $\Delta\sigma_{R,sk}$ has also changed, but it does not affect the values of $\lambda_{s,1}$. These values of $\lambda_{s,1}$ are given in [5] in Annex K, Table K.2, which is reproduced here in Table 6.

In Table 6 above is specified, in (1) to (4), the parameters of the S-N curves considered for assessment of, slopes k_{f1} , k_{f2} and number of cycles at the knee, N^* . However, N^* does not match with the value specified in the new S-N curves in Annex E, [5], $2 \cdot 10^6$ cycles. The same values than those in [2], Annex NN, are kept.

A solution for this apparent inconsistency is found in Note 2, where it is stated: "Different N^* values can be considered as follows: $\lambda_{s,1,N^*new} = \lambda_{s,1,N^*old} (N^*_{old}/N^*_{new})^{1/k_{f1}}$ ".

For a better understanding of this modification, it must be noticed that the aim of the $\lambda_{s,1}$ factor is to get the damage equivalent stress range, i.e., the stress range that leads to the same damage than that calculated with the Palmgren Miner rule, using the stress range histograms produced by the so-called traffic mixes. A general expression for this damage equivalent

TABLE 6.
 $\lambda_{s,1}$ values for simply supported and continuous members of railway bridges [5].

a) simply supported members				b) continuous members (interior span)			
	L [m]	STM	HTM		L [m]	STM	HTM
(1)	≤ 2	0.90	0.95	(1)	≤ 2	0.95	1.05
	≥ 20	0.65	0.70		≥ 20	0.50	0.55
(2)	≤ 2	1.00	1.05	(2)	≤ 2	1.00	1.15
	≥ 20	0.70	0.70		≥ 20	0.55	0.55
(3)	≤ 2	1.25	1.35	(3)	≤ 2	1.25	1.40
	≥ 20	0.75	0.75		≥ 20	0.55	0.55
(4)	≤ 2	0.80	0.85	(4)	≤ 2	0.75	0.90
	≥ 20	0.40	0.40		≥ 20	0.35	0.30
c) continuous members (end span)				d) continuous members (intermediate support area)			
	L [m]	STM	HTM		L [m]	STM	HTM
(1)	≤ 2	0.90	1.00	(1)	≤ 2	0.85	0.85
	≥ 20	0.65	0.65		≥ 20	0.70	0.75
(2)	≤ 2	1.05	1.15	(2)	≤ 2	0.90	0.95
	≥ 20	0.65	0.65		≥ 20	0.70	0.75
(3)	≤ 2	1.30	1.45	(3)	≤ 2	1.10	1.10
	≥ 20	0.65	0.70		≥ 20	0.75	0.80
(4)	≤ 2	0.80	0.90	(4)	≤ 2	0.70	0.70
	≥ 20	0.35	0.35		≥ 20	0.35	0.40

STM standard traffic mix

HTM heavy traffic mix

(1) Reinforcing steel, pre-tensioning (all), post-tensioning (tendons in plastic ducts and straight tendons in steel ducts); S-N curve with $k_{f1}=5$, $k_{f2}=9$ and $N^*=106$ (values may be changed due to changes in k_{f1} and k_{f2} or N^*)

(2) Post-tensioning (curved tendons in steel ducts); S-N curve with $k_{f1}=3$, $k_{f2}=7$ and $N^*=106$ (values may be changed due to changes in k_{f1} and k_{f2} or N^*)

(3) Couplers (prestressing steel); S-N curve with $k_{f1}=5$, $k_{f2}=5$ and $N^*=106$ (values may be changed due to changes in k_{f1} and k_{f2} or N^*)

(4) Couplers (reinforcing steel); welded bars including tack welding and butt joints; S-N curve with $k_{f1}=5$, $k_{f2}=5$ and $N^*=107$ (values may be changed due to changes in k_{f1} and k_{f2} or N^*)

NOTE 1 Interpolation between the given L-values according to formula (k.6) [5] may be carried out.

NOTE 2 Different N^* values can be considered as follows: $\lambda_{s,1,N^*_{new}} = \lambda_{s,1,N^*_{old}} (N^*_{old}/N^*_{new})^{1/k_{f1}}$

stress range, assuming proportionality between bending moment and stresses, is given below (Eq. 15):

$$\Delta\sigma_{equ} = \left(\sum_i^n \frac{\Delta\sigma_i^{k_{f1}}}{N^*} \right)^{1/k_{f1}} \quad (15)$$

Where $\Delta\sigma_i$ is the stress range of block i of the histogram, composed of n blocks. It is immediate to deduce that, keeping the same traffic mixes and therefore the values of $\Delta\sigma_i$, a change in the number of cycles N^* can be accounted for by the expression provided in Note 2 of Table 6.

11. REDUCTIONS OF MATERIALS AND IN-TURN CLIMATE IMPACT

Fatigue verification is not determinant for standard buildings, many road bridges, and several other structures. On the other hand, in railway bridges, support structures for wind turbines and other machinery, offshore structures, etc., fatigue usually have a significant impact in the design and hence in the material amount. Regarding this, the new Eurocode may lead to a non-negligible material volume reduction with the consequent favourable in-turn climate impact. A non-exhaustive summary is provided below.

- Shear reinforcement: Shear reinforcement was sometimes driven by fatigue in railway and even road bridges, as well as foundations for wind turbines and other machinery, mainly due to the significant reduction of the strut angle used at ULS verifications when verifying fatigue and the fatigue strength reduction due to the hook or bent at the links and stirrups. The possibility of a more refined calculation under service conditions of the strut angle, the optimization of the compressive strength reduction of concrete under transverse tensile stresses and the exclusion of the fatigue strength reduction due to the bent for depths larger than 600mm and diameters equal or less than 16mm may lead to local but non-negligible material savings.
- Welded reinforcement. The improvement of the S-N curves for reinforcing bars of diameters less or equal than 12mm, quite common in prestressed structures under dynamic loads will lead to some reduction of the amount of steel reinforcement or will allow the use of tack welding for reinforcement meshes and cages, rationalizing the production, which always has a positive impact in terms of sustainability.
- Fatigue of concrete. With the current formulation thicknesses of some slender webs and slabs of T-girders, box-girders, etc., of concrete railway bridges, and without a doubt thickness of support structures for wind turbines, which are driven by the fatigue verification of concrete under compression, can be reduced. The new formulation improves the compressive fatigue behaviour of concrete,

according to the trend in modern codes and standards such as Model Code 2010 [3].

As an example, fatigue strength of concrete C50/60 in [1], yields a $f_{ed,fat}$ of 22.67 Mpa, 45% of f_{ck} . Stress limit to avoid non-linear creep of concrete under the quasi-permanent combination of actions is, according to [1], $0.45 \cdot f_{ck}$. This means that stress control is determined in several cases by the fatigue verification provided in [1], not by the SLS verifications. Several precast and even in situ concrete bridges and other structures with decades in service may not comply with the current limits of [1]. A modification of this fatigue verification of concrete under compressive stress was mandatory and this improvement is consistent with the lack of fatigue related pathologies in bridges and support structures for wind turbines. For instance, in High-Speed Railway bridges built in Spain, some of them with more than 40 years in service, no concrete fatigue related pathologies are known by the authors.

Impact in concrete volume reduction for bridges will not be large, but some optimizations could be expected, especially for precast elements. This optimization will be more certain in case of support structures for wind turbines, although the application of [3] for the design of these structures has already led to important reductions of the concrete amount of these members. This conclusion could be extrapolated to other dynamically loaded structures, from crane bridge beams to offshore structures.

- Refined tools. The extension of the tools for the refined assessment of fatigue, such as the Palmgren-Miner rule, now just provided for bridges in [2], will also contribute to a more rational design of other structures cyclically loaded, allowing the optimization of the volume of materials.

12. CONCLUSIONS

This paper has carried out an in-depth review of the most relevant changes in the field of concrete fatigue in the new Eurocode 2 compared to its predecessor.

The first difference, more formal than technical but relevant in any case, is that in the new Eurocode 2 fatigue has its own chapter and an annex, which gives it a visibility and relevance that it did not have in the previous version of this standard. This is a clear demonstration of the importance that fatigue in concrete has acquired in recent years.

From a technical point of view, the most important change between the new Eurocode 2 and its predecessor lies in the improvement of the S-N curves of concrete in compression. After several decades of designing and building structures subjected to significant cyclic loading, mainly bridges and viaducts for railways and support structures for wind turbines, the virtual absence of pathologies is a clear indication that the current formulation was overly conservative. The new Eurocode 2 proposes curves that are more in line with reality (that is, less conservative), which will make it possible to optimize the design of structures, reducing their cost and increasing their sustainability.

Other tools, strongly supported by research and professional practice, have also been introduced to help optimize fatigue design. For example, the introduction of gradient redistribution of concrete under cyclic compressive loading, the possibility of not checking shear reinforcement hooks for fatigue if they meet certain requirements, optimization of the angle of the concrete strut to be considered in the verifications, etc.

In other cases, there are no substantial differences between the new Eurocode 2 and its predecessor, for example in the simplified verification of elements without shear reinforcement, multiaxial stress states or in the calculation of equivalent fatigue loads in road and railway bridges. In both cases, it is regrettable that the new standard has not been somewhat more daring, but precisely the correct behaviour of structures subjected to fatigue designed in recent decades has made it advisable to maintain the approach of the previous version.

Finally, it should be noted that one of the major new features of the new Eurocode 2 is the inclusion of an improved approach for fatigue design of joints between concretes of different ages.

References

- [1]. EN 1992-1-1: 2004. Eurocode 2 Design of concrete structures. Part 1-1 General rules and rules for buildings. European Committee for Standardization, Brussels (Belgium).
- [2]. EN 1992-2: 2005. Eurocode 2 Design of concrete structures. Part 2 Bridges – Design and detailing rules. European Committee for Standardization, Brussels (Belgium).
- [3]. Model Code 2010. FIB Model Code for Concrete Structures 2010. International Federation for Structural Concrete (FIB), Lausanne (Switzerland), 2012.
- [4]. ACI PRC-215-21. Concrete Structure Design for Fatigue Loading – Report. American Concrete Institute (ACI), Farmington Hills, (MI, USA), 2021.
- [5]. CEN FprEN 1992-1-1:2023 Eurocode 3- Design of concrete structures- Part 1-1: General rules and rules for buildings, bridges and civil engineering structures.
- [6]. EN 1991-1-4:2005+A1:2010. Eurocode 1: Actions on structures- Part 1-4: General actions – Wind actions. European Committee for Standardization, Brussels (Belgium), 2010.
- [7]. EN 1993-1-9:2005. Eurocode 3: Design of steel structures- Part 1-9: Fatigue. European Committee for Standardization, Brussels (Belgium), 2005.
- [8]. EN 1991-2:2003. Eurocode 1: Actions on structures- Part 2: Traffic loads on bridges. European Committee for Standardization, Brussels (Belgium), 2003.
- [9]. NS3473:2003. Concrete Structures – Design and Detailing Rules. Norwegian Standards, Oslo (Norway), 2003.
- [10]. Zanuy, C.; De la Fuente, P.; Albajar, L. (2007). "Effect of fatigue degradation of the compression zone of concrete in reinforced concrete sections". *Engineering Structures*, 29(11), 2908-2920. <https://doi.org/10.1016/j.engstruct.2007.01.030>
- [11]. EN 1990:2002+A1. Eurocode – Basis of structural design. European Committee for Standardization, Brussels (Belgium), 2005.
- [12]. Model Code 1990. Bulletin D'Information N° 213/214 CEB-FIB Model Code 1990. International Federation for Structural Concrete (FIB), Lausanne (Switzerland), 1993.
- [13]. UNE-EN IEC 61400-6:2020. Aerogeneradores. Parte 6: Requisitos de diseño de torres y cimientos (Ratificada por la Asociación Española de Normalización en abril de 2021.)
- [14]. DNV-ST-0126 Support structures for wind turbines. Standard. Edition 2021-12.
- [15]. (*) Background document to subsection 10.4, Annex C.4 and Annex E.4. Fatigue strength of reinforcing steel.
- (*) This document is available through the National members at CEN TC250/SC2.

Design provisions for anchorages and laps in the revised EC2

Disposiciones de diseño para anclajes y solapes en la revisión del EC2

John Cairns^{*,a}

^a Heriot-Watt University, Edinburgh UK

Recibido el 16 de diciembre de 2022; aceptado el 14 de febrero de 2023

ABSTRACT

The second generation of the Structural Eurocodes is expected to be published by 2026. This article describes design provisions for laps and anchorages of normal ribbed reinforcement in Sections 11.4 and 11.5 of FprEN_1992_1_1:2023, the forthcoming version of Eurocode 2, the European Code for Design of Concrete Structures. This article outlines why and how design provisions have been modified, demonstrates the physical rationale for the rules and notes the evidence on which the justification is based. It also indicates the impact of the revisions.

The article gives an overview of the factors influencing anchorage and lap strength and presents a historic perspective on the development of the revised rules. The influence of each factor as represented in current and revised Eurocode 2 are then compared. The revised rules are then validated against test databases for anchorages and for tension and compression laps, and the impact of the revisions on design practice for selected situations are briefly examined.

KEYWORDS: Structural concrete design, EC2, bond, anchorages, lap joints, lap splices, casting position.

©2023 Hormigón y Acero, the journal of the Spanish Association of Structural Engineering (ACHE). Published by Cinter Divulgación Técnica S.L. This is an open-access article distributed under the terms of the Creative Commons (CC BY-NC-ND 4.0) License

RESUMEN

La segunda generación de Eurocódigos Estructurales tiene prevista su publicación en 2026. En este artículo se describen las disposiciones de diseño para solapes y anclajes de armaduras nervadas normales de las secciones 11.4 y 11.5 del borrador final de la próxima versión del Eurocódigo 2, el Código Europeo para el Diseño de Estructuras de Hormigón. Este artículo describe por qué y cómo se han modificado las disposiciones de diseño, demuestra la justificación física de las normas y señala las pruebas en las que se basa la justificación. También indica el impacto de las revisiones.

El artículo ofrece una visión general de los factores que influyen en el anclaje y la resistencia de solape y presenta una perspectiva histórica del desarrollo de las normas revisadas. A continuación se compara la influencia de cada factor tal como se representa en las normas actuales y en las revisadas. Las normas revisadas se validan con bases de datos de ensayos de anclajes y solapes a tracción y compresión, y se examina brevemente el impacto de las revisiones en la práctica del diseño para situaciones seleccionadas.

PALABRAS CLAVE: Diseño de hormigón estructural, EC2, unión, anclaje, solape, empalme.

©2023 Hormigón y Acero, la revista de la Asociación Española de Ingeniería Estructural (ACHE). Publicado por Cinter Divulgación Técnica S.L. Este es un artículo de acceso abierto distribuido bajo los términos de la licencia de uso Creative Commons (CC BY-NC-ND 4.0)

1. INTRODUCTION

The second generation of the Structural Eurocodes is expected to be published by 2026. This article describes design provisions for laps and anchorages of normal ribbed reinforcement

in Sections 11.4 and 11.5 of FprEN_1992_1_1:2023 [1], the forthcoming version of Eurocode 2, the European Code for Design of Concrete Structures, which revises and enhances the current Standard EN1992_1_1:2004 (EC2) [2].

The basic expressions for design and anchorage which appear in EC2(2004) are essentially those proposed in the 1978 edition of the CEB-FIP Model Code [3] (MC78), although there were a few, generally modest, differences in the value of

* Persona de contacto / Corresponding author.
Correo-e / e-mail: civjcc@hw.ac.uk, civjcc@gmail.com (John Cairns).

coefficients. Since that time there has been a general increase in the strengths of both concrete and reinforcement used in construction. For example, the characteristic strength of reinforcement in many European countries was around 400 MPa in 1978 but is currently 500 MPa. The CEB Bulletin on High Performance Concrete [4] (CEB 1995) recommended that concrete grades be extended from the then limit of C80/100 up to C100/125, and that the validity of current rules for bond and anchorage should be reconsidered. New materials and technologies with differing bond and anchorage capabilities have been introduced, for example headed and post-installed bars, and design rules need to be extended to cover these innovations. Some aspects of current EC2 design rules appear inconsistent with recent research findings, for example, research has demonstrated a markedly lesser difference in capacity between lapped joints and anchorages than current requirements suggest. As a considerable amount of research into behaviour of anchorages and laps has been carried out over the past 50 years since MC78 was drafted, a significant revision of the rules in the first generation document was considered necessary.

Anchorage and laps of reinforcement attracted a substantial number of comments at the recently completed enquiry stage, and there is evidently a need to explain the basis for the revisions. The objectives of this article are to outline why and how design provisions have been modified, to demonstrate the physical rationale for the rules where appropriate, to note the evidence on which the justification is based and to indicate the impact of the revisions, with the overall aim of promoting an understanding of the justification for the new rules.

Throughout this article, “EC2” denotes the current version of the EC1992-1-1:2004 and “FprEC2” denotes the 2023 Formal Vote draft of the enhanced version. Equations, tables, and figures have been numbered sequentially in citation order in this article. References to equations, tables, and figures taken directly from FprEC2 are additionally given in {curly brackets}. It does not reproduce sections of the Code in detail and is intended to be read alongside the revised Code. At the time of writing the Formal Vote process is about to begin and it is possible that some minor adjustments will be introduced before a final version is published.

2. BOND, ANCHORAGES AND LAPS: GENERAL CONSIDERATIONS

Bond and anchorage are the terms used to denote the transfer of force between reinforcement and concrete. Design rules for anchorages and laps are found in sections {11.4} and {11.5} respectively in FprEC2. Anchorages transfer force from bar to concrete, for example at ends of members or where bars are curtailed where a member has sufficient capacity without their contribution; the force in an anchored bar reduces to zero over the anchorage length. Laps provide continuity of force in reinforcement, transferring force from one of a lapped pair to the other bars via the surrounding concrete; the force in a lapped pair remains approximately constant over the lap length.

Bond has conventionally been described as a shear stress on the nominal perimeter of a bar, calculated as the change

in bar force over a certain distance divided by the (nominal) area of bar surface over which this change takes place, Eq.1. This represents a major simplification as most bars produced today rely on the bearing of ribs rolled onto or indented into the surface of the bar during manufacture to transfer force. Although the transfer of force between reinforcement and concrete depends on adhesion and friction over the whole bar surface at low bond stress, as the ultimate limit state is approached bond relies increasingly on bearing of the ribs on the concrete. The definition of Eq. 1 is, nonetheless, a convenient one and is widely used.

$$f_b = \Delta\sigma_s A_s / (\pi \phi l_b) \quad (1)$$

where

f_b is the average bond stress over length l_b
 $\Delta\sigma_s$ is the change in bar stress over l_b
 A_s is the cross-sectional area of the bar
 ϕ is the nominal diameter of the bar
 l_b is the bond length over which $\Delta\sigma_s$ takes place

The simplicity of Eq. 1 can be misleading; the evaluation of bond resistance is complex, and while there has long been general agreement over the parameters which influence bond resistance, quantification of the magnitude of the contribution attributable to each parameter varies widely. The distribution of bond stress throughout an anchorage or lap length is non-uniform, a topic explored later in this article, see Figure 4. EC2 includes no less than 10 parameters for the calculation of anchorage or lap length. There are two broad forms of failure mode depending on whether or not concrete cover splits, and within the splitting mode there are a number of sub-modes dependent on section geometry. The one common conclusion on which all agree is that bond is not a fundamental property of the bar, as has been asserted in the past, but is a quantity influenced by bar and concrete section geometry, materials characteristics, and stress state.

Bond over a straight length of bar may be supplemented by other features which contribute to transfer of force between bar and concrete. These features may include welded cross bars, a hook or bend formed close to the end of the bar, a plate or head welded to the end of the bar, or in the case of bars in compression, bearing of the end of the bar on concrete. Because of the variation in bar concrete slip over a lap or anchorage length and differences in load-slip characteristics, the contributions of these other forms of anchorage cannot be directly summed with that of bond over the straight length of a bar, and it is necessary to consider their interaction to determine the combined resistance. Such analysis lies outside the scope of normal design, and for practical purposes a nominal allowance is given in Code rules to evaluate their contribution.

3. BACKGROUND TO THE REVISION AND DEVELOPMENT OF DESIGN EXPRESSION

A comprehensive reappraisal of provisions for laps and anchorages was initiated by *fib* TG4.5 (now TG2.5) and published in *fib* Bulletin 72 [5] in 2014. Bulletin 72 reported a

TABLE 1.
Summary of fit of Eq. 2 to test results [5].

Database	fib TG 4.5 ⁸				Amin ⁹
	Laps with links	Laps without links	Anchorage with links	Anchorage without links	Anchorage without links
Mean	1.00	0.97	0.98	0.93	1.01
Coefft. of Variation	0.132	0.150	0.176	0.118	0.16
Minimum	0.68	0.62	0.63	0.76	0.61
5% char. ratio	0.78	0.73	0.70	0.75	0.75
No. of results	288	255	18	21	164

detailed semi-empirical analysis in which a form of expression based on physical analysis of influencing parameters was calibrated using and validated against a database compiled by fib TG 4.5 comprising around 800 relevant results of tests on lapped joints and around 100 tests on end anchorages. Contributions of cover, secondary reinforcement and transverse compression are summative, in contrast to the multiplicative format in EC2. The format of the expression adopted reflects a view that the influence of each of these contributions acting in combination would tend to be equal to or less than the sum of their contributions taken individually, and that a factorial combination could potentially lead to less safe provisions. Limits were set on the range of accepted parameters to reflect normal practice as well as the limits to test parameters in the database: $15 \text{ MPa} < f_{cm} < 110 \text{ MPa}$, $0.5 \leq c_{min}/\phi \leq 3.5$, $c_{max}/c_{min} \leq 5.0$, $k_{tr} \leq 0.05$, $l_b \geq 10\phi$. The mean strength expression for bond, anchorages and laps proposed and validated in fib Bulletin 72, Eq. 2, is well regarded and subsequent studies have independently confirmed its suitability as the basis of design provisions [6],[7]. Equation 2 is suitable for evaluation both of anchorages of individual bars and for lapped pairs of bars. A summary of the statistical fit of Eq. 2 to test results compiled by fib TG4.5 [8] and by Amin [9] is shown in Table 1.

$$f_{stm} = 54 \left(\frac{f_{cm}}{54} \right)^{0.25} \left(\frac{l_b}{\phi} \right)^{0.55} \left(\frac{25}{\phi} \right)^{0.2} \left[\left(\frac{c_{min}}{\phi} \right)^{0.25} \left(\frac{c_{max}}{c_{min}} \right)^{0.1} + k_m K_{tr} \right] \quad (2)$$

where

- f_{stm} is the estimated stress developed in the bar (mean value)
- f_{cm} is the measured concrete cylinder compressive strength
- l_b and ϕ are the bond length and diameter of the lapped or anchored bar respectively,
- c_{max} and c_{min} are defined in Figure 1.
- $K_{tr} = n_l n_g A_{sv} / (l_b \phi n_i)$
- n_g is the number of groups of links within the lap or anchorage length,
- n_l is the number of legs of a link in each group which cross the potential splitting failure plane
- A_{sv} the area of each leg of a link, and
- n_s the number of bars lapped or anchored at the section
- n_b is the number of individual anchored bars or pairs of lapped bars alternatively, $K_{tr} = n_l A_{sv} / (s_v \phi n_b)$, where s_v is the spacing between groups of links
- k_m is an 'effectiveness factor' for link confinement

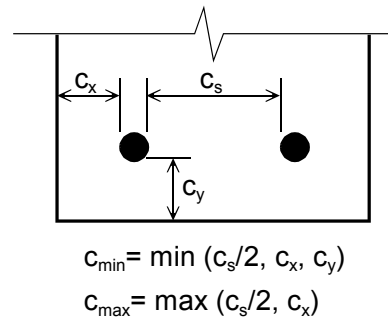


Figure 1. Definition of concrete cover dimensions.

Design values for bond stress in Bulletin 72 were derived from Eq. 2 in a relatively simple manner, assuming a normal distribution in the variability of tests results, determining a 95% lower bound characteristic value, and applying a partial safety coefficient of 1.5 to the characteristic value.

The derivation of design values for anchorage and lap length in FprEC2 has evolved through several stages since then. Mancini *et al* [10] subsequently performed a rigorous statistical analysis of the lap data compiled by fib TG4.5 and demonstrated that no significant trends of variation are found on the database. They note, however, that a log-normal distribution provided a better representation of the measured to estimated strength ratio of test results. A probabilistic calibration of the mean strength expression was performed defining the related model uncertainties, grounded on the experimental database, following the reliability format defined by Taerwe [11]. Focusing on ordinary structures with 50 years of service life, the accepted target level of reliability was taken to be $\beta = 3.8$. The semi-empirical Eq. 2 was processed accounting both for model uncertainties and random variability of concrete strength to derive a reliability-based design expression, although it was noted that concrete cover might also have been treated as a random variable. They noted that with EC2 provisions in which a uniform bond stress independent of the bar stress to be developed is assumed, reliability index β becomes significantly higher than the target 3.8 in case of low-stressed bars, but could become unconservative for high strength bars, thus prompting a move away from a notional average design bond strength towards direct calculation of anchorage and lap length. The analysis assumed that the variability assumed for concrete strengths

was sufficient to cover the weaker or less well compacted concrete found in ‘poor’ casting conditions, although this assertion appears not to have been verified against ‘top cast’ data available in the ACI408 database.

Vollum and Goodchild [12] refined the analysis of Mancini *et al* by dividing test results into four stress bands, namely $f_{st,test} < 300$ MPa, $300 \text{ MPa} \leq f_{st,test} < 400$ MPa, $400 \text{ MPa} \leq f_{st,test} < 500$ MPa and $f_{st,test} \geq 500$ MPa, where the stress $f_{st,test}$ is the measured lap strength. Each stress band was analysed following the procedure of Mancini *et al.* referred to in the preceding paragraph. It is apparent that the ratio of strength measured in tests to that estimated by Eq. 2 was greater and the scatter reduced for higher strength laps. They proposed a bond length coefficient of 67 for bars designed for the full 435 MPa design strength of Grade 500 bars, a lower value than that proposed by Mancini *et al.* However, for the weaker strength intervals as used in their analysis the reduced coefficient would provide insufficient safety. To allow for this a linear relationship between the stress developed and bond length was proposed for design strengths of less than 435MPa, the design strength of a Grade 500 bar. The difference in the proposals is shown schematically in Figure 2. The Vollum & Goodchild proposal is rather conservative for medium strength anchorages, and for a stress of 250 MPa would require an anchorage 43% longer than Mancini *et al.*

$$l_{bd}/\phi = 67 m (\gamma_c/1.5)^{0.64} (25/f_{ck})^{0.45} (\phi/25)^{0.36} / (\alpha_2 + \alpha_3) \quad (3a)$$

$$m = \text{Max}\{\sigma_{sd} / 435, (\sigma_{sd} / 435)^{1.82}\} \quad (3b)$$

$$\alpha_2 = (c_{min}/\phi)^{0.5} (c_{max}/c_{min})^{0.15} \quad (3c)$$

Where

- l_{bd} is the design value of anchorage length of reinforcing steel
- 67 is a dimensionless factor for calculating the design anchorage length.
- ϕ is the nominal bar diameter

- σ_{sd} is the design value of the reinforcing steel stress at the cross-section
- f_{ck} is the characteristic concrete compressive strength
- c_{min} and c_{max} are defined in Figure 1
- α_3 represents confinement from transverse or confining reinforcement

Equation 3 subsequently evolved, with modifications, into the design expression in FprEC2, Eq. 4. Indexes in Eq. 4 are rounded from those in Eq. 3: only nominal adjustments have been made to indices on concrete strength, bar size and minimum cover. Index n_σ is a Nationally Defined Parameter [NDP] with a constant recommended value of 1.5 [NDP], thus moderating the conservatism of the Vollum & Goodchild proposal for bar stresses less than 435 MPa Bond length coefficient k_{lb} is a Nationally Defined Parameter (NDP). Vollum and Goodchild recommended a value of 67 as a bond length coefficient, Eq. 3a. Their analysis was based on a benchmark cover ratio of $c_d/\phi = 1.0$ and a bar size factor $(\phi/25)$, whereas Eq. 4 {11.3} is based on a benchmark of $c_d/\phi = 1.5$ and a bar size factor $(\phi/20)$. Making allowance for these differences results in an equivalent bond length coefficient $k_{lb} = 67(1.0/1.5)^{0.5} (20/25)^{0.33} = 50.8$ and rounding leads to the recommended value of $k_{lb} = 50$ in Eq. 4. Parameter c_{max}/c_{min} has only a very modest influence on design anchorage length and has consequently been dropped. An evaluation of Eq. 4 is presented later.

$$l_{bd} = k_{lb} k_{cp} \phi \left(\frac{\sigma_{sd}}{435} \right)^{n_\sigma} \left(\frac{25}{f_{ck}} \right)^{\frac{1}{2}} \left(\frac{\phi}{20} \right)^{\frac{1}{3}} \left(\frac{1.5\phi}{c_d} \right)^{\frac{1}{2}} \geq 10 \phi \quad (4)[11.3]$$

- n_σ is the exponent to consider effect of steel stress on anchorage length, equivalent to m in Eq. 3. $n_\sigma = 1.5$ (recommended value) for persistent and transient conditions (formerly permanent and variable)
- c_d is similar to c_{min} in Figure 1 but with some additional limits
- k_{cp} is a coefficient accounting for casting effect on bond conditions

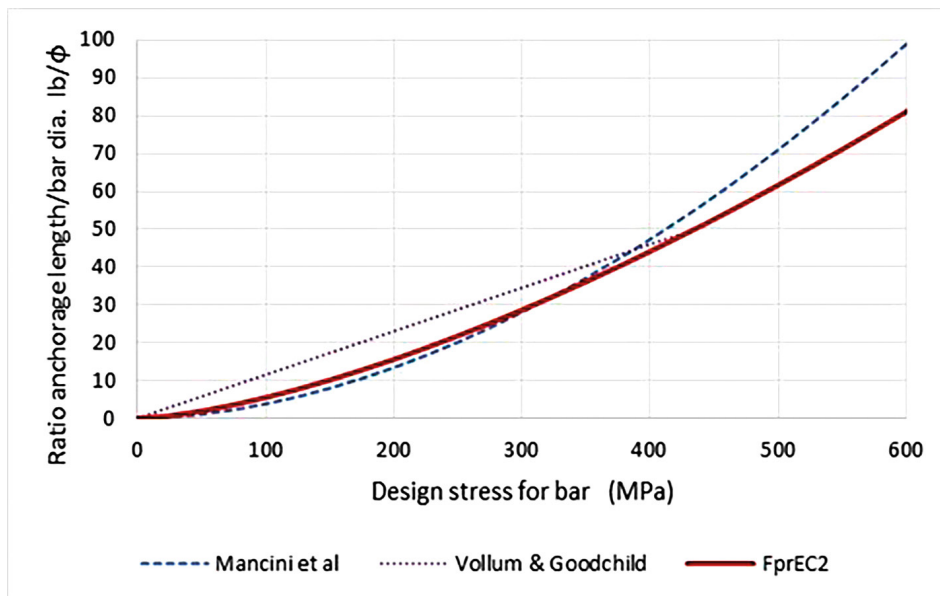


Figure 2. Comparison of proposals by Mancini *et al* [10], Vollum & Goodchild [12] and FprEC2 [1].

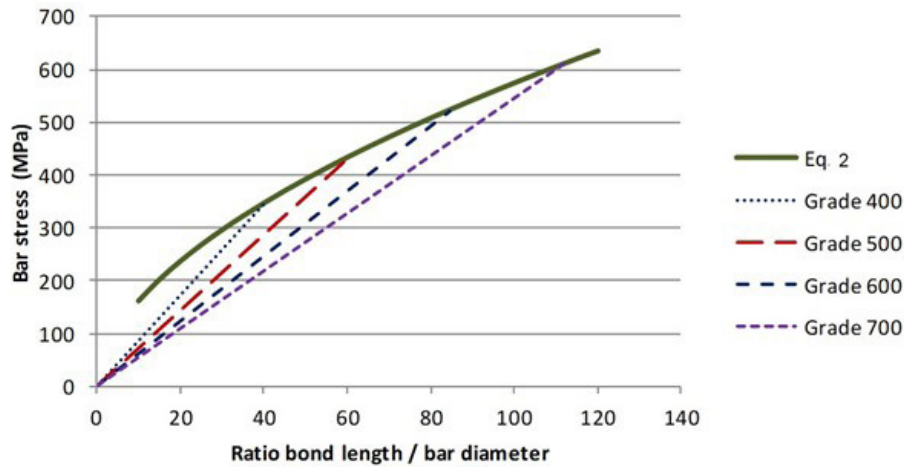


Figure 3. Influence of bond length on anchorage and lap strength.

$25/f_{ck}$ represents the influence of concrete strength
 $\phi/20$ represents the influence of bar size
 $1.5\phi/c_d$ represents splitting resistance provided by concrete cover.

4. ANCHORAGE LENGTHS OF STRAIGHT BARS IN TENSION IN FPREC2 {11.4.2}

The format of design provisions in FprEC2 is markedly different from that in EC2. Anchorage length is calculated directly from material properties and geometric parameters, in contrast to EC2 provisions where an ultimate bond strength and a basic anchorage length are first obtained (from Eqs. 8.2 and 8.3 respectively), the basic anchorage length then being modified by a set of α coefficients related to concrete cover, confining reinforcement, and transverse compression. Design bond length is no longer directly proportional to the stress to be anchored. In EC2 factors α_2 , α_3 and α_5 for the contribution of cover, secondary reinforcement or pressure were multiplicative, in FprEC2 they are now summative, following the approach adopted in Bulletin 72, Eq. 2. The revised provisions do not require calculation of a notional bond strength as in the earlier version, and therefore provide a more direct route to design anchorage length.

The elimination of ‘bond strength’ from the revised provisions was made for several reasons. Firstly, the more direct approach should improve ease of use. More fundamentally, the concept of a ‘bond strength’ is potentially misleading and, it may be asserted, has already led to a reduction in the level of safety provided by current provisions. Figure 3 illustrates the relationship between the mean stress developed in a lap/anchorage and bond length. The solid line represents the observed relationship between mean bar stress developed for a specific set of material properties and geometric parameters and bond length ratio according to Eq. 2. The gradient of the broken lines represents the average bond strength over the lap/anchorage length required to develop the design strength of bars of various Grades: there is a different

bond strength for each Grade. Neglect of this effect would mean that either longer bond lengths than necessary would be required for weaker bar Grades or that bond lengths would become increasingly non-conservative for stronger Grades. The concept of a bond stress on the perimeter of a bundle is also unsatisfactory, as discussed later.

Characteristic strength of ribbed bars was around 400MPa when MC78, which forms the basis of current EC2 design rules, was drafted. The main steel Grade in current practice is now 500MPa, an increase of 25%. To maintain a consistent level of safety, anchorages for Grade 500 bars should now be $(500/400)^{n_\sigma}$ or $(500/400)^m$ times longer than those for Grade 400 bars according to Eqs. 4 and 2 respectively. With n_σ set at the recommended value of 1.5 (Eq. 4) or $m = 1.82$ (Eq. 3), this corresponds to 40% or 50% increases in bond length. The increase in bond length required by current EC2 provisions has been only 25%. An increase of between 12% and 25% in bond lengths over EC2 values must therefore be expected for this reason.

Tabulated values for anchorage length l_b/ϕ are provided for Grade 500 bars in ‘good’ bond conditions covering a range of bar sizes and concrete strengths to cover the most common situations and facilitate application of these provisions, (Table 11.1). As coefficients k_{lb} and n_σ are both NDPs, tabulated values for l_b/ϕ are therefore also NDPs and anchorage lengths given by (Table 11.1) apply unless the National Annex gives different values. Tabulated values are conservative for $c_d > 1.5\phi$. However, if transverse reinforcement is provided or transverse compression is present, or if minimum cover $c_d > 1.5\phi$, a reduced anchorage length may be obtained through substitution of $c_{d,conf}$ in place of c_d in Eq. 4 (described later).

4.1. Influence of concrete strength

The influence of concrete strength on lap length is less strong in FprEC2. Bond failure typically occurs by splitting of the surrounding concrete cover unless minimum cover exceeds approximately 3-4 times bar diameter, very dense transverse reinforcement is provided, or transverse compression is present. Bond failure is consequently dependent on the tensile strength of concrete, which varies with $f_{ck}^{0.67}$ for concretes up

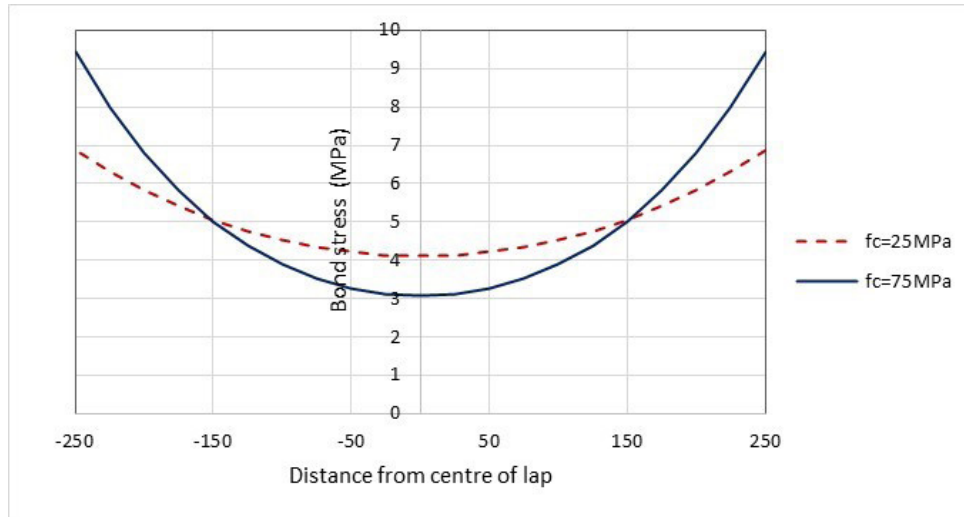


Figure 4. Variation in bond stress throughout a lap length.

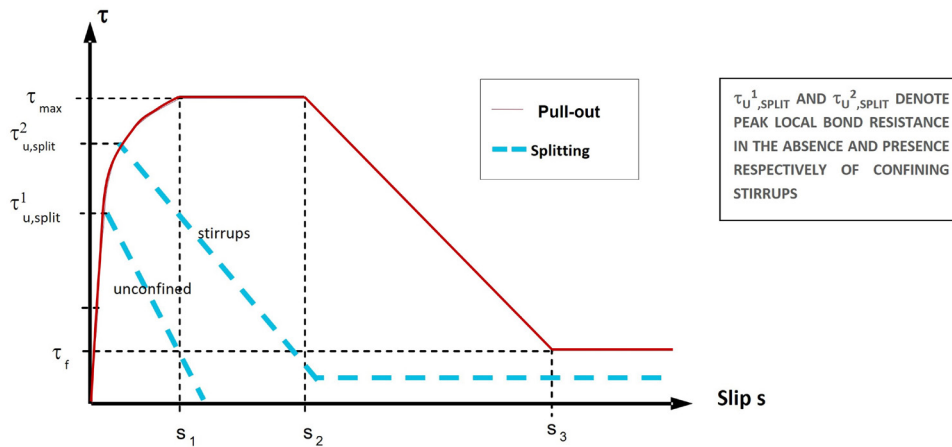


Figure 5. Local bond slip model, MC201014.

to and including Grade 50, FprEC2 [Table 5.1]. Bond strength was directly linked to concrete tensile strength in EC2, hence design anchorage length varied with $f_{ck}^{-0.67}$. The 0.67 index on f_{ck} is valid for short (5ϕ) bond lengths, but practical bond lengths commonly reach 40ϕ or longer. Bond stress along a long anchorage or lap is not uniform as suggested by Eq. 1 but varies over the bond length and is influenced by the bond-slip stiffness, which is itself dependent on concrete strength. Figure 4 compares bond stress distribution over a 40ϕ lap length of size 25 bars for concretes Grades C25 and C75 for a bar stress of 400 MPa. Stresses have been calculated using a linear elastic analysis similar to that used by Tepfers [13] and by Micaleff & Vollum [7], with bond-slip stiffness based on the local bond slip model for a splitting mode failure as given in the fib Model Code 2010 [14], Figure 5. Anchorage failure initiates near ends of the lap where bond stresses are highest. The bar stress developed over the end 5ϕ is 34% greater in the higher strength concrete. Tensile strength of a Grade C75 concrete is $(75/25)^{0.67}=2.1$ times that of a C25 concrete. Making allowance for the difference in bond stress distribution means that the stress anchored will increase by a factor of only $2.1/1.34=1.6$ as the 'peakier' bond stress distribution

of the higher stiffness/strength concrete partially offsets the enhancement provided by its higher concrete tensile strength. This increase is commensurate with $(75/25)^{0.45}$, and therefore consistent with Eq. 2.

The limitation that $25/f_{ck} \geq 0.3$ effectively sets a limit of 83.3MPa to f_{ck} , a value derived from analysis of experimental data, and is an increase on the current restriction of C60/75.

4.2. Concrete cover

Parameter $(1.5\phi/c_d)$ represents the contribution of passive confinement from concrete cover and replaces parameter α_2 in EC2 provisions. Parameter c_d is similar to c_{min} in Figure 1 but shall not exceed 3.75ϕ in calculations. Figure 6 compares the influence of minimum cover ratio c_d/ϕ on bond length in EC2 and FprEC2. Note that the benchmark ratio of $c_d = 1.5\phi$ for FprEC2 provisions differs from that for current EC2 provisions in which $c_d = \phi$. Figure 6 shows the revised provisions allow a more rapid reduction in anchorage length for smaller bars and higher covers. The upper limit to cover ratio $c_d = 3.75\phi$ corresponds to a change from splitting to pullout failure mode, above which the rate of increase in bond is probably negligible.

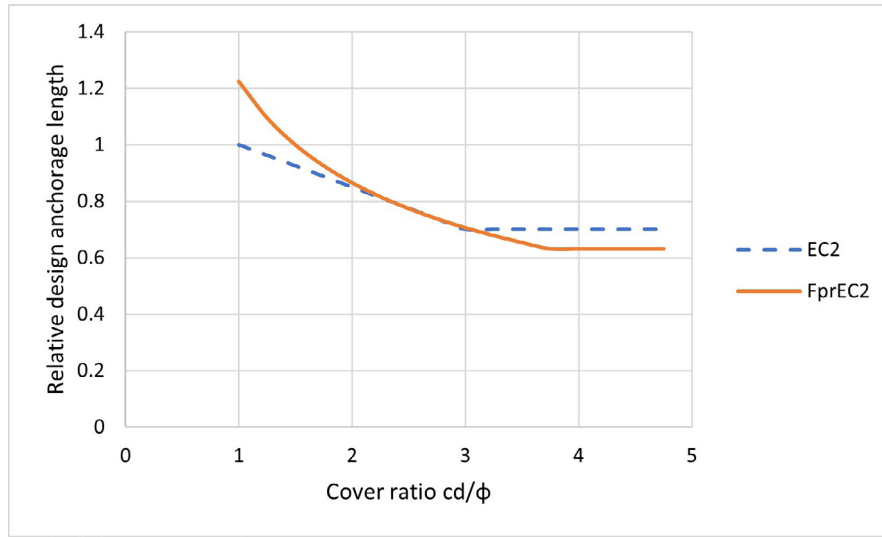


Figure 6. Influence of minimum cover/spacing ratio c_d/ϕ on anchorage length.

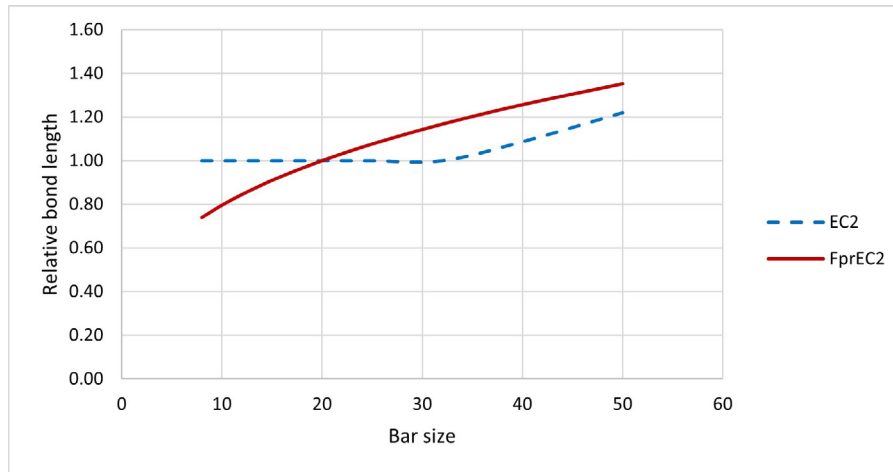


Figure 7. Influence of bar size on anchorage length (based to a ratio of 1.0 for size 20).

4.3. Bar size

The parameter $\phi/20$ in {Eq. 11.3} represents a size effect. It covers a wider range of bar sizes than parameter η_2 in the current version of EC2 which only affects bars larger than size 32, Figure 7. The requirement that $(\phi/20) \geq 0.6$ is derived from test data and effectively sets a lower limit of size 12 bars in the calculation and probably reflects the lower rib areas required for smaller size bars, FprEC2 Annex C. There are currently no provisions for indented bars larger than size 14 due to an absence of confirmatory test data, and there is a process to allow a country to extend the range via their National Annex once relevant data becomes available.

4.4. Transverse and confining reinforcement and transverse compression

If transverse reinforcement, confining reinforcement or transverse compression is present, or if minimum cover/spacing exceeds 1.5ϕ , a reduced anchorage length may be obtained through substitution of $c_{d,conf}$ in place c_d in Eq. 4 {11.3}, Eq. 5 {11.4}.

$$c_{d,conf} = \min\left\{c_x; c_y + 25 \frac{\phi_t^2}{s_t}; \frac{c_s}{2}; 3.75\phi\right\} + \Delta c_d \leq 6\phi \quad (5)\{11.4\}$$

$$\Delta c_d = (70 \rho_{conf} + 12 \sigma_{ccd} / \sqrt{f_{ck}})\phi \quad (5b)$$

ρ_{conf} represents the density of confining reinforcement,

$$\rho_{conf} = \frac{n_c \pi \phi_c^2}{4 n_b \phi s_c} \quad (5c)$$

ϕ_t and s_t are size and spacing respectively of transverse reinforcement

ϕ_c and s_c are size and spacing respectively of confining reinforcement

n_c is the number of legs of confinement reinforcement crossing the potential splitting failure surface

n_b is the number of anchored bars or pairs of lapped bars in the potential splitting failure surface

σ_{ccd} is the design value of the mean compression stress perpendicular to a free surface near bars to be anchored or spliced.

Confining reinforcement in which legs of links run perpendicular to a potential splitting failure surface is more effective

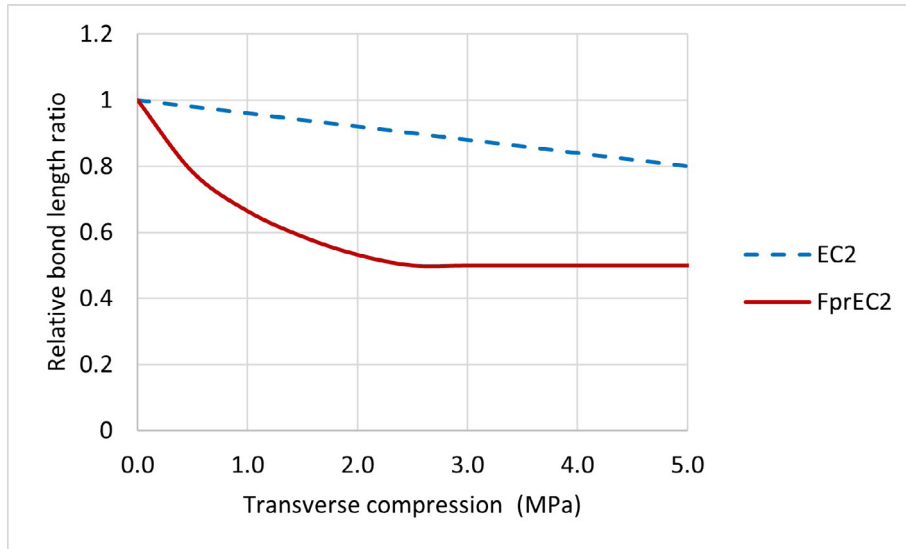


Figure 8. Influence of transverse compression on bond length.

than a similar quantity of transverse reinforcement in the form of distribution reinforcement in planar elements, {Figure 11.5}. Legs of links must be no further than 5ϕ distant from the anchored bar to be considered effective.

FprEC2 permits a more rapid reduction in design anchorage length than EC2 as transverse compression increases. Figure 8 provides a comparison for a size 20 bar in a Grade C40/50 concrete where $c_d=30\text{mm}$ and no transverse or confining reinforcement is present. The reduction is both more rapid at low transverse pressures and has a lower limit at higher values. Factor α_5 for transverse compression in EC2 appears to have been derived from tests in which a pullout failure mode predominated but this underestimates the enhancement for a splitting mode when cover is low, typically $c_d < \sim 3.75\phi$.

FprEC2 resolves two unsatisfactory details in EC2 rules for transverse or confining reinforcement. Firstly, EC2 does not recognize the possibility of a splitting surface forming parallel to transverse reinforcement through the plane of anchored bars which would not have intersected transverse reinforcement thereby rendering its contribution ineffective. Secondly, coefficient α_3 in EC2 for the contribution of transverse or confining reinforcement depends on the total area of that reinforcement within the anchorage or lap length. When link spacing has already been decided (to satisfy shear resistance for example) A_{st} and therefore α_3 are dependent on anchorage length and can only be determined once the anchorage length is known.

FprEC2 does not specify how to deal with situations where transverse compression acts over only part of the anchorage length. In circumstances where the anchorage cannot be accommodated within the bearing width l_{bw} it is suggested that the anchorage will have adequate strength provided Eq. 6 is satisfied:

$$\left(\frac{l_{bw}}{l_{bp}}\right)^{n_\sigma} + \left(\frac{l_{bd} - l_{bw}}{l_{b0} - l_{bw}}\right)^{n_\sigma} \geq 1.0 \quad (6)$$

l_{bw} is the length over which transverse compression is taken to act

l_{bp} is the required anchorage length if pressure σ_{ccd} acted over the entire anchorage length

l_{b0} is the required anchorage length if no transverse pressure were present.

It may be assumed that transverse compression disperses through concrete cover at an angle of 45° from ends of the bearing to determine l_{bw} , Figure 9.

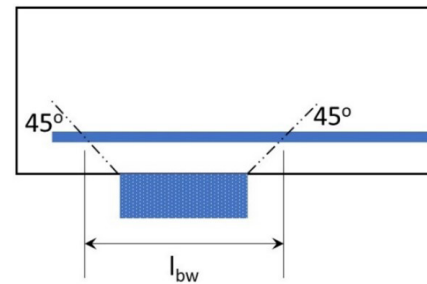


Figure 9. Determination of bearing length l_{bw} .

4.5. Casting position

The definition of a 'Poor' casting position for bars with an inclination less than 45° to the horizontal has been slightly modified in FprEC2 and bars up to 300 mm from the bottom of the formwork are now classified as in a 'Good' position, 50mm more than the value in EC2. Casting position factor k_{cp} for a 'Poor' casting position has been set to 1.2; factor $\eta_1 = 0.7$ on bond stress for a 'Poor' casting position in EC2 effectively resulted in a casting position factor of $1/0.7 = 1.43$ and so FprEC2 reduces additional anchorage length for 'Poor' conditions by 16%. Although 'top cast' reductions exceeding 50% are reported in some investigations, these are invariably obtained from tests on short bond lengths. Figure 10 provides a general plot of top cast ratios, i.e., the ratio of the anchorage capacity for a bar cast near the top of a pour to that of a similar bar cast near the bottom, reported in several investigations, di-

vided into three bond length ratio intervals. The lower bound to the top cast ratio is strongly dependant on bond length ratio. As the minimum anchorage length is set at 10ϕ , Eq. 4, results within the left column for $l_b/\phi \leq 10$ are not of practical significance. The average top cast ratio for bond lengths greater than 10ϕ comfortably exceeds 0.80. The lowest ratio in the middle interval is the average from two types of concrete from a 40 year old study, one of which had very high workability achieved without plasticisers, and thus unrepresentative of mix design today.

Recent work by Cairns and co-workers [15],[16], published too late for inclusion in FprEC2, demonstrates that the softer bond-slip stiffness in a poor casting position results in the top cast effect reducing with increasing anchorage length, and concludes that $k_{cp} = 1.0$ is reasonable for full strength laps of Grade 500 bars, with a higher factor required only for shorter/weaker laps, hence $k_{cp} = 1.2$ factor is conservative for full strength laps and anchorages of Grade 500 and above bars.

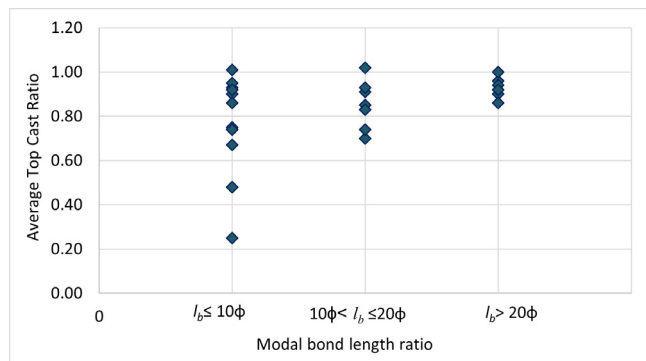


Figure 10. Influence of bond length on casting position observed in various investigations.

4.6. Bundled bars {11.4.3}

Equation 7 {11.6} for equivalent diameter of a bar bundle has been revised to address bundles containing a mix of bar sizes. Provisions now explicitly state that the equivalent diameter is to be used only when two or more bars in the bundle are anchored at a section, and that for a single bar forming part of a bundle the design anchorage length calculated by Eq. {11.3} should be based on its own diameter, covers, and confinement ratio for transverse/confining reinforcement. Research has confirmed that anchorage capacity is determined by the force to be transferred to/from a bar and not by a notional shear stress over the external perimeter of the bundle, hence equivalent diameter is only used when more than one bar is anchored at a section [17],[18].

$$\phi_b = \sqrt{\frac{4}{\pi} A_s} \quad (7)[11.6]$$

where A_s is the total area of all bars contained in the bundle.

4.7. Anchorage of bars with bends, hooks and U-loops {11.4.4, 11.4.5, 11.4.6}

As with bond, an end hook, bend or U-loop typically fails in a splitting mode unless concrete cover is relatively high, and its contribution is therefore controlled by the same concrete mate-

rial properties and geometric parameters as bond. Where a bar in tension terminates in a standard hook or bend anchorage length determined by Eq. {11.3} may be reduced by a length of 15 times the bar diameter and replaces the 30% reduction permitted by EC2 where minimum cover exceeds 3ϕ . The basis for the reduction is given in *fib* Bulletin 72. The revision generally permits shorter bond lengths where the stress to be anchored is below the design strength of a Grade 500 bar. It is not sensible that the contribution increases with increased bar strength as in EC2. Slip at the start of the bend would tend to reduce as bond length increases for higher strength bars, hence the contribution of the hook or bend would tend to reduce as bar stress increases. While it might be expected that a hook with α_{bend} exceeding 135° might provide a greater contribution than a bend with $\alpha_{bend} = 90^\circ$, this was not supported by experimental data and the same anchorage length reduction is therefore used for both shapes. A higher contribution of 20ϕ is permitted for U-loops however. Measurement of anchorage length is to the outside of the hook, bend or U-loop and is unchanged. As an alternative anchorage length may be based on the actual length of bar including the radiused part and the tail.

Anchorage of bars with welded transverse reinforcement {11.4.5} is treated in a similar manner to anchorage with hooks and bends, but as longitudinal and transverse bars may be of different diameter provisions are subject to a minimum amount of transverse reinforcement.

4.8. Anchorages with headed bars

This section is new. Provisions for headed bars have been derived through approaches developed for fastenings to concrete [19]. The head may be taken to anchor the design strength of a Grade 500 bar if a set of 'deemed to satisfy' criteria for minimum cover and spacing are satisfied, or a more detailed calculation may be undertaken. Bond over a straight length of bar may supplement head resistance to achieve the required anchorage capacity. As head resistance and bond resistance generally peak at different slips their individual peak resistances cannot simply be summed. The design bond length to provide the difference between design bar force and head capacity is accordingly increased by 10% above that calculated by Eq. 4.

4.9. Anchorage of bonded post-installed reinforcing steel {11.4.8}

This section is completely new. Straight lengths of bar may be installed by drilling an oversize hole into hardened concrete and bonding in an appropriate length of reinforcement with a suitable adhesive or mortar. Design provisions are broadly similar to those for cast in place bars, although additional limits on minimum cover are introduced mainly for reasons associated with the installation process. Such installations are generally undertaken by specialist sub-contractors. Design and installation of post-installed rebar is covered in detail in specialist documents such as the EOTA Report on Bonded Fasteners for Use in Concrete which should be consulted [20].

4.10. Compression anchorages {11.4.2(6)}

End bearing enhances the anchorage capacity of bars in compression, a contribution that FprEC2 now recognizes, and a

reduction of 15ϕ in the design anchorage length is permitted provided the end of the bar is no closer than 5ϕ (measured parallel to the bar axis) to a free surface, Figure 11: a shorter distance could result in an end cone failure at a reduced capacity. EC2 does not permit any reduction for an end bearing contribution. The basis for the reduction is given in *fib* Bulletin 72. Although there is no benefit to anchorage length in providing an end hook or bend to compression bars if the 5ϕ end distance criterion is satisfied, there may be a benefit for end distances between 3.5ϕ and 5ϕ . There may also be practical benefits for fixing reinforcement and in maintaining capacity in the event of accidental tension. There is some suggestion that an end hook or bend might be detrimental to anchorage as pressure in the hook could lead to prising off thin side covers; ACI318 [21] does not permit bends at the end of compression anchorages. Concrete cover, transverse and confining reinforcement, and transverse compression now influence compression anchorage length: this was not the case in EC2, presumably because of a lack of evidence when MC78 was drafted.

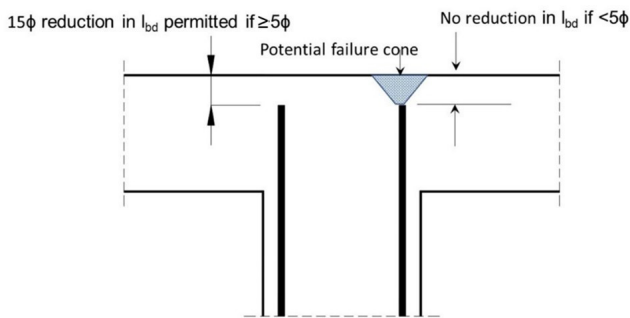


Figure 11. Minimum distance from end of compression bar to free face.

5. LAPS IN TENSION AND COMPRESSION

Laps, lapped joint and lapped splice are equivalent terms used to describe situations where the force in one set of bars is transferred to another set via the surrounding concrete to provide continuity of reinforcement. Lap lengths l_{sd} in FprEC2 are also based on Eqs 4 & 5 {11.3 & 11.4}, the expressions used for anchorages. Camps *et al* [22] compared design tension anchorage and lap lengths calculated according to EC2 and FprEC2. They noted that anchorages designed to FprEC2 tended to be longer than those designed to EC2, but that laps tended to be shorter, in one example by as much as 48%. They concluded on the basis of precedent that there should be a distinction between the k_{lb} value for anchorages and laps. Anchorage length l_{bd} in FprEC2 is multiplied by a factor k_{ls} , an NDP with a recommended value $k_{ls} = 1.2$, to obtain lap length, effectively a bond length coefficient of 60 for laps as opposed to the 50 for anchorages. This is a significant change from EC2 where lap length factor α_6 depends on the proportion of bars lapped at the section and varies from 1.2 where a maximum of 20% of the bars are lapped at a section to 1.5 where more than 50% of bars are lapped. Values for α_6 in EC2 were moderated from those in *fib* MC90, which formed the

basis of EC2 rules for bond, and had a maximum of $\alpha_6 = 2.0$. Early strength models by Tepfers [13] and by Ferguson [23] considered bond action to exert a hydraulic pressure around the bars, consequently the bursting force generated by bond in a direction perpendicular to a plane through the lapped pair would be double that exerted by a single anchored bar, Figure 12. These analyses also assumed bond generates a radial stress proportional to the local bond stress, from which it was concluded that in a splitting failure mode strength of a lap would be half that of an equivalent anchorage, and hence that lap lengths should be double those for single bar anchorages. Experimental evidence has since contradicted these models [24]. Investigations on tension laps by Cairns [25] and by Metelli [26] have demonstrated the proportion of bars lapped at a section has no appreciable influence on lap strength. Cairns also noted that the greater stiffness of a lapped pair over the lap length (compared to that of a continuous bar over the same distance) caused a small strength reduction when allowance was made for the increase in spacing of lapped pairs due to the greater stiffness of the lapped bars attracting a greater share of the total force. However, both studies also noted lap failure became less brittle as the proportion lapped reduced (see also following section on ductility).

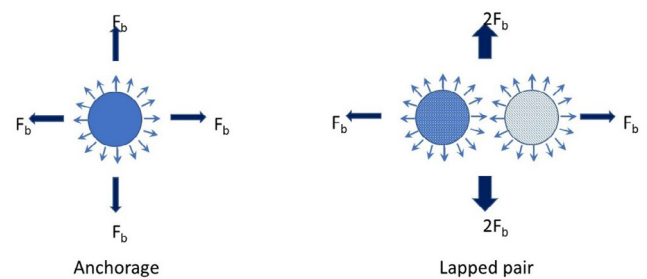


Figure 12. Historic hydraulic pressure analogy model.

Earlier drafts of FprEC2 did not include parameter k_{ls} for laps, but an evaluation carried out by Camps *et al* [22] at a late stage in the development of FprEC2 noted that this resulted in a lower safety margin for laps than for anchorages. The finding was not expected as Eq. 2, from which FprEC2 design expressions are derived, was found to be equally valid for both anchorages and laps, Table 1. Various North American studies have also moved away from the hydraulic pressure hypothesis and concluded that lap and anchorage lengths may be calculated by the same expression, and ACI 318 [21] allows lap lengths to be calculated using the same expressions as those for anchorages provided the area of reinforcement is at least double that required or no more than 50% of bars are lapped.

It is not clear whether the need to introduce k_{ls} is due to systemic or accidental factors. The index on the ratio l_{bd}/ϕ has been rounded down from the 'accurate' value of 1.82 proposed in *fib* Bulletin 72 [5] to 1.5 in FprEC2 introducing some conservatism at capacities below 435MPa, Figure 2. The average stress developed in tests without links or transverse pressure is 364MPa for anchorages, whereas that for laps is 424MPa. The difference in bar stress between the two groups may have produced a slight bias in favour of anchorages in Camps' analysis. Approximations in the transition from Eq. 2 to Eqs. 4 and 5 might accidentally have contributed to an apparent difference

between laps and anchorages. Eq. 2 must be rearranged to calculate the bond length required to develop a given bar stress, and indexes and coefficients have then been rounded in Eqs. 4 and 5 to obtain more ‘user friendly’ values. Due to the summative nature of the confinement terms in Eq. 2 this re-arrangement is not algebraically straightforward and is partly empirical. Whatever the reason, the evaluations presented later show that the introduction of $k_b = 1.2$ gives a more consistent margin of safety.

As with anchorages, where only a single bar within a bundle is lapped at a section design lap length should be based on the bars own diameter, covers, and confinement by secondary reinforcement.

In the calculation of bond lengths where only a portion of bars are lapped at a section, clear bar spacing c_s is the dimension of concrete between lapped pairs. Figure 13, equivalent to Figure {11.10} in FprEC2, shows dimension c_s where 50% of bars are lapped at a section and pairs of lapped bars are in contact.

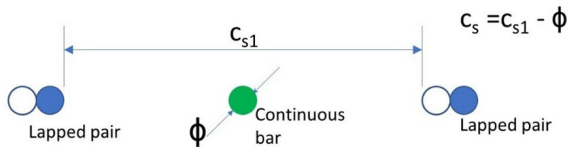


Figure 13. Definition of c_s where 50% of bars are lapped at a section.

The contribution of end bearing will frequently permit lap length of bars in compression to be reduced with no further reduction being gained by the presence of a hook or bend.

5.1. Laps using U-bar loops

U-bar loops are commonly used to provide tying and/or structural continuity between precast units. Failure may occur by crushing of the infill joint concrete or mortar within the loop, by splitting of the in-situ joint concrete in the plane of the overlapping loops, or by yielding and eventual rupture of reinforcement. The design philosophy requires that concrete failure does not occur before yielding of reinforcement [27]. The force to be resisted by the concrete strut is influenced by its inclination, represented by the ratio c_s/l_{sd} , and its resistance is determined by the properties of the joint infill concrete and the area of concrete mobilised. A minimum area of confining reinforcement is to be provided perpendicular to the plane of the loops to equilibrate the inclined compression struts, Figure 14.

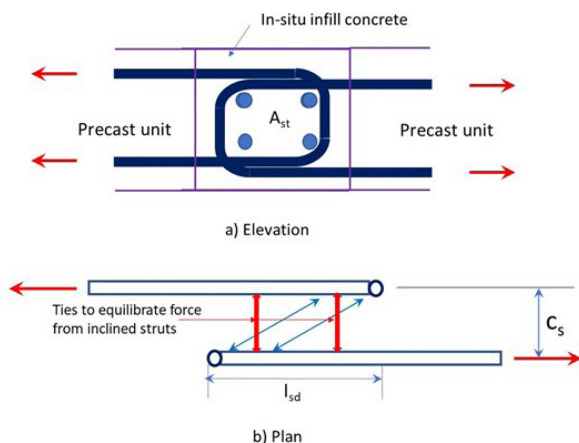


Figure 14. Strut and tie representation of forces at a U-bar lap.

6.

DUCTILITY AND REQUIREMENTS FOR ROBUSTNESS

The splitting mode of anchorage and lap failure may be extremely brittle. It is good practice to locate laps where bar stress is relatively low whenever possible. If, however, advantage is taken of moment redistribution or plastic analysis to improve structural efficiency, bars could be required to develop strains exceeding yield. FprEC2 introduces new provisions for tension laps located in the vicinity of a plastic hinge or yield line. Three alternatives are available in FprEC2 to provide the requisite deformation capacity and avert the risk of sudden collapse of the member:

- 1 increased confining reinforcement to counter the bursting forces generated by bond action and thus limit rate of loss of anchorage capacity in the event of capacity being reached.
- 2 restrictions on the proportion of bars lapped at a section to ensure continuous bars to accept a share of the load taken by a failing lap are present.
- 3 laps to be designed for a stress 20% above the design strength of the bar with the aim of ensuring that lapped bars can develop strains greater than ϵ_y , the strain at which appreciable plastic elongation starts to develop.

While some aspects of alternatives 1 & 2 are present in EC2 they appear to have been intended to address strength issues rather than deformation capacity.

7.

ASSESSMENT {APPENDIX I.11.4}

Equation 3 may also be used for assessment of anchorage and laps in existing construction. Cover and spacing dimensions from observations on existing structures may be used instead of those specified for construction. New expressions for anchorages and laps of hot-rolled plain surface bars are presented derived from work by Feldman *et al* [28].

8.

EVALUATION AGAINST TEST DATABASES

This section evaluates design rules for laps and anchorages in FprEC2 against test databases. Eq. {11.3} (Eq. 4 of this paper) has been re-arranged to estimate bar stress σ_s from dimensions and concrete strength given in the fibTG4.5 [8] and Amin [9] databases, Eq. 8. Dimension l_{bd} is the bond length in the test specimen. Characteristic concrete strength f_{ck} equals $f_{cm} - 5\text{MPa}$, the margin of 5MPa conservatively substituted for the 8MPa given in FprEC2 to account for tighter control in laboratory research compared to practical construction. Specimens in which $f_{ck} < 12\text{MPa}$ or $c_d < 0.95\phi$ have been filtered out as they lie outside the range covered by FprEC2 and normal practice, as do anchorage lengths $l_{bd} < 10\phi$ and lap lengths $l_{sd} < 15\phi$, although lengths down to 7.5ϕ have been retained for anchor-

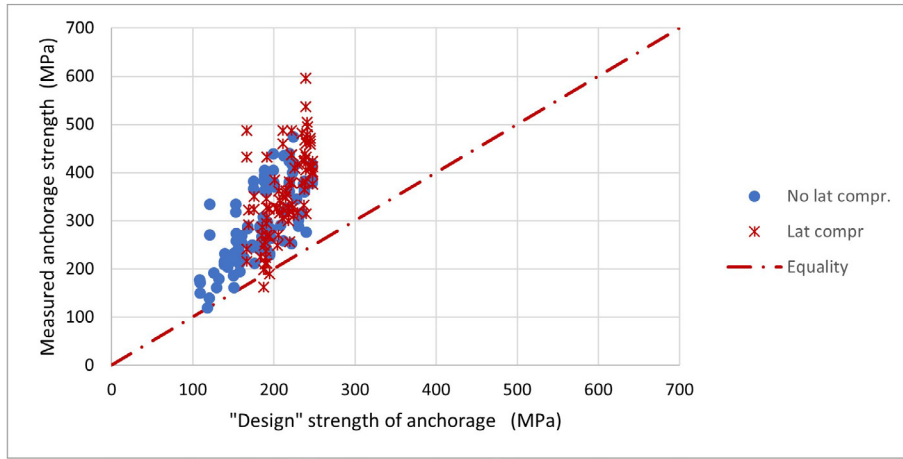


Figure 15. Evaluation of FprEC2 design rules for straight tension anchorages.

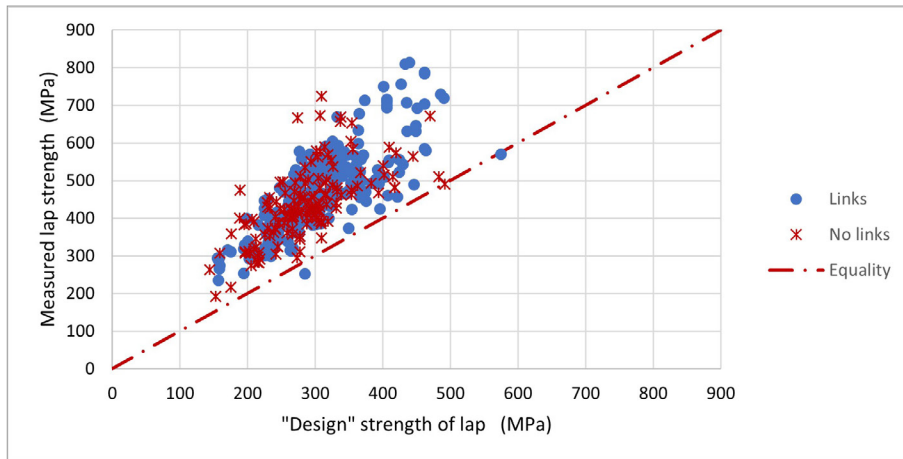


Figure 16. Evaluation of FprEC2 design rules for straight tension laps.

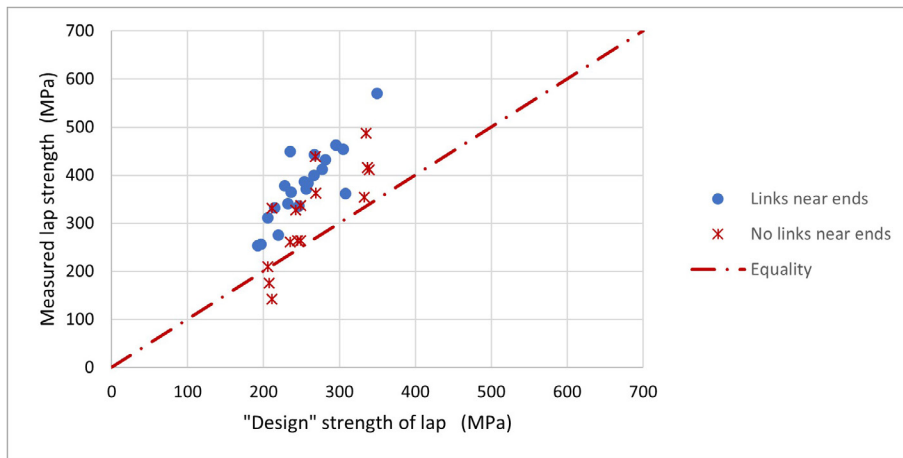


Figure 17. Evaluation of FprEC2 design rules for compression laps.

ages subject to transverse compression in view of a scarcity of data for longer lengths. Results for tension anchorages are plotted in Figure 15 and for tension laps in Figure 16. Results which plot above the chain-dashed line of equality are “safe”. A statistical summary is given in Table 2.

$$\sigma_s = 435 (k_{lb} k_{ls})^{-0.67} \left(\frac{l_{bd}}{\phi}\right)^{0.67} \left(\frac{f_{ck}}{25}\right)^{0.33} \left(\frac{20}{\phi}\right)^{0.22} \left(\frac{c_d}{1.5\phi}\right)^{0.33} \quad (8)$$

where
 $k_{lb} = 50$, $k_{ls} = 1.0$ and 1.2 for anchorages and laps respectively

Results for compression laps are presented in Figure 17. Here a length of 15ϕ is added to the lap length provided in tests, Eq. 9. Lap lengths down to 7.5ϕ and minimum cover down to 0.75ϕ are included in view of a scarcity of data for longer lengths and thicker covers. Two sets of results are plotted, one for specimens in which at least one link was located within the lap length and no further than 2ϕ or 50mm from the end of the lap [Figure 11.12], the other for specimens in which this requirement was not satisfied. All results for specimens in which the link location limit was satisfied lie in the ‘safe’ zone,

TABLE 2.
Statistical summary of design rules

	Tension Anchorages		Tension Laps		Compression laps	
	$\sigma_{ccd}=0$	$\sigma_{ccd}>0$	Links	No links	End links	No end links
Average	1.61	1.67	1.59	1.58	1.49	1.20
Std Dev.	0.31	0.35	0.20	0.28	0.16	0.26
CoV	0.19	0.21	0.13	0.17	0.11	0.22
Min	1.01	0.87	0.88	1.00	1.17	0.67
No. results	104	97	291	163	21	15
No. <1.0	0	2	1	0	0	2
% <1.0	0.0%	2.1%	0.3%	0.0%	0.0%	13.3%

but 2 out of the 15 results for specimens which did not satisfy the limit do not, and the average ratio of measured/design strength where links did not satisfy the limit is 20% below that for those which did.

$$\sigma_s = 435 (k_{lb} k_{ls})^{-0.67} \left(\frac{l_{bd}}{\phi} + 15 \right)^{0.67} \left(\frac{f_{ck}}{25} \right)^{0.33} \left(\frac{20}{\phi} \right)^{0.22} \left(\frac{c_d}{1.5\phi} \right)^{0.33} \quad (9)$$

The average ratio of measured to ‘design’ strength is consistent for all categories complying with FprEC2 provisions at around 1.6, Table 2. Test strength fell below design strength in 2 out of a total of 201 anchorage specimens. The two transverse compression tests falling below the equality line were from the same investigation with $l_{bd}/\phi = 8.6$ and a low concrete strength and do not comply with limits set in FprEC2. They only appear in this evaluation as the quantity of test data was somewhat limited. The single tension lap result in Figure 16 which falls below the equality line cannot be justified in a similar way and appears to be an outlier; the next lowest ratio is well above the equality line with a ratio of 1.07, and there is a clear gap between this individual result and the body of test data. This single result does not appear sufficient reason to further increase k_{ls} .

9. IMPACT OF CHANGES ON ANCHORAGE LENGTH

As stated earlier, bond and anchorage capacity are dependent on many factors. Differences in the format of design expressions between EC2 and FprEC2 means it is not possible to generalise the impact of differences between the two Codes. Selected comparisons for typical situations are presented here.

Figure 19 compares design anchorage lengths from EC2 and FprEC2 for anchorages in the beam section shown in Figure 18 where transverse compression is not present. Comparisons are presented for two concrete Grades, C25/30 and C60/75, and two bar sizes, 12 mm and 25 mm. Minimum cover $c_d=40$ mm in all cases. Confining reinforcement is size 8 bars at 200 mm centres. Three design anchorage lengths are plotted for each combination of bar size and concrete strength: design length from EC2, design length from FprEC2, and the design length from EC2 had it been revised to reflect the adjustment

to bond strength that should have been applied to maintain the margin of safety pertaining for a bar strength of 400 MPa after bar strength increased from 400 MPa to 500 MPa. An increase of 20%, midway between the values obtained for $n_\sigma=1.5$ and $n_\sigma=1.82$ has been applied.

Figure 19 shows that in good casting positions anchorage lengths have generally increased relative to EC2 where transverse compression is absent. However, had EC2 bond strengths been adjusted to take account of the increase in steel strength between the time EC2 rules were developed and the present day, the new rules would reduce anchorage lengths of small bars by around 15% and lead to an increase averaging around 10% for size 25 bars, with greater increases for larger sizes due to the wider range of influence of bar size in FprEC2, see Figure 7. Longer anchorage lengths are required in poor casting positions, Figure 20. Relative to current EC2 rules, anchorage lengths for small bars calculated to FprEC2 average around 15% shorter while lengths for size 25 bars are around 10% longer.

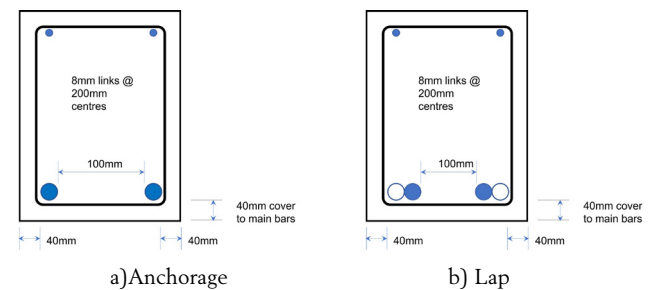


Figure 18. Sample beam sections.

Results of an analysis using the same parameters but with transverse compression $\sigma_{ccd}=1.0$ MPa are shown in Figure 21. As noted earlier, FprEC2 allows a more rapid reduction in bond length with increasing transverse reinforcement and transverse compression, and shorter anchorage lengths are permitted in most cases of the parameters selected here. Shorter anchorage lengths will generally result for directly supported end anchorages under the revised rules (provided the minimum anchorage length of 10ϕ is exceeded).

Figures 22 and 23 compare lap lengths in tension and in compression respectively where all bars are lapped at the same section, using the same parameters as the anchorage comparisons in Figures 19-21. FprEC2 generally results in shorter ten-

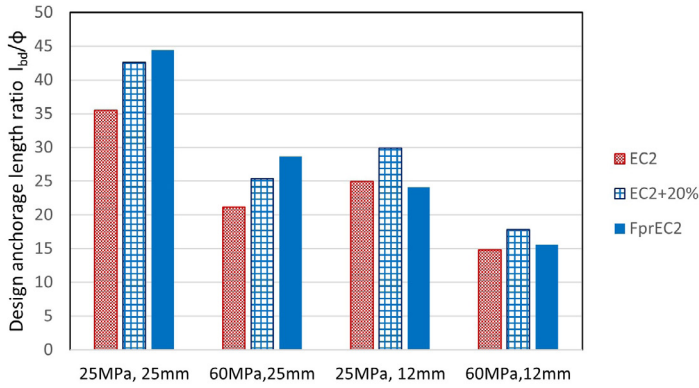


Figure 19. Comparison of design provisions, tension anchorages, good casting position.

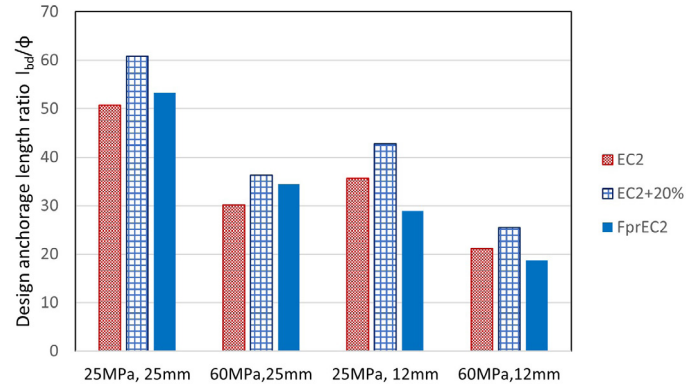


Figure 20. Comparison of design provisions, tension anchorages, poor casting position.

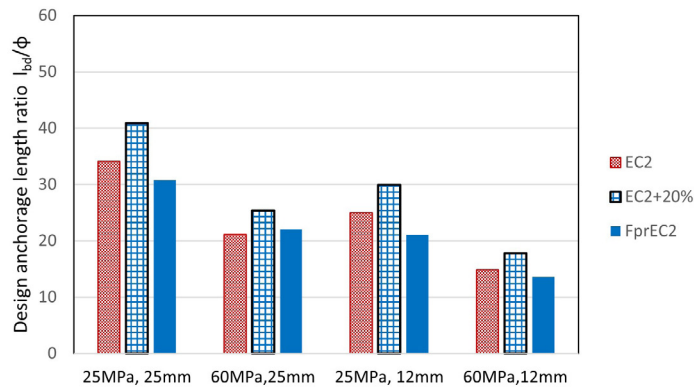


Figure 21. Comparison of design provisions, tension anchorages with transverse compression in a good casting position.

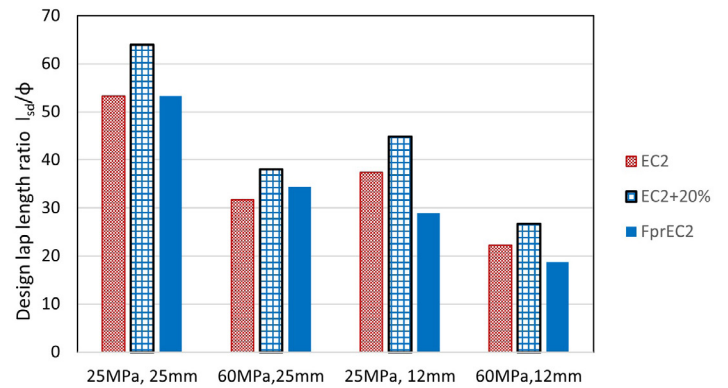


Figure 22. Comparison of design provisions, tension laps, good casting position.

sion lap lengths compared to EC2, and in all cases compared to EC2 adjusted for the increase in bar strength from 400 MPa to 500 MPa. There are marked reductions in all cases for compression laps as EC2 took no account of the contribution of end bearing.

10. CONCLUSIONS

This article has traced the development of provisions for anchorages and laps in the forthcoming revision to Eurocode2 for design of concrete structures and explained the main reasons for change. The format of expressions for design have changed and the several parameters influencing strength are now combined in a summative instead of a multiplicative way. Design anchorage and lap length are no longer proportional to the stress developed and now vary with $\sigma_{sd}^{1.2}$. While the influence of concrete strength has been reduced in the revision, the influence of confinement from cover, secondary reinforcement and transverse compression has increased. The bar size effect is not restricted to sizes above 32 and now influences a wider range of sizes. The contribution of end termination by a hook or bend or of welded transverse bars in a tension anchorage or lap is now a fixed length of 15ϕ rather than a 30% reduction. Provisions for com-

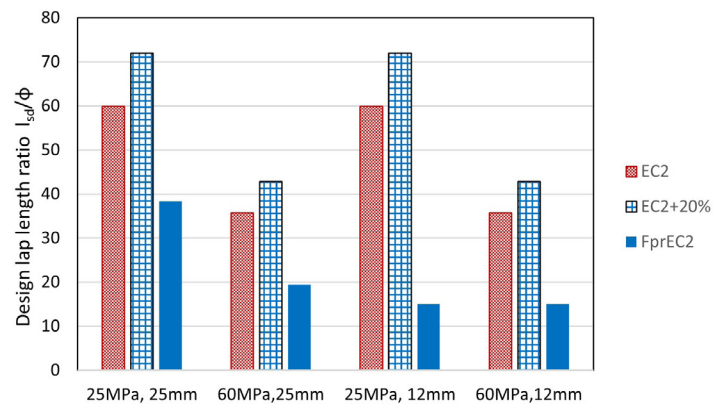


Figure 23. Comparison of design provisions, compression laps, good casting position.

pression laps have been made more consistent with those for tension laps and the contribution of end bearing is recognised.

Practical design of anchorages and laps has been and will continue to be based on an ultimate strength. However, it has been shown that bond-slip stiffness plays a significant role in performance and must be considered in the formulation of ultimate strength rules.

Revised design provisions are evaluated against two databases, one for anchorages and another for laps, and shown to be safe.

A few comparisons show that in the absence of transverse compression the new rules may lead to increased anchorage lengths for larger bar sizes and lower covers but will otherwise tend to result in shorter bond lengths.

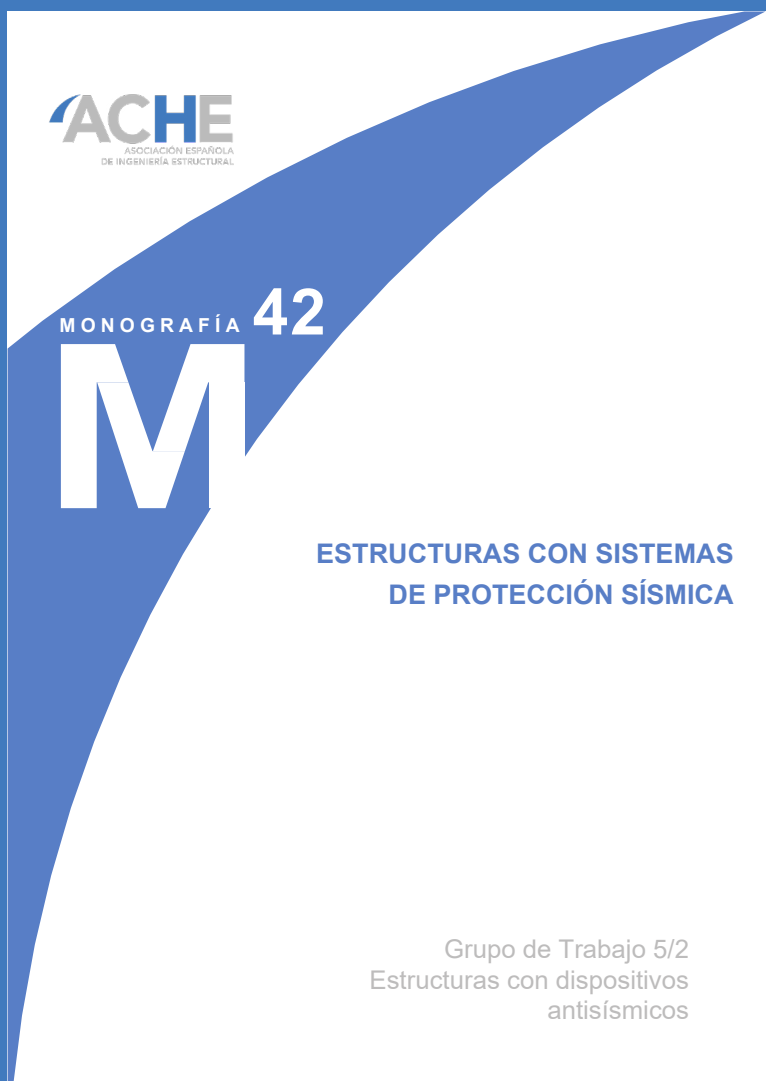
References

- [1] CEN/TC 250/SC 2 "Eurocode 2: Design of concrete structures — Part 1-1: General rules and rules for buildings, bridges and civil engineering structures". FprEN 1992-1-1:2023 as submitted to CEN/TC 250 for FV, Feb 2023. * This document is available through the National members of CEN TC250/SC2.
- [2] Eurocode 2: Design of concrete structures — Part 1-1: General rules and rules for buildings. BS EN 1992-1-1:2004. British Standards Institution London 2004. 225pp
- [3] CEB-FIP Model Code 78. CEB Lausanne 1978
- [4] CEB Bulletin 228. 'High Performance Concrete - Recommended extensions to the Model Code 90'. CEB Lausanne, 1995, 33 pp.
- [5] fib, Technical report bulletin 72 - Bond and anchorage of embedded reinforcement: background to the fib model code for concrete structures 2010, fib: Lausanne, Switzerland, 2014.
- [6] Schoening J Anchorages and laps in reinforced concrete members under monotonic loading. PhD Dissertation, University of Aachen, 2018
- [7] M. Micalef, R.L. Vollum, The effect of shear and lap arrangement on reinforcement lap strength, *Structure* 12 (2017) 253–264.
- [8] fib TG4.5 bond test database : may be obtained from: http://fibtg45.dii.unile.it/files%20scaricabili/Database_splacetest%20Stuttgart%20sept%202005.xls
- [9] Amin, R., 'End Anchorage at Simple Supports in Reinforced Concrete', Thesis presented for the Degree of PhD. London South Bank University, November 2009.
- [10] G. Mancini, V.I. Carbone, G. Bertagnoli, D. Gino, Reliability-based evaluation of bond strength for tensed lapped joints and anchorages in new and existing reinforced concrete structures, *Structural Concrete* (3/2018). 635-636 <https://doi.org/10.1002/suco.201700082>
- [11] Taerwe RL. Towards a consistent treatment of model uncertainties in reliability formats for concrete structures. In: CEB Bulletin d'Information No 219, Safety and Performance concepts, CEB, Lausanne; 1993. p. 5–61.
- [12] Vollum R, Goodchild C. Proposed EN 1992 tension lap strength equation for good bond. *Structures* 19 (2019) 5–18, 2018 Institution of Structural Engineers. Elsevier Ltd.
- [13] Tepfers, R. A. Theory of bond applied to overlapped reinforcement splices for deformed bars. Chalmers Technical University, Institution for Betonbyggnad. Publication 73:2, 328 pp, Gothenburg, 1973.
- [14] fib Model Code 2010. Ernst & Sohn, Berlin, 2013. 500pp. ISBN: 978-3-433-03061-5
- [15] Cairns J. Top cast effect: the influence of bond length. *Structural Concrete* 2021;1–14 <https://doi.org/10.1002/suco.202100376>
- [16] Cairns, J; Suryanto, B. Do design codes overestimate the influence of casting position? Proc Int Conf on Bond, Stuttgart, July 2022. IWB, Stuttgart, 2022. pp 1052-1064. <http://www.iwb.uni-stuttgart.de/publikationen/index.html>
- [17] Metelli G., Cairns J., Conforti A., & Plizzari G A. Local Bond Behavior of Bundled Bars: Experimental Investigation. *Structural Concrete* 2021. <https://doi.org/10.1002/suco.202000576>
- [18] Cairns J., Lap Splices of Bars in Bundles. *ACI Structural Journal*. Vol 110, no. 2. Mar 2013
- [19] Design of concrete anchorages in concrete. *Fib Bulletin* 58. Fib Lausanne, 2011.
- [20] Bonded Fasteners for Use in Concrete. European Assessment Document EAD 330499-01-0601. December 2018. Accessed from EAD 330499-01-0601 (eota.eu)
- [21] ACI Committee 318, "Building Code Requirements for Structural Concrete (ACI318-19) and Commentary," American Concrete Institute, Farmington Hills, MI, 2019
- [22] Camps B, Schoening J, Hegger J. Review of the design rules for anchorages and laps according to the draft of the second generation of Eurocode 2. Proc Int Conf on Bond, Stuttgart, July 2022. IWB, Stuttgart, 2022. pp490-505.
- [23] Ferguson P M, Thompson J N. Development for large high strength reinforcing bars. *Proc. ACI*. Vol 62 No.1, Jan 1965. pp 71-9 1.
- [24] Reynolds G C, Beeby A W. Bond strength of deformed bars. Proc Int Conf on Bond in Concrete, Ed Bartos P. Applied Science Publishers, London 1982. pp 434-445.
- [25] Cairns J. Staggered lap joints of tension reinforcement. *Structural Concrete*, Vol 15 no. 1. March 2014. <https://doi.org/10.1002/suco.201300041>
- [26] Metelli G, Cairns J, Plizzari G. The influence of percentage of bars lapped on performance of splices. *Materials and Structures* 48(9):2983-2996 • September 2015. <https://doi.org/10.1617/s11527-014-0371-y>
- [27] fib Bulletin 43. Structural connections for precast concrete buildings. fib Lausanne, Switzerland 2008. 360pp.
- [28] Feldman L, Cairns J. and Palmisano F. Codifying the development, splicing, and detailing of historical bar types for structural evaluation and rehabilitation. Proc Int Conf on Bond, Stuttgart, July 2022. IWB, Stuttgart, 2022. <http://www.iwb.uni-stuttgart.de/publikationen/index.html> pp956-967.

ACHE

MONOGRAFÍAS

PRÓXIMAMENTE



SECRETARÍA DE ACHE
Tel.: 91 336 66 98
www.e-ache.com

Contributions of the Future Eurocode 2 for Assessment of Existing Concrete Structures

Aportaciones del futuro Eurocódigo 2 para la evaluación de estructuras existentes de hormigón

Eduardo Díaz-Pavón Cuaresma^{*,a}, Raúl Rodríguez Escribano^a, Jorge Ley Urzaiz^a,
Pedro López Sánchez^b

^a Dr. Ingeniero de Caminos, Canales y Puertos. INTEMAC.

^b Dr. Ciencias Químicas. INTEMAC

Recibido el 8 de septiembre de 2022; aceptado el 17 de enero de 2023

ABSTRACT

This article highlights the most relevant aspects of the new generation of Eurocodes for the assessment of existing structures, and in particular those governing concrete structures. In this respect, the latest Eurocode 0 will include a new section (*prEN 1990-2. Basis of assessment and retrofitting of existing structures: general rules and actions*) covering the approaches and analysis methods that must be included in this type of assessment, while Eurocode 2 (*FprEN1992-1-1:2023 Design of concrete structures*) includes *Annex I: Assessment of existing structures*, which is informative and covers particular aspects of the assessment of concrete structures.

KEYWORDS: Existing structures, assessment, durability, reliability.

©2023 Hormigón y Acero, the journal of the Spanish Association of Structural Engineering (ACHE). Published by Cinter Divulgación Técnica S.L. This is an open-access article distributed under the terms of the Creative Commons (CC BY-NC-ND 4.0) License

RESUMEN

En el presente artículo se destacan los aspectos más relevantes de la nueva generación de Eurocódigos en lo relativo a la evaluación de estructuras existentes, y en particular, para aquellas de hormigón estructural. En este sentido el Eurocódigo 0 recogerá una nueva parte (*prEN 1990-2. Basis of assessment and retrofitting of existing structures: general rules and actions*) dedicada al planteamiento y análisis que deben recoger este tipo de evaluaciones, en tanto que el Eurocódigo 2 (*FprEN1992-1-1:2022 Design of concrete structures*) incorpora un anejo, el *Annex I: Assessment of existing structures*, de carácter informativo, en el que se recogen algunos aspectos particulares de dicha evaluación para las estructuras de hormigón.

PALABRAS CLAVE: Estructuras existentes, evaluación, durabilidad, fiabilidad.

©2023 Hormigón y Acero, la revista de la Asociación Española de Ingeniería Estructural (ACHE). Publicado por Cinter Divulgación Técnica S.L. Este es un artículo de acceso abierto distribuido bajo los términos de la licencia de uso Creative Commons (CC BY-NC-ND 4.0)

1. INTRODUCTION

The future Eurocode is sensitive, as it could not be otherwise, to the general interest in the evaluation of existing structures, while reflecting the current state of the art in relation to such evaluation.

In this regard, the new specification will subdivide Eurocode 0 into two parts¹. The first part would focus on design

issues (update of EN1990: *prEN1990:2020* [1]), while the second would cover the assessment of structures: *prEN1990-2. Basis of assessment and retrofitting of existing structures: general rules and actions* [2]. The latter document has been

1.- At the time of writing the enquiry stage currently is being completed and it is possible that some adjustments will be introduced before a final version is published. In particular, it is under discussion whether to include the provisions for existing structures in a separate part of EN1990 (in the current version, *prEN1990-2: 2022. Basis of structural and geotechnical assessment of existing structures*) or to include them in the current Eurocode 0, extending its scope and title to *prEN1990: 2022 Basis of structural and geotechnical design and assessment*.

* Persona de contacto / Corresponding author:
Correo-e / e-mail: ediazpavon@intemac.es (Eduardo Díaz-Pavón).

prepared by a horizontal group of TC250, WG2 Existing Structures, who had previously drafted *Technical Specification TS 17440* [3] forming the basis for *prEN1990-2*, dated July 2020.

In addition, *FprEn1992* [4] has included *Annex I Assessment of concrete existing structures* with informative purposes. It also has another informative annex - *Annex A Adjustment of partial factors for materials* - which incorporate specifications for the formulation of partial factors in concrete and reinforcement and states particular aspects of the assessment based on core sample tests.

This article aims to highlight the most relevant aspects of *Annex I*, as well as those of *Annex A*, logically based on the principles that should guide this type of assessment as set out in *prEN 1990-2* [2].

Based on the above, the article is divided into 4 sections:

- 1) *Preliminary considerations for the assessment of existing structures*: here *prEN1990-2* is referred, highlighting aspects that concern both the assessment and the investigation itself.
- 2) *The assessment of the strength of concrete in existing structures*, in accordance with *Annex A* and notes in *Annex I*.
- 3) Aspects to be taken into consideration in the *verification of existing concrete structures*, listed in *Annex I*.
- 4) Considerations on the *durability of existing concrete structures*, also listed in *Annex I*.

Throughout this article, equations, tables, and figures have been numbered sequentially in citation order in it. References to equations, tables, and figures taken directly from *FprEn1992* are additionally given. It does not reproduce sections of the Code in detail and is intended to be read alongside the revised Code.

2.

PRELIMINARY CONSIDERATIONS FOR THE ASSESSMENT OF EXISTING STRUCTURES

The design of a new structure is based on a set of requirements from which the structure is calculated, which then must be built and maintained in accordance with current criteria. As the regulatory criteria used at the time of design the existing structure may be very different than those at the time of assessment, new insight in material behaviour can result in requirements/regulations that differ from those applied during design in the past and should be taken into account in its assessment.

However, the information available will also differ, as it can usually be directly measurable, or at least, general information can be verified by inspection on the completed structure. Therefore, depending on the design and construction records, performed investigations, etc., more precise than that considered for design purposes. It means uncertainties are usually lower.

Finally, considerations regarding the structure's remaining service life are also different; and relative costs of an intervention are usually higher when an existing structure needs to be strengthened.

This means that assessments of these structures must be carried in a way different than that at the time of design.

The initial approach should entail the semi-probabilistic analyses that are normally used in the design of new structures, as they enable updating the overall safety level (β -value) and to update the partial factors based on additional information.

For this approach *prEN1990-2* [2] proposes different nomenclature for capacities and loads in Section 8.1, with an emphasis on differentiating the concepts of assessment and design:



Figure 1. Design plan of a bridge and the bridge built: An important difference between the design of a new structure and the assessment of an existing structure is the amount of information available, which in the latter usually allows lower uncertainties.

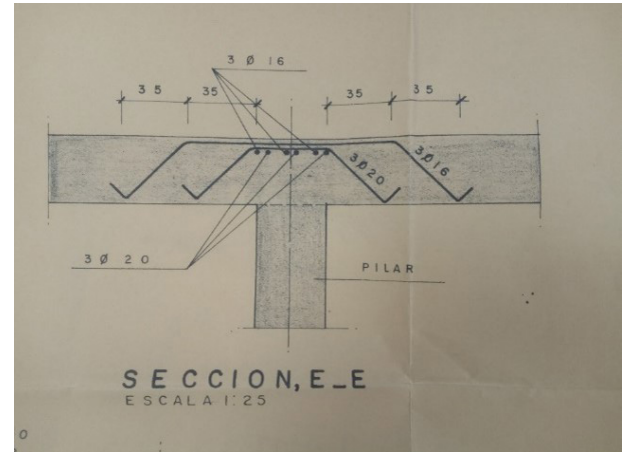
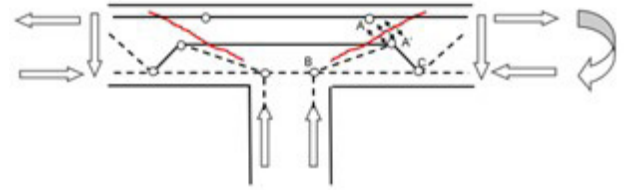


Figure 2. Example of punching failure in a slab due to a mistake in the placement of the specified reinforcement.

$$E_a \leq R_a \quad (1)$$

where

E_a is the assessment value of the effect of actions.

R_a is the assessment value of the resistance

NOTE E_a and R_a can be expressed as functions of the assessment values of the basic variables X_a (including the relevant partial factors, combination factors and conversion factors) as in formula (2) and (3).

$$E_a = E \{X_{a1}, X_{a2}, X_{a3}, \dots, X_{aj}\} \quad (2)$$

$$R_a = R \{X_{a1}, X_{a2}, X_{a3}, \dots, X_{aj}\} \quad (3)$$

With regard to the aforementioned partial factors, it is known (and explicitly stated in Eurocode 0, [1]) that they are set based on a certain *probability of failure* (normally by means of a reliability index, β) which is considered acceptable in terms of the consequences of such a failure (i.e. in terms of the accepted risk) over a given reference period. They also cover the uncertainties associated with the materials and actions, as well as those inherent to the resistance models and the effects of the actions included in the codes. As an example, for the design of new “conventional” structures within the framework of the Eurocodes (consequence class CC2), $\beta=3.8$ is generally considered for a reference period of 50 years and is associated with a service life failure probability of approximately 0.01%. In principle, this β -coefficient can be reduced in the case of a structure that has already been built by updating the safety coefficients; e.g. using the tools provided by Eurocode 0 [1] regarding reliability management.

However, it is particularly important to bear in mind that existing structures may have been designed and built with materials, techniques and construction specifications that are very

different to those covered by recent codes. Engineers must thus be particularly attentive to the validity of the verification models and their underlying assumptions. Aspects such as construction quality, the ductility of materials, the robustness of the structures, durability, etc., did not have the importance that they now do, given the evolution of knowledge and consequently of regulatory developments. Therefore, it requires a high degree of caution and experience to update the partial factors for assessment of existing structures.

In addition, other highly important aspects, especially for the assessment of existing structures, are not taken into account by means of these safety factors. They do not cover “*human error*”, which for designs are minimised through control activities (during design and construction phases). As the example in Figure 2, a defect in the placement of the reinforcement steel (the transverse reinforcement was too low and therefore not effective) caused the failure of the slab, which fortunately was detected and corrected despite the low warning capacity of punching shear failure (in this case, by demolishing and rebuilding the slab).

Therefore, a decisive aspect in the assessment of an existing structure is its investigation of its current condition. As specified in Annex A of prEN1990-2 [2]: *Guidance relating to the assessment process*, the investigation will depend on the type of structure (construction typology, period, etc.) and the information available, and should be carried out with the aim of updating knowledge about the structure, verifying its adequacy with the information available, and complementing this information with respect to aspects that may be incomplete for the appropriate analyses.

Furthermore, prEN1990-2 [2] supposes that such an investigation will be carried out by experienced and qualified personnel who are aware of the particular aspects that an assessment of each structure would entail.

Qualifications (experience and expertise) are essential to properly plan the investigation, whereby the configuration

of the structure to be assessed and its most likely failure modes are identified, followed by planning the appropriate on-site and office-based investigations. The quality of the results of the latter depends directly on the validity of the initial assumptions, which must be based on the structure itself. While for the analysis step, both the procedures and the calculation criteria are generally provided for in the standards, and the existing ones are generally applicable to design, these criteria are always qualitative in on-site investigations and are thus entrusted to the expert performing the assessment. Apart from some noteworthy attempts, neither there are references nor the standards included how to evaluate the influence of this information in the assessment. As an example, Section 3 of Eurocode 8, *UNE-EN 1998-3* [5] propose specific values for the frequency of the investigation according to different knowledge levels (KL), which are not usually practicable, and penalising the capacity of the structure by means of confidence coefficients (CF) when this investigation is not “complete”. Anyway assessment for seismic loads is not totally comparable to an assessment for static loads in ULS, and the knowledge level approach for ULS static design is still a challenge to be met.

It is nonetheless highlighted that the future Eurocode, in particular with *prEN 1990-2* [2]. Basis of assessment and retrofitting of existing structures: general rules and actions (with the format and/or location that is ultimately decided), together with *Annex I* of *FprEN1992-1-1*, are a first and great step towards assessment regulations, being one of the first design codes including a part on assessment and providing important tools for this type of concrete structure analysis.

3.

DESIGN STRENGTH OF CONCRETE

One of the key aspects in the evaluation of a concrete structure is the estimation of the concrete strength class, which is determined by measuring the concrete compressive strength.

The future Eurocode 2 [4] provides formulation to the characteristic strength of the concrete based on results obtained from cores, while allowing the engineer a more active role with respect to the uncertainties that have to be taken into account when determining the partial factor for concrete. To this end, Annex A outlines the different issues involved in obtaining these partial factors, while Annex I covers particular aspects of an assessment of existing structures.

Based on the formulation stated in the main text of *FprEN1992-1-1* (5.1.6) and the contents of *Annex A*, it is worth noting the factoring of concrete strength as the result of different log-normal distributions, which in the case of compression and bending are: that of the material itself on site (f_c), the effects of geometry (A_c), the effects on the strength model (θ) and that which takes into account casting of the concrete (η_{is}). This last coefficient allows the conversion between the resistance in the control tests and the resistance in the element, $f_{c,el}$. For each of them, the standard itself proposes bias coefficients, μ (or bias, i.e. ratio between the mean value and the characteristic value) and a variation coefficient, V (Table 1, which corresponds to Table A.3 of *prEN 1992-1-1* [4]).

TABLE 1. Statistical data assumed for the calculation of partial factor defined in *FprEN1992-1*. This table corresponds to Table A.3 of *FprEN 1992-1-1* [4].

	Coefficient of variation	Bias factor μ
Partial factor for reinforcement γ_s		
Yield strength f_y	$V_{fy} = 0.045$	$f_{ym}/f_{yk} = \exp(1.645V_{fy})$
Effective depth d	$V_d = 0.050$ ^b	$\mu_d = 0.95$ ^b
Model uncertainty	$V_{\theta s} = 0.045$ ^c	$\mu_{\theta s} = 1.09$ ^c
Coefficient of variation and bias factor of resistance for reinforcement	$V_{R_s} = 0.081$ ⁱ	$\mu_{R_s} = 1.115$ ⁱ
Partial factor for concrete γ_c		
Compressive strength f_c (control specimen)	$V_{fc} = 0.100$	$f_{cm}/f_{ck} = \exp(1.645V_{fc})$ ^d
In-situ factor $\eta_{is} = f_{c,ais}/f_c$ ^e	$V_{\eta_{is}} = 0.120$	$\mu_{\eta_{is}} = 0.95$
Concrete area A_c	$V_{Ac} = 0.040$	$\mu_{Ac} = 1.00$
Model uncertainty	$V_{\theta c} = 0.070$ ^f	$\mu_{\theta c} = 1.02$ ^f
Coefficient of variation and bias factor of resistance for concrete	$V_{RC} = 0.176$ ⁱ	$\mu_{RC} = 1.142$ ⁱ
Partial factor for shear and punching γ_v (see 8.2.2, 8.4, I.8.3.1, I.8.5)		
Compressive strength f_c (control specimen)	$V_{fc} = 0.100$	$f_{cm}/f_{ck} = \exp(1.645V_{fc})$ ^d
In-situ factor $\eta_{is} = f_{c,ais}/f_c$ ^e	$V_{\eta_{is}} = 0.120$	$\mu_{\eta_{is}} = 0.95$
Effective depth d	$V_d = 0.050$ ^b	$\mu_d = 0.95$ ^b
Model uncertainty	$V_{\theta v} = 0.107$ ^g	$\mu_{\theta v} = 1.10$ ^g
Residual uncertainties	$V_{res,v} = 0.046$ ^h	–
Coefficient of variation and bias factor of resistance for shear and punching (members without shear reinforcement)	$V_{RV} = 0.137$ ⁱ	$\mu_{RV} = 1.085$ ⁱ

^a The values in this column refer to ratio between mean value and values used in the design formulae (characteristic or nominal).

^b These values are valid for $d = 200$ mm. For other effective depths: $V_d = 0.05(200/d)^{2/3}$ and $\mu_d = 1 - 0.05(200/d)^{2/3}$.

^c The partial factor γ_s is calibrated for the case of pure bending according to 5.2.4 and 8.1.

^d This formula replaces relationship given in Table 5.1 for the purpose of Annex A.

^e In-situ factor η_{is} accounts for the difference between the actual *in-situ* concrete strength in the structure $f_{c,ais}$ and the strength of the control specimen f_c . For strength $f_{c,ais}$ assessed on extracted 2:1 cores according to EN 13791, see (7).

^f The partial factor γ_c is calibrated for the case of axial compression according to 5.1.6 and 8.1.

^g The partial factor γ_v is calibrated for the case of punching according to 8.4 and applies also for the case of shear without shear reinforcement according to 8.2.2 (similar statistical values).

^h The residual uncertainties refer to aggregate size, reinforcement area and spacing and column size.

ⁱ Based on the statistical values above and calculated using Formulae (A.2) and (A.3).

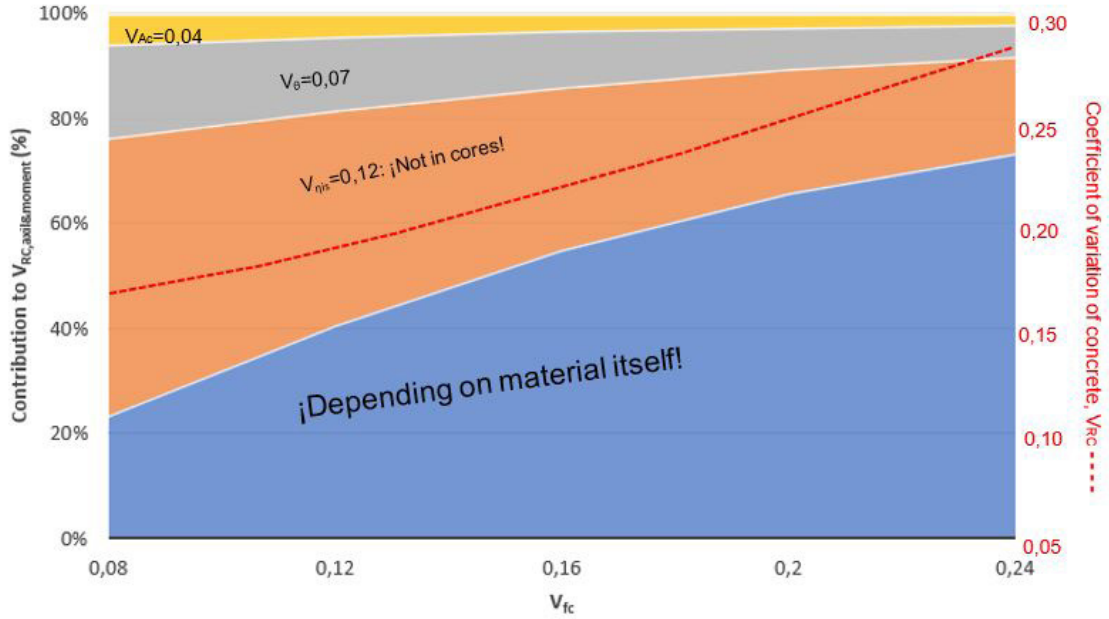


Figure 3. Contribution (in %) of different issues to total coefficient of variation of concrete, V_{RC} . V_{RC} obtained as function of the coefficient of variation of the material, V_{fc} (in red). $V_{Ac} = 0.04$, $V_{\theta} = 0.07$ and $V_{\eta_{is}} = 0.12$ are considered.

If the influence of these parameters in the design of a new structure are represented, the relationship shown in Figure 3 will be obtained as an expression of the coefficient of variation of concrete. Note the highly important influence of Eurocode 2 with respect to casting, a factor that logically disappears when strength is assessed on the basis of core sample tests, as the standard itself states below. Effects of casting are included in Annex I as part of k_{pfc} to obtain the characteristic strength, f_{ck} (see Table 3 further on).

The material's adjusted partial factor is thus obtained as shown below:

$$\gamma_M = \frac{e^{\alpha_R \beta_{igt} V_{RM}}}{\mu_{RM}} \quad (4)$$

where

index M is S for reinforcement, C for concrete in compression, and V for shear;

α_R is the sensitivity factor for resistance (0,8 according to Table A.3 of *FprEN1992-1-1*);

β_{igt} is the target value of the reliability index for the remaining service life (for example, 50 years) and taken into account the design situation (persistent or transient, fatigue or accidental)

V_{RM} is the coefficient of variation of the resistance which may be calculated from:

$$V_{RC} = \sqrt{V_{fc}^2 + V_{\eta_{is}}^2 + V_{Ac}^2 + V_{\theta C}^2} \quad (5)$$

$$V_{RC} = \sqrt{\left(\frac{V_{fc}}{3}\right)^2 + \left(\frac{V_{\eta_{is}}}{3}\right)^2 + V_d^2 + V_{\theta v}^2 + V_{res v}^2} \quad (6)$$

where the coefficients of variation of each uncertainty are defined in Table 1 (Table A.3 of *prEN 1992-1-1* [4]), as mentioned before, or updated.

μ_{RM} is the bias factor of the resistance and may be calculated from:

$$\mu_{RS} = \frac{f_{ym}}{f_{yk}} \mu_d \mu_{\theta S} \quad (7)$$

$$\mu_{RC} = \frac{f_{cm}}{f_{ck}} \mu_{\eta_{is}} \mu_{Ac} \mu_{\theta C} \quad (8)$$

$$\mu_{RV} = \left(\frac{f_{cm}}{f_{ck}} \mu_{\eta_{is}}\right)^{1/3} \mu_d \mu_{\theta v} \quad (9)$$

where the bias factors of each uncertainty are defined in Table 1 (Table A.3 of *prEN 1992-1-1* [4]) or updated.

In Annex A, Item 7, it is specified that in the assessment of existing structures based on the results of core sample tests, the intervention of the η_{is} factor is not considered. The reason is that $f_{c, is}$ is of interest for calculation purposes and is being obtained directly from the core sample tests, while the coefficient of variation and the bias factor are corrected to consider uncertainties inherent to statistical inference. As mentioned before, effects of coring and casting are included in Annex I as part of k_{pfc} (see Table 3, corresponding to Table I.2 in Annex I). In this case where compressive concrete strength is assessed according to *EN 13791: 2019* [6], Clause 8, to obtain the adjusted partial safety factor γ_c , formulae (5) to (9) should be replaced by:

$$V_{RC} = \sqrt{V_{fc \text{ is corr}}^2 + V_{Ac}^2 + V_{\theta C}^2} \quad (10)$$

$$V_{RC} = \sqrt{\left(\frac{V_{fc \text{ is corr}}}{3}\right)^2 + V_d^2 + V_{\theta v}^2 + V_{res v}^2} \quad (11)$$

$$\mu_{RC} = \mu_{fc \text{ is}} \mu_{Ac} \mu_{\theta C} \quad (12)$$

$$\mu_{RV} = \mu_{fc \text{ is}}^{1/3} \mu_d \mu_{\theta v} \quad (13)$$

where V_{Ac} , $V_{\theta C}$, μ_{Ac} , $\mu_{\theta C}$ are taken from Table A.3 of *prEN 1992-1-1* [4] or updated, and $V_{fc \text{ is corr}}$ and $\mu_{fc \text{ is}}$ are defined as:

$$V_{fc\ is\ corr} = \frac{k_{d,n}}{\alpha_R \beta_{igt}} V_{fc\ is} \quad (14)$$

$$\mu_{fc\ is} = e^{k_n} V_{fc\ is} \quad (15)$$

where:

$k_{d,n}$ is a parameter which depends on the number of samples, according to Table 2.

$V_{fc\ is}$ is the coefficient of variation of the core strength according to EN 13791: 2019 [6], but not smaller than 0,08.

k_n is the parameter which depends on the number of samples and has been used to calculate $f_{ck, is}$ according to EN 13791: 2019 [6]. See also Table 2.

TABLE 2.

Values of k_n and $k_{d,n}$ as function of the number of test results n used to evaluate the in-situ concrete compressive strength in the test region. This table corresponds to Table A.5 of *prEN 1992-1-1* [4].

n	8	10	12	16	20	30	∞
k_n	2.00	1.92	1.87	1.81	1.76	1.73	1.645
$k_{d,n}$ (for $\alpha_R \beta_{igt}=3.04$)	5.07	4.51	4.19	3.85	3.64	3.44	3.04

This approach is consistent with EN 13791: 2019 [6]. This is because the uncertainty associated with inferring the strength of the population from sampling as above is finally normalised, which when the dispersion of the concrete population is unknown (3rd row of Table 2) is done by means of Student's t-distribution with $n-1$ degrees of freedom. This formulation is limited to the coefficients resulting from using a $\beta=3.8$ reliability index, though this assumption is not explicitly stated in the standard.

Annex I proposes the use of clause (8) of the aforementioned EN 13791: 2019 [6] for the determination of the characteristic value of the in-situ compressive strength, $f_{ck, is}$, from cores. It points out that this strength must be corrected to obtain the characteristic strength, f_{ck} (to which the entire formulation of the articles including the strength of the concrete refers), by dividing it by a coefficient $k_{\mu, fc}$ (equation (16)), which is always less than 1 (Table 3):

$$f_{ck} = \frac{f_{ck\ is}}{k_{\mu, fc}} \quad (16)$$

TABLE 3.

Parameter $k_{\mu, fc}$ considering the representativeness of the in-situ compressive concrete strength assessed according to EN 13791: 2019 [6], clause 8. This table corresponds to Table I.2 of *prEN 1992-1-1* [4].

Regions and conditions of the structural member where the cores are extracted ^a	$k_{\mu, fc}$
a) Cores extracted only from the bottom parts of the concrete masses during casting (lower 70 % of the depth of concrete during casting) not necessarily representing the governing region for the verification	0.95
b) Cores extracted from different regions representing all conditions in the structural member, but not necessarily representing the governing region for the verification	0.90
c) Cores extracted from the region governing for the verification	0.85
NOTE The parameters given in Table I.2(NDF) apply unless a National Annex gives different values.	
^a The in-situ concrete compressive strength can exhibit significant variations depending on the location (strength typically smaller in the upper part of the element during casting)	

This factor $k_{\mu, fc}$ is the link between in situ measured characteristic strength and the characteristic strength to be used

for design. It is an important contribution of Annex I, since it is not covered in EN13791 and EN1992-1-1. It incorporates both the effect of the “damage” in the extraction ($\eta_{core-actual}$) and the effect of the casting (η_{is}). Specifically, it assigns an average value of 0.95 to the first of these, similar to that considered by the ACI (6%) [8] and somewhat more distinct to the 0.9 of the still recent EHE-08 [9] (currently replaced by *Código Estructural*, where in its art. 57.8 maintains the 10% difference between the concrete before placing and concrete in the cores, but including the effects of placing, as $k_{\mu, fc}$ does); in the second case, the parameters are contained in prEN 1992-1-1 [4].

Lastly, Section I.5.2.2. *Assessment assumptions* specifies the value of coefficients that influence the structural strength but depend on phenomena not directly related to concrete testing: one that accounts for the effect of brittle failure at non-uniform stress distribution in concrete, η_{cc} (not considered in current Eurocode), which in existing structures will normally have no influence ($\eta_{cc}=1$ for $f_{ck} < 40$ MPa [11]); and the other, k_{tc} , which considers the combination of the favourable effect of concrete strength gain over time due to hydration of the cement paste together with the reduction of concrete strength to take account the effects of sustained loads. With respect to the latter (already specified in current EN1922-1-1 as α_{cc} , though with different values), it is assumed that there is a “certain reduction” only when the overloads represent less than 20% of the total load [12]. For example, $k_{tc}=0.85$ in the limit case where permanent action (and/or variable actions of duration > 1 hour) represents 100 % of the total effect at assessment level. These values are consistent with those reported in the JCSS Probabilistic Model Code [13], where these effects are taken into account by means of $a(t, \tau) = a(t) \times a(\tau)$.

Though not commented in this paper, in Annex A and I of *prEN1992-1-1* steel guidance are also given to update the partial factors.

In summary, *prEN1992* [4] allows the designer a greater level of intervention in the partial factors to be considered for the resistance of the materials, as it includes a formulation and coefficients which, in the case of that obtained in concrete from the extraction of cores, are aligned with those used in other standards.

4.

VERIFICATION OF EXISTING CONCRETE STRUCTURES

Section I.8 of Annex A includes some particular aspects of the ULS verifications that may have to be taken into account in the assessment of an existing concrete structure, while I.9 covers those corresponding to the SLS. Following the numbering of the chapters in the main part of the code, section I.11 contains additional rules for reinforcement types (plain bars) and/or detailing of ribbed bars that do not meet modern code requirements.

4.1. Shear and punching

In Annex I, apart from some considerations of the effects of reinforcement corrosion which covered in the following sec-

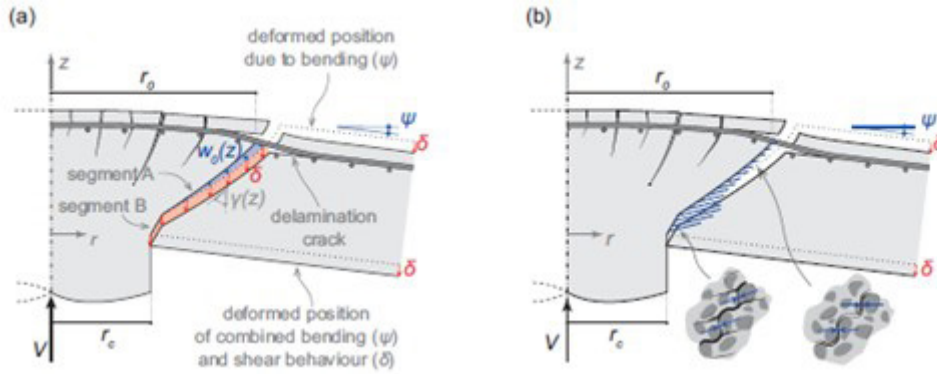


Figure 4. Theoretical principles of the mechanical model of Critical Shear Crack Theory: (a) kinematics of the critical shear crack at failure and resulting (b) internal stresses (extracted from the background document of *FprEN1992-1* [7]).

tion, probably the most relevant clauses of this Annex are those related to the shear and punching resistance. The formulation proposed is based on the *Critical Shear Crack Theory* (CSCT) (Figure 4) [7], both in Annex I and in the main text of *FprEN1992-1-1*.

Treatment of concrete members without shear reinforcement varies widely across different national and international standards: For the *Critical Shear Crack Theory* (CSCT), a shear failure criterion depending on the actual strain in the longitudinal reinforcement is considered, so that the strain ϵ_v must be determined.

According to Muttoni and Fernández Ruiz included in [7] for the strain in the reinforcement, ϵ_v , a linear relationship between the acting moment and the strain in the reinforcement can be assumed. ϵ_v can thus be calculated as:

$$\epsilon_v = \frac{M_E}{z A_s E_s} = \frac{M_E}{z \rho_l b_w d E_s} = \frac{V_E a_{cs}}{z \rho_l b_w d E_s} \quad (17)$$

where

- M_E is the acting bending moment at the control section;
- V_E is the acting shear force at the control section;
- $a_{cs} = |M_E / V_E|$ is the effective shear span at the control section;
- A_s is the area of the longitudinal reinforcement;
- ρ_l is the longitudinal reinforcement ratio;
- z is the effective level arm of the longitudinal internal forces;
- E_s is the modulus of elasticity of the longitudinal reinforcement.

Regarding the failure criterion, the original formulation used a hyperbolic failure [7].

In the case of shear, in *I.8.3. Shear*, the new formulation for elements without shear reinforcement is derived from that failure criterion. The shear stress resistance is computed as:

$$\tau_{Rd,c} = 0.33 \frac{\gamma_{def}^{2/3}}{\gamma_V^2} \frac{\sqrt{f_{ck}}}{1 + 24 \gamma_{def} \epsilon_v \frac{d}{d_{ag}}} \quad (18)$$

where

- d is the effective depth.
- ϵ_v is the strain in the longitudinal reinforcement at control section. For planar members, it refers to the principal

direction of the shear force, a non-linear cross-sectional analysis of the structure may be performed and the obtained internal forces as well as the strain ϵ_v may be averaged over the same width.

γ_{def} is a partial safety factor which covers the uncertainties related to the calculation of the deformation

NOTE

$\gamma_{def} = 1.33$ unless a National Annex gives a different value.

The proposal includes, as does the more simplified formulation in the main text in *FprEN1992*, the following:

- The consideration of a specific concrete reduction coefficient for the tangential stress verification, γ_V . This differentiation is in accordance with the dependence of concrete strength against shear stresses with the cube root of compressive strength. As γ_V is smaller than γ_C , this would imply lower uncertainties regarding the concrete's shear capacity.
- Consideration of the influence of the aggregate's size.

Both factors mean that the formulation generally produces results that are somewhat higher than those of the current Eurocode 2, except in cases of very small aggregate sizes (10 mm).

But as can be seen in formula (17), the formulation proposed in *Annex I* also takes into account the deformation of the tensioned reinforcement in the design section and not only with respect to the amount, as simplistically considered in most standards. This consideration is in line with the *Model Code 2010* [14] and may be of particular importance when elements present relatively minor bending (end columns of floor joists, shear verifications at the exit of abacus in reticular slabs, etc.) or in relatively high oversized elements (changes of use with overload reductions).

The importance of the effect of the deformation of the tensioned reinforcement can be seen in the graphs in Figure 5, which shows the shear resistance as a function of the effective shear span ($a_{cs} = M_d / V_d$) according to different formulations from current Eurocode 2 -*EN1992-1-1:2004*-; from the main text -*FprEN 1992-1-1*-; *Annex I*; and MC-2010. In all cases, a characteristic concrete strength $f_{ck} = 25$ MPa, a effective depth $d = 0.27$ m and a maximum aggregate size of $d_{ag} = 36$ mm were

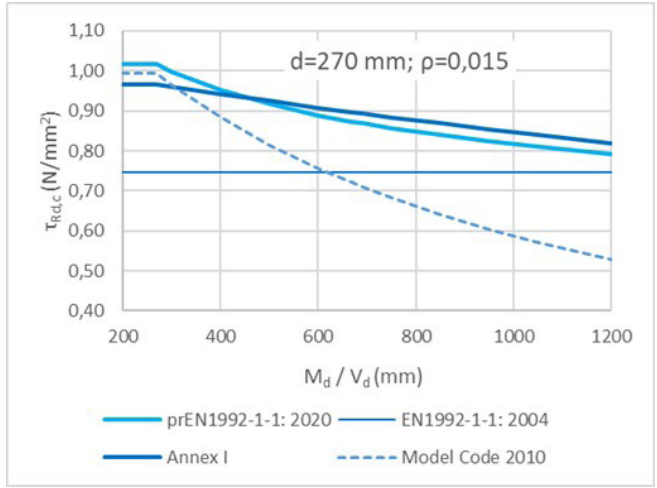
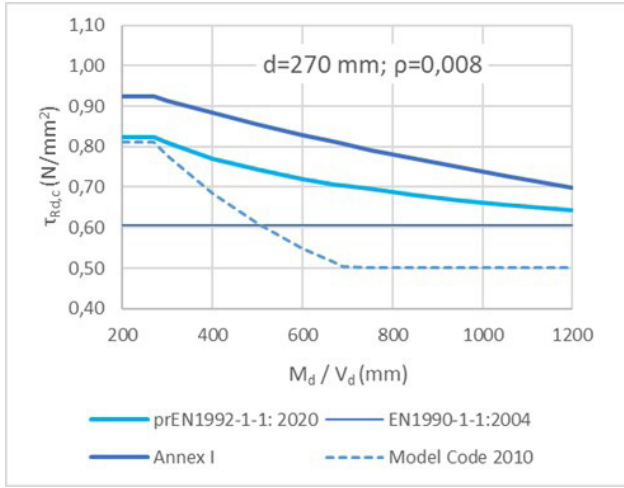


Figure 5. Effect of the effective shear span, $a_{cs} = M_d/V_d$, in concrete shear resistance, τ_{Rdc} , with different formulations for a effective depth $d = 0,27$ m.

considered. Regarding the partial factors, $\gamma_V=1.4$ is considered for prEN formulations, and $\gamma_C=1.5$ in the case of current Eurocode 2 and MC-2010. The results for two reinforcement ratios are shown, low ($\rho_1=0.008$) and high ($\rho_2=0.015$).

As shown in Figure 5, the proposed formulation has been found to be quite more favourable than the one in the current Eurocode. Furthermore, it is consistent with that of the Model Code (especially in the case of reduced effective shear span), although it gives substantially higher values for significant bending.

It is also worth noting the good approximation of the formulation of the main text -FprEN 1992-1-1- to the proposal in Annex I, derived from the original failure criterion, though the first one is the result of a simplification in that hyperbolic failure criterion, as explained hereafter.

Indeed, the formulation of Annex I implies that calculating the actual resistance, V_{Rd} , requires solving the set of formulae (17) and (18), which can be easily done iteratively, but it is not convenient for design.

For design purposes a closed-form expression is preferred. That is why FprEN1992-1-1 involves a simplification, using a parabolic curve instead of the hyperbolic one, which makes it possible to clear the resistant shear, τ_{Rd} , as a function of the effective shear span, a_{cs} . This results in a formulation similar to that currently used in EN1992-1-1:2004 [15], (8.27) in the main text of FprEN 1992-1-1, although instead of depending on the effective depth of the section, d , it depends on the aforementioned a_{cs} (clause (3) of 8.2.1):

$$\tau_{Rdc} = \frac{0.66}{\gamma_V} \left(100 \rho_l f_{ck} \frac{d_{dg}}{a_v} \right)^{1/3} \geq \tau_{Rdc,min} = \frac{11}{\gamma_V} \sqrt{\frac{f_{ck}}{f_{yd}} \frac{d_{dg}}{d}} \quad (19)$$

a_v is the mechanical shear span

$$a_v = \sqrt{\frac{a_{cs}}{4}} d \quad (20)$$

a_{cs} is the effective shear span.

$$a_{cs} = \left| \frac{M_{Ed}}{V_{Ed}} \right| \geq d \quad (21)$$

where:

As a first approximation and on the safety side, $a_{cs}=4d$ is considered, so that $a_v=d$. In addition, a minimum shear

resistance is given ((8.20) in the main text), which is obtained considering that the member reaches yielding of the flexural reinforcement and the shear resistance at the same load level.

Regarding punching, CSCT theory leads to a formulation in the articles which is completely different than the prior procedures in EN1992-1-1:2004 [15]. This entails changes even in the position of the verification section, which is now located $0.5d$ from the front of the column.

As for shear, the strains in the reinforcement are considered by a parameter a_p , obtained from the distances between the column axis and the locations where the bending moments in both directions are equal to zero. As a first approximation, a safe bound of $a_p = 8d$ is considered in the formulation from the main text (8.4.3), though it can be easily calculated (for regular slabs, a_{pi} may be approximated as $0.22L_i$ (where i refers to x and y axes); an elastic -uncracked- model is also proposed in the main text to obtain a_p).

According to Annex I, that formulation from the main text (8.4.3) can be used for assessment of existing structures, where it can also be considered the favourable effect of compressive membrane action around internal columns without significant opening, inserts or slab edges at a distance less than $5d_v$ from the control perimeter $b_{0,5}$, multiplying parameter a_p in formula by the following enhancement factor:

$$\eta_{pm} = \left(\frac{h}{d} \right)^{\sqrt{2}} \left(1.2 \frac{\sqrt{f_{ck}}}{\rho_l f_{yk}} \right)^{1/4} \geq 1 \quad (22)$$

Alternative, as for shear, the general method from CSCT theory is allowed in Annex I, both in terms of failure criterion and general definition of the load-rotation relationship. The shear stress resistance for punching is computed as:

$$\tau_{Rdc} = 0.75 \frac{\gamma_{def}^{2/3}}{\gamma_V^2} \frac{\sqrt{f_{ck}}}{1 + 15 \gamma_{def} \psi \frac{d_v}{d_{dg}}} \quad (23)$$

where

ψ in radians is the maximum rotation of the slab around the supported area. It may be calculated based on non-linear analysis of the structure and accounting for cracking,

tension-stiffening effects, yielding of the reinforcement membrane action and other non-linear effects relevant for providing an accurate assessment of the structure. The governing value of ψ is the maximum relative rotation between centre of the supporting area and a distance $2d_v$ from the control perimeter.

d_v , shear-resisting effective depth (potentially differing from the effective depth d to account for the penetration of the support and thus reducing the depth available to carry shear).

γ_{def} is a partial safety factor which covers the uncertainties related to the calculation of the deformation.

NOTE $\gamma_{def} = 1.33$ unless a National Annex gives a different value.

Though Eq (23) ((I.17) in Annex I) requires in general an iterative procedure to obtain the intersection between the hyperbolic curve of failure criterion and the load-rotation relationship, it produces more favourable results for small rotations ψ , as in the case of shear. In addition, for unusual geometries or reinforcement layout, a suitable load-rotation relationship can be obtained by non-linear analysis, taking into account slab continuity and membrane action, leading to a stiffer response of the slab, and then, higher punching resistance.

Regarding to slabs with punching shear reinforcement, some specifications are included that take into account the differences in the reinforcement details of existing structures in relation to the specifications in *FprEN1992-1-1* [4].

4.2. Serviceability Limit States

I.9 *Serviceability Limit States* indicates that in most cases SLS verifications may be performed using site-based observations and or measurements, instead of by calculations.

It is also noteworthy that when a reliability index lower than that usually considered for design purposes (according to *prEN 1990* [1]) is accepted in the ULS verifications, the stresses in the concrete and reinforcements under service loads (characteristic) must be within the values shown in Table 4.

TABLE 4. Limits on reinforcement and the concrete stresses at the characteristic combination of actions. This table corresponds to Table I.6 of *FprEN 1992-1-1* [4].

$\sigma_c \leq 0,60f_{ck}$	$\sigma_s \leq 0,80f_{yk}$	$\sigma_p \leq 0,80f_{pk}$
----------------------------	----------------------------	----------------------------

4.3. Anchorage of plain bars

The formulation in the articles of the main part of *FprEN1992-1* is restricted, as in the current Eurocode, to ribbed bars and tendons. However, for plain bars, reference is made to Annex I.

Before commenting on the formulation of the above-mentioned annex, it should be noted that the formulation of the main text in *FprEN1992* is already significantly different from the existing one, although it basically takes into account the same parameters (in particular the effect of the cover

- c_d - and of the bond conditions conditions depending on the position of the bar; other effects, such as the confinement or the shape of the anchorage, are considered by modifying c_d or the anchorage length itself - reducing it by 15Φ in the case of hooks). In addition, the type of situation for which the anchorage is checked (persistent and transient or accidental in nature).

This change in formulation takes into account the results of recent research findings [16] and [17], which are reliability-based. In practice, it results in a significant increase in anchorage lengths in most instances compared to the past formulae. For example, anchorage of a 20 mm diameter ribbed bar of a 250 MPa material (in *FprEN 1992-1-1* is declared that due to the database used to calibrate the formulation, it is valid for tensile stress in the bar not greater than 300 MPa) with 30 mm cover, in good bond conditions, which under the prevailing Eurocode would require 429 mm of straight extension, entails an increase of almost 34%, to 575 mm using the new formulation. For larger cover dimensions, the difference is much lower. Comparing the new approach to the Spanish regulation, *Código Estructural* [10], which allow the formulae of previous national codes (EHE-08 [9]) under some conditions, is even higher (300 mm compared to 575 mm -in fact, this value almost corresponds to the basic anchorage length for a bar B500 with the described conditions, which results 600 mm-).

For plain bars, usually anchored by hooks, the situation is even more unfavourable:

- For example, the reduction in anchorage tension due to the effect of the hook in I.11.4.2 is somewhat less than is currently the case (0.7). This reduction of the contribution of the hooks is based in the latest test on plain bars, which have confirmed that the effect of hooks is not as relevant as expected.
- More significant than the small reduction due to the effect of the hook is the anchorage length that is normal in relatively old structures, where the reinforcement covers are usually similar to the bar diameter. For example, for a plain bar 20 mm in diameter with a 20 mm cover and good bond conditions, concrete C25 and 260 MPa of steel stress, the anchorage length is 1.477 mm. This value should be compared with that which would be obtained from the application of the 1990 Model Code, MC-90 [18] (the most recent version, from 2010, does not include a formulation in this regard), whose formulation expressed 600 mm for this case, already somewhat higher than that which would result from the application of Instruction EH-68 [19] at a national level, the last one which considered the anchorage of plain bars (470 mm in the example). In this regard, the following graphs, extracted from the background of Annex I of *FprEN1992-1* [7], show the significant increase in anchorage length using the proposed formulation compared with that of MC-90 [18], at least for normal cases of relatively smaller covers. In fact, for poor bond conditions the differences become huge.

It should also be kept in mind that previous standards (for example, EH-39 [20] in Spain) went so far as to consider the bar anchored from the end of the hook, while not considering

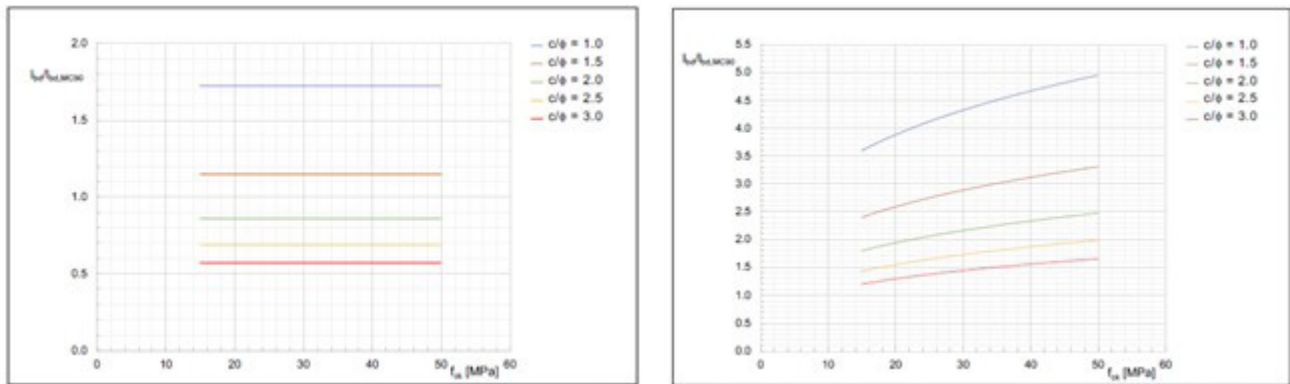


Figure 6. Influence of c/ϕ on $l_{bd,AnnexI} / l_{bd,MC90}$ for Good conditions position (GP, left) and Poor conditions position (PP, right), $\nu_c=1,5$, $\sigma_{sd}=200$ MPa (extracted from the background document of *FprEN1992-1* [7]).

the offset effect of bending moment laws (this concept was not taken into account in design until the publication of the ACI code of 1963 and, in Spain, until the aforementioned Instruction of 1968 was issued).

Under these conditions, the anchorage penalty found in the *Annex I* proposal may be of great importance. Of course, if for the assessment tensile stress the actual anchorage length is lower than l_{bd} , it doesn't mean that the relevant bars should not be taken into account for the verification but that the assessment stress should be reduced accordingly in order to have the actual anchorage length not lower than l_{bd} . This means that all bars present in the structure should be taken into account in the verifications but assuming for them a maximum stress consistent with the actual anchorage length that should not be lower than l_{bd} .

This only confirms that the reinforcement details of structures built with plain steel components (generally up to the 1960s), particularly those relating to anchorage and reinforcement overlaps, call for very strict reinforcement lengths, while raising significant uncertainties about the use of such reinforcements (e.g. in columns), which must be carefully considered in the assessment.

These results contrast with historic performance of concrete structures broadly, where no anchorage failures have been recorded. The surface oxidation that these bars generally present probably improves bond. This fact, combined with low stresses to which the anchoring components are normally subjected (especially at the end columns of beams and slab ribs or at overlaps), as well as the contribution of the hook at least in the ultimate limit state and given the presence of significant bending due to crushing of the concrete, are in principle much higher than those allowed by the standards (including EH-68 [19]), could explain these differences.

Anyway, all of the foregoing means that, in the opinion of the authors, it is necessary to warn of the need for an adequate analysis of aspects such as the contribution of all the reinforcement elements in horizontal structures, or of the longitudinal reinforcement in columns. The new formulation proposed in *FprEN1992-2* is the most advanced one and it is consistent with the reliability-based approach of the Eurocodes reliability-based, so it could afford a good approximation.

5. DURABILITY

Predictive methods for estimation of degradation processes in concrete are still under discussions and not generally accepted. This would lead to the situation that in engineering practice questions about remaining service life after presence of any deterioration or situations where, for instance, chloride fronts have almost reached the reinforcement, could not be predicted.

Then, neither *FprEN1992-1-1* [4] nor its Annex I lay out predictive methods for the estimation of the deterioration rates of an existing structure, and therefore of its residual service life, leading to the situation that for each specific case parties involved have to come to consensus on the required measures.

This is not a minor issue, as often in the structures under assessment -at least in Autor's experience, mostly in Spain- the carbonation front of the concrete has reached the position of the reinforcement (an example is shown in Figure 7, where the depth of the carbonate front was measured with a phenolphthalein solution, as is normally done) and its service life would be endangered. The Eurocode service life model considers two phases: the time to corrosion initiation, t_i (i.e. the time it takes for the attack front to reach the reinforcement), and the time to corrosion propagation leading to degradation, t_p (time to significant degradation of the structural element). For the example shown, the t_i has been consumed and since the latter depends mainly on the diameter of the reinforcement and the corrosion rate, measures must be taken to reduce it to the limits that allow the remaining service life to be admissible.



Figure 7. Example of a column where the carbonate concrete has reached the position of the rebars.



Figure 8. Different causes of deterioration of reinforced concrete: pitting corrosion (left), AAR (centre), acid attacks (right).

Under these conditions, decisions to try to comply with such standards may be excessive and possibly require the generalised protection of the structure. Such protection may be necessary in certain areas with unfavourable humidity conditions (e.g. damp rooms with an XC3 environment), but probably not in elements where the corrosion rate is very slow (e.g. in XC1 environments) and thus where the risk of structural and aesthetic consequences that may affect the structure's new service life are low.

The previous example highlights the differences between ULS and sustainability requirements. What actions are needed in each situation partly will depend on local building legislation. Fulfilling ULS requirements with sufficient confidence is generally what is stated in building legislation. Sustainability requirements are often less explicitly stated for existing construction, making it possible to distinguish between the different situations as described before.

Of concern are effects that must be considered in the assessment of structures deteriorated by durability defects (Section I.4.1.2): corrosion of reinforcements, sulphate attack (Delayed Ettringite Formation, DEF), Alkali-Aggregate reaction (AAR), acid attacks, etc. with some examples shown in [Figure 8](#).

These effects can include:

- Reduction of the concrete section due to spalling.
- Reduction of the cross-section of the reinforcement
- Reduction of its ductility. In the case of pitting corrosion, it may be necessary to stop its use because of the difficulties in detecting pitting (as its effect is local and often not accompanied by other forms of corrosion; it may not manifest itself externally), and because of the concentration of stresses around the pitting.
- Stress concentration due to localised corrosion (e.g. in prestressed steel).
- Stress corrosion cracking (e.g. in prestressed steel).
- Reduction of the bond between the reinforcement and the concrete.
- The loss of the concrete's properties (e.g. concrete's elastic modulus due to AAR).
- The loss of reinforcement properties (ductility from pitting corrosion) in relation to those deduced from the formulation of the articles.
- Cracking and expansion of concrete (e.g. due to DEF or AAR).

In addition, deterioration in the structure may influence the uncertainties of the strength models or the geometry itself.

These aspects need to be taken into account when updating the safety coefficients in a semi-probabilistic analysis.

To address reinforcement corrosion, the following considerations for testing purposes are proposed in I.8.1:

- An initial distinction is made between homogeneous and pitting corrosion. In relation to the former, the parameter P_x , *Corrosion Penetration Depth* is used. It is defined as the *loss in cross sectional radius of the bar due to homogeneous/uniform corrosion along the bar length; while pitting corrosion is defined as the form of localised corrosion that leads to the creation of cavities or crevices in the metal.*
- For reinforcement subjected to compression where the stirrups or ties are heavily corroded, reduced strength is possible due to the bars buckling prematurely.
- In shear-stressed elements, there is the possibility of premature failure of the stirrups due to corrosion (due to carbonation or pitting).
- For corrosion rates $P_x \geq 0.2-0.4$, cracks with an opening larger than 1 mm, or in the case of pitting corrosion:
 - A reduction of the maximum steel elongation is to be taken into account in the ULS verifications; as is a reduction of the concrete cross-section due to spalling of the cover.
 - A concentration of stresses in the pits.
- For homogeneous corrosion and low to medium corrosion rates ($P_x < 0.2-0.4$ or crack openings of less than 1 mm), it can be assumed that the stress-deformation diagram of the reinforcements is not affected and that the entire concrete section contributes to strength, although some reduced compressive strength due to cracking can be assumed.

In summary, though predictive methods for estimation of degradation processes in concrete are not included in a standard like Eurocode 2, the current draft of Annex I allows the assessment of structures without significant degradation.

6. CONCLUSIONS

In the previous sections, the most significant aspects of the assessment of existing concrete structures addressed in the future generation of Eurocodes have been presented. These are summarized as:

- *prEN1990-2* [2] sets out the criteria to be taken into account for the investigation and assessment of an existing structure and establishes differences with respect to the conventional design of new structures. In the opinion of the authors, particular importance should be given to knowledge of the structural configuration and most probable failure modes in the existing structure, as this establishes an essential basis for planning and carrying out verifications that are most appropriate and necessary in each case to quantify the safety, durability and functionality of the structure.
- *Annex I of FprEN1992* [4] complements these criteria for the specific case of concrete while emphasising the following aspects:
 - In relation to the materials, the procedure for obtaining the design strength of the concrete from the extraction of core samples is set out, which complements that of *Annex A*.
 - In relation to the shear and punching resistance of elements without transverse reinforcement, this *Annex I* proposes a formulation that in certain situations, like in the presence of elements with reduced reinforcement deformations, may allow for a greater contribution from concrete. This formulation, based on the *Critical Shear Crack Theory*, is also included in the main text, with some simplifications.
 - A particular aspect of existing concrete structures, and in particular those reinforced with plain steel bars, is the assessment of the anchorage conditions. In this regard, *Annex I* propose a formulation that, though is very advanced and consistent with the reliability-based approach of the Eurocodes, in the authors' view, should be applied with caution. The formulation reduces the strength contribution of the reinforcement in horizontal structures or contributions of longitudinal reinforcement in columns, which is why caution is recommended in its use and reliance on the expertise of technicians charged with conducting assessments: all bars present in the structure could be taken into account in the verifications but assuming for them a maximum stress consistent with the anchorage length given in the formulation proposed.
- When assessing existing structures, durability can be of particular importance. *Annex I* list some criteria that may guide considerations regarding structural deterioration. However, it does not propose a methodology for assessing the structure's remaining service life or measures that can be used to extend it, which are again left to the experience and knowledge of the technicians performing the assessments.

The future Eurocode will therefore standardise, at a European level, methods for the assessment of existing structures. *Annex I* is informative, so it depends on the adoption of individual countries as to whether this becomes the future standard in each one. This annex, together with *prEN 1990-2. Basis of assessment and retrofitting of existing structures: general rules and actions*, provide the basic principles of such assessments that are being developed in numerous forums. However, the proper application of this type of assessment requires

knowledge of the historical context within each country with respect to prior building codes and construction practice, in addition to those currently under development, as shown in the previous sections.

It must be highlighted that these new frameworks are a great step forward since it would be one of the first international design codes to specifically address assessment. However, there is still a long way to go including aspects such as the treatment of deteriorated or damaged structures, the definition of predictive methods for estimation of degradation processes, the consideration of the level of knowledge in the assessment, etc., that need to be further analyzed for their practical implementation. Hopefully in the next version of *EN1992-1-1* or a future amendment of the *FprEN1992-1-1* continued advancements can be made.

References

- [1] CEN/TC250. *prEN 1990:2020 Eurocode 0: Basis of structural and geotechnical design* (*)
 - [2] CEN/TC250. *prEN 1990-2 Eurocode 0: prEN 1990-2. Basis of assessment and retrofitting of existing structures: general rules and actions* (*)
 - [3] CEN/TS 17440. *Assessment and Retrofitting of Existing Structures*. Technical Specification. July 2020.
 - [4] CEN/TC250. *FprEN 1992-1-1 Eurocode 2: Design of concrete structures -Part 1-1: General rules and rules for buildings, bridges and civil engineering structures*. February 2023 (*)
 - [5] CEN/TC250. *prEN 1998-3 Eurocode 8: Design of structures for earthquake. Assessment and retrofitting of buildings* (*)
 - [6] EN 13791. *Assessment of in-situ compressive strength in structures and pre-cast concrete components*. August 2019.
 - [7] CEN/TC250. Background document to prEN 1992-1-1 ver. 2021-01. *Annex I. Assessment of Existing Structures* (N1074) (*)
 - [8] ACI Committee 214. 4-03. *Guide for obtaining cores and interpreting compressive strength results*. American Concrete Institute. Farmington Hills, Mich., 2003, 16pp. 2013.
 - [9] *Instrucción de Hormigón Estructural EHE-08*. Comisión Permanente del Hormigón. Ministerio de Fomento, Madrid, 2008.
 - [10] *Código Estructural*. Ministerio de Transportes, Movilidad y Agenda Urbana. Secretaría General Técnica. 2021.
 - [11] Moccia F, Yu Q., Fernández Ruiz M., Muttoni A. (2020) Concrete compressive strength: From material characterization to a structural value. *Structural Concrete*. July 2020. <https://doi.org/10.1002/suco.202000211>
 - [12] Tasevski, D., Fernández Ruiz, M., Muttoni, A. (2019) Assessing the compressive strength of concrete under sustained actions: Form refined models to simple design expressions. *FIB WILEY. Structural Concrete*, 2019; 20:971-985. <https://doi.org/10.1002/suco.201800303>
 - [13] Joint Committee in Structural Safety (JCSS). *Probabilistic Model Code. 2001*
 - [14] FIB. *Model Code for concrete structures 2010*. 2013.
 - [15] CEN/TC250. *EN 1992-1-1 Eurocode 2: Design of concrete structures -Part 1-1: General rules and rules for buildings*. 2004.
 - [16] Cairns, J., Feldman, L. (2018) Strength of laps and anchorages of plain bars. *Structural Concrete*. 2018. <https://doi.org/10.1002/suco.201700242>
 - [17] Palmisano, F., Greco, R., Biasi, M., Tondolo, F., & Cairns, J. (2020). Anchorage and laps of plain surface bars in R.C. structures. *Engineering Structures*, 213, [110603]. <https://doi.org/10.1016/j.engstruct.2020.110603>
 - [18] CEB-FIP. *Model Code 90*. 1993.
 - [19] *Instrucción para el proyecto y la ejecución de obras de hormigón en masa o armado, EH-68*. Ministerio de Fomento. España. Madrid, 1968.
 - [20] *Instrucción para el proyecto y ejecución de obras de hormigón EH-39*. Ministerio de Fomento. España. Burgos, 1939.
- (*) This document is available through the National members at CEN TC250/SC2 or other Committees and Subcommittees depending on the document.

Strengthening of Existing Concrete Structures with Fibre Reinforced Polymers (FRP) in the New Version of Eurocode 2

Refuerzo de estructuras existentes de hormigón con polímeros reforzados con fibras (PRF) en la nueva versión del Eurocódigo 2

Eva Oller^{*,a}, Ana de Diego^b, Lluís Torres^c, y Pedro Madera^d

^a Department of Civil and Environmental Engineering, Universitat Politècnica de Catalunya

^b Instituto de Ciencias de la Construcción Eduardo Torroja (IETCC), CSIC

^c Department of Mechanical Engineering and Industrial Construction, Universitat de Girona

^d Mapei

Recibido el 11 de agosto de 2022; aceptado el 5 de diciembre de 2022

ABSTRACT

This paper aims to introduce the content of Annex J “Strengthening of Existing Concrete Structures with CFRP” of Eurocode 2 [1]. This is first time that the design of adhesively bonded reinforcement with CFRP has been introduced in the European regulations through an informative annex. Annex J considers two different bonded strengthening techniques: externally bonded reinforcement (EBR) that consists of bonding CFRP strips or sheets to the surface of concrete elements, and near surface mounted reinforcement (NSM) that consists of embedded CFRP strips or rods to the slot cut in the concrete cover. Since, the content of Annex J is new, a summary and background related to all aspects required for designing CFRP strengthened systems for concrete structures, are given in this paper.

KEYWORDS: Strengthening, fibre reinforced polymer, externally bonded reinforcement, near surface bonded reinforcement, bond, reinforced concrete, prestressed concrete.

©2023 Hormigón y Acero, the journal of the Spanish Association of Structural Engineering (ACHE). Published by Cinter Divulgación Técnica S.L. This is an open-access article distributed under the terms of the Creative Commons (CC BY-NC-ND 4.0) License

RESUMEN

Este artículo tiene por objeto introducir el contenido del Anejo J del Eurocódigo 2 [1]: “Refuerzo de estructuras de hormigón existentes con CFRP”. Esta es la primera vez que el dimensionamiento de refuerzos adheridos con CFRP se introduce en la normativa europea a través de un anejo informativo. El Anejo J contempla dos técnicas de refuerzo adherido diferentes: el refuerzo adherido externamente (EBR) que consiste en pegar laminados o tejidos de CFRP a la superficie de los elementos de hormigón a reforzar, y el refuerzo insertado en el recubrimiento (NSM) que consiste en instalar el laminado o barra de CFRP en una ranura realizada en el recubrimiento del hormigón. Como el Anejo J en sí es una novedad, este artículo presenta un resumen de su contenido y algunos antecedentes relacionados con todos los aspectos necesarios para diseñar un sistema de refuerzo con CFRP para estructuras de hormigón.

PALABRAS CLAVE: Refuerzo, polímeros reforzados con fibras, refuerzo adherido externamente, refuerzo embebido en ranuras, adherencia, hormigón armado, hormigón pretensado.

©2023 Hormigón y Acero, la revista de la Asociación Española de Ingeniería Estructural (ACHE). Publicado por Cinter Divulgación Técnica S.L. Este es un artículo de acceso abierto distribuido bajo los términos de la licencia de uso Creative Commons (CC BY-NC-ND 4.0)

1. INTRODUCTION

Strengthening of existing reinforced and prestressed concrete structures might be necessary to restore or increase their

load-bearing capacity due to different reasons: an increase of load demand caused by a change of use, a loss of carrying capacity due to deterioration or structural damage, or to eliminate structural design or construction deficiencies.

* Persona de contacto / Corresponding author.
Correo-e / e-mail: eva.oller@upc.edu (Eva Oller Ibars).

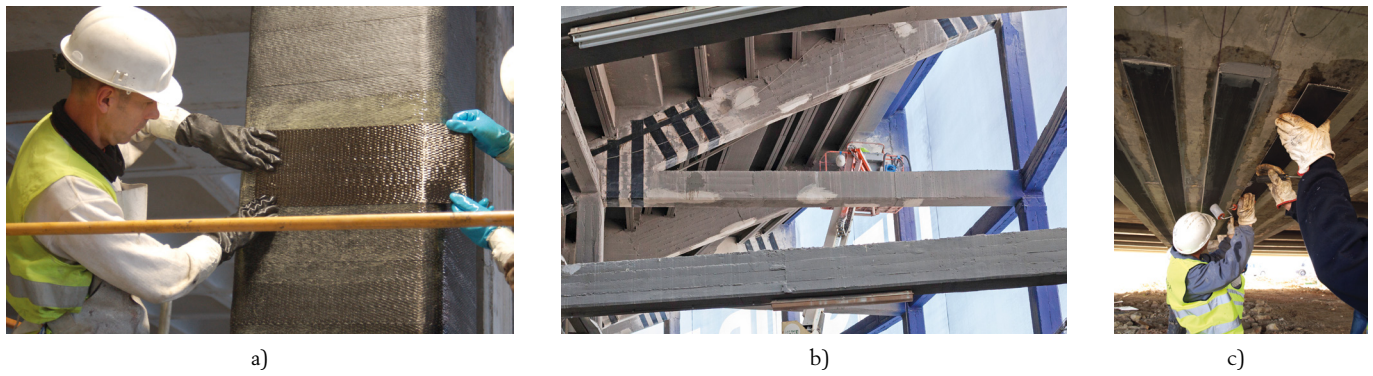


Figure 1. a) Flexural strengthening, b) shear strengthening, c) column confinement (courtesy of Mapei).



Figure 2. a) Externally bonded reinforcement (courtesy of Mapei), b) Near surface mounted reinforcement [16].

During the 1990's, fibre reinforced polymer (FRP) laminates, which were related to other industries such as aeronautics or sports, were introduced in the construction field to overcome the drawbacks of steel plates bonded to the tensile concrete surface, which were corrosion and weight among others.

FRP is the denomination of a composite material formed by a polymeric matrix reinforced with continuous glass (GFRP), basalt (BFRP), carbon (CFRP) or aramid (AFRP) fibres. Recently, other composites formed by natural fibres or PBO (polyphenylene bezobisoxazole) with a cementitious matrix [2,3] have been introduced in the strengthening field but with limited research applications. The first application of FRP strengthening in Europe was in 1991, in the Ibach bridge (Switzerland), a historic wooden bridge that was strengthened by externally bonded CFRP laminates [4]. Since then, the strengthening technique consisting on adhesively bonding a reinforcement (ABR) of FRP to an existing structure constitutes a well established technology. FRPs have been effectively applied as flexural strengthening, shear strengthening and confinement of columns (see Figure 1). There are many reasons of their increasing use, especially in aggressive environments, since they show a high strength-to-weight and stiffness-to-weight ratio, a potential high durability given by their resistance to corrosion, no need of scaffolding, reduction in labour costs, and versatility with practically unlimited availability of dimensions. However, FRP strengthened systems present also some drawbacks such as their reduced ductility due to their linear elastic behaviour up to failure, possible degradation under high temperatures depending on the glass transition temperature of the resin, and the cost of the material itself.

The future version of Eurocode 2 [1] will include an informative annex (Annex J) with the rules for strengthening existing plain, reinforced and prestressed normal weight concrete structures only with CFRP materials. This annex covers only CFRP materials because it is the most common fibre type in research and real applications. In addition, there is not enough experience in strengthening of special concrete structures, such as lightweight concrete or concrete with recycled aggregates.

Adhesively bonded reinforcement (ABR) gives wider applications for different methods and products. Annex J of Eurocode 2 [1] considers two possible applications: externally bonded reinforcement (EBR) [5–8] and near surface mounted reinforcement (NSM) [9–13]. EBR consists of strips or sheets bonded on the surface of a concrete support (see Figure 2a) and NSM consists of strips or bars applied in slot cuts in the concrete cover (see Figure 2b). Compared to EBR, the NSM technique provides better bond characteristics, the reinforcement can be anchored more easily to prevent debonding and it is more protected against mechanical damage or vandalism. Other strengthening techniques such as Textile Reinforced Mortar (TRM) [14], embedded through the section reinforcement [15] or other bonded configurations are not included in Annex J because there is not a consolidate experience with all of them. In addition, prestressed ABR is not considered for the same reason.

This paper aims to introduce the content of Annex J “Strengthening of Existing Concrete Structures with CFRP” of Eurocode 2 [1]. This is the first time that the design of CFRP strengthening systems has been introduced in European regulations. Model Code 2010 [17] included FRP reinforcement in two sections 5.5 “Non-metallic reinforcement” and 6.2 “Bond

of non-metallic reinforcement”, explaining the main principles of this technique. There are also some European guidelines such as DAfStb Heft 595 [18], TR-55 [19], CNR-DT-200 R1 2013 [20], AFGC [21], SIA [22] and GRECO [23]. The fib Bulletin 14 [24] was published in 2001 and gave detailed guidelines on the use of FRP externally bonded reinforcement, practical execution and quality control, based on the expertise of the members of fib TG9.3 “FRP Reinforcement for concrete structures”. The advance of the state-of-the-art of the last two decades was updated in fib Bulletin 90 [16] by fib TG5.1 (former TG9.3) in 2019. This document aimed to cover both externally bonded and near-surface mounted reinforcement for concrete structures. It was presented in a Eurocode-compatible format, with the objective of being also a background document for Annex J and to form the basis for the updating of the text on seismic retrofitting with composites in the next version of Eurocode 8. In addition, there is a background document of Annex J [25] with more details about the derivation of the formulations included in this paper.

2. BASIS OF DESIGN, MATERIALS AND DURABILITY

In general, the basis of design of concrete structures with conventional materials can be applied to reinforced (RC) and prestressed concrete (PC) strengthened with adhesively bonded CFRP reinforcement. However, there are some aspects such as the material safety factors that should be particularized for this case. Unless a National Annex gives different values, Table 1 complies the partial safety factors for ABR. As observed, safety factors are higher for in-situ wet lay-up sheets than for prefabricated strips and bars. These safety factors were obtained based on the regulations of prEN 1990:2020 [26] and the products considered in the determination of these factors were those used in the structural tests used in the calibration of approaches included in the subsections of Annex J related to Ultimate Limit States, Serviceability Limit States, Fatigue and Bond. The safety concept for bond is based on design assisted by testing. The safety factor for bond, γ_{BA} , was taken from [16], assuming failure in the concrete substrate or failure of the adhesive. This factor is the one specified in the main text of Eurocode 2 [1] for the design value of the ultimate bond stress.

TABLE 1. Partial safety factors for ABR strengthening [1].

Design situation	Tensile strength		Bond strength
	CFRP strips and bars	In-situ lay-up CF sheets	Failure in concrete or adhesive
Designation	γ_f		γ_{BA}
Persistent and transient	1.30	1.40	1.50
Accidental	1.10	1.15	1.15
Serviceability	1.00	1.00	1.00
Fatigue	1.30	1.40	1.50

In relation to the materials employed for strengthening, there is a different particularity in comparison with other construc-

tion materials. The system is made by the combination of fibres and a matrix, designed to work together, and with a specific binder applied to the surface of the support [16]. Therefore, only systems that have been tested and applied to real scale structures can be applied as ABR. In addition, the selection of the system type depends on the configuration and on the structure to be strengthened. A general description on FRP materials, systems and techniques can be found in fib Bulletin 90 [16]. The material properties should be given by the suppliers. The FRP strengthening systems shall comply with national or international product standards, such as ISO 10406 [27] that specify their geometrical, mechanical and technological properties. Annex J gives recommended values of some parameters where test procedures are not standardized yet.

Test procedures for the essential characteristics of construction products at European level, may be included in two types of technical specifications: European harmonised product standards or European Assessment Documents (EAD). EADs are currently under preparation for CFRP strengthening systems.

The design rules included in Annex J are for CFRP systems that accomplish the following conditions:

- interlaminar shear strength of CFRP strips according to EN ISO 14130 [28] shall be equal or larger than the adhesive bond strength for any system,
- mean modulus of elasticity of CFRP strips: $150\,000\text{ MPa} \leq E_f \leq 250\,000\text{ MPa}$,
- elastic stiffness per unit width of carbon fibre (CF) sheets: $20\text{ kN/mm} \leq E_f A_f/b_f \leq 400\text{ kN/mm}$,
- total CF cross section per unit width of CF sheets in the total of all layers determined in the direction of the tension action effect applied to the system: $100\text{ mm}^2/\text{m} \leq A_f/b_f \leq 1800\text{ mm}^2/\text{m}$.
- characteristic tensile strength of the adhesive f_{Atk} , determined in accordance with EN 1504-4 [29] shall be $f_{Atk} \geq 14\text{ N/mm}^2$.

Annex J requires the definition of the following properties for CFRP strips and sheets that are going to be used as ABR strengthening systems: f_{fuk} , characteristic short-term tensile strength of the ABR according to ISO 10406 [27]; η_f , reduction factor applied to the tensile strength; E_f , average mean modulus of elasticity of the ABR in the longitudinal direction; ε_{fuk} , characteristic ultimate strain; and A_f , cross sectional area. For strips A_f is taken as $b_f \cdot t_f$ (where b_f is the width and t_f is the thickness of the cross section). For sheets, A_f is obtained from relevant production data, considering $t_f = n_f^{k_f} A_f/b_f$ being n_f the number of layers, A_f/b_f the cross sectional area of the fibres per meter of a single layer of CF sheet, and $k_f = 0.85$ if the number of layers is higher than 3, or 1.00 otherwise. For the adhesive, Annex J requires the characteristic compressive strength, f_{Ack} , and the characteristic tensile strength, f_{Atk} , determined in accordance with EN 1504-4 [29].

FRP materials are linear elastic up to failure, as shown in the design stress-strain relationship in Figure 3.

The design tensile strength of the ABR system shall be obtained as:

$$f_{fud} = \frac{\eta_f f_{fuk}}{\gamma_f} \quad (1)$$

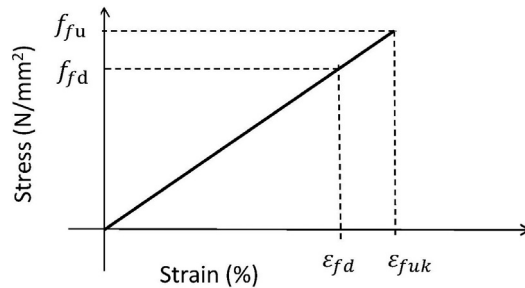


Figure 3. Design stress-strain relationship for the CFRP strengthening system [16].

where: f_{fuk} is the characteristic tensile strength, γ_f is the partial safety factor, and η_f is a reduction factor applied to the tensile strength of the ABR for the relevant exposure conditions in accordance with ISO 10406 [27], and may be taken as 0.7 unless more accurate information is available.

In a similar manner to conventional RC and PC structures, durability of the strengthened structure, and in particular of the CFRP system and adhesive should be ensured during lifetime according to the exposure classes. The FRP-concrete interface is the critical component of the system since the transfer of stresses occurs through it, and bond quality is affected by the environmental conditions. Therefore, additional protective measures should be included to ensure durability if necessary.

Special attention should be paid to the exposure of the strengthened element to direct UV radiation, penetration of moisture and temperature.

3. STRUCTURAL ANALYSIS

According to Annex J, members strengthened with ABR should not be analysed using linear elastic analysis with limited redistribution or plastic analysis, since the CFRP systems are linear elastic up to failure.

The glass transition temperature usually ranges from 50 to 80°C for epoxy and for processed FRP elements ranges from 130 to 140°C. This means that in the event of fire, protection systems may be required in such a way that service temperature is limited with respect to the glass transition temperature. During fire, the CFRP strengthening system will be lost due to the weakening of the adhesive. If this is the case, the existing structure should bear this accidental design situation without collapse, complying with the robustness requirement. This is similar to other accidental situations such as vandalism, blast or impact, where the design engineer should verify the structure against accidental loss of FRP.

4. ULTIMATE LIMIT STATES

4.1. Bending with and without axial forces

When strengthening in flexure RC or PC sections, the design of the required ABR area can be obtained by applying sec-

tional equilibrium and compatibility conditions, in a similar manner than conventional concrete elements but with an additional reinforcement, assuming that the slip between the CFRP reinforcement and the concrete substrate is neglected, that is, full composite action between the CFRP and the substrate. The strain state of the unstrengthened element before strengthening should be considered since the strains from additional bending effects after strengthened should be superimposed to the existing ones when verifying the capacity of the strengthened element. Fib bulletin 90 [16] recommends the process given by the flow chart of Figure 4.

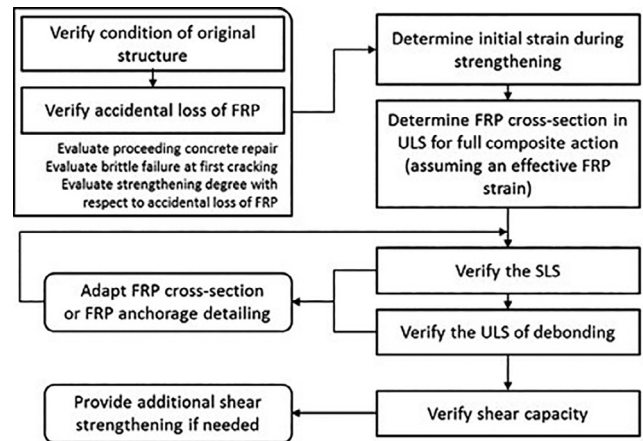


Figure 4. Design process when strengthening a section in flexure recommended by fib Bulletin 90 [16].

When designing the CFRP strengthening system, it is desirable that the strengthened element fails in a ductile manner after steel yielding. So, the governing modes of failure of a flexural element will be steel yielding followed by concrete crushing or steel yielding followed by FRP rupture. As observed in many experimental programs, debonding of the CFRP strengthening system might occur before reaching a classical failure mode (see Figure 5). Debonding is more common in externally bonded reinforcement and might initiate at any location different from the critical section considered to design the flexural strengthening system. To avoid this type of premature failure, debonding should be checked following the procedure described in Section 7 of this paper.

Usually, the reason for strengthening is motivated by strength increase to comply with ULS requirements. However, sometimes the serviceability limit state governs the design,

and larger amounts of CFRP than those required for ULS should be applied.

Provisions of Annex J for flexural strengthening with and without axial forces for both EBR and NSM are in accordance with fib Bulletin 90 [16].



Figure 5. Debonding of the CFRP strengthening system [30].

4.2. Confinement

It is well known that confinement can enhance the load bearing capacity of axial loaded members.

Concrete confined by FRP behaves differently from concrete confined by steel. Due to the linear elastic behaviour up to failure, FRP apply an ever-increasing confinement pressure to the concrete core. The stress–strain behaviour of FRP-confined concrete typically displays an approximately bilinear ascending response, and ultimate capacity is governed by tensile failure of the FRP (Figure 6). The ultimate strength of the confined concrete is closely related with the rupture strain of the FRP reinforcement. Many experimental studies have shown that the rupture strain values of FRP jackets are consistently lower than the ultimate tensile strain obtained by standard tensile testing of FRP coupons [31,32]. The ratio between the two values is called strain efficiency factor. There are a number of possible reasons for this premature failure of the FRP jacket, such as the multiaxial stress state, stress concentrations due to concrete failure, or the jacket curvature, especially at corners with low radius.



Figure 6. Failure mode of FRP confined concrete.

Current international design guidelines provide predictive design equations to calculate the ultimate strength and strain of FRP confined concrete columns subjected to pure axial load, as a function of the confining pressure applied by the FRP jacket. It is known that the confinement of non-circular columns is less efficient than the confinement of circular columns [33–35] (see Figure 7a). In a circular cross section, the jacket exerts a uniform confining pressure over the entire perimeter. In the case of a rectangular cross section, the confining action is mostly concentrated at the corners. The predictive equations found in the design guides are mostly based on approaches deduced for circular columns and then modified by a shape factor, usually defined as the ratio of the effectively confined area to the gross area.

Annex J gives provisions to consider the effect of concrete confinement achieved by bonding hoop CFRP around existing columns (see Figure 7b and 7c). Since the formulations have an empirical basis, Annex J limits them to columns with a diameter greater than 150 mm and with characteristic concrete strength less than 50 MPa. Experimental studies outside this range are scarce and show that the effect of confinement is very limited in high strength concrete.

In addition, the first-order eccentricity of the axial load must meet the condition $e_0 / D_{eq} \leq 0.20$ and the slenderness satisfy the condition $l_0 / D_{eq} \leq 40$.

For the application of the equations given in Annex J to rectangular sections the rounding radius of the corners must be $r_c \geq 20$ mm and the aspect ratio $h / b \leq 2$.

According to Annex J, the increase in compressive strength of concrete due to CFRP confinement can be calculated as follows:

For circular columns:

$$\Delta f_{cd} = 0 \quad \text{for} \quad \frac{t_f f_{tud}}{D f_{cd}} < 0.07 \quad (2)$$

$$\Delta f_{cd} = k_{cc} \frac{t_f}{D} f_{tud} \quad \text{for} \quad \frac{t_f f_{tud}}{D f_{cd}} \geq 0.07 \quad (3)$$

with $k_{cc} = 2.5$ unless more accurate information is available.

In the case of discontinuous and/or helical wrapping the value of f_{tud} in equations (2) and (3) should be multiplied by the efficiency factor k_h (see Figure 7b and 7c):

$$k_h = \left(1 - \frac{(s_f - b_f)}{2D} \right)^2 \left(\frac{1}{1 + (\tan \beta_f)^2} \right) \quad (4)$$

For rectangular columns:

$$\Delta f_{cd} = 0 \quad \text{for} \quad \left(\frac{b}{h} \right)^2 k_e \frac{t_f k_r f_{tud}}{D_{eq} f_{cd}} < 0.07 \quad (5)$$

$$\Delta f_{cd} = k_{cc} \left(\frac{b}{h} \right)^2 k_e \frac{t_f}{D_{eq}} k_r f_{tud} \quad \text{for} \quad \left(\frac{b}{h} \right)^2 k_e \frac{t_f k_r f_{tud}}{D_{eq} f_{cd}} \geq 0.07 \quad (6)$$

where:

$k_{cc} = 1.5$ unless more accurate information is available.

$$D_{eq} = \frac{2bh}{b+h} \quad (7)$$

$$k_e = 1 - \frac{(b-2r_c)^2 + (h-2r_c)^2}{3bh} \quad (8)$$

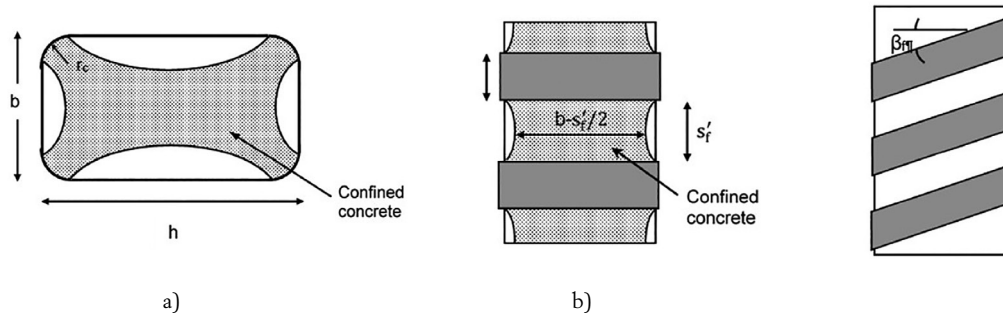


Figure 7. a) Effectively confined section in a rectangular section; b) confinement with discrete strips and c) with helically bonded strips, adapted from [16].

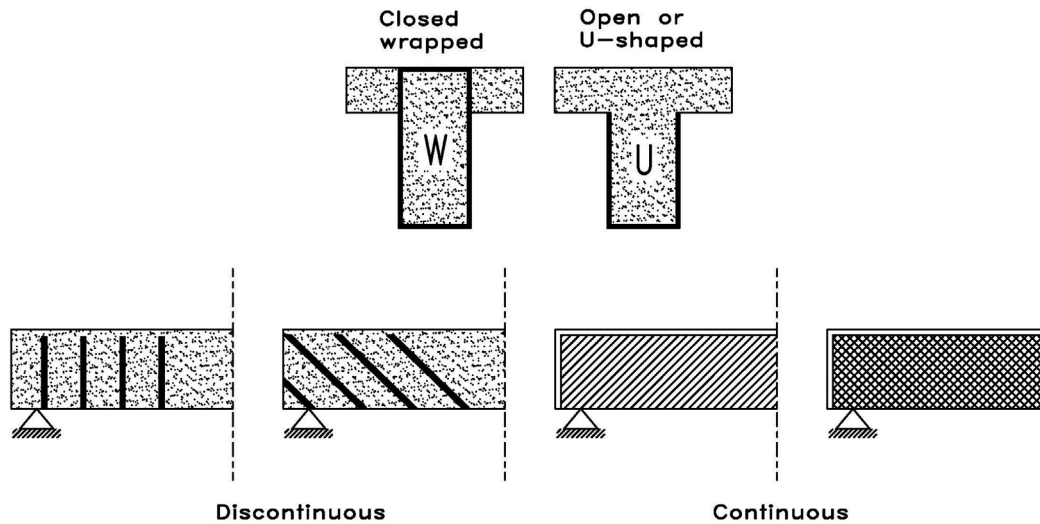


Figure 8. Shear strengthening configurations.

$$k_r = \begin{cases} 1.0 \left(\frac{r_c}{50} \right) \left(2 - \frac{r_c}{50} \right) & \text{for } r_c \leq 50 \text{ mm} \\ 1.0 & \text{for } r_c \geq 50 \text{ mm} \end{cases} \quad (9)$$

k_e is the ratio between effectively confined area and gross area (see Figure 7a).

k_r is a reduction factor that takes into account that, for rectangular sections, the smaller the corner radius the lower the rupture strain of the FRP jacket.

For discontinuous and/or helical wrapping on rectangular columns the value of f_{jud} in equations (5) and (6) should be multiplied by k_h according to (10):

$$k_h = \left(1 - \frac{(s_f - b_j)}{2b} \right) \left(1 - \frac{(s_f - b_j)}{2h} \right) \left(\frac{1}{1 + (\tan \beta_j)^2} \right) \quad (10)$$

The above equations largely align with the provisions of *fib* bulletin 90 [16]. Equations (3) and (6) implicitly include a strain efficiency factor equal to 0.5, in accordance with [16], for circular and square or rectangular sections with a corner radius $r_c \geq 50$ mm.

However, while in [16] the factor k_{cc} is 3.3, according to the original model of Lam and Teng [32], Annex J indicates that the value of k_{cc} can be taken as 2.5 for circular columns and 1.5 for square and rectangular columns unless more accurate information is available.

4.3. Shear

In a RC or PC element, the shear strength should be checked by following the general provisions of §8.2 of new Eurocode 2 [1], without considering the flexural CFRP ABR (if this is the case) in the contribution of the longitudinal reinforcement. If the design shear stress is higher than the shear strength, then shear strengthening is required, and the section can be strengthened by EBR or NSM techniques.

Externally bonded CFRP shear strengthening can be performed in two different configurations (see Figure 8): a) sheets fully wrapping the section (closed wrapped); b) sheets or L-shaped strips bonded on the lateral sides and the bottom surface of the beam (open or U-shaped systems). The side-bonded configuration, which consists of bonding sheets or strips in the lateral faces of the section is not allowed since they are prompt to debond at both sides of the critical shear crack once it opens and widens. The sheets and strips can be bonded in a continuous or discontinuous configuration.

Closed wrapped CFRP configurations fail due to fibre rupture, sometimes initiated near the corner of the sections that have been rounded to avoid sharp zones that may lead to fibre rupture. Open or U-shaped configurations are susceptible of debonding once a critical shear crack opens and propagates. Then, if the bonded length of each strip at the upper side of the crack (for the U-shaped) is not long enough to anchor the tensile force of the FRP, the laminate debonds suddenly

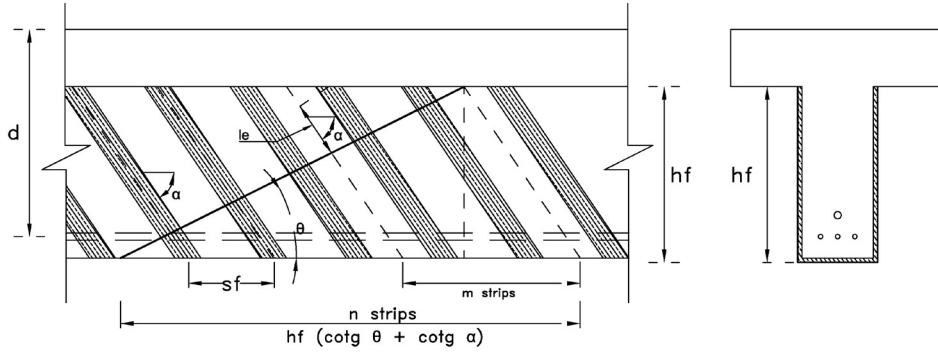


Figure 9. n and m parameters in a CFRP shear-strengthened beam [1].

before reaching its ultimate tensile strength. This debonding failure mode should be considered in the calculation of the shear capacity of the strengthened element and can be delayed or can be avoided by using appropriate anchorage devices. Annex J recommends the application of anchorage devices when strengthening T-shaped cross sections.

The total shear strength of a section strengthened with CFRP may be taken as:

$$\tau_{Rd,CFRP} = \tau_{Rd} + \tau_{Rd,f} \leq 0.5 v f_{cd} \quad (11)$$

where:

τ_{Rd} is the design shear strength according to Section 8.2 of Eurocode 2 [1].

$$\tau_{Rd,f} = \frac{A_f}{s_f} \frac{f_{wd}}{b_w} (\cot\theta + \cot\alpha_f) \sin\alpha_f \quad (12)$$

$$\frac{A_f}{s_f} = \begin{cases} \frac{2t_f b_f}{s_f} & \text{for discrete CFRP strips or CF sheets} \\ 2t_f \sin\alpha_f & \text{for continuous CF sheets} \end{cases} \quad (13)$$

α_f is the angle formed between the CFRP system and the longitudinal member axis;

f_{wd} is the design shear strength of the CFRP system.

θ should be taken as 45 degrees for the calculation of τ_{Rd} and $\tau_{Rd,f}$ unless more rigorous analysis is undertaken.

Formulations to assess the contribution of the CFRP strip or sheet to the total shear strength consider the different type of configurations. For closed CFRP systems, the design shear strength is defined as Equation (14).

$$f_{wd} = 0.8 k_r f_{ud} \quad (14)$$

Where:

f_{ud} should be determined using Equation (1) and k_r should be determined using Equation (9).

For open discrete CFRP systems, debonding should be taken in consideration and the shear strength can be obtained through Equation (15) and (16), depending on the length of the strip above the critical shear crack and the maximum bond length, $l_{bf,max,k}$. In any case, the shear strength f_{wd} is limited by Equation (14).

f_{wd} is determined by Equation (15) if the anchorage length into the compression zone of the member of all CFRP strips, l_{bf} is less than $l_{bf,max,k}$.

$$f_{wd} = \frac{2}{3} \frac{n s_f}{l_{bf,max,k} [(\cot\theta + \cot\alpha_f) \sin\alpha_f]} f_{bfRd} \quad (15)$$

f_{wd} is determined by Equation (16) if the anchorage length into the compression zone of the member of some CFRP strips, l_{bf} is less than $l_{bf,max,k}$.

$$f_{wd} = \left[1 - \left(1 - \frac{2}{3} \frac{n s_f}{l_{bf,max,k} [(\cot\theta + \cot\alpha_f) \sin\alpha_f]} \right) \frac{m}{n} \right] f_{bfRd} \quad (16)$$

where the parameters m and n are defined in Equation (17) and (18), and in Figure 9. The maximum bond length $l_{bf,max,k}$ and the anchorage resistance f_{bfRd} shall be determined according to §8 of this paper.

$$n = \text{integer} \left(\frac{h_f (\cot\theta + \cot\alpha_f)}{s_f} \right) \quad (17)$$

$$m = \text{integer} \left(\frac{l_{bf,max,k} (\cot\theta + \cot\alpha_f) \sin\alpha_f}{s_f} \right) \quad (18)$$

The open continuous sheet system can be treated as a particular case of the discontinuous case with $s_f = b_f / \sin\alpha_f$. Then, $n s_f = h_f (\cot\theta + \cot\alpha_f)$, $m s_f = l_{bf,max,k} (\cot\theta + \cot\alpha_f) \sin\alpha_f$ and $m/n = l_{bf,max,k} \sin\alpha_f / h_f$ [16].

D'Antino and Triantafillou [36] performed an assessment of five design guidelines (EN 1998-3 [37], ACI 440.2 R-08 [38], DAfStb Heft 595 [18], TR-55 [19], CNR-DT/200-R1.2013 [20]) and a new proposed model, based on the German guideline [18], which is very similar to the proposal included in Annex J. The assessment was performed with a database of 229 RC shear - strengthened beams that failed in shear. They concluded that all models tend to underestimate the FRP shear strength for the completely wrapped configuration. However, models were more accurate for the U-shaped configuration. The proposal gave conservative results (mean value of the experimental to theoretical ratio $MV=1.77$ and coefficient of variation $COV=2.21$ for U-shaped and $MV=3.51$ and $COV=4.32$ for wrapped).

In the framework of TG1, Oller and Kotynia presented in [39] an analysis of the performance of different existing

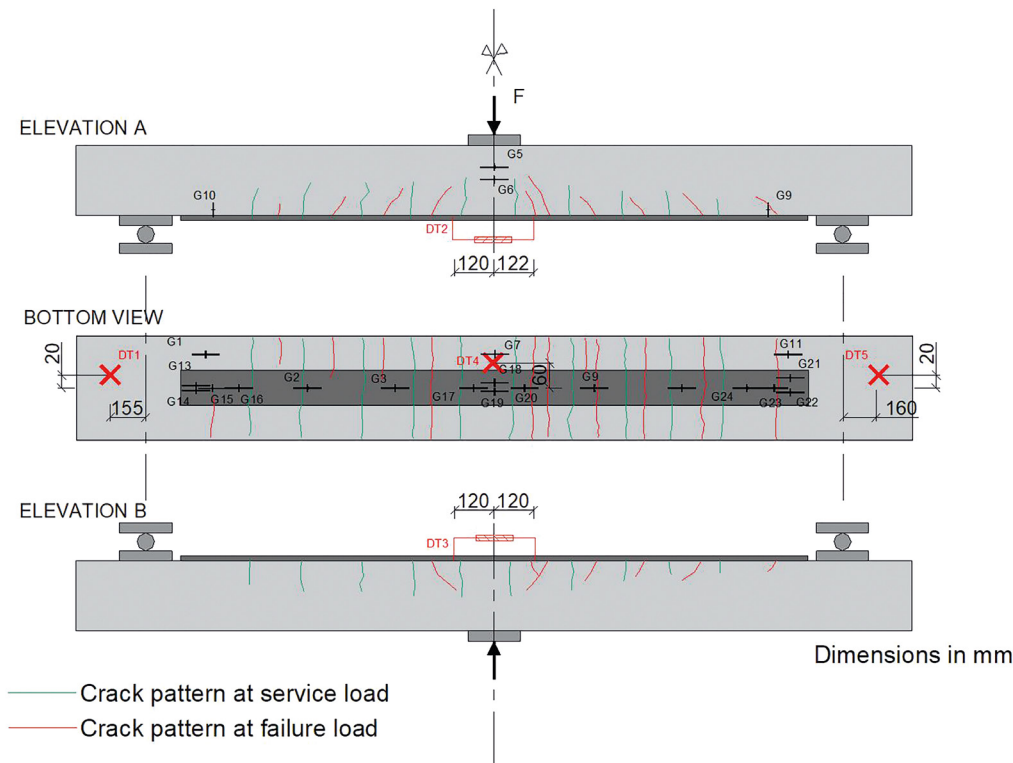


Figure 10. Example of cracking pattern after strengthening [30].

formulations to quantify the FRP contribution to the shear strength of RC elements strengthened in shear by externally bonded FRP sheets [16,18–20,24,40–48]. A large database of 555 tests (355 with rectangular section and 200 with T-section) has been assembled distinguishing between the shape of the section, the existence of internal transverse reinforcement and the FRP configurations. Selected beams with a/d higher than 2.5, that were well-documented, and which had a rectangular (276) or a T (180) cross-section, were externally strengthened in a closed (71 R + 68 T), open (114 R + 98 T) or side bonded (91 R + 14 T) configuration with FRP wet lay-up or pultruded strips in a continuous or discontinuous manner, and with or without internal transverse steel reinforcement. In general, predictions for all models were more conservative for beams without transverse reinforcement. In some cases, predictions were unsafe for beams with transverse reinforcement, showing a possible interaction with the internal transverse reinforcement which is not considered in the experimental FRP contribution to the shear strength.

For closed FRP configurations, models generally assumed failure at the bottom corner of the section and predictions were very conservative where failure was experimentally observed along the web. This is the case of the formulation included in Annex J, with a mean value of the experimental to the theoretical ultimate shear force ranging between 1.21 and 2.91 for beams without transverse reinforcement and coefficient of variation (COV) ranging from 38 to 49%. For beams with rectangular section with internal stirrups and continuous CFRP configuration, the mean value is less conservative than for the remaining cases, 0.83 with a similar COV. For open configurations, results depended mainly on the assumed bond model and are more accurate than in the previous case, showing for

some models unsafe predictions for the continuous FRP system applied in beams with transverse reinforcement. This is the case of the formulation of Annex J, where $MV = 0.85$ and 0.53 for rectangular beams with internal stirrups and with a discontinuous and continuous CFRP configuration, respectively.

According to fib Bulletin 90 [16], the contribution of anchored NSM reinforcement to the shear capacity of the element can be approximately computed with the same model of EBR.

4.4. Torsion, Punching and Design with strut-and-tie models

Annex J doesn't give provisions for CFRP strengthening in torsion or in punching-shear. There is not enough data in the literature to include provisions related to both torsion and punching-shear.

5. SERVICEABILITY LIMIT STATES

The verification of serviceability limit states (SLS) considers the limitation of stresses to avoid steel yielding, damage or excessive creep of concrete, adhesives or FRP, or creep rupture of FRP, limitation of cracking and deflections. In some cases, SLS governs the design of the strengthening system, even the main purpose was the strength increase. The previous state of stresses and deflections should be considered in the verification of the SLS.

Under service load conditions, stresses in the concrete and in the longitudinal reinforcement of the strengthened struc-

ture are limited according to the main text of Eurocode. As a result of the limitations of the longitudinal tensile steel reinforcement stresses, the stress in the FRP should be limited due to compatibility reasons. Therefore, under the characteristic combination of loading, the stress in the EBR or NSM CFRP reinforcement should be limited to:

$$\sigma_f \leq 0.8 f_{yk} \frac{E_f}{E_s} \quad (19)$$

In relation to cracking, it has been observed experimentally that the presence of the CFRP strengthened systems induces the appearance of new cracks in between the existing ones due to the additional tensile stress transfer from the CFRP system to the concrete (see Figure 10). These new cracks usually show smaller crack widths and might be less conditioning than for the unstrengthened element.

The strengthened element should fulfil the deflection limitations given by the main text of Eurocode 2 [1]. Deflections of beams or slabs strengthened with ABR may be estimated by ignoring the slip between the CFRP and concrete and transforming the area of CFRP to steel by taking account of the modular ratio, as considered in Annex J [1]. Deflections can be obtained for instance, by the double integration of the curvature, determined by a cross-section analysis along the RC element. In relation to long-term effects, they can be considered by considering the quasi-permanent load combinations and the modular ratios that consider the creep coefficient. However, there are limited existing studies about the long-term behaviour of concrete elements strengthened with FRP [49–51].

6. FATIGUE

Fatigue damage is not significant if the strengthened structure is exposed to typical service load ranges, but damage can occur if the load range exceeds 60% of load at first yield [52]. For this reason, special care should be taken in consideration, if the increase of service loading in the strengthened structures is significantly high. According to fib Bulletin 90 [16], in such cases under fatigue loading, failure occurs due to fracture of the longitudinal tensile reinforcement. Despite that FRP has an excellent fatigue strength, fatigue of bond should be considered since the loss of bond may lead to higher stresses in the longitudinal reinforcement with increased number of cycles.

6.1. Fatigue of externally bonded reinforcement (EBR) systems

For EBR, Annex J presents a basic and a refined analysis for fatigue analysis for EBR CFRP systems, which is based on [18]. The basic analysis verifies that no damage due to cycling loading occurs, by limiting the increment of CFRP tensile forces in between cracks or at the laminate end to the elastic zone of the bond stress-slip relationship. Fatigue checking for EBR may be omitted if Equation (20) is accomplished. If this is the case, the upper load is limited by the load associated

to the maximum bond stress. Then, strains are in the elastic range and no damage occurs.

$$\Delta F_{fE, equ} \leq \Delta F_{fRd, fat1} = 0.35 f_{ctm, surf}^{1/4} f_{bRd} b_f t_f \quad (20)$$

where:

$$\Delta F_{fE, equ} = \max \{ b_f t_f \Delta f_{fEd, max}; F_{fEd, cr} \} \quad (21)$$

f_{bRd} is the limiting design strength of the bond in the area being considered, calculated according Equation (33).

$f_{ctm, surf}$ is the mean value of the tensile strength at the surface that can be determined by testing or estimated by Equation (31).

$\Delta f_{fEd, max}$ is the maximum difference in CFRP stress under the relevant load combination between cracks given by Equation (39).

$F_{fEd, cr}$ is the force in the CFRP at the first crack of the strengthened area.

If Equation (20) is not accomplished, the refined analysis should be performed. In the refined analysis, the fatigue range S is used to obtain the tolerable number of cycles based on the $S-N$ curve. As explained in [25], the refined analysis uses the $S-N$ curve determined by some experimental data [53–58]. The number of load cycles needed for reaching a debonded length of 30 mm are calculated from the experimental programs of [53,54,57,58] by linear interpolation using the bond length and the number of cycles until completely debonding. For fitting the curve $S-N$, the unified related load ranges $S_{o,i}$, at a lower load level of 0, and the corresponding number of cycles N_{30} is needed. $S_{o,i}$ is determined in a projection analysis using the Goodman relation. S_o is the difference between the maximum and minimum load related to the monotonic quasi-static load carrying capacity of the interface. The curve $S-N$ has been obtained fitted to the experimental data.

Under the frequent combination, the following condition, Equation (22), should be checked:

$$\Delta F_{fEd, fat} \leq \Delta F_{fRd, fat2} = \alpha_{fat2} \frac{\Delta F_{fk, B}}{\gamma_{BA}} \quad (22)$$

where:

$\Delta F_{fEd, fat}$ is the design force range due to forces at the crack edge, $\Delta f_{f, max} - \Delta f_{f, min}$

$\Delta f_{f, min}$ is the minimum value of $b_f \cdot t_f \cdot \Delta f_{fEd}$ under the relevant fatigue load combination specified in Clause 10.2 of the main text of Eurocode 2 [1].

$\Delta f_{f, max}$ is the maximum value of $b_f \cdot t_f \cdot \Delta f_{fEd}$ under the relevant fatigue load combination specified in Clause 10.2 of the main text of Eurocode 2 [1].

$\Delta f_{fk, B} = b_f t_f \Delta f_{fEd}$ where $\Delta f_{fk, B}$ is calculated according Equation (44).

$$\alpha_{fat2} = -c_{fat} \frac{\Delta F_{f, max}}{\Delta F_{fRd}} + c_{fat} \quad (23)$$

$$\alpha_{fat} = 0.35 \left(\frac{N^*}{2 \cdot 10^6} \right)^{-\frac{1}{k_3}} \quad (24)$$

N^* is the number of stress cycles.

$$k_{f3} = \begin{cases} 23.2 & \text{for } N^* > 2 \cdot 10^6 \\ 23.2 & \text{for } N^* \leq 2 \cdot 10^6 \end{cases} \quad (25)$$

6.2. Fatigue of near surface mounted reinforcement (NSM) CFRP strips

In relation to fatigue of near surface mounted reinforcement, there is a low number of available tests (see [59]). Therefore, it is not possible to specify an S-N curve for this case, and then it is not possible to extrapolate the number of load cycles higher than that given in the tests results, which is $2 \cdot 10^6$ cycles. Annex J states that near surface mounted strips are adequate for fatigue under the frequent load combination given in Clause 10 of the main text, if the following conditions are accomplished:

- 1) The number of stress cycles is less than $2 \cdot 10^6$.
- 2) The maximum force in the NSM CFRP system, considering also the shift of the tension envelope into account does not exceed $F_{f,NSM,max}$ given by Equation (26).

$$F_{f,NSM,max} = 0.6 f_{bjRd} b_f t_f \quad (26)$$

- 3) The strip stress range $\Delta\sigma_f$ accomplishes the condition given by Equation (27).

$$\Delta\sigma_f = \frac{\Delta F_{f,max} - \Delta F_{f,min}}{b_f t_f} \leq \frac{500}{t_f} \quad (27)$$

7. BOND AND ANCHORAGE OF ADHESIVELY BONDED CFRP SYSTEMS

7.1. Anchorage of externally bonded reinforcement (EBR)

The existing experimental research in beams externally strengthened by plate bonding has commonly shown the

appearance of premature failures due to loss of bond that involve the laminate debonding before reaching the design failure load (Figure 5). As mentioned in Oller *et al.* [60, 61], this debonding failure mode was observed in 375 well-documented FRP flexural strengthened beams without external anchorages assembled in a database. Bond failure implies the complete loss of bond between reinforcement and concrete substrate. Debonding can occur through the FRP, the adhesive, or the concrete cover, or in the FRP-adhesive or adhesive-concrete interfaces. The most common case is debonding along the concrete surface which is the weakest material in tension.

In flexural strengthening, laminate debonding can initiate at an intermediate section along the span at flexural or flexural-shear cracks along the span (intermediate crack IC debonding) or at the laminate end (end debonding) (see Figure 11). Even though both initiation points are critical for design or verification purposes, tests results compiled in the database of Oller [30] have shown that IC debonding is more common (70% of specimens) than end debonding (30% of specimens). For IC debonding, the laminate detachment involves a thin layer of the concrete due to the predominance of bond stresses and propagates towards the laminate end. A shear induced crack separation can also be observed due to the movement of the crack edges produced by the shear force. This latter case, will be treated separately even it initiates along the span length. In relation to end debonding, two types of failures can be observed according to *fib* Bulletin 90 [16]. The first one, named interfacial debonding at the anchorage zone, is related to the combination of bond and normal stresses at the laminate end, and usually involves the concrete layer adjacent to the adhesive interface and propagates from the laminate end to midspan. The second one is related to the shear deficiency of the RC element and is named end cover separation. This failure involves the ripping-off of the concrete cover along the longitudinal tensile reinforcement. Both failure modes can be avoided by providing end anchoring devices or shear strengthening in the second case.

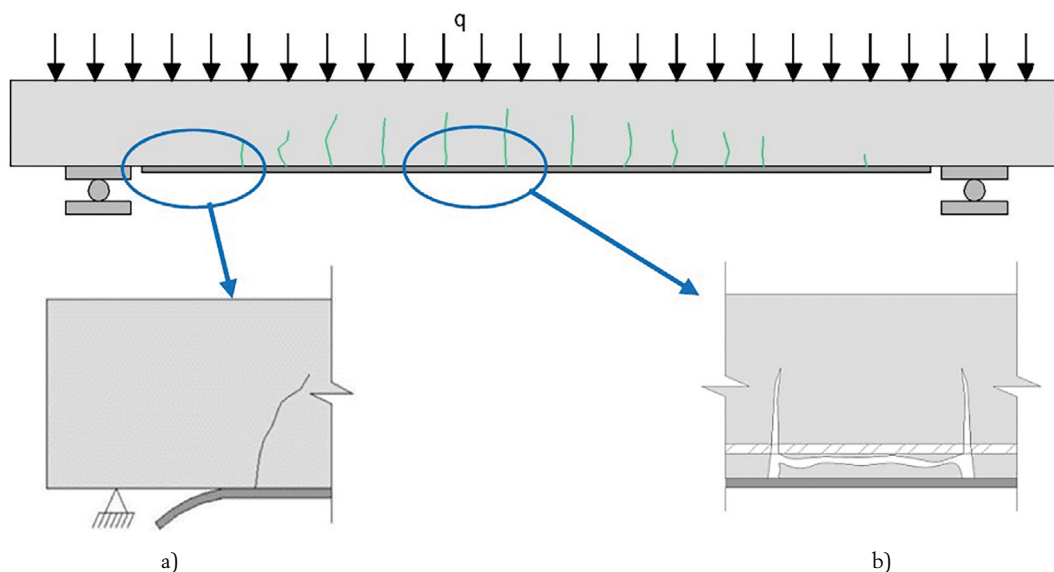


Figure 11. Debonding failure modes: a) end debonding, b) intermediate crack debonding.

For bond verifications, two areas will be distinguished: the end anchorage zone and the remaining length of the element. At the anchorage zone, the force of the CFRP at the outermost bending crack should be anchored along the length from this point to the CFRP laminate end. This element can be assumed as a pure shear specimen. In addition, end cover separation should also be checked. In the remaining beam length, intermediate crack debonding should be checked in between each pair of subsequent cracks. For each intermediate crack element, the increment of tensile forces in the CFRP laminate between both crack tips should be transferred by bond to the structural element.

The behaviour of a bonded joint can be described through the governing equations obtained from equilibrium and compatibility assuming a bond-slip relationship as the constitutive behaviour of the interface, which in this case can be assumed as a bilinear law (see Figure 12) defined by Equation (28).

$$\tau_f(s_f) = \begin{cases} \left(1 - \frac{s_f}{s_{f0}}\right) \tau_{f1} & \text{where } s_f < s_{f0} \\ 0 & \text{where } s_f \geq s_{f0} \end{cases} \quad (28)$$

where:

τ_{f1} is the maximum bond stress. The characteristic value, τ_{f1k} , is given by Equation (29).

$$\tau_{f1k} = 0.37 k_{sys,b1} (f_{cm} f_{ctm,surf})^{0.5} \quad (29)$$

s_{f1} is the slip associated to the maximum bond stress.

s_{f0} is the ultimate slip. The characteristic value, s_{f0k} , is given by Equation (30).

$$s_{f0k} = 0.2 k_{sys,b2} \quad (30)$$

$k_{sys,b1}$ is a constant that can be taken as 1.0 unless more accurate information is available based on production data of the EBR system.

$k_{sys,b2}$ is a constant that can be taken as 1.0 unless more accurate information is available based on production data of the EBR system.

f_{cm} is the mean concrete compressive strength.

$f_{ctm,surf}$ is the surface tensile strength of the prepared concrete surface to be bonded. If it cannot be determined, it can be estimated as a function of the position during concreting (top, side or bottom) according Equation (31).

$$f_{ctm,surf} = f_{ctm} \begin{cases} 0.3 + 0.6 \left(\frac{f_{ck}}{60} - 0.2\right) & \text{top} \\ 0.4 + 0.5 \left(\frac{f_{ck}}{60} - 0.2\right) & \text{side} \\ 0.6 + 0.3 \left(\frac{f_{ck}}{60} - 0.2\right) & \text{bottom} \end{cases} \quad (31)$$

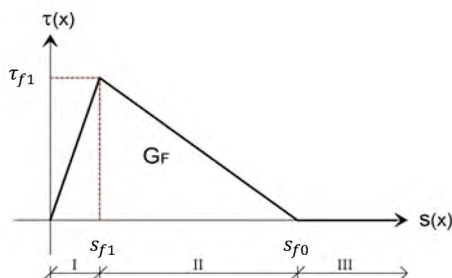


Figure 12. Bilinear bond-slip relationship for the interface.

7.1.1. End anchorage

Annex J presents two methods to check end debonding: a refined method and a simplified method. Both methodologies are based on the bilinear bond-slip law given in Figure 12.

a) Refined method

For the simplified bond-slip relationship, the tensile stress σ_f that can be anchored at the single crack may be determined as a function of the bond length $x = l_{bf}$ (see Equation 32).

$$f_{bf}(l_{bf}) = \sqrt{\frac{E_f \tau_{f1} - s_{f0}}{\tau_f}} \sin \left(\sqrt{\frac{\tau_{f1}}{E_f \tau_f s_{f0}}} l_{bf} \right) \quad (32)$$

Equation (32) can be replaced by a quadratic parabola as shown by Equation (33) where for design purposes, the characteristic values affected by the partial safety coefficient of bond, γ_{BA} , are used.

$$f_{bf,rd}(l_{bf}) = \sqrt{\frac{\eta_{cc} k_{tc} k_{tt}}{\gamma_{BA}}} f_{bfk,max} \begin{cases} \left(2 - \frac{l_{bf}}{l_{bf,max,k}}\right) & \text{where } l_{bf} < l_{bf,max,k} \\ 1 & \text{where } l_{bf} \geq l_{bf,max,k} \end{cases} \quad (33)$$

The maximum characteristic tensile stress that can be anchored is $f_{bfk,max}$ given by Equation (34).

$$f_{bfk,max} = \sqrt{\frac{E_f \tau_{f1k} - s_{f0k}}{t_f}} \quad (34)$$

Values of η_{cc} , k_{tc} , and k_{tt} are defined in accordance with Section 5.1.6 of [1].

The effective bonded length $l_{bfk,max}$, given by Equation (35), is the bond length beyond which the transfer force remains almost constant and is the minimum length that ensures the transfer of the maximum force or stress between the CFRP laminate and the concrete substrate.

$$l_{bfk,max,k} = \frac{\pi}{2} \sqrt{\frac{E_f \tau_f s_{f0k}}{t_{f1k}}} = \frac{2}{k_{sys,b3}} \sqrt{\frac{E_f \tau_f s_{f0k}}{t_{f1k}}} \quad (35)$$

where:

$k_{sys,b3}$ is a constant that can be taken as 1.0 unless more accurate information is available based on production data of the EBR system.

b) Simplified method

Equation (33) can be simplified with the following definitions of the maximum characteristic tensile stress to be anchored $f_{bfk,max}$ and the effective bonded length $l_{bf,max}$.

$$f_{bfk,max,k} = \frac{0.2}{\gamma_{BA}} \sqrt{\frac{E_f (f_{cm} f_{ctm,surf})^{0.5}}{t_f}} \quad (36)$$

$$l_{bfk,max,k} = 1.5 \sqrt{\frac{E_f t_f}{E_f (f_{cm} f_{ctm,surf})^{0.5}}} \quad (37)$$

The simplified approach was assessed on the basis of a wide experimental database with more than 280 bond tests [62] on concrete elements strengthened with FRP strips or sheets with the following parameters: mean concrete strength, $f_{cm} = 15\text{-}62$ N/mm²; modulus of elasticity of the FRP, $E_f = 82\text{-}400$ GPa; FRP laminate thickness, $t_f = 0.083\text{-}1.6$ mm ; 1-3 layers of sheets, also used in the *fib* Bulletin 90 [16].

In any case, according to [26], the EBR shall be anchored from the section where the existing structure is able to carry the design load forces without any additional strengthening system.

7.1.2. Intermediate crack debonding

To avoid intermediate crack debonding, there are two approaches according to the state-of-the-art and the existing guidelines: a) to limit the maximum CFRP strain or stress [16,20,48,63–65] or b) to limit the increment of the tensile forces for each pair of adjacent cracks [60,61,66–69], which is a more accurate approach based on bond transfer. Annex J is based in the second approach. The formulation presented in this Annex to avoid intermediate crack debonding is based on a refined model included in the DAfStb [18] and in *fib* Bulletin 90 [16] with several simplifications. The mechanical model was developed by Finckh and Zilch [68] and its simplification was developed in [70].

The anchorage capacity between flexural cracks shall be enough to transfer the increment of tensile forces along the crack spacing. Therefore, the design value of the increment of CFRP laminate tensile stresses in between two adjacent cracks, Δf_{fEd} , should be limited to the bond strength in between these two sections, Δf_{fRd} , according to Equation (38), which should not be applied if the strain in the CFRP laminate exceeds 10 mm/m or if it exceeds the ultimate strain.

$$\Delta f_{fEd} \leq \Delta f_{fRd} \quad (38)$$

where:

$$\Delta f_{fEd} = \frac{F_{fEd,b} - F_{fEd,a}}{b_f t_f} \quad (39)$$

being $F_{fEd,a}, F_{fEd,b}$ the tensile forces at two adjacent cracks a and b, respectively.

According to Annex J, Δf_{fEd} and Δf_{fRd} should be calculated using the minimum crack spacing, $s_{cr,min}$, given by Equation (40) unless a more accurate analysis has been performed.

$$s_{cr,min} = 1.5 \frac{M_{cr}}{0.85 h F_{bsm}} \quad (40)$$

where:

M_{cr} is the cracking bending moment of the unstrengthened section according to [1].

F_{bsm} is the bond strength per length of the longitudinal reinforcing steel according to Equation (41).

$$F_{bsm} = \sum_{i=1}^n n_{s_i} \phi_i \pi f_{bsm} \quad (41)$$

$$F_{bsm} = \begin{cases} k_{vb1} 0.43 f_{cm}^{2/3} & \text{for ribbed bars} \\ k_{vb2} 0.28 f_{cm}^{1/2} & \text{for plain bars} \end{cases} \quad (42)$$

k_{vb1} and k_{vb2} are parameters that depend on the bond conditions (for good conditions $k_{vb1}=k_{vb2}=1.0$ and for medium bond conditions, $k_{vb1}=0.7$ and $k_{vb2}=0.5$).

The bond strength between two adjacent cracked sections, Δf_{fRd} , can be obtained from Equation (43). It is constant for each pair of cracks, and considers the effects of bond friction, $\Delta f_{fk,F}$, clamping curvature of the beam, $\Delta f_{fk,C}$, and adhesive bond resistance between cracks, $\Delta f_{fk,B}$.

$$\Delta f_{fRd} = \frac{1}{\gamma_{BA}} \left((\eta_{cc} k_{tc} k_{ti})^{0.5} \Delta f_{fk,B} + \Delta f_{fk,F} + \Delta f_{fk,C} \right) \quad (43)$$

$$\Delta f_{fk,B} = 0.84 k_{sys,b1} \sqrt{f_{cm} f_{ctm,surf}} \frac{s_{cr,min}^{0.5}}{t_f} \quad (44)$$

$$\Delta f_{fk,F} = f_{cm}^{-0.9} \frac{s_{cr,min}^{4/3}}{t_f} \quad (45)$$

$$\Delta f_{fk,C} = \frac{k_h}{h_f} \frac{s_{cr,min}^{0.5}}{t_f} \quad (46)$$

where:

k_h is a parameter equal to 2000 for reinforced concrete (RC) elements and 0 for prestressed concrete (PC) elements

$$h_f = \min\{100 \text{ mm}, h\}$$

η_{cc} , k_{tc} , k_{ti} are defined in accordance with Section 5.1.6 of the main text of [1].

D'Antino and Triantafillou [36] performed an assessment of 11 analytical models for evaluating the effective strain in FRP strengthening systems or the increment of the FRP force along the crack spacing to prevent intermediate crack debonding and the model. The assessment was performed through the results of 154 RC beams collected from the literature. According to [36], the simplified and detailed approaches given by the German DAfStb [18], which is a similar approach to that given by Eurocode 2 [1] provide highly underestimated effective strain values. However, the German models were calibrated for applications of CFRP strips and do not cover other cases with different geometrical or mechanical characteristics of the strengthening system, that were included in the database.

Finckh and Zilch [68] also applied their model, which is the original bases of the model included in DAfStb [18], to a database of 151 bending tests on single-span beams with CFRP strips that belong to a larger database of 473 tests with beams strengthened with CFRP sheets, steel or GFRP plates. Their comparison shows that the model fits very well with average tests values and that in most cases the mean values are not below the characteristic values.

7.1.3. End cover separation

To avoid end cover separation, that is the detachment of the concrete layer beneath the reinforcement near the supports, the maximum design force at the end of the CFRP reinforcement should be lower than the value that generates this premature failure mode (see Equation (47)). The proposal included in Annex J for this limitation is in accordance to DAfStb [18] and has been included in *fib* Bulletin 90 [16].

$$V_{Ed} \leq V_{Rd,cfE} = \left(0.11 + 2.2 \frac{(100 \rho_l)^{0.15}}{\alpha_{fE}^{0.36}} \right) (100 \rho_l f_{ch})^{1/3} b_w d \quad (47)$$

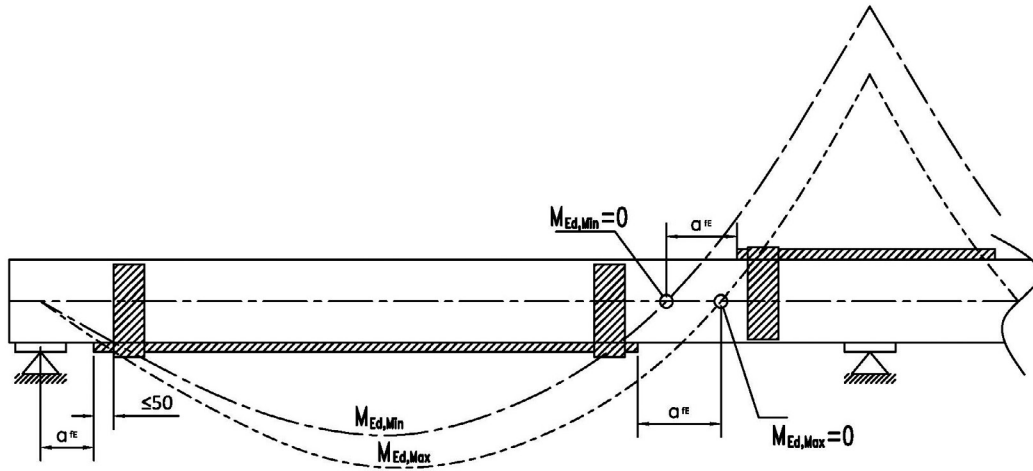


Figure 13. End concrete cover separation. Location of the shear strengthening system if required (adapted from Annex J).

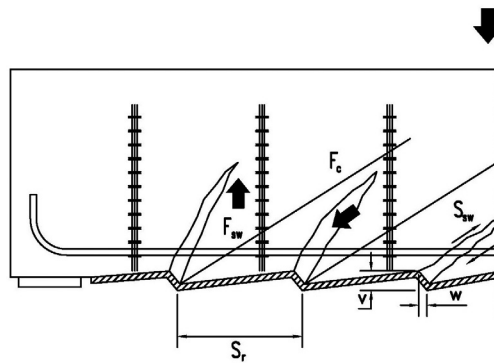


Figure 14. Shear induced separation, adapted from [18].

where:

α_{fe} is the distance between the laminate end and the point of zero bending moment, and the remaining parameters are the longitudinal reinforcement ratio (ρ_l), the characteristic compressive concrete strength (f_{ck}), the web width (b_w) and the effective depth (d).

If Equation (47) is not met, it is required to provide shear strengthening at the end of the longitudinal CFRP laminate with enough anchorage provisions (see Figure 13).

7.1.4. Shear induced separation

Shear induced separation refers to the delamination caused by the relative displacements in the crack tips between the crack edges due to the shear forces (Figure 14). This occurs if the strut and tie system is subjected to a high level of stresses (Figure 15). The CFRP laminate does not debond if Equation (48) and (49) are accomplished.

$$\frac{\tau_{Ed} \sigma_{swd}}{\tau_{R,d}} \leq \begin{cases} 75 \text{ MPa} & \text{for ribbed steel bars} \\ 25 \text{ MPa} & \text{for plain round steel bars} \end{cases} \quad (48)$$

$$\tau_{Ed} \leq 0.33 f_{ck}^{2/3} \quad (49)$$

Where:

τ_{Ed} and σ_{swd} can be calculated according to the provisions of the general document of Eurocode 2 [1].

Adhesively bonded reinforcement may be required if the previous equations are not met to ensure that the tensile

forces are transferred to the compression zone of the member. The design force for the shear EBR system can be obtained as the maximum of two components. The first component corresponds to the distribution of the design value of the total applied shear force over the elastic stiffness and the second one is the difference between the design value of the total applied shear force and the design value of the shear strength of the transverse reinforcement (see Equation (50)).

$$\tau_{Ed,f} = \max \left\{ \begin{array}{l} \frac{E_f A_f}{E_f A_f + E_s A_s} \tau_{Ed} \\ \tau_{Ed} - \tau_{Rd,sv} \end{array} \right. \quad (50)$$

7.2. Anchorage of near surface mounted reinforcement (NSM)

In relation to the anchorage of near surface mounted reinforcement, the formulation of Annex J is based again on the German DAfStb guideline [18] and on the fib Bulletin 90 [16]. As stated by Blaschko [71], it is assumed an effective composite action between the strengthening system and the concrete support that leads to a short anchorage length. Therefore, it is only required to check the anchorage length from the section where the near surface mounted reinforcement is not needed for the load carrying capacity.

According to Annex J, the design bond capacity per strip should be defined by Equation (51).

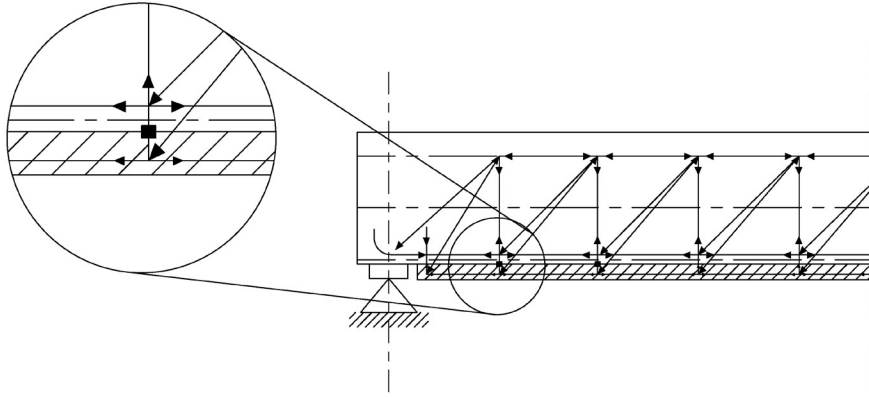


Figure 15. Strut-and-tie model with the mechanism for transferring tensile forces (adapted from *fib* Bulletin 90 [16]).

$$F_{bfRd} = \begin{cases} 0.95 b_f \tau_{Ed} \sqrt[4]{a_r} l_{bf} (0.4 - 0.0015 l_{bf}) & \text{for } l_{bf} \leq 115 \text{ mm} \\ 0.95 b_f \tau_{bAd} \sqrt[4]{a_r} l_{bf} (26.2 + 0.065 \tanh(\frac{a_r}{70}) (l_{bf} - 115)) & \text{for } l_{bf} > 115 \text{ mm} \end{cases} \quad (51)$$

being a_r the distance from the longitudinal axis of the strip to the free edge, which may not be larger than 150 mm.

The maximum design strength of the adhesive for the NSM systems, τ_{bAd} can be obtained by Equation (52).

$$\tau_{bAd} = \frac{1}{\gamma_{BA}} \min \left\{ \begin{array}{l} \alpha_{bA} 0.6 \sqrt{2 f_{Atk} - 2 \sqrt{f_{Atk}^2 + f_{Ack} f_{Atk} + f_{Ack}} f_{Atk}} \\ \alpha_{bC} 4.5 f_{cm}^{0.5} \end{array} \right. \quad (52)$$

where: f_{Ack} and f_{Atk} are the characteristic compressive and tensile strength of the adhesively, respectively, defined in Section 2 as a requirement of Annex for the design of ABR; α_{bA} may be taken as 0.5 unless the more accurate information is available based on production data of NSM CFRP strips; and α_{bC} may be taken as $(\eta_{cc} \cdot k_{cc} \cdot k_{tt})^{0.5}$ unless the more accurate information is available based on production data of NSM CFRP strips.

Factors 0.6 and 4.5 of Equation (52) have been calibrated by bond tests with CFRP strips with 10-30 mm width and 1-3 mm thickness. For round or square bars both factors should be recalibrated.

The NSM anchorage should accomplish the provisions for end cover separation given in 7.1.3 and shear induced separation given in 7.1.4.

8. DETAILING AND OTHER RULES

8.1. Detailing for flexural strengthening with adhesively bonded reinforcement (ABR)

In the case of flexural strengthening with externally bonded reinforcement (EBR), Annex J recommends that the maximum spacing between strips, from centre to centre, should be lower than 0.2 times distance between points of zero moments; 3 times the thickness of the slab; 0.4 times the cantilever length and 400 mm.

The distance of the longitudinal edge of the strip from the member edge should be at least equivalent to the nominal concrete cover of the internal reinforcement.

Fib bulletin 90 [16] gives additional detailing rules on the location, arrangement and limitations for the FRP reinforcement required. Some of these rules are important to avoid premature debonding of the strengthened system.

For NSM CFRP systems, slots cut into the cover concrete should be located such that the cover is not adversely compromised when considering the accuracy of installation equipment along with adequate tolerance for installation.

Annex J provides Table 2 with some geometrical recommendations for NSM reinforcement. Slot dimensions, distance from the slot to the edge of the element and spacing between adjacent slots are important details to avoid premature debonding failure of the strengthened element.

8.2. Permissible parameters

Annex J give additional permissible parameters such as the radius of bending, the number of sheets and strips, and lapping of the closed wrapped systems for shear strengthening or confinement.

In the case of straight prefabricated ABR CFRP bars, bending radius should be larger than 1000 times their thickness, unless stresses that arise from the bending process are considered in determining the tensile strength f_{fuk} .

In relation to the number of allowed layers, no more than five layers of CF sheets should be bonded for flexural or shear strengthening and no more than ten layers for column confinement. In the case of CFRP strips, no more than two layers should be bonded and the maximum thickness of the CFRP strip cross section should not exceed 3 mm (excluding adhesive). For the NSM systems, no more than one strip or bar should be bonded per slot.

When strengthening beams in shear or in the case of column confinement with a closed wrapped system, overlapping of the sheets or slips should be considered.

Conclusions

This paper summarizes the content of the informative Annex J, developed by CEN/TC250/SC2/WG1/TG1 and Pro-

TABLE 2.
Geometrical limits for NSM CFRP reinforcement in the form of bars or strips

Geometrical limits	Square NSM CFRP bars	Round NSM CFRP bars	NSM CFRP strips
b_{slot} (slot width)	$t_f + 2 \leq b_{slot} \leq t_f + 6$	$t_f + 2 \leq b_{slot} \leq t_f + 6$	$t_f + 2 \leq b_{slot} \leq t_f + 4$
t_{slot} (slot thickness)	$b_f + 1 \leq t_{slot} \leq b_f + 3$ $t_f \leq b_f$	$\phi_f + 1 \leq t_{slot} \leq \phi_f + 3$	$b_f \leq t_{slot} \leq b_f + 2$
a_r (distance from the slot to the edge of the NSM)		$a_r \geq 4 b_f$	
s_f (centre-to-centre spacing of CFRP reinforcement)		$max \{ 3 b_{slot} ; d_g \} \leq s_f \leq min \{ 0.2 l_{ob} ; 3 h \}$	

ject Team 3, that for the first time incorporates in Eurocode 2 provisions the design of strengthening existing concrete structures with CFRP adhesively bonded systems. More detailed information about the formulations included in this Annex can be found in the *fib* Bulletin 90 [16], published in 2019, which was also intended to serve as a background document.

CFRP laminates or bars are linear elastic up to failure. Therefore, linear elastic analysis with limited redistribution or plastic analysis are not allowed.

Annex J includes design provisions for strengthening existing reinforced or prestressed concrete structures in flexure, shear or confinement with passive EB or NSM CFRP reinforcements. When designing CFRP strengthening systems in flexure or shear, the laminate might debond before reaching the ultimate bending moment or shear force. This premature failure mode should be correctly predicted during design, especially in the externally bonded case, more prompt to debond than the NSM since it is only bonded by one side of the strip.

Despite the FRP system might be design to increase the strength of the existing concrete cases, SLS might governs the design and should also be checked.

Acknowledgements

The authors acknowledge the support provided by Spanish Ministry of Science and Innovation (MCIN/ AEI) and by the European Funds for Regional Development in the following projects during their collaboration in the CTN140/SC2 and in the CEN/TC250/SC2/WG1/TG1 (Eva Oller): BIA2015-64672-C4-1-R, RTI2018-097314-B-C21, and PID2020-119015GB-C22.

References

[1] European Committee for Standardization CEN, Eurocode 2: Design of concrete structures — Part 1-1: General rules — Rules for buildings, bridges and civil engineering structures, prEN 1992-, 2022. (*)

[2] C. Carloni, S. Verre, L.H. Sneed, L. Ombres, Open issues on the investigation of PBO FRCM-Concrete debonding, *Compos. Struct.* 299 (2022). <https://doi.org/10.1016/j.compstruct.2022.116062>.

[3] L.H. Sneed, T. D'Antino, C. Carloni, C. Pellegrino, A comparison of the bond behavior of PBO-FRCM composites determined by double-lap and single-lap shear tests, *Cem. Concr. Compos.* 64 (2015) 37–48. <https://doi.org/10.1016/j.cemconcomp.2015.07.007>.

[4] U. Meier, M. Deuring, H. Meier, G. Schwegler, Strengthening of structures with CFRP laminates: research and applications in Switzerland, in: *Proc. 1st Int. Conf. Adv. Compos. Mater. Bridg. Struct.*, 1992: pp. 243–251.

[5] Meier U, Bridge repair with high performance composite materials, *Mater. Und Tech.* 4 (1987) 125–128. <http://libra.msra.cn/Publication/2795762/bridge-repair-with-high-performance-composite-materials>.

[6] B. Täljsten, Strengthening of concrete structures for shear with bonded CFRP-fabrics, *Proc. US-Canada-Europe Work. Bridg. Eng.* (1997) 57–64.

[7] L.C. Bank, *Composites for Construction: Structural Design with FRP Materials*, 2007. <https://doi.org/10.1002/9780470121429>.

[8] J.G. Teng, J.F. Chen, S.T. Smith, L. Lam, FRP : Strengthened RC Structures, 2002. <https://doi.org/10.1002/pi.1312>.

[9] R. Parretti, A. Nanni, Strengthening of RC members using near-surface mounted FRP composites: Design overview, *Adv. Struct. Eng.* 7 (2004) 469–483. <https://doi.org/10.1260/1369433042863198>.

[10] L. De Lorenzis, J.G. Teng, Near-surface mounted FRP reinforcement: An emerging technique for strengthening structures, *Compos. Part B Eng.* 38 (2007) 119–143. <https://doi.org/10.1016/j.compositesb.2006.08.003>.

[11] J.M. Sena Cruz, J.A.O. Barros, R. Gettu, Á.F.M. Azevedo, Bond Behavior of Near-Surface Mounted CFRP Laminate Strips under Monotonic and Cyclic Loading, *J. Compos. Constr.* 10 (2006) 295–303. [https://doi.org/10.1061/\(asce\)1090-0268\(2006\)10:4\(295\)](https://doi.org/10.1061/(asce)1090-0268(2006)10:4(295)).

[12] I.A. Sharaky, M. Baena, C. Barris, H.E.M. Sallam, L. Torres, Effect of axial stiffness of NSM FRP reinforcement and concrete cover confinement on flexural behaviour of strengthened RC beams: Experimental and numerical study, *Eng. Struct.* 173 (2018) 987–1001. <https://doi.org/10.1016/j.engstruct.2018.07.062>.

[13] J. Gómez, L. Torres, C. Barris, Characterization and simulation of the bond response of NSM FRP reinforcement in Concrete, *Materials (Basel)*. 13 (2020). <https://doi.org/10.3390/MA13071770>.

[14] T.C. Triantafyllou, *Textile Fibre Composites in Civil Engineering*, 2016. <https://doi.org/10.1016/C2014-0-01415-3>.

[15] P. Valerio, T.J. Ibell, A.P. Darby, Deep embedment of FRP for concrete shear strengthening, *Proc. Inst. Civ. Eng. Struct. Build.* 162 (2009) 311–321. <https://doi.org/10.1680/stbu.2009.162.5.311>.

[16] fib Task group 5.1, *FIB Bulletin 90, Externally applied FRP reinforcement for concrete structures*, Lausanne, Switzerland, 2019.

[17] Fédération Internationale du Béton, *fib Model Code for Concrete Structures 2010*, Ernst & Sohn, 2013.

[18] German Committee for Reinforced Concrete, *DAfStb Heft 595 Erläuterungen und Beispiele zur DAfStb-Richtlinie Verstärken von Betonbauteilen mit geklebter Bewehrung*, Berlin, Germany, 2013.

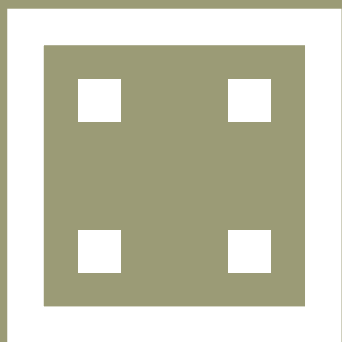
- [19] C.S.T.R. 55, Design guidance for strengthening concrete structures using fibre composite materials, London, Great Britain, 2012.
- [20] CNR (National Research Council) Advisory Committee on technical recommendations for construction, Istruzioni per la Progettazione, l'Esecuzione ed il Controllo di Interventi di Consolidamento Statico mediante l'utilizzo di Compositi Fibrorinforzati, CNR-DT200, Rome, Italy, 2013.
- [21] Association Française de Génie Civil, AFGC Réparation et renforcement des structures en béton au moyen des matériaux composites. Recommandations provisoires, 2011.
- [22] Schweizerischer Ingenieur und Architektenverein, SIA166 Klebebewehrungen (Eternally bonded reinforcement), 2004.
- [23] Earthquake and protection planning organization, Greek Seismic Assessment Retrofit Code GRECO, 2013.
- [24] fib Task Group 9.3 FRP Reinforcement for Concrete Structures, Externally bonded FRP reinforcement for RC structures (2001). Technical report on the design and use of externally bonded fibre reinforced polymer reinforcement (FRP EBR) for reinforced concrete structures, Fib Bulletin 14., 2001.
- [25] European Committee for Standardization CEN, Background document for pr EN1992-1-1:2021, 2021. (*)
- [26] prEN 1990:2020: Eurocode – Basis of structural and geotechnical design, (2020). (*)
- [27] ISO/TC 71/SC 6 Non-traditional reinforcing materials for concrete structures, ISO 10406-1. Fibre-reinforced polymer (FRP) reinforcement of concrete Test methods Part 1: FRP bars and grids, 2015.
- [28] ISO/TC 61/SC 13 Composites and reinforcement fibres, ISO 14130:1997 Fibre-reinforced plastic composites — Determination of apparent interlaminar shear strength by short-beam method, 1997.
- [29] European Committee for Standardization CEN, EN 1504-4: 2004 Products and systems for the protection and repair of concrete structures - Definitions, requirements, quality control and evaluation of conformity - Part 4: Structural bonding, 2004.
- [30] E. Oller, Peeling failure in beams strengthened by plate bonding. A design proposal, Universitat Politècnica de Catalunya, 2005.
- [31] A. de Diego, Á. Arteaga, J. Fernández, Strengthening of square concrete columns with composite materials. Investigation on the FRP jacket ultimate strain, Compos. Part B Eng. 162 (2019) 454–460. <https://doi.org/10.1016/j.compositesb.2019.01.017>.
- [32] L. Lam, J.G. Teng, Design-oriented stress-strain model for FRP-confined concrete, Constr. Build. Mater. 17 (2003) 471–489. [https://doi.org/10.1016/S0950-0618\(03\)00045-X](https://doi.org/10.1016/S0950-0618(03)00045-X).
- [33] T.M. Pham, M.N.S. Hadi, Stress Prediction Model for FRP Confined Rectangular Concrete Columns with Rounded Corners, J. Compos. Constr. 18 (2014). [https://doi.org/10.1061/\(asce\)cc.1943-5614.0000407](https://doi.org/10.1061/(asce)cc.1943-5614.0000407).
- [34] B. Shan, F.C. Gui, G. Monti, Y. Xiao, Effectiveness of CFRP Confinement and Compressive Strength of Square Concrete Columns, J. Compos. Constr. 23 (2019). [https://doi.org/10.1061/\(asce\)cc.1943-5614.0000967](https://doi.org/10.1061/(asce)cc.1943-5614.0000967).
- [35] A. de Diego, S. Martínez, V.J. Castro, L. Echevarría, F.J. Barroso, J.P. Gutiérrez, Experimental investigation on the compressive behaviour of FRP-confined rectangular concrete columns, Arch. Civ. Mech. Eng. 22 (2022). <https://doi.org/10.1007/s43452-022-00450-4>.
- [36] T. D'Antino, T.C. Triantafyllou, Accuracy of design-oriented formulations for evaluating the flexural and shear capacities of FRP-strengthened RC beams, Struct. 17 (2016) 425–442. <https://doi.org/10.1002/suco.201500066>.
- [37] Comité Européen de Normalisation (CEN), Eurocode 8. Design of structures for earthquake resistance. Part 3. Assessment and retrofitting of buildings, EN 1998-3, Brussels, 2005.
- [38] A.C.I. (ACI) ACI Committee 440, Guide for the design and construction of externally bonded FRP systems for strengthening concrete structures, ACI 440.2R, 2008.
- [39] E. Oller, R. Kotynia, A. Mari, Assessment of the existing models to evaluate the shear strength contribution of externally bonded FRP shear reinforcements, Compos. Struct. 266 (2021). <https://doi.org/10.1016/j.compstruct.2021.113641>.
- [40] G. Monti, M. Liotta, Tests and design equations for FRP-strengthening in shear, Constr. Build. Mater. 21 (2007) 799–809. <https://doi.org/10.1016/j.conbuildmat.2006.06.023>.
- [41] A. Carolin, B. Täljsten, Theoretical study of strengthening for increased shear bearing capacity, J. Compos. Constr. 9 (2005) 488–496. [https://doi.org/10.1061/\(ASCE\)1090-0268\(2005\)9:6\(488\)](https://doi.org/10.1061/(ASCE)1090-0268(2005)9:6(488)).
- [42] J.F.F. Chen, J.G.G. Teng, Shear capacity of FRP-strengthened RC beams: FRP debonding, in: Constr. Build. Mater., 2003: pp. 27–41. [https://doi.org/10.1016/S0950-0618\(02\)00091-0](https://doi.org/10.1016/S0950-0618(02)00091-0).
- [43] Japan Society of Civil Engineers, Recommendation for design and construction of concrete structures using continuous fibre reinforcing materials, Concrete E, Tokyo (Japan), 1997.
- [44] T.C. Rousakis, M.E. Saridaki, S.A. Mavrothalassitou, D. Hui, Utilization of hybrid approach towards advanced database of concrete beams strengthened in shear with FRPs, Compos. Part B Eng. 85 (2016) 315–335. <https://doi.org/10.1016/j.compositesb.2015.09.031>.
- [45] R. Kotynia, Shear strengthening of RC beams with polymer composites, Lodz University of Technology, 2011.
- [46] A. Mofidi, O. Chaallal, Shear Strengthening of RC Beams with EB FRP: Influencing Factors and Conceptual Debonding Model, J. Compos. Constr. 15 (2011) 62–74. [https://doi.org/10.1061/\(ASCE\)CC.1943-5614.0000153](https://doi.org/10.1061/(ASCE)CC.1943-5614.0000153).
- [47] C. Pellegrino, C. Modena, Fiber-reinforced polymer shear strengthening of reinforced concrete beams: Experimental study and analytical modeling, ACI Struct. J. 103 (2006) 720–728. <https://www.scopus.com/inward/record.url?eid=2-s2.0-33748587309&partnerID=40&md5=fdb67a21a2eb606f645b2bd1b5d1fd9e>.
- [48] ACI Committee 440, ACI 440.2R-17, Guide for the Design and Construction of Externally Bonded FRP Systems for Strengthening Concrete Structures, Farmington Hills, Michigan, USA, 2017.
- [49] S. Jiang, W. Yao, J. Chen, S. Tao, Time dependent behavior of FRP-strengthened RC beams subjected to preload: Experimental study and finite element modeling, Compos. Struct. 200 (2018) 599–613. <https://doi.org/10.1016/j.compstruct.2018.05.110>.
- [50] M. Moawad, M. Baena, C. Barris, L. Torres, H.E.M. Sallam, Time-dependent behavior of NSM strengthened RC beams under sustained loading, Eng. Struct. 247 (2021). <https://doi.org/10.1016/j.engstruct.2021.113210>.
- [51] A. Mari, E. Oller, J.M. Bairán, N. Duarte, A.R. Mari, E. Oller, J.M. Bairán, N. Duarte, Simplified method for the calculation of long-term deflections in FRP-strengthened reinforced concrete beams, in: Int. Symp. Fiber Reinf. Polym. Reinf. Concr. Struct., 2013: pp. 147–149. <https://doi.org/10.1016/j.compositesb.2012.07.003>.
- [52] Y.J. Kim, P.J. Heffernan, Fatigue Behavior of Externally Strengthened Concrete Beams with Fiber-Reinforced Polymers: State of the Art, J. Compos. Constr. 12 (2008) 246–256. [https://doi.org/10.1061/\(asce\)1090-0268\(2008\)12:3\(246\)](https://doi.org/10.1061/(asce)1090-0268(2008)12:3(246)).
- [53] L. Bizindavyi, K.W. Neale, M.A. Erki, Experimental Investigation of Bonded Fiber Reinforced Polymer-Concrete Joints under Cyclic Loading, J. Compos. Constr. 7 (2003) 127–134. [https://doi.org/10.1061/\(asce\)1090-0268\(2003\)7:2\(127\)](https://doi.org/10.1061/(asce)1090-0268(2003)7:2(127)).
- [54] C. Carloni, K. V. Subramaniam, M. Savoia, C. Mazzotti, Experimental determination of FRP-concrete cohesive interface properties under fatigue loading, Compos. Struct. 94 (2012) 1288–1296. <https://doi.org/10.1016/j.compstruct.2011.10.026>.
- [55] H. Budelmann, et al., Praxisgerechte Bemessungsansätze für das wirtschaftliche Verstärken von Betonbauteilen mit geklebter Bewehrung - Verbundtragfähigkeit unter dynamischer Belastung, DAfStb H. 593. (2013).
- [56] T. Leusmann, Das Verbundtragverhalten geklebter Kohlefaserkunststoffe auf Beton unter schwingender Beanspruchung Thon Leusmann, Technische Universität Braunschweig., 2015.
- [57] J. Dai, Y. Saito, T. Ueda, Y. Sato, Static and fatigue bond characteristics of interfaces between CFRP sheets and frost damage experienced concrete, in: Am. Concr. Institute, ACI Spec. Publ., 2005: pp. 1515–1530. <https://doi.org/10.14359/14907>.
- [58] E. Ferrier, D. Bigaud, P. Hamelin, L. Bizindavyi, K.W. Neale, Fatigue of CFRPs externally bonded to concrete, Mater. Struct. 38 (2005) 39–46. <https://doi.org/10.1007/bf02480573>.
- [59] B. M., Zum tragverhalten von betonbauteilen mit in schlitz eingekeblten CFK-lamellen, Munich TU, 2001.
- [60] E. Oller Ibars, D. Cobo Del Arco, A.R. Mari Bernat, Design proposal to avoid peeling failure in FRP-strengthened reinforced concrete beams, J. Compos. Constr. 13 (2009). [https://doi.org/10.1061/\(ASCE\)CC.1943-5614.0000038](https://doi.org/10.1061/(ASCE)CC.1943-5614.0000038).
- [61] E. Oller, A.R. Mari, L. Bellido, Design method for flexural strengthening with fiber reinforced polymer (FRP) laminates avoiding its premature debonding, Inf. La Construcción. 65 (2013) 519–531. <https://doi.org/10.3989/ic.12.087>.

- [62] M. Bilotta, A., Ceroni, F., Nigro, E. And Pecce, Design by testing procedure of debonding load for RC elements strengthened with EBR FRP materials, in: C. R. Sen, R. Seracino, C. Shield and W. Gold (eds), Tampa, Florida (Ed.), Proc. 10th FRPRCS Int. Symp. ACI SP-275 Fiber-Reinforced Polym. Reinf. Concr. Struct., 2011.
- [63] J.G. Teng, S.T. Smith, J. Yao, J.F. Chen, Intermediate crack-induced debonding in RC beams and slabs, *Constr. Build. Mater.* 17 (2003) 447–462. [https://doi.org/10.1016/S0950-0618\(03\)00043-6](https://doi.org/10.1016/S0950-0618(03)00043-6).
- [64] X.Z. Lu, Studies of FRP-concrete interface, Tsinghua University, Beijing, China, 2004.
- [65] J.C. López González, Estudio de la redistribución tensional en la interfase FRP-Hormigón, Universidad Politécnica de Madrid, 2012.
- [66] R. Niedermeier, Envelope line of tensile forces while using externally bonded reinforcement., TU München, Munchen, 2000.
- [67] S. Matthys, Structural behaviour and design of concrete members strengthened with externally bonded FRP reinforcement, University of Ghent, Belgium, 2000.
- [68] W. Finckh, K. Zilch, Strengthening and Rehabilitation of Reinforced Concrete Slabs with Carbon-Fiber Reinforced Polymers Using a Refined Bond Model, *Comput. Civ. Infrastruct. Eng.* 27 (2012) 333–346. <https://doi.org/10.1111/j.1467-8667.2011.00752.x>.
- [69] Japan Society of Civil Engineers, Recommendations for upgrading of concrete structures with use of continuous fiber sheets, *JSCE Concr. Eng. Ser.* 41 (2001).
- [70] G. Zehetmaier, K. Zilch, Interaction between internal bars and externally FRP Reinforcement in RC Members, in: Proc. Sixth Int. Symp. FRP Reinf. Concr. Struct., Singapore, 2003: pp. 397–406.
- [71] M. Blaschko, Bond Behaviour of CFRP Strips Glued into Slits, in: Proc. Sixth Int. Symp. FRP Reinf. Concr. Struct., Singapore, 2003: pp. 205–214.

*This document is available through the National members at CEN TC250/SC2

2nd generation of Eurocode 2 on concrete structures

"Hormigón y Acero", with ACHE, will organize an event on October 17th in Madrid to present the main technical content of Eurocode 2, explained in the monographic issue 299-300 of the journal, with the participation of Hans Ganz, Aurelio Muttoni, John Cairns, Fabienne Robert and several members of the Spanish UNE CTN140/SC2.



EUROCODES

EN 1992

Design of concrete structures

Design of Steel Fibre Reinforced Concrete Structures According to the Annex L of the Eurocode-2 2023

Diseño de estructuras de hormigón reforzado con fibras de acero según el Anejo L del nuevo Eurocódigo-2 2023

de la Fuente, A.^a, Monserrat-López, A.^{*b}, Tošić, N.^a, Serna, P.^c

^a Department of Civil and Environmental Engineering, UPC-BarcelonaTECH.

^b Department of Civil and Environmental Engineering, UPC-BarcelonaTECH; Postdoctoral Margarita Salas Fellowship funded by UPV.

^c Institute of Concrete Science and Technology ICITECH Universitat Politècnica de València.

Recibido el 20 de febrero de 2023; aceptado el 30 de marzo de 2023

ABSTRACT

The Annex L of FprEN 1992-1-1:2023 (EC-2) provides provisions for the design of Steel Fibre Reinforced Concrete (SFRC) structures. This Annex is supported by a comprehensive background document (BD) that gathers the main outcomes of the research carried out on SFRC during the last thirty years. This paper aims to cover the sections of Annex L and supplement those with scientific literature, to help readers reach a deeper understating of the fundamentals and specific details of the proposed formulations and rules.

KEYWORDS: Fibre reinforced concrete, design, standardization, Eurocode 2, steel fibre.

©2023 Hormigón y Acero, the journal of the Spanish Association of Structural Engineering (ACHE). Published by Cinter Divulgación Técnica S.L. This is an open-access article distributed under the terms of the Creative Commons (CC BY-NC-ND 4.0) License

RESUMEN

El Anexo L del FprEN 1992-1-1:2023 (EC-2) plantea disposiciones para el diseño de estructuras de hormigón reforzado con fibras de acero (SFRC). Este anexo está respaldado por un sólido documento de antecedentes (BD) que recopila los principales resultados de las investigaciones realizadas sobre SFRC durante los últimos treinta años. Este artículo tiene como objetivo cubrir las secciones del Anexo L y complementarlas con literatura científica para permitir que los lectores profundicen en los fundamentos y detalles específicos de las formulaciones y reglas establecidas.

PALABRAS CLAVE: Hormigón reforzado con fibras, diseño, estandarización, Eurocódigo 2, fibras de acero.

©2023 Hormigón y Acero, la revista de la Asociación Española de Ingeniería Estructural (ACHE). Publicado por Cinter Divulgación Técnica S.L. Este es un artículo de acceso abierto distribuido bajo los términos de la licencia de uso Creative Commons (CC BY-NC-ND 4.0)

I. INTRODUCTION

Provisions for the structural design of Steel Fibre Reinforced Concrete (SFRC) members were included in both FprEN 1992-1-1:2023 (Annex L) [1] and FprEN 1992-1-2:2023 (Annex B) [2]. This has been the result of increasing demand for regulations of this materials from the construction sector; well-established knowledge on the mechanical properties of SFRC derived from the research and wide variety of successful existing applications (Figure 1) and the future perspectives for the material [3].

In this regard, chronologically at European level, the DBV 2001 [4] was the first to introduce design provisions for SFRC structures in Germany, followed by the RILEM TC 162-TDF in 2003 [5], the Italian CNR-DT/204/2006 in Italy [6] and the EHE-08 in Spain [7]. Within these 20 years, other European countries have regulated the design of SFRC structures. Even, in some national regulations (i.e., Italy, Spain and Sweden [6–8]), the use of other types of fibre materials (mainly synthetic-based) for partially replacing the ordinary steel reinforcement are regulated by including specifications related to the mechanical properties of these materials. In the same line, the fib Model Code 2010 [40], also covers the use of SFRC (and other types of FRCs).

Furthermore, the type of reinforcement for concrete has

* Persona de contacto / Corresponding author.
Correo-e / e-mail: andrea.monserrat@upc.edu (Andrea Monserrat-López).

proved to have a significant impact on the sustainability performance of the structure. Some researchers were focused on quantifying the sustainability performance -considering economic, environmental and social indicators- of concrete structures reinforced with different types and configuration of reinforcements (including traditional RC, SFRC, and hybrid solutions) [9–11]. The outcomes of these analyses prove—and confirm—that the sustainability performance of SFRC and hybrid reinforced (steel fibres + steel rebar) concrete solutions are promising.

This paper is aimed to cover—not exhaustively—the features included in the Annexes L and B of the FprEN 1992-1-1:2023 [1] and FprEN 1992-1-2:2023 [2], respectively (both referred to as EC-2 hereafter), and complement those with justifications and explanations supported by the Background Document (BD) to Annex L [12] and scientific literature, when necessary.

2. DESIGN BASIS - SAFETY FORMAT

The design approach for SFRC structures proposed in the EC-2 is aligned with the partial safety format described in Eurocode 0 [13]. In this regard, the material partial safety factor (γ_{sf}) for SFRC to be considered for both compression and tensile mechanical properties is established as 1.50 for both persistent and transient situation in ULS, 1.20 for accidental situations and 1.00 for SLS. These safety factors are equivalent to those suggested in the EC-2 for reinforced and/or prestressed concrete structures.

As acknowledged in the BD and other relevant literature dealing with the design basis FRC [12,14], the post-cracking (residual hereinafter) tensile properties of this material are known to be subjected to several sources of uncertainty. Fibre distribution and orientation anisotropy are the dominant sources of variability that lead to a total scatter in the notched beam test EN 14651 [15] ranging between 10% to 30% [16,17] depending on the amount of fibres, fresh concrete properties, and other aspects [18]. This scatter observed in the EN 14651 beams tends to be superior to that observed in the final structure due to the usually larger volume of SFRC involved in the cracked areas of the latter. The combined use of: characteristic values of the residual flexural tensile strength ($f_{R,k}$); orientation factors (k_o) [19–21] and the factor k_G for taking into account the decrease of variability with the increase of the size of cracked areas (with respect to the EN 14651 beam, $125 \times 150 \text{ mm}^2$), allows for designs that meet the structural reliability levels widely accepted for traditional reinforced concrete (RC) structures [22].

In specific structures or components, different partial safety factors might be required for optimization purposes or to meet other failure consequences classes (with other reliability levels associated). To this end, FORM [23] has been already implemented to calibrate γ_{sf} for precast FRC tunnel linings [24] and for FRC elements without transversal reinforcement [25]. Alternatively, and specifically oriented to non-linear structural analysis, the method proposed in [26] to calibrate the global resistance safety factor -and reported in the Annex F of the EC-2- was satisfactorily used and implemented in SFRC flat slabs [27–29]. The test up to failure of the SFRC flat slab (200 mm thickness, and four bays of $5 \times 6 \text{ m}$) presented in [29] (see

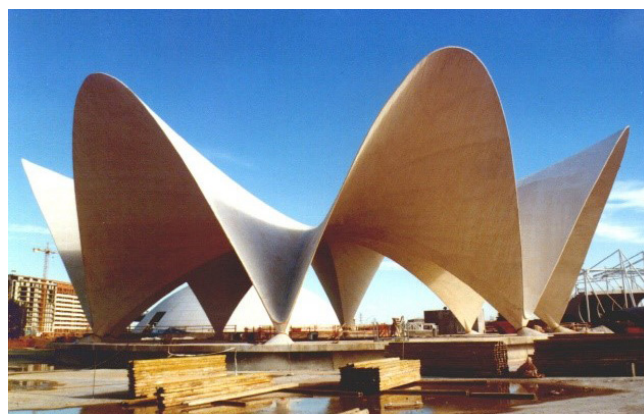
Figure 2) proved that the design carried out combining FE-based non-linear models and the safety factor calibration approach [26] lead to safe-side results for the ultimate load [30].



(a)



(b)

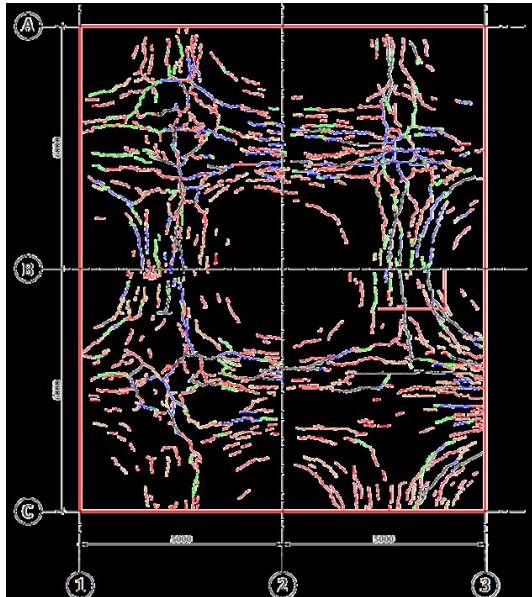


(c)

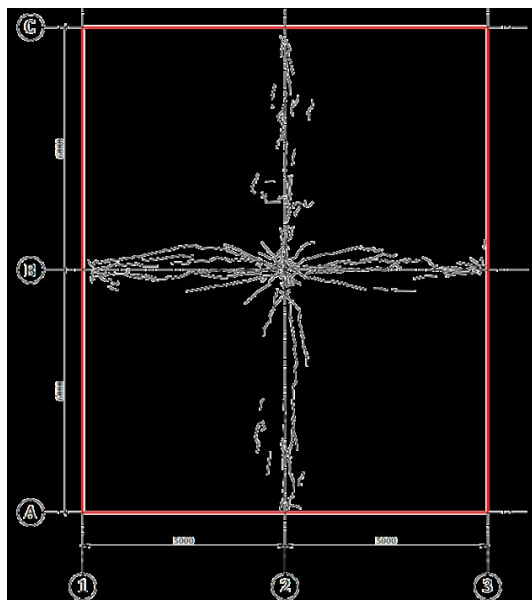
Figure 1. Different existing applications of SFRC in (a) underground construction (tunnel vertical shaft in Barcelona, Spain), (b) building column-supported flat slab (LKS Headquarters Building in Mondragón, Spain) and (c) architectural applications (Culvert of the Oceanographic Restaurant in Valencia, Spain).



(a)



(b)



(c)

Figure 2. Real-scale test of the SFRC flat slab reported in [29]: (a) application of the live load, and final crack patterns of the (b) bottom and (c) upper sides of the slab.

3. MATERIALS

3.1. General aspects

The EC-2 explicitly refers to steel fibres (SF) that follow the requirements of the EN 14889-1 [31] as concrete reinforcement with the capacity to replace or complement the ordinary steel reinforcement. SFs are seen as a material that enhances the residual capacity of the resulting SFRC composite for both compression (confinement effect) and tension (cracking control, ductility and energy absorption capacity).

The adequate selection of both fibre geometry and strength for a specific mix design can lead to an efficient application. The best solution requires a compromise among the targeted effect of the fibres in different limit states. In this regard, and in general terms, short and thin fibres might be suitable for initial crack control while these not affect significantly the workability of the composite. On the opposite, long and slender –with performant anchorages– fibres might be suitable when higher residual tensile strength of the SFRC is required for crack control in SLS and bearing capacity in ULS. In this case, the impact on workability may be significant. These tendencies are more evident for high fibres' dosages, and the mechanical effects tend to be empowered with the matrix quality [32]. The workability reduction has to be compensated using plasticizer admixtures, and, for high fibres dosages, the mix design has to be adapted with finer granulometries.

3.2. Strength and ductility classification

In general, the addition of fibres does not modify matrix properties as density, both compressive and tensile (pre-cracked) strengths, elastic modulus, and shrinkage for the range of strength classes (SC) identified in the Annex L (Table 1.2).

Concerning creep, both compressive and tensile (pre-cracking) creep of SFRC can be computed according to 5.1 of the EC-2. However, if tensile-creep is expected to be a design determining parameter in any limit state, tests must be conducted following a standardized testing configuration and procedure [33–35] to quantify its time-dependent magnitude (see Figure 3). According to [36], tensile-creep of SFRC may be significant in elements with both low degree of redundancy and low amounts of longitudinal reinforcement.

Assuming these starting points, EC-2 typifies the SFRC SC based on the residual flexural strength (f_R) of the composite determined according to EN 14651 [15] (see Figure 4). The characteristic values of the residual flexural strengths for crack mouth opening displacements (CMODs) of 0.5 mm and 2.5 mm, $f_{R,1k}$ and $f_{R,3k}$, are the relevant design, strength characterization and quality control parameters of the SFRC [37]. This statistical values of f_R account for the sources of variability of samples of the same and of different batches. $f_{R,1k}$ and $f_{R,3k}$ shall be computed considering that: f_R follows a log-normal probability density distribution according to EN 1990 [13] (5% quantile, 75% of confidence level); and that the standard deviation of f_R is unknown unless explicitly agreed. Criteria to determine the statistic properties of f_R and to assess the population standard deviation could be found in [38,39].

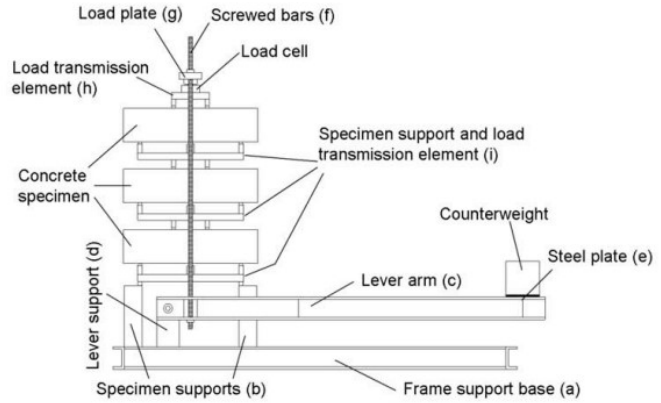


Figure 3. Test configuration for quantifying creep time-dependant phenomena in pre-cracked FRC beams subjected to long-term flexure [33–35].

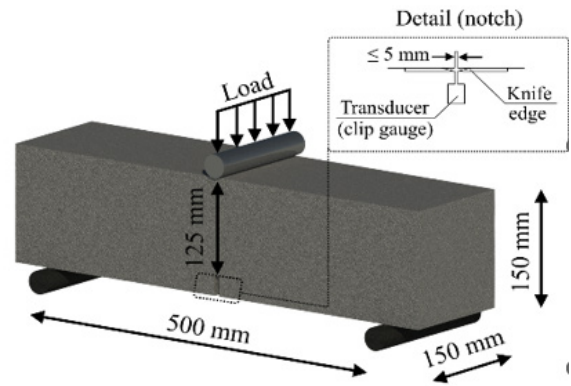


Figure 4. Test setup according to EN 14651 [15].

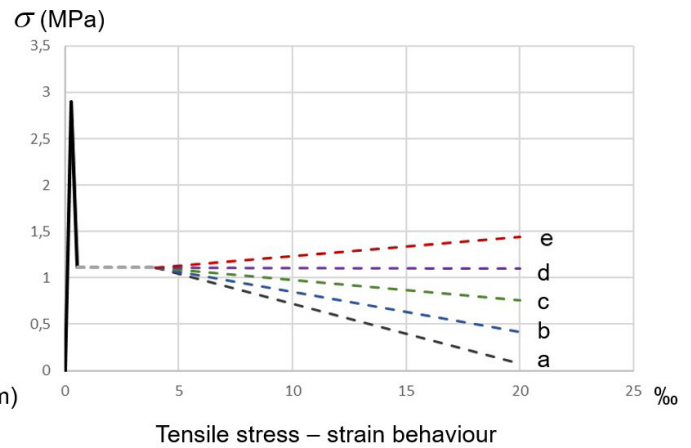
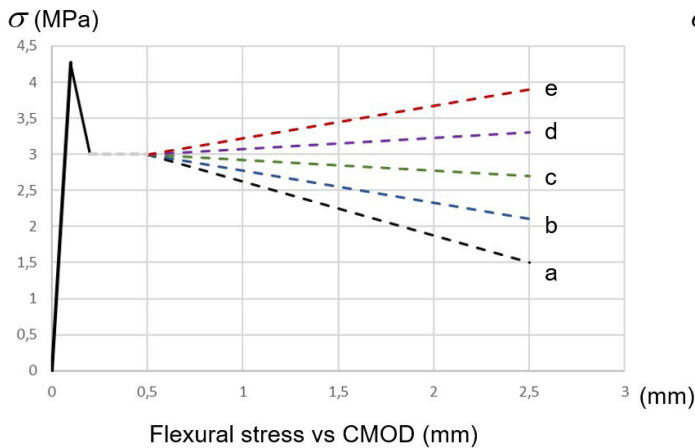


Figure 5. Limits for the ductility classes in the EN 14651 [15]: (a) flexural test for a FRC corresponding to a SC 3, and (b) the resultant tensile stress/strain law evaluated according to EC-2.

The value of $f_{R,1k}$ establish the strength class: SC (1.0; 1.5; 2.0; 2.5; 3.0; 3.5; 4.0; 4.5; 5.0; 6.0; 7.0; 8.0) and the ductility class is denominated by a letter “a”, “b”, “c”, “d” or “e” when the ratio $f_{R,3k} / SC$ exceeds the values of 0.5; 0.7; 0.9; 1.1 or 1.3 respectively. Figure 5 represents an example for those limits by means of a qualitative tensile stress-CMOD relationship.

This SFRC classification criteria is non-coincident with the initial proposal in the MC2010 [40], where the ductility class is defined, with the same limits, but based on the $f_{R,3k} / f_{R,1k}$ ratio instead of the $f_{R,3k} / SC$ ratio. In this sense, the EC-2 criterion is oriented to accept the compensation of a low ductility by an increase in strength. For instance, a concrete SC4

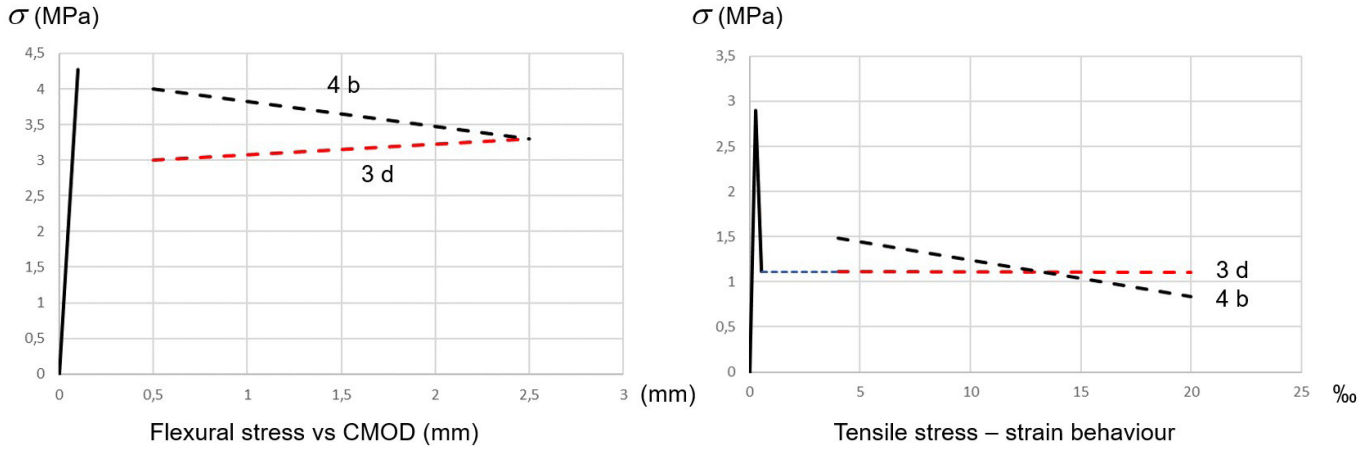


Figure 6. Example of accepted FRC concretes when a SC3d class is prescribed.

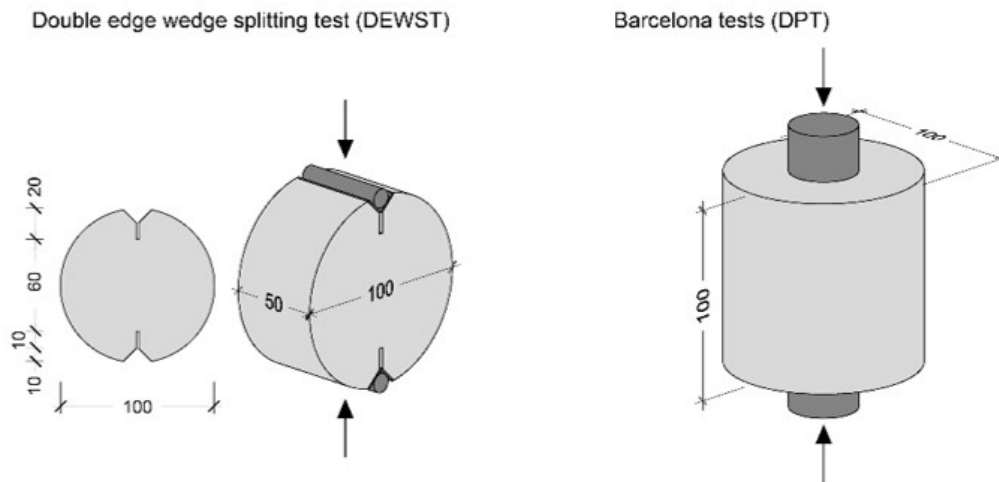


Figure 7. Dimensions and boundary conditions for the DEWST and DPT.

b could be accepted as a SC3 d as shown in Figure 6.

Even if the EC-2 does not make any explicit mention, only for quality control (QC) purposes, alternative tests as the DEWS [41] and the Double Punching Test (DPT, or BCN test) [42–44] (see Figure 7) may be used provided an statistically coherent and robust correlation [45] with the notched beam EN-14651 [15] has been established for the SFRC under characterization.

3.3. Design assumptions for the material

As per cross-sectional analysis and design, the design values of the service and ultimate residual strength of SLS (f_{Ftsd}) and ULS (f_{Ftud}), respectively, should be computed with Eq. 1 and 2, respectively.

$$f_{Ftsd} = f_{Fts,ef} / \gamma_{SF} = k_o k_G 0.37 f_{R,1k} / \gamma_{SF} \quad (1)$$

$$f_{Ftud} = f_{Ftu,ef} / \gamma_{SF} = k_o k_G 0.33 f_{R,3k} / \gamma_{SF} \quad (2)$$

where k_o is the factor that relates the fibre orientation expected in the real structure with that existing in the notched beam EN-14651 [15] and k_G is the factor accounting for the effect of member size.

The Annex L suggests considering $k_o = 0.5$ unless otherwise is specified in the same Annex L or verified by testing, with final values always smaller than 1.7. Likewise, for bending, shear and torsion forces $k_o = 1.0$ may be used when S2-S4 consistency classes (according to EN 206 [46]) are achieved.

The orientation factor can be assessed by means of representative tests [20]: cutting and testing beams from the real structure and/or using non-destructive tests based on the inductive properties of the SFRC [47–50]. Concerning the latter, the SFRC flat slab constructed and tested up to failure reported in [29] was cored for characterizing the amount, distribution and orientation of fibres with a portable inductive device (see Figure 8). The orientation factor pattern was posteriorly computed by means of the results obtained. An equivalent approach was conducted in SFRC slabs [46] with conclusive results towards the alternative use of these non-destructive techniques.

The size effect on the magnitude of variation coefficient of the SFRC residual tensile properties is considered through the coefficient $k_G (=1.0 + 0.5 A_{ct} \leq 1.5)$, which depends on the area of the tension zone (A_{ct}) involved in the flexural failure mechanism –of the structural system in equilibrium. This consideration makes it possible to utilize the residual tensile capacity up to 90% of the average strength [22,40]. This as-

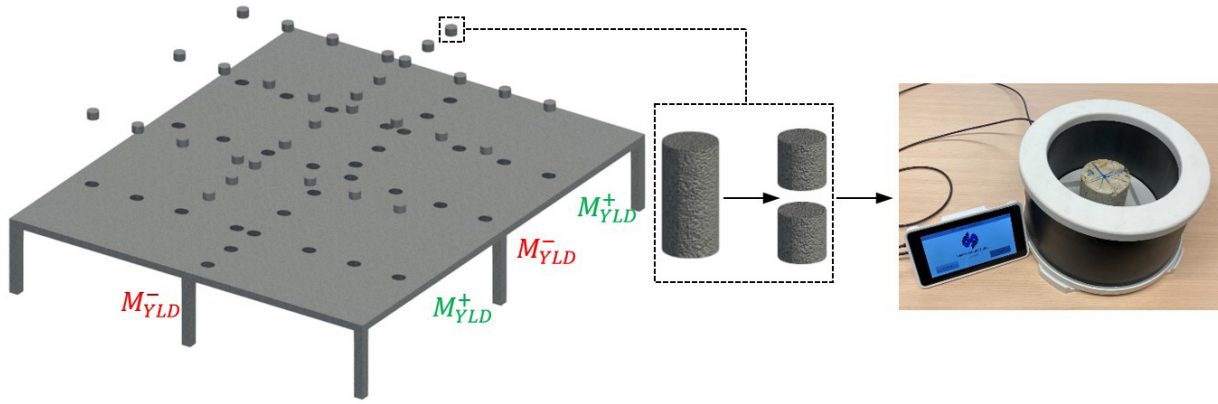


Figure 8. Cored flat slab and inductive testing for determining the amount, distribution and orientation of fibres.

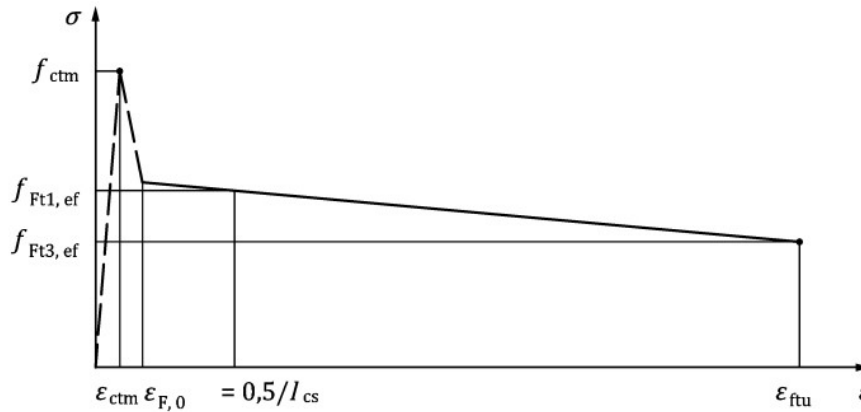


Figure 9. Tri-linear stress-strain constitutive law for simulating the mechanical response of SFRC subjected to uniaxial tension.

sumption is based on the fact that the scatter of the residual tensile strength of the SFRC decreases with the increase of the volume of material subjected to tension involved in the failure mechanism (i.e., length of the yield line). For local failure mechanisms—independently of the structural redundancy- and small cracked areas, a $k_G = 1.0$ shall be considered.

The relation $f_{R,1k}/f_{ctk,0.05} \geq 0.5$ must be satisfied to guarantee material ductility to avoid either a fragile response in case of lightly reinforced elements or any crack localization. Considering that the characteristic value of the residual tensile strength for SLS (f_{Ftsk}) is $0,40 f_{R,1k}$ (assuming $k_o = k_G = 1.0$), the ratio $f_{R,1k}/f_{ctk,0.05} \geq 0.5$ results in $f_{Ftsk}/f_{ctk,0.05} \geq 0.2$ and, thus, that the residual tensile capacity of the SFRC must be equal or superior than 20% of $f_{ctk,0.05}$.

In local analyses, for critical cross-sections responsible for the structural equilibrium—of part or the entire structure—, the contribution of fibres has to be disregarded. Likewise, this applies to tying systems for robustness of building (L.12.5) and for connections and supports subjected to compression (L.13.2).

3.4. Stress-strain relation for structural analysis

For structural analysis by means of using numerical tools, a tri-linear constitutive law is proposed (see Figure 9 and Eq. 3-6) for simulating the uniaxial stress-strain of SFRC subjected to tension. The pre-cracking and crack initiation stage are

assimilated to the response of a plain concrete (PC), and the residual response is simulated through a linear strain softening or hardening—depending on the SFRC strength class—until reaching the ultimate tensile uniaxial strain of the material (ϵ_{ftu}). This approach is similar to that proposed in the *fib* Model Code 2010 and the *fib* Bulletin 105 [32,40].

$$f_{Ft1,ef} = k_o k_G 0.37 f_{R,1k} \quad (3)$$

$$f_{Ft3,ef} = k_o k_G (0.57 f_{R,3k} - 0.26 f_{R,1k}) \quad (4)$$

$$\epsilon_{F,0} = 1,2 \epsilon_{ctm} = f_{ctm} / E_{cm} \quad (5)$$

$$\epsilon_{F,0} = \frac{w_u}{l_{cs}} \leq 2,5 \frac{mm}{l_{cs}} < \epsilon_{Fud} = 0.02 \quad (6)$$

In Eq. 3 and 4, k_o is the fibre orientation factor and k_G is the factor accounting for the effect of member size. In Eq. 6, the structural characteristic length l_{cs} is obtained as $l_{cs} = \min(h; s_{r,m,cal,F})$ for members subjected to combined axial and bending and as $l_{cs} = s_{r,m,cal,F}$ for members subjected to uniaxial tension ($s_{r,m,cal,F}$ is the mean crack spacing, see Eq. 16). As it can be observed, l_{cs} can be considered as a double factor considering size effect and synergy of the fibres and rebars contributions. In structural elements with SFRC where cracking pattern is mainly governed by the rebars, l_{cs} is computed as the cracks spacing. For low or not reinforced SFRC, l_{cs} is evaluated as the element depth, as the equivalent hinge length.

When EN 14651 [15] specimens are considered $l_{cs} = 125$ mm as applied in Figure 9. The structural characteristic length l_{cs} is considered jointly with the maximum crack opening (w_u) adopted for ULS to transform the localized crack opening in equivalent strain.

In the case of the stress-strain relation of SFRC subjected to short-term uniaxial compression, the same expression than for PC may be used, but by providing modifications in the compressive strain at mean compressive strength ($\epsilon_{c1}(\%_0) = 0.7f_{cm}^{1/3} (1+0.03f_{R,1k})$) and in the ultimate compressive strain ($\epsilon_{c1} = k \epsilon_{c1}$, where $k = 1 + 20/\sqrt{(82-2.2 f_{R,1k})}$) [51–53].

3.5. Properties of SFRC at high temperature

The Annex B of the FprEN 1992-1-2:2023 [2] provides additional provisions to FprEN 1992-1-1:2023 Annex L [1] for the design of SFRC subjected to high temperatures. Only in this subsection, the Clauses cited are specifically referred to FprEN 1992-1-2:2023 [2].

Strength and deformation properties of SFRC in compression at elevated temperatures may be assumed as those for PC and computed according to the provisions provided in Clause 5. As per uniaxial tension SFRC properties at elevated temperatures, the stress-strain relationships proposed in the Annex L of FprEN 1992-1-1:2023 [1] can be considered; nonetheless, the strength parameters (f_{cm} , $f_{F1,ef}$ and $f_{F3,ef}$) must be affected by a reduction coefficient $f_{ct,\theta}/f_{ctk,0.05}$ ($f_{ct,\theta}$ being the uniaxial tensile strength of concrete at temperature θ) to take into consideration the degradation of the mechanical properties caused by high elevated temperatures. In any case, if design methods given in Clauses 6 and 7 are used, any contribution of fibres shall be neglected.

A formulation to compute the reduction coefficient $f_{ct,\theta}/f_{ctk,0.05}$ is proposed in Clause 5, nevertheless, alternative formulations for deriving the constitutive law for SFRC subjected to uniaxial tensions at high temperatures may be considered provided the results are within the range of experimental evidence. To this end, the research and methods reported in [54–57] might be of reference for this purpose. Likewise, test procedures as those proposed in the RILEM Recommendation TC 129 MHT-part 4 [58] might also provide support to derive the pre- and post-cracking tensile properties of the SFRC subjected to high temperatures.

4. DURABILITY

The second generation of EC-2 brings a radically new concept of design for/verification of durability through the introduction of Exposure Resistance Classes (ERCs) based on performance [1, 12, 59], introduced for carbonation and chloride-induced corrosion (environmental exposure conditions XC, XD and XS). At the same time, an informative Annex P is offered to National Standardization Bodies (NSBs) that actually contains the approach for durability of the current EC-2 [60].

Nonetheless, whichever approach is adopted by an NSB, the concrete cover due to durability requirements, $c_{min,dur}$, in the case of SFRC applies only to the embedded reinforcement.

In other words, for a given element type and environmental exposure conditions, $c_{min,dur}$ is unaffected by the presence of SFs. The only limitation placed on minimum cover in the case of SFRC is to avoid fibre accumulation. Therefore, a minimum cover of $c_{min} = 20$ mm to embedded reinforcement is prescribed for SFRC elements.

Hence, a conservative approach has been adopted – any potential benefit in terms of durability offered by SF inclusion has been neglected as $c_{min,dur}$ is determined in the same way as for an equivalent RC element [61]. At the same time, even though SFs close to the element surface may corrode and cause rust stains, spalling of concrete is unlikely to occur since generated tensile stresses caused by corrosion-derived products from SFs are low due to the small diameter of the fibres [12, 62].

However, the fact that an outer “layer” of fibres might corrode in an SFRC element has caused the adoption of two design approaches which take this into account, differentiating between SFRC elements designed to be uncracked and cracked.

In the case of SFRC elements under environmental exposure conditions XC2–XC4, XD1–XD3, and XS1–XS3, designed to be uncracked at the serviceability limit state (SLS), when verifying those at the ultimate limit state (ULS), the tensile strength of SFRC at the greatest distance from the neutral axis shall be disregarded within a “sacrificial” layer of $c_{f,dur} = 10$ mm from the exposed surface [1] (see Figure 10). It should be noted that this refers to the verification of ULS and the cracked state of the cross-section. The justification for such an approach for uncracked elements is found in recent studies that have shown a modification of bond between the fibres and the matrix in this outermost layer, in particular due to wet–dry exposures [63, 64]. If this occurs, either a decrease/loss of bond may happen, or its increase, which may lead to fibre rupture.

In the case of SFRC elements under environmental exposure conditions XC2–XC4, XD1–XD3, and XS1–XS3, designed to be cracked at the serviceability limit state (SLS), when verifying those at ULS and SLS, the tensile strength of SFRC at the greatest distance from the neutral axis shall be disregarded within a “sacrificial” layer of $c_{f,dur} = k_{dur}c_{min,dur}$ from the exposed surface [1] (see Figure 10). The recommended value of k_{dur} is 0.50, unless defined differently by a National Annex. This provision does not apply for stainless steel fibres nor during the construction phase. The provision rely on relatively recent literature [63–65].

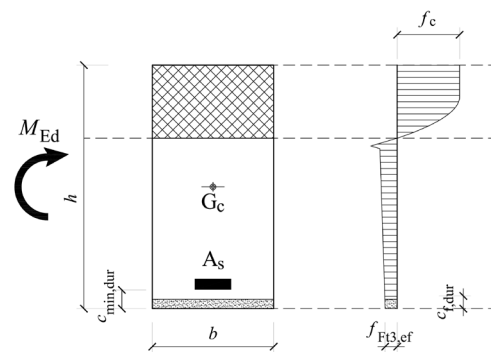


Figure 10. Definition of the “sacrificial” layer $c_{f,dur}$.

One of the main benefits of SFRC, i.e. reduced crack widths, may be taken into account for reducing the depth of the “sacrificial” layer $c_{f,dur}$:

$$c_{f,dur} = k_{dur} c_{min,dur} \frac{w_{k,cal}}{w_{lim,cal}} \geq 10 \text{ mm} \quad (7)$$

where $w_{k,cal}$ and $w_{lim,cal}$ are the calculated and maximum permissible characteristic crack widths, i.e. the “sacrificial” layer depth can be reduced in proportion to the reduction of crack width relative to the limit.

It should be noted that the adopted approach disregards the potential corrosion of SFs on lateral surfaces of linear elements such as beams (i.e. no reduction of tensile strength is considered along the width of a section).

5. STRUCTURAL ANALYSIS – PLASTIC ANALYSIS

The combination of SFRC and longitudinal ordinary reinforcement –both with the suitable SC and quantity, respectively– has proven to provide sufficient rotation capacity of the bending-controlling cross-sections to allow for bending moment redistribution in statically indeterminate structures [14,27,30,32,66].

In this regard, the Annex L allows for a non-linear structural plastic analysis –or linear analysis with limited redistribution of forces– in ULS without a direct check of the capacity rotation in elements without ordinary reinforcement in (1) foundations and slabs supported directly on ground (even without ordinary reinforcement) and (2) for statically indeterminate rafts and pile-supported slabs. For the second group, a SFRC ductility class “c” is necessary and, if the member is needed for structural stability, a ratio $k_G \cdot f_{R,3k} / f_{ctm,fl} \geq 1.0$ (equivalent to bending-hardening response) is required. For this second group of elements, including elevated slabs, the rotation capacity is not necessary to be checked in (1) two-way systems with $L_x/L_y \leq 1.5$ and $A_s \geq A_{s,min}$, and (2) in both one- and two-way systems with $L_x/L_y > 1.5$ and $A_s \geq \alpha_{duct} \cdot A_{s,min}$. $A_{s,min}$ as per Clause L.12 (L_x/L_y). α_{duct} to be considered as 2.0 unless other recommended values are provided within National Annex.

For elements not fulfilling these sets of conditions, the compatibility between the ductility provided by the critical sections and that required for the plastic mechanism assumed (or redistribution level considered) must be checked accordingly. To this end, analyses as conducted in [67] [68] could be used to quantify the rotational capacity of critical SFRC cross-sections.

It must be remarked that, for members not fulfilling these conditions simultaneously, Annex L emphasizes that crack localization effects and, consequently, local reduction of the ductility could occur even if the minimum longitudinal reinforcement $A_{s,min}$ (according to L.12.1) is guaranteed. This aspect has been proved experimentally [69–75] and numerically [68] for statically both determinate and indeterminate beams.

Furthermore, the potential local variations of the residual tensile capacity of the SFRC should be considered appropriately as large cracked sections might present non-uniform ductility capacity.

6. ULTIMATE LIMIT STATES

6.1. Bending

The Annex L provides two simplified stress-strain constitutive models for simulating the residual tensile stress-strain response of SFRC members: a rigid-plastic behaviour and a bi-linear behaviour (see Figure 11).

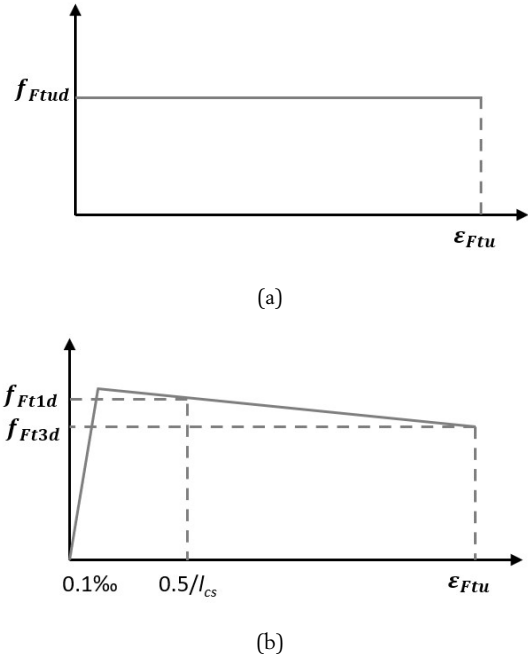


Figure 11. Simplified stress distributions for SFRC: (a) rigid-plastic distribution; (b) bi-linear distribution.

Referred to the bi-linear simplified stress distributions, the residual tensile strength and are defined according to:

$$f_{Ft1d} = f_{Ft1,ef} / \gamma_{SF} \quad (8)$$

$$f_{Ft3d} = f_{Ft3,ef} / \gamma_{SF} \quad (9)$$

The rigid-plastic approach proposed by the Annex L for flexural ULS design is consistent with the rigid-plastic constitutive model provided by the *fib* Model Code [40], which identifies the unique reference value f_{Ftud} as $f_{R3d}/3$ (Formula 5.6-4 in the *fib* Model Code [40]). This approach has proved to be reliable for evaluating the flexural strength of SFRC beams according to [76] and [71,77]. Based on the dataset of 53 SFRC beams assessed in [76], the mean of the model error (ratio of experimental-to-estimated flexural strength) for the *fib* Model Code [40] is 1.011 (coefficient of variation of the model of 8.0%). In addition, the trend of this error reduces with the increase of the SFRC residual flexural strength. Regarding RC beams with fibres, the *fib* Model Code predictions are also consistent according to the experimental program reported in [71,77] carried out on 42 standard beams with different types of fibres and longitudinal reinforcement ratios. Moreover, only for low longitudinal reinforcement ratios (around 0.5%) the addition of fibres significantly improves the flexural strength at ULS.

This rigid-plastic approach can be used for ductility classes a, b and c; for classes d and e, this approach should only be used to determine the ULS moment capacity at the design tensile strain limit ϵ_{Ftud} .

For sectional analysis at ULS (see Figure 12), fibre effect in SFRC is considered as a constant stress under the neutral axis corresponding to the residual tensile strength in uniaxial tension (according to the rigid-plastic model). In compression, parabola-rectangle or rectangular stress distribution proposed for PC can be assumed for SFRC by modifying the compressive strain at the peak stress ($\epsilon_{c2} = 0.0025$) and the ultimate compressive strain ($\epsilon_{cu} = 0.006$). These modifications of compressive strains are based on the studies carried out by Ruiz et al. [51–53] and de la Rosa et al. [78].

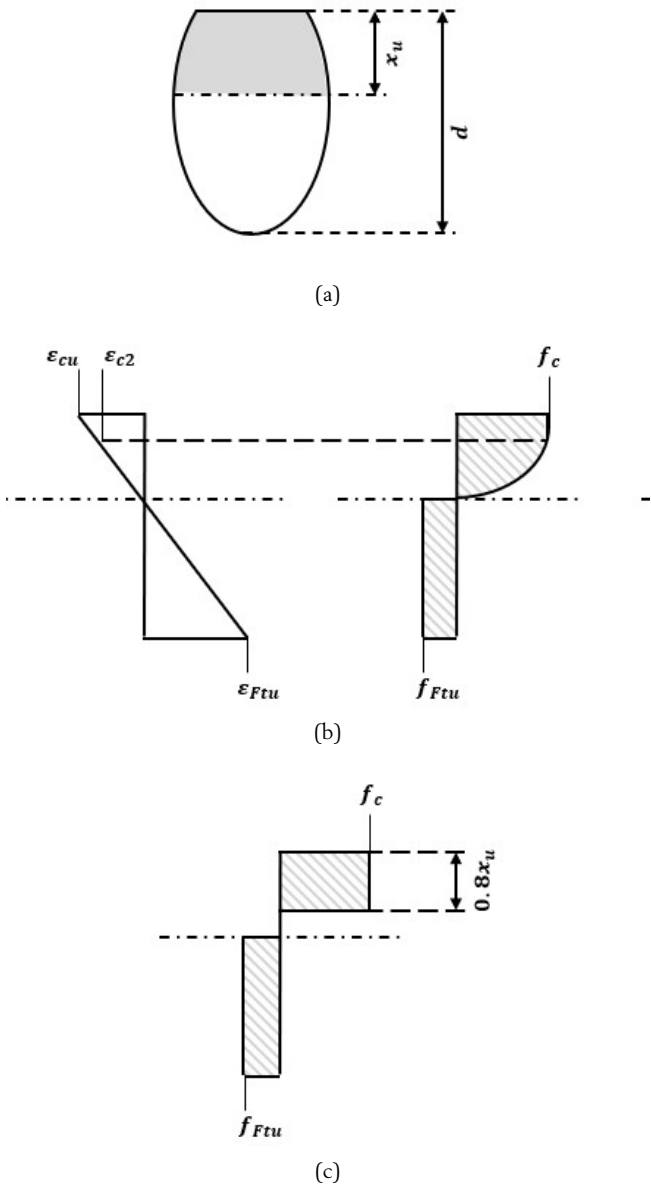


Figure 12. (a) Cross SFRC section; (b) strain distribution in SFRC section; (c) parabola-rectangle stress distribution in compression and constant stress in tension; (d) rectangular stress distribution in compression and constant stress distribution in tension.

6.2. Shear

The presence of steel fibres enhance the shear resistance of SFRC members since these are effective in controlling the opening of inclined cracks induced by shear stresses [79]. In fact, fibres allow a multiple and stable shear crack progression, delaying the formation of a single critical shear crack [80,81]. Hence, the addition of fibres improves the shear transfer across cracks, which results in an improvement of the aggregate interlock capacity [82] and, as a result, in an increase of the shear strength of SFRC members, as it is shown in Figure 13 [80,83–85] and Figure 14 [83,86].

In the Annex L, the shear strength formulation provided for RC members without shear reinforcement is modified to consider the fibre effect in SFRC members according to:

$$\tau_{Rd,cF} = \eta_{cF} \tau_{Rd,c} + \eta_F \tau_{Ftud} \geq \eta_{cF} \tau_{Rd,c,min} + \eta_F f_{Ftud} \quad (10)$$

where $\tau_{Rd,cF}$ is the design shear stress resistance of SFRC members without shear reinforcement, $\tau_{Rd,c}$ is the design shear stress resistance of RC members without shear reinforcement, $\tau_{Rd,c,min}$ is the minimum design shear stress resistance allowing to avoid a detailed verification for shear, $\eta_{cF} = \max(1.2 - 0.5 f_{Ftuk}; 0.4) \leq 1.0$ and $\eta_F = 1.0$.

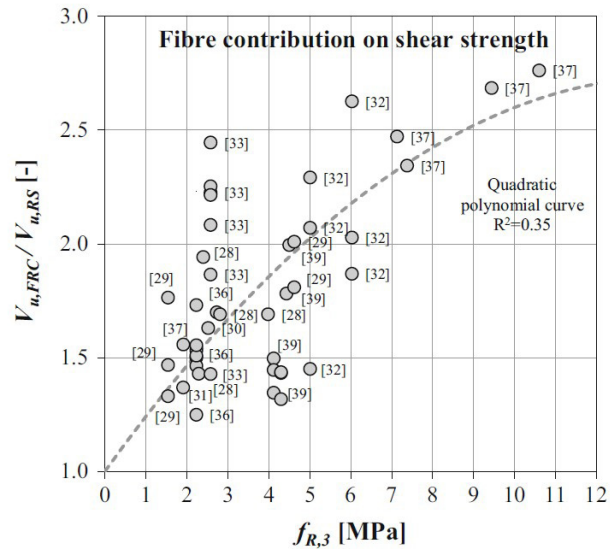


Figure 13. Increase in shear strength due to the effect of fibres in FRC members [87].

As it can be seen, the effect of fibres is described by an additional strength term f_{Ftud} and by introducing the parameter η to express that the fibre reinforcement term is not fully additive to the ordinary reinforced concrete contribution [12]. As for this, the shear strength of RC members is derived from the original formulation of the Critical Shear Crack Theory (CSCT) [88], whose failure criterion describes the shear resistance as a function of the reinforcement strain.

According to the CSCT, the shear resistance of members without stirrups is dependent on the critical shear crack width and on its roughness, since both parameters—influenced by the strain of the reinforcement, the size effect and the aggregate size— govern the aggregate interlock capacity. On this basis,

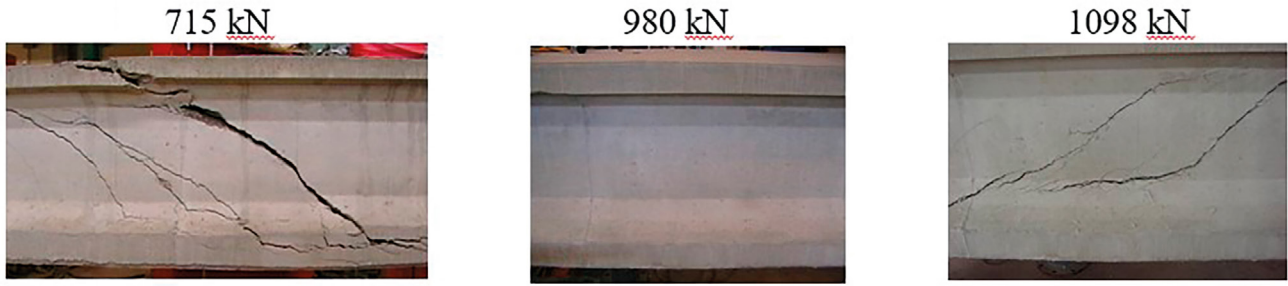


Figure 14. Shear crack patterns in prestressed beams with the same amount of transversal ordinary steel reinforcement for: (a) no fibres at 715 kN and SFRC for (b) 980 kN and (c) 1098 kN. [83,86].

close-form expressions for the calculation of the shear strength are proposed considering an improved general failure criterion—based on the refinement of the mechanical of the CSCT [89]—in combination with the load-deformation relationship. These new expressions have been validated considering a database with 669 shear tests resulting in good agreement when compared with test results and with no trends for the parameters investigated—shear span-to-effective depth ratio, longitudinal reinforcement, effective depth, width-to-effective depth ratio, compressive strength of the material, aggregate size [12].

Regarding the performance of SFRC members, a comprehensive shear database of 171 elements (93 in FRC and their 78 related in RC) was analysed in [87] to allow the development and validation of shear formulations. In this sense, it has been proved that the ratio shear span-to-effective depth ratio, the longitudinal reinforcement and the compressive strength of the material have similar influence on the shear strength both in RC and FRC members; however, it is different in the case of the size effect in shear. Related to this, the experimental results reported in [81] proved that fibres substantially mitigate the size effect in shear, showing that for effective depths above 1 m this effect is quite limited. Nevertheless, further studies are necessary to confirm this trend.

For SFRC members with shear reinforcement, Annex L also considers the fibre effect by an additional strength and by introducing the parameter f_{Ftud} to express that the fibre reinforcement and reinforced concrete contributions are not fully additive. The formulation provided results in:

$$\tau_{Rd,sF} = (\eta_{sw} \rho_w f_{ywd} + \eta_F f_{Ftud}) \cot \theta \geq \rho_w f_{ywd} \cot \theta \quad (11)$$

where $\tau_{Rd,sF}$ is the design shear stress resistance of SFRC members with shear reinforcement, ρ_w is the shear reinforcement ratio, f_{ywd} is the design yield strength of the shear reinforcement, f_{Ftud} is the design ultimate residual strength of ULS, θ is the angle of the compression field, $\eta_{sw} = 0.75$ and $\eta_F = 1.0$.

6.3. Punching shear

Several studies [90–93] have confirmed the effect of fibres for increasing the punching shear strength of SFRC slabs as well as their deformational capacity. This improvement is due to the bridging action of the fibres after the cracking of the concrete matrix [94]. Although this particular mechanical behaviour of

SFRC slabs, code provisions have been adapted from the formulation of the RC elements [94]. Nevertheless, several specific models for punching shear of slab-column connections for elements with fibres have been proposed over the last decades [91,95–97]. In this regard, [94] gathers 140 test results from 13 different studies for assessing the punching shear strength of SFRC slab-column connections based on the CSCT [98,99]. It was confirmed that the concrete contribution to the punching strength decreases with the increase of the slab rotation, whereas the contribution of the fibres increases with it (see Figure 15).

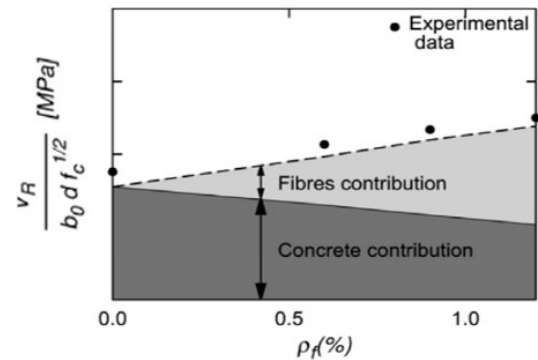


Figure 15. Fibres contribution to the punching shear strength for elements tested by Swamy and Ali [100] as reported in [94].

In a similar way that in the case of shear, the Annex L provides a punching shear formulation based on the CSCT considering an additional contribution to the punching shear stress resistance due to the presence of fibres. However, this contribution is not fully additive, as it is considered the parameter $\eta_c = 0.4$. For SFRC without shear reinforcement, the punching shear resistance is obtained according to:

$$\tau_{Rd,cF} = \eta_c \tau_{Rd,c} + \eta_F f_{Ftud} \geq \eta_c \tau_{Rdc,min} + f_{Ftud} \quad (12)$$

where $\tau_{Rd,cF}$ is the design punching shear stress resistance of SFRC members without shear reinforcement, $\tau_{Rd,c}$ is the design punching shear stress resistance of RC members without shear reinforcement, f_{Ftud} is the design ultimate residual strength of ULS, $\tau_{Rdc,min}$ is the minimum design punching shear stress resistance allowing to avoid a detailed verification for punching shear, $\eta_c \leq 1.0$ and $\eta_F = 0.4$.

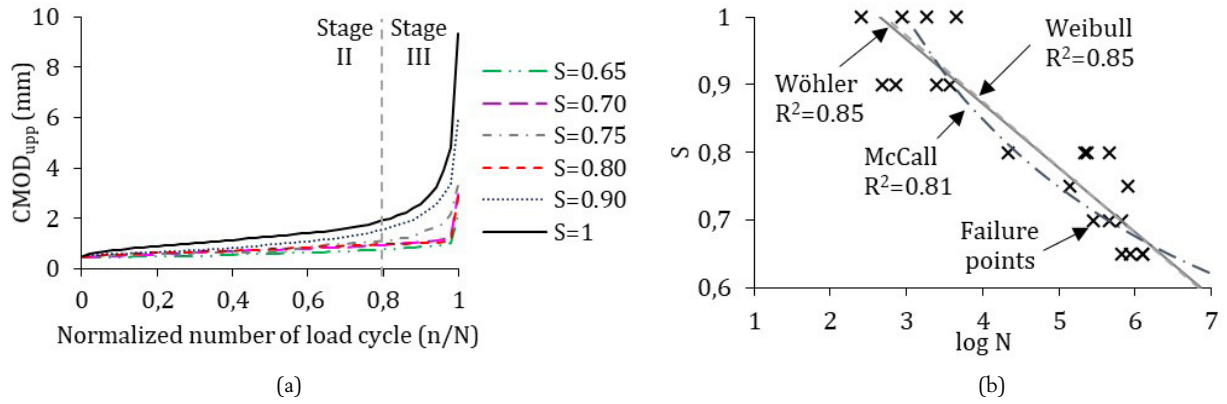


Figure 16. (a) CMOD - n/N for different S and (b) different semi-probabilistic approaches for fitting the S - log N curves obtained experimentally.

In the case of elements with shear reinforcement, the contribution is also not fully additive and the punching shear resistance is obtained as follows:

$$\tau_{Rd,csF} = \eta_c \tau_{Rd,c} + \eta_s \rho_w f_{yw} + \eta_F f_{Ftud} \geq \rho_w f_{yw} + \eta_F f_{Ftud} \quad (13)$$

where $\tau_{Rd,csF}$ is the design punching shear stress resistance of SFRC members with shear reinforcement, $\tau_{Rd,c}$ is the design punching shear stress resistance of RC members without shear reinforcement, ρ_w is the shear reinforcement ratio, f_{yw} is the design yield strength of the shear reinforcement, f_{Ftud} is the design ultimate residual strength of ULS, $\eta_c \leq 1.0$, $\eta_s = 0.75$ and $\eta_F = 0.4$.

6.4. Torsion

The provisions for torsion follow the philosophy adopted for shear: consideration of fibres as a smeared/distributed reinforcement and a reduction of the reinforced concrete (RC) contribution to torsion resistance as it is not considered fully additive with the fibre contribution:

$$\tau_{t,Rd,swF} = \eta_{sw} \tau_{t,Rd,sw} + \eta_F f_{Ftud} \geq \tau_{t,Rd,sw} \quad (14)$$

$$\tau_{t,Rd,slF} = \eta_{sw} \tau_{t,Rd,sl} + \eta_F f_{Ftud} \geq \tau_{t,Rd,sl} \quad (15)$$

where $\tau_{t,Rd,swF}$ and $\tau_{t,Rd,sw}$ are the torsional capacities of SFRC and RC, respectively, when governed by the yielding of the shear reinforcement; $\tau_{t,Rd,slF}$ and $\tau_{t,Rd,sl}$ are the torsional capacities of SFRC and RC, respectively, when governed by the yielding of the longitudinal reinforcement; f_{Ftud} is the design ultimate residual strength of SFRC; $\eta_{sw} = 0.75$ and $\eta_F = 1.0$. The torsional capacities $\tau_{t,Rd,sw}$ and $\tau_{t,Rd,sl}$ are calculated as for RC members according to the main text of EC-2 [1].

Additionally, when an SFRC member is subjected to a combination of torsion and shear and/or bending, two approaches are possible:

- considering that the fibre contribution is used to resist only torsional effects, or
- considering that the fibre contribution is used to resist only shear and/or bending effects (disregarding the fibre contribution to resisting torsional effects).

The provisions were tested on only a small number of available results [101], but a large safety margin was observed, justifying the approach [12].

6.5. Fatigue

Due to divergences found within the literature concerning the performance fatigue of FRC, the CEN/TC250/SC2 agreed on disregarding any potential contribution of steel fibres in compressive and/or tensile fatigue-induced stresses unless this contribution is proved by testing.

In this regard, there already exist SFRC structures designed to be subjected to fatigue-inducing loads, and allowed to crack in service conditions, as for instance: (1) rail-tracks embedded SFRC platforms [102,103], (2) floors and pavements [104] – the Spanish ROM 4.1-94 [105] allows the use of steel fibres as unique reinforcement of concrete pavements subjected to aggressive marine environments in combination with heavy static and dynamic loads–, (3) precast concrete towers for wind turbines [106], and others. Likewise, within the literature, there are several experimental programs and semi-probabilistic models on fatigue performance of cracked SFRC members subjected to direct tension [107,108], compression [109,110] and flexural [111–115] fatigue. Experimental constitutive crack mouth opening displacement (CMOD) - number of fatigue cycles (n) for pre-cracked SFRCs beams subjected to fatigue (Figure 16a) were provided in [114]. Likewise, several semi-probabilistic models (Figure 16b) that relate the load level (S) with the number of cycles to failure (N) were fitted based on experimental results.

As noted by the CEN/TC250/SC2, the scientific literature and current state-of-art on fatigue performance of SFRC allow confirming the marked stochastic nature –specially in pre-cracked elements subjected to direct tension or flexure– of the fatigue response of SFRC. Likewise, it is confirmed that there are numerous variables (i.e., pre-crack width, frequency and load range, amount and type of fibres, and others) which makes it difficult, at the current extent of knowledge, the derivation of general and robust conclusions and, thus, standardized provisions for fatigue of SFRC components.

7. SERVICEABILITY LIMIT STATES (SLS)

7.1. Crack control

One of the most well-known and proven benefits of using SFRC is crack control – the decrease of crack spacing and consequent decrease of crack widths. The new EC-2 presents an updated refined control of cracking relative to the current version, but the verification philosophy remains the same: a characteristic crack width is obtained by multiplying the calculated mean crack spacing $s_{r,m,cal}$ with the difference between the mean strain in the reinforcement and the mean strain in concrete ($\varepsilon_{sm} - \varepsilon_{cm}$) and multiplied by a factor k_w (1.7 if not specified otherwise by a National Annex) converting the mean crack width into a characteristic crack width (in fact the new EC-2 introduces one more factor $k_{1/r}$ that takes into account the increase in crack width due to curvature).

For SFRC, two cases are considered: (1) a multi-crack pattern associated to a presence of conventional reinforcement at a spacing $\leq 10\emptyset$ and (2) a single-crack pattern when the spacing of conventional reinforcement is larger than $10\emptyset$. In the first case, the expression for $s_{r,m,cal}$ for RC is converted into $s_{r,m,cal,F}$ by multiplication of the second term of the original equation by $(1 - \alpha_f)$:

$$\tau_{r,m,cal,F} = 1.5 c + \frac{k_{fl} k_b}{7.2} \frac{\phi}{\rho_{p,eff}} (1 - \rho_f) \quad (16)$$

where c is the clear cover of the longitudinal reinforcement, k_{fl} is a factor accounting for the cross-section area in tension, k_b is a factor accounting for bond conditions, ϕ is the bar diameter, $\rho_{p,eff}$ is the reinforcement ratio of the effective tensile zone and $(1 - \rho_f)$ is an expression accounting for the crack arresting effect of SFRC as:

$$\alpha_f = \frac{f_{Fr1,ef}}{f_{ctm}} \leq 1.0 \quad (17)$$

In other words, the ratio of the effective residual strength associated to SLS (and a strain $0.5/l_{cs}$) to the axial tensile strength determines the crack spacing reduction, with a minimum value of $1.5c$ at $f_{Fr1,ef} = f_{ctm}$. The performance of the expression was validated on experimental results [116].

In the second case of elements with a single-crack pattern, the calculated mean crack spacing is given simply as:

$$s_{r,m,cal,F} = h - x \quad (18)$$

where x is the depth of the compression zone.

A final important point is that the conversion factor k_w is 1.7 and 1.3 for cases (1) and (2), i.e. multi-crack and single-crack patterns, respectively (though these values can be changed as the Annex L is informative and clause 9.2.3(2) of the main text declares k_w a nationally determined parameter with a recommended value of 1.7).

7.2. Deflection control

The Annex L does not explicitly deal with deflection control nor provide direct guidance or provision for indirect or direct

deflection control of SFRC members. Considering that, except for lightly reinforced SFRC members subject to clause L.14, all SFRC members compliant with provisions of Annex L will be reinforced with at least the minimum longitudinal steel reinforcement, it is safe to assume that the general ζ -method of interpolating curvatures (or deflections) [1] is applicable to SFRC members as well.

In particular, at the fibre and fibre–matrix level, no significant effect of steel fibre and fibre–matrix creep is observed at normal temperatures [117]. However, at the structural level, several phenomena should be considered. Firstly, the presence of steel fibres will affect the tension stiffening, i.e. the contribution of concrete in tension between two cracks (affecting the ζ interpolation coefficient), and secondly, the moment of inertia of a “fully cracked” SFRC section will be larger than a corresponding RC one due to the presence of fibres.

Although there is still no direct integration of these aspects into the ζ -method, some research exists showing the way forward. Namely, in [118] an extension of the so-called tension chord model (TCM) to SFRC to model the tension stiffening effect is proposed. This model allowed to define tension stiffening stresses for minimum and maximum crack spacing scenarios. Following this result, in [119] the TCM model for SFRC to calculating instantaneous deflections of members in bending was applied; however, not following the approach of the ζ -method but the deflection calculation method originally proposed in [120].

Therefore, work remains in this regard, both at the experimental level as full-scale sustained load tests on SFRC are scarce [121–123], as well as with regards to models that need to be developed.

8. DETAILING OF MEMBERS AND PARTICULAR RULES

8.1. General rules for minimum reinforcement

The residual bending capacity in ULS of a SFRC cross-section subjected to bending (and a concomitant design axial force, N_{Ed}) shall be superior to its cracking bending capacity (Eq. 19) to guarantee a ductile response immediately after the cracking.

$$M_{R,min}(N_{Ed}) \geq M_{cr}(N_{Ed}) \quad (19)$$

For computing $M_{R,min}$, the effective residual tensile strength of the SFRC in ULS ($f_{Ftu,ef}$) can be considered. The reduced $A_{s,min}$ due to the contribution of the fibres that satisfies Eq. 19 shall be compliant with the criteria presented in subsection 8.2.

The similar approach shall be considered for cross-sections subjected to pure tensile axial force ($M_{Rd} = 0$) by computing $A_{s,min}$ through the application of Eq. 19. $N_{R,min}$ and N_{cr} are the pure tensile capacity of SFRC in ULS and against cracking, respectively.

$$N_{R,min} \geq N_{cr} \quad (20)$$

Similarly, the effective contribution of fibres can be considered in ULS for shear and torsion resistant mechanisms. The



a)



b)



c)



d)

Figure 17. SFRC segments subjected to loading transient situations inducing bending forces: (a) demoulding; (b) stacking; (c) manipulation and (d) final transport operation.

minimum shear reinforcement ratio ($\rho_{Fw,min}$) in SFRC elements requiring shear or torsion reinforcement can be computed by means of Eq. 21.

$$\rho_{Fw,min} = \rho_{w,min} - \frac{f_{Ftu,ef}}{f_{yk}} \geq 0 \quad (21)$$

where $\rho_{w,min}$ being the minimum transverse reinforcement, f_{yk} the characteristic value of the steel (bars) yielding strength, and $f_{Ftu,ef} \geq 0.08 \cdot \sqrt{f_{ck}}$.

The minimum torsion reinforcement ratio ($\rho_{Fw,min}$) for SFRC requiring longitudinal and transverse reinforcement can be computed –for both types of reinforcements– according to Eq. 22.

$$\rho_{Fw,min} \geq \rho_{w,min} - \frac{f_{Ftu,ef}}{f_{yk}} \geq 0.3 \frac{f_{ctm}}{f_{yk}} \quad (22)$$

8.2. Particular rules for minimum reinforcement

For *beams*, the $A_{s,min}$ –minimum longitudinal reinforcement as per sectional ductility according to 9.2.2 of EC-2– should be always guaranteed independently of the structural redundancy level of the beam. Contrarily, both the shear and torsion reinforcement can be totally replaced by the contribution of fibres if $f_{Ftu,ef}/f_{yk} \geq \rho_{Fw,min}$ and the other general rules presented in 8.1 are fulfilled.

In case of slabs, the Annex L allows for partial replacement of the longitudinal reinforcement, and for a reduction of $A_{s,min}$

so that $A_{s,min} \geq k_{AS} A_{s,min}$ (0.5 unless a country's National Annex establishes a different value). The secondary reinforcement in one-way slabs may be fully replaced by steel fibres. Regarding shear reinforcement, this may be fully replaced by steel fibres if the inequalities $f_{Ftu,ef}/f_{yk} \geq \rho_{Fw,min}$ and $f_{Ftu,ef} \geq 0.08 \cdot \sqrt{f_{ck}}$ are satisfied.

Finally, for walls and deep beams, both vertical ($A_{s,min,v}$) and horizontal ($A_{s,min,h}$) minimum reinforcement computed according to Eq. 19 may be fully replaced.

9. LIGHTLY REINFORCED SFRC STRUCTURES

The Clause L.14 covers the design and detailing of structural SFRC elements reinforced with longitudinal reinforcement inferior to $A_{s,min}$. This clause may be only applied to statically indeterminate structures –some of those are identified in the Clause L.14.1.

As per understanding of the authors of this paper, other elements as those (1) designed no to crack –in either transient or permanent loading situations– and (2) that both the SFRC SC and ductility are sufficient to prevent the element from a fragile response in the unlikely event of cracking could also be covered by Clause L.14. This would be the case of, for example, precast SFRC segments for tunnel linings (Figure 17) since

these undergo transient loading situations (i.e., demoulding, staking, transport, manipulation) in which the segments are statically supported and subjected to bending [124–129].

It is remarked that ductility should be ensured -providing a suitable combination of fibres and longitudinal reinforcement- to avoid structural collapse in case of brittle failure in members constructed with crack-controlling joints. Likewise, it is emphasized that –independently of the minimum longitudinal reinforcement designed for both ductility and strength requirements– the reinforcement for SLS of cracking and for any local/global ULS must be designed accordingly.

For elements without longitudinal reinforcement, the residual shear strength of the SFRC in ULS ($\tau_{R,d,cF}$) may be taken as f_{Tud} . Likewise, the Annex L remarks that lightly reinforced SFRC elements subjected to punching are not covered and have to be assessed by rigorous analyses.

Apart from other provisions within this Clause L.14, the Annex L specifies minimum SFRC strength and ductility classes for foundations directly on ground (1b), foundations on piles (2c) and tunnel lining segments without additional longitudinal reinforcement (4c). The latter specification is aligned with the recommendations gathered *fib* Bulletin 83 [130] and with outcomes reported in [131–133].

10. CONCLUSIONS

Since the DBV 2001 [4], the first national standard regulating the structural use of steel fibres, to the recently approved Spanish Structural Code 2020 [134], the Annex L of the new EC-2 represents a compendium of experience and knowledge related to the structural use (design, execution and quality control) of SFRC and a reference for the European countries.

The Annex L provides guide to design SFRC structures of any typology and of any structural responsibly (consequence failure class). Therefore, as SFRC has been introduced in the harmonized European guidelines for the first time, in order to adopt a prudent approach among the numerous member countries of CEN, the Annex L has the status of an Informative Annex and each CEN member has to decide its status within the country.

The scientific community is intensively researching on open topics to provide methods and tools that allow optimized design of SFRC components by considering the resistant mechanisms more accurately, as well as improved quality control procedures. A significant part of this research is promoted and boosted by the construction sector, which has seen interest in this material due to the identified (and proved) technical benefits as well as the enhanced sustainability performance respect to existing alternatives in a large variety of applications.

Notation

A_{ct} Tension area of the concrete cross section
 A_s Cross-sectional area of ordinary reinforcement
 $A_{s,min}$ Minimum cross-sectional area of reinforcement
 M_{cr} Cracking moment of the section in presence of the simultaneous axial force N_{Ed}

$M_{R,min}$ Bending strength of the section with $A_{s,min}$ in presence of the simultaneous axial force N_{Ed}
 N_{Ed} Design value of the applied axial force
 c Concrete cover
 c Minimum concrete cover
 c Minimum concrete cover c due to durability requirement
 d Effective depth of a cross section
 E_c Secant modulus of elasticity of concrete
 f_{cm} Compressive strength of concrete
 f_{ctm} Characteristic concrete cylinder compressive strength
 $f_{ct,0}$ Mean concrete cylinder compressive strength
 $f_{ctk,0.05}$ Characteristic axial tensile strength of concrete (5% fractile)
 f_{ctm} Mean axial tensile strength of concrete
 $f_{ctm,fl}$ Mean flexural tensile strength of concrete
 $f_{ct,\theta}$ Tensile strength of concrete at temperature θ
 $f_{Fts,ef}$ Effective value of the service residual strength (SFRC)
 f_{Ftsd} Design value of the service residual strength (SFRC)
 f_{Ftsk} Characteristic value of the service residual strength (SFRC)
 $f_{Ftu,ef}$ Effective value of the ultimate residual strength (SFRC)
 f_{Ftud} Design value of the ultimate residual strength (SFRC)
 f_{Ftuk} Characteristic value of the ultimate residual strength (SFRC)
 f_R Residual flexural strength (SFRC)
 $f_{R,ld}$ Design value of the residual flexural strength for crack mouth opening displacements of 0.5 mm (SFRC)
 $f_{R,1k}$ Characteristic value of the residual flexural strength for crack mouth opening displacements of 0.5 mm (SFRC)
 $f_{R,3d}$ Design value of the residual flexural strength for crack mouth opening displacements of 2.5 mm (SFRC)
 $f_{R,3k}$ Characteristic value of the residual flexural strength for crack mouth opening displacements of 2.5 mm (SFRC)
 f_{Rk} Characteristic value of the residual flexural strength (SFRC)
 f_{yk} Characteristic value of yield strength of reinforcement
 f_{ywd} Design yield strength of shear reinforcement
 h Overall depth of a cross section
 k_G Factor accounting for the effect of member size (SFRC)
 k_o Fibre orientation factor (SFRC)
 l_{cs} Structural characteristic length
 $s_{rm,cal,F}$ Calculated mean crack spacing (SFRC)
 $w_{k,cal}$ Calculated crack width
 $w_{lim,cal}$ Limiting crack width to be compared with the calculated crack width $w_{k,cal}$
 w_u Maximum crack opening at the ultimate limit state (SFRC)
 x Depth of concrete in compression
 x_u Depth of the neutral axis at the ultimate limit state after redistribution
 γ_{SF} Partial factor for fibers in concrete
 ϵ_{c1} Compressive strain in the concrete at mean compressive strength
 ϵ_{c2} Compressive strain in the concrete at the peak stress f_c
 ϵ_{cm} Mean strain in the concrete between cracks at the same level of ϵ_{sm}
 ϵ_{ctm} Mean strain in the concrete at peak stress f_{ctm}
 ϵ_{cu} Ultimate compressive strain in the concrete
 $\epsilon_{F,0}$ Strain in the concrete equal to $2 \cdot \epsilon_{ctm}$ (SFRC)
 ϵ_{Ftu} Ultimate tensile strain in concrete (SFRC)
 ϵ_{Ftud} Design value of the ultimate tensile strain in concrete (SFRC)
 ϵ_{sm} Mean strain in the reinforcement closest to the most tensioned concrete surface under the relevant

	combination of actions.
θ	Angle between the compression field and the member axis
$\rho_{p,eff}$	Tensile reinforcement ratio accounting for the different bond properties of reinforcing bars referred to the effective concrete area
ρ_w	Shear reinforcement ratio
$\rho_{Fw,min}$	Minimum shear reinforcement ratio (SFRC)
$\rho_{w,min}$	Minimum shear reinforcement ratio
$\rho_{Rd,c}$	Design stress resistance of members without shear reinforcement
$\rho_{Rd,cF}$	Design stress resistance of members without shear reinforcement (SFRC)
$\rho_{Rd,csF}$	Design stress resistance of planar members with shear reinforcement (SFRC)
$\rho_{Rd,sF}$	Design stress resistance of members with shear reinforcement (SFRC)
$\rho_{Rde,min}$	Minimum shear stress resistance allowing to avoid a detailed verification of shear (SFRC)
\emptyset	Diameter of a reinforcing bar

References

- [1] FprEN 1992-1-1:2023, Eurocode 2: Design of concrete structures – Part 1-1: General rules, rules for buildings, bridges and civil engineering structures, CEN, Brussels, 2023. This document is available through the National members at CEN TC250/SC Eurocode 2.
- [2] FprEN 1992-1-2:2023, Eurocode 2: Design of concrete structures – Part 1-2: General rules - Structural fire design, CEN, Brussels, 2023. This document is available through the National members at CEN TC250/SC Eurocode 2.
- [3] M. di Prisco, G. Plizzari, L. Vandewalle, Fibre reinforced concrete: new design perspectives, *Mater. Struct.* 42 (2009) 1261–1281. <https://doi.org/10.1617/s11527-009-9529-4>.
- [4] DBV-Merkblatt, *Stahlfaserbeton*, 2001.
- [5] RILEM TC162-TDF, Test and design methods for steel fibre reinforced concrete σ - ε design method, *Mater. Struct. Constr.* 36 (2003) 560–567. <https://doi.org/10.1617/14007>.
- [6] CNR-DT 204/2006, Guide for the Design and Construction of Fiber-Reinforced Concrete Structures, Rome, 2007.
- [7] EHE, Instrucción de Hormigón Estructural (EHE-08), 2008. <https://doi.org/10.1017/CBO9781107415324.004>.
- [8] SS 812310, Fibre Concrete - Design of Fibre Concrete Structures, 2014.
- [9] A. de la Fuente, A. Blanco, J. Armengou, A. Aguado, Sustainability based-approach to determine the concrete type and reinforcement configuration of TBM tunnels linings. Case study: Extension line to Barcelona Airport T1, *Tunn. Undergr. Sp. Technol.* 61 (2017) 179–188. <https://doi.org/10.1016/j.tust.2016.10.008>.
- [10] A. de La Fuente, M.D.M. Casanovas-Rubio, O. Pons, J. Armengou, Sustainability of Column-Supported RC Slabs: Fiber Reinforcement as an Alternative, *J. Constr. Eng. Manag.* 145 (2019) 1–12. [https://doi.org/10.1061/\(ASCE\)CO.1943-7862.0001667](https://doi.org/10.1061/(ASCE)CO.1943-7862.0001667).
- [11] I. Josa, A. de la Fuente, M.M. del M. Casanovas-Rubio, J. Armengou, A. Aguado, Sustainability-oriented model to decide on concrete pipeline reinforcement, *Sustain.* 13 (2021) 3026. <https://doi.org/10.3390/su13063026>.
- [12] CEN/TC 250/SC 2/WG 1, Background Document for prEN 1992-1-1:2021, Brussels, 2021. This document is available through the National members at CEN TC250/SC Eurocode 2.
- [13] EN 1990, Eurocode - Basis of structural design, CEN, Brussels, 2002.
- [14] M. Di Prisco, M. Colombo, D. Dozio, Fibre-reinforced concrete in fib Model Code 2010: principles, models and test validation, *Struct. Concr.* 14 (2013) 342–361. <https://doi.org/10.1002/SUCO.201300021>.
- [15] EN 14651, Test method for metallic fibred concrete — Measuring the flexural tensile strength (limit of proportionality (LOP), residual), *Br. Stand. Inst.* (2005). <https://doi.org/9780580610523>.
- [16] G. Tiberti, F. Germano, A. Mudadu, G.A. Plizzari, An overview of the flexural post-cracking behavior of steel fibre reinforced concrete, *Struct. Concr.* 19 (2018) 695–718. <https://doi.org/10.1002/suco.201700068>.
- [17] E. Galeote, Á. Picazo, M.G. Alberti, A. De La Fuente, A. Enfedaque, J. Gálvez, A. Aguado, Statistical analysis of an experimental database on residual flexural strengths of fiber reinforced concretes: Performance-based equations, *Struct. Concr.* (2022) 1–14.
- [18] S.H.P. Cavalaro, A. Aguado, Intrinsic scatter of FRC: an alternative philosophy to estimate characteristic values, *Mater. Struct. Constr.* 48 (2015) 3537–3555. <https://doi.org/10.1617/s11527-014-0420-6>.
- [19] P. Martinelli, M. Colombo, A. de la Fuente, S. Cavalaro, P. Pujadas, M. di Prisco, Characterization tests for predicting the mechanical performance of SFRC floors: design considerations, *Mater. Struct. Constr.* 54 (2021). <https://doi.org/10.1617/s11527-020-01598-2>.
- [20] P. Martinelli, M. Colombo, P. Pujadas, A. de la Fuente, S. Cavalaro, M. di Prisco, Characterization tests for predicting the mechanical performance of SFRC floors: identification of fibre distribution and orientation effects, *Mater. Struct. Constr.* 54 (2021). <https://doi.org/10.1617/s11527-020-01593-7>.
- [21] G. Žirgulis, O. Švec, E.V. Sarmiento, M.R. Geiker, A. Cwirzen, T. Kanstad, Importance of quantification of steel fibre orientation for residual flexural tensile strength in FRC, *Mater. Struct. Constr.* 49 (2016) 3861–3877. <https://doi.org/10.1617/S11527-015-0759-3/METRICS>.
- [22] M. di Prisco, P. Martinelli, D. Dozio, The structural redistribution coefficient KRd: a numerical approach to its evaluation, *Struct. Concr.* 17 (2016) 390–407. <https://doi.org/10.1002/SUCO.201500118>.
- [23] JCSS, Probabilistic Model Code, 2001.
- [24] V. Cugat, S.H.P.P. Cavalaro, J.M. Bairán, A. de la Fuente, Safety format for the flexural design of tunnel fibre reinforced concrete precast segmental linings, *Tunn. Undergr. Sp. Technol.* 103 (2020) 103500. <https://doi.org/10.1016/j.tust.2020.103500>.
- [25] J.M. Bairán, N. Tošić, A. De La Fuente, Reliability-based assessment of the partial factor for shear design of fibre reinforced concrete members without shear reinforcement, *Mater. Struct. Constr.* 54 (2021) 185. <https://doi.org/10.1617/s11527-021-01773-z>.
- [26] V. Cervenka, Reliability-based non-linear analysis according to fib Model Code 2010, *Struct. Concr.* 14 (2013) 19–28. <https://doi.org/10.1002/SUCO.201200022>.
- [27] L. Facconi, G. Plizzari, F. Minelli, Elevated slabs made of hybrid reinforced concrete: Proposal of a new design approach in flexure, *Struct. Concr.* 20 (2019) 52–67. <https://doi.org/10.1002/SUCO.201700278>.
- [28] A. Nogales, A. de la Fuente, Numerical-aided flexural-based design of fibre reinforced concrete column-supported flat slabs, *Eng. Struct.* 232 (2021). <https://doi.org/10.1016/j.engstruct.2020.111745>.
- [29] S. Aidarov, F. Mena, A. de la Fuente, Structural response of a fibre reinforced concrete pile-supported flat slab: full-scale test, *Eng. Struct.* 239 (2021). <https://doi.org/10.1016/j.engstruct.2021.112292>.
- [30] S. Aidarov, N. Tošić, A. de la Fuente, A limit state design approach for hybrid reinforced concrete column-supported flat slabs, *Struct. Concr.* 23 (2022) 3444–3464. <https://doi.org/10.1002/SUCO.202100785>.
- [31] EN 14889-1, Fibres for concrete - Part 1: Steel fibres, Brussels, 2006.
- [32] fib Bulletin 105, Fibre Reinforced Concrete, Lausanne, 2023.
- [33] E. Garcia-Taengua, S. Arango, J.R. Martí-Vargas, P. Serna, Flexural creep of steel fiber reinforced concrete in the cracked state, *Constr. Build. Mater.* 65 (2014) 321–329. <https://doi.org/10.1016/j.conbuildmat.2014.04.139>.
- [34] A. Llano-Torre, P. Serna Ros, S.H. Palarissi Cavalaro, International round robin test on creep behavior of FRC supported by the RILEM TC 261-CCF, FRC Mod. Landscape. BEFIB 2016. Proc. 9th RILEM Int. Symp. Fibre Reinf. Concr. (2016) 127–140. <https://upcommons.upc.edu/handle/2117/94235> (accessed February 18, 2023).
- [35] A. Llano-Torre, P. Serna, S.H.P. Cavalaro, International Round-Robin Test on Creep Behaviour of FRC - Part 2: An Overview of Results and Preliminary Conclusions, RILEM Bookseries. 36 (2022) 291–306. https://doi.org/10.1007/978-3-030-83719-8_26/COVER.
- [36] G. Plizzari, P. Serna, Structural effects of FRC creep, *Mater. Struct. Constr.* 51 (2018) 1–11. <https://doi.org/10.1617/s11527-018-1290-0>.
- [37] P. Serna, S. Arango, T. Ribeiro, A.M. Núñez, E. Garcia-Taengua, Structural cast-in-place SFRC: Technology, control criteria and recent applications in Spain, *Mater. Struct. Constr.* 42 (2009) 1233–1246. <https://doi.org/10.1617/S11527-009-9540-9/METRICS>.

- [38] E.S. Bernard, G.G. Xu, Estimation of Population Standard Deviation for Post-Crack Performance of Fiber-Reinforced Concrete, *Adv. Civ. Eng. Mater.* 6 (2017) 68–82.
- [39] E.S. Bernard, G.G. Xu, Normality of post-crack performance data for fiber-reinforced concrete, *Adv. Civ. Eng. Mater.* 8 (2019) 145–157.
- [40] FIB, fib Model Code for Concrete Structures 2010, International Federation for Structural Concrete (fib), Lausanne, 2013. <https://doi.org/10.1002/9783433604090>.
- [41] M. Di Prisco, L. Ferrara, M.G.L. Lamperti, Double edge wedge splitting (DEWS): An indirect tension test to identify post-cracking behaviour of fibre reinforced cementitious composites, *Mater. Struct. Constr.* 46 (2013) 1893–1918. <https://doi.org/10.1617/S11527-013-0028-2/METRICS>.
- [42] C. Molins, A. Aguado, S. Saludes, Double punch test to control the energy dissipation in tension of FRC (Barcelona test), *Mater. Struct. Constr.* 42 (2009) 415–425. <https://doi.org/10.1617/s11527-008-9391-9>.
- [43] P. Pujadas, A. Blanco, S.H.P.P. Cavalaro, A. De La Fuente, A. Aguado, Multidirectional double punch test to assess the post-cracking behaviour and fibre orientation of FRC, *Constr. Build. Mater.* 58 (2014) 214–224. <https://doi.org/10.1016/j.conbuildmat.2014.02.023>.
- [44] P. Pujadas, A. Blanco, S. Cavalaro, A. De La Fuente, A. Aguado, New Analytical Model To Generalize the Barcelona Test Using Axial Displacement, *J. Civ. Eng. Manag.* 19 (2013) 259–271. <https://doi.org/10.3846/13923730.2012.756425>.
- [45] E. Galeote, A. Blanco, S.H.P.P. Cavalaro, A. de la Fuente, Correlation between the Barcelona test and the bending test in fibre reinforced concrete, *Constr. Build. Mater.* 152 (2017) 529–538. <https://doi.org/10.1016/j.conbuildmat.2017.07.028>.
- [46] EN 206, Concrete - Specification, performance, production and conformity, CEN, Brussels, 2013.
- [47] J.M. Torrents, A. Blanco, P. Pujadas, A. Aguado, P. Juan-García, M.Á. Sánchez-Moragues, Inductive method for assessing the amount and orientation of steel fibers in concrete, *Mater. Struct. Constr.* 45 (2012) 1577–1592. <https://doi.org/10.1617/s11527-012-9858-6>.
- [48] A. Blanco, P. Pujadas, A. De La Fuente, S.H.P. Cavalaro, A. Aguado, Assessment of the fibre orientation factor in SFRC slabs, *Compos. Part B Eng.* 68 (2015) 343–354. <https://doi.org/10.1016/j.compositesb.2014.09.001>.
- [49] S.H.P. Cavalaro, R. López, J.M. Torrents, A. Aguado, Improved assessment of fibre content and orientation with inductive method in SFRC, *Mater. Struct. Constr.* 48 (2015) 1859–1873. <https://doi.org/10.1617/s11527-014-0279-6>.
- [50] S.H.P. Cavalaro, R. López-Carreño, J.M. Torrents, A. Aguado, P. Juan-García, Assessment of fibre content and 3D profile in cylindrical SFRC specimens, *Mater. Struct. Constr.* 49 (2016) 577–595. <https://doi.org/10.1617/s11527-014-0521-2>.
- [51] P.G. Ruiz, M.F. Muttoni, A. and Gambarova, Relationship between non-linear creep and cracking of concrete under uniaxial compression, *J. Adv. Concr. Technol.* 5 (2007) 383–393.
- [52] G. Ruiz, A. de la Rosa, E. Poveda, R. Zanon, M. Schäfer, S. Wolf. Compressive behaviour of steel-fibre reinforced concrete in Annex L of new Eurocode 2, *Hormigón y Acero* (2022). <https://doi.org/10.33586/hya.2022.3092>
- [53] G. Ruiz, Á. de la Rosa, S. Wolf, E. Poveda, Model for the compressive stress-strain relationship of steel fiber-reinforced concrete for non-linear structural analysis, *Hormigón y Acero*. 69 (2018) 75–80. <https://doi.org/10.1016/J.HYA.2018.10.001>.
- [54] M. Colombo, M. Di Prisco, R. Felicetti, SFRC exposed to high temperature: Hot vs. residual characterization for thin walled elements, *Cem. Concr. Compos.* 58 (2015) 81–94. <https://doi.org/10.1016/J.CEMCONCOMP.2015.01.002>.
- [55] F. Di Carlo, A. Meda, Z. Rinaldi, Evaluation of the bearing capacity of fiber reinforced concrete sections under fire exposure, *Mater. Struct. Constr.* 51 (2018) 1–12. <https://doi.org/10.1617/S11527-018-1280-2/FIGURES/13>.
- [56] R. Serafini, R.R. Agra, R.P. Salvador, A. De La Fuente, A.D. De Figueiredo, Double Edge Wedge Splitting Test to Characterize the Design Postcracking Parameters of Fiber-Reinforced Concrete Subjected to High Temperatures, *J. Mater. Civ. Eng.* 33 (2021). [https://doi.org/10.1061/\(ASCE\)MT.1943-5533.0003701](https://doi.org/10.1061/(ASCE)MT.1943-5533.0003701).
- [57] R. Serafini, R.R. Agra, J. Bitencourt L.A.G., A. de la Fuente, A.D. de Figueiredo, Bond-slip response of steel fibers after exposure to elevated temperatures: Experimental program and design-oriented constitutive equation, *Compos. Struct.* 255 (2021). <https://doi.org/10.1016/j.compstruct.2020.112916>.
- [58] R.T. 129-M.T. methods for mechanical properties of concrete at High temperatures, Part 4: Tensile strength for service and accident conditions, *Mater. Struct.* 33 (2000) 219–223.
- [59] C. Andrade, D. Izquierdo, Durability and Cover Depth Provisions in Next Eurocode 2. Background Modelling and Calculations and Cover Depth Provisions, *Hormigón y Acero*. (2023). <https://doi.org/https://doi.org/10.33586/hya.2023.3102>.
- [60] EN 1992-1-1, Eurocode 2: Design of concrete structures - Part 1-1: General rules and rules for buildings, CEN, Brussels, 2004.
- [61] S.C. Paul, G.P.A.G. van Zijl, B. Šavija, Effect of fibers on durability of concrete: A practical review, *Materials* (Basel). 13 (2020) 1–26. <https://doi.org/10.3390/ma13204562>.
- [62] P.S. Mangat, K. Gurusamy, Chloride diffusion in steel fibre reinforced marine concrete, *Cem. Concr. Res.* 17 (1987) 385–396. [https://doi.org/10.1016/0008-8846\(87\)90002-0](https://doi.org/10.1016/0008-8846(87)90002-0).
- [63] V. Marcos-Meson, Durability of steel fibre reinforced concrete in corrosive environments, Technical University of Denmark, 2019.
- [64] P. Hagelia, Deterioration Mechanisms and Durability of Sprayed concrete for Rock Support in Tunnels, Technical University of Delft, 2011.
- [65] V. Marcos-Meson, A. Michel, A. Solgaard, G. Fischer, C. Edvardsen, T.L. Skovhus, Corrosion resistance of steel fibre reinforced concrete - A literature review, *Cem. Concr. Res.* 103 (2018) 1–20. <https://doi.org/10.1016/J.CEMCONRES.2017.05.016>.
- [66] H. Salehian, J.A.O. Barros, Assessment of the performance of steel fibre reinforced self-compacting concrete in elevated slabs, *Cem. Concr. Compos.* 55 (2015) 268–280. <https://doi.org/10.1016/J.CEMCONCOMP.2014.09.016>.
- [67] P. Schumacher, Rotation capacity of self-compacting steel fibre reinforced concrete, TU Delft, 2006.
- [68] A. Nogales, N. Toši, | Albert De La Fuente, N. Tošić, A. de la Fuente, Rotation and moment redistribution capacity of fiber-reinforced concrete beams : Parametric analysis and code compliance, *Struct. Concr.* (2021) 1–20. <https://doi.org/10.1002/suco.202100350>.
- [69] H.C. Mertol, E. Baran, H.J. Bello, Flexural behavior of lightly and heavily reinforced steel fiber concrete beams, *Constr. Build. Mater.* 98 (2015) 185–193. <https://doi.org/10.1016/J.CONBUILD-MAT.2015.08.032>.
- [70] A.N. Dancygier, E. Berkover, Cracking localization and reduced ductility in fiber-reinforced concrete beams with low reinforcement ratios, *Eng. Struct.* 111 (2016) 411–424. <https://doi.org/10.1016/J.ENG-STRUCT.2015.11.046>.
- [71] A. Conforti, R. Zerbino, G. Plizzari, Assessing the influence of fibers on the flexural behavior of reinforced concrete beams with different longitudinal reinforcement ratios, *Struct. Concr.* 22 (2021) 347–360. <https://doi.org/10.1002/SUCO.201900575>.
- [72] P. Visintin, M.S. Mohamad Ali, T. Xie, A.B. Sturm, Experimental investigation of moment redistribution in ultra-high performance fibre reinforced concrete beams, *Constr. Build. Mater.* 166 (2018) 433–444. <https://doi.org/10.1016/J.CONBUILD-MAT.2018.01.156>.
- [73] D.Y. Yoo, D.Y. Moon, Effect of steel fibers on the flexural behavior of RC beams with very low reinforcement ratios, *Constr. Build. Mater.* 188 (2018) 237–254. <https://doi.org/10.1016/J.CONBUILD-MAT.2018.08.099>.
- [74] T. Markić, A. Amin, W. Kaufmann, T. Pfyl, Strength and Deformation Capacity of Tension and Flexural RC Members Containing Steel Fibers, *J. Struct. Eng.* 146 (2020) 04020069. [https://doi.org/10.1061/\(ASCE\)ST.1943-541X.0002614](https://doi.org/10.1061/(ASCE)ST.1943-541X.0002614).
- [75] T. Markić, A. Amin, W. Kaufmann, T. Pfyl, Discussion on “Assessing the influence of fibers on the flexural behavior of reinforced concrete beams with different longitudinal reinforcement ratios” by Conforti et al. [structural concrete, 2020], *Struct. Concr.* 22 (2021) 1888–1891. <https://doi.org/10.1002/suco.202000488>.
- [76] S.J. Foster, A. Parvez, Assessment of model error for reinforced concrete beams with steel fibers in bending, *Struct. Concr.* 20 (2019) 1010–1021. <https://doi.org/10.1002/SUCO.201800090>.
- [77] A. Conforti, R. Zerbino, G. Plizzari, Influence of steel, glass and polymer fibers on the cracking behavior of reinforced concrete beams under flexure, *Struct. Concr.* 1 (2018) 133–143.
- [78] Á. de la Rosa, G. Ruiz, E. Poveda, Study of the Compression Behavior of Steel-Fiber Reinforced Concrete by Means of the Response Surface

- Methodology, Appl. Sci. 2019, Vol. 9, Page 5330. 9 (2019) 5330. <https://doi.org/10.3390/APP9245330>.
- [79] W. Kaufmann, A. Amin, A. Beck, M. Lee, Shear transfer across cracks in steel fibre reinforced concrete, *Eng. Struct.* 186 (2019) 508–524. <https://doi.org/10.1016/J.ENGSTRUCT.2019.02.027>.
- [80] F. Minelli, G.A. Plizzari, On the effectiveness of steel fibers as shear reinforcement, *ACI Struct. J.* 110 (2013) 2013. <https://doi.org/10.14359/51685596>.
- [81] F. Minelli, A. Conforti, E. Cuenca, G. Plizzari, Are steel fibres able to mitigate or eliminate size effect in shear?, *Mater. Struct. Constr.* 47 (2014) 459–473. <https://doi.org/10.1617/S11527-013-0072-Y/METRICS>.
- [82] J. Navarro-Gregori, E.J. Mezquida-Alcaraz, P. Serna-Ros, J. Echegaray-Oviedo, Experimental study on the steel-fibre contribution to concrete shear behaviour, *Constr. Mater.* 112 (2016) 100–111. <https://doi.org/10.1016/J.CONBUILDMAT.2016.02.157>.
- [83] E. Cuenca, On shear behavior of structural elements made of steel fiber reinforced concrete, *Universitat Politècnica de València*, 2015.
- [84] A. Amin, S.J. Foster, Shear strength of steel fibre reinforced concrete beams with stirrups, *Eng. Struct.* 111 (2016) 323–332. <https://doi.org/10.1016/J.ENGSTRUCT.2015.12.026>.
- [85] J.A.O. Barros, S.J. Foster, An integrated approach for predicting the shear capacity of fibre reinforced concrete beams, *Eng. Struct.* 174 (2018) 346–357. <https://doi.org/10.1016/J.ENGSTRUCT.2018.07.071>.
- [86] E. Cuenca, P. Serna, Failure modes and shear design of prestressed hollow core slabs made of fiber-reinforced concrete, *Compos. Part B Eng.* 45 (2013) 952–964. <https://doi.org/10.1016/J.COMPOSITESB.2012.06.005>.
- [87] E. Cuenca, A. Conforti, F. Minelli, G.A. Plizzari, J. Navarro Gregori, P. Serna, A material-performance-based database for FRC and RC elements under shear loading, *Mater. Struct. Constr.* 51 (2018) 11. <https://doi.org/10.1617/s11527-017-1130-7>.
- [88] A. Muttoni, M.F. Ruiz, Shear strength of members without transverse reinforcement as function of critical shear crack width, *ACI Struct. J.* 105 (2008) 163–172. <https://doi.org/10.14359/19731>.
- [89] FIB Bulletin 85, Towards a rational understanding of shear in beams and slabs, Lausanne, 2018.
- [90] S.D.B. Alexander, S.H. Simmonds, Punching Shear Tests of Concrete Slab-Column Joints Containing Fiber Reinforcement, *Struct. J.* 89 (1992) 425–432. <https://doi.org/10.14359/3027>.
- [91] M.H. Harajli, D. Maalouf, H. Khatib, Effect of fibers on the punching shear strength of slab-column connections, *Cem. Concr. Compos.* 17 (1995) 161–170. [https://doi.org/10.1016/0958-9465\(94\)00031-S](https://doi.org/10.1016/0958-9465(94)00031-S).
- [92] P.J. McHarg, W.D. Cook, D. Mitchell, Y.S. Yoon, Benefits of concentrated slab reinforcement and steel fibers on performance of slab-column connections, *ACI Struct. J.* 97 (2000) 225–234. <https://doi.org/10.2/JQUERY.MINJS>.
- [93] M.Y. Cheng, G.J. Parra-Montesinos, Evaluation of Steel Fiber Reinforcement for Punching Shear Resistance in Slab-Column Connections—Part I: Monotonically Increased Load, *ACI Struct. J.* 107 (2010) 101–109.
- [94] L.F. Maya, M. Fernández Ruiz, A. Muttoni, S.J. Foster, Punching shear strength of steel fibre reinforced concrete slabs, *Eng. Struct.* 40 (2012) 83–94. <https://doi.org/10.1016/J.ENGSTRUCT.2012.02.009>.
- [95] R. Narayanan, I.Y.S. Darwish, Punching shear tests on steel-fibre-reinforced micro-concrete slabs, <https://doi.org/10.1680/Macr.1987.39.138.42>. 39 (2015) 42–50. <https://doi.org/10.1680/MACR.1987.39.138.42>.
- [96] K.K. Choi, M.M. Reda Taha, H.G. Park, A.K. Maji, Punching shear strength of interior concrete slab-column connections reinforced with steel fibers, *Cem. Concr. Compos.* 29 (2007) 409–420. <https://doi.org/10.1016/J.CEMCONCOMP.2006.12.003>.
- [97] H. Higashiyama, A. Ota, M. Mizukoshi, Design Equation for Punching Shear Capacity of SFRC Slabs, *Int. J. Concr. Struct. Mater.* 5 (2011) 35–42. <https://doi.org/10.4334/IJCSM.2011.5.1.035>.
- [98] A. Muttoni, Punching shear strength of reinforced concrete slabs without transverse reinforcement, *ACI Struct. J.* 105 (2008) 440–450. <https://doi.org/10.14359/19858>.
- [99] J.T. Simões, M. Fernández Ruiz, A. Muttoni, Validation of the Critical Shear Crack Theory for punching of slabs without transverse reinforcement by means of a refined mechanical model, *Struct. Concr.* 19 (2018) 191–216. <https://doi.org/10.1002/SUCO.201700280>.
- [100] R.N. Swanmy, S.A.R. Ali, Punching Shear Behavior of Reinforced Slab-Column Connections Made with Steel Fiber Concrete, *J. Proc.* 79 (1982) 392–406. <https://doi.org/10.14359/10917>.
- [101] V.V. Oettel, Torsionstragverhalten von stahlfaserbewehrten Beton-, Stahlbeton und Spannbetonbalken, TU Braunschweig, 2016.
- [102] M. Tarifa, X.X. Zhang, G. Ruiz, E. Poveda, Full-scale fatigue tests of precast reinforced concrete slabs for railway tracks, *Eng. Struct.* 100 (2015) 610–621. <https://doi.org/10.1016/J.ENGSTRUCT.2015.06.016>.
- [103] M. Domingo, G. Ramos, Á.C. Aparicio, Use of fiber reinforced concrete in bridges – Metrorrey Line 2 case study, *Eng. Struct.* 276 (2023) 115373. <https://doi.org/10.1016/J.ENGSTRUCT.2022.115373>.
- [104] B. Belletti, R. Cerioni, A. Meda, G. Plizzari, Design Aspects on Steel Fiber-Reinforced Concrete Pavements, *J. Mater. Civ. Eng.* 20 (2008) 599–607. [https://doi.org/10.1061/\(ASCE\)0899-1561\(2008\)20:9\(599\)](https://doi.org/10.1061/(ASCE)0899-1561(2008)20:9(599)).
- [105] Puertos del estado, ROM 4.1-94: Guidelines for the design and construction of port pavements, 1994.
- [106] The Concrete Center, Concrete Towers for Onshore and Offshore Wind Farms, 2007.
- [107] G.A. Plizzari, S. Cangiano, S. Alleruzzo, The Fatigue Behaviour of Cracked Concrete, *Fatigue Fract. Eng. Mater. Struct.* 20 (1997) 1195–1206. <https://doi.org/10.1111/J.1460-2695.1997.TB00323.X>.
- [108] J. Zhang, H. Stang, V.C. Li, Experimental Study on Crack Bridging in FRC under Uniaxial Fatigue Tension, *J. Mater. Civ. Eng.* 12 (2000) 66–73. [https://doi.org/10.1061/\(ASCE\)0899-1561\(2000\)12:1\(66\)](https://doi.org/10.1061/(ASCE)0899-1561(2000)12:1(66)).
- [109] L. Saucedo, R.C. Yu, A. Medeiros, X. Zhang, G. Ruiz, A probabilistic fatigue model based on the initial distribution to consider frequency effect in plain and fiber reinforced concrete, *Int. J. Fatigue.* 48 (2013) 308–318. <https://doi.org/10.1016/J.IJFATIGUE.2012.11.013>.
- [110] A. Medeiros, X. Zhang, G. Ruiz, R.C. Yu, M.D.S.L. Velasco, Effect of the loading frequency on the compressive fatigue behavior of plain and fiber reinforced concrete, *Int. J. Fatigue.* 70 (2015) 342–350. <https://doi.org/10.1016/J.IJFATIGUE.2014.08.005>.
- [111] J.-L. Granju, P. Rossi, P. Rivillon, G. Chanvillard, B. Mesureur, A. Turatsinze, Delayed behaviour of cracked SFRC beams, Fifth Int. RILEM Symp. Fibre-Reinforced Concr. (2000) 511–520.
- [112] F. Germano, G. Tiberti, G. Plizzari, Post-peak fatigue performance of steel fiber reinforced concrete under flexure, *Mater. Struct. Constr.* 49 (2016) 4229–4245. <https://doi.org/10.1617/S11527-015-0783-3/METRICS>.
- [113] S.J. Stephen, R. Gettu, Fatigue fracture of fibre reinforced concrete in flexure, *Mater. Struct. Constr.* 53 (2020) 1–11. <https://doi.org/10.1617/S11527-020-01488-7/METRICS>.
- [114] D.M. Carlesso, S. Cavalaro, A. de la Fuente, Flexural fatigue of pre-cracked plastic fibre reinforced concrete: Experimental study and numerical modeling, *Cem. Concr. Compos.* 115 (2021). <https://doi.org/10.1016/j.cemconcomp.2020.103850>.
- [115] H. Fataar, R. Combrinck, W.P. Boshoff, An Experimental Study on the Flexural Fatigue Behaviour of Pre-cracked Steel Fibre Reinforced Concrete, *RILEM Bookseries.* 36 (2022) 155–165. https://doi.org/10.1007/978-3-030-83719-8_14/COVER.
- [116] G. Tiberti, F. Minelli, G. Plizzari, Cracking behavior in reinforced concrete members with steel fibers: A comprehensive experimental study, *Cem. Concr. Res.* 68 (2015) 24–34. <https://doi.org/10.1016/J.CEMCONRES.2014.10.011>.
- [117] N. Tošić, S. Aidarov, A. de la Fuente, Systematic Review on the Creep of Fiber-Reinforced Concrete, *Materials (Basel).* 13 (2020) 5098.
- [118] A. Amin, S.J. Foster, M. Watts, Modelling the tension stiffening effect in SFR-RC, *Mag. Concr. Res.* 68 (2016) 339–352. <https://doi.org/10.1680/mac.15.00188>.
- [119] A. Amin, S.J. Foster, W. Kaufmann, Instantaneous deflection calculation for steel fibre reinforced concrete one way members, *Eng. Struct.* 131 (2017) 438–445. <https://doi.org/10.1016/j.engstruct.2016.10.041>.
- [120] A. Kenel, P. Nellen, A. Frank, P. Marti, Reinforcing steel strains measured by Bragg grating sensors, *J. Mater. Civ. Eng.* 17 (2005) 423–431. [https://doi.org/10.1061/\(ASCE\)0899-1561\(2005\)17:4\(423\)](https://doi.org/10.1061/(ASCE)0899-1561(2005)17:4(423)).
- [121] K.H. Tan, P. Paramasivam, K.C. Tan, Instantaneous and long-term deflections of steel fiber reinforced concrete beams, *ACI Struct. J.* 91 (1994) 384–393.
- [122] K.H. Tan, P. Paramasivam, K.C. Tan, Creep and shrinkage deflections of RC beams with steel fibers, *J. Mater. Civ. Eng.* 6 (1994) 474–494.
- [123] E. Vasanelli, F. Micelli, M.A. Aiello, G. Plizzari, Long term behavior of FRC flexural beams under sustained load, *Eng. Struct.* 56 (2013) 1858–1867. <https://doi.org/10.1016/j.engstruct.2013.07.035>.

- [124] G.A. Plizzari, G. Tiberti, Steel fibers as reinforcement for precast tunnel segments, *Tunn. Undergr. Sp. Technol.* 21 (2006) 438–439. <https://doi.org/10.1016/j.tust.2005.12.079>.
- [125] B. Chiaia, A.P. Fantilli, P. Vallini, Evaluation of minimum reinforcement ratio in FRC members and application to tunnel linings, *Mater. Struct. Constr.* 40 (2007) 593–604. <https://doi.org/10.1617/s11527-006-9166-0>.
- [126] B. Chiaia, A.P. Fantilli, P. Vallini, Combining fiber-reinforced concrete with traditional reinforcement in tunnel linings, *Eng. Struct.* 31 (2009) 1600–1606. <https://doi.org/10.1016/j.engstruct.2009.02.037>.
- [127] A. Caratelli, A. Meda, Z. Rinaldi, P. Romualdi, Structural behaviour of precast tunnel segments in fiber reinforced concrete, *Tunn. Undergr. Sp. Technol.* 26 (2011) 284–291. <https://doi.org/10.1016/j.tust.2010.10.003>.
- [128] A. Caratelli, A. Meda, Z. Rinaldi, Design according to MC2010 of a fibre-reinforced concrete tunnel in Monte Lirio, Panama, *Struct. Concr.* 13 (2012) 166–173. <https://doi.org/10.1002/SUCO.201100034>.
- [129] A. la Fuente, P. Pujadas, A. Blanco, A. Aguado, A. De la Fuente, P. Pujadas, A. Blanco, A. Aguado, Experiences in Barcelona with the use of fibres in segmental linings, *Tunn. Undergr. Sp. Technol.* 27 (2012) 60–71. <https://doi.org/10.1016/j.tust.2011.07.001>.
- [130] FIB Bulletin 83, *Precast Tunnel Segments in Fibre-Reinforced Concrete*, International Federation for Structural Concrete (fib), Lausanne, 2018.
- [131] F. Di Carlo, A. Meda, Z. Rinaldi, Design procedure for precast fibre-reinforced concrete segments in tunnel lining construction, *Struct. Concr.* 17 (2016) 747–759. <https://doi.org/10.1002/SUCO.201500194>.
- [132] L. Liao, A. de la Fuente, S. Cavalaro, A. Aguado, Design of FRC tunnel segments considering the ductility requirements of the Model Code 2010, *Tunn. Undergr. Sp. Technol.* 47 (2015) 200–210. <https://doi.org/10.1016/j.tust.2015.01.006>.
- [133] L. Liao, A. de la Fuente, S. Cavalaro, A. Aguado, Design procedure and experimental study on fibre reinforced concrete segmental rings for vertical shafts, *Mater. Des.* 92 (2016) 590–601. <https://doi.org/10.1016/j.matdes.2015.12.061>.
- [134] Código Estructural, 2020.

Compressive Behaviour of Steel-Fibre Reinforced Concrete in Annex L of New Eurocode 2

Comportamiento en compresión del hormigón reforzado con fibras de acero según el Anejo L del nuevo Eurocódigo 2

Gonzalo Ruiz^{*,a}, Ángel de la Rosa^a, Elisa Poveda^a, Riccardo Zanon^b,
Markus Schäfer^b, & Sébastien Wolf^c

^aETS de Ingenieros de Caminos, C. y P., Universidad de Castilla-La Mancha, Avda. Camilo José Cela s/n, 13071 Ciudad Real, Spain

^bDepartment of Engineering, University of Luxembourg, 6 rue Richard Coudenhove-Kalergi, L-1359 Luxembourg

^cArcelorMittal Fibres, Route de Finsterthal, L-7769 Bissen, Luxembourg

Recibido el 15 de julio de 2022, aceptado el 8 de diciembre de 2022

ABSTRACT

This paper describes the model for the compressive stress-strain behaviour of steel-fibre reinforced concrete (SFRC) in Annex L of the new Eurocode 2 (CEN, Eurocode 2: Design of concrete structures. Part 1-1: General rules – Rules for buildings, bridges and civil structures, prEN 1992-1-1: 2022; EC2 in short), developed within CEN TC250/SC2/WG1/TG2 – Fiber reinforced concrete. The model uses functions obtained from correlations with an extensive database comprised of 197 well-documented SFRC compressive tests and 484 flexural tests. We detailedly explain the model and derive the strain values for the parabola-rectangle model for ULS of SFRC in Annex L. In addition, we also use the model and the correlations with the database to provide a link between the compressive and the flexural performance classes in EC2, which allows a complete definition of any particular SFRC. Likewise, we derive parabola-rectangle strain values for each flexural performance class, which is mainly advantageous for the stronger flexural performance classes. Finally, we give an example showing the enhancement in strength and ductility of a composite steel-SFRC section endorsed with the new model, which results of 15% and 100%, respectively.

KEYWORDS: Compressive model for SFRC in Annex L of Eurocode 2, combined compression/flexural classification for any SFRC, relevant strains for ULS calculation, impact of the ductility and toughness enhancement of composite steel-SFRC sections on Eurocode 4.

©2023 Hormigón y Acero, the journal of the Spanish Association of Structural Engineering (ACHE). Published by Cinter Divulgación Técnica S.L. This is an open-access article distributed under the terms of the Creative Commons (CC BY-NC-ND 4.0) License.

RESUMEN

Este artículo describe la nueva ley tensión-deformación en compresión para hormigón reforzado con fibras de acero (HRFA) que propone el Anejo L del nuevo Eurocódigo 2 (CEN, Eurocódigo 2: Diseño de estructuras de hormigón. Parte 1-1: Reglas generales – Reglas para edificios, puentes y estructuras civiles, prEN 1992-1-1: 2022; en breve, EC2), desarrollado dentro del grupo de trabajo CEN TC250/SC2/WG1/TG2 – Hormigón reforzado con fibras. La nueva ley utiliza funciones obtenidas a través de correlaciones con una extensa base de datos compuesta por ensayos de HRFA bien documentados, 197 a compresión y 484 a flexión. En el artículo explicamos detalladamente la nueva ley, y deducimos los nuevos valores de deformación para la ley parábola-rectángulo en ELU para HRFA en el Anejo L. Además, también usamos la nueva ley y las correlaciones con la base de datos para vincular las clases de compresión y flexión del EC2, lo cual permite una definición completa de cualquier HRFA. Del mismo modo, deducimos nuevos valores de deformación para la ley parábola-rectángulo en ELU para cada clase de flexión, que añaden ductilidad a las clases de flexión más resistentes. Finalmente, incluimos un ejemplo que muestra la mejora en resistencia y ductilidad de una sección mixta de acero-HRFA calculada con la nueva

* Persona de contacto / Corresponding author.
 Correo-e / e-mail: Gonzalo.Ruiz@uclm.es (Gonzalo Ruiz).



ley, que resulta ser un 15% más resistente y un 100% más dúctil que la misma sección con hormigón sin fibras de la misma clase de compresión.

PALABRAS CLAVE: Ley tensión-deformación en compresión para HRFA en el Anejo L del Eurocódigo 2, clasificación combinada compresión/flexión para cualquier HRFA, deformaciones relevantes para el cálculo de ELU, repercusión en la mejora de la ductilidad y tenacidad de secciones mixtas acero-HRFA en el Eurocódigo 4.

©2023 Hormigón y Acero, la revista de la Asociación Española de Ingeniería Estructural (ACHE). Publicado por Cinter Divulgación Técnica S.L. Este es un artículo de acceso abierto distribuido bajo los términos de la licencia de uso Creative Commons (CC BY-NC-ND 4.0).

1 INTRODUCTION

The superior ductility and toughness provided by steel-fibre reinforcement to flexural elements are well known, mainly due to the higher residual flexural tensile strength after cracking [1–6]. This is achieved because steel fibres give the capacity to the concrete to overtake tension, and this capacity is increased in correlation with the fibres' type, the steel wire tensile strength, and the dosage rate of steel fibres in the concrete mix. This enables the use of steel-fibre reinforced concrete (SFRC) in many structural applications [1, 3, 7–9], mainly when controlling the cracking processes is a must [1, 10], like in tunnel lining segments [1, 11–20], industrial floors [1, 21, 22], elevated slabs, bearing rafts on ground, and on piles [23, 24], precast pipes [25] and others. This is why SFRC is included in several structural concrete design codes and regulations [26–35], although they only consider the response to tension and its influence on bending.

It is also known that increasing the compression strength of the concrete involves an increase in the flexural strength, and in turn, the addition of steel fibres increases the capacity of deformation and ductility when the maximum flexural load is exceeded [36]. There is much research that analyzes the flexural behaviour of SFRC in terms of tension, deformation and crack mouth opening displacement using relationships that take into account the characteristics associated with the reinforcement of the fibre [1, 2, 6, 37–47], principally the dosage rate, slenderness, and steel wire tensile strength.

On the other hand, the ductility and toughness increase after the maximum load of SFRC in compression has been thoroughly reported [48–64], and there are several compressive stress-strain models developed so far [50, 52, 54, 57, 58, 64–69]. Regrettably, most of them were calibrated with limited data, and their predictions failed when checked against other experimental sources, as pointed out by Bencardino *et al.* [70]. However, they reported that the model of Barros *et al.* [57] is very accurate. Indeed, it gave good results when used by Yoo *et al.* [36] to model the flexural and compressive strengths of concrete reinforced with amorphous steel fibres.

Disregarding the effective contribution of the fibres in compression when designing structural elements may lead to a waste of the capabilities of the material. For instance, additional ductility and toughness in compression may facilitate that steel elements in composite sections can work at their limits [71, 72]. Besides, as flexural and compressive behaviours of SFRC are interconnected, it follows that proper classification of SFRC requires establishing a link between the compression and flexural strength classes, which is not done in the current normative [26, 27]. All the above considered, Task Group CEN TC250/SC2/WG1/TG2, responsible for the new Annex

L on SFRC, decided to study the compressive capacities of the material and draft a model that could account for them in a technological fashion. The outcome is the model in the draft of Annex L of the new Eurocode 2 [73] (EC2 in short). It is based on functions obtained from correlations with an extensive database comprised of 197 well-documented SFRC compressive tests and 484 flexural tests [1, 56, 57, 61, 62, 70, 74–88]. Detailed derivations of these functions are reported in [89–91].

The following section succinctly describes the stress-strain model as it appears in Annex L of EC2 [73]. For the sake of consistency, along with brevity in the description, the new model is based on the σ_c - ϵ_c equation for plain concrete proposed by Sargin [92] and implemented in Formula 5.6 of Section 5.1.6 (3) of EC2 [73]. The new model just changes the expressions for some of the coefficients in Formula 5.6 to account for the increased toughness and ductility of SFRC due to fibres. Subsequently, we comprehensively explain the model in a closed form and justify the strain values given for ULS calculations (Section 3). In Section 4 we provide a discussion based on the link between compressive and flexural classification (Subsection 4.1), the ductility in compression including the strain values defining the new expressions for each flexural performance class (4.2), and the impact of SFRC ductility on composite beams designed in accordance to Eurocode 4 [93] (4.3). Finally, we draw some conclusions in Section 5.

2 COMPRESSIVE BEHAVIOUR OF SFRC IN ANNEX L

2.1. Stress-strain relationship in compression for non-linear structural analysis of SFRC

The stress-strain relation for non-linear structural analysis of SFRC in Annex L of the new EC2 (version of November 10, 2022) [73], section L.5.5.2 (2), reads as follows:

“The relation between σ_c and ϵ_c in compression in Formula (5.6) may be used to model the response of SFRC to short-term uniaxial compression provided the following modifications in the parameters are made:

$$\epsilon_{c1} (\%0_0) = 0.7 f_{cm}^{1/3} (1 + 0.03 f_{R,1k}) \quad (1)$$

and, for $\epsilon_{c1} < \epsilon_c \leq \epsilon_{cu1}$:

$$k = 1 + \frac{20}{\sqrt{82 - 2.2 f_{R,1k}}} \quad \text{and} \quad \epsilon_{cu1} = k \epsilon_{c1} \quad (2)$$

where f_{cm} and $f_{R,1k}$ must be inserted in MPa in Eqs. 1 and 2.

2.2. Stress distribution for SFRC in compression in ULS

Annex L also allows accounting for the superior toughness and ductility of SFRC in ULS —as compared to plain concrete— by enlarging the strain parameters that define the stress distribution. This is done in Section L.8.1 (4), which reads as follows:

“The stress distribution according to Formula (8.4) may be modified for SFRC by applying $\epsilon_{c2} = 0.0025$ and $\epsilon_{cu} = 0.006$.”

These parameters are 0.0020 and 0.0035, respectively, for concrete without fibres.

3. EXPLANATION AND JUSTIFICATION OF THE COMPRESSIVE STRESS-STRAIN MODEL FOR SFRC IN ANNEX L

3.1. Stress-strain relationship in compression

The new σ_c - ϵ_c relationship for SFRC is built on the compressive model for plain concrete proposed by Sargin [92] and implemented in EC2 [73], Formula 5.6, that is:

$$\frac{\sigma_c}{f_{cm}} = \frac{k\eta - \eta^2}{1 + (k-2)\eta} \quad (3)$$

where f_{cm} is the mean compressive strength (given in Table 5.1 of EC2 [73]); k is a parameter enforcing that the secant elastic modulus of the curve is E_{cm} , and is given by:

$$k = 1.05 \epsilon_{c1} \frac{E_{cm}}{f_{cm}} \quad (4)$$

where ϵ_{c1} is the compressive strain corresponding to the concrete strength, i.e. the peak of the curve, and is obtained as:

$$\epsilon_{c1} [\text{‰}] = 0.7 f_{cm}^{1/3} \leq 2.8\text{‰} \quad (5)$$

Equation 5 needs that f_{cm} is in MPa. Note that k in Eq. 4 is non-dimensional whatever the system of units is used, but it would need that E_{cm} is in GPa and f_{cm} in MPa in case ϵ_{c1} is given in per mill as per Eq. 5.

Variable η of Eq. 3 is the ratio between the compressive strain, ϵ_c , and the compressive strain at the peak, ϵ_{c1} :

$$\eta = \frac{\epsilon_c}{\epsilon_{c1}} \quad (6)$$

where ϵ_c has the following limit value:

$$\epsilon_c < \epsilon_{cu1} [\text{‰}] = 2.8 + 14 (1 - f_{cm}/108)^4 \leq 3.5\text{‰} \quad (7)$$

which requires that f_{cm} is in MPa. Having the above definitions into account, Eq. 3 describes a non-dimensional stress-strain curve whose abscissa and ordinate are η and σ_c/f_{cm} , respectively. The dimensional stress-strain curve for plain concrete given by Eq. 3 is shown in Figure 1.

The new stress-strain relation for SFRC uses Eq. 3 but modifies the values of some of the parameters to account for

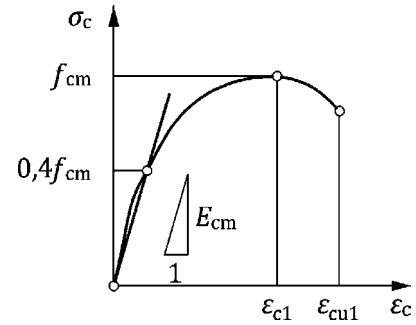


Figure 1. Stress-strain relation for plain concrete in compression (Figure 5.1, EC2 [73]).

the additional toughness and ductility provided by the steel fibres. The SFRC model keeps the values for f_{cm} and E_{cm} of the base concrete since it is proven that fibres have little influence on them [89–91]. However, the strain for the peak of the curve, ϵ_{c1} , is increased as expressed in Eq. 1. The unit increase of the strain for the maximum stress is $0.03f_{R,1k}$ ($f_{R,1k}$ in MPa), as disclosed in [91]. The rest of the curve parameters in Eq. 3 remain the same for the ramp-up part of the stress-strain curve, that is for $\epsilon_c \leq \epsilon_{c1}$ (or $\eta \leq 1$).

The downward stretch of the curve after ϵ_{c1} can also be represented using Eq. 3 provided a new value for the parameter k is taken, as expressed in Eq. 2. Note that with this new value for k the stress-strain curve has a maximum at $\epsilon_c = \epsilon_{c1}$ ($\eta = 1$), and intercepts the abscissa at $\epsilon_c = \epsilon_{cu1}$, where $\epsilon_{cu1} = k \epsilon_{c1}$ ($\eta_u = k$). So, the new value for k in Eq. 2 represents the increase in the critical strain relative to ϵ_{c1} [89, 91].

It bears emphasis that parameter k takes the following values for the two stretches—ascending and descending branches—of the stress-strain curve:

$$k = \left\{ \begin{array}{ll} 1.05 \epsilon_{c1} \frac{E_{cm}}{f_{cm}} & \text{for } \epsilon_c \leq \epsilon_{c1} \\ 1 + \frac{20}{\sqrt{82 - 2.2 f_{R,1k}}} (f_{R,1k} \text{ in MPa}) & \text{for } \epsilon_{c1} < \epsilon_c \leq \epsilon_{cu1} \end{array} \right\} \quad (8)$$

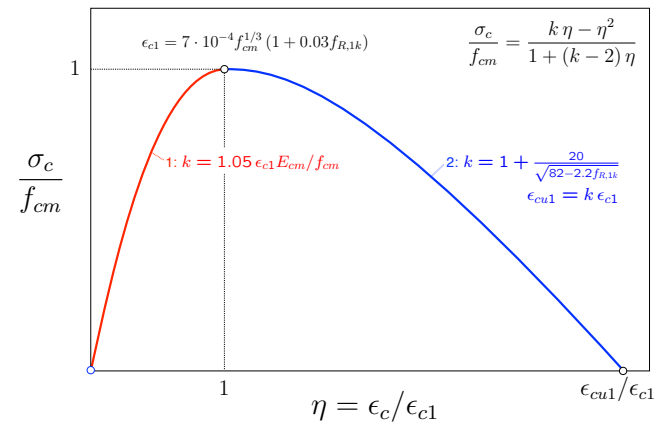


Figure 2. Non-dimensional stress-strain relationship for SFRC.

The new stress-strain curve for SFRC is plotted in Figure 2. Note that Figure 2 includes the equations and variables to be applied for building the complete compressive stress-strain model for SFRC.

The database we used for the multivariate analysis and subsequent model derivation contains results of SFRC with hooked-end fibres only. Thus, the equations derived in papers [89–91] are valid for this type of SFRC. However, the compressive σ - ϵ curve in Annex L is a function of $f_{R,1k}$ only (see Eqs. 1 and 2), which is a parameter that depends mainly on the compressive strength of the base concrete and the interface properties of the fibre [90], and very little on the hooks at the ends or the shape of the fibre. Therefore, the new compressive model can be used for SFRC reinforced with any type of steel fibre.

Previous versions of this stress-strain curve did not use Eq. 3 for the descending stretch, but an inverted parabola with the maximum in the peak of the compressive strength [89–91], which expression is:

$$\frac{\sigma_c}{f_{cm}} = 1 - \frac{1}{4} (\eta - 1)^2 \left(1 - \frac{\sigma_R}{f_{cm}} \right) \quad (9)$$

where σ_R was called the residual compressive strength and is the value that the stress takes for $\eta = 3$. It was defined so because there was not a single stress-strain curve in the database that did not reach at least a final strain three times larger than the strain at the peak, which served to define a reference point to obtain the energy per unit volume absorbed in the database tests, which were called W_{c1} from 0 to ϵ_{c1} , and W_{c2} from ϵ_{c1} to $3 \epsilon_{c1}$. Besides, it seemed reasonable to define a *residual* compressive strength since it was analogous to the *residual* flexural strengths, $f_{R,i}$, which are accepted as relevant SFRC parameters defining the tensile behaviour. The intercept of Eq. 9 with the η -axis is $\eta_u (= k)$, and can be written as a function of σ_R as:

$$\eta_u = 1 + \frac{2}{\sqrt{1 - \sigma_R/f_{cm}}} \quad (10)$$

Likewise, Eq. 9 expressed as a function of η_u is:

$$\frac{\sigma_c}{f_{cm}} = 1 - \left(\frac{\eta - 1}{\eta_u - 1} \right)^2 \quad (11)$$

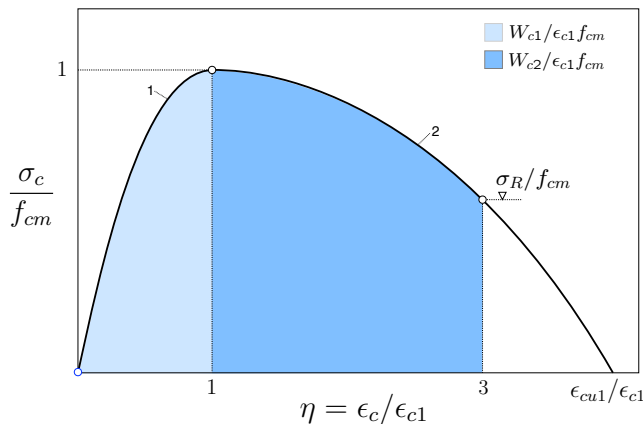


Figure 3. Schematic representation of the stress-strain relationship for SFRC previously proposed in [89–91].

Discussions within TG2 led to looking for an expression for the descending branch that allowed a very short description of the σ - ϵ model, with few or no new variables involved. This is why we opted for using Eq. 3 also for the second

stretch of the new model since the curve is very similar to the parabola given by Eqs. 9 and 11. Eq. 3 has a maximum at $\eta = 1$ and intercepts the η -axis at $\eta = k$, and so it was only necessary to change the meaning of k after the peak, taking it as η_u (Eq. 10). Besides, detailed derivations using the response-surface methodology—a multivariate regression tool—applied to the database disclosed that σ_R depends mainly on the characteristic residual flexural strength for a crackmouth opening displacement of 0.5 mm, $f_{R,1k}$, the expression for it being:

$$\frac{\sigma_R}{f_{cm}} = 0.1839 + 0.02203 f_{R,1k} \quad (12)$$

where $f_{R,1k}$ must be introduced in MPa (Eq. 16 in [91]). Such derivation was made by fitting the energy absorbed by the tests in the database between ϵ_{c1} and $3 \epsilon_{c1}$, W_{c2} , which is related to the residual compressive strength as:

$$\frac{\sigma_R}{f_{cm}} = \frac{3W_{c2}}{2f_{cm}\epsilon_{c1}} - 2 \quad (13)$$

Inserting Eq. 12 in Eq. 10 yields:

$$\eta_u = 1 + \frac{20}{\sqrt{82 - 2.2 f_{R,1k}}} \quad (14)$$

which is the value that should be used for k in the descending stretch of the compressive stress-strain model given by Eq. 3.

3.2. Stress distribution in ULS

For the design of cross sections in ULS, EC2 Section 8.1.2 (1) [73] proposes using a parabola-rectangle stress distribution (see Figure 4c), defined as:

$$\eta_u = \begin{cases} f_{cd} [1 - (1 - \epsilon_c/\epsilon_{c2})^2] & \text{for } 0 \leq \epsilon_c \leq \epsilon_{c2} \\ f_{cd} & \text{for } \epsilon_{c2} \leq \epsilon_c \leq \epsilon_{cu} \end{cases} \quad (15)$$

where ϵ_{c2} and ϵ_{cu} are 0.0020 and 0.0035, respectively, for concrete without fibres. Alternatively, a rectangular stress block distribution as given in Figure 4d may be assumed, as stated in section 8.1.2 (2).

Annex L accounts for the enhancement of toughness and ductility in compression provided by the fibre by increasing the strains defining the stress distribution, ϵ_{c2} and ϵ_{cu} , to 0.0025 and 0.0060, respectively.

These new values for ϵ_{c2} and ϵ_{cu} for SFRC are based on the observed behaviour of the SFRCs in the database. In particular, the energy consumption up to ϵ_{c2} increases 45% in average compared to the corresponding base concrete (see Table 1). As fibres have little effect on the compressive strength, the toughness increase up to the peak of the parabola, and subsequently the new strain that corresponds with the peak, can be obtained by multiplying the strain for the peak stress of the base concrete—without fibres—times W_{f1}° ($= W_{f1}/W_{c1}$, see Table 1):

$$\epsilon_{f2} = \epsilon_{c2} W_{f1}^{\circ} \quad (16)$$

where ϵ_{f2} is the strain for the peak of the parabola for the concrete with fibres (we use subscript 'f' instead of 'c' to specify that we refer to concrete reinforced with steel fibres). The re-

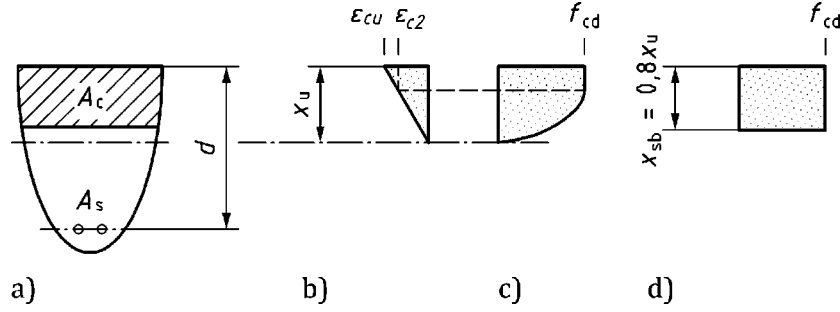


Figure 4. Stress distributions within the compression zone: a) cross section; b) assumed strain distribution; c) parabola-rectangle stress distribution; d) rectangular stress distribution. (Figure 8.2, EC2 [73])

sult is 0.0029, rounded down to 0.0025, which is finally taken as ϵ_{c2} for ULS calculations in SFRC.

Regarding the value for ϵ_{cu} with fibres, it is figured out by enforcing that the rectangular part consumes the same energy as the post-peak stretch of the new stress-strain curve (Eq. 9) up to $3\epsilon_{f2}$. The energy consumed in this stretch is, on average, $2.83 W_{c1}$, which is 183% more energy than consumed up to the peak by the corresponding base concrete, Table 1. For the parabola-rectangle law of Eq. 15, this can be expressed as:

$$W_{f2}^o = \frac{W_{f2}}{W_{c2}} = \frac{f_{fd}(\epsilon_{fu} - \epsilon_{f2})}{\frac{2}{3} f_{cd} \epsilon_{c2}} \quad (17)$$

where again we use subscript 'f' instead of 'c' to refer to SFRC (for instance, ϵ_{fu} means ϵ_{cu} for the SFRC). As stated above, the strength increase due to fibres is small and can be neglected (i.e. $f_{fd} = f_{cd}$ in Eq. 17). Then:

$$W_{f2}^o = \frac{3}{2} \left(\frac{\epsilon_{fu}}{\epsilon_{f2}} - 1 \right) \frac{\epsilon_{f2}}{\epsilon_{c2}} \quad (18)$$

Table 1: Statistics of the unit toughness increase for SFRC.

	Mean	(Std. dev.)	[Min.–Max.]
$W_{f1}^o (=W_{f1}/W_{c1})$	1.45	(0.52)	[0.91–3.73]
$W_{f2}^o (=W_{f2}/W_{c2})$	2.83	(1.09)	[1.12–5.49]

where the ratio $\epsilon_{f2}/\epsilon_{c2}$ equals W_{f1}^o (Eq.16). Then, solving for $\epsilon_{fu}/\epsilon_{f2}$ in Eq. 18 we get:

$$\frac{\epsilon_{fu}}{\epsilon_{f2}} = \frac{2}{3} \frac{W_{f2}^o}{W_{f1}^o} + 1 \quad (19)$$

Introducing the values in Table 1 for W_{f1}^o and W_{f2}^o we get a ratio of 2.30. Taking ϵ_{f2} ($=\epsilon_{c2}$ for a SFRC) as 0.0029 (as derived above) we get that ϵ_{fu} ($=\epsilon_{cu}$ for a SFRC) is 0.0067, whereas for $\epsilon_{f2} = 0.0025$ we obtain $\epsilon_{fu} = 0.0057$. So, finally we round the result and take 0.0060 as the value of ϵ_{cu} for a SFRC.

Note that values for W_{f1}^o and W_{f2}^o in Table 1 are the average values of the stress-strain curves of the database disregarding dependencies on fibre content, fibre quality, etc., and we assume that the toughness of the parabola-rectangle curve for plain concrete increases according to them. In other words, we get ϵ_{c2} and ϵ_{cu} for an SFRC by enforcing that the parabola and the rectangle yield the same energy enhancement as the average of the curves in the database. Observe that absolute-

ly none of the SFRC specimens in the compressive database broke before reaching a strain of $3\epsilon_{f1}$, and most of them continued deforming way ahead of this value. Therefore, the mean values for W_{f1}^o and W_{f2}^o in Table 1 are on the safe side, and thus the new strain figures for SFRC in the curve defined in Eq. 15, namely 0.0025 and 0.0060, are on the safe side too.

4. DISCUSSION

4.1. Compressive and flexural SFRC classification

The new model for the compressive stress-strain behaviour in SFRC in Annex L allows a complete description of the material response, as can be seen graphically in Figure 5. The upper part plots the flexural stress versus the crack opening curves in non-dimensional format for several of the flexural performance classes (see Table 2, which reproduces Table L.2 of Annex L). These are called performance classes, but actually they only depend on the residual flexural strengths $f_{R,1k}$ and $f_{R,3k}$ experimentally determined according to EN 14651 [35]. The classification is based on a number—called SC (or σ_{SC} in this paper) for strength class—that corresponds to the minimum value required for $f_{R,1k}$ in MPa, and a letter associated to the ratio $f_{R,3k}/\sigma_{SC}$. For instance, class 4.0 b means that $\sigma_{SC} = 4.0$ MPa $\leq f_{R,1k} < 4.5$ MPa and $0.7 \leq f_{R,3k}/\sigma_{SC} < 0.9$ (see Table 2).

The lower part of Figure 5 plots the new compressive stress-strain law in Annex L as described in Section 2 and explained in Section 3. The plot is in a non-dimensional format, the abscissa and ordinate representing ϵ_c/ϵ_{c1} ($=\eta$) and σ_c/f_{cm} , respectively. Note that the intercept of the curve with the horizontal axis is equal to η_u ($=k$). Since both ϵ_{c1} and k depend directly on $f_{R,1k}$ through Eqs. 1 and 2, respectively, it would seem that there is no reason to add any additional number or letter to the SFRC classification. However, an SFRC has to define the *compressive* class along with the flexural performance class since it is apparent that the *compressive* strength correlates with the residual flexural strengths. The new compressive model in Annex L does not contain information about this correlation *per se*, but the *multivariate analyses reported in [89–91]* provide it. There it was found that the expression for the residual compressive strength as a function of the flexural behaviour is:

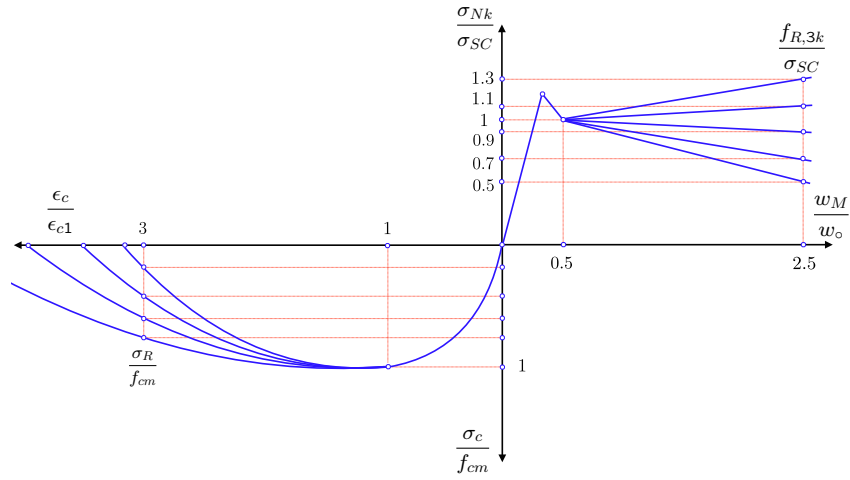


Figure 5. Description of the flexural/compression behaviour of SFRC and meaning of the material classification.

TABLE 2.

Performance classes for SFRC in MPa as defined in Table L.2 of EC2 [73].

Ductility classes	Strength classes SC ($f_{R,1k} \geq SC$)												Analytical formulae
	1.0	1.5	2.0	2.5	3.0	3.5	4.0	4.5	5.0	6.0	7.0	8.0	
a	0.5	0.8	1.0	1.3	1.5	1.8	2.0	2.3	2.5	3.0	3.5	4.0	$f_{R,3k} \geq 0.5 SC$
b	0.7	1.1	1.4	1.8	2.1	2.5	2.8	3.2	3.5	4.2	4.9	5.6	$f_{R,3k} \geq 0.7 SC$
c	0.9	1.4	1.8	2.3	2.7	3.2	3.6	4.1	4.5	5.4	6.3	7.2	$f_{R,3k} \geq 0.9 SC$
d	1.1	1.7	2.2	2.8	3.3	3.9	4.4	5.0	5.5	6.6	7.7	8.8	$f_{R,3k} \geq 1.1 SC$
e	1.3	2.0	2.6	3.3	3.9	4.6	5.2	5.9	6.5	7.8	9.1	10.4	$f_{R,3k} \geq 1.3 SC$

TABLE 3.

Performance classes for SFRC related with their residual flexural and compressive strengths (in MPa).

Ductility classes		Strength classes SC ($f_{R,1k} \geq SC$)											
		1.0	1.5	2.0	2.5	3.0	3.5	4.0	4.5	5.0	6.0	7.0	8.0
a:	$f_{R,3k}$	0.5	0.8	1.0	1.3	1.5	1.8	2.0	2.3	2.5	3.0	3.5	4.0
	f_{cm}	22	25	28	30	32	35	36	37	40	43	46	48
	σ_R	4	5	6	7	8	9	10	11	12	13	15	17
b:	$f_{R,3k}$	0.7	1.1	1.4	1.8	2.1	2.5	2.8	3.2	3.5	4.2	4.9	5.6
	f_{cm}	31	34	36	38	40	42	43	45	46	49	51	53
	σ_R	6	7	8	9	10	11	12	13	14	15	17	19
c:	$f_{R,3k}$	0.9	1.4	1.8	2.3	2.7	3.2	3.6	4.1	4.5	5.4	6.3	7.2
	f_{cm}	40	42	44	46	47	49	50	51	53	55	56	58
	σ_R	8	9	10	11	12	13	14	15	16	17	19	21
d:	$f_{R,3k}$	1.1	1.7	2.2	2.8	3.3	3.9	4.4	5.0	5.5	6.6	7.7	8.8
	f_{cm}	49	51	52	53	55	56	57	58	59	60	62	63
	σ_R	10	11	12	13	14	15	15	16	17	19	21	23
e:	$f_{R,3k}$	1.3	2.0	2.6	3.3	3.9	4.6	5.2	5.9	6.5	7.8	9.1	10.4
	f_{cm}	58	59	60	61	62	63	64	64	65	66	67	68
	σ_R	12	13	14	15	15	16	17	18	19	21	23	25

$$\sigma_R = -1.77 + 1.807 f_{R,1k} + 9.12 \frac{f_{R,3k}}{f_{R,1k}} \quad (20)$$

where the residual flexural strengths are introduced in MPa to obtain σ_R in MPa. Both $f_{R,1k}$ and $f_{R,3k}$ are the only significant parameters to get σ_R . Interestingly, they are also the parameters defining the flexural performance class.

On the other hand, Eq. 12 already expresses the result obtained for σ_R/f_{cm} . It should be noted that only $f_{R,1k}$ was disclosed

as a significant parameter to obtain the non-dimensional version of σ_R in Eq. 12. Combining Eqs. 12 and 20, the relation between the compressive strength and the residual flexural strengths follows as:

$$f_{cm} = \frac{-1.77 + 1.807 f_{R,1k} + 9.12 \frac{f_{R,3k}}{f_{R,1k}}}{0.1839 + 0.02203 f_{R,1k}} \quad (21)$$

TABLE 4.

Performance classes for SFRC related with their relevant strains both for the parabola-rectangle model in ULS, ϵ_{f2} and ϵ_{fu} , and for the stress-strain general model, ϵ_{f1} and ϵ_{fu1} , (strains in ‰; SC in MPa).

Ductility classes	Strength classes SC ($f_{R,1k} \geq SC$)												
	1.0	1.5	2.0	2.5	3.0	3.5	4.0	4.5	5.0	6.0	7.0	8.0	
a: $\epsilon_{f2} = \epsilon_{f1}$	2.0	2.1	2.3	2.4	2.4	2.5	2.6	2.7	2.8	2.9	3.0	3.2	
ϵ_{fu}	5.0	5.3	5.6	5.9	6.1	6.3	6.6	6.8	7.0	7.4	7.7	8.1	
ϵ_{fu1}	6.6	7.0	7.4	7.7	8.1	8.4	8.7	9.0	9.3	9.9	10.4	11.0	
b: $\epsilon_{f2} = \epsilon_{f1}$	2.3	2.4	2.5	2.5	2.6	2.7	2.8	2.8	2.9	3.0	3.1	3.3	
ϵ_{fu}	5.6	5.9	6.1	6.3	6.5	6.7	6.9	7.1	7.3	7.7	8.0	8.4	
ϵ_{fu1}	7.4	7.7	8.0	8.3	8.6	8.9	9.2	9.5	9.8	10.3	10.8	11.4	
c: $\epsilon_{f2} = \epsilon_{f1}$	2.5	2.5	2.6	2.7	2.8	2.8	2.9	3.0	3.0	3.1	3.2	3.4	
ϵ_{fu}	6.1	6.3	6.5	6.7	6.9	7.1	7.3	7.4	7.6	8.0	8.3	8.6	
ϵ_{fu1}	8.0	8.3	8.6	8.9	9.1	9.4	9.7	9.9	10.2	10.7	11.2	11.7	
d: $\epsilon_{f2} = \epsilon_{f1}$	2.6	2.7	2.8	2.8	2.9	3.0	3.0	3.1	3.1	3.2	3.3	3.5	
ϵ_{fu}	6.5	6.7	6.9	7.1	7.2	7.4	7.6	7.7	7.9	8.2	8.6	8.9	
ϵ_{fu1}	8.5	8.8	9.1	9.3	9.6	9.8	10.1	10.3	10.6	11.1	11.6	12.1	
e: $\epsilon_{f2} = \epsilon_{f1}$	2.8	2.8	2.9	3.0	3.0	3.1	3.1	3.2	3.2	3.3	3.4	3.5	
ϵ_{fu}	6.9	7.0	7.2	7.4	7.5	7.7	7.9	8.0	8.2	8.5	8.8	9.1	
ϵ_{fu1}	9.0	9.3	9.5	9.7	10.0	10.2	10.4	10.7	10.9	11.4	11.9	12.4	

where residual flexural strengths are introduced in MPa to obtain f_{cm} in MPa. This formula depends on the ratio $f_{R,3k}/f_{R,1k}$, and thus it is only valid for SFRC with hooked-end fibres since the database in [89–91] contain results for this type of SFRC only.

Equation 21 gives an estimate of the compressive strength needed to obtain a definite flexural performance class with SFRC with hooked-end fibres, defined by the desired residual flexural strengths. Table 3 arrays all the estimates given by Eqs. 20 and 21 for each flexural performance class of Annex L. In each cell of the matrix, we give the estimate for the compressive strength f_{cm} needed to obtain the desired flexural performance class along with an estimate for the residual compressive strength. For instance, Table 3 indicates that you need at least a C35/45 (whose minimum f_{cm} is 43 MPa) to produce a class 4.0 b, whereas the expected minimum value for σ_R is 12 MPa. So, the complete classification of this SFRC should be C35/45 4.0 b. It bears emphasis that obtaining flexural performance class 4.0 b with a compressive class below C35/45 may be rather difficult.

4.2. Ductility in compression

The deformability in compression of SFRCs of each performance class can be estimated using the new stress-strain model in Annex L. Indeed, Eqs. 1 and 2 allow obtaining ϵ_{c1} and ϵ_{cu1} values for each flexural performance class, see Table 4 (we use subscript 'f' instead of 'c' to name parameters of a SFRC). Note that these strain values depend jointly on the compressive strength and the residual flexural strengths.

As aforementioned, Annex L follows the core of EC2 [73] in providing two constant values for the strains determining the parabola-rectangle used in ULS, namely ϵ_{f2} and ϵ_{fu} (again, subscript 'f' is for SFRC). It is done so for the sake of brevity and consistency since mirroring the structure of EC2 [73] for plain concrete avoids new formulas or parameters and subsequent definitions. However, it is also possible to give defining strains for the parabola-rectangle model for each performance class. It is appropriate to do so since ULS calculations may also

benefit from having selected a flexural performance class for the SFRC element or structure under study. To do this, we assume that ϵ_{f2} takes the same value as ϵ_{f1} . Then, we can use Eq. 19 to calculate ϵ_{fu} for each class, but in its dimensional version:

$$\frac{\epsilon_{fu}}{\epsilon_{f2}} = \frac{2}{3} \frac{W_{f2}}{W_{f1}} + 1 \quad (22)$$

where W_{f1} and W_{f2} are now calculated with the complete stress-strain model (Subsection 3.1) but assuming that the up and down stretches are perfect parabolas. Additionally, as W_{f2} is the energy per unit volume absorbed between ϵ_{f1} and $3\epsilon_{f1}$, we assume that the detracted area between $3\epsilon_{f1}$ and $k\epsilon_{f1}$ can be calculated as if it was a triangle. The result for ϵ_{fu} is:

$$\frac{\epsilon_{fu}}{\epsilon_{f2}} = \frac{2}{3} \left((k-1) - \frac{3}{4} (k-3) \frac{\sigma_R}{f_{cm}} \right) + 1 \quad (23)$$

where k is the value for the downward stretch of the curve (Eq. 2), which coincides with the nondimensional strain of the intercept with the abscissa ($k = \eta_u$). Table 4 arrays the results of Eq. 23 for each performance class.

The constant values for ϵ_{f2} and ϵ_{fu} that Annex L, section L.8.1 (4), proposes, namely 0.0025 and 0.0060, roughly coincide with these of classes 3.0 a, 2.0 b, and 1.0 c. So, using the proposed constant strains leads to slightly overestimating the ductility for weaker classes and underestimating it for the stronger ones, actually the majority of them. For instance, these strains for class 1.0 a are 0.0020 and 0.0050, whereas for class 8.0 e are 0.0035 and 0.0091. It bears emphasis that all these strain values are on the safe side since absolutely none of the SFRC specimens in the compressive database broke before reaching a strain of $3\epsilon_{f1}$, and most of them continued deforming way ahead this value [89–91].

4.3. Outlook about the impact of SFRC ductility on Eurocode 4

The benefits of an increased concrete ductility conferred by the addition of steel fibre reinforcement have consequences

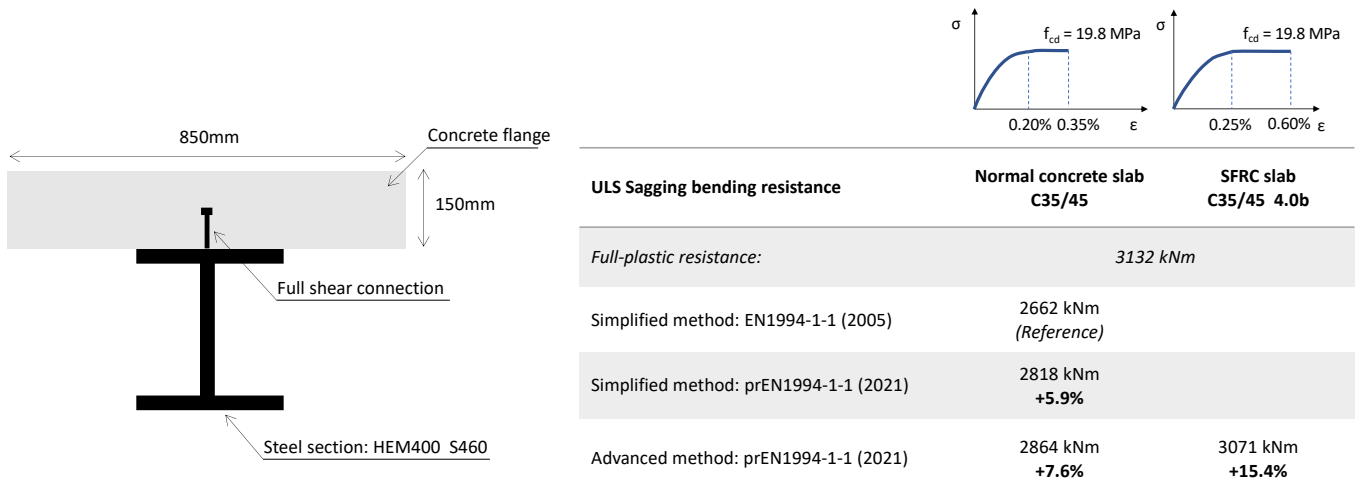


Figure 6. Steel-concrete composite section considered in the example.

which reach beyond concrete structures according to Eurocode 2 [27]. For instance, the maximum compression strain of plain concrete in concrete ($\epsilon_{cu} = 0.0035$ for normal strength concrete in accordance with Eurocode 2 [27] and EC2 [73]) plays a relevant role also for the design of steel-concrete composite structures in accordance with Eurocode 4 [93].

For several composite cross-section configurations in fact the concrete component may reach its ultimate compressive strain before the structural steel component develops enough strain to reach yielding in most of the steel section, thus full plastic capacity may not be reached.

This aspect is explicitly considered when the strain-based resistance of the cross-section is performed (a recent review of strain-limited design method for composite beam sections is given by Zhang [71] and Schäfer *et al.* [72]). The described phenomenon depends on different effects that impact the rotation capacity, as the position of the plastic neutral axis, material strength and geometry of the cross-section. Thus when reaching the concrete ultimate strain before the plastic moment resistance of the steel section is attained, a concrete compression failure may occur in the compression zone even if the cross-section satisfies the Class 2 requirements (criteria to prevent local buckling effects in the steel sections prior to reaching of the plastic resistance, EN1993-1-1 [94]). On a general basis, a strain-based resistance with the stress-strain curves in accordance with EN 1992-1-1 [27] for concrete and reinforcement steel and EN1993-1-1 [94] for the stress-strain curve of structural steel would be required to consider the limited rotation capacity of the section due to the restrictions by the concrete. In addition, for composite beams with partial shear interaction, the strain discontinuity appearing in the composite connection shall be considered. To avoid this effort for practical design, Eurocode 4 [93] provides a simplified design method based on the full-plastic cross-section moment resistance introducing a reduction factor β . The reduction factors were derived by a large parametric study comparing the plastic and strain-limited resistance for a large spectrum of composite cross-sections and material combinations. For current Eurocode 4 [93] this study was provided by

Hanswille *et al.* [95] and newer investigation for the second generation of Eurocode 4, prEN1994-1-1 [96], can be found in Schäfer *et al.* [97].

Furthermore, the use of steel grades such as S500 or higher (already foreseen in product standards [98], design codes for steel structures and the second generation of Eurocodes) requires developing higher strains to reach yielding. At increasing strain the cases of premature compression concrete failure become even more relevant, reducing the interest of high steel strength with composite structures.

The following configurations may lead to a limitation of the plastic moment resistance (a more detailed discussion of the configurations is given in [99]):

1. composite beam with a limited effective width of the concrete flange (e.g. edge beams, due to openings in the slab, use of precast slab elements);
2. composite beams with high strength steel (in particular for S420 or higher grades);
3. composite beams with an intensive concrete contribution (e.g. for partially encased composite beams with a large amount of reinforcement, fully encased composite beams such as filler beam decks and shallow-floor beams);
4. composite beams with asymmetric steel sections having a bottom flange area significantly higher than the top flange;
5. composite beams with hybrid steel sections having a bottom flange resistance significantly higher than the top flange;
6. concrete encased composite columns without external steel tube.

To quantify the impact that higher concrete ductility obtained by steel fibre reinforcement would bring for steel-concrete composite structures a calculation example is proposed corresponding to case 2 of above list. A typical composite beam cross-section with a standard profile and a concrete flange on top of the upper steel flange is considered (see Figure 6). Complete interaction with full shear connection is assumed. The example considers sagging bending moment, therefore with the concrete component being entirely under compression.

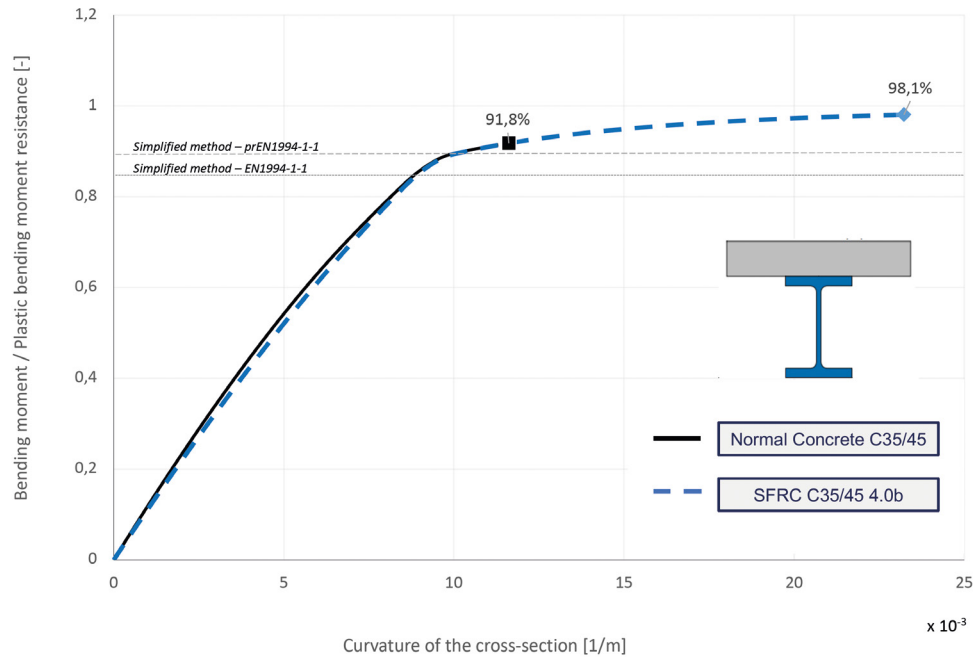


Figure 7. Moment-curvature diagram of the cross-section of Figure 6 with different types of concrete slab.

The simplified method is based on a plastic stress block distribution assuming the whole cross-section attaining the plastic resistance, whereas the reduction factor β for the deep-lying neutral axis is applied as in the current design provisions of current Eurocode 4 [93] for the normal strength concrete. The simplified method is also applied with the reduction factor β proposed in the future version of the design code based on Schäfer *et al.* [97].

The advanced method foresees an integration of the material laws over the cross-section. The calculation is performed both with the non-linear stress-strain relationship according to subsection 3.1 as well as for the parabola rectangle explained in subsection 3.2, and with f_{cd} obtained following the provisions in the draft of the new Eurocode 4 [96] for calculation of the resistance of a cross-section of this type [97], for a compressive strength class C35/45. The results have a maximum difference of 2% (the energy consumption of both models is the same for the selected class C35/45 4.0 b) and for sake of simplicity only the ones obtained with the parabola-rectangle are reported in Figure 6. For the steel material, the quadrilinear stress-strain relationship has been used according to [97].

Since steel is very ductile and can reach very large elongations before rupture, in this kind of cross-sections under sagging bending moment the maximum resistance is reached when the top fibre attains the maximum admissible concrete compressive strain (ultimate strain). Figure 7 shows that beside an improvement of the bending moment resistance, a remarkable increase of the section ductility is achieved. This leads to significant higher cross-section rotation capacity in plastic hinges when using SFRC than the one of plain concrete thanks to a pronounced yielding plateau which is more than doubled. The beneficial effects of this increased ductility will not be discussed here, but is focus of ongoing research and is hinted that it may contribute in redistributing bending mo-

ments in continuous systems and ensuring ductility of specific shear connection configurations.

As a conclusion, the increased concrete ductility achieved by SFRC in compression is promising for the optimization of some specific steel-concrete composite structures. For a future deployment of higher strengths for the structural steel sections (both for columns and beam applications) and the more and more widespread use of cross-section configuration with limited rotation capacity an increased concrete ductility appears essential.

It shall be reminded that the considerations exposed in this chapter have focused on the impact of the improved compression behaviour of SFRC compared to concrete without fibres: other advantages are of course expected by the improved tensile behaviour (crack limitation, durability, shear connection resistance), possibly an additional reason to combine these materials in steel-concrete composite structures.

5. CONCLUSIONS

Annex L of the new EC2 [73] considers the enhancement in ductility and toughness in compression due to fibres. It proposes to use the same stress-strain formulas for the compressive behaviour of plain concrete in the core of EC2 [73] but changes the strain parameters to account for the ductility increase. In particular, parameter k is used to define the initial slope of the curve in the ramp-up stretch, up to the stress peak, but changes after the peak to represent the intercept of the downward curve with the strain axis, and so it defines the energy consumption of the material after the peak. Similarly, Annex L also enlarges the strain values needed for the ULS calculation of SFRC sections. In this paper, we give detailed derivations

of all the expressions in Annex L related to the compressive SFRC behaviour, which are based on a multivariate analysis of a large database [89–91].

In addition, we provide formulas to calculate the compressive strength needed to get a desired flexural performance class since the compressive behaviour of a base concrete is correlated with the residual flexural strengths of the corresponding SFRC. We give compressive strength values for each flexural performance class defined in Annex L of the new EC2 [73], which may be very useful to design a SFRC.

Regarding the strain values for ULS calculations, Annex L mirrors the approach for plain concrete and gives constant values of the parameters defining the parabola-rectangle model, ϵ_{c2} and ϵ_{cu} , for any SFRC. However, we propose particular values of these parameters for each flexural performance class, to take better advantage of the ductility increase of SFRC in stronger classes.

Finally, we highlight the importance of accounting for the real SFRC ductility in composite structures since the low deformation capacity of plain concrete makes that steel elements cannot be used to their limits. We provide an example of a composite beam with a deep neutral axis and high steel strength, which resists 15.4% more load and duplicates its rotation capacity with the new provisions in Annex L.

Acknowledgements

The authors gratefully acknowledge the financial support from the *Ministerio de Ciencia e Innovación*, Spain, through grants PID2019-110928RB-C31 and RTC- 2017-6736-3, and the *Junta de Comunidades de Castilla-La Mancha*, Spain, through grant SBPLY/19/180501/000220.

Nomenclature

CMOD	Crack mouth opening displacement
E_{cm}	Mean elastic modulus of concrete/SFRC in 150 300 mm ² cylinders
EC2	New Eurocode 2 (final draft, version 2022-11) [73]
f_{cd}	Design value of concrete/SFRC compressive strength
f_{fd}	Design value of SFRC compressive strength ¹
f_{cm}	Mean compressive strength of concrete/SFRC in 150 x 300 mm ² cylinders
$f_{R,1k}$	Characteristic residual flexural strength for a crack mouth opening displacement of 0.5 mm
$f_{R,3k}$	Characteristic residual flexural strength for a crack mouth opening displacement of 2.5 mm
k	Coefficient
SC	Strength class
SFRC	Steel-fibre reinforced concrete
ULS	Ultimate limit state
W_{c1}	Volumetric deformation work in pre-peak branch of concrete/SFRC in 150 × 300 mm ² cylinders (from $\epsilon_c = 0$ to $\epsilon_c = \epsilon_{c1}$)

1 Annex L does not use parameters with subscript *f* for referring to SFRC but uses subscript *c* for plain concrete and SFRC. However, the complete definition and derivation of the compressive model need to differentiate between both types of materials since we require to refer to a base concrete (*c*) and the SFRC resulting from reinforcing it with steel fibres (*f*).

W_{c2}	Volumetric deformation work in post-peak branch of concrete/SFRC in 150×300 mm ² cylinders (from $\epsilon_c = \epsilon_{c1}$ to $\epsilon_c = \epsilon_{cu1}$)
W_{f1}	Volumetric deformation work in pre-peak branch of SFRC in 150 × 300 mm ² cylinders (from $\epsilon_f = 0$ to $\epsilon_f = \epsilon_{f1}$)
W_{f2}	Volumetric deformation work in post-peak branch of SFRC in 150 × 300 mm ² cylinders up to 3 ϵ_{f1} (from ϵ_{f1})
$W_{f1}^0 = \frac{W_{f1}}{W_{c1}}$	Non-dimensional volumetric deformation work in pre-peak branch of SFRC
$W_{f2}^0 = \frac{W_{f2}}{W_{c2}}$	Non-dimensional volumetric deformation work in post-peak branch of SFRC
w_M	Crack mouth opening displacement, CMOD
$w_o = 1 \text{ mm}$	Coefficient to keep non-dimensionality
ϵ_c	Compressive strain in concrete/SFRC
ϵ_{c1}	Compressive strain in concrete/SFRC when the stress reaches the compressive strength in the stress-strain model for non-linear analysis
ϵ_{cu1}	Ultimate compressive strain in concrete/SFRC in the stress-strain model for non-linear analysis
ϵ_{c2}	Compressive strain in concrete/SFRC when the stress reaches the compressive strength in the ULS model
ϵ_{cu}	Ultimate compressive strain in concrete/SFRC in the ULS model
ϵ_f	Compressive strain in SFRC
ϵ_{f1}	Compressive strain in SFRC when the stress reaches the compressive strength in the stress-strain model for non-linear analysis
ϵ_{f2}	Compressive strain in SFRC when the stress reaches the compressive strength in the ULS model
ϵ_{fu}	Ultimate compressive strain in SFRC in the ULS model
ϵ_{fu1}	Ultimate compressive strain in SFRC in the stress-strain model for non-linear analysis
$\eta = \frac{\epsilon_c}{\epsilon_{c1}}$	Non-dimensional compressive strain in concrete/SFRC
$\eta_u = \frac{\epsilon_{cu1}}{\epsilon_{c1}}$	Non-dimensional ultimate compressive strain in concrete/SFRC in the stress-strain model for non-linear analysis
σ_c	Stress in concrete/SFRC
σ_{cd}	Design value of compressive stress in concrete/SFRC
σ_f	Stress in SFRC
σ_{Nk}	Characteristic nominal/flexural stress
σ_R	Compressive residual strength
σ_{SC}	Strength class, SC

References

- [1] G. Tiberti, F. Germano, A. Mudadu, G. Plizzari, An overview of the flexural post-cracking behavior of steel fiber reinforced concrete, *Structural Concrete* 19 (2018) 695–718. <https://doi.org/10.1002/suco.201700068>
- [2] N. Buratti, B. Ferracuti, M. Savoia, Concrete crack reduction in tunnel linings by steel fibre-reinforced concretes, *Construction and Building Materials* 44 (2013) 249–259. <https://doi.org/10.1016/j.conbuildmat.2013.02.063>
- [3] M. di Prisco, G. Pizzari, L. Vandewalle, Fibre reinforced concrete: New design perspectives, *Materials and Structures* 42 (9) (2009) 1261–1281. <https://doi.org/10.1617/s11527-009-9529-4>

- [4] F. Altun, T. Haktanir, K. Ari, Effects of steel fiber addition on mechanical properties of concrete and RC beams, *Construction and Building Materials* 21 (2007) 654–661. <https://doi.org/10.1016/j.conbuildmat.2005.12.006>
- [5] B. Xu, H. Shi, Correlations among mechanical properties of steel fiber reinforced concrete, *Construction and Building Materials* 23 (12) (2009) 3468–3474. <https://doi.org/10.1016/j.conbuildmat.2009.08.017>
- [6] S. Lee, C. J.Y., F. Vecchio, Simplified diverse embedment model for steel fiber-reinforced concrete elements in tension, *ACI Materials Journal* 110 (4) (2013) 403–412.
- [7] A. Naaman, H. Reinhardt, High performance fiber reinforced cement composites–HPFRCC4, in: A. Naaman, H. Reinhardt (Eds.), *RILEM Proceedings, PRO 30*, RILEM Publications SARL, 2003.
- [8] J. Walraven, Fibre reinforced concrete: A material in development, in: *Conference in Structural Applications of Fiber Reinforced Concretes*, Barcelona, Spain, 2007, pp. 199–213.
- [9] Fibre reinforced concrete: Challenges and opportunities, in: J. Barros (Ed.), *8th RILEM International Symposium (BEFIB 2012)*, Guimaraes, Portugal, RILEM Publications SARL, 2012.
- [10] J. Deluce, F. Vecchio, Cracking behavior of steel fiber-reinforced concrete members containing conventional reinforcement, *ACI Structural Journal* 110 (3) (2013) 481–490.
- [11] A. Caratelli, A. Meda, Z. Rinaldi, Design according to MC2010 of a fibre-reinforced concrete tunnel in Monte Lirio, Panama, *Structural Concrete* 13 (3) (2012) 166–173. <https://doi.org/10.1002/suco.201100034>
- [12] A. De La Fuente, P. Pujadas, A. Blanco, A. Aguado, Experiences in Barcelona with the use of fibres in segmental linings, *Tunnelling and Underground Space Technology* 27 (1) (2012) 60–71. <https://doi.org/10.1016/j.tust.2011.07.001>
- [13] H. Mashimo, N. Isago, T. Kitani, T. Endou, Effect of fiber reinforced concrete on shrinkage crack of tunnel lining, *Tunnelling and Underground Space Technology* 21 (3–4) (2006) 382–3.
- [14] H. Mashimo, N. Isago, T. Kitani, Numerical approach for design of tunnel concrete lining considering effect of fiber reinforcements, *Tunnelling and Underground Space Technology* 19 (4–5) (2004) 454–5.
- [15] L. Sorelli, F. Toutlemonde, On the design of steel fibre reinforced concrete tunnel lining segments, in: *XI International Conference on Fracture*. Turin, Italy, 2005.
- [16] R. Gettu, B. Barragán, T. García, J. Ortiz, R. Justa, Fiber concrete tunnel lining, *Concrete International* 28 (8) (2006) 63–69.
- [17] G. Tiberti, G. Plizzari, J. Walraven, C. Blom, Concrete tunnel segments with combined traditional and fibre reinforcement, in: *Tailor Made Concrete Structures – New Solutions for Our Society (fib Symposium)*. Amsterdam, The Netherlands, 2008, pp. 605–610.
- [18] R. Burgers, J. Walraven, G. Plizzari, G. Tiberti, Structural behaviour of SFRC tunnel segments during TBM operations, in: *World Tunnel Congress ITA-AITES*. Prague, Czech Republic, 2007, pp. 1461–1467.
- [19] T. Kasper, C. Edvardsen, G. Wittneben, D. Neumann, Lining design for the district heating tunnel in Copenhagen with steel fibre reinforced concrete segments, *Tunnelling and Underground Space Technology* 23 (5) (2008) 574–587.
- [20] A. Caratelli, A. Meda, Z. Rinaldi, P. Perruzza, P. Romualdi, Precast tunnel segment in fibre reinforced concrete., in: *Concrete Engineering for Excellence and Efficiency (fib Symposium)*. Prague, Czech Republic, 2011, pp. 579–582.
- [21] A. Meda, G. Plizzari, A new design approach for SFRC slabs on grade based on fracture mechanics, *ACI Structural Journal* 101 (3) (2004) 298–303. <https://doi.org/10.14359/13089>
- [22] B. Belletti, R. Cerioni, A. Meda, G. Plizzari, Design aspects on steel fiber reinforced concrete pavements, *Journal of Materials in Civil Engineering* 20 (9) (2008) 599–607. [https://doi.org/10.1061/\(ASCE\)0899-1561\(2008\)20:9\(599\)](https://doi.org/10.1061/(ASCE)0899-1561(2008)20:9(599))
- [23] J. Michels, D. Waldmann, S. Maas, A. Zürbes, Steel fibers as only reinforcement for flat slab construction – Experimental investigation and design, *Construction and Building Materials* 26 (1) (2012) 145–155. <https://doi.org/10.1016/j.conbuildmat.2011.06.004>
- [24] M. Soutsos, T. Le, A. Lampropoulos, Flexural performance of fibre reinforced concrete made with steel and synthetic fibres, *Construction and Building Materials* 36 (2012) 704–710. <https://doi.org/10.1016/j.conbuildmat.2012.06.042>
- [25] A. De La Fuente, R. Escariz, A. De Figueiredo, C. Molins, A. Aguado, A new design method for steel fibre reinforced concrete pipes, *Construction and Building Materials* 30 (2012) 547–555. <https://doi.org/10.1016/j.conbuildmat.2011.12.015>
- [26] *fib Bulletins* 65 & 66, Model Code 2010, Final Draft, International Federation for Structural Concrete, *fib*. Lausanne, Switzerland, 2012.
- [27] EN 1992-1-1, Eurocode 2: Design of Concrete Structures, European Committee for Standardization–CEN, 2020.
- [28] UNI 11039-2, Steel Fibre Reinforced Concrete–Test Method for Determination of First Crack Strength and Ductility Indexes, Italian Standardization Body–UNI, 2003.
- [29] Guide for the Design and Construction of Fiber-Reinforced Concrete Structures, Italian Standardization Body–UNI, 2003.
- [30] DAFStb TR SFRC Draft, DAFStb Technical Rule on Steel Fibre Reinforced Concrete, Deutscher Ausschuss für Stahlbeton (DAFStb), 2012.
- [31] EHE 08, Instrucción de Hormigón Estructural, Ministerio de Fomento. Secretaria General Técnica, 2008.
- [32] RILEM TC 162 TDF, Test and design methods for steel fibre reinforced concrete. Design of steel fibre reinforced concrete using the σw method: Principles and applications, *Materials and Structures* 35 (5) (2002) 262–278.
- [33] RILEM TC 162 TDF, Test and design methods for steel fibre reinforced concrete. $\sigma - \epsilon$ design method. Final recommendation, *Materials and Structures* 36 (8) (2003) 560–567.
- [34] RILEM TC 162 TDF, Test and design methods for steel fibre reinforced concrete. $\sigma - \epsilon$ design method. Recommendation, *Materials and Structures* 33 (2) (2000) 75–81.
- [35] EN14651, Test Method for Metallic Fibre Concrete–Measuring the Flexural Tensile Strength (Limit of Proportionally (LOP), Residual), European Committee for Standardization, Brussels, 2005.
- [36] D. Yoo, N. Banthia, Experimental and numerical analysis of the flexural response of amorphous metallic fiber reinforced concrete, *Materials and Structures* 50 (64) (2017).
- [37] S. Yazici, G. Inan, V. Tabak, Effect of aspect ratio and volume fraction of steel fiber on the mechanical properties of SFRC, *Construction and Building Materials* 21 (2007) 1250–1253. <https://doi.org/10.1016/j.conbuildmat.2006.05.025>
- [38] R. Swamy, P. Mangat, A theory for the flexural strength of steel fiber reinforced concrete, *Cement and Concrete Research* 4 (2) (1974) 313–325.
- [39] J. Olesen, Crack propagation in fiber-reinforced concrete beams, *Journal of Engineering Mechanics* 127 (3) (2001) 272–280. [https://doi.org/10.1061/\(ASCE\)0733-9399\(2001\)127:3\(272\)](https://doi.org/10.1061/(ASCE)0733-9399(2001)127:3(272))
- [40] M. Pajak, T. Ponikiewski, Flexural behavior of self-compacting concrete reinforced with different types of steel fibers, *Construction and Building Materials* 47 (2013) 397–408. <https://doi.org/10.1016/j.conbuildmat.2013.05.072>
- [41] D. Yoo, N. Banthia, J. Yang, Y. Yoon, Mechanical properties of corrosion-free and sustainable amorphous metallic fiber-reinforced concrete, *ACI Materials Journal* 113 (5) (2016) 633–643. <https://doi.org/10.14359/51689108>
- [42] P. Marti, T. Pfy, V. Sigrist, T. Ulaga, Harmonized test procedures for steel fiber-reinforced concrete, *ACI Materials Journal* 96 (6) (1999) 676–686. <https://doi.org/10.14359/794>
- [43] P. Stroeven, Stereological principles of spatial modeling applied to steel fiber-reinforced concrete in tension, *ACI Materials Journal* 106 (3) (2009) 213–222.
- [44] J. Voo, S. Foster, Variable engagement model for fibre reinforced concrete in tension, in: *Uniciv Report R-420*. School of Civil and Environmental Engineering, University of New South Wales, Sydney, NSW, Australia, 2003, pp. 86–96.
- [45] T. Leutbecher, E. Fehling, Crack width control for combined reinforcement of rebars and fibers exemplified by ultra-high-performance concrete, in: *Uniciv Report R-420*. School of Civil and Environmental Engineering, fib Task Group 8.6, Ultra High Performance Fiber Reinforced Concrete–UHPFRC, 2008, pp. 1–28.
- [46] S. Lee, J. Cho, F. Vecchio, Diverse embedment model for steel fiber-reinforced concrete in tension: Model development, *ACI Materials Journal* 108 (5) (2011) 516–525.
- [47] S. Lee, J. Cho, F. Vecchio, Diverse embedment model for steel fiber-reinforced concrete in tension: Model verification, *ACI Materials Journal* 108 (5) (2011) 526–535.
- [48] ACI 544.4R-88, Design Considerations for Steel Fiber Reinforced Concrete, Tech. rep., American Concrete Institute (1999).
- [49] S. Shah, P. Stroeven, D. Dalhuisen, P. Van Stekelenburg, Complete stress-strain curves for steel fibre reinforced concrete in uniaxial tension and compression, *Testing and Test Methods of Fibre Cement Composites* (1978) 399–408.
- [50] M. A. Tasdemir, A. Ilki, M. Yerlikaya, Mechanical behaviour of steel fibre reinforced concrete used in hydraulic structures, in: *International Conference of Hydropower and Dams, HYDRO 2002*, 2002, pp. 159–166.
- [51] F. Bayramov, M. A. Tasdemir, A. Ilki, M. Yerlikaya, Steel fibre reinforced concrete for heavy traffic load conditions, in: *9th International Symposium on Concrete Roads*, 2004, pp. 73–82.
- [52] L. Hsu, C. Hsu, Complete stress-strain behavior of high-strength concrete under compression, *Magazine of Concrete Research* 46 (169) (1994) 301–312. <http://dx.doi.org/10.1680/mac.1994.46.169.301>

- [53] A. Someh, N. Saeki, Prediction for the stress-strain curve of steel fiber reinforced concrete, in: Proceedings Japan Concrete Institute, Vol. 18, 1994, pp. 1149–1154.
- [54] M. Mansur, M. Chin, T. Wee, Stress-strain relationship of high-strength fiber concrete in compression, *ASCE Journal of Materials in Civil Engineering* 11 (1999) 21–29. [https://doi.org/10.1061/\(ASCE\)0899-1561\(1999\)11:1\(21\)](https://doi.org/10.1061/(ASCE)0899-1561(1999)11:1(21))
- [55] M. Nataraja, N. Dhang, A. Gupta, Stress-strain curves for steel-fiber reinforced concrete under compression, *Cement and Concrete Composites* 21 (5–6) (1999) 383–390. [https://doi.org/10.1016/S0958-9465\(99\)00021-9](https://doi.org/10.1016/S0958-9465(99)00021-9)
- [56] R. Neves, J. Fernandes de Almeida, Compressive behaviour of steel fibre reinforced concrete, *Structural Concrete* 6 (1) (2005) 1–8. <https://doi.org/10.1680/stco.2005.6.1.1>
- [57] J. Barros, J. Figueiras, Flexural behavior of SFRC: Testing and modeling, *Journal of Materials in Civil Engineering* 11 (4) (1999) 331–339. [https://doi.org/10.1061/\(asce\)0899-1561\(1999\)11:4\(331\)](https://doi.org/10.1061/(asce)0899-1561(1999)11:4(331))
- [58] R. Neves, Modelling the Compressive Behaviour of Steel Fibre Reinforced Concrete, Master Thesis, Instituto Superior Técnico, Lisbon, 2000.
- [59] D. Fanella, A. Naaman, Stress-strain properties of fiber reinforced mortar in compression, *ACI Journal* 82 (4) (1985) 475–483.
- [60] D. Otter, A. E. Naaman, Steel fibre reinforced concrete under static and cyclic compressive loading, in: RILEM Symposium FRC 86, Devel. in Fibre Reinforced Cement and Concrete, Vol. 1, 1986.
- [61] K. Marar, O. Eren, T.Çelik, Relationship between impact energy and compression toughness energy of high-strength fiber-reinforced concrete, *Materials Letters* 47 (2001) 297–304.
- [62] J. Thomas, A. Ramaswamy, Mechanical properties of steel fiber-reinforced concrete, *Journal of Materials in Civil Engineering* 19 (2007) 385–392. [https://doi.org/10.1061/\(ASCE\)0899-1561\(2007\)19:5\(385\)](https://doi.org/10.1061/(ASCE)0899-1561(2007)19:5(385))
- [63] L. Daniel, A. Loukili, Behavior of high-strength fiber-reinforced concrete beams under cyclic loading, *ACI Structural Journal* 99 (3) (2002) 248–256. <https://doi.org/10.14359/11908>
- [64] G. Williamson, The effect of steel fibers on the compressive strength of concrete, in: *Fiber Reinforced Concrete – ACI Symposium Publication*, Vol. 44, American Concrete Institute, 1974, pp. 195–207.
- [65] P. Soroushian, C. Lee, Constitutive modeling of steel fiber reinforced concrete under direct tension and compression, in: *Fibre Reinforced Cements and Concretes, Recent Developments*. University of Wales, College of Cardiff, School of Engineering, United Kingdom, 1989, pp. 363–375.
- [66] A. Ezeldin, P. Balaguru, Normal and high strength fiber reinforced concrete under compression, *Journal of Materials in Civil Engineering* 4 (4) (1992) 415–429. [https://www.doi.org/10.1061/\(ASCE\)0899-1561\(1992\)4:4\(415\)](https://www.doi.org/10.1061/(ASCE)0899-1561(1992)4:4(415))
- [67] Y. Ou, M. Tsai, K. Liu, K. Chang, Compressive behavior of steel fiber reinforced concrete with a high reinforcing index, *Journal of Materials in Civil Engineering* 24 (2) (2011) 207–215. [https://doi.org/10.1061/\(ASCE\)MT.1943-5533.0000372](https://doi.org/10.1061/(ASCE)MT.1943-5533.0000372)
- [68] L. Taerwe, Influence of steel fibres on strain-softening of high-strength concrete, *Materials Journal* 88 (6) (1992) 54–60. <http://hdl.handle.net/1854/LU-204450>
- [69] B. Hughes, N. Fattuhi, Stress-strain curves for fiber reinforced concrete in compression, *Cement and Concrete Research* 7 (2) (1977) 173–183. [https://doi.org/10.1016/0008-8846\(77\)90028-X](https://doi.org/10.1016/0008-8846(77)90028-X)
- [70] F. Bencardino, L. Rizzuti, G. Spadea, Experimental tests vs. theoretical modeling for FRC in compression, *FramCoS*, 2007, pp. 159–166.
- [71] Q. Zhang, Moment and Longitudinal Resistance for Composite Beams Based on Strain Limited Design Method, Ph.D. thesis, Université du Luxembourg (2020).
- [72] M. Schäfer, Q. Zhang, M. Braun, M. Banfi, Limitations of plastic bending resistance for composite beams deviated from strain-limitation, *Journal of Constructional Steel Research* 180 (2021) 106562. <https://doi.org/10.1016/j.jcsr.2021.106562>
- [73] CEN, Eurocode 2, Design of concrete structures. Part 1-1: General rules – Rules for buildings, bridges and civil structures, prEN 1992-1-1: 2022, version of November 10, 2022, available at both UNE and CEN websites (2022).
- [74] S. Lee, J. Oh, J. Cho, Compressive behavior of fiber-reinforced concrete with end-hooked steel fibers, *Materials* 8 (4) (2015) 1442–1458. <https://doi.org/10.3390/ma8041442>
- [75] F. Bencardino, L. Rizzuti, G. Spadea, R. Swamy, Stress-strain behavior of steel fiber-reinforced concrete in compression, *Journal of Materials in Civil Engineering* 20 (2008) 255–263.
- [76] P. Song, S. Hwang, Mechanical properties of high-strength steel fiber-reinforced concrete, *Construction and Building Materials* 18 (9) (2004) 669–673. <https://doi.org/10.1016/j.conbuildmat.2004.04.027>
- [77] F. Bayramov, C. Tasdemir, M. Tasdemir, Optimisation of steel fibre reinforced concretes by means of statistical response surface method, *Cement and Concrete Composites* 26 (2004) 665–675. [https://doi.org/10.1016/S0958-9465\(03\)00161-6](https://doi.org/10.1016/S0958-9465(03)00161-6)
- [78] B. Jo, Y. Shon, Y. Kim, The evaluation of elastic modulus for steel fiber reinforced concrete, *Russian Journal of Nondestructive Testing* 37 (2001) 152–161. <https://doi.org/10.1023/A:1016780124443>
- [79] F. Aslani, S. Nejadi, Self-compacting concrete incorporating steel and polypropylene fibers: Compressive and tensile strengths, moduli of elasticity and rupture, compressive stress-strain curve, and energy dissipated under compression, *Composites Part B: Engineering* 53 (2013) 121–133. <https://doi.org/10.1016/j.compositesb.2013.04.044>
- [80] Y. Şahin, F. Köksal, The influences of matrix and steel fibre tensile strengths on the fracture energy of high-strength concrete, *Construction and Building Materials* 25 (4) (2011) 1801–1806. <https://doi.org/10.1016/j.conbuildmat.2010.11.084>
- [81] P. Cachim, J. Figueiras, P. Pereira, Fatigue behavior of fiber-reinforced concrete in compression, *Cement and Concrete Composites* 24 (2) (2002) 211–217.
- [82] B. Barragán, R. Gettu, M. Martín, R. Zerbinò, Uniaxial tension test for steel fibre reinforced concrete — A parametric study, *Cement and Concrete Composites* 25 (7) (2003) 767–777. [https://doi.org/10.1016/S0958-9465\(02\)00096-3](https://doi.org/10.1016/S0958-9465(02)00096-3)
- [83] A. Medeiros, X. Zhang, G. Ruiz, R. Yu, M. de Souza Lima Velasco, Effect of the loading frequency on the compressive fatigue behavior of plain and fiber reinforced concrete, *International Journal of Fatigue* 70 (2015) 342–350. <https://doi.org/10.1016/j.ijfatigue.2014.08.005>
- [84] H. Dhonde, Y. Mo, T. Thomas, C. Hsu, J. Vogel, Fresh and hardened properties of self-consolidating fiber-reinforced concrete, *ACI Materials Journal* 104 (5) (2007) 491–500.
- [85] K. Marar, O. Eren, I. Yitmen, Compression specific toughness of normal strength steel fiber reinforced concrete (NSSFRC) and high strength steel fiber reinforced concrete (HSSFRC), *Materials Research* 14 (2) (2011) 239–247. <https://doi.org/10.1590/S1516-14392011005000042>
- [86] F. Wafa, S. Ashour, Mechanical properties high strength fiber reinforced concrete, *ACI Materials Journal* 89 (5) (1992) 449–455.
- [87] M. Tabatabaiean, A. Khaloo, A. Joshaghani, E. Hajibandeh, Experimental investigation on effects of hybrid fibers on rheological, mechanical, and durability properties of high-strength SCC, *Construction and Building Materials* 147 (2017) 497–509. <https://doi.org/10.1016/j.conbuildmat.2017.04.181>
- [88] F. Köksal, A. İlki, M. Tasdemir, Optimum mix design of steel-fibre-reinforced concrete plates, *Arabian Journal for Science and Engineering* 38 (11) (2013) 2971–2983. <https://doi.org/10.1007/s13369-012-0468-y>
- [89] G. Ruiz, Á. De La Rosa, S. Wolf, E. Poveda, Model for the compressive stress-strain relationship of steel fiber-reinforced concrete for non-linear structural analysis, *Hormigón y Acero* 69-Suppl. 1 (2018) 75–80. <https://doi.org/10.1016/j.hya.2018.10.001>
- [90] G. Ruiz, Á. De La Rosa, E. Poveda, Relationship between residual flexural strength and compression strength in steel-fiber reinforced concrete within the new Eurocode 2 regulatory framework, *Theoretical and Applied Fracture Mechanics* 103 (2019) 102310. <https://doi.org/10.1016/j.tafmec.2019.102310>
- [91] Á. De La Rosa, G. Ruiz, E. Poveda, Study of the compression behavior of steel-fiber reinforced concrete by means of the response surface methodology, *Applied Sciences* 9:24 (2019) 5330. <https://doi.org/10.3390/app9245330>
- [92] M. Sargin, Stress-strain Relationship for Concrete and the Analysis of Structural Concrete Sections, Studies series, Solid Mechanics Division, University of Waterloo, 1971.
- [93] EN 1994-1-1, Design of Composite Steel and Concrete Structures, European Committee for Standardization–CEN, 2013.
- [94] EN 1993-1-1, Design of Steel Structures: General rules and rules for buildings, European Committee for Standardization–CEN, 2005.
- [95] G. Hanswille, G. Sedlacek, D. Anderson, The use of steel grades S460 and S420 in composite structures, Tech. rep., ECCS-EUROFER improvements by TC11 to Eurocode 4 (1996).
- [96] CEN, Eurocode 4, Design of composite steel and concrete structures. Part 1-1: Part 1-1: General rules and rules for buildings, prEN 1994-1-1: 2022, available through the National members at CEN TC250/SC4 until approved as EN (2022).
- [97] M. Schäfer, Q. Zhang, M. Banfi, Background document on materials and limits for plastic moment resistance, Tech. rep., European Mandate M515, CEN/TC250/SC4.T6, CEN-Documents CEN/TC250/SC4 (February 2022).
- [98] EN 10025, Hot rolled products of structural steels, European Committee for Standardization–CEN, 2019.
- [99] M. Schäfer, Q. Zhang, Zur dehnungsbegrenzten Momenten Tragfähigkeit von Flachdecken in Verbundbauweise – Grenzen der plastischen Bemessung, *Stahlbau* 88 (7) (2019) 653–664.

Embedded Fibre Reinforced Polymer (FRP) Reinforcement in Concrete Structures According to the New Version of Eurocode 2

Armaduras de polímeros reforzados con fibras (PRF) para estructuras de hormigón en la nueva versión del Eurocódigo 2

Eva Oller^{*,a}, Lluís Torres^b, Ana de Diego^c

Department of Civil and Environmental Engineering, Universitat Politècnica de Catalunya
Department of Mechanical Engineering and Industrial Construction, Universitat de Girona
Instituto de Ciencias de la Construcción Eduardo Torroja (IETCC), CSIC

Recibido el 11 de agosto de 2022; aceptado el 5 de diciembre de 2022

ABSTRACT

The new version of Eurocode 2 will include for the first time an informative annex, Annex R “Embedded FRP reinforcement”, to design reinforced concrete structures with fibre reinforced polymer (FRP) reinforcement. FRP embedded reinforcement has some advantages such as their low susceptibility to corrosion, high-strength, and low life-cycle cost. FRP rebars can be used as longitudinal or transverse reinforcement in a similar way than conventional steel rebars. However, in the design of FRP reinforced concrete structures, some particular aspects related to the reinforcement properties must be taken into account, among which it is worth highlighting their linear elastic behaviour until failure, their relatively low modulus of elasticity or their behaviour under sustained stresses. Since, the content of Annex R is new, a summary and background related to all aspects required for designing with FRP reinforcement are given in this paper.

KEYWORDS: Embedded FRP reinforcement, fibre reinforced polymer, reinforced concrete, Eurocode 2.

©2023 Hormigón y Acero, the journal of the Spanish Association of Structural Engineering (ACHE). Published by Cinter Divulgación Técnica S.L. This is an open-access article distributed under the terms of the Creative Commons (CC BY-NC-ND 4.0) License

RESUMEN

La nueva versión del Eurocódigo 2 incluirá por primera vez un anejo informativo, el Anejo R “Armadura embebida de FRP”, para diseñar estructuras de hormigón armado con armaduras de polímeros reforzados con fibras. Estas armaduras tienen ventajas como su baja susceptibilidad a la corrosión, elevada resistencia y bajo coste de ciclo de vida. Las barras de FRP se pueden utilizar como armadura longitudinal o transversal de manera similar a las barras de acero convencionales. No obstante, en el cálculo de las estructuras de hormigón armadas con barras de FRP, hay algunos aspectos específicos que deben ser tenidos en cuenta, entre los que cabría destacar su comportamiento elástico lineal hasta rotura, su relativamente bajo módulo de elasticidad o su comportamiento con carga mantenida a largo plazo. Dado que el contenido del Anejo R es nuevo, en este artículo se proporciona un resumen del mismo y los antecedentes relacionados con todos los aspectos necesarios para dimensionar con armadura de FRP.

PALABRAS CLAVE: Armadura interna de FRP, polímeros reforzados con fibras, hormigón armado, Eurocódigo 2.

©2023 Hormigón y Acero, la revista de la Asociación Española de Ingeniería Estructural (ACHE). Publicado por Cinter Divulgación Técnica S.L. Este es un artículo de acceso abierto distribuido bajo los términos de la licencia de uso Creative Commons (CC BY-NC-ND 4.0)

1. INTRODUCTION

Fibre reinforced polymer (FRP) embedded reinforcement can be an alternative to conventional steel reinforcement in con-

crete structures exposed to aggressive environments, where magnetic neutrality is required, or in some applications where good cuttability may be an advantage (for instance, a “soft eye” area of a diaphragm wall that will be cut by a Tunnel

* Persona de contacto / Corresponding author:
Correo-e / e-mail: eva.oller@upc.edu (Eva Oller Ibars).

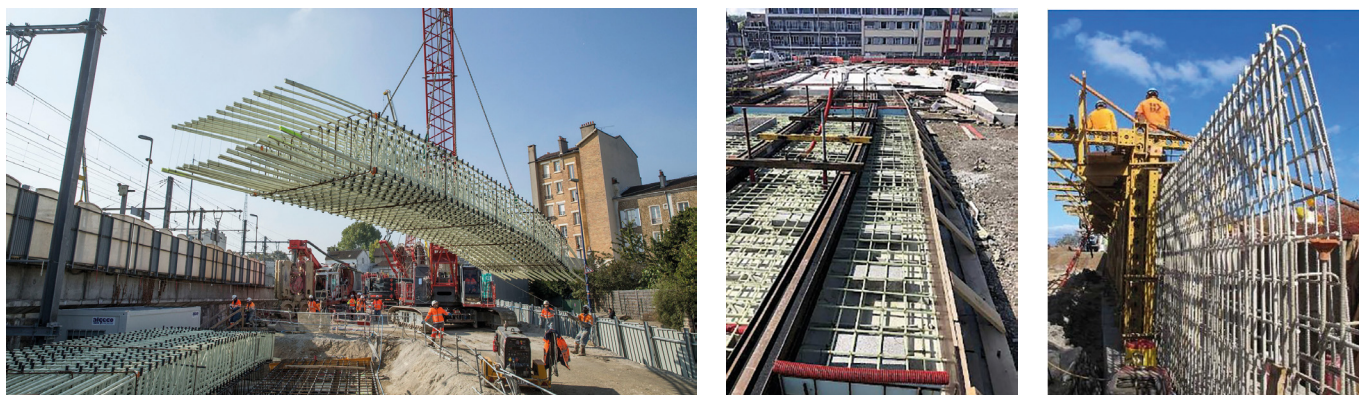


Figure 1. Real applications of FRP embedded reinforcement. a) Metro of Paris (courtesy of Schöck), b) Tramway in Liège (Belgium) (courtesy of Sireg), c) Highway sea wall in Maui (courtesy of Owens Corning) [8].

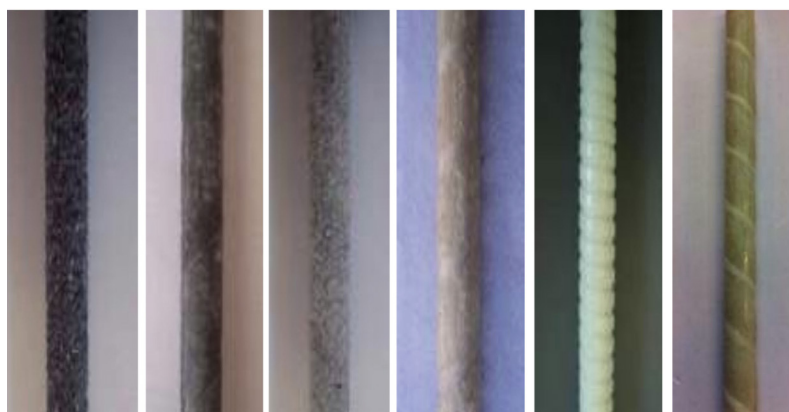


Figure 2. FRP reinforcement [9].

Boring Machine). Its low susceptibility to corrosion leads to longer service life, less maintenance and low life-cycle cost. Additionally, they present low density (ease of handling) and high fatigue endurance [1–5]. FRP rebars appeared in the market in the early 1990s. The first design guidelines for FRP reinforced concrete (RC) were introduced in Japan in 1997 [6]. Most initial applications of FRP reinforcement in concrete were made in Japan but nowadays there are applications worldwide (see Figure 1).

FRP reinforcement consists of continuous fibres of glass (in the case of GFRP), carbon (CFRP), basalt (BFRP) or aramid (AFRP) embedded in a polymeric resin. The fibres contribute with a high-strength and high-stiffness, and the matrix bind the fibres together and transfer the forces between fibres. FRP embedded reinforcement bars are usually manufactured through a pultrusion process where fibres are pulled and impregnated in a resin bath before curing by heat. To increase bond between bar and concrete, there are different surface treatments, such as sand coating, performing surface indentations, over-moulding a new surface on the bar or a combination of these techniques [4,7] (see Figure 2).

The basic principles of design for steel RC can be applied to FRP RC elements, however, the changes in properties of FRP reinforcement may have a different influence on the design [10,11]. Unlike steel, FRP reinforcement behaves linear elastic up to failure and does not yield. Additionally, FRPs subjected to constant stresses may present creep rupture, i.e.

failure at a lower strength than the short-term strength, which can be influenced by adverse environments [4,12]. The linear behaviour of the FRP reinforcement up to high failure stresses leads to a different response of FRP RC members.

The modulus of elasticity of the FRP embedded reinforcement, and in particular for GFRP or BFRP, is much lower than that of steel. This affects bending and shear design, as well as serviceability conditions. Despite the absence of yielding, a proper design leads the FRP RC members to exhibit large deformability at failure. However, the low stiffness of FRP reinforcement may result in large crack widths and deflections, making the design often governed by serviceability requirements [13].

In recent years, concrete structures with embedded FRP reinforcement have successfully been applied in many projects all over the world, nevertheless, the lack of codes and standards equivalent to those for steel has been recognized as a limitation for its normalized use. Annex R of Eurocode 2 (FprEN 1992-1-1:2021) [14] is an informative annex that includes guidance for the design of new RC structures with FRP embedded reinforcement in the form of bars or mesh. Despite the several types of fibres, only glass (GFRP) and carbon (CFRP) reinforcement is covered by this annex. Although there are some recommendations for the use of prestressed FRP reinforcement [15,16] in the final version of Annex R it has been considered that there is not enough experience to cover it. Annex R applies only to normal weight concrete elements and not to lightweight concrete or con-

crete with recycled aggregates, as well as elements subjected predominantly to static loads, that is, with a maximum stress range of 10 % of $f_{fjk,100a}$ (long-term tensile strength, see Section 3) with a maximum stress $0.5f_{fjk,100a}$ for a maximum of 2×10^6 cycles.

This paper aims to introduce the content of Annex R [14] since this is the first time that the design of FRP embedded reinforcement has been introduced in Eurocodes. Model Code 2010 [17] already introduced FRP reinforcement in the chapter of Materials (section on Non-metallic reinforcement) and Interface characteristics (section on Bond of non-metallic reinforcement). There are also some existing guidelines or codes such as the ACI 440.1R-15 [3] (which is currently developed as a Code), CSA S806-12 [18], CNR-DT 203/2006 [19] and JSCE [6]. The fib Bulletin 40 [4] was published in 2007 and gave the background of the main physical and mechanical properties of FRP reinforcing bars, as long as the design models to verify the ultimate and serviceability limit states. This fib bulletin was based on the expertise of the members of fib TG9.3 "FRP Reinforcement for concrete structures". In addition, there is a background document of Annex R [20] with more details about its content.

2. BASIS OF DESIGN

In general, the basis of design of concrete structures with conventional materials can be applied to concrete structures reinforced with FRP longitudinal rebars or transverse stirrups. However, there are some aspects, such as the material safety factors, that should be particularized for this case. Unless a National Annex gives different values, Table 1 gives the partial safety factors for FRP reinforcement that consider also model uncertainty.

These partial safety factors have been obtained assuming a reliability index $\beta = 3.8$ and are based on the characteristic long-term strength of the FRP reinforcement, $f_{fjk,100a}$, which will be defined in §3, and on the short-term strength, f_{fjk} . According to the mentioned background document of Eurocode 2 [20], a reduction can be applied if the supplier can demonstrate the required reliability.

For beams with FRP transverse reinforcement, it has been observed experimentally that the strength in the bent area reduces in comparison to that in the straight part of the stirrup [21–24]. This reduction is a function of the geometry, the material properties and the manufacturing process. Long term reductions between straight and bent shapes are expected as well.

TABLE 1. Partial safety factors for FRP embedded reinforcement [14].

Design situation	γ_{FRP}
ULS (Persistent and transient)	1.50
Accidental	1.10
Serviceability	1.00

3. MATERIALS

The design rules in Annex R are for members reinforced with embedded FRP reinforcement that meet the following conditions:

- Minimum modulus of elasticity of $E_{FR} \geq 40000 \text{ N/mm}^2$
- Ratio of $f_{fjk,100a}/E_{FR} \geq 0.005$
- Minimum long term bond strength of $f_{bd,100a} \geq 1.5 \text{ MPa}$
- Characteristic compressive strength of concrete $f_{ck} \geq 20 \text{ MPa}$
- Members with longitudinal reinforcement ratio $\rho_l \leq 0.05$

The previous limits have been selected to reflect the values of testing specimens used for the calibration of the formulations. These values correlate with products widely available on the market and cover all usual types of reinforcement (ARFP, GFRP, CFRP, BFRP). The limit for the ratio of the long-term strength and the elastic modulus is given to avoid brittle failure. The lower limit on compressive strength of concrete results from the limit on the parameter $f_{bd,100a}$. The maximum reinforcement ratio ρ_l was introduced to avoid an excessive amount of reinforcement and facilitate constructability and placement of concrete.

Annex R requires the definition of the following properties of FRP systems for design according to Eurocode 2 [14]: $f_{fjk,0}$, characteristic short-term tensile strength of the FRP and E_{FR} tensile modulus of elasticity of the FRP, both determined according to ISO 10406-1 [25]; and nominal diameter.

When designing a concrete structure with FRP reinforcement, the designer should specify the following properties, that should be provided by the manufacturer to ensure a performance as assumed in design: section sizes and tolerances; minimum characteristic short-term and long-term tensile strength ($f_{fjk,0}$ and $f_{fjk,100a}$, respectively); tensile modulus of elasticity, E_{FR} ; long-term bond strength, $f_{bd,100a}$; strain at design tensile strength of FRP shear reinforcement, ϵ_{fjwRd} ; installation temperature; maximum and minimum temperature of the FRP reinforcement for the design lifetime of the structure; exposure classification; and durability requirements.

The provision of the design properties that should be considered by the manufacturer is given in the Annex because there is not yet a European Standard or execution standard, or European Assessment Document (EAD), for FRP reinforcement.

As previously mentioned, the behaviour of FRP reinforcement under tension is linear elastic and should only be considered as tension reinforcement. In addition, due to the effect of creep rupture under sustained stresses, there might be a significant reduction in the strength over the time.

For this reason, in relation to the design assumptions for the mechanical properties of the embedded FRP reinforcement, the design tensile strength of embedded FRP reinforcement shall be taken as:

$$f_{fd} = \frac{f_{fjk,100a}}{\gamma_{FRP}} \quad (1)$$

where:

$f_{fjk,100a}$ is the design long-term strength, that can be obtained through tests or either by eq. (2) when it is not directly deter-

mined by production data. The long-term tensile strength is evaluated as the characteristic value of the stress leading to a 5% probability of a failure under 100 years of sustained stress in 40°C wet concrete.

$$f_{fjk,100a} = C_t C_c C_e f_{fjk0} \quad (2)$$

C_t is the factor that considers the temperature effects and can be defined as:

$C_t = 1.0$ for indoor and underground environments,

$C_t = 0.8$ for outdoor members if heating through solar radiation cannot be excluded;

C_c is the ratio between the strength under sustained load and the strength under short-term load, that may be determined according to ISO 10406-1 [25]. This value shall be taken as 0.35 for GFRP reinforcement and 0.8 for CFRP reinforcement, unless more accurate values are determined.

C_e is the ratio between the strength before ageing and after ageing, and may be determined according to the test concept in ISO 10406-1 [25] with exposure to 60°C for a duration of 3000 h. The value shall be taken as 0.7, unless more accurate values are determined.

The design long-term tensile strength considers the decrease in the short-term tensile strength due to sustained stresses, time, temperature and environmental influence. The previous coefficients are conservative and more accurate values can be obtained by performing tests defined in the EAD to directly obtain them. The background document of Eurocode 2 [20] describes tests methods to obtain in a direct way the value of $f_{fjk,100a}$, following tests setups from ISO 10406-1 [25] or comparable international standards [20]. These methods are based on the principles of linear reduction of the residual tensile strength in a time logarithmic scale and the time-temperature shift (i.e. an increase of temperature in the test is equivalent to a certain increase of time in the original temperature). This way $f_{fjk,100a}$ can be extrapolated from tests results with shorter times (i.e. some months)

Without tests and by using eq. (2), a typical design value for the long-term strength of a GFRP rebar in an outdoor element and in a persistent ULS situation might be calculated as indicated in eq. (3). A conservative value for design is obtained.

$$f_{fid} = \frac{f_{fjk,100a}}{\gamma_{FRP}} = \frac{C_t C_c C_e f_{fjk0}}{\gamma_{FRP}} = \frac{0.8 \cdot 0.35 \cdot 0.7}{1.5} = 0.13 f_{fjk0} \quad (3)$$

The stress-strain relationship for FRP embedded reinforcement is linear elastic up to failure. Figure 3 shows the characteristic short-term tensile stress f_{fjk0} , the long-term tensile strength $f_{fjk,100a}$ and the design value of the tensile strength, f_{fid} .

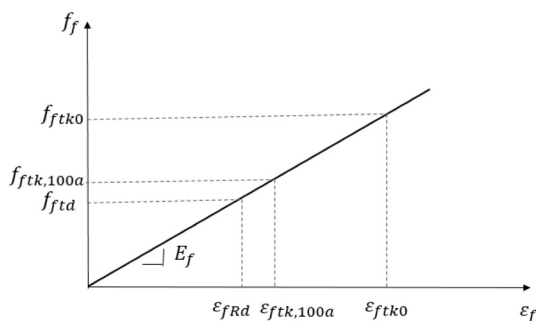


Figure 3. Stress-strain relationship for FRP embedded reinforcement.

Annex R gives also mean values of the FRP density for design purposes (2000 kg/m³ for GFRP and 1650 kg/m³ for CFRP reinforcement) and the coefficient of thermal expansion in the longitudinal direction (5·10⁻⁶ K⁻¹ for GFRP and 0 for CFRP bars).

4. DURABILITY

Durability conditions for design are defined by the main text of Eurocode 2 [14]. However, Annex R gives some provisions related to the concrete cover for reinforced concrete structures with FRP reinforcement. The nominal concrete cover, c_{nom} , is the sum of the minimum value, c_{min} , plus an allowance in design for deviation, as for steel RC members, ΔC_{dev} . The minimum concrete cover is defined as eq. (4).

$$c_{min} = \max \{c_{min,dur} + \Sigma \Delta c; c_{min,b}; 10 \text{ mm}\} \quad (4)$$

In particular, for FRP reinforcement, $c_{min,dur}$, which is the minimum cover required for environmental conditions, is set to zero because corrosion induced by carbonation or chlorides does not occur for FRP reinforcement.

Unless more accurate information based on tests is available, the cover for transmission of forces by bond between reinforcement and concrete should be taken as $c_{min,b} \geq 2\phi$, being ϕ the bar diameter. At least the minimum cover for the FRP reinforcement shall be taken as $c_{min,b} \geq 1.5\phi$ and $c_{min,b} \geq 10$ mm. The concrete cover due to bond requirements may be higher than for steel reinforcement (where the minimum is 1ϕ), because of possibly higher splitting forces. According to the background document [20], for the same force to be anchored, higher slip values and higher splitting forces may occur for FRP reinforcement because of the lower modulus of elasticity and the bar surface.

One issue to keep in mind regarding corrosion is that CFRP reinforcement can form an electrical circuit which can cause corrosion in steel reinforcement in case of an electrical conductive contact. For this reason, direct contact of CFRP and steel reinforcement should be avoided.

Annex R does not address directly all the effects that might induce the deterioration of FRP in concrete (effect of water, chlorides, alkali, sustained stress, ultraviolet radiation, carbonation, acid attack, thermal actions). This might be justified by the limited design data available that can be used by design engineers related to this topic as mentioned in fib Bulletin 40 [4]. This is due to the lack of international agreement on FRP durability test methods, variability in production and variability in fibres, resin and FRP types.

5. STRUCTURAL ANALYSIS

As explained in §3, FRPs are a linear elastic material up to failure. Therefore, linear elastic analysis with limited redistribution and plastic analysis shall not be undertaken for the case of RC elements with FRP embedded reinforcement. In

addition, design with strut and tie models and stress fields for concrete elements with FRP reinforcement are not covered by this Eurocode [14].

6. ULTIMATE LIMIT STATES

6.1. Bending with and without axial forces

The design of longitudinal FRP embedded reinforcement for bending, follows equilibrium and compatibility as in a reinforced concrete elements with conventional reinforcement [3,4,10]. FRP RC sections may fail either by crushing of the concrete or FRP rupture and both modes of failure are accepted in Annex R. The main particularities are that FRP reinforcement does not yield as in the case of steel and additionally it is available in a large variety of properties (short-term strength, long-term strength, modulus of elasticity) all of them having incidence on the design [11]. The absence of yielding limits the tensile strain in FRP reinforcement to the design rupture strain, $\varepsilon_{fr,d}$ (see Figure 3).

Compression reinforcement is assumed to not contribute to the strength of the element. For columns or elements subjected to compression axial forces, unless more rigorous analysis is undertaken the benefit of the confining effect of FRP reinforcement should be reduced by the ratio E_{fr}/E_s in any direction that confinement is considered. This is because confinement is less effective for materials with lower modulus of elasticity [20,26].

6.2. Shear

Existing studies [27–31] have shown that the same shear resisting mechanisms can be assumed to develop in beams with FRP reinforcement and in beams with conventional steel reinforcement. However, the resisting mechanisms degrade at higher rates than in conventional RC beams because, FRP reinforced beams develop larger and deeper cracks [32], and less shear can be transferred by aggregate interlock. Therefore, provisions of §8.2 of the main text of Eurocode 2 [14] can be applied to elements with FRP longitudinal reinforcement by applying some modifications that are explained in this section. As a summary, the procedure to verify the shear strength of linear members and the out-of-plane shear strength of planar members consists of three different steps:

Step 1. If the design average shear stress over the cross-section, τ_{Ed} , is lower than the minimum shear resistance, $\tau_{Rdc,min}$, a detailed verification of the shear resistance may be omitted.

$$\tau_{Ed} \leq \tau_{Rdc,min} \quad (5)$$

where:

τ_{Ed} is the average shear stress defined as eq. (6):

$$\tau_{Ed} \begin{cases} \frac{V_{Ed}}{b_w z} & \text{for linear members} \\ \frac{V_{Ed}}{z} & \text{for planar members} \end{cases} \quad (6)$$

being:

- V_{Ed} the design shear force at the control section for linear elements
- V_{Ed} the design shear force per unit width at the control section for planar elements
- b_w is the width of the cross-section of linear members and is the smallest width of the cross-section between the tension chord and the neutral axis for sections with variable width.
- z is the lever arm defined as $z = 0.9 d$, where d is the effective depth, that is the distance between the most compressed fibre to the centroid tensile reinforcement.
- $\tau_{Rdc,min}$ is the minimum shear resistance of elements with FRP longitudinal reinforcement without transverse stirrups, based on the Critical Shear Crack Theory (CSCT) and is given by eq. (7):

$$\tau_{Rdc,min} = \frac{11}{\gamma_v} \sqrt{\frac{f_{ck}}{f_{tk0}} \frac{E_{fr}}{E_s} \frac{d_{dg}}{d}} \quad (7)$$

where:

- γ_v is the partial safety factor defined in Table 1 of §2.
- f_{ck} is the characteristic value of the concrete compressive strength.
- f_{tk0} is the characteristic short-term strength of the FRP embedded reinforcement given by the manufacturer (see Figure 3).
- E_{fr} is the modulus of elasticity of the FRP reinforcement.
- d_{dg} is a size parameter that describes the failure zone roughness, which is a function of D_{lower} , the smallest value of the aggregate size.

$$d_{dg} = \begin{cases} 16mm + D_{lower} \leq 40mm & \text{for concrete with } f_{ck} \leq 60 \text{ MPa} \\ 16mm + D_{lower} (60/f_{ck})^2 \leq 40mm & \text{for concrete with } f_{ck} > 60 \text{ MPa} \end{cases} \quad (8)$$

Step 2. If the design average shear stress over the cross-section, τ_{Ed} , is lower than the design value of the shear resistance, τ_{Rdc} , no calculated shear reinforcement is required (see §8.2.2 of [14]).

$$\tau_{Ed} \leq \tau_{Rdc} \quad (9)$$

In this case, for elements without shear reinforcement, the formulas provided in §8.2.2 of the main text of Eurocode 2 [14], to obtain the ultimate shear strength, can be adapted for the FRP embedded reinforcement by reducing the longitudinal reinforcement ratio ρ_{lf} by the ratio E_{fr}/E_s . This is to account for the lower stiffness of the FRP reinforcement in comparison with conventional steel. This modification is also applied in other codes or guidelines such as the ACI440.1R-15[3], CNR-DT203/2006 [19] and JSCE [33]. Therefore, τ_{Rdc} , can be obtained as eq. (10):

$$\tau_{Rdc} = \frac{0.66}{\gamma_v} \left(100 \rho_{lf} \frac{E_{fr}}{E_s} f_{ck} \frac{d_{dg}}{d} \right)^{1/3} \geq \tau_{Rdc,min} \quad (10)$$

where:

$$\rho_{lf} = \frac{A_{f1}}{b_w d} \quad (11)$$

A_{f1} is the effective area of the FRP longitudinal embedded reinforcement.

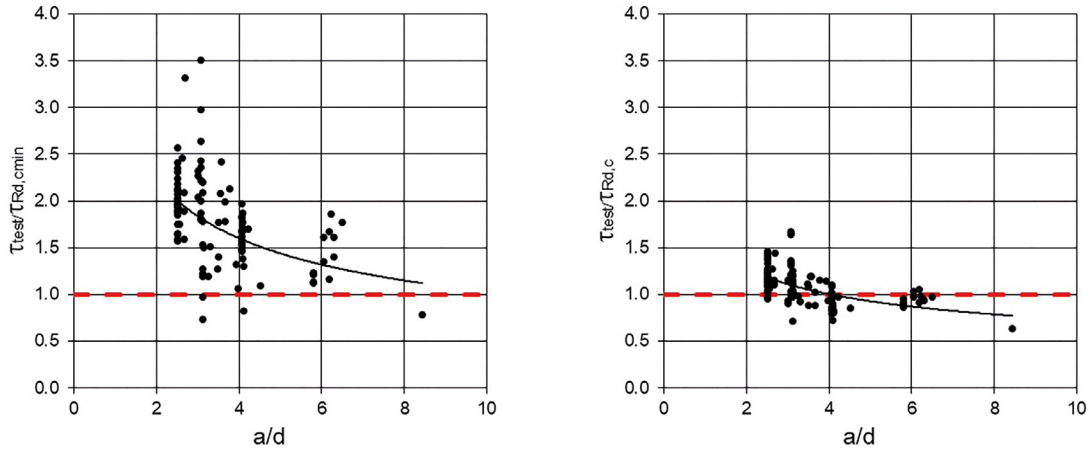


Figure 4. a) Experimental average shear stress vs. minimum shear strength, including trend, b) Experimental average shear stress vs. shear strength for elements without FRP shear reinforcement, including trend.

In the presence of tensile forces, equations given in §8.2.2 should not be applied if the height of the compression zone in the cracked state of the section is less than $0.1d$.

Step 3. If eq. (9) is not satisfied, shear reinforcement is required. Then, provisions of §8.2.3 of the Eurocode [14] can be applied, but with the following modifications in order to adapt the formulation to the case with FRP longitudinal and transverse embedded reinforcement.

First of all, the shear stress resistance perpendicular to the longitudinal member axis shall be calculated according to eq. (12):

$$\tau_{Rd,f} = \tau_{Rd,c} + \rho_w f_{fwRd} \cot \theta \leq 0.17 f_{cd} \quad (12)$$

where:

$$f_{fwRd} = f_{fwk,100a} / \gamma_{FRP} \leq \varepsilon_{fwRd} E_{fwr} \quad (13)$$

$f_{fwk,100a}$ is the characteristic long-term shear strength of the FRP shear reinforcement

γ_{FRP} is the partial safety factor given in Table 1.

E_{fwr} is the modulus of elasticity of the FRP shear reinforcement.

$$\varepsilon_{fwRd} = 0.0023 + 1/15 E_{fwr} A_{fr} (0.8 d)^2 10^{-15} \leq 0.007 \quad (14)$$

θ is the inclination of the compression field, and $\cot \theta$ should be considered as eq. (15):

$$\cot \theta = 0.8 \quad (15)$$

For the inclination of the struts, θ , Kurth et al. [34,35] developed a formula to determine this inclination based on the compression field theory. The calculated inclination ranged between 20° and 50° . The cotangent of the inclination is then used to compute the contribution of the shear stress resistance provided by the shear reinforcement. In a pragmatic sense, the cotangent of the inclination may be taken as 0.8, since this is a value on the safe side.

As explained in the background document [20], a data-

base of shear tests without transverse reinforcement, compiled by Kurth [34], has been used to verify eq. (7). The experimental ultimate shear strength has been compared to the minimum shear resistance, with mean values for the material properties and without applying the partial safety factor, obtaining a safer estimated for longitudinal reinforcement with characteristic short term tensile strengths of 1400 N/mm^2 . In addition, the experimental shear strength has been compared with the predicted value obtaining a good agreement. There are also other published database, such as that of [36] and [37]. In this paper, the same comparison has been done but with the database compiled in Mari et al. [36], observing the same conservative trend for the minimum shear resistance, as shown in Figure 4a. When predicting the shear strength with the database of beams with longitudinal FRP reinforcement and without FRP stirrups, a good agreement is observed (see Figure 4b). The mean value (MV) of the experimental average shear stress to the theoretical shear strength ratio is 1.07 and the coefficient of variation (CoV) is 17.59%.

The formulation for the shear resistance in conventional RC elements with transverse reinforcement is based on a strut-and-tie model, where the concrete contribution is included through the $\cot \theta$ and the shear capacity is limited by stirrups yielding and by the carrying capacity of the struts. This approach cannot be directly applied to the FRP shear reinforcement because of it is linear elastic up to failure. In addition, it has been observed in some tests that a shear compression failure can occur before failure of the FRP transverse reinforcement. To take this into account, the shear strain in the reinforcement should be limited. Kurth et al. [35] proposed a strain limit that depends on the flexural stiffness. In addition, the capacity of the compression struts is modified because the larger deformations expected when using FRP reinforcement. Therefore, the efficiency factor for the capacity of the concrete strength is reduced to $\nu = 0.35$.

For elements with transverse FRP reinforcement, and based on the previous statements, an initial formulation which is a modification of the strut-and-tie model was firstly developed. However, when applying this formulation to the database compiled by Kurth [34], results are very conserv-

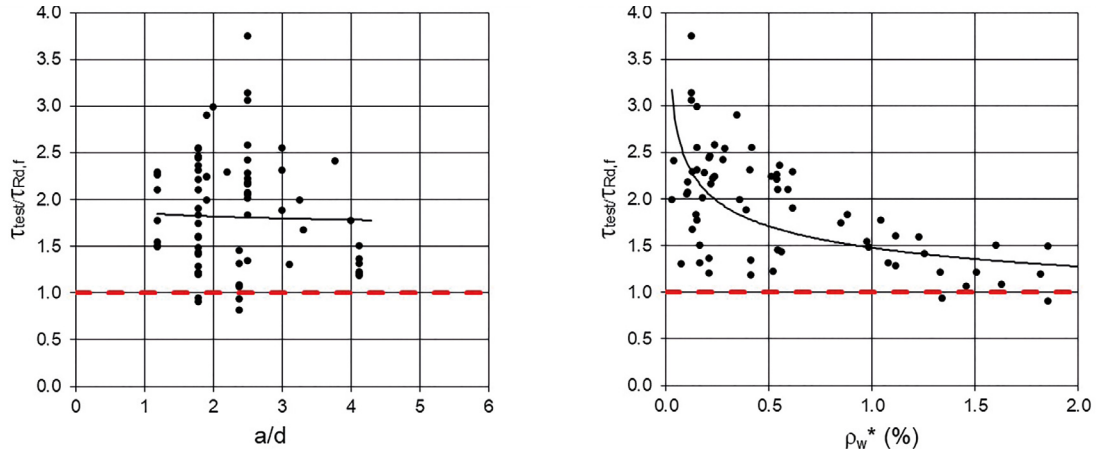


Figure 5. Experimental average shear stress to shear strength ratio for elements with FRP longitudinal and shear reinforcement vs a/d (a) and vs ρ_w^* , including trends.

ative, especially for small shear reinforcement ratios, where sometimes it was lower than the strength given by eq. (10). Then, to avoid an uneconomical design, an additive approach derived by Kurth et al. [34,35] and given by eq. (12) has been included in Annex R.

According to the experimental program performed by Szech and Kotynia [38] of 22 beams, very small values of the shear strength are obtained when neglecting the concrete contribution to the shear strength of beams with FRP stirrups. The real θ achieved in their tests was much lower than the assumed $\cot\theta = 0.8$. So the calculated shear stresses obtained according eq. (12) are within a safe range.

Eq. (12) has been applied to the database compiled in Oller et al. [39] obtaining a mean value of the experimental shear stress to the theoretical shear strength ratio of 1.93 with a coefficient of variation of 36%, which is conservative. Figure 5 shows this ratio plotted as a function of the shear span to effective depth ratio and as a function of a modified transverse shear reinforcement ratio ($\rho_w^* = \rho_w E_{frw}/E_c$) observing a decreasing trend in this last case. In addition, almost all the specimens show a conservative ratio above 1.0.

For shear between web and flanges, provisions in §8.2.5 of [14] may be used by replacing f_{yd} by f_{fd} , $\cot\theta = 1.0$, and $v = 0.35$.

In relation to shear at interfaces, §8.2.6 of [14] may also be used but after applying some changes. As mentioned in [14], the shear at the interfaces should be checked if the static equilibrium depends on the shear transfer across a given interface. Then, the shear transfer should accomplish eq. (16):

$$\tau_{Edi} \leq \tau_{Rdi} \quad (16)$$

where:

τ_{Edi} is the design value of the shear stress in an interface given by:

$$\tau_{Edi} = \frac{V_{Edi}}{A_i} \quad (17)$$

V_{Edi} is the shear force parallel to the interface.

A_i is the area of the interfaces according to §8.2.6.

τ_{Rdi} is the design shear resistance at the interface that can be calculated by eq. (18) if reinforcement is not required.

$$\tau_{Rdi} = c_{v1} \frac{\sqrt{f_{ck}}}{\gamma_c} + \mu_v \sigma_n \leq 0.17 f_{cd} \quad (18)$$

where the definition of the parameters can be found in §8.2.6.

Finally, the provisions of the main text of Eurocode 2 related to not ensure yielding of the reinforcement crossing the interface due to insufficient anchorage do not apply for FRP reinforcement.

6.3. Torsion

The provisions for torsion of the main text of Eurocode 2 [14] are valid for elements with FRP reinforcement but after applying some changes, related to the definition of the longitudinal and transverse strength of the FRP rebars, because of their linear elastic performance. These changes mainly consists of replacing the longitudinal steel yielding f_{yd} by the design tensile strength of the FRP reinforcement, f_{fd} , and the transverse steel yielding f_{ywd} by the design strength value of the FRP transverse reinforcement, f_{frw} .

Therefore, for a single cell, thin-walled section of a sub-section with a constant effective wall thickness, t_{eff} , the design torsional strength can be calculated as eq. (19):

$$\tau_{t,Rd} = \min \{ \tau_{t,Rd,sw} ; \tau_{t,Rd,sl} ; \tau_{t,Rd,max} \} \quad (19)$$

where:

$$\tau_{t,Rd,sw} = \cot\theta \frac{A_{fw}}{t_{eff} S} f_{frw} \quad (20)$$

$$\tau_{t,Rd,sl} = \frac{\sum A_{fl} f_{fd}}{t_{eff} u_k \cot\theta} \quad (21)$$

$$\tau_{t,Rd,max} = \frac{v f_{cd}}{\cot\theta + \tan\theta} \quad (22)$$

being:

$$\cot\theta = 1.0 \quad (23)$$

f_{juRd} is given by eq. (13), but should be limited to $f_{juRd} \leq 0.004 E_{juR}$.

f_{jd} is given by eq. (1), but should be limited to $f_{jd} \leq 0.004 E_{juR}$.

u_k is the perimeter of the area A_k , which is the area enclosed by the centre-lines of the connecting walls, including inner hollow areas.

t_{eff} is the effective wall thickness that may be taken as A/u , being A , the total area of the cross-section, including inner hollow areas and u , the outer perimeter of the cross-section.

$$\nu = 0.35 \quad (24)$$

For combined shear and torsion, the compatibility of strains has to be ensured because different approaches have been applied for shear and for torsion. In addition, the transverse reinforcement should be the sum of the reinforcement required for shear and for torsion.

6.4. Punching

The provisions for the punching-shear for slabs without shear reinforcement of §8.4.3 of [14] and with shear reinforcement of §8.4.3 of [14] shall not be applied to concrete slabs with longitudinal FRP reinforcement. This is because there is not enough database to validate any proposal. There are only few existing studies related to punching-shear with FRP embedded reinforcement.

7.

SERVICEABILITY LIMIT STATES (SLS)

Since the behaviour of FRP RC members is governed by the same principles of steel RC [2,11], the general equations in the main text of Eurocode 2 [14] apply. Again, the possible difference in the design solution will be due to the different properties of FRP reinforcement with respect to steel one. The design of FRP concrete is often controlled by SLS due to the lower modulus of elasticity in comparison with steel reinforcement.

7.1. Stress limitation and crack control

Stresses in concrete and reinforcement are limited in a similar way to steel RC members.

For elements with FRP embedded reinforcement, cracking shall be usually limited for appearance conditions to $w_{lim,cal} = 0.40$ mm. In the absence of appearance conditions this limit may be relaxed.

Table 2 and Table 3 provide the verifications, stress and crack width limitations for elements reinforced with FRP according to Annex R. These tables are an adaptation from Tables 9.1 (NDP) and 9.2 (NDP) from the main text [14]. As observed, since FRP embedded reinforcement does not have corrosion problems, there is no need to limit the crack width for durability reasons, only for appearance, or in environments with freeze/thaw, and where wheel loads are present.

TABLE 2.

Verifications, stress and crack width limits for appearance according to Annex R [14].

Verification	Calculation of minimum reinforcement according to §9.2.2	Verification of width according to §9.2.3	Verification of reinforcement stresses to avoid failure at SLS
Combination of for calculating σ_f	Cracking forces according to §9.2.2	Quasi-permanent combination of	Characteristic combination of
Limiting value of σ_f	$\sigma_f \leq f_{jd}$	$w_{lim,cal} = 0.4$ mm $\sigma_f \leq f_{jd}$	$\sigma_f \leq 0.8 f_{jd}$

TABLE 3.

Verifications, stress and crack width limits for durability according to Annex R [14].

Exposure class	Concrete members with FRP reinforcement	
	Combination of actions	
	Quasi-permanent	Characteristic
XC, XF, XD	$w_{lim,cal} = 0.4$ mm ^{d)}	$\sigma_c \leq 0.6 f_{ck}$ ^{a),b)}

- No limitation in serviceability conditions is necessary for stresses under bearings, partially loaded areas and plates of headed bars.
- The compressive stress σ_c may be increased to $0.66 f_{ck}$ if the cover is increased by 10 mm or confinement by the transverse reinforcement is provided.
- In absence of appearance conditions, fasteners, punctual wheel pressure, lap splice or freeze thaw, this limit may be relaxed to values up to 0.7 mm.

The provisions relevant to steel reinforcement for the calculation of minimum reinforcement areas (§9.2.2) and refined control of cracking (§9.2.3) may be applied to concrete with FRP reinforcement by replacing the parameters corresponding to steel reinforcement by those corresponding to FRP, under the assumption that the bond behaviour of both types of reinforcement are similar.

7.2. Deflection control

Existing equations for the calculation of deflections of FRP RC members are based on the same principles as for steel RC structures. Being the deformability an issue of major importance for FRP RC structures, a significant number of studies about their short-term deflections have been carried out [13,40–43]. With different levels of approximation, either double integration of curvatures or constant average stiffness along the member, the proposals lead to acceptable predictions [3,44–46].

Although less work has been done on long-term deflections, some proposals have also been presented [47–51]. Since long term curvatures (and deflections) of RC members are highly dependent on the reinforcement stiffness, $E_f A_f$, differences in behaviour with respect to steel RC arise from possible changes in that value. Similarly to short-term deflections, application of general analytical procedures provides reasonable predictions [51]. A practical alternative consists

on the use of multiplicative coefficients to obtain long-term deflections from the short-term ones. Some proposals of multiplicative coefficients have been presented, either empirically modifying the values for steel RC [3,52] or analytically deducing factors from the general equations [47,51]. Some larger deviations may appear in the case of empirical methods [51].

Annex R proposes the application of the general method for deflection calculations in §9.3.4 of Eurocode 2 [14]. The simplified approach for deflections of steel RC building structures given in §9.3.3 of Eurocode 2 does not apply to FRP embedded reinforcement.

Likewise, the limits of span to effective depth ratios calibrated for steel RC flexural members given in section §9.3.2 do not apply to FRP RC structures. Some proposals with different levels of approximation and different framework (i.e. ACI, Eurocode) can be found in the literature as in [3,43,53,54].

8. BOND AND ANCHORAGE OF FRP REINFORCEMENT

According to Annex R, the provisions related to detailing with FRP reinforcement apply only to straight rebars. The main text of Eurocode 2 [14] is valid for spacing between FRP embedded rebars.

In relation to the permissible mandrel diameters for bent rebars, the minimum diameter shall avoid damage of the FRP reinforcement and failure in the concrete inside the bend of the bar (crushing, splitting or spalling). To accomplish the first condition, the mandrel diameter may be found in the Technical Product Specification and should be at least:

$$\phi_{mand,min} = \begin{cases} 4\phi & \text{for } \phi \leq 16 \text{ mm} \\ 7\phi & \text{for } \phi > 16 \text{ mm} \end{cases} \quad (25)$$

The verification of the concrete inside the bend may be omitted (provided that $f_{fd} \leq 25f_{cd}$ and $\gamma_c \leq 1.5$): for stirrups that accomplish conditions described in §12.3.3 of [14]; for standard hook and bend anchorage; if $c_x \geq 1.5\phi$ from an edge parallel to the bend and a clear distance between bars $c_s \geq 3\phi$ according to Figure 6c of [14]; or for all bends with an angle $\alpha_{bend} \leq 45^\circ$ at a clear distance $c_x \geq 2.5\phi$ from an edge parallel to the bent, a clear distance between bars $c_s \geq 5\phi$ and a length $\geq 2\phi$ of the straight segments between multiple bends.

For the remaining cases, the design value of the stress in the FRP rebar should accomplish eq. (26) to avoid concrete failure inside the bend area.

$$\sigma_{fd} \leq 25 f_{cd} \quad (26)$$

One of the main limitations of the thermosetting rebars, which are the commercial FRP rebars, is bending at the construction site or re-bending which is not possible. The thermosetting based bars cannot bend once the matrix has solidified because they are fully cross-linked. Then, these thermosetting rebars should be manufactured with the required length and their bent configurations, and bending

should only be done under controlled factory and controlled temperature conditions. There are also some additional limitations related to the number of bends per rebar, to the bent radius and to the spacing between two successive bends. Lap splices are required to overcome these problems which consume more material [55].

When anchoring FRP reinforcement in tension and compression, provisions of the main text of Eurocode 2 [14] may be applied except for the modifications included in Annex R. It is only possible to anchor the rebars by following only 3 of the 6 methods described in [14]. These methods are anchorage of straight bars, bend and hooks and loops (see Figure 6).

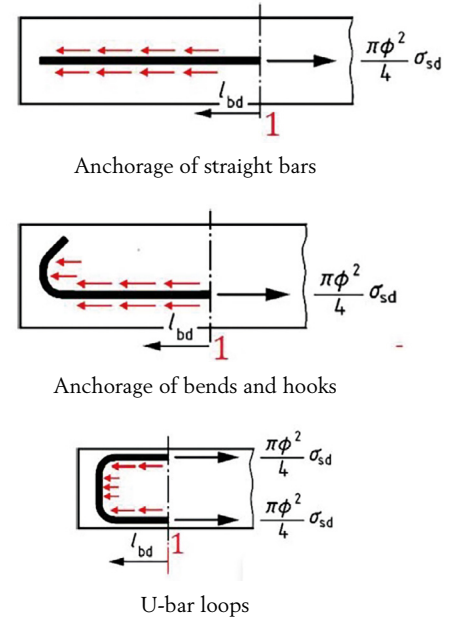


Figure 6. Methods for anchoring FRP reinforcement [14].

Eq. (27) can be applied to determine the anchorage length of FRP reinforcement.

$$l_{bd} = k_{lb} k_{cp} \phi \left(\frac{\sigma_{fd}}{217} \right)^{\eta_\sigma} \left(\frac{25}{f_{ck}} \right)^{1/2} \left(\frac{\phi}{25} \right)^{1/3} \left(\frac{1.5\sigma}{25} \right)^{1/2} \geq \left\{ \frac{10\phi}{4} \frac{\sigma_{fd}}{f_{bd,100a}} \right. \quad (27)$$

where:

$$\eta_\sigma = \begin{cases} 1.0 & \text{for } \sigma_{fd} \leq 217 \text{ MPa} \\ 1.5 & \text{for } \sigma_{fd} > 217 \text{ MPa} \end{cases} \quad (28)$$

$f_{bd,100a}$ may be taken as 1.5 MPa unless there is more accurate information based on production data. This value has been conservatively defined for $f_{ck} = 20 \text{ MPa}$.

$$c_d = \min \{0.5 c_s ; c_x ; c_y\} \quad (29)$$

Figure 7 gives the definition of the parameters cover and clear distance between rebars, to obtain c_d .

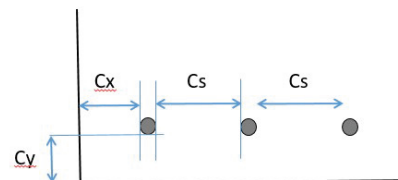


Figure 7. Concrete cover and clear distance between rebars to calculate c_d [14].

k_{cp} is a coefficient that accounts for casting effects on bond conditions. $k_{cp}=1.0$ for bars with good bond conditions, $k_{cp}=1.2$ for poor bond conditions, and $k_{cp}=1.4$ for all bars executed under bentonite or similar slurries.

k_{lb} is equal to 50 for persistent and transient design situations or 35 for accidental design situations unless a National Annex gives different values.

If the clear distance between FRP reinforcement bars $c_s < 7.5\phi$, concrete cover spalling shall be prevented by limiting the design strain to $\varepsilon_{FR,d} \leq 0.0035$ in straight bars or with confining of the anchorage zone.

Laps splices for FRP reinforcement shall be placed in the zone where the stress in the reinforcement at ultimate limit state is less than 80% of the design strength.

The provisions of §11.4.4 of [14] for anchorage with bents and hooks, of §11.4.6 and of §11.5.4 for anchorage and lap splices with U-bar loops, respectively, may be applied with the assumption, that only the straight part is considered determining the anchorage length and that the design long-term tensile strength $f_{FR,d}$ is considered.

The general provisions for bundles in anchorage or lap splices should not be applied for FRP reinforcement.

Provisions of this section have been checked in the background document [20] through a database of 126 available tests from 15 authors with GFRP-reinforced lap splices. Part of this database was previously analysed by [56]. According to this data, the influence of concrete strength and diameter is similar to that of reinforcing steel. Due to different surface preparations and to the different products tested, it is not clear enough the influence of the concrete cover and the bar spacing. The maximum strain limit for unconfined lap splices was given according to this database.

9. DETAILING OF MEMBERS WITH FRP REINFORCEMENT

Detailing of the RC elements with FRP reinforcement should be consistent with the design models and rules included in Annex R. In general, detailing given in the main text of Eurocode 2 [14] can be applied except for the specific modifications given in Annex R, after applying the following changes: steel yielding, f_{yk} , is replaced by the design FRP tensile strength, $f_{FR,d}$; the elasticity modulus of steel, E_s , is replaced by the modulus of FRP, E_{FR} ; and the area of tensile steel reinforcement, A_s , is replaced by the area of FRP, A_f . Annex R only provides rules for straight FRP rebars.

The minimum area of FRP reinforcement for elements under pure tension is given by eq. (30).

$$A_{f,min} = A_c f_{ctm} / f_{FR,d} \quad (30)$$

The minimum reinforcement shall be anchored and lapped following the previous section and considering a stress level of $f_{FR,d}$.

9.1. Beams

In the case of beams with FRP longitudinal and transverse embedded reinforcement, reinforcement should be detailed following the requirements of Table 12.1 (NDP) of the main text of Eurocode 2 [14], but using $s_{max,l} < 250$ mm.

Some rules are given for the minimum reinforcement: 1) it should be distributed over the width and proportionally over the height of the tension zone; 2) it should be fully provided between the supports; and 3) the area required for lever arm must be provided for the total length of the lever arm.

When distributing the longitudinal reinforcement, for members with constant depth, the bending moment law should be shifted at a distance a_l , that for members with and without shear reinforcement, it may be assumed $a_l = d$.

The shear reinforcement shall only consist of a combination of stirrups/links (enclosing the longitudinal tension reinforcement and the compression zone) or cages/ladders properly anchored in the compression and tension zones

Anchorage with headed bars or welded/connected transverse reinforcement are generally not considered for FRP reinforcement.

Laps on legs of stirrups in shear reinforcement may be used and designed according to the previous section of this paper and considering a stress level equal to the design tensile strength, $f_{FR,d}$.

Annex R does not give provisions for the additional suspension reinforcement for indirect support of loads (i.e. intersection of primary and secondary beams or hanging loads).

9.2. Slabs

In the case of slabs with FRP longitudinal and transverse embedded reinforcement, reinforcement should be detailed following the requirements of Table 12.2 (NDP) of the main text of Eurocode 2, but using $s_{max,slab}, s_{max,l}, s_{max,bu}, s_{max,tr} < 250$ mm.

The minimum height of the concrete slab is 200 mm if shear reinforcement is provided.

In relation to the shear reinforcement, the maximum longitudinal spacing $s_{max,l}$ of shear stirrups is $0.3d$ instead of $0.75d$.

Annex R does not give provisions for the minimum area of reinforcement for robustness in case of progressive collapse utilising FRP reinforcement in slabs. In addition, some of the rules for shear reinforcement do not apply in the case of FRP, in particular, rules are not provided for using FRP reinforcement for punching-shear, since there is not enough experience.

9.3. Columns and foundations

Although design criteria for columns and foundations can be found elsewhere (e.g. ACI 440.11-22 [57]), the new Eurocode 2 [14] does not provide rules for using FRP reinforcement under compression or for their use in foundations.

9.4. Other elements

For walls and deep beams, provisions of the main text can be used but using $s_{max,l} < 250$ mm. No changes are required with

respect to the main text, when using FRP reinforcement for tying systems for robustness of buildings, supports, bearings and expansions joints.

For precast concrete elements and structures, the rules given in §13 of the main text, can be applied when using FRP reinforcement with some restrictions. Most of them are related with the fact that prestressing with FRP is not covered by Annex R.

10. CONCLUSIONS

The purpose of this paper is to summarize the content of the informative Annex R, developed by CEN/TC250/SC2/WG1/TG1 and Project Team 3, in the new Eurocode 2 [14] provisions for the design with embedded FRP reinforcement. In addition, there is also a background document [20] that provides additional explanations and supporting information about Annex R.

The provisions of Annex R for verifying the ultimate limit states are an adaptation of the main text to the particular case of FRP reinforcement.

The main differences between FRP and conventional steel reinforcement are that FRPs are anisotropic linear elastic up to failure and have lower modulus of elasticity. The design tensile strength of the FRP rebar is defined as the long-term tensile strength affected by a safety factor. This long-term tensile strength considers the decrease in the short-term tensile strength due to time, temperature and environmental influence.

For the ULS of shear, for elements with transverse reinforcement, an initial formulation which was a modifications of the strut-and-tie model was firstly developed. However, results were very conservative when applying the formulation to a database compiled by Kurth [34]. To avoid an uneconomical design, an additive approach, derived by Kurth et al. [34,35] was included, in Annex R.

Due to the lower modulus of elasticity, serviceability limit states may often govern the design of FRP RC members. Limitation of cracking is mainly due appearance conditions, since FRP rebars present low susceptibility to corrosion.

Acknowledgements

The authors acknowledge the support provided by Spanish Ministry of Science and Innovation (MCIN/ AEI) and by the European Funds for Regional Development in the following projects during their collaboration in the CTN140/SC2 and in the CEN/TC250/SC2/WG1/TG1 (Eva Oller), BIA2015-64672-C4-1-R, RTI2018-097314-B-C2 and PID2020-119015GB-C22.

The authors would like to acknowledge the companies Schöck, Sireg and Owens Corning for their courtesy supporting pictures of real applications of FRP embedded reinforcement.

References

- [1] L.C. Bank, Composites for Construction: Structural Design with FRP Materials, 2007. <https://doi.org/10.1002/9780470121429>.
- [2] C. Barris, L. Torres, C. Miàs, I. Vilanova, Design of FRP RC beams for serviceability requirements, *J. Civ. Eng. Manag.* 18 (2012) 843-857.
- [3] A.C.I. (ACI) ACI Committee 440, Guide for the Design and Construction of Structural Concrete Reinforced with Fiber Reinforced Polymer (FRP Bars). ACI440.1R-15, ACI-440.1R, Farmington Hills, Michigan, USA, 2015.
- [4] fib T.G. 9.3, Bulletin 40. FRP reinforcement in RC structures., Lausanne, Switzerland, 2007.
- [5] K. Pilakoutas, M. Guadagnini, K. Neocleous, L. Taerwe, Design guidelines for FRP reinforced concrete structures, in: *Proc. Adv. Compos. Constr.*, Bath, 2007.
- [6] Japan Society of Civil Engineers, Recommendations for design and construction of concrete structures using continuous fiber reinforcing materials, Concrete E, Japan, 1997.
- [7] G. Fava, V. Carvelli, M.A. Pisani, Remarks on bond of GFRP rebars and concrete, *Compos. Part B Eng.* 93 (2016) 210–220. <https://doi.org/10.1016/j.compositesb.2016.03.012>.
- [8] Association Française de Genie Civil, Utilisation d'armatures composites (à fibres longues et à matrice organique) pour le béton armé, 2021.
- [9] M. Baena Muñoz, Study of bond behaviour between FRP reinforcement and concrete, University of Girona, 2010. <http://www.tdx.cat/handle/10803/7771>.
- [10] K. Pilakoutas, M. Guadagnini, K. Neocleous, S. Matthys, Design guidelines for FRP reinforced concrete structures, *Proc. Inst. Civ. Eng. Struct. Build.* 164 (2011) 255–263. <https://doi.org/10.1680/stbu.2011.164.4.255>.
- [11] L. Torres, K. Neocleous, K. Pilakoutas, Design procedure and simplified equations for the flexural capacity of concrete members reinforced with fibre-reinforced polymer bars, *Struct. Concr.* 13 (2012) 119–129. <https://doi.org/10.1002/suco.201100045>.
- [12] A.C.I. ACI Committee 440, Guide for the Design and Construction of Structural Concrete Reinforced with Fiber-Reinforced Polymer (FRP) Bars (ACI 440.1R-15), American Concrete Institute, 2015.
- [13] S. Matthys, L. Taerwe, Concrete Slabs Reinforced with FRP Grids. I: One-Way Bending, *J. Compos. Constr.* 4 (2000) 145–153. [https://doi.org/10.1061/\(asce\)1090-0268\(2000\)4:3\(145\)](https://doi.org/10.1061/(asce)1090-0268(2000)4:3(145)).
- [14] European Committee for Standardization CEN, Eurocode 2: Design of concrete structures — Part 1-1: General rules — Rules for buildings, bridges and civil engineering structures, prEN 1992-, 2022.*
- [15] ACI 440 American concrete Institute, ACI 440.4R-04. Prestressing concrete structures with FRP tendons, 2004.
- [16] American Association of State Highway and Transportation Officials., Guide specifications for the design of concrete bridge beams prestressed with carbon fiber-reinforced polymer (CFRP) systems, 2018.
- [17] Fédération Internationale du Béton, fib Model Code for Concrete Structures 2010, Ernst & Sohn, 2013.
- [18] Canadian Standards Association (CSA), Design and Construction of Building structures with Fibre-Reinforced Polymer, CAN/CSA S806-12., 2012.
- [19] CNR-DT 203/2006, Guide for design and construction of concrete structures reinforced with fiber-reinforced polymer bars, Rome, Italy, 2006.
- [20] European Committee for Standardization CEN, Background document for pr EN1992-1-1:2021, 2021. (*)
- [21] T. Nagasaka, H. Fukuyama, M. Tanigaki, Shear performance of concrete beams reinforced with FRP stirrups, Detroit, Michigan, 1993.
- [22] E.F.G. Shehata, Fiber reinforced polymer (FRP) for shear reinforcement in concrete structures, University of Manitoba, Manitoba, Canada, 1999.
- [23] E.A. Ahmed, E. El-Salakawy, B. Benmokrane, Shear performance of RC bridge girders reinforced with carbon FRP stirrups, *J. Bridg. Eng.* 15 (2010) 44–54.
- [24] E.C. Bentz, L. Massam, M.P. Collins, Shear Strength of Large Concrete Members with FRP Reinforcement, *J. Compos. Constr.* 14 (2010) 637–646. [https://doi.org/10.1061/\(ASCE\)JC.1943-5614.0000108](https://doi.org/10.1061/(ASCE)JC.1943-5614.0000108).
- [25] ISO/TC 71/SC 6 Non-traditional reinforcing materials for concrete structures, ISO 10406-1. Fibre-reinforced polymer (FRP) reinforcement of concrete Test methods Part 1: FRP bars and grids, 2015.
- [26] B.S. Hamad, A.A. Rteil, Comparison of Roles of FRP Sheets, Stirrups, and Steel Fibers in Confining Bond Critical Regions, *J. Compos.*

- Constr. 10 (2006) 330–336. [https://doi.org/10.1061/\(asce\)1090-0268\(2006\)10:4\(330\)](https://doi.org/10.1061/(asce)1090-0268(2006)10:4(330)).
- [27] N. Duranovic, K. Pilakoutas, P. Waldron, Tests on concrete beams reinforced with glass fibre reinforced plastic bars, in: Japan Concrete Institute (Ed.), Proc. 3rd Int. Symp. Non-Metallic FRP Reinf. Concr. Struct., Sapporo, Japan, Japan, 1997: pp. 479–486.
- [28] M. Guadagnini, K. Pilakoutas, P. Waldron, Shear Resistance of FRP RC Beams: Experimental Study, *J. Compos. Constr.* 10 (2006) 464–473. [https://doi.org/10.1061/\(ASCE\)1090-0268\(2006\)10:6\(464\)](https://doi.org/10.1061/(ASCE)1090-0268(2006)10:6(464)).
- [29] A.K. El-Sayed, E. El-Salakawy, B. Benmokrane, Mechanical and structural characterization of new carbon FRP stirrups for concrete members, *J. Compos. Constr.* 11 (2007) 352–362.
- [30] N.A. Hoult, E.G. Sherwood, E.C.C. Bentz, M.P. Collins, Does the use of FRP reinforcement change the one-way shear behaviour of reinforced concrete slabs?, *J. Compos. Constr.* 12 (2008) 125–133. [https://doi.org/10.1061/\(ASCE\)1090-0268\(2008\)12:2\(125\)](https://doi.org/10.1061/(ASCE)1090-0268(2008)12:2(125)).
- [31] C. S., D.B. M., P. K., Z. E., G. M., Experimental Analysis of Shear Resisting Mechanisms in FRP RC Beams with Shear Reinforcement, *J. Compos. Constr.* 24 (2020) 4020037. [https://doi.org/10.1061/\(ASCE\)CC.1943-5614.0001046](https://doi.org/10.1061/(ASCE)CC.1943-5614.0001046).
- [32] A.K. Tureyen, R.J. Frosch, Shear Tests of FRP-Reinforced Concrete Beams without Stirrups, *ACI Struct. J.* 99 (2003) 427–434.
- [33] JSCE Japanese Society of Civil Engineers, Recommendations for upgrading of concrete structures with use of continuous fiber sheets, 2000.
- [34] M. Kurth, Zum Querkrafttragverhalten von Betonbauteilen mit Faserverbundkunststoff-Bewehrung, Rheinisch-Westfälische Technische Hochschule Aachen, 2012.
- [35] M. Kurth, J. Hegger, Querkrafttragfähigkeit von Betonbauteilen mit Faserverbundkunststoff-Bewehrung – Ableitung eines Bemessungsansatzes, *Bauingenieur*. 88 (2013).
- [36] A. Mari, A. Cladera, E. Oller, J. Bairán, A. Mari, A. Cladera, E. Oller, J.M. Bairan, Shear design of FRP reinforced concrete beams without transverse reinforcement, *Compos. Part B Eng.* 57 (2014) 228–241. <https://doi.org/10.1016/j.compositesb.2013.10.005>.
- [37] H. Baghi, J.A.O. Barros, M. Kaszubska, R. Kotynia, Shear behavior of concrete beams reinforced exclusively with longitudinal glass fiber reinforced polymer bars: Analytical model, *Struct. Concr.* 19 (2018) 162–173. <https://doi.org/10.1002/suco.201700175>.
- [38] D. Szczech, R. Kotynia, Shear tests on GFRP reinforced concrete beams, in: AMCM' 2020 10th Int. Conf. Adv. Model. New Concepts, 2020: pp. 113–114.
- [39] E. Oller, A. Mari, J.M.J.M. Bairán, A. Cladera, Shear design of reinforced concrete beams with FRP longitudinal and transverse reinforcement, *Compos. Part B Eng.* 74 (2015) 104–122. <https://doi.org/10.1016/j.compositesb.2014.12.031>.
- [40] R. Masmoudi, M. Thériault, B. Benmokrane, Flexural behavior of concrete beams reinforced with deformed fiber reinforced plastic reinforcing rods, *ACI Struct. J.* 95 (1998) 665–676. <https://doi.org/10.14359/580>.
- [41] M. Pecce, G. Manfredi, E. Cosenza, Experimental Response and Code Models of GFRP RC Beams in Bending, *J. Compos. Constr.* 4 (2000) 182–190. [https://doi.org/10.1061/\(asce\)1090-0268\(2000\)4:4\(182\)](https://doi.org/10.1061/(asce)1090-0268(2000)4:4(182)).
- [42] C. Barris, L. Torres, A. Turon, M. Baena, A. Catalan, An experimental study of the flexural behaviour of GFRP RC beams and comparison with prediction models, *Compos. Struct.* 91 (2009) 286–295. <https://doi.org/10.1016/j.compstruct.2009.05.005>.
- [43] P.H. Bischoff, Reevaluation of Deflection Prediction for Concrete Beams Reinforced with Steel and Fiber Reinforced Polymer Bars, *Struct. Eng.* 131 (5) (2005) 752–767.
- [44] Fédération Internationale du Béton, fib Model Code for Concrete Structures 2010. vol. 1., Lausanne, Switzerland, 2013.
- [45] CEN, European Committee for Standardization, (CEN) European Committee for Standardization, Eurocode 2: Design of concrete structures. Part 1-1: General rules and rules for buildings, *Eur. Com. Stand.* (2016). [https://doi.org/\[Authority: The European Union Per Regulation 305/2011, Directive 98/34/EC, Directive 2004/18/EC\]](https://doi.org/[Authority: The European Union Per Regulation 305/2011, Directive 98/34/EC, Directive 2004/18/EC]).
- [46] P.H. Bischoff, S.P. Gross, Equivalent Moment of Inertia Based on Integration of Curvature, *J. Compos. Constr.* 15 (2011) 263–273. [https://doi.org/10.1061/\(asce\)cc.1943-5614.0000164](https://doi.org/10.1061/(asce)cc.1943-5614.0000164).
- [47] L. Torres, C. Miàs, A. Turon, M. Baena, A rational method to predict long-term deflections of FRP reinforced concrete members, *Eng. Struct.* 40 (2012) 230–239. <https://doi.org/10.1016/j.engstruct.2012.02.021>.
- [48] V. Brown, Sustained load deflections in GFRP-reinforced concrete beams, in: 3rd Int. RILEM Symp. Non-Metallic Reinf. Concr. Struct., 1997: pp. 495–502.
- [49] M. Arockiasamy, S. Chidambaram, A. Amer, M. Shahawy, Time-dependent deformations of concrete beams reinforced with CFRP bars, *Compos. Part B Eng.* 31 (2000) 577–592. [https://doi.org/10.1016/S1359-8368\(99\)00045-1](https://doi.org/10.1016/S1359-8368(99)00045-1).
- [50] C. Miàs, L. Torres, A. Turon, C. Barris, Experimental study of immediate and time-dependent deflections of GFRP reinforced concrete beams, *Compos. Struct.* 96 (2013) 279–285. <https://doi.org/10.1016/j.compstruct.2012.08.052>.
- [51] C. Miàs, L. Torres, A. Turon, I.A. Sharaky, Effect of material properties on long-term deflections of GFRP reinforced concrete beams, *Constr. Build. Mater.* 41 (2013) 99–108. <https://doi.org/10.1016/j.conbuildmat.2012.11.055>.
- [52] ACI Committee 318, Building Code Requirements for Structural Concrete, 2014.
- [53] S. Veysey, P.H. Bischoff, Designing FRP reinforced concrete for deflection control, *Am. Concr. Institute, ACI Spec. Publ.* 1 (2011) 33–55. <https://doi.org/10.14359/51682413>.
- [54] C. Barris, L. Torres, J. Comas, C. Miàs, Cracking and deflections in GFRP RC beams: an experimental study, *Compos. Part B Eng.* 55 (2013) 580–590.
- [55] M. El-Tahan, K. Galal, V.S. Hoa, New thermoplastic CFRP bendable re-bars for reinforcing structural concrete elements, *Compos. Part B Eng.* 45 (2013) 1207–1215. <https://doi.org/10.1016/j.compositesb.2012.09.025>.
- [56] M. Rakhshanimehr, S.R. Mousavi, M.R. Esfahani, S. Farahi Shahri, Establishment and experimental validation of an updated predictive equation for the development and lap-spliced length of GFRP bars in concrete, *Mater. Struct. Constr.* 51 (2018). <https://doi.org/10.1617/s11527-018-1137-8>.
- [57] ACI (American Concrete Institute), Building Code Requirements for Structural Concrete Reinforced with Glass Fiber-Reinforced Polymer (GFRP) Bars, ACI 440.11, 2022.

*This document is available through the National members at CEN TC250/SC2

Eurocode Practice: Design of Fastenings for Use in Concrete in Accordance with Eurocode 2

Práctica del Eurocódigo: Diseño de fijaciones para uso en hormigón de acuerdo con el Eurocódigo 2

Dr. Jörg Appl^a, & Antonio Cardo Fernández^{*b}

^a *Dr. Civil Engineer. Senior Technical Marketing Manager. Hilti Germany AG.*

^b *MSc. Civil Engineer. Engineering Competence Center Manager. Hilti Española S.A.*

Recibido el 29 de septiembre de 2022; aceptado el 20 de marzo de 2023

SUMMARY

Since 1997, the design of fastenings for anchoring in concrete has been regulated at European level by Annex C of the European Technical Approval Guideline and the subsequently published, supporting and referenced “Technical Report” TR029 and TR045 or by the pre-standard series CEN/TS 1992-4. The new EN 1992-4 standard, which is published in 2017 and has been formally accepted by the CEN members in the voting process. It summarizes the existing design rules while taking into account state of the art and applies to all main fasteners used in construction engineering. It is far more comprehensive in terms of the fastening systems it covers, and the load conditions it takes into consideration. Consequently, it represents an important and necessary step in harmonizing the design of fasteners for use in concrete. The following paper briefly presents the contents of the new European Standard EN 1992-4 “Design of fasteners for use in concrete” and the major changes that have been introduced compared to CEN/TS 1992-4 and ETAG 001, Annex C.

There is an added chapter regarding “post-installed rebar anchorage length”, which is covered by FprEN 1992-1-1:2023 [15]. This application is used for design of rigid connections between concrete members.

KEYWORDS: EN 1992-4, EN 1992-1-1, concrete fasteners, post-installed rebar, anchor.

©2023 Hormigón y Acero, the journal of the Spanish Association of Structural Engineering (ACHE). Published by Cinter Divulgación Técnica S.L. This is an open-access article distributed under the terms of the Creative Commons (CC BY-NC-ND 4.0) License

RESUMEN

Desde 1997, el diseño de las fijaciones para el anclaje en hormigón está regulado a nivel europeo por el Anexo C de la Directriz Europea de aprobación técnica y los “Informes técnicos” TR029 y TR045 publicados posteriormente, de apoyo y referenciados o por la serie prenorma CEN/TS 1992-4. La nueva norma EN 1992-4, que se publica en 2017, ha sido aceptada formalmente por los miembros del CEN en el proceso de votación. Resume las reglas de diseño existentes teniendo en cuenta el estado de la técnica y se aplica a todos los principales anclajes utilizados en la ingeniería de la construcción. Es mucho más completo en términos de los sistemas de fijación que cubre y las condiciones de carga que tiene en cuenta. En consecuencia, representa un paso importante y necesario en la armonización del diseño de anclajes para su uso en hormigón. El artículo presenta brevemente el contenido de la nueva Norma Europea EN 1992-4 “Diseño de fijaciones para uso en hormigón” y los principales cambios que se han introducido en comparación con CEN/TS 1992-4 y ETAG 001, Anexo C.

Hay un capítulo añadido con respecto a la “longitud de anclaje de las barras corrugadas post-instalada”, que está cubierto por la nueva EN1992-1-1. Esta aplicación se utiliza para el diseño de conexiones rígidas entre elementos de hormigón.

PALABRAS CLAVE: EN 1992-4, EN 1992-1-1, fijaciones en hormigón, barras corrugadas post-instaladas, anclaje.

©2023 Hormigón y Acero, the journal of the Spanish Association of Structural Engineering (ACHE). Published by Cinter Divulgación Técnica S.L. This is an open-access article distributed under the terms of the Creative Commons (CC BY-NC-ND 4.0) License

* Persona de contacto / *Corresponding author*:
Correo-e / *e-mail*: Antonio.Cardo@hilti.com (Antonio Cardo Fernández)

1.

INTRODUCTION

Since 1997, the design of fastenings for anchoring in concrete has been regulated at European level by Annex C of the European Technical Approval Guideline [1] and the subsequently published, supporting and referenced “Technical Report” TR029 [2] and TR045 [3] or by the pre-standard series CEN/TS 1992-4 [4]. The new EN 1992-4 standard [18], which was published in 2017, has been formally accepted by the CEN members in the voting process. It summarizes the existing design rules while taking into account state of the art and applies to all fasteners either cast into concrete or installed in hardened concrete. It is far more comprehensive in terms of the fastening systems it covers, and the load conditions it takes into consideration. Consequently, it represents an important and necessary step in harmonizing the design of fasteners for use in concrete. The following paper briefly presents the contents of the new European Standard EN 1992-4 “Design of fasteners for use in concrete” [18] and the major changes that have been introduced compared to CEN/TS 1992-4 [4] and ETAG 001, Annex C [1].

There is an added chapter regarding “post-installed rebar anchorage length”, which is covered by FprEN 1992-1-1:2023 [15]. This application is used for design of rigid connection between concrete members.

2

EN 1992-4 [18]

2.1. General

While the CEN/TS series 1992-4 [4] consists of 5 parts with approximately 170 pages, EN 1992-4 [18] is considerably shorter but technically much more comprehensive. The abridged background information will be still available as supplementary documents as part of the CEN/TR 17080 “Anchor channels – Supplementary rules”, CEN/TR 17081 “Design based on plasticity theory” and CEN/TR 17079 “Redundant systems”.

EN 1992-4 [18] applies to cast-in place systems such as anchor channels, headed bolts, headed studs in combination

with welded steel plates, mechanical fasteners such as metal expansion anchors, undercut anchors, concrete screws and post-installed chemical fasteners such as bonded anchors and bonded expansion anchors. Cast-in place systems, which are embedded in precast concrete elements under controlled production, and which are only used temporarily for the lifting and transportation of pre-cast elements, are covered in the document CEN/TR 15728: 2008 [5] “Design and use of inserts for lifting and handling precast concrete elements”.

2.1.1. Anchor channels, headed bolts and headed anchors

Anchor channels consist of a cold-formed or hot-rolled, V-shaped or U-shaped steel profile with special anchoring elements that are attached directly to the inside of the formwork (Figure 1). The open steel profiles are filled with foam or provided with environmentally compatible foam filling with pull-out tape to prevent concrete from penetrating the channel during the casting process. Once the filling has been stripped and removed, the fixtures can be attached using special T-headed bolts. Anchor channels are usually held in place by headed bolts or studs which are either welded, forged or screwed on. Depending on the product, the anchor channel can only be loaded perpendicularly to the axis of the channel because transferring forces along the length of the channel is only achieved by way of friction between the T-headed bolt and the lip of the rail, and the magnitude of friction is uncertain. To transfer loads along the length of the channel there are special channels or special T-headed bolts to guarantee an interlock connection which transfers the loads. EN 1992-4 [18] does not cover shear in the direction of the longitudinal axis of anchor channels.

Headed stud anchors consist of a steel plate with a headed studs welded on it. Headed studs are also made of ribbed or profiled rebar and are arc-welded to the anchor plate.

2.1.2. Mechanical fasteners

The fasteners covered by EN 1992-4 [18] can be divided into different groups:

- **Metal expansion anchors** (Figure 2a/2c)

In the case of torque-controlled fasteners (Figure 2a) a hole is drilled, the fastener is inserted into the drill hole and anchored by tightening the screw or nut with a cal-



Figure 1. Anchor channel before installation (left) and after installation (right).

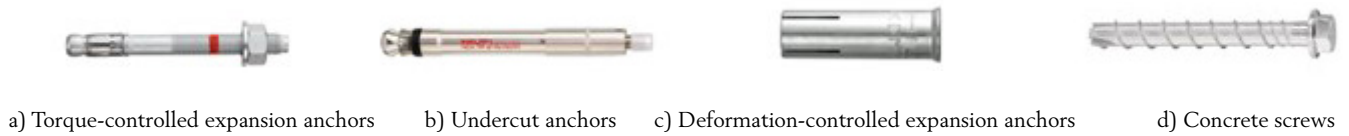


Figure 2. Mechanical fastening systems

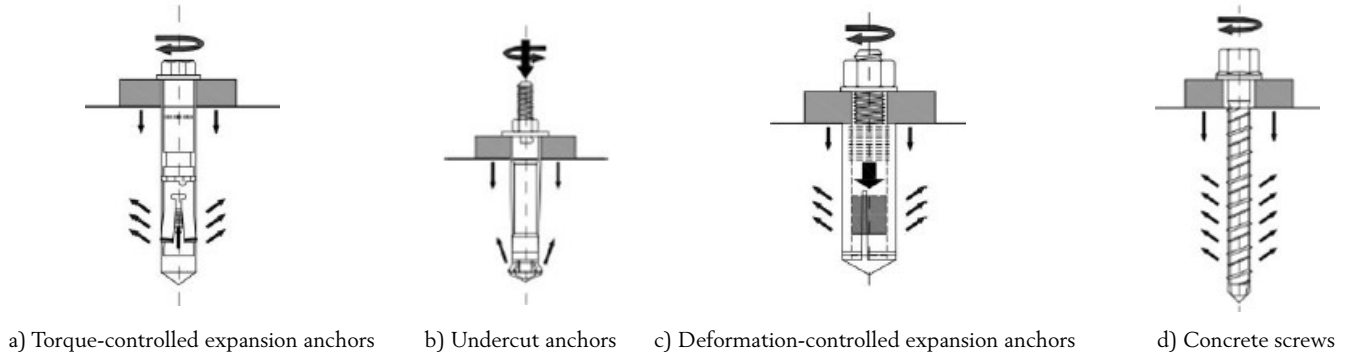


Figure 2. Mechanical fastening systems. Load transfer to concrete mechanism. Source [19].

ibrated torque wrench. A tensile force is produced in the bolt, the cone at the tip of the anchor is drawn into the expansion sleeve and forced against the sides of the drilled hole. Deformation-controlled anchors (Figure 2c) comprise an expansion sleeve and cone. They are set in place by expanding the sleeve through controlled deformation. This is achieved either by driving the cone into the sleeve or the sleeve over the cone.

- **Undercut anchors** (Figure 2b)
As with cast-in-place systems, undercut anchors develop a mechanical interlock between anchor and the base material. To do this, a cylindrically drilled hole is modified to create a notch, or undercut, of a specific dimension at a defined location either by means of a special drilling apparatus, or by the undercutting action of the anchor itself. In case of self-undercutting the undercut is generated using the expansion element inserted into the pre-drilled hole. Use of rotary-impact action permits the expansion element to simultaneously undercut the concrete and widen to their fully installed position. The cone bolt provides at its end space for the drilling dust which accu-

mulates during formation of the undercut. This process results in a precise match between the undercut form and the anchor geometry.

- **Concrete screws** (Figure 2d)
Concrete screws or screw anchors are typically hardened to permit the thread to engage the base material during installation. They are installed in drilled holes. The thread pitches at the tie may be provided with special cutting surface and or geometries in order to assist the process of cutting threads in the wall of the drilled hole. They may be driven by mean of special impact driver or, in other systems with a conventional drill equipped with an adapter. The diameter of the drilled hole is matched to the geometry of the screw so that the thread cuts into the concrete and an external force can be transferred to the concrete through this positive interlocking connection.

2.1.3. Chemical fasteners

- **Bonded anchors:**
Bonded anchors are available in various systems. A distinction is made between anchors in which the mortar

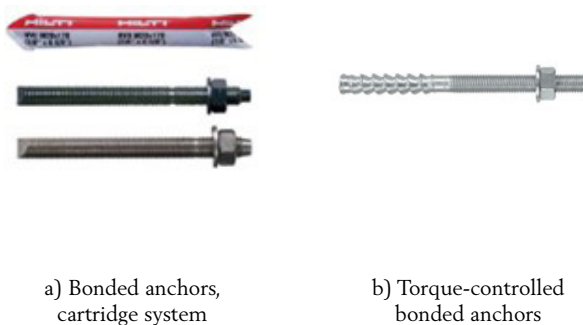


Figure 3. Chemical fastening systems.

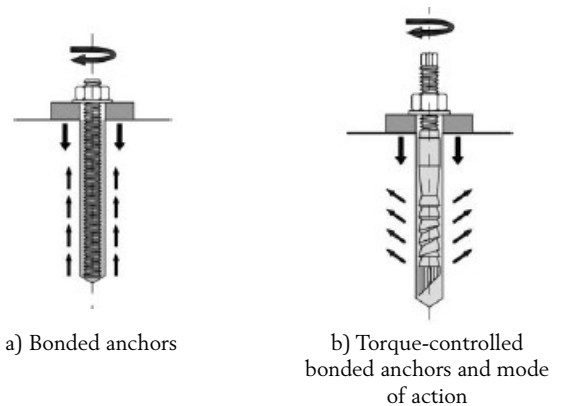


Figure 3. Chemical fasteners. Load transfer to concrete mechanism. Source [19].

EN 1992-4

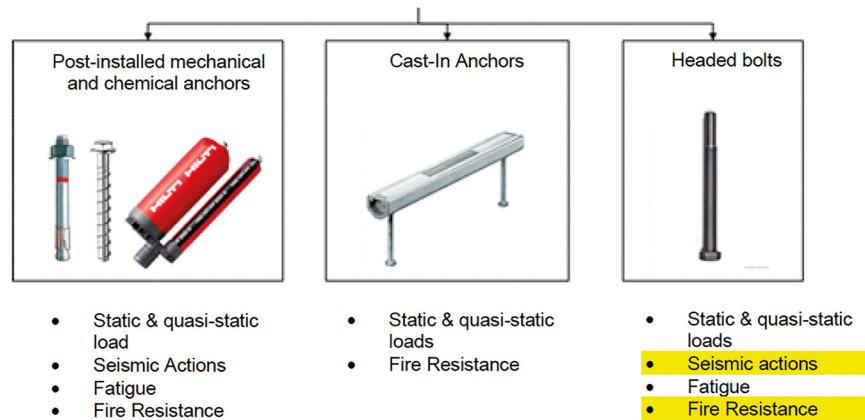


Figure 4. Verifications for different fasteners in accordance with EN 1992-4 [18].

is contained in plastic or glass capsules (Figure 3a) and injection systems in which the mortar is delivered in cartridges. Irrespective of the system, forces are applied from the threaded rod to the mortar via mechanical interlocking and to the anchor base via micro-interlock, friction and bonding between the mortar and hole wall.

Torque-controlled bonded anchors:

Torque-controlled expansion anchors use an anchor rod with multiple cones (Figure 3b). They are coated and can be protected with a wire sleeve if necessary. When a tension force is applied to the anchor rod, the cones are drawn into the mortar, which acts as an expansion sleeve. This results in expansion and frictional forces between the mortar and the borehole wall, sufficient enough to induce a tensile force to the base material regardless of the adhesive effect of the mortar.

2.2. Field of Application

The basic requirement for the usage of EN 1992-4 [18] is an European Technical Approval ETA (until June 2013), called Assessment (since July 2013) of the covered fastening systems on the basis of the applicable European Technical Approval Guideline ETAG [6] (until June 2013), called European Assessment Document (EAD) [7] (since July 2013).

The Guideline or Assessment document specifies the requirements and acceptance criteria which must be fulfilled by the fastening system. Based on this approach, tests need to be carried out in order to assess the suitability of the system and determine the permissible conditions of use. The tests involve, among other things, low-strength and high-strength concrete, with tests being carried out on both cracked or non-cracked concrete, depending on the intended application range. The effects of possible deviations during installation of the fastening system, such as borehole tolerances, level of borehole cleaning, extent of expansion, positioning of anchors with respect to reinforcing bars (reinforcing contact), the impact of moisture and concrete temperature on the load-bearing behavior of the fastener should be checked specifically, where relevant. The tests also take into account the impact of sustained and/or variable loads on the fasteners.

Gross installation errors cannot and are not covered by these tests. EADs are produced by the European Organization for Technical Assessment (EOTA). The EOTA works closely with the European Committee for Standardization CEN.

The design in accordance with EN 1992-4 [18] is based on the characteristic resistance and spacing of the fasteners as specified in the Approval/Assessment. EN 1992-4 [18] is intended for the design of fastenings which connect structural and non-structural components with structural components, in which the failure of fastenings will:

- result in a complete or partial collapse of the structure.
- cause risk to human life or
- lead to significant economic loss.

The design in accordance with EN 1992-4 [18] can be applied to both new buildings and existing structures which are covered by EN 1992 (Eurocode 2, concrete structures) and EN 1994 (Eurocode 4, composite structures). For applications where special conditions may apply, e.g. nuclear power plants or civil defense structures, modifications and supplements of the design may be necessary.

Fastenings can be designed as both single fasteners and groups of fasteners for anchoring in concrete, whereby it is assumed that only fasteners of the same type, manufacturer, diameter and anchoring depth are used within a group. With the introduction of EN 1992-4 [18], the permissible concrete strength classes C20/25 to C50/60 [6] will also be extended to C12/15 to C90/105 if the fasteners qualify for these concrete strength classes in accordance with [7].

For a group of fastenings, the loads are transferred to the individual anchors by means of a common fixture – usually a steel plate. Although the design of the fixture itself is not considered in EN 1992-4 [18], the design must, nevertheless, correspond to the standard to be applied. The load transfer from anchor group to the supports of the reinforced concrete structure has to be verified for both the ultimate limit state and the serviceability limit state in accordance with EN 1992-1-1 [8].

Fasteners must be designed for static, quasi-static, dynamic (fatigue and earthquakes) and fire actions. Whether and to what extent a fastener qualifies for the above-mentioned ac-

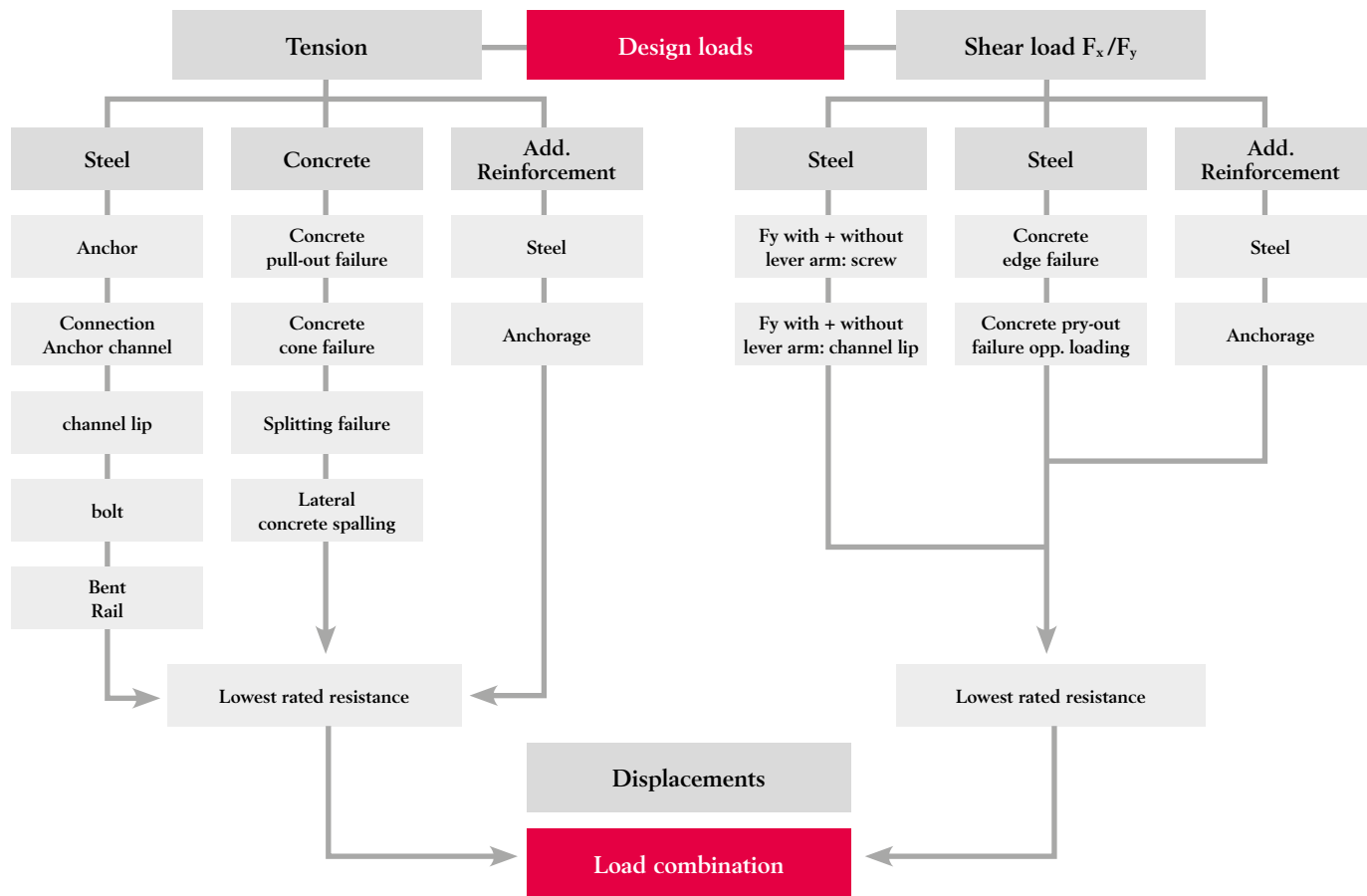


Figure 5. Possible failure modes for anchor channels.

tion effects can be derived from the product-related approval/assessment (ETA). Figure 4 shows the verifications that will be covered taking account of the different types of fastening systems in accordance with EN 1992-4 [18].

The load-bearing characteristics of fasteners can be significantly influenced by cracks due to tension loads. Fasteners can generally be qualified and approved for cracked and/or non-cracked concrete. It is therefore up to the designer to decide which national standards need to be taken into consideration and, consequently, which usage conditions need to be assumed for specific reinforced concrete components. In the design of flexural or tension components, it will be prudent to assume that concrete is cracked. Tensile Stresses caused by restraint will often exceed the low tensile strength of concrete.

If non-cracked concrete conditions are assumed and fasteners with an ETA for non-cracked concrete are selected, verification needs to be provided in accordance with EN 1992-4 [18] that no cracks will appear in the anchorage area of the fastener for the entire service life of the fastener. To avoid such complex verification – if this is at all possible – fasteners suitable for use in cracked concrete are generally preferred.

2.3. Basis of design

Verification for the following two states needs to be performed:

- Ultimate limit state.
- Serviceability limit state.

For the ultimate limit state, it must be shown that the value of the design actions does not exceed the value of the design resistance, whereby the failure mode with the mathematically lowest resistance value is decisive for the design.

In the serviceability limit state, it shall be shown that the displacement occurring under characteristic actions is not larger than the admissible displacement. The admissible displacement depends on the item to be fastened and must be specified by the structural engineer. The functionality of the component being fastened also needs to be observed when subjected to displacement. The characteristic displacements as given in the approval/assessment can generally be interpolated linearly, but in the case of combined tension and shear loads they should be added vectorially.

Optimum and sufficiently safe utilization of the fastener is only possible if the design takes into account the loading direction (tension load, shear load, combined tension and shear load) as well as the type of action (predominantly static, dynamic, variable, etc.) and differentiates the different modes of failure. In 1995 the Committee Euro-International du Béton (CEB) published a design method based on the CC-method [9] (concrete capacity) that meets the above requirements. In 1997 this design concept was fully adopted by the EOTA. This basic approach or its philosophy to other fastening systems can be found in the European standard EN 1992-4 [18].

For post-installed mechanical and chemical fasteners under tension loads, the CC method [9] differentiates between

steel failure, pull-out failure, concrete cone failure, splitting as well as blow-out failures of headed studs near to an edge. For shear loads, the differentiated modes of failure include steel failure (bolt shearing or bending failure), concrete edge failure and pry-out failure. Where existing reinforcement in the concrete member is utilized in the design for the above-mentioned fasteners, such reinforcement also needs to be verified against steel and anchorage failure.

The CC method [9] optimally utilizes the performance capabilities for the given marginal conditions but can also be considered as relatively complex as the load-bearing capacity of fasteners is described for all loading directions and all modes of failure. This is illustrated in Figure 5, which shows schematically the flowchart for the required verifications for anchor channels.

Various manufacturers have developed design software to simplify the design process. Such design programs make it possible to solve almost every fastening task quickly while optimizing the utilization rate and thus the required number of fasteners.

Unlike CEN/TS [4] or [2], EN 1992-4 [18] is adapted to the current state of the art and the regulatory framework of the Construction Products Ordinance. This has resulted in both minor and major changes. In the following section, only the major differences will be discussed.

2.4. Technical changes

2.4.1. Consideration of the effect of sustained tension loads

Fasteners must ensure a safe load transfer over many years. Therefore, its long-term behavior is of interest. In case of verification of the failure mode “combined pull-out and concrete cone failure” of chemical fasteners, EN 1992-4 [18] contains an additional coefficient ψ_{sus} (not present in [1] and [4]), which is intended to take account of the effect of a tension load acting permanently on the fastener (sustained loading). It decreases the adhesive strength of the chemical fastener and therefore the resistance. The coefficient is product-specific and should be given in the product-related European Technical Assessment (ETA). It is included in the design by considering the ratio of the value of sustained loading related to the value of short-term loading. If no value is specified in the ETA for chemical anchors, a default coefficient of $\psi_{sus} = 0,6$ is assumed.

There is currently no qualification guideline to describe how this value must be derived. As long as this remains the case, the design in accordance with EN 1992-4 [18] for a specific product with the total effect of the sustained load results in a load reduction of 40% compared to [1] and [4].

2.4.2. Consideration of the excess force on the concrete breakout body subjected to a moment

When a fastening consisting of two anchors is subjected to a bending moment, a couple is set up consisting of a tensile force in the anchor and a compressive force beneath the fixture (Figure 6). If the tensile force in the anchor exceeds the concrete cone breakout capacity, then a concrete cone failure will occur. In this situation however the concrete cone failure load may be influenced by the adjacent compression stress block beneath the fixture. According to [10], the impact depends to a large extent

on the lever arm between the resulting tension and compression forces (z) in relation to the radius of the expected breakout cone ($r = 1.5 h_{ef}$, with h_{ef} = anchoring depth of the fastener).

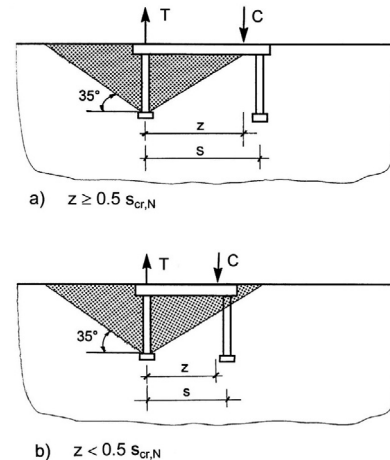


Figure 6. Impact of a bending moment acting on the anchor plate on the concrete breakout load of the tensioned fasteners [10].

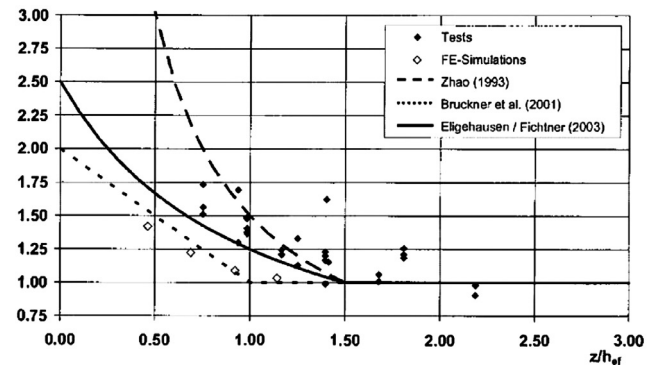


Figure 7. Impact of a compression force beneath the anchor plate on the concrete breakout load as a function of the ratio between the inner lever arm z and the anchoring depth h_{ef} due to an applied bending moment.

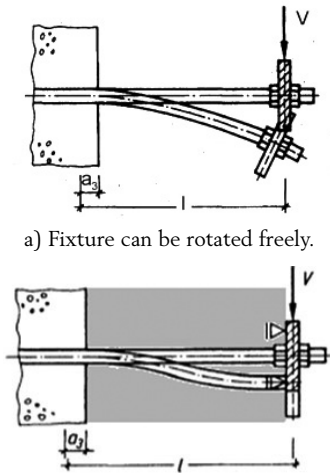
It is determined using the coefficient $\psi_{M,N} (= 2 - z / 1.5h_{ef})$. The smaller the difference between the resulting compression and tension force, the greater the increase in the load required to precipitate concrete cone failure (Figure 7). The coefficient can be between 1.0 and 2.0 in accordance with EN 1992-4 [18]. This behavior can only be incorporated to a limited extent in the design and only in the cases of large edge distances, for example. Important studies have already been made in this regard in [8], [10] and [11].

2.4.3. Consideration of the supporting effect of a mortar bed (shimming)

When designing a fastener or providing verification for steel failure under an acting shear load, a distinction must be made between a “shear load without lever arm” and a “shear load with lever arm”. Until now, the design method for “shear load without lever arm” can only be used if the fixture is made of metal and positioned directly against the concrete. Compensation layers or shims were only covered up to $t = 3\text{mm}$ while this value was already increased to $d/2$ in [1] and [4] (d = nominal diameter of the anchoring element [mm]). If this

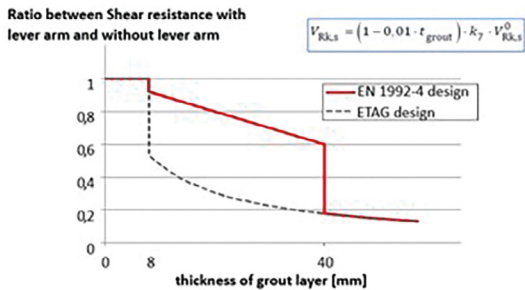
was not the case, the design had to be assumed as “shear load with lever arm”, which results in significantly lower resistance values with respect to “steel failure” due to bending stresses.

EN 1992-4 [18] provides the option of taking account of the supporting effect of a mortar bed under the fixture up to a maximum thickness of $t = 40$ mm. This only applies if it can be demonstrated that no cracks can be expected in the concrete (non-cracked concrete). In accordance with EN 1992-4 [18], verification will be provided within the limits of the layer thickness of $0.5d < t < 40$ mm as “shear load without lever arm” where the resistance value for this type of failure is linearly reduced within the said limits. For a mortar layer thickness of $t = 40$ mm, there will be a 40% reduction in the resistance value compared to a shear load without a lever arm and without shims. (Figure 8).



b) Supporting effect of the mortar bed up to $t = 40$ mm, schematic, non-cracked concrete.

EN 1992-4 vs. ETAG design (for e.g. $d = 16$ mm)



- *Key restrictions:
- 1) At least 2 anchors in group
 - 2) No tension/moment
 - 3) Uncracked concrete situation
 - 4) t_{grout} is no bigger than 40mm and $\leq 5d$.
 - 5) Grout strength > 30 Mpa, and rough surface

c) Example for Anchor Diameter 16 mm.

Figure 8. Fastening under shear load with lever arm.

If the value of the characteristic cylinder compressive strength f_{ck} of the mortar being used is less than 30 N/mm² (MPa), the linear reduction is already within the limits of

$0 < t < 40$ mm.

For a ratio of embedment depth (h_{ef}) to diameter (d) $h_{ef}/d < 5$ and a concrete strength class less than C20/25, a reduction in the resistance value for the failure type “steel failure without lever arm” of 20% is recommended.

2.4.4. Consideration of failure modes under combined tension and shear loads

The load-bearing behavior of fasteners under combined tension and shear loads lies somewhere between the behavior for centric tension and shear loads and depends on the angle of action. The same modes of failure occur as for tension or shear loads. The following failure combinations are possible:

- a) Steel failure under tension and shear load
- b) Concrete breakout failure under tension load and steel failure under shear load
- c) Concrete breakout failure under tension and shear load
- d) Steel failure under tension load and concrete failure under shear load.

Until now, the individual modes of failure under combined tension and shear loads have not been fully considered on the basis of a trilinear interaction equation (Figure 9). According to EN 1992-4, the combined action should be calculated separately, once for concrete-related failures and once for steel failures, with the smallest value of both interaction curves providing the design value. This technically correct approach results in significantly higher resistance values (Figure 10) than in the original equation ([1] and [4]).

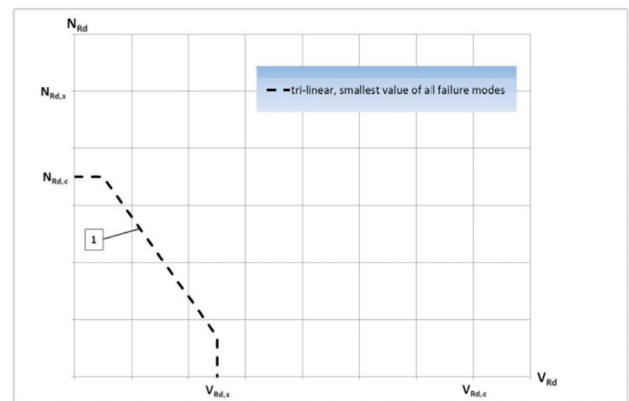


Figure 9. Trilinear interaction diagram for fasteners based on [1], taken from [13].

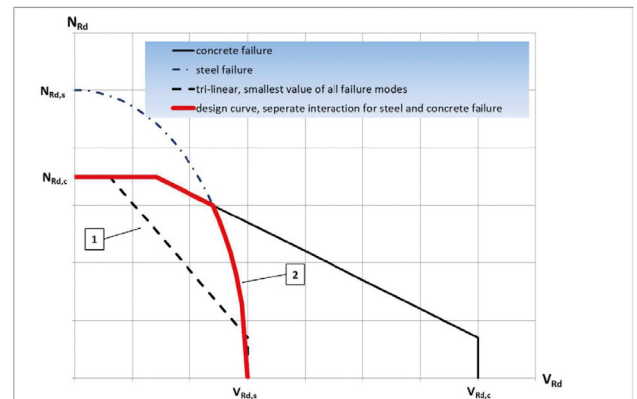


Figure 10. Interaction diagram in accordance with EN 1992-4 taking into account the different modes of failure, taken from [13].

2.4.5. Consideration of edge reinforcement for the concrete edge failure

Fasteners close to the edge under shear load perpendicular to the edge can fail due to concrete breakage (concrete edge failure) before reaching the steel load-bearing capacity. Coefficient $\psi_{re,V}$ in EN 1992-4 takes into account the increase in the concrete edge failure load based on the type of edge reinforcement in place. If there is no available edge reinforcement or shear reinforcement, the coefficient is 1 (Figure 11a). The approach is identical to [1] and [4]. Whereas in [1] and [4], when edge reinforcement is provided, the basic characteristic resistance for the failure type “concrete edge failure” is increased by 20% ($\psi_{re,V} = 1.2$), in EN 1992-4 [18], the effect of edge reinforcement is ignored (Figure 11b) because there is no a clear strut & tie model to verify how it happens when a shear reinforcement is available (Figure 11c). If staggered shear reinforcement is available ($a \leq 100\text{mm}$ and $a \leq 2c_1$ with $c_1 = \text{edge distance in [mm]}$) and verification is provided for cracked concrete, the basic value is increased by 40%. This corresponds to the approach of [1] and [4].

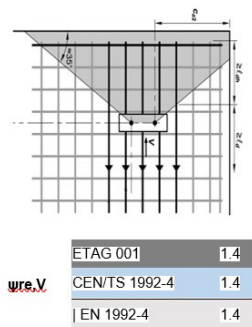
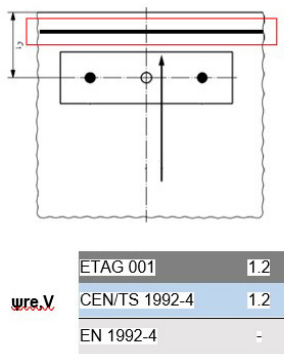
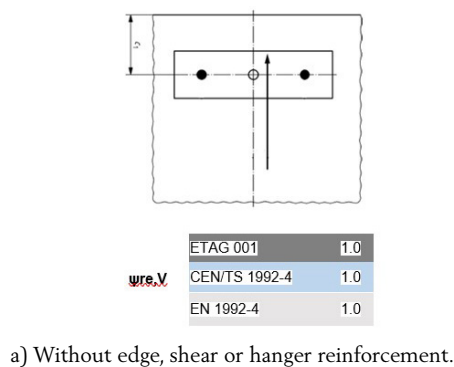


Figure 11. Type of edge reinforcement and its impact on the concrete edge load.

2.4.6. Consideration of the concrete edge load for shear loads parallel to or at an angle to the edge

The coefficient ψ_{α} takes into account the angle α that the acting shear force forms with the direction perpendicular to the free edge. If the force acts parallel to the edge ($\alpha = 90^\circ$), the failure-inducing force acting perpendicular to the edge in accordance with [11] is approximately 50% of the load. This means that the shear force that can be absorbed when applied parallel to the edge with the same edge distance is approximately twice as great as the load applied perpendicular to the edge. To date, the approach in accordance with [1] and [4] resulted in a 2.5-fold shear force under the above-mentioned marginal conditions. In accordance with EN 1992-4 [18], the original value of 90° in [11] is reverted while the equation for the calculation of the coefficient ψ_{α} has been modified accordingly. Consequently, the concrete edge failure load for a shear force acting obliquely to the edge produces up to 20% (90°) less resistance values according to EN 1992-4 [18] compared to [1] and [4], and as the angle decreases, the difference becomes smaller.

2.4.7. Impact of the conversion of the original concrete compressive strength measured on cubes with an edge length of 200mm

The original equations for determining concrete-related failure loads, such as concrete cone failure and concrete edge failure, were determined by taking into account the concrete compressive strength measured on concrete cubes with an edge length of 200 mm. In the context of transferring the design concept to other fastening systems or guidelines, the corresponding equations were given with reference to a concrete compressive strength – measured on concrete cubes with an edge length of 150mm.

As part of the revisions made to the European Standard, the equations in question were adjusted to reflect the cylinder compressive strength (150mm x 300mm). Based on this adjustment, up to 4% lower resistance values are calculated than for [1] and [4] in accordance with EN 1992-4 [18] – using the equation referred to.

3 FASTENING DESIGN IN FPEN 1992-1-1:2023 [15]

There is a fastening application which is not covered by EN1992-4 [18]. This application is the rigid connection between structural concrete elements using post-installed reinforcement bars. This application is covered, as a novelty, in FprEN 1992-1-1:2023 [15] (Art. 11.4.8). These connections are made with deformed reinforcement bars ($f_{yk} \leq 500 \text{ MPa}$) and mortars (epoxies, vinylesters, etc) in existing concrete structures to resist mainly static loads. (Figure 12).

The reason for not covering these topics in EN1992-4 is that the approach, in relation to the classical theory of anchors on which EN1992-4 is based, is different. The two main differences are:

Post-installed reinforcement bars (Rebar) are stressed by tension-compression loads. Not shear loads as an anchor.

Concrete cone failure or combined pullout and concrete cone failure, which are typical failure mode in classical the-

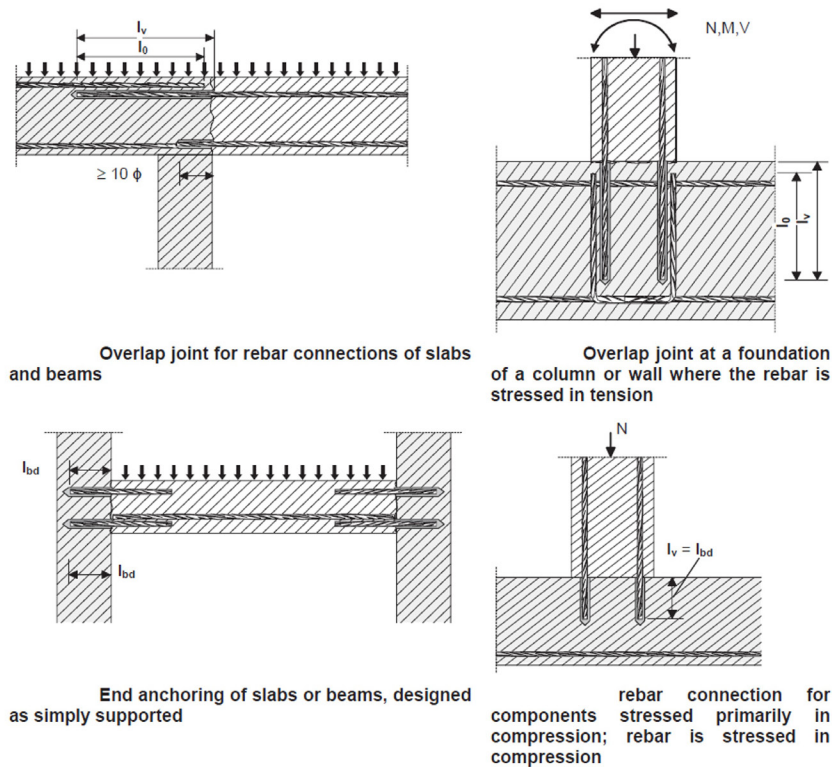


Figure 12. Examples of post-installed rebar connections include EAD 330087-00-0601 "Systems for Post-Installed rebar connections with mortar". Source [16].

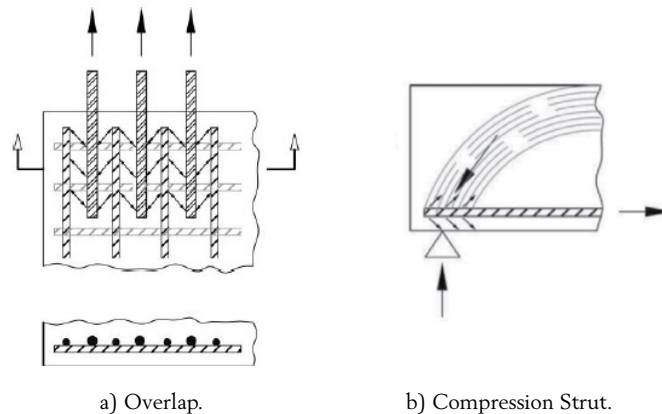


Figure 13. Situations to avoid concrete cone failure or combined pullout and concrete cone failure with post installed rebar. Source [19].

ory of anchors, are prevented by the existing reinforcement, which takes tension loads as an overlap with post-installed rebar or by a compression strut. (Figure 13).

This sketch clarifies this last topic

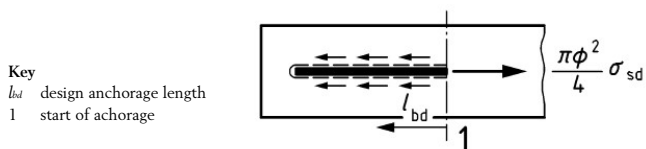


Figure 14. Sketch Anchorage of bonded post-installed reinforcement. Source [15].

The start of anchorage refers to the cross section where the reinforcement force is fully transferred to the concrete in compression. (Figure 14).

3.1. Design Anchorage length calculation

Calculation of design anchorage length for post-installed rebar is described in Art. 11.4.8 FprEN 1992-1-1:2023 [15].

Formula (1) is used according to [15]:

$$l_{bd,pi} = \frac{l_{bd}}{k_{b,pi}} \geq 10\phi \alpha_{lb} \quad (1)$$

Where:

$l_{bd,pi}$ is anchorage length for a post-installed rebar with ϕ diameter.

$k_{b,pi}$ is bond efficiency factor. This factor depends on bonding properties of mortar, which are evaluated with test regarding European Assessment Document EAD 330087-00-0601. This factor appears in European Technical Product Specification (European Technical

Table 11.1 (NDP) — Anchorage length of straight bars divided by diameter l_{bd}/ϕ

ϕ [mm]	Anchorage length l_{bd}/ϕ							
	f_{ck}							
	20	25	30	35	40	45	50	60
≤ 12	47	42	38	36	33	31	30	27
14	50	44	41	38	35	33	31	29
16	52	46	42	39	37	35	33	30
20	56	50	46	42	40	37	35	32
25	60	54	49	46	43	40	38	35
28	63	56	51	47	44	42	40	36
32	65	58	53	49	46	44	41	38

NOTE The values of Table 11.1 (NDP) are derived from Formula (11.3). This table is valid for $\alpha_s = 1,5\phi$; $\sigma_{sd} = 435$ MPa and for bars in good bond conditions. For bars in poor bond conditions in concrete members the values should be multiplied by 1,2.

Table 1. Anchorage length of straight bars. (It corresponds to Table 11.11 in [15]).

Approval) (ETA) of mortar. This factor could take values between 0.71 to 1.

α_{lb} factor accounting for cracks along the bar which may be taken as $\alpha_{lb} = 1,5$ in general or as given in the European Technical Product Specification of mortar.

l_{bd} is the anchorage length for a cast-in rebar with ϕ diameter. There are important changes regarding this topic in FprEN 1992-1-1:2023 [15]. There are two calculation methods:

Simplified Method: Using Table 1 based in f_{ck} of concrete and Table 1. Anchorage length of straight bars. (It corresponds to Table 11.11 in [15])

Detailed Method: Design anchorage length should be calculated with formula (2) according to [15].

$$l_{bd} = k_{lb} k_{cp} \phi \left(\frac{\sigma_{sd}}{435} \right)^{n_s} \left(\frac{25}{f_{ck}} \right)^{1/2} \left(\frac{\phi}{20} \right)^{1/5} \left(\frac{1,5\phi}{c_d} \right)^{1/2} \geq 10\phi \quad (2)$$

where:

c_d is the concrete cover. This is $\text{Min}(0,5 c_s, c_x, c_y)$ (Figure 15).

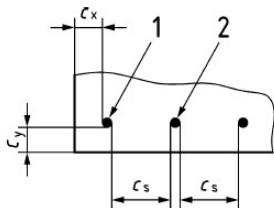


Figure 15. Concrete cover definition. Source [15].

σ_{sd} is the tension/compression stress in rebar in MPa.
 f_{ck} is the characteristic concrete strength in MPa.
 ϕ is the diameter rebar in mm.
 k_{cp} is the coefficient accounting for casting effects on bond conditions.

k_{lb} is the factor depending design situation (50 for persistent and transient design situations. 35 for accidental design situations).

3.2. Post Installed Rebar Installation

It is important to note that design of post-installed reinforcing bars according to FprEN 1992-1-1:2023 [15] assumes that the installation is performed according to the manufacturer's installation instructions by qualified personnel and inspection of the installation is carried out by appropriately qualified personnel.

Installation procedure of post-installed rebars involves the realization of drill holes in the concrete. The realization of drill holes close to each other or close to the concrete edge can cause cracks in the concrete that could significantly reduce the tension strength of post-installed rebars.

That is why Article 11.4.8 [15] indicates minimum distances at the concrete edge of the post-installed rebars depending on the drilling method used (rotary percussion drilling with electropneumatic hammer, rotary drilling with diamond coring, compressed air drilling), if drilling is guided with a drilling aid, etc. (Table 2 and Figure 16).

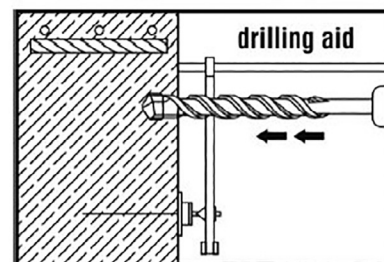


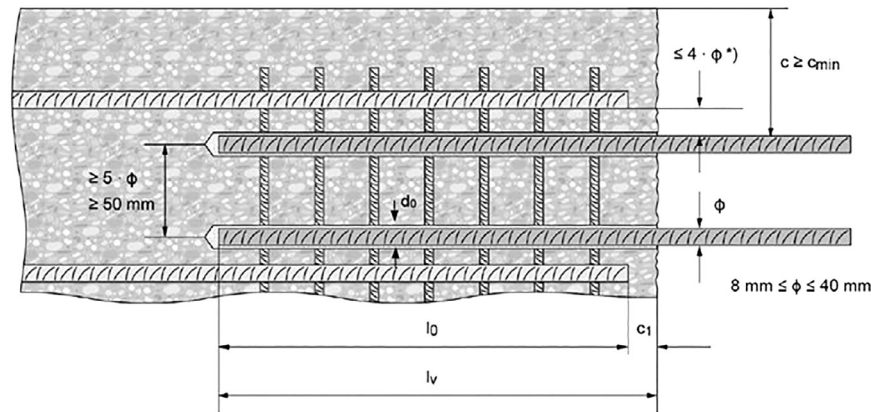
Figure 16. Example of drilling aid. Source [16].

There are also limitations with the minimum distance between post-installed rebars $c_{s,pir} = \max(4\phi; 40 \text{ mm})$ and between post-installed and cast-in rebars $c_s = \max(2\phi; 20 \text{ mm})$.

Table 11.2 — Minimum concrete cover $c_{min,b}$ for post-installed reinforcing steel bars

Drilling method	Bar diameter	$c_{min,b}$	
		without drilling aid	with drilling aid
Rotary percussion drilling / Hammer drilling and diamond coring/drilling	$\phi < 25$ mm	30 mm + 0,06 $l_{bd,pi} \geq 2\phi$	30 mm + 0,02 $l_{bd,pi} \geq 2\phi$
	$\phi \geq 25$ mm	40 mm + 0,06 $l_{bd,pi} \geq 2\phi$	40 mm + 0,02 $l_{bd,pi} \geq 2\phi$
Compressed air drilling	$\phi < 25$ mm	50 mm + 0,08 $l_{bd,pi}$	50 mm + 0,02 $l_{bd,pi}$
	$\phi \geq 25$ mm	60 mm + 0,08 $l_{bd,pi} \geq 2\phi$	60 mm + 0,02 $l_{bd,pi} \geq 2\phi$

Table 2. Minimum concrete cover for post-installed rebar. (it corresponds to Table 11.1. in [15]).



*) If the clear distance between lapped bars exceeds $4 \cdot \phi$, then the lap length shall be increased by the difference between the clear bar distance and $4 \cdot \phi$.

- c concrete cover of post-installed rebar
- c_1 concrete cover at end-face of existing rebar
- c_{min} minimum concrete cover according to Table B3 and to EN 1992-1-1
- ϕ diameter of reinforcement bar
- l_0 lap length, according to EN 1992-1-1 for static loading and according to EN 1998-1, chapter 5.6.3 for seismic loading
- l_v embedment length $\geq l_0 + c_1$
- d_0 nominal drill bit diameter

Figure 17. General construction rules for post-installed rebars. Source [17].

These minimum distances could be specified in European Technical Product Specification of the mortar. (Figure 17)

CONCLUSIONS

EN1992-4 represents the state of the art regarding the design of concrete fasteners, being fully consistent with the rest of the Eurocodes series.

The design according to EN1992-4 [18] is only possible for those fasteners with an ETA approval, in which EN1992-4 [18] is specified as the design method.

At the technical level, EN1992-4 [18] does not introduce very significant changes in relation to ETAG 001 [1] or CEN/TS 1992-4 [4], which it replaces, however, the level of acceptance and mandatory compliance will necessarily be higher.

There are two new aspects to take account in design of fasteners in concrete:

- Consideration of the effect of sustained tension loads for chemical anchors due to creep effect.

- Consideration of strenght contribution of reinforcement close to fasteners.

FprEN 1992-1-1:2023 [15] includes, as a novelty, anchorage length calculation of post-installed rebars, not included in EN1992-4 [18], which is used for design of rigid connections between concrete members.

References

- [1] ETAG 001, European Technical Approval Guideline – Metal anchors for use in concrete, Annex C, Design methods for anchorages, amended 2010, Edition 1997.
- [2] European Organization for Technical Approval (EOTA), Technical Report TR029: Design of bonded anchors, Edition June 2007, amended September 2010.
- [3] European Organization for Technical Approval (EOTA), Technical Report TR045: Design of metal anchors for use in concrete under seismic actions, Edition February 2013.
- [4] European Committee for Standardization CEN, CEN / TS 1992-4 provisions: Design of fastenings for use in concrete.
- [5] European Committee for Standardization CEN / TR 15728: 2008: Design and use of inserts for lifting and placing concrete precast concrete.
- [6] ETAG 001, European Technical Approval Guideline – Metal anchors for use in concrete, Amended 2013, Edition 1997.

- [7] European Organization for Technical Assessment (EOTA), European Assessment Document, EAD: Mechanical fasteners for use in concrete, 10/2016.
- [8] Eurocode 2 (EN 1992-1-1): Design of concrete structures - Part 1-1: General rules and rules for buildings. 2004
- [9] Fuchs, W., Eligehausen, R. : The CC method for calculating the concrete breakout load of anchors, concrete and reinforced concrete 90 (1995), H.1 S.6-9, H2, p.38-44 , H3, S73-76.
- [10] Zhao, G. : Load-bearing behavior of headed stud anchors positioned away from the edge in concrete breakout failures. Dissertation, University of Stuttgart, 1993. Dissertation, University of Stuttgart, 1993.
- [11] Bruckner, M., Eligehausen R., Ozbolt, J. : Influence of the bending compressive stresses on the concrete cone capacity. In Eligehausen, R. (Editor), Connections between Steel and Concrete. Rilem Publications s.a.r.l. Cadhan Cedex, 2001.
- [12] Eligehausen, R., Fichtner, S. : Influence of the axial distance on the concrete breakout load of fasteners under a bending moment. Report, Institute for Materials in Construction, University of Stuttgart, not published.
- [13] Sippel, M. : Fasteners and anchors – design based on new standard EN 1992-4, 2nd annual meeting of DAfStb 2014.
- [14] Fuchs W. : Load-bearing behavior of fasteners under shear loads in non-cracked concrete. Dissertation, University of Stuttgart, 1990.
- [15] CEN. FprEN1992-1-1:2023. Eurocode 2: Design of concrete structures-Part 1-1: General rules and rules for buildings, bridges and civil engineering structures.
(*) This document is available through the National members at CEN TC250/SC2
- [16] European Assessment Document EAD 330087-00-0601"Systems for Post-Installed rebar connections with mortar". EOTA. 2018..
- [17] European Technical Approval ETA-20/0540 Hilti HIT-RE500 V4 Injection Mortar. EOTA. 2021.
- [18] Eurocode 2 (EN1992-4). Design of concrete structures - Part 4: Design of fastenings for use in concrete. 2008.
- [19] Special Activity Group 4. Convener: Eligehausen, R. : Bulletin 58 "Design of anchorages in concrete". Fédération International du Béton (fib). 2011.

Some Highlights on the New Version of EN 1992-1-2 (Eurocode 2, Fire part).

Algunos aspectos destacados de la nueva versión de la norma EN 1992-1-2 (Eurocódigo 2, parte de fuego)

Sergio Carrascón^a, Fabienne Robert^b, Carlos Villagrà^{*,c}

^a Spanish Institute of Cement and its Applications (IECA)

^b CERIB, Fire Testing Centre

^c Eduardo Torroja Institute of Construction Sciences

Recibido el 3 de agosto de 2022; aceptado el 31 de marzo de 2023

SUMMARY

The revision process of Eurocode 2 relating to concrete structural design is ready for the final step, the Formal Vote in CEN TC 250 Structural Eurocodes at the beginning of 2023. This paper summarizes the main changes and new developments presented by this revision in FprEN 1992-1-2 regarding the version currently in force. It's mainly focused in the introduction on some changes in the structure of the document and the reduction of the number of Nationally Determined Parameters (NDPs). Additionally, some changes and novelties in the properties of concrete, reinforcing and prestressing steel with temperature are commented. Another important point is the novelties in the design and verification methods (tables, simplified and advanced), focusing on the simplified methods and an analytical formulation to find the temperature in rectangular and circular cross-sections. Finally, the new approach in the treatment of concrete spalling that simplifies and clarifies the measures to avoid it and new developments in the Annexes section are discussed.

KEYWORDS: EN 1992-1-2, concrete structures, fire design, design methods, spalling.

©2023 Hormigón y Acero, the journal of the Spanish Association of Structural Engineering (ACHE). Published by Cinter Divulgación Técnica S.L. This is an open-access article distributed under the terms of the Creative Commons (CC BY-NC-ND 4.0) License

RESUMEN

El proceso de revisión del Eurocódigo 2 relativo al diseño estructural de hormigón está listo para el último paso, la votación formal en el CEN TC 250 *Structural Eurocodes* a principios de 2023. Este documento resume los principales cambios y novedades que presenta esta revisión de FprEN 1992-1-2 con respecto a la versión actualmente en vigor. Se centrará principalmente en la introducción en algunos cambios en la estructura del documento y en la reducción del número de Parámetros de Determinación Nacional (PDN). Además, se comentan algunos cambios y novedades en las propiedades del hormigón, las armaduras y el acero de pretensado con la temperatura. Otro punto importante son las novedades en los métodos de diseño y verificación (tablas, simplificado y avanzado), centrándose en los métodos simplificados y en una formulación analítica para hallar la temperatura en secciones rectangulares y circulares. Por último, se discute el nuevo enfoque en el tratamiento del desconchado del hormigón (spalling) que simplifica y aclara las medidas para evitarlo y las novedades en la sección de Anexos.

PALABRAS CLAVE: EN 1992-1-2, estructuras de hormigón, diseño frente a incendio, métodos de cálculo, spalling.

©2023 Hormigón y Acero, the journal of the Spanish Association of Structural Engineering (ACHE). Published by Cinter Divulgación Técnica S.L. This is an open-access article distributed under the terms of the Creative Commons (CC BY-NC-ND 4.0) License

* Persona de contacto / Corresponding author:
Correo-e / e-mail: carlosv@ietcc.csic.es (Carlos Villagrà)

1 INTRODUCTION

The revision process of Eurocode 2 [1] relating to concrete structural design is ready for the final step, the Formal Vote in CEN TC 250 Structural Eurocodes at the beginning of 2023. This paper summarizes the main changes and new developments presented by this revision in prEN 1992-1-2 [2] about the version currently in force.

2 STRUCTURE AND GENERAL ISSUES OF prEN 1992-1-2

It has a structure very similar to the rest of the Eurocodes, with the particularities of the design of concrete structures against fire. It can be summarized in the following sections:

- Chapter 1. Introduction.
- Chapter 2. Scope.
- Chapter 3. Normative references.
- Chapter 4. Terms, definitions and symbols.
- Chapter 5. Basis of design.
- Chapter 6. Material properties.
- Chapter 7. Tabulated design data.
- Chapter 8. Simplified design methods.
- Chapter 9. Advanced design methods.
- Chapter 10. Detailing.
- Chapter 11. Rules of spalling.
- Annex A (normative): Lightweight aggregate concrete.
- Annex B (informative): Properties at high temperature of steel fibres reinforced concrete.
- Annex C (informative): Recycled aggregate concrete structures.

- Annex D (normative): Buckling of columns under fire conditions.
- Annex E (informative): Load-bearing solid walls – complementary tables.
- Bibliography.

One of the premises to be fulfilled in this revision of the Eurocodes was the reduction of Nationally Determined Parameters (NDPs) to a minimum. In the introduction, the parameters of national determination that are contemplated in [2] are defined, having been reduced from eighteen to four as could see in Table 1.

3 CHANGES CONCERNING BASIS OF DESIGN AND MATERIAL PROPERTIES

In the next bullet list, the main changes in basis of design and materials properties are listed:

- In Chapter 4, one important change should be highlighted: the introduction in the project guidelines of a section on spalling where a definition of severe spalling is introduced and reference is made to chapter 10 where rules to avoid it are given.
- Chapter 5, in its general section, introduces lightweight aggregates (material properties and specific rules for spalling in Annex A), steel fibres for concrete reinforcement (design rules in Annex B) and recycled aggregates (design rules in Annex C).
- In [1], for the evaluation of the characteristic strength of normal concrete as a function of temperature and for application in the simplified methods at sectional level,

No.	Clause in EN 1992-1-2:2004	Corresponding clause in prEN 1992-1-2:2023	Parameter	Recommended value	Category of NDP	Status
	e.g. 2.3(1)	e.g. 4.3(1)	e.g. characteristic values of self-weight	e.g. nominal value	Essential NDP	Retained
					Other NDP	Removed
						New
1	2.1.3 (2)	4.3 (2)	values of D_{s1} and D_{s2}		Other NDP	Removed
2	2.3 (2)	4.5 (1)	partial safety factor for the material properties	Recommended value $\gamma_{M,fi}=1$	Essential NDP	Retained
					Other NDP	Removed
3	3.2.3 (5)	5.3.2.1	class N and class X reduction factor for steel		Other NDP	Removed
4	3.2.4 (2)	5.3.3.1	Class A or B for prestressing steel		Other NDP	Removed
5	3.3.3 (1)	5.2.2	thermal conductivity of concrete		Other NDP	Removed
6	4.1 (1)		use of advanced calculation method		Other NDP	Removed
7	4.5.1 (2)	section 10	moisture content		Other NDP	Removed
8	5.2 (3)[refers to (2.4.2 note 2)]	6.2(1)	partial factor for combination of actions	Recommended value $\eta_{1f}=0,7$	Essential NDP	Retained
9	5.3.2 (2)	6.3.2	first order eccentricity max		Other NDP	Removed
10	5.6.1 (1)	6.6.1 (1)	class WA, WB, WC		Other NDP	Removed
11	5.7.3 (2)	6.7.3	plastic rotation		Other NDP	Removed
12	6.1 (5)	5.3.1.1	reduction factor HSC		Other NDP	Removed
13	6.2 (2)	new section 10	methods against spalling		Other NDP	Removed
14	6.3.1 (1)	5.2.2	thermal conductivity for HSC		Other NDP	Removed
15	6.4.2.1 (3)		k factor		Other NDP	Removed
16	6.4.2.2 (2)		k factor		Other NDP	Removed
17		9.2(1)	coefficient anchorage length		Essential NDP	New
18		10 (10)	minimum content of kpp monofilament fibres	$k_{pp} = 2 \text{ kg/m}^3$	Other NDP	New

Table 1. Former and current NDP.

Concrete temp. θ	$k_{c,\theta} = f_{c,\theta}/f_{ck}$			$\epsilon_{c1,\theta}$	$\epsilon_{cu1,\theta}$
	$f_{ck} < 70$ MPa Siliceous aggregates	Calcareous aggregates	$f_{ck} \geq 70$ MPa any type of aggregates		
[°C]	[-]	[-]	[-]	[-]	[-]
1	2	3	4	5	6
20	1.00	1.00	1.00	0.0025	0.0200
100	1.00	1.00	1.00	0.0040	0.0225
200	0.95	0.97	0.75	0.0055	0.0250
300	0.85	0.91	0.75	0.0070	0.0275
400	0.75	0.85	0.75	0.0100	0.0300
500	0.60	0.74	0.60	0.0150	0.0325
600	0.45	0.60	0.45	0.0250	0.0350
700	0.30	0.43	0.30	0.0250	0.0375
800	0.15	0.27	0.15	0.0250	0.0400
900	0.08	0.15	0.08	0.0250	0.0425
1 000	0.04	0.06	0.04	0.0250	0.0450
1 100	0.01	0.02	0.01	0.0250	0.0475
1 200	0.00	0.00	0.00	-	-

Table 2: New version of reduction factor for concrete strength in compression. Reproduction of Table 5.1 of FprEN1992-1-2:2023 [2].

there is a curve that represents the coefficient as a function of the type of aggregate.

On the other hand, there is a table giving the reduction strength factor for High Strength Concrete (HSC) for the three different classes of HSC. In the new version there is only one table (Table 2) for the reduction factor $k_{c,\theta}$, and other parameters of stress-strain relationship with two columns for normal concrete (under 70 MPa) for calcareous aggregates and for siliceous aggregates and the third column is for HSC (from 70 to 100 MPa).

One reference for these changes, could be [3].

- In [4], a specific informative annex is provided specifying the strength of concrete during its cooling phase. To harmonize the different parts of Eurocodes, the Horizontal Fire Group has suggested incorporating the informative annex in EN1992-1-2 [1]. This one has been adapted to cover both siliceous and calcareous aggregates and has been simplified to become one unique clause. The decision was taken by an agreement between the members of the Horizontal Fire Group.
- Another interesting new feature is the introduction of values for the concrete strength in the cooling phase, depending on the maximum temperature reached during the heating phase (Extract 1 in Appendix to this paper).
- In [1] two different curves for thermal conductivity at elevated temperatures are provided and finally an interval of values is adopted but giving the possibility to take any specific curve within the interval in the scope of national annex (NDP). This situation has led to many curves across Europe. The new curve presented as an analytical expression is included in Extract 2 of the Appendix to this paper. For further information, see 5.2.2 in the Background Document for prEN 1992-1-2:2022.[5]

4

CHANGES CONCERNING TABULATED DATA

In chapter 6, new tables have been introduced for ease of use. The following general rules are given:

Concretes of usual density between 2000 and 2600 kg/m³.

- If the cross-section is variable along length, the minimum dimensions and axis distance of reinforcement shall be applied for the most unfavourable cross-section.
- For concretes with $f_{ck} \geq 70$ MPa, they should only be checked for R-values up to R120.
- There is a risk of severe spalling if the limitation rules to avoid spalling (Chapter 10) are not complied with.
- If the minimum values of the tabulated data are taken, no additional checks for torsion, shear, and reinforcement anchorage should be carried out.
- All tables in Chapter 6 are calculated with a load level $\eta_{fi} = 0.7$.

The design Table 5.2a in EN1992-1-2 [1] gives in some cases results on the unsafe side compared to advance design method, see explanations according to Method A. Thus the table is restricted to columns with $l_{0,fi}/l_0 = 0.5$. To increase the ease of use for designing columns, a rule defining a fictitious replacement effective length is established and the tables and Formula (6.7) in [2] may be used for other values of this ratio. Then, should be calculated according to Formula (6.6) in [2] using the value of axial resistance of the column at ambient temperature conditions N_{Rd} for a modified effective length $l_{0'} = 2l_{0,fi}$.

For columns, there is a definition of the effective column lengths to consider second order effects in case of fire (Figure 1).

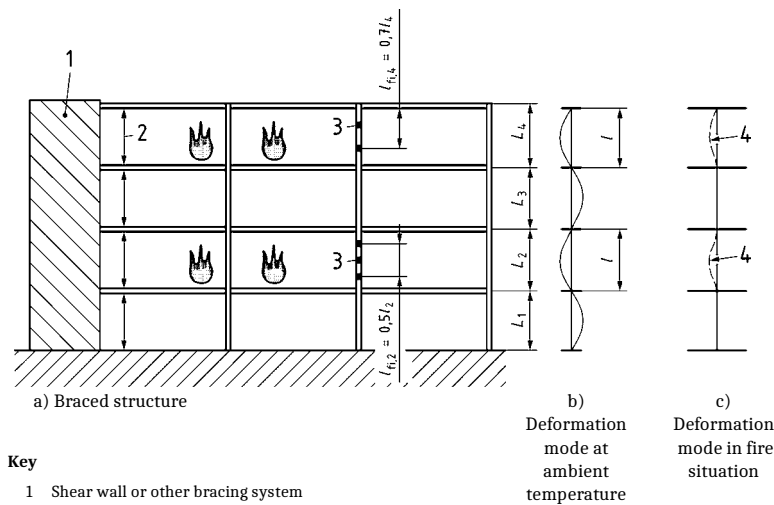


Figure 1. Effective length $l_{0,fi}$ for columns. Reproduction of Figure 6.3 [2].

According to 6.1 (2) of [2], Tabulated design data is considered to generally give conservative results compared to relevant tests or simplified or advanced design methods. This is in line with the concept of Levels-of-Approximation, presented e.g. in FIB Model Code 2010 in the Section “Basic Principles” [6]. Several studies with comparing calculations indicate that Method A in tendency leads to less conservative results than other design methods for $l_{0,fi} = l_0$, and also for $l_{0,fi} = l_0$. Furthermore, the extensively validated Annex D is available for columns with $l_{0,fi} = l_0$, and for $l_{0,fi} = 0.7l_0$.

In method A, two tables are provided (one for columns with fire exposure on four faces and one for a single exposed face) for $l_{0,fi}/l_0 = 0.5$, the number of μ_{fi} values having been increased for ease of use (Table 3).

A new methodology has been set up to develop tables for braced or unbraced columns given in Annex D when $l_{0,fi} = 0$ or $l_{0,fi} = 0.7l_0$.

To increase the ease of use for designing load bearing walls exposed to fire, the tabulated data for load bearing walls were extended. The table for load bearing walls in [1] contains three load degrees and two different maximum lengths at ambient temperature linked to different maximum lengths in case of fire. The table was transferred from DIN 4102-4 [7] without justifying the load degrees. For further information, see 6.4 in the Background Document for prEN 1992-1-2:2022 [5].

In walls, the table for solid load-bearing walls exposed to fire on one or two sides has been modified, increasing the values of μ_{fi} for ease of use (Tables 4 and 5) and splitting the table according to the effective length.

5 CHANGES CONCERNING THE TREATMENT OF SPALLING

A new chapter 10 has been added which clarifies the rules to assess spalling.

Many tests have been performed on concrete structural elements these last decades. However test reports on fire resistance tests on structural elements with detailed concrete mix and characteristic strength are not so well documented or publicly available. Further to a state of the art performed within CEN TC 250/SC2/WG1/TG5 and then the threshold of concrete strength for which no experimental evidence or addition of polypropylene is asked, is switched from C80 to C60.

In [1], moisture content is a key parameter to consider the occurrence of explosive spalling. Moisture content is undeniably one of the main parameters influencing fire spalling of concrete, but it cannot be taken as the only parameter and many arguments are in favour of eliminating the moisture threshold:

- It is controversial, below which moisture content spalling is “unlikely to occur”. Since a European agreement for the value of μ_{fi} could not be reached, the decision was left to national annexes (in the present version of EN1992-1-2 [1], varies from 2% to 4%).
- Scientific results indicate that spalling may appear from different moisture content values depending on the concrete composition, strength, section geometry, load... At first glance, a general fixed moisture limit for spalling seems like a good idea but this is not supported by the literature as so many inter-dependent factors are involved in the phenomenon. For further information, see chapter 10 in the Background Document for prEN 1992-1-2:2022 [5].
- Even if the temperature, relative humidity (climate history) and age of concrete are known, it is a very difficult task to determine the moisture content of the concrete.
- While moisture gradients do appear instead of uniform moisture contents, nothing is said about where (at the surface, in depth...) and when (3 months after casting, at equilibrium?) the moisture content should be measured or estimated.
- The designer has difficulties predicting what will be the moisture content in the built element, and cannot influence it.

Standard fire resistance	Minimum dimensions (mm)		
	Column width b_{min} /axis distance a of the main reinforcement		
	$\mu_n = 0,2$	$\mu_n = 0,5$	$\mu_n = 0,7$
1	2	3	4
R 30	200/25	200/25	200/32 300/27
R 60	200/25	200/36 300/31	250/46 350/40
R 90	200/31 300/25	300/45 400/38	350/53 450/40 ^a
R 120	250/40 350/35	350/45 ^a 450/40 ^a	350/57 ^a 450/51 ^a
R 180	350/45 ^a	350/63 ^a	450/70 ^a
R 240	350/61 ^a	450/75 ^a	-

NOTE 1 For prestressed columns, the increase of axis distance according to 6.2 (2) should be noted.
NOTE 2 Table 6.1 has been generated from Formula (6.6) with $l_{0,fi} = 3$ m.
NOTE 3 Table 6.1 can be used for columns exposed on two parallel sides

^a Minimum 8 bars

Standard fire resistance	Minimum dimensions (mm)		
	Column width b_{min} /axis distance a of the main reinforcement		
	$\mu_n = 0,2$	$\mu_n = 0,5$	$\mu_n = 0,7$
1	2	3	4
R 30	100/10	120/15	130/25
R 60	110/10	130/15	140/25
R 90	120/20	140/25	155/25
R 120	150/25	160/30	175/35
R 180	185/45	200/50	230/55
R 240	230/60	240/65	290/70

Table 3. Tables of method A for columns exposed to fire on four sides (upper table) and one side (lower table). Reproduction of Tables 6.1 and 6.2 [2].

Standard fire resistance	Minimum dimensions (mm)			Standard fire resistance	Minimum dimensions (mm)		
	Wall thickness h_w /axis distance a				Wall thickness h_w /axis distance a		
	$\mu_{fi} = 0,2$	$\mu_{fi} = 0,5$	$\mu_{fi} = 0,7$		$\mu_{fi} = 0,2$	$\mu_{fi} = 0,5$	$\mu_{fi} = 0,7$
Exposed on one side				Exposed on both sides			
1	2	3	4	5	6	7	8
REI 30	100/10	110/10	120/10	R 30	100/10	120/10	130/10
REI 60	110/10	120/15	130/20	R 60	120/15	155/20	170/25
REI 90	120/20	135/25	140/30	R 90	140/20	185/30	210/35
REI 120	135/25	150/30	160/35	R 120	165/30	210/40	240/45
REI 180	155/35	170/40	180/45	R 180	200/45	250/50	280/55
REI 240	180/40	200/45	210/50	R 240	250/50	305/55	340/60

Table 4. Minimum dimensions and axis distances for load-bearing reinforced concrete walls exposed on one long side (left) or on both sides (right) with $l_0 \leq 4.5$ m for ambient temperature conditions and $l_{0,fi} \leq 2.5$ m for fire situations. Reproduction of Table 6.4 [2].

It is favoured to delete the moisture content threshold and to give general recommendations when a high moisture content is expected.

Firstly, Table 6 shows the spalling verification rules according to the requested fire resistance, the environmental circumstances of the structure and the compressive strength of the concrete and the types of concrete additions.

Standard fire resistance	Minimum dimensions (mm)			Standard fire resistance	Minimum dimensions (mm)		
	Wall thickness h_w /axis distance a				Wall thickness h_w /axis distance a		
	$\mu_{fi} = 0,2$	$\mu_{fi} = 0,5$	$\mu_{fi} = 0,7$		$\mu_{fi} = 0,2$	$\mu_{fi} = 0,5$	$\mu_{fi} = 0,7$
Exposed on one side				Exposed on both sides			
1	2	3	4	5	6	7	8
REI 30	80/10	90/10	100/10	R 30	90/10	100/10	110/10
REI 60	90/10	100/10	110/15	R 60	110/10	125/15	140/20
REI 90	100/10	110/15	120/20	R 90	125/15	155/25	170/30
REI 120	120/15	120/20	130/25	R 120	140/25	175/35	200/40
REI 180	150/20	150/25	150/30	R 180	175/30	215/40	240/45
REI 240	170/25	175/30	175/35	R 240	200/35	250/45	280/50

Table 5. Minimum dimensions and axis distances for load-bearing reinforced concrete walls exposed on one long side (left) or on both sides (right) with $l_0 \leq 2.5$ m for ambient temperature conditions and $l_{0,fi} \leq 1.25$ m for fire situations. Reproduction of table 6.6 [2].

Verification for spalling	
R15	Verification of spalling may be omitted except Clause 10(2)
— structures in a water saturated environment — insulating permanent formwork which prevents concrete from drying	Specific assessment of spalling should be undertaken or polypropylene fibres should be specified See Clause 10(7), (8), (9) or (10)
$f_{ck} < 70$ MPa and silica fume content < 6 % by weight of cement	Verification of spalling may be omitted except Clause 10(3) and (5)
$f_{ck} < 70$ MPa and silica fume content ≥ 6 % by weight of cement or $f_{ck} \geq 70$ MPa	Specific assessment of spalling should be undertaken or polypropylene fibres should be specified See Clause 10(7), (8), (9) or (10)

Table 6. Overview of the rules for spalling. Reproduction of Table 10.1 [2].

Standard fire resistance	Minimum web thickness $b_{w,min}$ (mm)	Minimum web thickness $b_{w,min}$ for a distance of $2h$ from an intermediate support in continuous isolated members
R 30	80	80
R ≥ 60	100	120

Table 7. Special rules for isolated members with thin web. Reproduction of Table 10.2 [2].

In [Extract 3](#) of the Appendix to this paper, content from [\[2\]](#) is included that is referred to [Table 6](#).

In a second table ([Table 7](#)), the specific cases in which special measures have to be taken for beams with small web dimensions are shown.

6 CHANGES CONCERNING SIMPLIFIED DESIGN METHODS

The major change in chapter 7 related to simplified design method is that the Isotherm 500 method disappears as such. However, an improved version of the “zone method” is given.

In [\[1\]](#), the zone method consists of dividing the section into strips of equal width (zones), determining the average

temperature of each zone and, from this, determining the strength of the concrete. From the contributions of each zone, the resistance capacity of the section is determined, disregarding a rim zone, determined by the parameter a_r . The contribution of the reinforcement is evaluated considering the exact temperatures in the rebars.

The major drawback of this method is the determination of the section temperatures. In [\[1\]](#), different temperature profiles at different time instants are given for several typical cross-section profiles. Some of these profiles are shown in [Figure 2](#). The problem with this method is that the determination of the temperatures at each point is not very precise, which leads to some uncertainty in the calculation of the temperature of the reinforcement, for example. On the other hand, if the section considered in the project does not coincide exactly with one of those recorded in the current Annex A, it is difficult to make an accurate estimate of the temperature and the associated

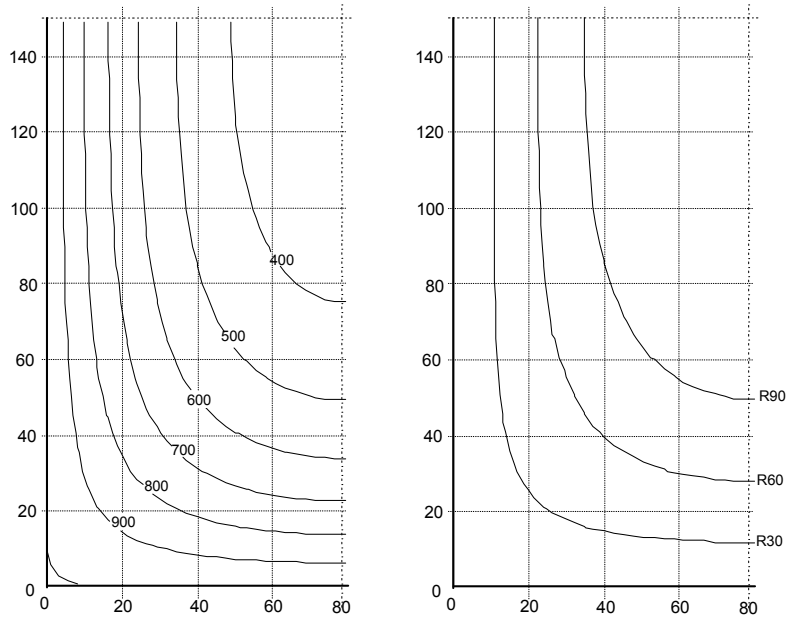


Figure 2. Isotherms ($t=90\text{min}$) and Isotherm 500 positions for different times. Reproduction of Figures A5 and A6 [1].

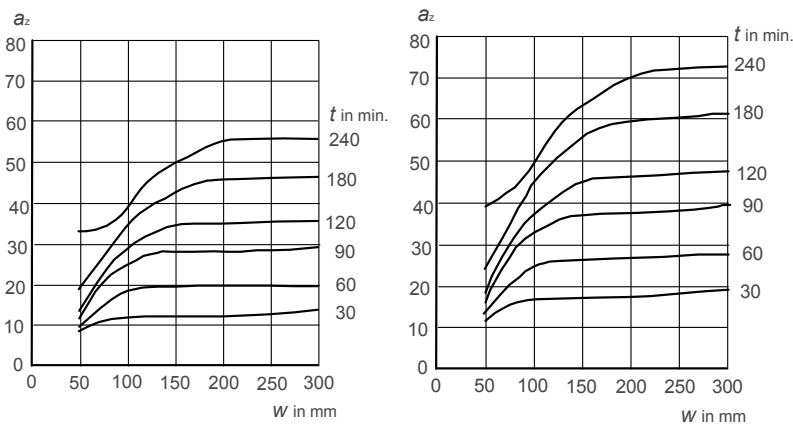


Figure 3. Reduction in cross-section a_z , of a beam or slab using siliceous aggregate concrete (left). Reduction in cross section a_z , of a column or wall using siliceous aggregate concrete (right). Reproduction of Figure B.5 [1].

resistance. With this approach, the calculation using the zone method is really laborious.

This is where one of the most important changes of [2] appears. Now, the calculation of the temperature is done employing analytical expressions. The proposed models allow the most common cases to be solved: rectangular section elements, cylindrical section elements, walls and slabs... The other major change is the determination of the parameter a_z , which is used in the improved zone method. Previously it was done from a series of abacuses (Figure 3), while now it is calculated from analytical expressions¹.

Although the a_z parameter is also defined in [2], it appears that its definition is a bit different from [1]. In the current version, it simply appears as a parameter in the calculation. In [2] it is called “rim zone” and, according to [5], for a wall of

¹ Strictly speaking, in [1] the calculation of a_z is already done using analytical expressions (from which come those of [2]). However, these expressions depend on the terms $k_c(\theta)$, the reduction coefficients for concrete. The calculation of $k_c(\theta)$ is complex because it depends on the temperature in the centre of the zone, which, as mentioned above, must be calculated graphically.

thickness $2w$ with both sides exposed, a_z can be determined with the following expression:

$$(2w - 2a_z) \cdot f_c(\theta_M) = \int_{-w}^w f_c(\theta(x)) dx \quad (1)$$

The idea behind equation (1) is that a_z gives the thickness of a strength-equivalent element with reduced cross-section, by deducting the thickness a_z from the original cross-section. For supports exposed on all four sides, [5] gives an analogous expression. Equations (8) and (9) are the analytical approximation of (1).

6.1. Calculation procedure in the new Eurocode [2]

In the new Eurocode, for the verification of the fire resistance, the following procedures are given:

- Tabulated methods (chapter 6).
- Simplified methods (chapter 7), which are divided for the cases of bending and bending and axial load in:
 - Simplified verification.

- Refined verification.
- Advanced methods (chapter 8).

The changes in the tabulated methods have already been listed in section 4.

As indicated in the introduction, the most significant change has been in the simplified methods. What used to be the Isotherm 500 method and the zone method have converged into analytical methods, with two levels of complexity.

Finally, the changes in advanced methods are mainly due to changes in material models. As in [1], what is set out in Chapter 8 are general guidelines for the calculation of temperatures and structural response by numerical methods, based on the models established in Chapter 5.

Assessment by simplified methods

The new Eurocode, as in the current version, considers the cases of bending, bending and axial load, shear and torsion. However, it focuses on bending and bending-compression behaviour, leaving shear and torsional verification as a series of additional checks.

The procedure is almost the same for both bending and bending and axial load checks:

1. Determination of temperatures
2. Structural analysis
 1. Calculation of the reduced cross-section (determination of the parameter a_z). In the case of bending, the a_z parameter is determined by dividing the section into parallel zones of equal width, while in the case of bending and axial loading, the cross-section of the member should be discretized into a grid of small elemental zones (see Figure 7.9 of [2]) each characterized by area A_{cij} .
 2. Verification of the structural behaviour:
 - Simplified verification
 - Refined verification

This procedure is basically the same as the one to be followed in [1]; the key changes are in how both the temperatures and the rim zone are determined. In both cases, there has been a move from graphical methods to analytical methods.

Calculation of section temperature

In [2], it is now possible to calculate the temperature of each point of the section utilizing a series of analytical expressions.

Equations (2) to (7), which reproduce part of equations (7.1) to (7.11) of [2], do not actually have a physical meaning, but are mathematical expressions that try to adjust the temperature values of a section to those calculated by numerical methods from the material models of [2]. In particular, according to the background document [5], the conditions adopted are:

- emissivity of concrete surfaces, 0.7 (5.2.1 of [2])
- convection factor of exposed surfaces, 25W/(m²K) (7.2.1. (3) of [2])
- thermal conductivity of concrete is as given in 5.2.2 of [2]
- specific heat of concrete is as given in 5.2.3 of [2] with moisture content 1.5%.

- density of concrete is as indicated in 5.2.4 of [2]; the reference value at 20°C is 2300 kg/m³.

In addition, in [5], it can be seen that the fit between the numerical and the analytical model is rather good, with an error threshold for both concrete and steel strength of 0.1. Temperature deviations, when they occur, are always on the safe side.

For sections with a rectangular cross-section²:

- Unidirectional temperature distribution:

$$\theta_1(x,t) = 345 \cdot \log_{10} \left(\frac{7(t - \Delta t)}{60} + 1 \right) \cdot \exp \left(-x \sqrt{\frac{k}{t}} \right) \quad (2)$$

where:

- t is the duration of the standard fire (in seconds), $t \geq 1800$ s;
- x is the distance from the exposed surface (in m);
- Δt represents a delay between the temperature in the fire compartment and the concrete surface temperature as an approximation for the effects of convection and radiation, $\Delta t = 720$ s;
- k is an adjust coefficient as a function of density of concrete. It should be taken as $k = 3 \times 10^6$ s/m². Additional information is given in the background document [6].
- Fire on two opposite sides:

$$\theta_2(y,t) = \theta_1(y,t) + \theta_1(b-y,t) \quad (3)$$

$$\theta_2(z,t) = \theta_1(z,t) + \theta_1(h-z,t) \quad (4)$$

In these equations, x and z refer to the two directions (horizontal or vertical, respectively) of the section under consideration. Each equation therefore represents the temperature distribution in each direction (cases A and B of [2], 7.2.3 (1)).

- Four-sided fire:

$$\theta(y,z,t) = \theta_2(y,t) + \theta_2(z,t) - \frac{\theta_2(y,t) \cdot \theta_2(z,t)}{\theta_1(0,t)} + \Delta\theta(y',z',t) + 20^\circ\text{C} \quad (5)$$

- Three-sided fire:

$$\theta(y,z,t) = \theta_2(y,t) + \theta_1(z,t) - \frac{\theta_2(y,t) \cdot \theta_1(z,t)}{\theta_1(0,t)} + \Delta\theta(y',z',t) + 20^\circ\text{C} \quad (6)$$

In the above equations, the term $\Delta\theta$ considers the increase in temperatures due to the effect of the corners:

$$\Delta\theta(y',z',t) = \left[345 \log_{10} \left(\frac{8t}{60} + 1 \right) - \theta_1(0,t) \right] \frac{(a_c - y')(a_c - z')}{a_c^2} \quad (7)$$

where the term a_c is a parameter that depends on the duration of the fire under consideration.

Calculation of the reduced cross-section

In this part, there are also considerable changes compared to [1]. On the one hand, what has been done is a generalization of the zone method of [1]. On the other hand, the parameter a_z is now determined by the following expressions:

² Similarly, the temperature can be calculated analytically for elements with a circular cross-section. For simplicity, the expressions for circular cross-sections have not been included in this article, as they are similar to those for rectangular cross-sections

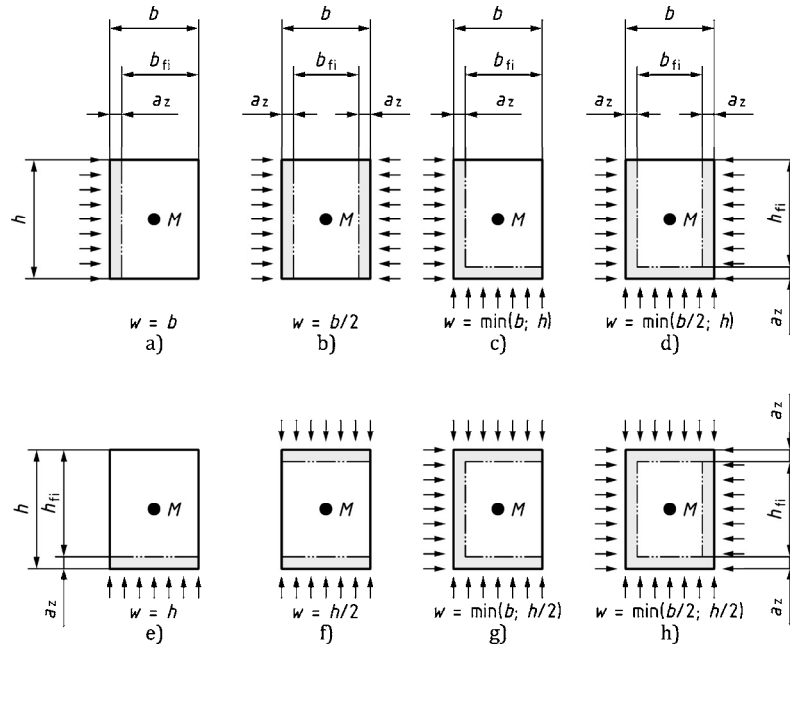


Figure 4. Determination of parameter w . Reproduction of Figure 7.5 [2].

$$a_z = \begin{cases} 0.011 \sqrt{1 + \frac{t-27}{27} \sqrt{\frac{w}{0.0125}}} & \text{for } 0.075 \leq w < 0.20 \\ 0.011 \sqrt{1 + 4 \frac{t-27}{27}} & \text{for } \geq 0.02 \end{cases} \quad (8)$$

which in [2] is used to determine a_z in a simplified way. Here, a_z depends uniquely on the time considered, t , and the w parameter³. In [1], w was obtained from an abacus, whereas now its determination has been simplified and is taken directly from a Figure, as appropriate case (Figure 4). It is important to note that in this expression, a_z does not depend on zone division. However, a_z can be determined more precisely by dividing the section into strips (or squares in the case of columns).

The expressions to determine a_z from the zones are similar to those that already existed, with the difference that now they are expressed in a more compact form and depend solely on the resistance of the concrete at each point. For the case of division into vertical zones, the next equation is used:

$$a_z = w \left(1 - \frac{\left(1 - \frac{0.02}{n} \right) \sum_{i=1}^n f_{cd,\theta}(\theta_i)}{f_{cd,\theta}(\theta_M)} \right) \quad (9)$$

where n is the number of zones into which the section is divided, $f_{cd,\theta}(\theta_i)$ is the concrete strength at temperature θ_i at the centroid of the zone i . $f_{cd,\theta}(\theta_M)$ is the concrete strength at point M , the centre of the section. This expression is actually not new, but brings together in a more compact form several expressions that were already present in [1].

³ w is a cross-sectional dimension used to obtain the reduced cross-section depending on the fire exposure and the cross-section geometry.

As can be seen, the advantage of using this expression compared to [1] is, except for the w parameter, that the rest of the values can be calculated directly and accurately, which allows, in addition to speeding up the calculation, to test different options in the search for an optimum solution. In addition, the parameter w is constant for each case analysed and is obtained in a simple way from Figure 7.5 of [2] (Figure 4).

Verification of the structural behaviour

Bending.

Once the temperatures and the thickness of the section area to be discounted have been determined, the last step is to calculate the resistant capacity of the section. A simplified assessment and a refined verification method are provided.

The expression for the calculation of the bending capacity, in the simplified form of [2] is:

$$M_{Rd,fi} = \frac{\gamma_s}{\gamma_{s,fi}} \frac{\sum_i^n f_{sy,\theta,i}}{n_{st} f_{yk}} M_{Ed} \frac{A_{s,prov}}{A_{s,req}} \quad (10)$$

With this expression⁴, what is done is to correct the calculation moment in normal situation, with the relation between the resistance in case of fire against temperatures, the ratio between the steel area designed strictly (to building code specifications) and the real one, and the relation of the partial coefficients of the material. It must be considered that to be

⁴ In [1] there is an equation very similar to (10) (eq. (E.4)). The resisting moment is evaluated by correcting the bending moment by, among other factors, the ratio $(d-a)/d$, where a is a parameter that homogenizes the reinforcement, depending on temperatures and corner effects. As explained above, it is difficult to obtain the precise temperature in the bars, and corner effects are considered as a simple correction. In [2], this correction is made by calculating the steel strengths as a function of temperature, which can now be accurately determined.

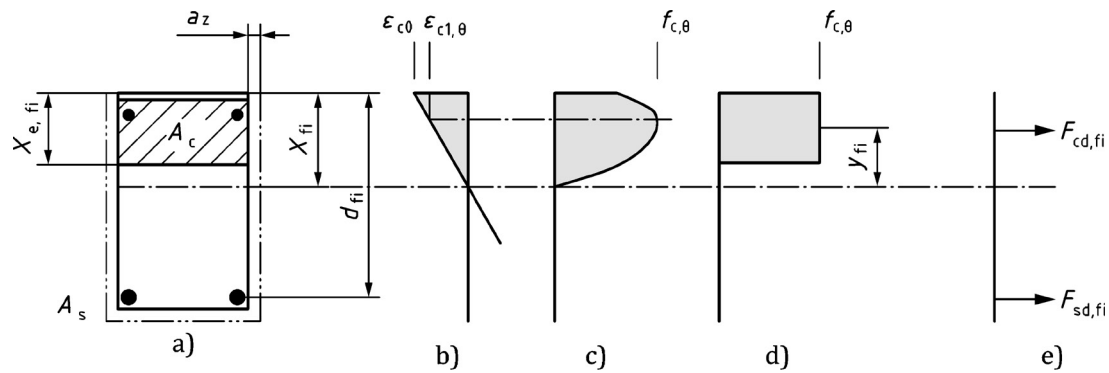


Figure 5. Stresses and strains in bending. Reproduction of Figure 7.7 [2].

able to evaluate the resistance capacity of a section by this method, a series of conditions must be fulfilled. The main one is that $A_{s,prov}/A_{s,req} < 1.3$ to make sure that the compression zone is not decisive.

If the conditions are not met, or if a more accurate verification is desired, then the refined verification method must be used. This consists of evaluating the equilibrium of forces in the section, considering the loss of resistance capacity of the reinforcement, the rim zone to be discounted, and taking as the strength of the concrete that which is reached at the point as a function of the temperature ($f_{c,\theta}(\theta_M)$). The parameters to be considered are those shown in Figure 5. The maximum section strain and the depth of the compressed block are also given.

This method is basically the convergence between the 500 Isotherm method and zone method of [1]. The zone to be discarded is now given by a_z and not by the 500 °C isotherm. The residual strength value of the entire undamaged zone is $f_{c,\theta}(\theta_M)$, instead of $f_{cd,20}$.

Bending and axial loading

In the case of supports, there are also expressions for the calculation by the simplified and refined method. However, these are no longer as simple as in the case of simple bending. The simplified method would be equivalent to the refined method for the bending case, where the equilibrium of forces in the section has to be evaluated, considering the properties of the materials in case of fire, and the different components of the eccentricity (first order, geometric imperfections, thermal...). The refined method is basically the same as the one already present in [1]. It consists of determining the moment-curvature curve of the section and, from this, ultimate moment capacity ($M_{Rd,fi}$), as a combination of the ultimate first order moment ($M_{0,Rd,fi}$) and the nominal second order moment ($M_{2,fi}$). The main difference with [1] is that, as the temperatures of each point of the section can be calculated analytically, it is much easier to establish the moment-curvature diagram of the section at a given instant.

7

CONCLUSIONS

The following key changes of the new draft [2] can be highlighted:

- harmonized structure / table of contents [2] with other fire parts;
- amended and improved simplified design methods, especially the determination of the temperature through analytical expressions, makes it possible to simplify and automate the calculation. In addition, it allows the search for optimal solutions and more precise results to be obtained because new tables for columns and walls with more parameters are included;
- ensured consistency between tabulated design data, simplified and advanced design methods;
- properties of steel fibre reinforced concrete at high temperature;
- properties of recycled aggregate concrete at high temperature;
- specific rules for avoiding / controlling spalling.

Moreover, through the reduction of the number of alternative application rules, the clarification of the use and scope of tabulated data, the reduction of NDPs, and the reduction of the volume of text by about 25%, ease of use has been enhanced.

References⁵

- [1] CEN, EN 1992-1-2:2004 Eurocode 2: Design of concrete structures - Part 1-2: Structural fire design. Brussels: CEN, 2004.
- [2] CEN, *FprEN 1992-1-2:2023 Eurocode 2: Design of concrete structures - Part 1-2: Structural fire design. Brussels: CEN, 2023.
- [3] P. Pimienta, *Physical properties and behaviour of high-performance concrete at high temperature: State-of-the-art report of the RILEM technical committee 227-HPB*. Cham, Switzerland: Springer, 2019.
- [4] CEN, EN 1994-1-2:2005 Eurocode 4: Design of Composite Steel and Concrete Structures - Part 1-2: Structural Fire Design. Brussels: CEN, 2005.

5 Documents marked with (*) are available through the National members at CEN TC250/SC2

- [5] CEN, *Background document for prEN 1992-1-2:2022. Brussels: CEN, 2022.
- [6] FIB, *FIB Model Code for Concrete Structures*. Lausanne: Ernst & Sohn, 2010.
- [7] DIN, *Fire behavior of building materials and building components - Part 4: Synopsis and application of classified building materials, components and special components*, DIN. Berlin, 2014.

APPENDIX

EXTRACTED TEXT OF FPEN 1992-1-2:2023.

(6) For thermal actions in accordance with prEN 1991-1-2:2021, 5.3 (Physically based models), when considering the cooling phase, the strength of concrete heated to a maximum temperature $\theta_{c,max}$ and having cooled down to 20 °C may be taken according to Formula (5.8):

$$f_{c,\theta,20\text{ °C}} = \varphi f_{ck} \quad (5.8)$$

where for:

— $f_{ck} < 70$ MPa

$$\varphi = f_{c,\theta_{max}}/f_{ck} \quad \text{for } 20\text{ °C} \leq \theta_{max} < 100\text{ °C} \quad (5.8a)$$

$$\varphi = (-0,0005 \times \theta_{max} + 1,05) (f_{c,\theta_{max}}/f_{ck}) \quad \text{for } 100\text{ °C} \leq \theta_{max} < 300\text{ °C} \quad (5.8b)$$

$$\varphi = 0,9 (f_{c,\theta_{max}}/f_{ck}) \quad \text{for } \theta_{max} \geq 300\text{ °C} \quad (5.8c)$$

Extract 1: Concrete strength in the cooling phase. Text extract taken from article 5.2.3 (2) [2].

(1) The thermal conductivity λ_c of concrete may be taken as:

$$\lambda_c = 2 - 0,2451 (\theta_c/100) + 0,0107 (\theta_c/100)^2 \text{ W/(m K)} \quad \text{for } \theta_c \leq 140\text{ °C} \quad (5.1a)$$

$$\lambda_c = -0,02604 \theta_c + 5,324 \text{ W/(m K)} \quad \text{for } 140 < \theta_c < 160\text{ °C} \quad (5.1b)$$

$$\lambda_c = 1,36 - 0,136 (\theta_c/100) + 0,0057 (\theta_c/100)^2 \text{ W/(m K)} \quad \text{for } 160\text{ °C} \leq \theta_c \leq 1\,200\text{ °C} \quad (5.1c)$$

Extract 2: Definition of conductivity λ_c function of temperature θ_c . Text extract taken from article 5.2.2 (1) [2].

(2) For performance requirements R15, verification for spalling may be omitted except for isolated members with webs thinner than 80 mm and $f_{ck} \geq 70$ MPa.

(3) A specific assessment of spalling should be undertaken (see (7), (8) or (9)), or polypropylene fibres should be specified for the concrete mix according to (10), under any one of the following conditions due to the expected high moisture content or specific behaviour:

- structures in a water saturated environment;
- insulating permanent formwork which prevents concrete from drying.

(4) When using tabulated design data (Clause 6), verification of spalling may be omitted for $f_{ck} < 70$ MPa, provided that the maximum content of silica fume is less than 6 % by weight of cement except for (3) above.

NOTE 2 Tabulated data have been developed based on fire tests or on calculations calibrated against full scale fire resistance tests, including tests where spalling occurred. Hence the effects of spalling are covered by tabulated data.

(5) When using simplified design methods or advanced design methods, verification of spalling may be omitted for $f_{ck} < 70$ MPa, provided that the maximum content of silica fume is less than 6 % by weight of cement except in the case of (3) and in the case of isolated members with three sides exposed, whose dimensions do not comply with Table 10.2. In these cases, a specific assessment of spalling should be undertaken (see (7), (8) or (9)), or polypropylene fibres should be specified for the concrete mix according to (10).

NOTE 3 When columns are highly loaded, it can result in higher susceptibility to spalling.

(6) For $f_{ck} \geq 70$ MPa or contents of silica fume above 6 % by weight of cement, a specific assessment of spalling should be undertaken (see (7), (8) or (9)), or polypropylene fibres should be specified for the concrete mix according to (10).

(7) The application of protective layers may be used to mitigate severe spalling (see 4.12).

(8) The effect on performance (R and/or EI) due to severe spalling may be taken into account by considering the loss of strength either at member or at structure level. This loss of strength may be assessed using a reduced effective cross-section, where the spalled layer of concrete is omitted when calculating the strength. The extent of the spalled layer of concrete may be based on experimental assessment according to (9).

(9) When assessment based on experimental evidence is required, it should be obtained from tests representative of the conditions of the structural member in terms of geometry, stress and moisture content.

(10) When polypropylene fibres are used to mitigate severe spalling, a minimum content k_{pp} of monofilament fibres with diameter less than or equal to 50 μm should be specified for the concrete mix. Alternative contents or diameters may be specified if experimental evidence according to (9) is provided.

NOTE 4 The value of k_{pp} is 2,0 kg/m³, unless the National Annex gives a different value.

Extract 3: Clauses referred in Table 6. Text extract taken from article 10 [2].

